Journal of Immunology Research

Natural Products as Targeted Modulators of the Immune System 2021

Lead Guest Editor: Kai Wang
Guest Editors: Michael A. Conlon, Wenkai Ren, and Tomasz Baczek

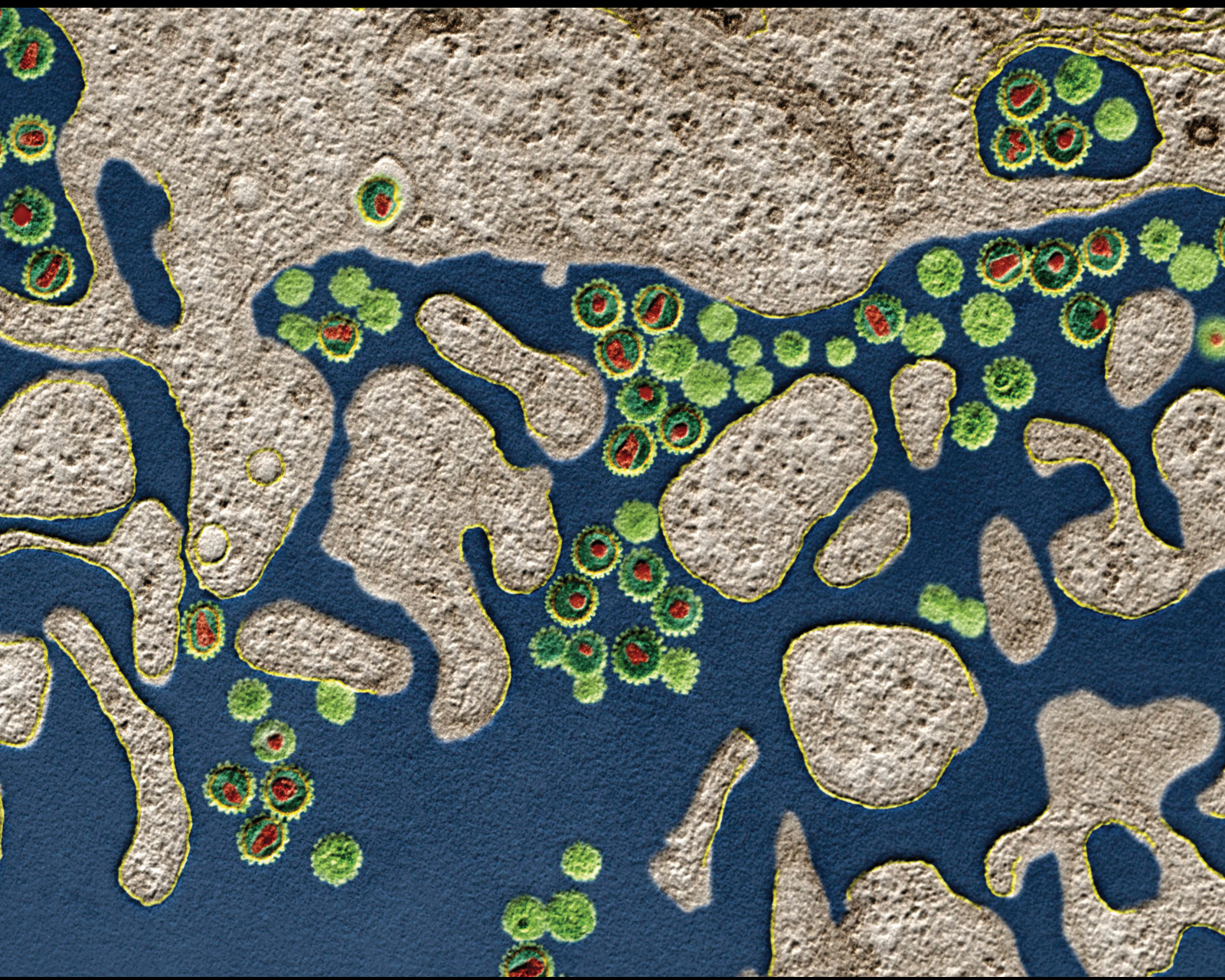

Natural Products as Targeted Modulators of the Immune System 2021

Journal of Immunology Research

Natural Products as Targeted Modulators of the Immune System 2021

Lead Guest Editor: Kai Wang
Guest Editors: Michael A. Conlon, Wenkai Ren, and Tomasz Baczek

Contents

Hindawi
Journal of Immunology Research
Volume 2021, Article ID 4560012, 10 pages
https://doi.org/10.1155/2021/4560012

Review Article

Pharmacological Actions, Molecular Mechanisms, Pharmacokinetic Progressions, and Clinical Applications of Hydroxysafflor Yellow A in Antidiabetic Research

Xilan Zhang[1], **Dayue Shen**[1], **Yating Feng**[1], **Yuanping Li**[2] and **Hui Liao**[2]

[1]*School of Pharmacy, Shanxi Medical University, Taiyuan 030001, China*
[2]*Department of Pharmacy, Fifth Hospital of Shanxi Medical University (Shanxi Provincial People's Hospital), Taiyuan 030012, China*

Correspondence should be addressed to Hui Liao; huiliao@263.net

Received 29 July 2021; Revised 1 November 2021; Accepted 16 November 2021; Published 13 December 2021

Academic Editor: Kai Wang

Hydroxysafflor yellow A (HSYA), a nutraceutical compound derived from safflower (*Carthamus tinctorius*), has been shown as an effective therapeutic agent in cardiovascular diseases, cancer, and diabetes. Our previous study showed that the effect of HSYA on high-glucose-induced podocyte injury is related to its anti-inflammatory activities via macrophage polarization. Based on the information provided on PubMed, Scopus and Wanfang database, we currently aim to provide an updated overview of the role of HSYA in antidiabetic research from the following points: pharmacological actions, molecular mechanisms, pharmacokinetic progressions, and clinical applications. The pharmacokinetic research of HSYA has laid foundations for the clinical applications of HSYA injection in diabetic nephropathy, diabetic retinopathy, and diabetic neuropathy. The application of HSYA as an antidiabetic oral medicament has been investigated based on its recent oral delivery system research. *In vivo* and *in vitro* pharmacological research indicated that the antidiabetic activities of HSYA were based mainly on its antioxidant and anti-inflammatory mechanisms via JNK/c-jun pathway, NOX4 pathway, and macrophage differentiation. Further anti-inflammatory exploration related to NF-κB signaling, MAPK pathway, and PI3K/Akt/mTOR pathway might deserve attention in the future. The anti-inflammatory activities of HSYA related to diabetes and diabetic complications will be a highlight in our following research.

1. Introduction

Hydroxysafflor yellow A (HSYA) is a single chalcone glycoside compound [1] which is derived from safflower (*Carthamus tinctorius*), a traditional Chinese herb (Figure 1) [2]. The most general and traditional method of extracting HSYA is water immersion. However, many other extraction systems have been developed such as smashing tissue extraction, microwave extraction, ultrasound extraction, and Soxhlet extraction [3]. HSYA has been commonly used in China to treat cardiovascular disease (CVD) [4]. Our recent literature research provides a number of articles and reviews describing novel applications of HSYA towards various diseases such as cancer and diabetes, beyond their conventional use against CVD (Figure 1).

According to the International Diabetes Federation, the number of adults diagnosed with diabetes has increased from 285 million in the year 2009 to 463 million in the year 2019, 95% of which are type 2 diabetes mellitus (T2DM) patients [5]. Diabetes is associated with accelerated rates of macrovascular and microvascular complications [6]. Macrovascular complications affect the heart, brain, and peripheral arteries and are termed CVD, cerebrovascular disease, and peripheral vascular disease, respectively [7]. Diabetes-related macrovascular complications are responsible for the impaired quality of life, disability, and premature death

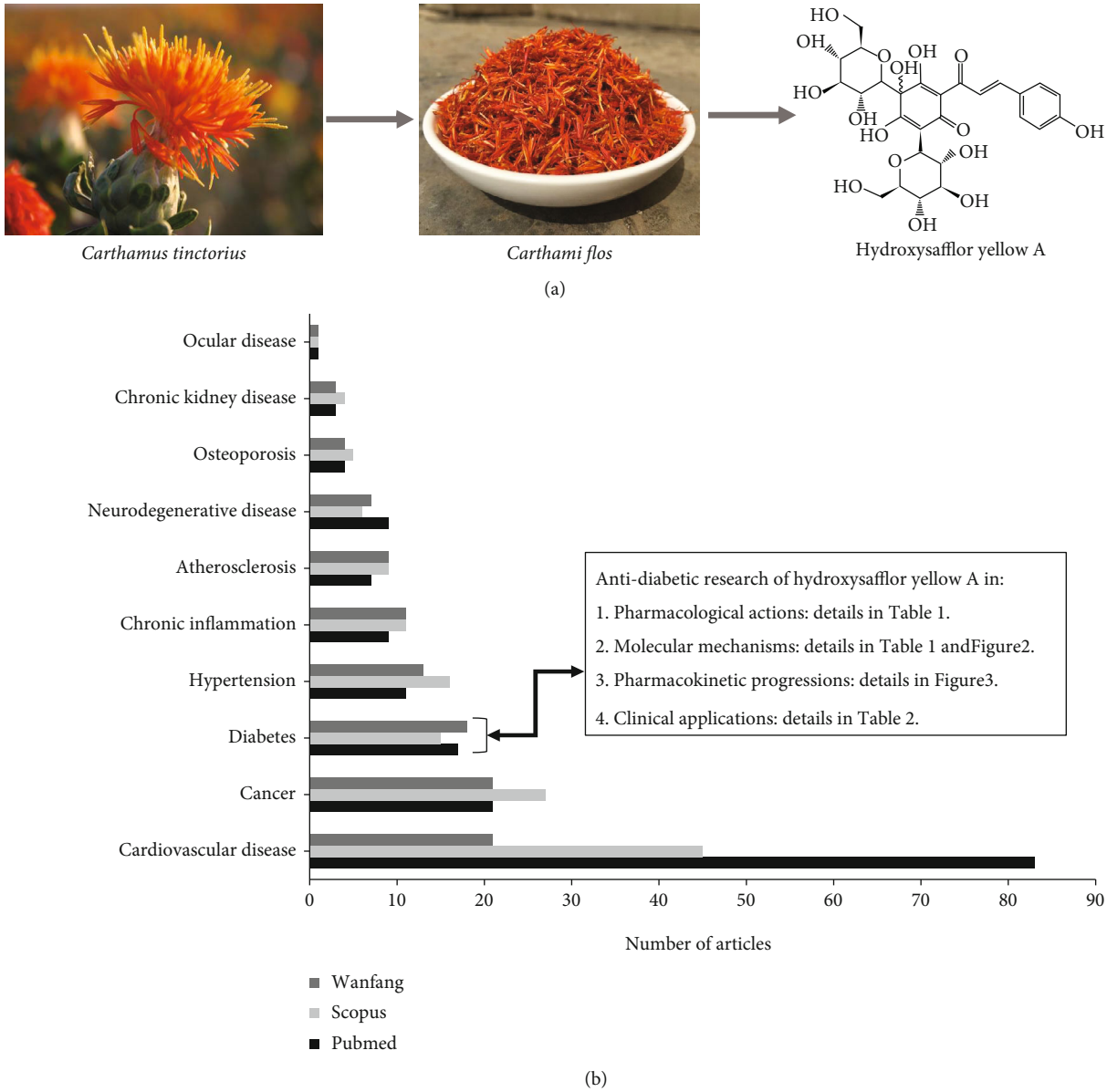

Figure 1: The source, structure, and literature research of hydroxysafflor yellow A: (a) the source and structure of hydroxysafflor yellow A; (b) the research articles of the top ten diseases related to hydroxysafflor yellow A. Abbreviation: Wanfang: Wanfang Data.

associated with diabetes [8, 9]. Microvascular complications affect the retina which is the inner part of the eye, the kidneys, and peripheral nerves. The resulting conditions are known as diabetic retinopathy, diabetic nephropathy (DN), and diabetic neuropathy, respectively [7]. In a study involving 689 individuals with T2DM obtained at baseline, the occurrences of microvascular complications observed during a median follow-up of 10.5 years were as follows: 206 patients had DN, 161 patients had retinopathy, and 179 patients had neuropathy [10].

Specifically, T2DM is characterized by chronic systemic inflammation alongside hyperglycemia and insulin resistance in the body [11]. Clinical data analysis showed that elevated C-reactive protein (CRP), tumor necrosis factor- (TNF-) α, and interleukin- (IL-) 6 were the most common inflammation indicators in diabetes-related angiopathies [12]. Related research suggested that HSYA could inhibit the apoptosis of pancreatic β-cells, and this might be the underlying mechanisms through which HSYA regulates glycolipid metabolism in T2DM rats [13]. Our previous study indicated that HSYA had direct protective effects on high glucose- (HG-) induced podocyte injury and indirect protective effects by regulating macrophage M1/M2 polarization [14]. These effects were related to its antioxidant and anti-inflammatory activities *in vitro* [15].

In this article, we first reviewed the *in vivo* and *in vitro* antidiabetic pharmacological actions and antidiabetic molecular mechanisms of HSYA. Based on signal research in the application of HSYA in the treatment of inflammation-related diseases, possible anti-inflammatory pathways involved in antidiabetic effects were discussed. The clinical applications of HSYA in diabetic macrovascular

and microvascular complications were then summarized based on its recent pharmacokinetic progression. Finally, possible application of HSYA as an antidiabetic oral medicament was investigated.

2. Antidiabetic Pharmacological Research and Related Mechanisms

2.1. In Vivo Antidiabetic Research. T2DM was induced in rats by feeding high-fat diet (HFD) for four weeks followed by intraperitoneal injection of streptozocin (STZ). The established models were treated with HSYA for eight weeks while metformin was used as positive control. The results showed that the underlying mechanisms of HSYA in T2DM rats were related to the following activities: the direct or indirect inhibition of pancreatic β-cell apoptosis, the improvement of insulin resistance, and the regulation of glycolipid metabolism [13].

Also, in the treatment of HFD- and STZ-induced T2DM rats by HSYA, renal protective effects were observed based on the improvement of renal functions including serum creatinine (Scr), blood urea nitrogen (BUN), glomerular volume, podocyte number, and cell apoptosis markers. Furthermore, in the HSYA treatment group, the levels of TNF-α and the inflammatory products, including free fatty acids (FFA) and lactic dehydrogenase (LDH), were significantly decreased. Regarding oxidative stress markers, the level of superoxide dismutase (SOD) markedly increased in the HSYA treatment group, while the level of malondialdehyde (MDA) in the serum and kidney tissue evidently decreased [16].

In STZ-induced type 1 diabetes mellitus (T1DM) rats, a diabetic wound model was established by full-thickness excisional wounds that extended through the panniculus carnosus with a biopsy punch. Topical application of HSYA significantly enhanced the wound closure rate, and the time taken for complete wound closure was 17 days, whereas 30 days was needed for complete wound closure with phosphate-buffered saline (PBS) treatment [17].

2.2. In Vitro Antidiabetic Research. In vitro antidiabetic studies were conducted on seven different cell lines: rat INS-1 insulinoma cells [18], mice MPC-5 podocyte cells [14], human umbilical vein endothelial cells (HUVECs) [17, 19], human brain microvascular endothelial cells (HBMECs) [20], 3T3-L1 preadipocytes and adipocytes [21], and RAW264.7 macrophage cells [14, 17].

The loss of functional insulin-producing β-cells is a hallmark of diabetes; therefore, understanding the cellular biology of the pancreas is crucial. Rat insulinoma INS-1 cells are widely used to study glucose-stimulated insulin secretion [22]. DN is one of the microvascular complications of diabetes and is a main cause of end-stage nephropathy. The most common clinical feature of DN is progressive proteinuria which is related to podocyte function. Podocyte plays an important role in maintaining the integrity and function of the glomerular filtration barrier. MPC-5 cell line is also widely used to evaluate renal injury *in vitro* [23]. Related research showed that HG-induced apoptosis of podocytes and pancreatic β-cells was reversed by HSYA [14, 18].

In diabetic patients, hyperglycemia-induced endothelial injury results in all kinds of vascular complications [24]. *In vitro* research showed that HG increased HUVEC apoptosis, vascular permeability, monocyte adhesion, the formation of reactive oxygen species (ROS), and the expression of NADPH oxidase 4 (NOX4) protein. The increased vascular injury by HG was attenuated by HSYA [19]. Another *in vitro* research showed that HSYA could inhibit methylglyoxal-induced injury in cultured HBMEC, which was associated with its antiglycation effect. Methylglyoxal is mainly formed from the degradation of glucose and glycated proteins [20].

For both diabetic wounds and DN progression, a central feature is the persistence of chronic inflammation, which is partly due to the prolonged presence of proinflammatory macrophages [25, 26]. In HG- and lipopolysaccharide-(LPS-) induced RAW264.7 macrophage cells, HSYA showed its anti-inflammatory effects by decreasing TNF-α, IL-1β, and nitric oxide (NO) levels [14, 17]. From Table 1, we could see that the main antidiabetic mechanism of HSYA is through its anti-inflammatory activity.

2.3. Anti-Inflammatory Signals in Antidiabetic Research of HSYA. So far, our review has shown that the antidiabetic mechanisms of HSYA are related to the following signals: c-jun NH2-terminal kinases/c-jun (JNK/c-jun) pathway [18], NOX4 pathway [19], macrophage polarization [14], and phosphoinositide 3-kinase/protein kinase B (PI3K/Akt) pathway [13]. HSYA also showed its ability to cause a decrease in oxidative stress factors such as ROS [18, 19] and hydrogen peroxide (H_2O_2) [19].

Inflammation is closely linked to the pathogenesis of diabetes, and chronic inflammation is one of the main causes of insulin resistance. Proinflammatory mediators can be related to obesity and induce insulin resistance in adipose tissue. Signaling pathways of transcription factors, particularly nuclear factor-κB (NF-κB) signaling, are involved in insulin sensitivity [27]. NF-κB plays a crucial role in the development of diabetic complications because of its involvement in the expression of genes that are responsible for the damage of organs such as the brain, liver, heart, muscles, endothelium, adipose tissue, and pancreas by inflammation, apoptosis, and oxidative stress [28].

The role of NF-κB signal in the antidiabetic activities of HSYA has not been previously reported. Figure 2 indicates that NF-κB signal plays an important role in the use of HSYA to treat other inflammatory diseases [29–38]. This might provide some research points to explore anti-inflammatory mechanisms of HSYA in the treatment of diabetes and diabetes complications.

2.4. Possible Anti-Inflammatory Mechanisms in Antidiabetic Research of HSYA. In Figure 2, organ damages treated by HSYA via the NF-κB pathway include brain damages such as ischemia reperfusion-injury, traumatic brain injury, ischemic stroke, and Alzheimer's disease (AD) [29–32]; lung injury such as fetal lung fibroblasts, chronic obstructive pulmonary disease, and acute respiratory distress syndrome

Table 1: Summary of pharmacological effects and mechanisms of HSYA on diabetes and diabetes complications.

Disease	Species/strains	Effective dose/concentration	Route	Positive control	Intervention time	Main improved results	Mechanisms/pathways	Reference
Diabetes	HFD- and STZ-induced T2DM rats	120 mg/kg	i.g.	Metformin as positive control	8 weeks	Pancreatic β-cell apoptosis↓, FBG↓, IR↓, TG↓, TC↓, LDLC↓, glycogen synthase↑, hepatic glycogen↑	Regulation on glycolipid metabolism via PI3K/Akt pathway	[13]
Diabetes	HG-induced rat INS-1 insulinoma cells (pancreatic β-cells)	800 μM		N-Acetylcysteine as oxidative stress scavenger control	72 hours	Pancreatic β-cell apoptosis↓, ROS↓, MDA↓, CAT↑, GSH-px↑, SOD↑	Antioxidative effects via JNK/c-jun pathway	[18]
Diabetic nephropathy	HFD- and STZ-induced T2DM rats	120 mg/kg	i.g.		8 weeks	Scr↓, UN↓, TG↓, TC↓, LDLC↓, FBG↓, TNF-α↓, LDH↓, FFA↓, MDA↓, SOD↑	Antioxidative and anti-inflammation effects	[16]
Diabetic nephropathy	HG-induced mice MPC-5 podocyte cells and HG-induced mice RAW264.7 cells	100 μM, 200 μM		Kaempferol as positive control	24 hours	Podocyte apoptosis↓ In podocytes: TNF-α↓, IL-1β↓ In RAW264.7 cells: TNF-α↓, iNOS↓, IL-1β↓ CD206↑, Arg-1↑	Anti-inflammation effects directly on podocyte cells and indirectly via macrophage polarization	[14]
Diabetic vascular injury	HG-induced HUVECs	10 μM, 25 μM, 50 μM			24, 48, and 72 hours	HUVEC hyperpermeability↓, HUVEC apoptosis↓, VCAM-1↓, ICAM-1↓, E-selectin↓, NOX4↓, ROS↓, H_2O_2↓	Anti-inflammation effects via the NOX4 pathway	[19]
Diabetic vascular injury	Methylglyoxal-induced HBMECs	10, 50, and 100 μM			24 hours	HBMEC apoptosis↓, caspase-3↓, AGEs↓	Antiglycation effects	[20]
Diabetic wound	STZ-induced T1DM rats	2 mg/mL	vs ext	Hydrogel as positive control	30 days	Wound closure↑, granulation tissue formation↑, collagen disposition↑, secretion of VEGF↑, TGF-β1↑		[17]
Diabetic wound	HUVECs and LPS-induced RAW264.7 cells	0.4, 0.8, and 1.6 mM			60 and 96 hours	NO production↓, HEK migration↑, HUVEC tube formation↑	Anti-inflammation effects	[17]
Diabetic obesity	3T3-L1 preadipocytes and adipocytes	100 mg/L			24 hours	PPARγ2 promoter activities↑, PPARγ2↑	Increasing the expression of insulin signaling pathway-related genes	[21]

Abbreviations: T1DM: type 1 diabetes mellitus; T2DM: type 2 diabetes mellitus; HFD: high-fat diet; STZ: streptozotocin; FBG: fasting blood glucose; IR: insulin resistance; TG: triglyceride; TC: total cholesterol; LDLC: low-density lipoprotein cholesterol; DN: diabetic nephropathy; ROS: reactive oxygen species; SOD: superoxide dismutase; CAT: catalase; GSH-px: glutathione peroxidase; MDA: malondialdehyde; Scr: serum creatinine; UN: urea nitrogen; LDH: lactate dehydrogenase; FFA: free fatty acids; NOX4: NADPH oxidase 4; H_2O_2: hydrogen peroxide; HG: high glucose; HBMECs: human brain microvascular endothelial cells; HUVECs: human umbilical vein endothelial cells; VCAM-1: vascular cell adhesion molecule-1; ICAM-1: intercellular adhesion molecule-1; iNOS: inducible nitric oxide synthase; TNF-α: tumor necrosis factor-α; CD206: mannose receptor; Arg-1: arginase-1; IL-1β: interleukin-1β; LPS: lipopolysaccharide; AGEs: advanced glycation end-products; VEGF: vascular growth factors; TGF-β1: transforming growth factor-β1; NO: nitric oxide; HEKs: human epithelial keratinocytes; PPARγ2: peroxisome proliferator-activated receptor-γ2.

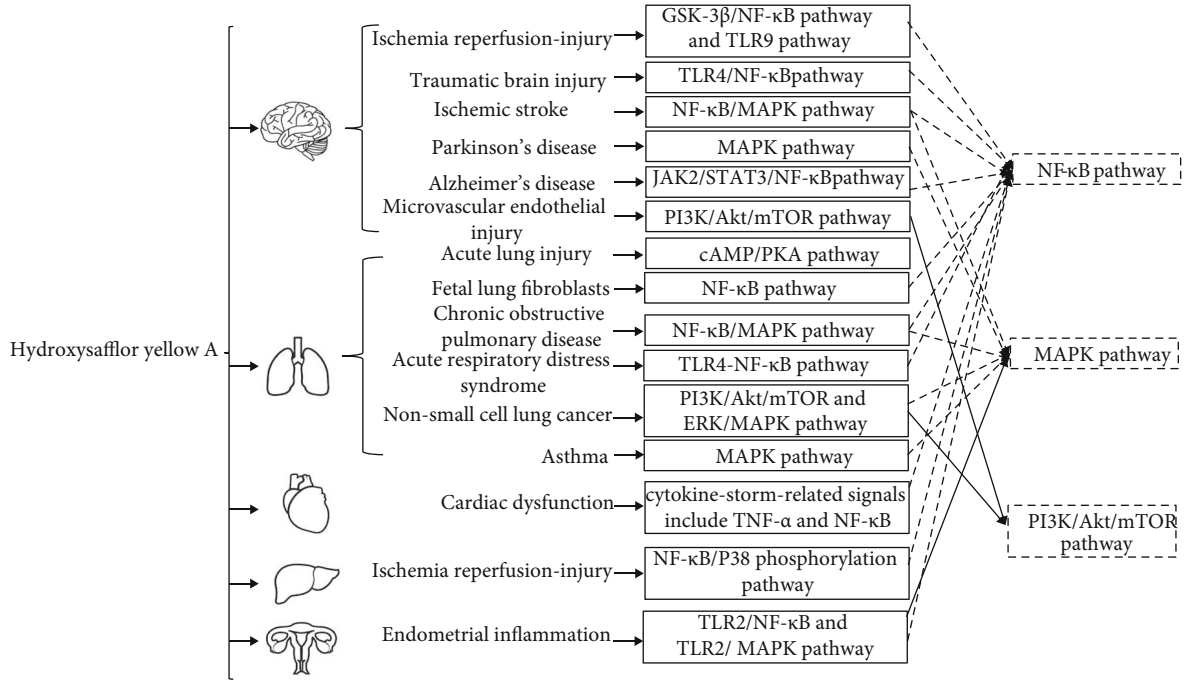

Figure 2: The molecular mechanisms of hydroxysafflor yellow A in the treatment of inflammation-related diseases. Abbreviations: GSK3β: glycogen synthase kinase-3β; NF-κB: nuclear factor-κB; TLR9: toll-like receptor 9; TLR4: toll-like receptor 4; TLR2: toll-like receptor 2; MAPK: mitogen-activated protein kinase; JAK2: Janus kinase 2; STAT3: signal transducers and activators of transcription 3; PI3K: phosphatidylinositol 3-kinase; Akt: protein kinase B; mTOR: mammalian target of rapamycin; cAMP: cyclic adenosine monophosphate; PKA: protein kinase A; ERK: extracellular signal-regulated kinase; TNF-α: tumor necrosis factor-α.

[33–35]; cardiac dysfunction [36]; liver ischemia reperfusion-injury [37]; and endometrial inflammation [38].

It is reported that AD and T2DM share many common features including inflammation, oxidative stress, and neuronal degeneration [39]. β-Amyloid- (Aβ-) mediated inflammation plays a critical role in the initiation and progression of AD. HSYA protects Aβ-induced AD model by inhibiting inflammatory response, which may involve inhibiting the activation of the NF-κB pathway [32]. The NF-κB signaling pathway will be the first research point for our team in future studies on the antidiabetic mechanisms of HSYA.

Mitogen-activated protein kinase (MAPK) pathway and phosphoinositide 3-kinase/protein kinase B/mammalian target of rapamycin (PI3K/Akt/mTOR) pathway are two other important signals indicating the intervention of HSYA in the treatment of Parkinson's disease (PD) [40], asthma [41], non-small-cell lung cancer [42], and brain microvascular endothelial injury [43]. It is reported that activated MAPK may be associated with both inflammation and energy metabolism in mice, rats, and humans fed with HFD for a short or long term [44]. A case-control study including 248 cases of T2DM and 101 controls showed that genetic variations in the PI3K/Akt/mTOR signaling pathway may be associated with increasing risk of obesity and diabetes [45]. Our previous discussion showed that HSYA could promote the activation of PI3K/Akt and inhibit the apoptosis of pancreatic β-cells in HFD- and STZ-induced T2DM rats [13]. Further research on the relationship between HSYA and PI3K/Akt/mTOR signal in diabetic complications should be conducted.

Other inflammation signals, including toll-like receptor 9 (TLR9) signal and cyclic adenosine monophosphate/protein kinase A (cAMP/PKA) signal, were observed in ischaemic cortex after cerebral ischaemia and reperfusion and acute lung injury [46, 47]. TLRs are a family of pattern recognition receptors that play a critical role in innate immune response. Recently, studies have reported the important role of TLR4 pathway in insulin resistance [27]. TLRs can be proposed as new targets in the intervention of HSYA in diabetes. The important roles of cAMP/PKA signal in the cognitive impairment of diabetic rats may suggest its involvement in the antidiabetic mechanism of HSYA.

3. Pharmacokinetic Progressions

3.1. Pharmacokinetics of Intravenous Administration

3.1.1. In Healthy Humans. 36 healthy volunteers were recruited in a single-center, open-label, single-dose, and multiple-dose study. It was found that the area under the curve (AUC) of plasma concentration at different time points and time to peak plasma concentration (Cmax) were linearly related to the dose ranging from 25 to 75 mg in a single administration of HSYA and the elimination half-life was about 3.91–4.18 h. When HSYA was administered for 7 d (50 mg/d) continuously, Cmax and AUC decreased significantly and the elimination half-life was prolonged from 3.91 h to 4.41 h [48].

Table 2: The RCT research of SYI (90% HSYA) in the treatment of diabetes and diabetes complications.

	Diseases	RCT research	Main improved clinical indicators	Mechanism research	Reference
Microvascular complications	Diabetic nephropathy	Early stage: $n = 535$ (control: $n = 532$)	Serum creatinine	SOD, MDA, TNF-α, IL-6, and IL-10	[55]
		End stage: $n = 50$ (control: $n = 50$)	24 h proteinuria, urea nitrogen		[56]
	Diabetic retinopathy	$n = 92$ (control: $n = 76$)	Serum vascular endothelial growth factor and endostatin		[57]
	Diabetic neuropathy	$n = 41$ (control: $n = 41$)	Tendon reflexes and EMG nerve conduction velocity		[58]
Macrovascular complications	Cardiovascular disease	Unstable angina pectoris: $n = 42$ (control: $n = 42$)	Number and duration of angina pectoris		[59]
	Cerebrovascular disease	Acute cerebral infarction: $n = 40$ (control: $n = 40$)	NIHSS score		[60]
	Peripheral vascular disease	Diabetic foot ulcers: $n = 20$ (control: $n = 20$)	Wagner classification		[61]

Abbreviations: RCT: randomized controlled trial; SYI: safflower yellow injection; HSYA: hydroxysafflor yellow A; SOD: superoxide dismutase; MDA: malondialdehyde; TNF-α: tumor necrosis factor-α; IL-6: interleukin-6; IL-10: interleukin-10; EMG: electromyogram; NIHSS: National Institute of Health Stroke Scale.

Pharmacokinetic studies in healthy humans have shown that the metabolic process in the body after intravenous administration of HSYA conforms to the two-compartment model, indicating that HSYA can be quickly distributed in many organs including the heart, liver, spleen, lungs, brain, intestines, and kidneys [49]. The distribution of HSYA in the kidneys is more than that of the other organs [3]. The excretion of HSYA is mainly from the kidneys, and the cumulative excretion rate of HSYA in urine 24 h after intravenous administration is up to 88.6% [3, 49]. According to the above characteristics, the pharmacokinetic indexes of HSYA in DN patients are different from those of the healthy volunteers.

3.1.2. In Renal Insufficient Patients. It was found that the Cmax and AUC of HSYA in the diabetic impaired renal function group increased and the apparent volume of distribution and clearance rate reduced significantly after a single administration. The results showed that impaired renal function affected pharmacokinetic indicators [50].

Relevant studies have shown that after administering HSYA intravenously for 1 h, the average blood concentration of HSYA in renal insufficient patients was equivalent to 2.64 times that of patients with normal renal functions [51]. It is suggested that the dosage and frequency of administration should be adjusted according to the blood concentration when HSYA is used in DN patients.

3.1.3. In Patients with Traumatic Brain Injury. A sensitive, rapid, and reliable liquid chromatography-tandem mass spectrometry method was applied to investigate the pharmacokinetics of HSYA in patients with traumatic brain injury (TBI). The results demonstrated that some HSYA crossed the blood-brain barrier after administration. This study provides evidence to better understand the pharmacokinetics and potential clinical guidance for TBI treatment [52].

3.1.4. Clinical Antidiabetic Applications. Safflower yellow injection (SYI) containing 90% HSYA (45 mg HSYA per 50 mg SYI) has been widely used clinically [53]. In line with clinical guidelines and expert consensus [54], the use of SYI is becoming more and more standardized. Randomized controlled trials (RCTs) of SYI in the treatment of diabetes complications are summarized in Table 2 [55–61].

It can be observed from Table 2 that HSYA has effects on microvascular complications as well as macrovascular complications. Among these complications, HSYA was mostly used in the early stage of DN, and the mechanism research showed that HSYA had anti-inflammatory activity by decreasing TNF-α levels in DN patients [62]. There is no clinical anti-inflammatory research about HSYA on diabetic retinopathy, diabetic neuropathy, etc. The development of further clinical applications of HSYA may need to be carried out alongside its clinical anti-inflammatory effects.

It is said that the age of natural antioxidant compounds in the treatment of diabetic complications is coming [63]. HSYA injection has made some progress in the treatment of different diabetic complications. But from the perspective of patients, it is obvious that an oral drug is more convenient than an injection.

3.2. Pharmacokinetics of Oral Administration

3.2.1. In Healthy Humans. The pharmacokinetics of HSYA in 12 healthy volunteers after a single oral administration of HSYA was investigated. The plasma pharmacokinetics of HSYA after oral administration in the 12 healthy subjects showed that the component was absorbed quickly, with a peak time of 1 h and a short elimination half-life of approximately 2.6–3.5 h [64]. HSYA is relatively polar and easily catabolized and metabolized in the gastrointestinal tract and liver, leading to its rapid elimination, short half-life, and low bioavailability under oral or intragastric administration conditions [49]. The clinical use of HSYA as an oral preparation is being hindered by its low bioavailability, and hence, there is the need for an improvement of its oral bioavailability.

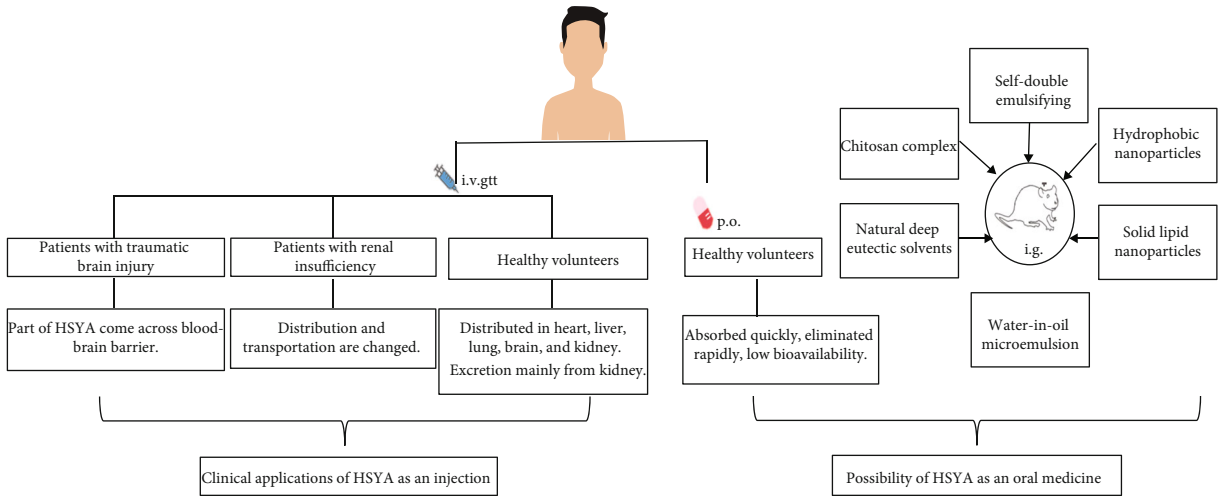

Figure 3: Clinical applications and possible medicine development of HSYA based on human and animal pharmacokinetic research. Abbreviation: HSYA: hydroxysafflor yellow A.

3.2.2. Oral Delivery System Research. Fortunately, research on the delivery system of HSYA made it possible to develop it into an oral medicament. Some oral delivery systems of HSYA are shown in Figure 3. They are water-in-oil microemulsion [65], self-double-emulsifying [66], hydrophobic nanoparticles [67], chitosan complex [68], solid lipid nanoparticles [69], and natural deep eutectic solvents [70].

Related research suggested that shell nanoparticles are a highly effective delivery system for resveratrol, another natural compound, due to their significant effects in increasing the bioavailability and anti-inflammation activity [71]. We look forward to a suitable delivery system for HSYA, which will improve not only its bioavailability but also its anti-inflammatory activity in the near future.

4. Conclusion

HSYA, a major active component from safflower plant, has drawn more interest in recent years for its multiple pharmacological actions. We aim to provide an updated overview of HSYA in diabetes and diabetic complications from these four points: pharmacological actions, molecular mechanisms, pharmacokinetic progressions, and clinical applications. Anti-inflammation mechanism plays an important role in the antidiabetic pharmacological actions of HSYA. Further anti-inflammation research should pay attention to more inflammation signals such as NF-κB pathway and MAPK pathway. The pharmacokinetic properties of HSYA enhanced its wide clinical use as an injection to treat diabetic complications. Based on the development of drug delivery systems, HSYA could be expected as an oral drug with improved bioavailability and improved anti-inflammatory activity.

Data Availability

All authors declare that the readers can access the conclusions from the three figures and two tables. All of the figures and tables are summarized based on the references.

Conflicts of Interest

The authors declare that there is no conflict of interest regarding the publication of this paper.

Authors' Contributions

Xilan Zhang and Dayue Shen contributed equally to this work.

Acknowledgments

This study was supported by Wu Jieping Medical Foundation (No. 320.6750.2021-08-10) and Key R & D Project of Shanxi Province (International Scientific and Technological Cooperation, Independent Topics, No. 201903D421061).

References

[1] X. Xue, Y. Deng, J. Wang et al., "Hydroxysafflor yellow A, a natural compound from Carthamus tinctorius L with good effect of alleviating atherosclerosis," *Phytomedicine*, vol. 91, pp. 1–15, 2021.

[2] J. Hou, C. Wang, M. Zhang et al., "Safflower yellow improves the synaptic structural plasticity by ameliorating the disorder of glutamate circulation in A$\beta_{1\text{-}42}$-induced AD model rats," *Neurochemical Research*, vol. 45, no. 8, pp. 1870–1887, 2020.

[3] F. Zhao, P. Wang, Y. Jiao, X. Zhang, D. Chen, and H. Xu, "Hydroxysafflor yellow A: a systematical review on botanical resources, physicochemical properties, drug delivery system, pharmacokinetics, and pharmacological effects," *Frontiers in Pharmacology*, vol. 11, pp. 1–21, 2020.

[4] M. Z. Hu, Z. Y. Zhou, Z. Y. Zhou et al., "Effect and safety of hydroxysafflor yellow A for injection in patients with acute ischemic stroke of blood stasis syndrome: a phase II, multicenter, randomized, double-blind, multiple-dose, active-controlled clinical trial," *Chinese Journal of Integrative Medicine*, vol. 26, no. 6, pp. 420–427, 2020.

[5] Y. H. Wong, S. H. Wong, X. T. Wong et al., "Genetic associated complications of type 2 diabetes mellitus: a review," *Panminerva Medical*, 2021.

[6] V. S. Tanwar, M. A. Reddy, and R. Natarajan, "Emerging role of long non-coding RNAs in diabetic vascular complications," *Frontiers in Endocrinology (Lausanne)*, vol. 12, pp. 1–19, 2021.

[7] R. Pradeepa and V. Mohan, "Prevalence of type 2 diabetes and its complications in India and economic costs to the nation," *European Journal of Clinical Nutrition*, vol. 71, no. 7, pp. 816–824, 2017.

[8] E. D. Canto, A. Ceriello, L. Rydén et al., "Diabetes as a cardiovascular risk factor: an overview of global trends of macro and micro vascular complications," *European Journal of Preventive Cardiology*, vol. 26, no. 2, pp. 25–32, 2019.

[9] D. Zhou, Z. Huang, X. Zhu, T. Hong, and Y. Zhao, "Combination of endothelial progenitor cells and BB-94 significantly alleviates brain damage in a mouse model of diabetic ischemic stroke," *Experimental and Therapeutic Medicine*, vol. 22, no. 1, pp. 1–11, 2021.

[10] C. R. L. Cardoso, N. C. Leite, and G. F. Salles, "Importance of hematological parameters for micro- and macrovascular outcomes in patients with type 2 diabetes: the Rio de Janeiro type 2 diabetes cohort study," *Cardiovascular Diabetology*, vol. 20, no. 1, pp. 1–13, 2021.

[11] R. I. Mota, S. E. Morgan, and E. M. Bahnson, "Diabetic vasculopathy: macro and microvascular injury," *Current Pathobiology Reports*, vol. 8, no. 1, pp. 1–14, 2020.

[12] M. C. Nwadiugwu, "Inflammatory activities in type 2 diabetes patients with co-morbid angiopathies and exploring beneficial interventions: a systematic review," *Frontiers in Public Health*, vol. 8, pp. 1–15, 2021.

[13] M. Lee, H. Li, H. Zhao, M. Suo, and D. Liu, "Effects of hydroxysafflor yellow A on the PI3K/AKT pathway and apoptosis of pancreatic β-cells in type 2 diabetes mellitus rats," *Diabetes, Metabolic Syndrome and Obesity: Targets and Therapy*, vol. 13, pp. 1097–1107, 2020.

[14] Y. Li, D. Zheng, D. Shen, X. Zhang, X. Zhao, and H. Liao, "Protective effects of two safflower derived compounds, kaempferol and hydroxysafflor yellow A, on hyperglycaemic stress-induced podocyte apoptosis via modulating of macrophage M1/M2 polarization," *Journal of Immunology Research*, vol. 2020, pp. 1–11, 2020.

[15] H. Liao, Y. Li, X. Zhai et al., "Comparison of inhibitory effects of safflower decoction and safflower injection on protein and mRNA expressions of iNOS and IL-1β in LPS-activated RAW264.7 cells," *Journal of Immunology Research*, vol. 2019, pp. 1–11, 2019.

[16] M. Lee, H. Zhao, X. Liu et al., "Protective effect of hydroxysafflor yellow A on nephropathy by attenuating oxidative stress and inhibiting apoptosis in induced type 2 diabetes in rat," *Oxidative Medicine and Cellular Longevity*, vol. 2020, pp. 1–11, 2020.

[17] S. Q. Gao, C. Chang, X. Q. Niu, L. J. Li, Y. Zhang, and J. Q. Gao, "Topical application of hydroxysafflor yellow A accelerates the wound healing in streptozotocin induced T1DM rats," *European Journal of Pharmacology*, vol. 823, pp. 72–78, 2018.

[18] Y. Zhao, H. Sun, X. Li, Y. Zha, and W. Hou, "Hydroxysafflor yellow A attenuates high glucose-induced pancreatic β-cells oxidative damage via inhibiting JNK/c-jun signaling pathway," *Biochemical and Biophysical Research Communications*, vol. 505, no. 2, pp. 353–359, 2018.

[19] S. Chen, J. Ma, H. Zhu, S. Deng, M. Gu, and S. Qu, "Hydroxysafflor yellow A attenuates high glucose-induced human umbilical vein endothelial cell dysfunction," *Human and Experimental Toxicology*, vol. 38, no. 6, pp. 685–693, 2019.

[20] W. Li, J. Liu, P. He et al., "Hydroxysafflor yellow A protects methylglyoxal-induced injury in the cultured human brain microvascular endothelial cells," *Neuroscience Letters*, vol. 549, pp. 146–150, 2013.

[21] K. Yan, X. Wang, H. Zhu et al., "Safflower yellow improves insulin sensitivity in high-fat diet-induced obese mice by promoting peroxisome proliferator-activated receptor-γ2 expression in subcutaneous adipose tissue," *Journal of Diabetes Investigation*, vol. 11, no. 6, pp. 1457–1469, 2020.

[22] A. Acosta-Montalvo, C. Saponaro, J. Kerr-Conte, J. H. M. Prehn, F. Pattou, and C. Bonner, "Proglucagon-derived peptides expression and secretion in rat insulinoma INS-1 cells," *Frontiers in Cell and Developmental Biology*, vol. 8, pp. 1–11, 2020.

[23] H. Wang, Y. Zhang, F. Xia, W. Zhang, P. Chen, and G. Yang, "Protective effect of silencing Stat1 on high glucose-induced podocytes injury via Forkhead transcription factor O1-regulated the oxidative stress response," *BMC Molecular and Cell Biology*, vol. 20, no. 1, pp. 1–15, 2019.

[24] H. Chen, Z. Feng, L. Li, and L. Fan, "MicroRNA-9 rescues hyperglycemia-induced endothelial cell dysfunction and promotes arteriogenesis through downregulating Notch1 signaling," *Molecular and Cellular Biochemistry*, vol. 476, no. 7, pp. 2777–2789, 2021.

[25] J. Hu, L. Zhang, C. Liechty et al., "Long noncoding RNA _GAS5_ regulates macrophage polarization and diabetic wound healing," *Journal of Investigative Dermatology*, vol. 140, no. 8, pp. 1629–1638, 2020.

[26] J. Zhao, J. Chen, Y. Y. Li, L. L. Xia, and Y. G. Wu, "Bruton's tyrosine kinase regulates macrophage-induced inflammation in the diabetic kidney via NLRP3 inflammasome activation," *International Journal of Molecular Medicine*, vol. 48, no. 3, pp. 1–12, 2021.

[27] H. Zand, N. Morshedzadeh, and F. Naghashian, "Signaling pathways linking inflammation to insulin resistance," *Diabetes and Metabolic Syndrome: Clinical Research and Reviews*, vol. 11, Suppl 1, pp. S307–S309, 2017.

[28] R. Sahukari, J. Punabaka, S. Bhasha, V. S. Ganjikunta, S. K. Ramudu, and S. R. Kesireddy, "Plant compounds for the treatment of diabetes, a metabolic disorder: NF-κB as a therapeutic target," *Current Pharmaceutical Design*, vol. 26, no. 39, pp. 4955–4969, 2020.

[29] X. Yang, L. Chen, Y. Li et al., "Protective effect of hydroxysafflor yellow A on cerebral ischemia reperfusion- injury by regulating GSK3β-mediated pathways," *Neuroscience Letters*, vol. 736, pp. 1–9, 2020.

[30] J. Xu, T. Zhan, W. Zheng et al., "Hydroxysafflor yellow A acutely attenuates blood-brain barrier permeability, oxidative stress, inflammation and apoptosis in traumatic brain injury in rats1," *Acta Cirúrgica Brasileira*, vol. 35, no. 12, pp. 1–8, 2021.

[31] J. Li, S. Zhang, M. Lu et al., "Hydroxysafflor yellow A suppresses inflammatory responses of BV2 microglia after oxygen-glucose deprivation," *Neuroscience Letters*, vol. 535, pp. 51–56, 2013.

[32] Z. H. Zhang, L. J. Yu, X. C. Hui et al., "Hydroxy-safflor yellow A attenuates A$\beta_{1\text{-}42}$-induced inflammation by modulating the JAK2/STAT3/NF- κ B pathway," *Brain Research*, vol. 1563, pp. 72–80, 2014.

[33] S. Liu, Y. Wang, H. Wen, X. Sun, and Y. Wang, "Hydroxysafflor yellow A inhibits TNF-α-induced inflammation of human fetal lung fibroblasts via NF-κB signaling pathway," *Evidence-*

based Complementary and Alternative Medicine, vol. 2019, pp. 1–9, 2019.

[34] M. Jin, C. J. Xue, Y. Wang et al., "Protective effect of hydroxysafflor yellow A on inflammatory injury in chronic obstructive pulmonary disease rats," *Chinese Journal of Integrative Medicine*, vol. 25, no. 10, pp. 750–756, 2019.

[35] Y. Zhang, L. Song, R. Pan, J. Gao, B. X. Zang, and M. Jin, "Hydroxysafflor yellow A alleviates lipopolysaccharide-induced acute respiratory distress syndrome in mice," *Biological & Pharmaceutical Bulletin*, vol. 40, no. 2, pp. 135–144, 2017.

[36] X. T. Wang, Z. Peng, Y. Y. An et al., "Paeoniflorin and hydroxysafflor yellow A in Xuebijing injection attenuate sepsis-induced cardiac dysfunction and inhibit proinflammatory cytokine production," *Frontiers in Pharmacology*, vol. 11, pp. 1–19, 2021.

[37] S. Jiang, Z. Shi, C. Li, C. Ma, X. Bai, and C. Wang, "Hydroxysafflor yellow A attenuates ischemia/reperfusion-induced liver injury by suppressing macrophage activation," *International Journal of Clinical and Experimental Pathology*, vol. 7, no. 5, pp. 2595–2608, 2014.

[38] S. He, X. Wang, Z. Liu et al., "Hydroxysafflor yellow A inhibits staphylococcus aureus-induced mouse endometrial inflammation via TLR2-mediated NF-kB and MAPK pathway," *Inflammation*, vol. 44, no. 3, pp. 835–845, 2021.

[39] E. Lazar, A. Sherzai, J. Adeghate, and D. Sherzai, "Gut dysbiosis, insulin resistance and Alzheimer's disease: review of a novel approach to neurodegeneration," *Frontiers in Bioscience-Scholar*, vol. 13, no. 1, pp. 17–29, 2021.

[40] X. Yang, Y. Li, L. Chen et al., "Protective effect of hydroxysafflor yellow A on dopaminergic neurons against 6-hydroxydopamine, activating anti-apoptotic and anti-neuroinflammatory pathways," *Pharmaceutical Biology*, vol. 58, no. 1, pp. 686–694, 2020.

[41] M. Zheng, X. Guo, R. Pan, J. Gao, B. Zang, and M. Jin, "Hydroxysafflor yellow a alleviates ovalbumin-induced asthma in a guinea pig model by attenuateing the expression of inflammatory cytokines and signal transduction," *Frontiers in Pharmacology*, vol. 10, pp. 1–12, 2019.

[42] M. Jiang, L. Y. Zhou, N. Xu, and Q. An, "Hydroxysafflor yellow a inhibited lipopolysaccharide-induced non-small cell lung cancer cell proliferation, migration, and invasion by suppressing the PI3K/AKT/mTOR and ERK/MAPK signaling pathways," *Thoracic Cancer*, vol. 10, no. 6, pp. 1319–1333, 2019.

[43] G. Yang, N. Wang, S. W. Seto, D. Chang, and H. Liang, "Hydroxysafflor yellow a protects brain microvascular endothelial cells against oxygen glucose deprivation/reoxygenation injury: involvement of inhibiting autophagy via class I PI3K/Akt/mTOR signaling pathway," *Brain Research Bulletin*, vol. 140, pp. 243–257, 2018.

[44] Z. Wang, M. Zhu, M. Wang et al., "Integrated multiomic analysis reveals the high-fat diet induced activation of the MAPK signaling and inflammation associated metabolic cascades via histone modification in adipose tissues," *Frontiers in Genetics*, vol. 140, pp. 243–257, 2018.

[45] X. Yin, Z. Xu, Z. Zhang et al., "Association of PI3K/AKT/mTOR pathway genetic variants with type 2 diabetes mellitus in Chinese," *Diabetes Research and Clinical Practice*, vol. 128, pp. 127–135, 2017.

[46] Z. Gong, J. Pan, X. Li, H. Wang, L. He, and Y. Peng, "Hydroxysafflor yellow A reprograms TLR9 signalling pathway in ischaemic cortex after cerebral ischaemia and reperfusion," *CNS & Neurological Disorders-Drug Targets*, vol. 17, no. 5, pp. 370–382, 2018.

[47] C. Wang, Q. Huang, C. Wang et al., "Hydroxysafflor yellow A suppress oleic acid-induced acute lung injury via protein kinase A," *Toxicology and Applied Pharmacology*, vol. 272, no. 3, pp. 895–904, 2013.

[48] C. Y. Li, J. G. Yin, J. Zhang et al., "Pharmacokinetic profiles of hydroxysafflor yellow A following intravenous administration of its pure preparations in healthy Chinese volunteers," *Journal of Ethnopharmacology*, vol. 162, pp. 225–230, 2015.

[49] L. Wu, A. Kang, S. J. Le, and Y. P. Tang, "Research progress on process of hydroxyl safflower yellow A in vivo," *Chinese Traditional Patent Medicine*, vol. 42, no. 1, pp. 150–155, 2020.

[50] G. Lyu, X. Sun, Y. Li, S. Liu, and A. Wang, "Pharmacokinetics of safflower yellow in the diabetes mellitus patients with renal impairment," *World Clinical Drugs*, vol. 39, no. 9, pp. 625–629, 2018.

[51] J. Wang, F. Liu, C. Xi, M. Li, and H. Gao, "Concentration determination of hydroxysafflor yellow A in the plasma of the patients with renal insufficiency by HPLC method," *Pharmaceutical Care and Research*, vol. 16, no. 1, pp. 48–51, 2016.

[52] C. Sheng, W. Peng, Z. Xia, and Y. Wang, "Plasma and cerebrospinal fluid pharmacokinetics of hydroxysafflor yellow A in patients with traumatic brain injury after intravenous administration of Xuebijing using LC-MS/MS method," *Xenobiotica*, vol. 50, no. 5, pp. 545–551, 2020.

[53] H. Ao, W. Feng, and C. Peng, "Hydroxysafflor yellow A: a promising therapeutic agent for a broad spectrum of diseases," *Evidence-based Complementary and Alternative Medicine*, vol. 2018, pp. 1–17, 2018.

[54] K. Chen, C. Fu, W. Cong, and Y. Liu, "Chinese expert consensus on the clinical application of safflower yellow," *Chinese Journal of Integrated and Traditional and Western Medicine*, vol. 37, no. 10, pp. 1167–1173, 2017.

[55] S. Xu, Z. Zhu, Y. Zhang, R. Ye, Q. Feng, and H. Zeng, "Effect of safflower yellow pigment injection on stage III diabetic nephropathy:a systematic review," *Traditional Chinese Drug Research & Clinical Pharmacology*, vol. 30, no. 2, pp. 232–238, 2019.

[56] S. Wu, B. Zeng, and S. Lin, "Clinical observation of diabetic nephropathy renal failure treated with safflower yellow pigment injection," *Chinese Community Doctors*, vol. 35, no. 11, pp. 99–101, 2019.

[57] L. Xiong and Y. Dong, "Safflower yellow injection in the treatment of diabetic retinopathy in type 2 diabetes patients," *World Clinical Drugs*, vol. 35, no. 4, pp. 206–209, 2014.

[58] X. Zhang, "Effect of safflower yellow pigment injection on diabetic peripheral neuropathy," *Cardiovascular Disease Journal of Integrated Traditional Chinese and Western Medicine*, vol. 4, no. 20, p. 189, 2016.

[59] H. Yang, "Therapeutic effect of safflower yellow pigment injection on type 2 diabetes mellitus complicated with unstable angina pectoris," *Chinese Community Doctors*, vol. 14, no. 6, p. 210, 2012.

[60] X. Xiong, "Clinical efficacy of safflower yellow injection in the treatment of diabetes with acute cerebral infarction," *Journal of Liaoning University of TCM*, vol. 20, no. 3, pp. 157–159, 2018.

[61] X. Wu, "40 cases of diabetic foot ulcer treated with safflower yellow pigment injection," *Guide of Chinese Medicine*, vol. 11, no. 4, pp. 289-290, 2013.

[62] M. Yin, "Influence of carthamin yellow pigment injection on oxidative stress indexes and inflammatory factors of patients with early diabetic nephropathy," *Journal of Clinical Medicine in Practice*, vol. 22, no. 23, pp. 51–54, 2018.

[63] T. Caro-Ordieres, G. Marín-Royo, L. Opazo-Ríos et al., "The coming age of flavonoids in the treatment of diabetic complications," *Journal of Clinical Medicine*, vol. 9, no. 2, pp. 1–30, 2020.

[64] A. D. Wen, J. Yang, Y. Y. Jia et al., "A rapid and sensitive liquid chromatography-tandem mass spectrometry (LC- MS/MS) method for the determination of hydroxysafflor yellow A in human plasma: application to a pharmacokinetic study," *Journal of Chromatography B*, vol. 876, no. 1, pp. 41–46, 2008.

[65] J. Qi, Q. Zhuang, W. Wu et al., "Enhanced effect and mechanism of water-in-oil microemulsion as an oral delivery system of hydroxysafflor yellow A," *International Journal of Nanomedicine*, vol. 6, pp. 985–991, 2011.

[66] M. Han, C. Q. Tong, L. Lv, L. Tang, Y. Fang, and J. Q. Gao, "Enhanced absorption of hydroxysafflor yellow A using a self-double-emulsifying drug delivery system: in vitro and in vivo studies," *International Journal of Nanomedicine*, vol. 7, pp. 4099–4107, 2012.

[67] L. Z. Lv, C. Q. Tong, J. Yu, M. Han, and J. Q. Gao, "Mechanism of enhanced oral absorption of hydrophilic drug incorporated in hydrophobic nanoparticles," *International Journal of Nanomedicine*, vol. 8, pp. 2709–2717, 2013.

[68] G. N. Ma, F. L. Yu, S. Wang, Z. P. Li, X. Y. Xie, and X. G. Mei, "A novel oral preparation of hydroxysafflor yellow A base on a chitosan complex: a strategy to enhance the oral bioavailability," *AAPS PharmSciTech*, vol. 16, no. 3, pp. 675–682, 2015.

[69] B. Zhao, S. Gu, Y. Du, M. Shen, X. Liu, and Y. Shen, "Solid lipid nanoparticles as carriers for oral delivery of hydroxysafflor yellow A," *International Journal of Pharmaceutics*, vol. 535, no. 1–2, pp. 164–171, 2018.

[70] X. Tong, J. Yang, Y. Zhao et al., "Greener extraction process and enhanced in vivo bioavailability of bioactive components from Carthamus tinctorius L. by natural deep eutectic solvents," *Food Chemistry*, vol. 348, pp. 1–7, 2021.

[71] Y. Liu, X. Liang, Y. Zou, Y. Peng, D. J. McClements, and K. Hu, "Resveratrol-loaded biopolymer core-shell nanoparticles: bioavailability and anti-inflammatory effects," *Food & Function*, vol. 11, no. 5, pp. 4014–4025, 2020.

Hindawi
Journal of Immunology Research
Volume 2021, Article ID 2549541, 11 pages
https://doi.org/10.1155/2021/2549541

Research Article

Supplemental *Bacillus subtilis* PB6 Improves Growth Performance and Gut Health in Broilers Challenged with *Clostridium perfringens*

Yan Liu,[1] **Song Zhang**,[2,3] **Zheng Luo**,[3] **and Dan Liu**[1]

[1]*State Key Laboratory of Animal Nutrition, College of Animal Science and Technology, China Agricultural University, Beijing, China*
[2]*Department of Animal Resource & Science, Dankook University, Cheonan, Choongnam 330–714, Republic of Korea*
[3]*Kemin (China) Technologies Co. Ltd., 25 Qinshi Road, Sanzao, Zhuhai 519040, China*

Correspondence should be addressed to Dan Liu; liud@cau.edu.cn

Received 24 July 2021; Revised 15 September 2021; Accepted 29 September 2021; Published 27 October 2021

Academic Editor: Kai Wang

Clostridium perfringens (CP) is the principal pathogenic bacterium of chicken necrotic enteritis (NE), which causes substantial economic losses in poultry worldwide. Although probiotics are known to provide multiple benefits, little is known about the potential effects of *Bacillus subtilis* (*B. subtilis*) application in preventing CP-induced necrotic enteritis. In this study, 450 male Arbor Acres broilers were divided into 5 experimental treatments: A: basal diet (control group); B: basal diet and CP challenge (model group); C: CP challenge+10 mg/kg enramycin (positive control group); D: CP challenge+4×10^7 CFU/kg of feed *B. subtilis* PB6 (PB6 low-dosage group); and E: CP challenge+6×10^7 CFU/kg of feed *B. subtilis* PB6 (PB6 high-dosage group). There were 6 replicate pens per treatment with 15 broilers per pen. The present research examined the effect of *Bacillus subtilis* PB6 (*B. subtilis* PB6) on growth performance, mRNA expression of intestinal cytokines and tight junctions, and gut flora composition in broilers challenged with CP. The entire experiment was divided into two phases: the non-CP challenge phase (d0–18) and the CP challenge phase (d18–26). PB6 did not increase the growth performance during the first stage, but the PB6 high-dosage group was found to have larger body weight gain and ADFI during the CP challenge stage. Feed supplementation with PB6 reduced the lesion score of challenged chicks, with increased tight junction-related gene expression (*occludin* and *ZO-1*) and decreased *TNF-α* expression compared with CP-infected birds. A decrease in the abundance of *Clostridium XI*, *Streptococcus*, and *Staphylococcus* was observed after CP infection ($P < 0.05$), while supplementation with PB6 restored the ileal microbial composition. In conclusion, administration of *B. subtilis* PB6 improved growth performance, enhanced intestinal barrier function, and mitigated intestinal inflammation/lesions, which might be due to its restoring effects on the ileal microbial composition in CP-challenged broilers.

1. Introduction

Necrotic enteritis (NE) is a serious bacterial disease in poultry that causes devastating financial losses. *Clostridium perfringens* (CP), an anaerobic gram-positive bacterium, is the major pathogen of NE. In fact, CP is one of the gut symbiotic bacteria of birds, and healthy birds normally harbor 10^4 CFU of CP/g of digesta in their intestine. CP is an opportunistic pathogen in some conditions, such as dietary nutrient risks (unbalanced diet formulation, antinutritional factors, and quality of raw materials), disease challenges (coccidiosis, infectious bursal virus), and inadequate management (high temperature), with increased proliferation to ~10^7 to 10^9 CFU/g of digesta [1], which leads to clinical signs of NE. In poultry production, subclinical NE leads to significant economic losses due to lesions in the small intestine, which in turn reduces body weight gain (BWG) and impairs the feed conversion ratio (FCR) [2]. Chickens are a reservoir of CP, and contaminated chicken products also represent a potential public food safety threat [3]. In human medicine,

Clostridial-contaminated food can be treated with surgical debridement and oral antibiotic therapy. However, antibiotic resistance among anaerobic bacteria, such as *Clostridial* species, is increasing worldwide [4]. Therefore, an efficient and natural method to overcome NE for chicken production in the postantibiotic age is warranted.

Probiotic supplementation has been demonstrated to be an efficient natural approach for regulating intestinal flora in humans and farm animals, which can act as follows: (a) a sustainer of the intestinal microflora ecosystem to maintain beneficial microflora colonization and inhibit pathogen proliferation, (b) a digestive booster to increase endogenous digestive enzyme activities and indigestion and reduce indigestible nutrient fermentation by depressing the activity of bacterial enzymes, and (c) a positive immune modulator by maintaining intestinal integrity [5]. Meanwhile, qualified probiotics have the capacity to overcome erratic elements, such as gastric acids, bile acids, endogenous proteases, and competition with other microorganisms. Consequently, *Bacillus subtilis* (*B. subtilis*) is a widely adopted probiotic bacterial species with many advantages. As a spore-forming facultative anaerobe, it has strong heat resistance and can last for 8 minutes at a high temperature of 113°C, which increases its possibility of survival during feed processing. At the same time, *Bacillus* spores have strong stress resistance and can survive in the gastrointestinal environment under harsh conditions, such as low pH and bile salts [6]. As a symbiotic bacterium, *B. subtilis* PB6 (ATCC-PTA 6737) has been proven to produce antibacterial substances and has a wide range of activities against numerous strains *in vitro*, including *Campylobacter* spp. and *Clostridium* spp. [7]. Moreover, research has demonstrated that supplementation with *B. subtilis* PB6 alleviates CP-induced gut lesions and also strengthens intestinal barrier function in broilers [8]. However, the potential effects of *B. subtilis* PB6 administration on gut microbiota composition and intestinal inflammatory damage in CP-challenged birds remain elusive. Here, we sought to determine the influence of *B. subtilis* PB6 administration on growth performance, lesion scores, intestinal tight junctions (TJs), proinflammatory cytokines, and gut microbiota composition in broilers challenged with CP.

2. Materials and Methods

2.1. Animals, Diets, and Housing. In total, 450 male Arbor Acres broilers were separated into 5 experimental groups, each of which was replicated 6 times for 15 broilers per replicate. The experiments were ethically approved by the Animal Care and Use Committee of China Agricultural University. All treatments were as follows: A: basal diet; B: basal diet+CP challenge; C: CP challenge+10 mg/kg enramycin; D: CP challenge+4×10^7 CFU/kg of *B. subtilis* PB6; and E: CP challenge+6×10^7 CFU/kg of *B. subtilis* PB6. The original strain of *B. subtilis* PB6 was obtained from Kemin China Technologies Co., Ltd., Zhuhai, China. Broilers were raised in a controlled environment and allowed *ad libitum* access to water and feed. Repetitions of different treatments were equally distributed among the cages as much as possible to reduce variations at the cage level. The entire experiment was divided into two phases: the non-CP challenge phase (d0–18) and the CP challenge phase (d18–26).

Table 1: Basal diet composition (as-fed basis).

Ingredient (%)	Basal diet
Corn	57.52
Soybean meal (CP > 46%)	36.20
Soy oil	2.14
Limestone	1.13
Dicalcium phosphate	1.97
Salt	0.35
Methionine (99%, DL-form)	0.19
Choline (50%)	0.25
Vitamin premix[1]	0.025
Mineral premix[2]	0.2
Ethoxyquin (66%)	0.03
Total	100.00
Calculated composition[3] (%)	
Crude protein	21.0
ME (kcal/kg)	2950
Ca	1.00
AP	0.45
Lys	1.11

[1]Provided per kg of diet: vitamin premix (1 kg) contained the following: vitamin A, 50 MIU; vitamin D_3, 12 MIU; vitamin K_3, 10 g; vitamin B_1, 10 g; vitamin B_2, 32 g; vitamin B_{12}, 0.1 g; vitamin E, 0.2 MIU; biotin, 0.5 g; folic acid, 5 g; pantothenic acid, 50 g; niacin, 150 g copper, 4 g; zinc, 90 g; iron, 38 g; manganese, 46.48 g; selenium, 0.1 g; iodine, 0.16 g; cobalt, 0.25 g. [2]Provided per kg of diet: 150 g copper, 4 g; zinc, 90 g; iron, 38 g; manganese, 46.48 g; selenium, 0.1 g; iodine, 0.16 g; cobalt, 0.25 g. [3]Calculated value based on the analyzed data for the experimental diets.

All diets were designed following the instructions of NRC (1994) and the Chinese chicken feeding standard (NY/T-33–2004) (Table 1). The CP challenge was performed on the basis of the study of Liu et al. [9].

A field strain of CP type A (CVCC2030) was cultured on tryptone-sulfite-cycloserine agar, and a single colony was then inoculated into a cooked meat medium and subsequently cultured in an incubator at 37°C for 8 hours. In the infected groups, chickens were orally inoculated with 1 ml bacterial solution containing 10^8 CFU/ml CP once a day from Day 19 to Day 25. Chickens in the basal diet group were subjected to the same gavage procedure described above but with a sterilized medium.

2.2. Growth Performance. The mortality rate was recorded throughout the experiment. Body weights of chickens were measured on Day 0, on Day 18, and on the last day (Day 26). Feed intake (FI), body weight gain (BWG), and the feed conversion ratio (FCR) were calculated and recorded for further analysis.

2.3. Lesion Score. Intestinal scoring was evaluated on Day 26. A randomly selected chicken of each repetition was killed by cervical dislocation and then underwent intestinal scoring. The intestines were cut open and scored for NE lesions.

Table 2: Sequences for real-time PCR primers.

Genes	Primer sequence (5′–3′)	Accession no.
β-Actin	F: GAGAAATTGTGCGTGACATCA R: CCTGAACCTCTCATTGCC	L08165
Occludin	F: ACGGCAGCACCTACCTCAA R: GGGCGAAGAAGCAGATGAG	D21837.1
ZO-1	F: CTTCAGGTGTTTCTCTTCCTCCTC R: CTGTGGTTTCATGGCTGGATC	XM_413773
TRL4	F: GTTCCTGCTGAAATCCCAAA R: TATGGATGTGGCACCTTGAA	NM_001030693
IL-1β	F: ACTGGGCATCAAGGGCTA R: GGTAGAAGATGAAGCGGGTC	NM_204524
TNF-α	F: GAGCGTTGACTTGGCTGTC R: AAGCAACAACCAGCTATGCAC	NM_204267
IFN-γ	F: TAACTCAAGTGGCATAGATGTGGAAG R: GACGCTTATGTTGTTGCTGATGG	NM_008337

[1]Abbreviation: ZO-1: zonula occludens-1; TRL4: Toll-like receptor-4; IL-1β: interleukin-1β; TNF-α: tumor necrosis factor-α; IFN-γ: interferon-γ.

Specifically, after intestinal observation, the intestinal lesions were rated from 0 to 4 points according to the method of Dahiya et al. [10].

2.4. Proinflammatory Cytokine and Tight Junction Protein Gene Expression. Jejunum samples were collected from broilers that were randomly selected from each replicate on Day 26 and stored at -80°C for RNA extraction. RNA extraction, reverse transcription, and quantification methods were performed according to Wang et al. [11]. In short, total RNA extraction was performed with a TRIzol reagent, and RNA quality and concentration were detected by a NanoDrop spectrophotometer (ND-2000 UV-Vis; Thermo Scientific Inc.). RNA reverse transcription and real-time fluorescence quantification were carried out with Takara reagents following the manufacturer's instructions (Takara Biotechnology Inc.). An ABI 7500 Real-Time PCR System (Applied Biosystems) was used for real-time fluorescence quantitative detection. β-Actin was used as a reference gene to normalize the relative RNA expression. The primer sequences for β-actin, occludin, ZO-1, TLR4, IL-1β, TNF-α, and IFN-γ are listed in Table 2. Each sample was measured in triplicate, and the average value was calculated. The $2^{-\Delta\Delta}$Ct method was used to calculate the relative mRNA expression of target genes [12].

2.5. Pyrosequencing of Ileal Microbiota. On Day 26, broiler ileal digesta were sampled. DNA was extracted from ileal digesta using a QIAamp® Fast DNA Stool Mini Kit (Qiagen Ltd., Germany) according to the guidelines. According to the specifications outlined by Illumina, all DNA samples were pretreated for MiSeq compositional sequencing. The V3-V4 region of the 16S rRNA gene was amplified, and Illumina index primers were attached in two separate PCRs.

FLASH software (v1.2.7) was used to generate raw tags [13]. Effective tags were obtained by the UCHIME algorithm [14] and QIIME (v1.7.0) analysis [15]. UPARSE software (v7.0.1001) was used to analyze sequences, and the sequences were clustered at 97% similarity as operational taxa (OTUs). The GreenGene database was used to compare sequences and classify the different classification levels of these sequences. Microbial diversity was detected through QIIME software and Python scripts.

2.6. Statistical Analysis. The data, including growth performance, lesion scores, and the gene expression of both intestinal tight junctions and proinflammatory cytokines collected for quantitative parameters, were analyzed using analysis of variance (ANOVA) under a completely randomized design. Significant differences among the treatments were measured using Duncan's multiple comparison and were declared when $P < 0.05$.

3. Results

3.1. Effects of Bacillus subtilis PB6 on Growth Performance in Broilers Challenged with Clostridium perfringens. As shown in Table 3, before the birds were challenged by CP (Days 1–18), no differences were detected among the treatment groups ($P > 0.05$). However, during the CP challenge period, CP infection significantly reduced BWG and ADFI ($P < 0.05$) and tended to increase FCR ($P = 0.062$) compared to the control group. However, the addition of enramycin numerically increased the BWG of CP-infected chicks ($P > 0.05$). Moreover, the addition of a low dosage of *B. subtilis* PB6 increased the BWG ($P < 0.05$) and tended to increase the ADFI ($P > 0.05$) of CP-challenged chicks, while the addition of a high dosage of *B. subtilis* PB6 significantly increased the BWG and ADIF of CP-challenged chicks ($P < 0.05$).

3.2. Effects of Bacillus subtilis PB6 on Intestinal Lesions and Gene Expression in Broilers Challenged with Clostridium perfringens. As shown in Table 4, CP infection significantly increased the intestinal lesion score compared to the control group ($P < 0.05$). However, dietary addition of enramycin and low and high dosages of *B. subtilis* PB6 significantly reduced the intestinal lesion score of CP-infected broilers ($P < 0.05$).

Table 3: The effect of *B. subtilis* supplementation on growth performance and mortality in CP-challenged broilers.

Treatment[1]	Control group	CP-challenged model group	Antibiotics (positive control group)	*B. subtilis* PB6 low-dosage group	*B. subtilis* PB6 high-dosage group	SEM[2]	*P* value[3]
d1-d18 nonchallenge phase							
BWG (g)	36.06	35.47	35.44	35.14	35.58	0.25	0.86
FI (g)	51.61	50.87	51.65	51.79	51.97	0.44	0.95
FCR	1.43	1.44	1.46	1.48	1.46	0.01	0.50
Mortality rate	0.00	0.00	0.00	0.00	0.00	0.00	1.00
d19-d26 challenge phase							
BWG (g)	66.12^{a}	54.95^{c}	59.21^{bc}	61.62^{ab}	62.86^{ab}	1.087	0.009
FI (g)	109.55^{a}	99.90^{bc}	98.35^{c}	106.30^{ab}	108.41^{a}	1.305	0.007
FCR	1.66	1.83	1.67	1.73	1.73	0.02	0.062
Mortality rate (%)	2.22	3.49	1.11	4.45	3.58	0.907	0.821
Overall							
BWG (g)	46.47^{a}	42.21^{c}	43.67^{bc}	44.31^{abc}	45.02^{ab}	0.394	0.004
FI (g)	71.66^{a}	67.84^{b}	67.81^{b}	70.66^{ab}	71.51^{a}	0.544	0.026
FCR	1.55	1.61	1.55	1.6	1.59	0.009	0.151
Mortality rate (%)	2.22	3.49	1.11	4.45	3.58	0.907	0.821

[1]Treatment information: control group: basal diet; CP-challenged model group: basal diet and CP challenge; antibiotics (positive control group): CP challenge+10 mg/kg enramycin; *B. subtilis* PB6 low-dosage group: CP challenge+4×10^7 CFU/kg of feed *B. subtilis* PB6; *B. subtilis* PB6 high-dosage group: CP challenge+6×10^7 CFU/kg of feed *B. subtilis* PB6. BWG: body weight gain; FI: feed intake; FCR: feed conversion ratio. [2]Standard error of the means; $n = 6$ chickens/group. [3]Mean values within a column with unlike superscripts letters (a, b, and c) are significantly different ($P < 0.05$).

Table 4: Intestinal lesion score and relative mRNA expression of intestinal tight junction proteins and proinflammatory cytokines in broilers.

Treatment[1]	Control group	CP-challenged model group	Antibiotics (positive control group)	*B. subtilis* PB6 low-dosage group	*B. subtilis* PB6 high-dosage group	SEM[2]	*P* value[3]
Occludin	1.11^{ab}	0.50^{c}	1.39^{a}	0.75^{bc}	0.65^{bc}	0.093	0.009
ZO-1	1.04^{c}	1.43^{bc}	1.68^{abc}	2.54^{a}	2.01^{ab}	0.145	0.009
TRL4	1.1	1.06	0.98	1.38	1.24	0.069	0.335
IL-1β	1.32	2.04	1.47	2.14	2.87	0.199	0.106
TNF-α	1.06^{ab}	1.45^{a}	0.93^{b}	1.33^{a}	0.95^{b}	0.083	0.022
IFN-γ	1.12	1.83	1.15	1.68	1.76	0.137	0.289
Lesion score[4]	0.00^{d}	1.25^{a}	0.33^{c}	0.75^{b}	0.66^{b}	0.088	<0.001

[1]Treatment information: control group: basal diet; CP-challenged model group: basal diet and CP challenge; antibiotics (positive control group): CP challenge+10 mg/kg enramycin; *B. subtilis* PB6 low-dosage group: CP challenge+4×10^7 CFU/kg of feed *B. subtilis* PB6; *B. subtilis* PB6 high-dosage group: CP challenge+6×10^7 CFU/kg of feed *B. subtilis* PB6. ZO-1: zonula occludens-1; TRL4: Toll-like receptor-4; IL-1β: interleukin-1β; TNF-α: tumor necrosis factor-α; IFN-γ: interferon-γ. [2]Standard error of the means; $n = 6$ chickens/group. [3]Mean values within a column with unlike superscripts letters (a, b, and c) are significantly different ($P < 0.05$). [4]0 = no gross lesions; 0.5 = severely congested serosa and mesenteric hyperemia; 1 = thin-walled and brittle intestines with small hemorrhagic spots (>5); 2 = small amounts of gas production and focal necrotic lesions; 3 = large amount of gas-filled intestines and necrotic plaques.

Compared to the control group, CP challenge led to a significant decrease in jejunum mRNA expression of occludin ($P < 0.05$) and tended to upregulate TNF-α expression ($P > 0.05$). Nevertheless, supplementation with enramycin upregulated occludin expression and downregulated TNF-α expression in the jejunum of CP-infected birds ($P < 0.05$). Moreover, the infected broilers fed a diet with a low dosage of *B. subtilis* PB6 showed the highest ZO-1 mRNA expression among all groups ($P < 0.05$) and had relatively higher occludin expression than CP-infected birds ($P > 0.05$). Infected birds fed a diet with a high dosage of *B. subtilis* PB6 had lower expression of TNF-α ($P < 0.05$) and relatively higher occludin expression ($P > 0.05$) than infected birds fed a basal diet.

3.3. The Quality of Gut Microbiota Sequencing Data. After the OTUs were assigned and chimeras were removed, 1,965,036 effective sequences were obtained from 30 ileal samples, and 56,143 sequences were shared by a single sample. The read length ranged from 220 to 500 base pairs (bp), and the median read length was 427 bp. OTU numbers were identified. As shown in Figure 1(a), 109 OTUs were shared by five groups, and 112, 32, 111, 24, and 93 OTUs were exclusive in each group.

3.4. Effects of Bacillus subtilis PB6 on the Intestinal Bacterial Structure and Diversity in Broilers Challenged with Clostridium perfringens. Phylum-level microbiota analysis showed that *Firmicutes* (89.97%), *Proteobacteria* (7.67%), and *Bacteroidetes* (1.78%) (Figure 1(b)) were the three most dominant phyla, accounting for 99.42% of all sequences in the groups. Supplementation with enramycin reduced *Firmicutes* abundance in the ileum. As shown in Figure 1(c), the analysis of the ileal community at the genus level revealed that *Lactobacillus* (69.63%), *Clostridium XI* (11.70%), *Escherichia* (4.24%), *Streptococcus* (1.92%), and *Brevundimonas* (1.44%) were the five dominant genera.

Further statistics were carried out to identify differences in the ileal community at the genus level among the groups, which are shown in Figure 1(d). CP challenge significantly decreased the abundance of *Clostridium XI*, *Streptococcus*, and *Staphylococcus* in comparison with the control group ($P < 0.05$), while supplementation with enramycin and low-dosage *B. subtilis* PB6 raised these bacterial abundances to levels similar to those of nonchallenge birds ($P > 0.05$). The birds fed high-dosage *B. subtilis* PB6 had more *Clostridium XI* than the other groups ($P < 0.05$). LEfSe analysis showed that 18 differentially abundant bacterial clades were distributed to all taxonomic levels (LDA score > 3.0) among the 5 treatments (Figure 2(a)). The highest relative abundances of *Clostridium XI*, *Peptostreptococcaceae*, *Desulfovibrionaceae*, and *Staphylococcus* were indicated in the control group among all treatments (LDA score > 3.0). Moreover, supplementation with enramycin increased the relative abundances of *Bosea* and *Xanthomonadaceae* (LDA score > 3.0). Supplementation with a low dosage of *B. subtilis* PB6 increased *Streptococcus* abundance (LDA score > 3.0), while supplementation with a high dosage of *B. subtilis* PB6 increased *Clostridia* abundance (LDA score > 3.0). Figure 2(b) shows the ileal microbial alpha diversity. There were no significant differences in the diversity indexes (Shannon) among all groups ($P > 0.05$). Beta diversity was demonstrated via PCoA in Figure 2(c), showing no distinguishable clustering of the ileal samples in different treatments.

4. Discussion

Pathogenic bacteria, such as *Clostridium perfringens* (CP), can cause imbalances in animal homeostasis and damage to the body and severely affect animal growth performance [16]. A large amount of evidence has shown that probiotics are beneficial for improving the growth performance of animals under both the pathogen-infected and noninfected conditions, which may be due to the compounds secreted by probiotics, such as digestive enzymes, antibacterial substances, and/or other growth-promoting factors, such as short-chain fatty acids [17, 18]. As a widely used probiotic, *Bacillus subtilis* PB6 has been proven to improve broiler/-animal feed intake, increase body weight, and reduce FCR

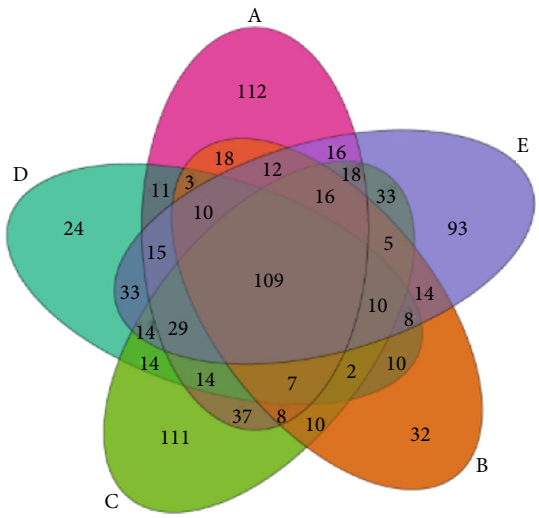

(a)

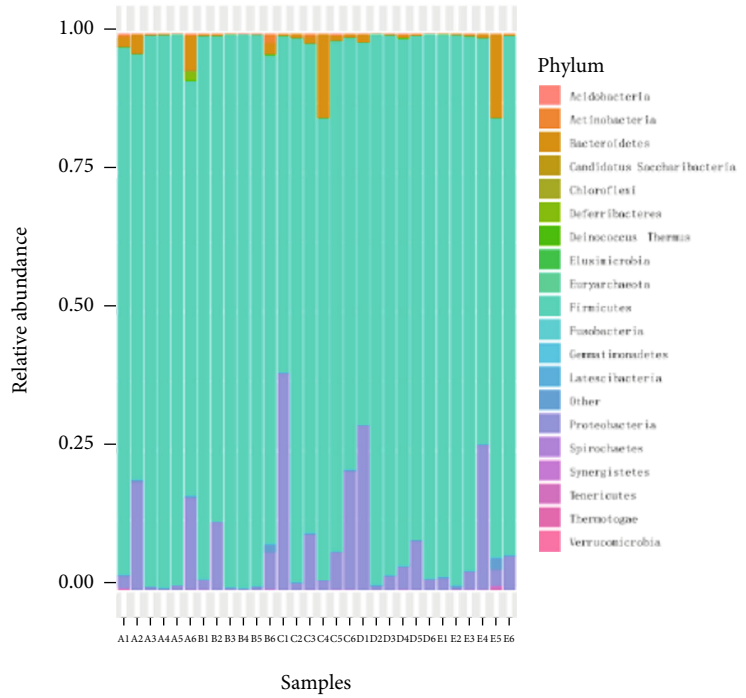

(b)

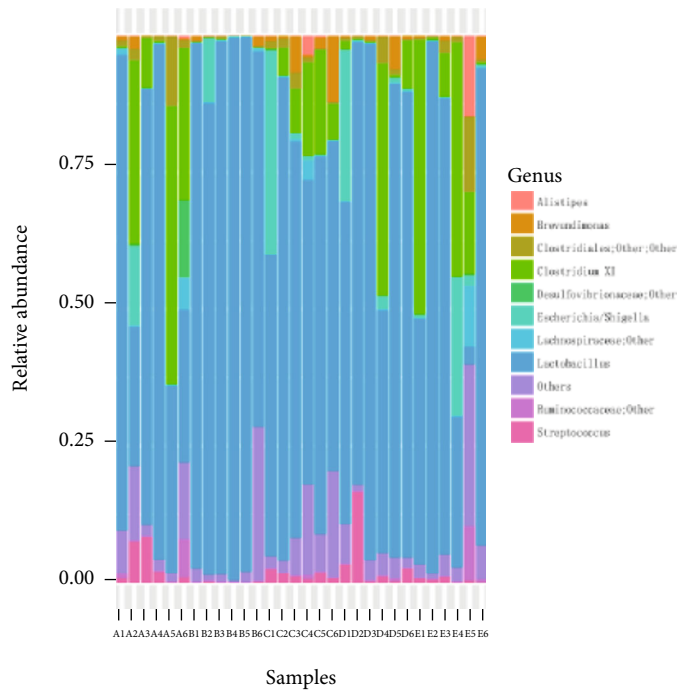

(c)

Figure 1: Continued.

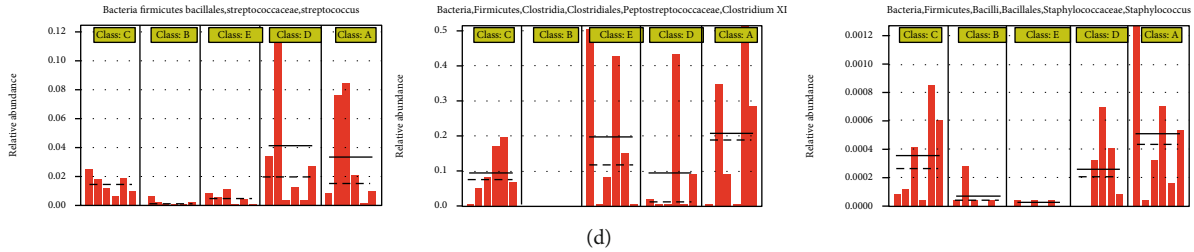

(d)

Figure 1: Effects of *Bacillus subtilis* PB6 on the intestinal bacterial structure in broilers challenged with *Clostridium perfringens*. (a) Venn diagrams showing the shared OTUs between the five different treatments. (b) Effects of relative abundance (%) of ileal bacterial taxa at the phylum level of broilers. (c) Relative abundance (%) of ileal bacterial taxa at the genus level of broilers. (d) The relative abundance (%) of ileal bacterial taxa at the genus level of *Streptococcus*, *Clostridium XI*, and *Staphylococcus* in broilers. Treatment information: A: basal diet; B: basal diet and CP challenge; C: CP challenge+10 mg/kg enramycin (positive control group); D: CP challenge+4×10^7 CFU/kg of feed *B. subtilis* PB6 (PB6 low-dosage group); E: CP challenge+6×10^7 CFU/kg of feed *B. subtilis* PB6 (PB6 high-dosage group).

[19, 20]. In the present study, we also found that adding 4×10^7 and 6×10^7 CFU/kg *B. subtilis* PB6 to the diet could mitigate the negative effects of CP infection on broiler BWG and FCR, particularly with the addition of a high dose. In addition, we found that *B. subtilis* PB6 exerted a better growth-promoting effect on CP-infected broilers than enramycin, which is commonly used in CP prevention, ultimately confirming the growth-promoting effect of *B. subtilis* PB6. However, other studies showed that the growth-promoting effect of *B. subtilis* PB6 was not significant [21], and these inconsistent results across studies may be due to the breeding environment, animal species, additive dosage, or operating procedures.

CP can produce various toxins, bacteriocins, and collagenolytic enzymes after colonization [22]. These active substances affect tight junctions and their components, such as occludin and junction adhesion molecules (JAMs), by altering the transmembrane pores and extracellular matrix of intestinal cells, leading to compromised integrity of the lamina propria [23]. The above alterations are accompanied by activation of the mucosal immune response; subsequently, many proinflammatory cytokines are secreted, such as TNF-α and IL-1β [24]. These cytokines can induce the rearrangement of tight junctions and damage the intestinal barrier, thereby causing a vicious cycle over the host and even a systemic infection [22]. In line with other studies [25–27], our results noted that CP infection caused severe physical damage to the intestine of broilers, significantly raised intestinal lesion scores, inhibited the gene expression of the intestinal TJ protein occludin, and upregulated the expression of the proinflammatory cytokine TNF-α. These abnormal physiological alterations may be important factors in the reduction of growth performance of broilers infected with CP. Furthermore, we found that enramycin and *B. subtilis* PB6 could variously increase the expression of the TJ proteins occludin and ZO-1 in CP-infected broilers and reduce the expression of the inflammatory factor TNF-α. This indicates that the addition of enramycin and *B. subtilis* PB6 can restore the intestinal physical barrier and reduce intestinal inflammation, thus helping to decrease the intestinal lesion scores and recover the physiological function of the damaged intestine. In agreement with our findings, Jayaraman et al. and Belote et al. reported that supplementation with *B. subtilis* PB6 and enramycin prevented CP-induced NE and decreased lesion scores and also improved intestinal health in challenged broilers [8, 28]. Enramycin can kill pathogenic bacteria by directly inhibiting their cell wall formation, thereby reducing the damage caused by pathogens to the body [28]. However, in addition to competitive rejection, probiotics can also exert their growth-promoting effects through immune regulation, secretion of antibacterial molecules, and enhancement of the body's antioxidant capacity. In this study, *B. subtilis* PB6 exerted its immunomodulatory effect by downregulating the expression of TNF-α in the intestine of CP-infected broilers and simultaneously upregulating the expression of occludin and ZO-1. TNF-α is produced by activated monocytes/macrophages and is synthesized in large quantities during the acute phase of bacterial infection, subsequently promoting the activation of downstream immune cells, such as T cells, thus intensifying the inflammatory response and harming the host [29]. Similarly, recent studies have shown that *B. subtilis* can reduce intestinal inflammation by modifying the polarization of macrophages, inhibiting the expression of TNF-α, and thus protecting the body from bacterial infections [30]. As the main components of epithelial tight junctions, the improved mRNA expression of occludin and ZO-1 can enhance intestinal barrier function and protect intestinal health [31, 32]. Studies have also found that the culture supernatant of *B. subtilis* can upregulate the expression of tight junction proteins and mucin 2 in HT-29 cells *in vitro*, but the specific metabolites are not yet known, and further exploration is needed [33].

The intestinal microbial community, which is regulated by many factors, such as food [34], age [35], and additives [36], is very important for the growth and health of broilers due to its ability to promote nutrient digestion and regulate the immune system [37]. In general, the diversity of gut microbiota is closely related to pathogen resistance. The intestinal microbiome can be affected by many factors, such as pathological conditions, antibiotic therapy, dietary supplementation, and housing environment [38]. Recently, Fasina

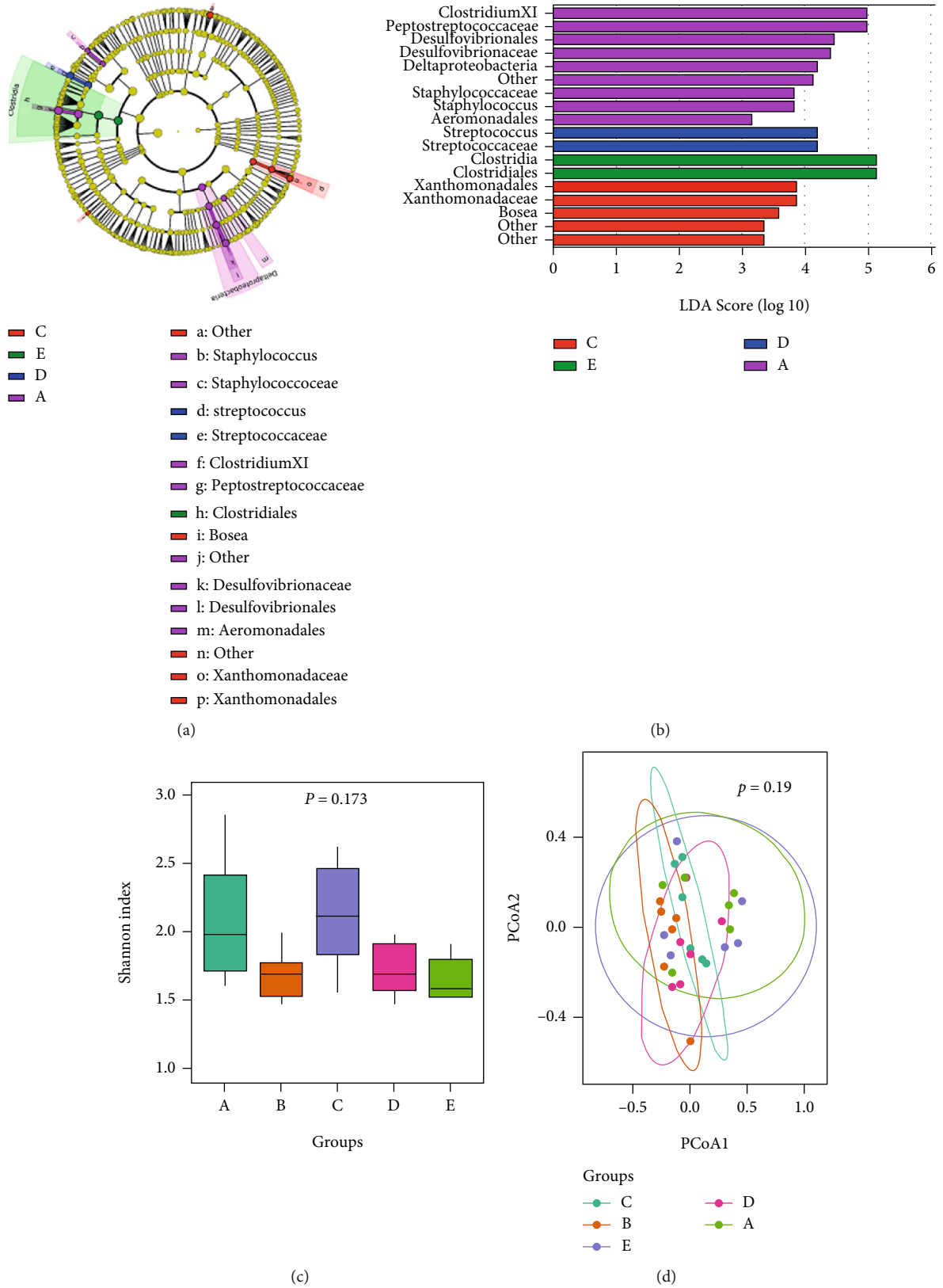

Figure 2: Effects of *Bacillus subtilis* PB6 on intestinal bacterial diversity in broilers challenged with *Clostridium perfringens*. (a) Diversity and composition of ileal microbiota (LEfSe score) in broilers. (b) Diversity and composition of ileal microbiota (circular cladogram) in broilers. (c) Alpha diversity analysis (Shannon) of ileal microbiota in broilers. (d) Beta diversity analysis (PCoA) of ileal microbiota in broilers. Treatment information: A: basal diet; B: basal diet and CP challenge; C: CP challenge+10 mg/kg enramycin (positive control group); D: CP challenge+4 × 10^7 CFU/kg of feed *B. subtilis* PB6 (PB6 low-dosage group); E: CP challenge+6 × 10^7 CFU/kg of feed *B. subtilis* PB6 (PB6 high-dosage group).

et al. [39] and Li et al. [40] reported that CP infection dramatically reduced the α-diversity index of the broiler intestinal microbial community. However, Xu et al. [41] and Zhang et al. [42] indicated the opposite result, which revealed that CP infection significantly increased the α-diversity index of the gut microbial community. Moreover, some studies found that CP infection did not affect either the α- or β-diversity index [43, 44], which is in agreement with the current results. Those authors considered that the discrepancy might be attributed to the following: (a) the different sections of the ileum in which the digesta were collected, (b) diverse CP strains and diet types, and (c) the different durations of CP challenge. Relevant references are limited, and further trials are required.

Studies have shown that the abundance of intestinal *Clostridium XI* is significantly increased, accompanied by decreased gene expression of TNF-α and a decreased inflammation index in the colon after treatment with probiotics in a colitis mouse model [45]. Consistently, we found a higher abundance of *Clostridium XI* in the ileum of broilers in the control group, enramycin supplementation group, and low- and high-dosage *B. subtilis* PB6 supplementation groups, accompanied by a decrease in TNF-α expression and reduced intestinal lesions. Therefore, we speculate that a high abundance of *Clostridium XI* may inhibit intestinal inflammation. LEfSe analysis showed that *Streptococcus* was significantly enriched in the low-dose *B. subtilis* PB6 supplementation group. *Streptococcus* contains many probiotic strains, such as *Streptococcus thermophilus*. Recent studies have found that *Streptococcus thermophilus* can increase the expression of the tight junction proteins ZO-1 and ZO-2 in high-fat diet mice and maintain the expression of ZO-1 in a human intestinal epithelial cell line infected with *E. coli* [46–48]. Therefore, in this experiment, the increased expression of ZO-1 in the intestine of broilers in the low-dose *B. subtilis* PB6 supplementation group may be related to the increased abundance of *Streptococcus*. A previous study showed that *Bosea* contains strains that can secrete a variety of cellulolytic enzymes [49]. In this experiment, enramycin treatment significantly increased the abundance of *Bosea* in the intestine of CP-infected broilers. Thus, the ability of *Bosea* to decompose cellulose and improve the utilization of feed nutrients may be one of the reasons for the increased body weight of broilers in the enramycin group. *Staphylococcus*, as a conditional pathogen, is generally considered harmful to the host, but the reason for its decreased abundance in the ileum of CP-infected broilers remains unclear. This may be due to the occupying effect of CP that inhibits the reproduction of *Staphylococcus*. *Desulfovibrionaceae* and *Xanthomonadaceae* are currently less studied. However, one study found that *Xanthomonadales* is enriched in mice inoculated with Chinese propolis [50], but its function is unclear.

5. Conclusion

In summary, administration of *B. subtilis* PB6 can improve growth performance by enhancing intestinal barrier function, mitigating intestinal inflammation/lesions, and reshaping the ileal microbial composition in CP-challenged birds.

Abbreviations

BWG: Body weight gain
ADFI: Average daily feed intake
ZO-1: Zonula occludens-1
TRL4: Toll-like receptor-4
IL-1β: Interleukin-1β
TNF-α: Tumor necrosis factor-α
IFN-γ: Interferon-γ.

Data Availability

The data used to support the findings of this study are available from the corresponding author upon request.

Conflicts of Interest

The authors declare that they have no conflicts of interest.

Acknowledgments

This study was supported by the Shandong Provincial Key R&D Program (2019JZZY020602) and the China National Key R&D Program during the 13th Five-Year Plan Period (Grant No. 2017YFE0129900).

References

[1] R. B. Williams, "Intercurrent coccidiosis and necrotic enteritis of chickens: rational, integrated disease management by maintenance of gut integrity," *Avian Pathology*, vol. 34, no. 3, pp. 159–180, 2005.

[2] Y. A. Attia, H. F. Ellakany, A. A. El-Hamid, F. Bovera, and S. Ghazaly, "Control of *Salmonella enteritidis* infection in male layer chickens by acetic acid and/or prebiotics, probiotics and antibiotics," *Arch Geflügelk*, vol. 76, pp. 239–245, 2013.

[3] M. Lindström, A. Heikinheimo, P. Lahti, and H. Korkeala, "Novel insights into the epidemiology of *Clostridium perfringens* type A food poisoning," *Food Microbiology*, vol. 28, no. 2, pp. 192–198, 2011.

[4] P. R. Murray, K. S. Rosenthal, and M. A Pfaller, *Medical Microbiology*, Elsevier Health Sciences, Philadelphia, 2015.

[5] S. M. Aziz Mousavi, H. Mahmoodzadeh Hosseini, and S. A. Mirhosseini, "A review of dietary probiotics in poultry," *Journal of Applied Biotechnology Reports*, vol. 5, no. 1, pp. 48–54, 2018.

[6] S. Shivaramaiah, N. R. Pumford, M. J. Morgan et al., "Evaluation of _Bacillus_ species as potential candidates for direct-fed microbials in commercial poultry," *Poultry Science*, vol. 90, no. 7, pp. 1574–1580, 2011.

[7] A. Y.-L. Teo and H.-M. Tan, "Inhibition of Clostridium perfringens by a novel strain of Bacillus subtilis isolated from the gastrointestinal tracts of healthy chickens," *Applied and Environmental Microbiology*, vol. 71, no. 8, pp. 4185–4190, 2005.

[8] S. Jayaraman, G. Thangavel, H. Kurian, R. Mani, R. Mukkalil, and H. J. P. Chirakkal, "_Bacillus subtilis_ PB6 improves intestinal health of broiler chickens challenged with _Clostridium perfringens_ -induced necrotic enteritis," *Poultry Science*, vol. 92, no. 2, pp. 370–374, 2013.

[9] D. Liu, S. Guo, and Y. Guo, "Xylanase supplementation to a wheat-based diet alleviated the intestinal mucosal barrier impairment of broiler chickens challenged by Clostridium perfringens," *Avian pathology*, vol. 41, no. 3, pp. 291–298, 2012.

[10] J. P. Dahiya, D. Hoehler, D. C. Wilkie, A. G. Van Kessel, and M. D. Drew, "Dietary glycine concentration affects intestinal Clostridium perfringens and lactobacilli populations in broiler chickens[1]," *Poultry Science*, vol. 84, no. 12, pp. 1875–1885, 2005.

[11] W. Wang, Z. Li, Q. Han, Y. Guo, B. Zhang, and R. D'inca, "Dietary live yeast and mannan-oligosaccharide supplementation attenuate intestinal inflammation and barrier dysfunction induced by Escherichia coli in broilers," *The British Journal of Nutrition*, vol. 116, no. 11, pp. 1878–1888, 2016.

[12] K. J. Livak and T. D. J. M. Schmittgen, "Analysis of relative gene expression data using real-time quantitative PCR," *Methods*, vol. 25, pp. 402–408, 2001.

[13] T. Magoč and S. L. Salzberg, "FLASH: fast length adjustment of short reads to improve genome assemblies," *Bioinformatics*, vol. 27, no. 21, pp. 2957–2963, 2011.

[14] R. Edgar, B. J. Haas, J. C. Clemente, C. Quince, and R. Knight, "UCHIME improves sensitivity and speed of chimera detection," *Bioinformatics*, vol. 27, no. 16, pp. 2194–2200, 2011.

[15] J. G. Caporaso, J. Kuczynski, J. Stombaugh et al., "QIIME allows analysis of high-throughput community sequencing data," *Nature Methods*, vol. 7, no. 5, pp. 335-336, 2010.

[16] U. Ramlucken, S. O. Ramchuran, G. Moonsamy, R. Lalloo, M. S. Thantsha, and C. Jansen van Rensburg, "A novel *Bacillus* based multi-strain probiotic improves growth performance and intestinal properties of *Clostridium perfringens* challenged broilers," *Poultry Science*, vol. 99, no. 1, pp. 331–341, 2020.

[17] Y. Wang and Q. Gu, "Effect of probiotic on growth performance and digestive enzyme activity of Arbor Acres broilers," *Research in Veterinary Science*, vol. 89, no. 2, pp. 163–167, 2010.

[18] A. J. H. Maathuis, D. Keller, and S. Farmer, "Survival and metabolic activity of the GanedenBC30 strain of Bacillus coagulans in a dynamic in vitro model of the stomach and small intestine," *Beneficial Microbes*, vol. 1, no. 1, pp. 31–36, 2010.

[19] S. Jiraphocakul, T. W. Sullivan, and K. M. Shahani, "Influence of a dried *Bacillus subtilis* culture and antibiotics on performance and intestinal microflora in turkeys," *Poultry Science*, vol. 69, no. 11, pp. 1966–1973, 1990.

[20] T. Melegy, N. F. Khaled, R. El-Bana, and H. Abdellatif, "Effect of dietary supplementation of Bacillus subtilis PB6 (CLOSTAT™) on performance, immunity, gut health and carcass traits in broilers," *Journal of American Science*, vol. 7, 2011.

[21] A. Y. Teo and H.-M. Tan, "Evaluation of the performance and intestinal gut microflora of broilers fed on corn-soy diets supplemented with Bacillus subtilis PB6 (CloSTAT)," *Journal of Applied Poultry Research*, vol. 16, pp. 296–303, 2007.

[22] Z. Mora, M. E. Macías-Rodríguez, J. Arratia-Quijada, Y. S. Gonzalez-Torres, K. Nuño, and A. Villarruel-López, "Clostridium perfringens as foodborne pathogen in broiler production: pathophysiology and potential strategies for controlling necrotic enteritis," *Animals*, vol. 10, no. 9, 2020.

[23] W. A. Awad, C. Hess, and M. Hess, "Enteric pathogens and their toxin-induced disruption of the intestinal barrier through alteration of tight junctions in chickens," *Toxins*, vol. 9, no. 2, p. 60, 2017.

[24] M. Flores-Díaz, E. Barquero-Calvo, M. Ramírez, and A. Alape-Girón, "Role of Clostridium perfringens toxins in necrotic enteritis in poultry," in *Microbial Toxins*, P. Gopalakrishnakone, B. Stiles, A. Alape-Girón, J. D. Dubreuil, and M. Mandal, Eds., pp. 119–134, Dordrecht, Netherlands, 2016.

[25] M. Lu, R. W. Li, H. Zhao et al., "Effects of *Eimeria maxima* and *Clostridium perfringens* infections on cecal microbial composition and the possible correlation with body weight gain in broiler chickens," *Research in Veterinary Science*, vol. 132, pp. 142–149, 2020.

[26] H. Wang, X. Ni, X. Qing et al., "Probiotic enhanced intestinal immunity in broilers against subclinical necrotic enteritis," *Frontiers in Immunology*, vol. 8, 2017.

[27] H. Lee, S. Lee, S. Kim et al., "Asymptomatic Clostridium perfringens inhabitation in intestine can cause inflammation, apoptosis, and disorders in brain," *Foodborne Pathogens and Disease*, vol. 17, no. 1, pp. 52–65, 2020.

[28] B. L. Belote, A. Tujimoto-Silva, P. H. Hümmelgen et al., "Histological parameters to evaluate intestinal health on broilers challenged with *Eimeria* and *Clostridium perfringens* with or without enramycin as growth promoter," *Poultry Science*, vol. 97, no. 7, pp. 2287–2294, 2018.

[29] N. H. Ruddle, "Tumor necrosis factor (TNF-α) and lymphotoxin (TNF-β)," *Current Opinion in Immunology*, vol. 4, no. 3, pp. 327–332, 1992.

[30] L. Guo, M. Meng, Y. Wei et al., "Protective effects of live combined and in polymicrobial sepsis through modulating activation and transformation of macrophages and mast cells," *Frontiers in Pharmacology*, vol. 9, 2019.

[31] P. D. Cani, S. Possemiers, T. Van de Wiele et al., "Changes in gut microbiota control inflammation in obese mice through a mechanism involving GLP-2-driven improvement of gut permeability," *Gut*, vol. 58, no. 8, pp. 1091–1103, 2009.

[32] S. Oh-I, H. Shimizu, T. Sato, Y. Uehara, S. Okada, and M. Mori, "Molecular mechanisms associated with leptin resistance: n-3 polyunsaturated fatty acids induce alterations in the tight junction of the brain," *Cell Metabolism*, vol. 1, no. 5, pp. 331–341, 2005.

[33] Y. Li, T. Zhang, C. Guo et al., "Bacillus subtilis RZ001 improves intestinal integrity and alleviates colitis by inhibiting the Notch signalling pathway and activating ATOH-1," *Pathogens and Disease*, vol. 78, no. 2, 2020.

[34] K. Wang, Z. Wan, A. Ou et al., "Monofloral honey from a medical plant, Prunella vulgaris, protected against dextran sulfate sodium-induced ulcerative colitis via modulating gut microbial populations in rats," *Food & Function*, vol. 10, no. 7, pp. 3828–3838, 2019.

[35] J. Xiong, L. Xuan, W. Yu, J. Zhu, Q. Qiu, and J. Chen, "Spatiotemporal successions of shrimp gut microbial colonization: high consistency despite distinct species pool," *Environmental Microbiology*, vol. 21, no. 4, pp. 1383–1394, 2019.

[36] D. J. Schwartz, A. E. Langdon, and G. Dantas, "Understanding the impact of antibiotic perturbation on the human microbiome," *Genome Medicine*, vol. 12, no. 1, 2020.

[37] K. Y. Choi, T. K. Lee, and W. J. Sul, "Metagenomic analysis of chicken gut microbiota for improving metabolism and health of chickens - a review," *Asian-Australasian Journal of Animal Sciences*, vol. 28, no. 9, pp. 1217–1225, 2015.

[38] A. Corrigan, M. de Leeuw, S. Penaud-Frézet, D. Dimova, and R. A. Murphy, "Phylogenetic and functional alterations in bacterial community compositions in broiler ceca as a result of

mannan oligosaccharide supplementation," *Applied and Environmental Microbiology*, vol. 81, no. 10, pp. 3460–3470, 2015.

[39] Y. O. Fasina, M. M. Newman, J. M. Stough, and M. R. Liles, "Effect of _Clostridium perfringens_ infection and antibiotic administration on microbiota in the small intestine of broiler chickens," *Poultry Science*, vol. 95, no. 2, pp. 247–260, 2016.

[40] Z. Li, W. Wang, D. Liu, and Y. Guo, "Effects of Lactobacillus acidophilus on gut microbiota composition in broilers challenged with Clostridium perfringens," *PLoS One*, vol. 12, no. 11, article e0188634, 2017.

[41] S. Xu, Y. Lin, D. Zeng et al., "_Bacillus licheniformis_ normalize the ileum microbiota of chickens infected with necrotic enteritis," *Scientific Reports*, vol. 8, no. 1, 2018.

[42] B. Zhang, Z. Lv, Z. Li, W. Wang, G. Li, and Y. Guo, "Dietary l-arginine supplementation alleviates the intestinal injury and modulates the gut microbiota in broiler chickens challenged by Clostridium perfringens," *Frontiers in Microbiology*, vol. 9, 2018.

[43] D. Stanley, A. L. Keyburn, S. E. Denman, and R. J. Moore, "Changes in the caecal microflora of chickens following *Clostridium perfringens* challenge to induce necrotic enteritis," *Veterinary Microbiology*, vol. 159, no. 1-2, pp. 155–162, 2012.

[44] D. Stanley, S.-B. Wu, N. Rodgers, R. A. Swick, and R. J. Moore, "Differential responses of cecal microbiota to fishmeal, Eimeria and Clostridium perfringens in a necrotic enteritis challenge model in chickens," *PLoS One*, vol. 9, no. 8, article e104739, 2014.

[45] M. C. S. Mendes, D. S. Paulino, S. R. Brambilla, J. A. Camargo, G. F. Persinoti, and J. B. C. Carvalheira, "Microbiota modification by probiotic supplementation reduces colitis associated colon cancer in mice," *World Journal of Gastroenterology*, vol. 24, no. 18, pp. 1995–2008, 2018.

[46] D. Briskey, M. Heritage, L.-A. Jaskowski et al., "Probiotics modify tight-junction proteins in an animal model of nonalcoholic fatty liver disease," *Therapeutic Advances in Gastroenterology*, vol. 9, no. 4, pp. 463–472, 2016.

[47] S. Resta-Lenert and K. E. Barrett, "Live probiotics protect intestinal epithelial cells from the effects of infection with enteroinvasive Escherichia coli (EIEC)," *Gut*, vol. 52, no. 7, pp. 988–997, 2003.

[48] Q. Zeng, X. He, S. Puthiyakunnon et al., "Probiotic mixture Golden Bifido prevents neonatal Escherichia coli K1 translocation via enhancing intestinal defense," *Frontiers in Microbiology*, vol. 8, 2017.

[49] A. A. Houfani, T. Větrovský, P. Baldrian, and S. Benallaoua, "Efficient screening of potential cellulases and hemicellulases produced by *Bosea* sp. FBZP-16 using the combination of enzyme assays and genome analysis," *World Journal of Microbiology and Biotechnology*, vol. 33, 2017.

[50] K. Wang, X. Jin, Q. Li et al., "Propolis from different geographic origins decreases intestinal inflammation and Bacteroides spp. populations in a model of DSS-induced colitis," *Molecular nutrition & food research*, vol. 62, no. 17, 2018.

Hindawi
Journal of Immunology Research
Volume 2021, Article ID 9659304, 11 pages
https://doi.org/10.1155/2021/9659304

Research Article

Network Pharmacology Analysis of the Identification of Phytochemicals and Therapeutic Mechanisms of *Paeoniae Radix Alba* for the Treatment of Asthma

Jingwei Wang,[1,2,3] Ling Peng,[4] Lu Jin,[1] Huiying Fu,[1,2,3] and Qiyang Shou[1,2,3]

[1]*Second Clinical Medical College, Zhejiang Chinese Medical University, China*
[2]*Academy of Chinese Medical Science, Zhejiang Chinese Medical University, China*
[3]*Zhejiang Provincial Key Laboratory of Sexual Function of Integrated Traditional Chinese and Western Medicine, Hangzhou, China*
[4]*Department of Respiratory Disease, Zhejiang Provincial People's Hospital, Hangzhou, Zhejiang Province, China*

Correspondence should be addressed to Huiying Fu; fhy131@126.com and Qiyang Shou; sqy133@126.com

Jingwei Wang and Ling Peng contributed equally to this work.

Received 29 June 2021; Accepted 17 August 2021; Published 14 September 2021

Academic Editor: Kai Wang

Background. *Paeoniae Radix Alba* (PRA), the root of the plant *Paeonia lactiflora* Pall., has been suggested to play an important role for the treatment of asthma. A biochemical understanding of the clinical effects of *Paeoniae Radix Alba* is needed. Here, we explore the phytochemicals and therapeutic mechanisms via a systematic and comprehensive network pharmacology analysis. *Methods*. Through TCMSP, PubChem, GeneCards database, and SwissTargetPrediction online tools, potential targets of active ingredients from PRA for the treatment of asthma were obtained. Cytoscape 3.7.2 was used to determine the target of active ingredients of PRA. Target protein interaction (PPI) network was constructed through the STRING database. The Gene Ontology (GO) biological process and Kyoto Encyclopedia of Genes and Genes (KEGG) pathway enrichment analysis were analyzed through the biological information annotation database (DAVID). *Results*. Our results indicate that PRA contains 21 candidate active ingredients with the potential to treat asthma. The enrichment analysis of GO and KEGG pathways found that the treatment of asthma by PRA may be related to the process of TNF (tumor necrosis factor) release, which can regulate and inhibit multiple signaling pathways such as ceramide signaling. *Conclusions*. Our work provides a phytochemical basis and therapeutic mechanisms of PRA for the treatment of asthma, which provides new insights on further research on PRA.

1. Introduction

Asthma is a common condition due to chronic inflammation of the lower respiratory tract [1]. Asthma exhibits recurrent episodes of wheeze, cough, chest tightness, and shortness of breath. It arises from heterogenic gene-environment interactions which are not fully understood. Airway hyperresponsiveness, reversible airflow obstruction, and bronchial hyperresponsiveness are characteristic features of asthma [2]. Most asthma is associated with sensitization of the airways to common allergens. Upon exposure to allergen, early response was the result of activation of airway mast cells in an IgE-dependent way with release of the rapidly acting granule-associated preformed mediators, as histamine and tryptase, to contract airway smooth muscle, promote vascular leakage, and stimulate mucus secretion. Allergic response such as interleukins- (IL-) 4, IL-5, IL-6, and TNF-α, in concert with the inflammatory mediators, stimulates the recruitment and activation of secondary effector cells, starting with neutrophils, followed by eosinophils and then T lymphocytes to cause late-phase airway narrowing and airway hyperresponsiveness [3]. This in turn produces long-term changes in the structure of the affected organs and substantial abnormalities in their function, which impact the quality of life.

Table 1: Candidate active ingredients of PRA.

Mol ID	Molecule name	OB (%)	DL
MOL001902	3β,23-Dihydroxy-oleana-11,13(18)-dien-28-oic acid	21.53	0.75
MOL001910	11Alpha,12alpha-epoxy-3beta-23-dihydroxy-30-norolean-20-en-28,12beta-olide	64.77	0.38
MOL001911	Albiflorin R1	21.29	0.82
MOL001912	Albiflorin R1_qt	26.18	0.34
MOL001918	Paeoniflorgenone	87.59	0.37
MOL001919	(3S,5R,8R,9R,10S,14S)-3,17-Dihydroxy-4,4,8,10,14-pentamethyl-2,3,5,6,7,9-hexahydro-1H-cyclopenta[a]phenanthrene-15,16-dione	43.56	0.53
MOL001921	Lactiflorin	49.12	0.8
MOL001924	Paeoniflorin	53.87	0.79
MOL001925	Paeoniflorin_qt	68.18	0.4
MOL001928	Albiflorin_qt	66.64	0.33
MOL001929	Alexandrin	20.63	0.62
MOL001930	Benzoyl paeoniflorin	31.27	0.75
MOL001933	Oxypaeoniflorin	21.88	0.78
MOL000211	Mairin	55.38	0.78
MOL000263	Oleanolic acid	29.02	0.76
MOL000358	Beta-sitosterol	36.91	0.75
MOL000359	Sitosterol	36.91	0.75
MOL000422	Kaempferol	41.88	0.24
MOL000492	(+)-Catechin	54.83	0.24
MOL000551	Hederagenol	22.42	0.74
MOL000357	Sitogluside	20.63	0.62

Traditional Chinese medicine (TCM) has a long-lasting history of using herbal medicine in the treatment of various respiratory diseases [4]. There is increasing scientific evidence supporting the use of TCM for the treatment of asthma. Possible mechanisms include anti-inflammation, inhibition of airway smooth muscle contraction, and immunomodulation [5]. *Paeoniae Radix Alba* (Bai Shao, also known as Chinese peony), the root of the perennial herbaceous plant *Paeonia lactiflora* Pall. of the buttercup family, has the effects of nourishing blood and regulating menstruation, restraining yin and antiperspirant, softening liver and relieving pain, and suppressing liver-yang [6]. Our previous studies investigated the antiallergic role of total glucosides of peony, indicating that total glucosides of peony have an effect on the allergic reaction of mice [7]. Thus, we speculate that the total glucosides of peony should have a therapeutic effect on asthma. In this study, network pharmacology was utilized to analyse the active ingredients, drug targets, and key pathways of PRA for the treatment of asthma.

2. Methods

2.1. Composition of Chinese Medicine White Peony. TCMSP database was used to obtain the pharmaceutical ingredients with "*Paeoniae Radix Alba*" as the key word. The ingredients that meet the criteria with oral biological degree (OB) > 20% and drug – like properties (DL) > 0.18 at the same time were selected as the active ingredients of PRA. Effective active ingredients of PRA contained in the database were queried and screened.

2.2. Prediction of Small Molecule Target Protein. Based on the TCMSP and DrugBank databases, target proteins corresponding to small molecules were sorted out, while components without target proteins and duplicate targets were deleted. Using the UniProt (http://www.uniprot.org/) database, screened targets are converted into gene names, full protein names are corresponded to the gene abbreviations, and the component target-gene data table is made.

2.3. Chemical-Gene Network Analysis. According to the chemical molecule-gene relationship obtained by the analysis, component target-gene data were imported into the Cytoscape 3.7.2 software. The data were analyzed and displayed graphically in the form of a network diagram. Different nodes are used to represent data types, and connections are used to represent interaction relationships. Topological analysis is performed, and the core target of PRA is selected according to the node degree. The node degree is one of the main data methods to determine the key nodes. The higher the node degree, the more important the role of the node in the network.

2.4. Asthma Gene Acquisition and Analysis. The UniProt database (https://www.uniprot.org/) and TTD data (https://db.idrblab.org/ttd/) database were searched for asthma-related targets. Duplicate targets were deleted, and information acquired were collected.

Table 2: Target-gene pairs of active ingredients of PRA.

Target gene	Gene name
26S proteasome non-ATPase regulatory subunit 3	PSMD3
5-Hydroxytryptamine 2A receptor	HTR2A HTR2
5-Hydroxytryptamine receptor 3A	HTR3A
Acetylcholinesterase	ACHE
Activator of 90 kDa heat shock protein ATPase homolog 1	AHSA1
Aldo-keto reductase family 1 member C3	AKR1C3
Alpha-1D adrenergic receptor	ADRA1B
Androgen receptor	AR
Antileukoproteinase	**SLPI**
Apoptosis regulator BAX	BAX
Apoptosis regulator Bcl-2	BCL2
Arachidonate 5-lipoxygenase	ALOX5
Aryl hydrocarbon receptor	AHR
Beta-2 adrenergic receptor	ADRB2 ADRB2R, B2AR
Beta-lactamase	blaC
Calmodulin	CAMKK2
Caspase-3	CASP3
Caspase-8	CASP8
Caspase-9	CASP9 MCH6
Catalase	CAT
Cell division control protein 2 homolog	CDC42
CGMP-inhibited 3′,5′-cyclic phosphodiesterase A	PDE3A
Coagulation factor VII	F7
Coagulation factor Xa	F10
Cytochrome P450 1A1	CYP1A1
Cytochrome P450 1A2	CYP1A2
Cytochrome P450 1B1	CYP1B1
Cytochrome P450 3A4	CYP3A4
Cytochrome P450-cam	camC
Dipeptidyl peptidase IV	DPP4
DNA topoisomerase II	TOP2
Dopamine D1 receptor	DRD5 DRD1B, DRD1L2
E-Selectin	SELE
Estrogen receptor	ESR1
Gamma-aminobutyric acid receptor subunit alpha-1	GABRA1
Gamma-aminobutyric-acid receptor alpha-2 subunit	GABRA2
Gamma-aminobutyric-acid receptor alpha-3 subunit	GABRA3
Gamma-aminobutyric-acid receptor alpha-5 subunit	GABRA5
Glutathione S-transferase Mu 1	GSTM1
Glutathione S-transferase Mu 2	GSTM2
Glutathione S-transferase P	GSTP1
Heat shock protein HSP 90	HSP90AA1 HSP90A, HSPC1, HSPCA
Heme oxygenase 1	HMOX1 HO, HO1
Hyaluronan synthase 2	HAS2
Inhibitor of nuclear factor kappa-B kinase subunit beta	IKBKB
Insulin receptor	INSR
Intercellular adhesion molecule 1	ICAM1
Interleukin-6	IL6

Table 2: Continued.

Target gene	Gene name
Interstitial collagenase	MMP1
Lipopolysaccharide-binding protein	LBP
Microtubule-associated protein 2	Map2
Mineralocorticoid receptor	NR3C2
Mitogen-activated protein kinase 8	MAPK8
Monocyte differentiation antigen CD14	CD14
mRNA of PKA catalytic subunit C-alpha	PRKACA
Muscarinic acetylcholine receptor M1	CHRM1
Muscarinic acetylcholine receptor M2	CHRM2
Muscarinic acetylcholine receptor M3	CHRM3
Muscarinic acetylcholine receptor M4	CHRM4
Mu-type opioid receptor	OPRM1 MOR1
NAD(P)H dehydrogenase [quinone] 1	NQO1 DIA4, NMOR1
Neuronal acetylcholine receptor protein, alpha-7 chain	CHRNA7 NACHRA7
Neuronal acetylcholine receptor subunit alpha-2	CHRNA2
Nitric-oxide synthase, inducible	NOS2
Nitric-oxide synthase, endothelial	NOS3
Nuclear receptor coactivator 2	**NCOA2**
Nuclear receptor subfamily 1 group I member 2	NR1I2
Pancreatic alpha-amylase	AMY2A
Peroxidase C1A	PRXC1A
Peroxisome proliferator activated receptor gamma	PPARG
Phosphatidylinositol-4,5-bisphosphate 3-kinase catalytic subunit, gamma isoform	PIK3CG
Potassium voltage-gated channel subfamily H member 2	KCNH2 ERG, ERG1, HERG
Progesterone receptor	PGR
Prostaglandin G/H synthase 1	PTGS1
Prostaglandin G/H synthase 2	PTGS2
Protein kinase C-alpha type	PRKCA
RAC-alpha serine/threonine-protein kinase	AKT1
Retinoic acid receptor RXR-alpha	RXRA
Serine/threonine-protein phosphatase 2B catalytic subunit alpha isoform	PPP3CA
Serum paraoxonase/arylesterase 1	PON1
Signal transducer and activator of transcription 1-alpha/beta	STAT1
Sodium channel protein type 5 subunit alpha	SCN5A
Sodium-dependent noradrenaline transporter	SLC6A2
Solute carrier family 2, facilitated glucose transporter member 4	SLC2A4
Thrombin	F2
Transcription factor AP-1	JUN
Transcription factor p65	RELA
Transforming growth factor beta-1	TGFB1
Trypsin-1	PRSS1
Tumor necrosis factor	TNF

2.5. Gene Pathway and Function Analysis. The DAVID database (https://david.ncifcrf.gov/) and Metascape database (https://metascape.org/) were used to analyze the GO function and KEGG pathway enrichment analysis of the potential targets of PRA for the treatment of asthma. GOTERM_BP_DIRECT (biological process), GOTERM_CC_DIRECT (cell composition), and GOTERM_MF_DIRECT (molecular function) are saved in Gene_Ontology; KEGG_PATH-WAY was saved in Pathways.

3. Results

3.1. Screening of Active Ingredients of Paeonia. Oral administration is the most common route of traditional Chinese

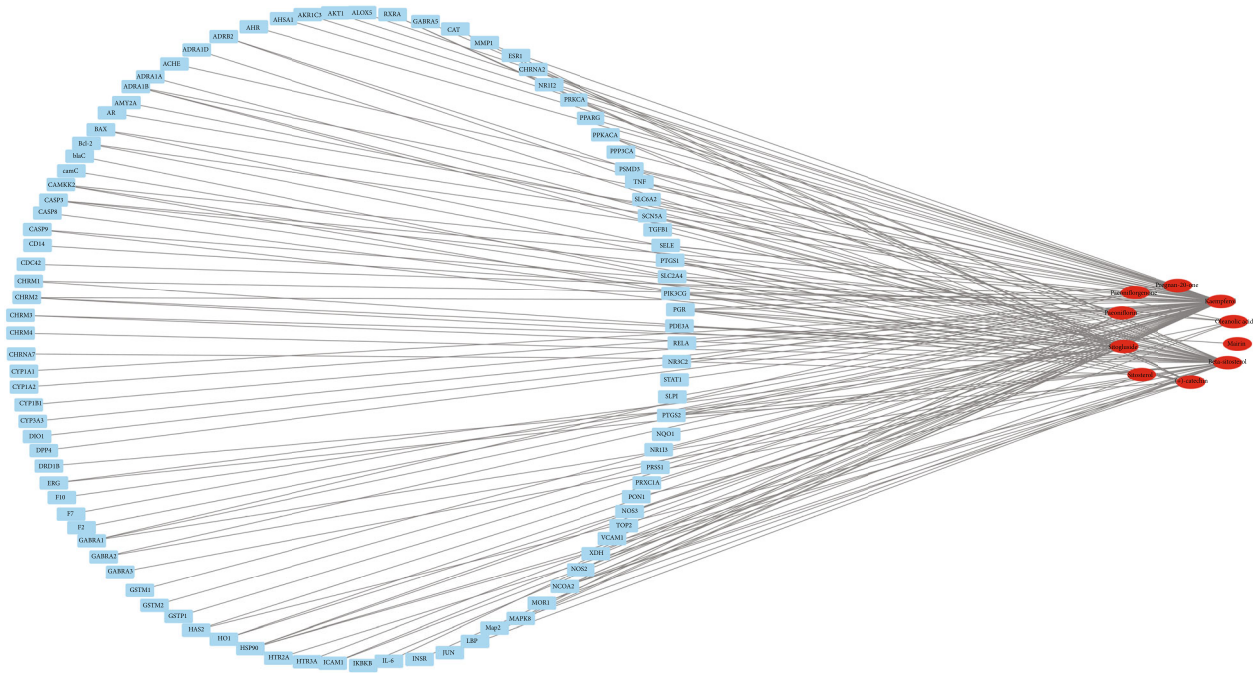

Figure 1: Part of main active ingredients of PRA.

Table 3: Degree of top 5 chemicals and target proteins of PRA.

Gene	Degree	Molecule	Degree
PGR	6	Kaempferol	63
NCOA2	5	Beta-sitosterol	39
HSP90	4	Sitogluside	17
PTGS1	4	(+)-Catechin	11
PTGS2	4	Oleanolic acid	6

Medicine preparations. OB is an effective index to evaluate the clinical efficacy of traditional Chinese medicine. Through the TCMSP database, combined with "OB > 20%" and "DL > 0.18", 21 active ingredients in PRA that can be orally absorbed were screened out, as shown in Table 1.

3.2. Target Prediction Results of Active Ingredients in White Peony. Reverse docking through the SwissTargetPrediction website was used using "*Homo sapiens*." Target proteins of the active ingredients were screened, and gene target corresponding to each ingredient was acquired. A total of 147 targets after removing 90 targets were sort out, and the target-gene pairs were obtained, which are shown in Table 2.

3.3. Small Molecule Target Protein. Based on the TCMSP and DrugBank databases, the target protein relationship of each chemical small molecule after integration was obtained. Figure 1 is a network diagram of the effective small chemical molecules and target proteins contained in PRA. The network diagram contains 42 nodes (10 small chemical molecules and 96 target proteins) and 145 edges. Table 3 shows the degree table of the small chemical molecules and target proteins of PRA. In this network, kaempferol with the highest degree of connectivity regulates 63 target proteins, followed by beta-sitosterol, sitogluside, (+)-catechin, etc. The target protein with the highest degree of connectivity is PGR, which is regulated by 6 small chemical molecules, followed by NCOA2, HSP90, PTGS1, PTGS2, and so on.

3.4. Functional Analysis. Based on the DAVID tool, the GO function and KEGG pathway enrichment analysis of the target genes of PRA were performed, and the significance threshold was selected as the correction (Benjamini P value < 0.01). Figure 2 is the GO analysis diagram. The most significant biological processes are cellular response to organic cyclic compound, response to lipopolysaccharide, and response to toxic substance. Figure 3 shows the enrichment of the first 30 pathways. The most significant pathways are toxoplasmosis, Toll-like receptor signaling, osteoclast differentiation, apoptosis, and the Chagas disease. The interaction between related proteins can be classified into positive regulation of vasoconstriction, toxoplasmosis, and estrogen metabolic process, as shown in Figure 4, among which the most widely involved is the vasoconstriction.

3.5. Key Gene Screening of Asthma. We searched for disease targets in databases as Delegated Database Tree (DDT), DrugBank, and DisGeNET, and a total of 153 asthma-related targets were obtained. The intersection of these targeted genes with the previous targets of the active substance of PRA was analyzed. Finally, 13 genes are both target genes (Table 4). KEGG enrichment analysis was performed on these 13 key genes, and $P < 0.05$ was chosen as the threshold, which is shown in Table 5. Through the enrichment analysis of the coacting targets, the red node in Figure 5 indicates the key upregulated gene of asthma, which only contains *TNF*. We believe that only *TNF* is the key gene in the treatment of asthma with white peony drugs, and some downregulated

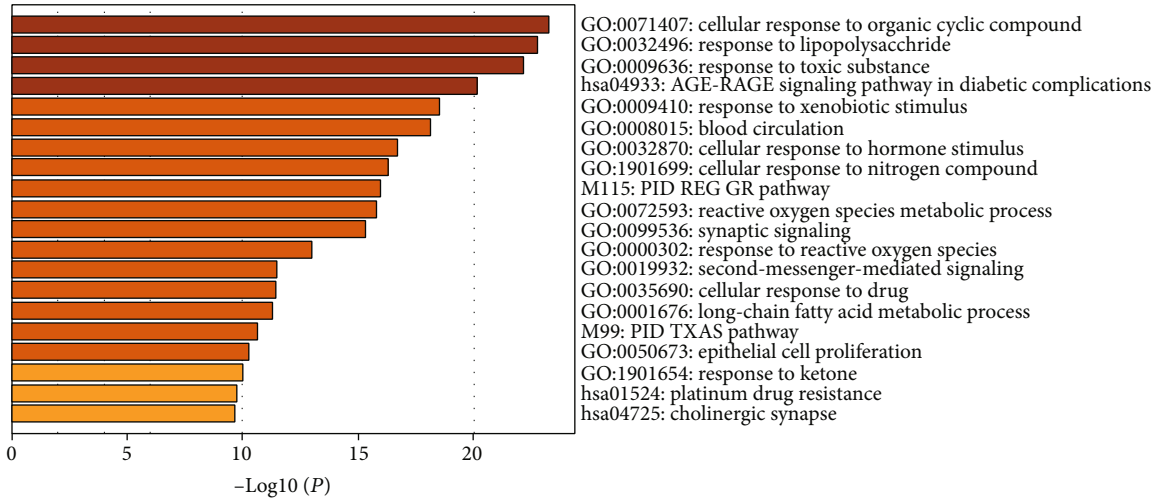

(a)

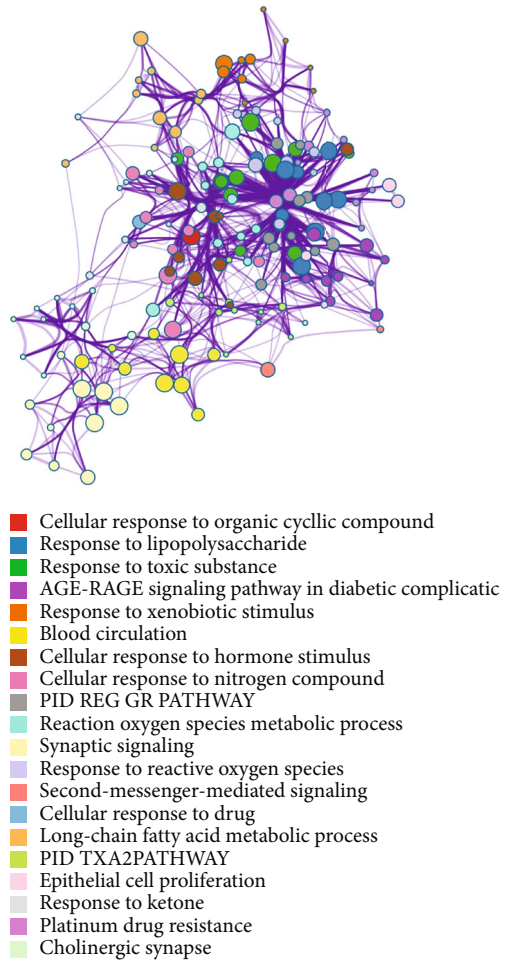

(b)

Figure 2: Graph of the GO function analysis bar and PPI. (a) GO analysis. (b) PPI network.

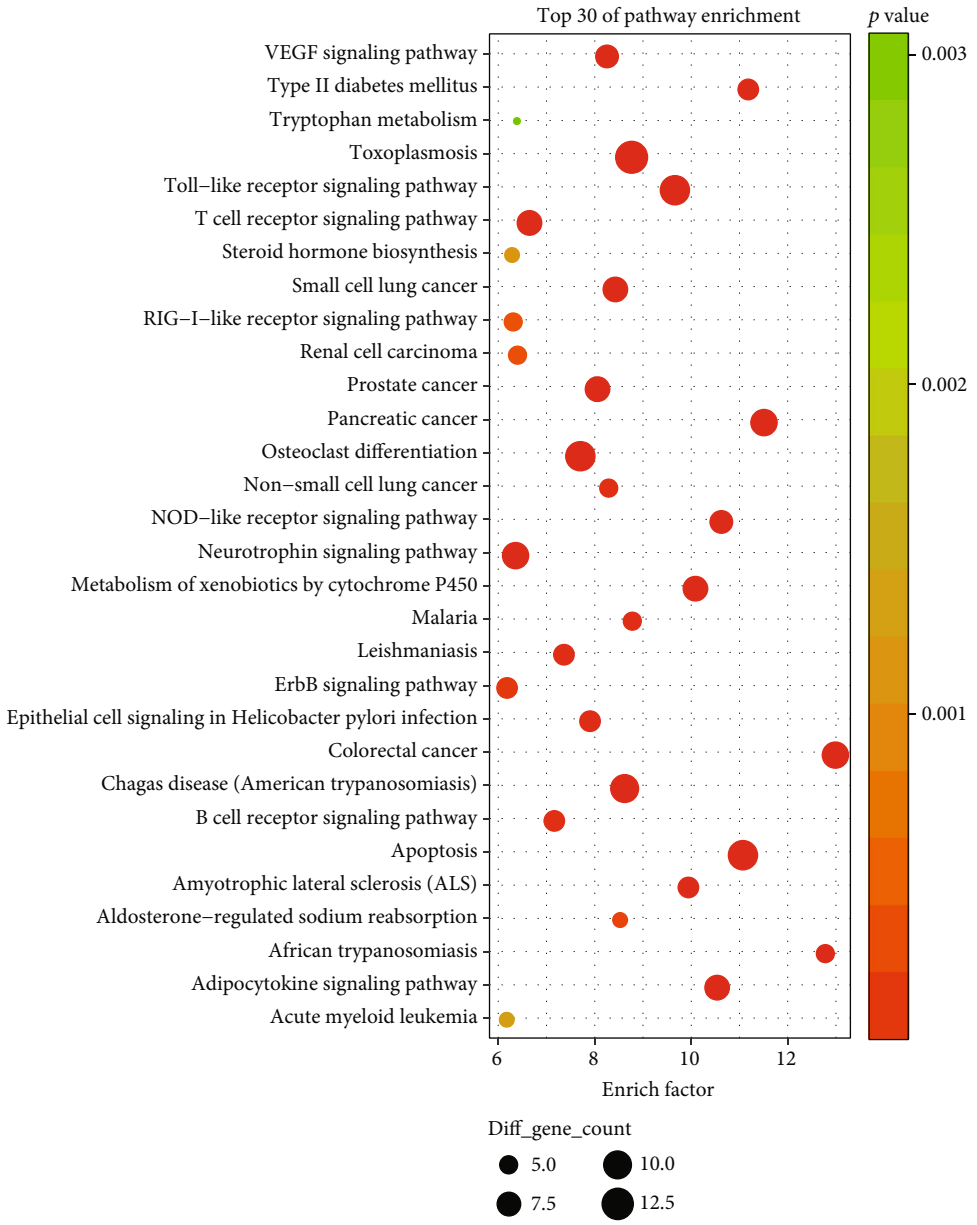

Figure 3: KEGG-enriched bubble chart.

genes such as IL-4 and IL-13 will affect the regulation of asthma.

4. Discussion

Asthma is a chronic disease characterized by inflammation hyperreactivity of the airways [8]. It is a complex syndrome with many clinical phenotypes in adults and children, which consists different phenotypes that share common features with distinct etiologies and pathophysiological pathways leading to disease [9]. The inhaled allergen encounters antigen presenting cells (APCs) in the airways. After recognizing the antigen and being activated by APCs, naïve T cells differentiate into Th2 cells, and the activated Th2 cells stimulate B cells to form IgE. IgE molecules then bind to IgE receptors on mast cells. The IgE crosslinking of allergens and mast cells will release biologically active mediators (histamine and leukotrienes) through degranulation, leading to direct symptoms of allergies [10]. Mast cells also release chemokines, which help the recruitment of inflammatory cells, especially eosinophils, which secret IL-5 to promote their proliferation and differentiation from bone marrow progenitor cells [11]. The activated eosinophils will release toxic particles and oxygen-free radicals, which leads to tissue damage and promotes the development of chronic inflammation.

The human TNF-α gene is about 2.76 kb in length and consists 4 exons and 3 introns. It is closely linked to the MHC gene group and is located on the 6^{th} and 17^{th} chromosomes, respectively. The natural form of TNF-α exerts its biological effects is a homotrimer. TNF-α is mainly produced and secreted by activated alveolar macrophages with a variety of biologically active cytokines, which can stimulate

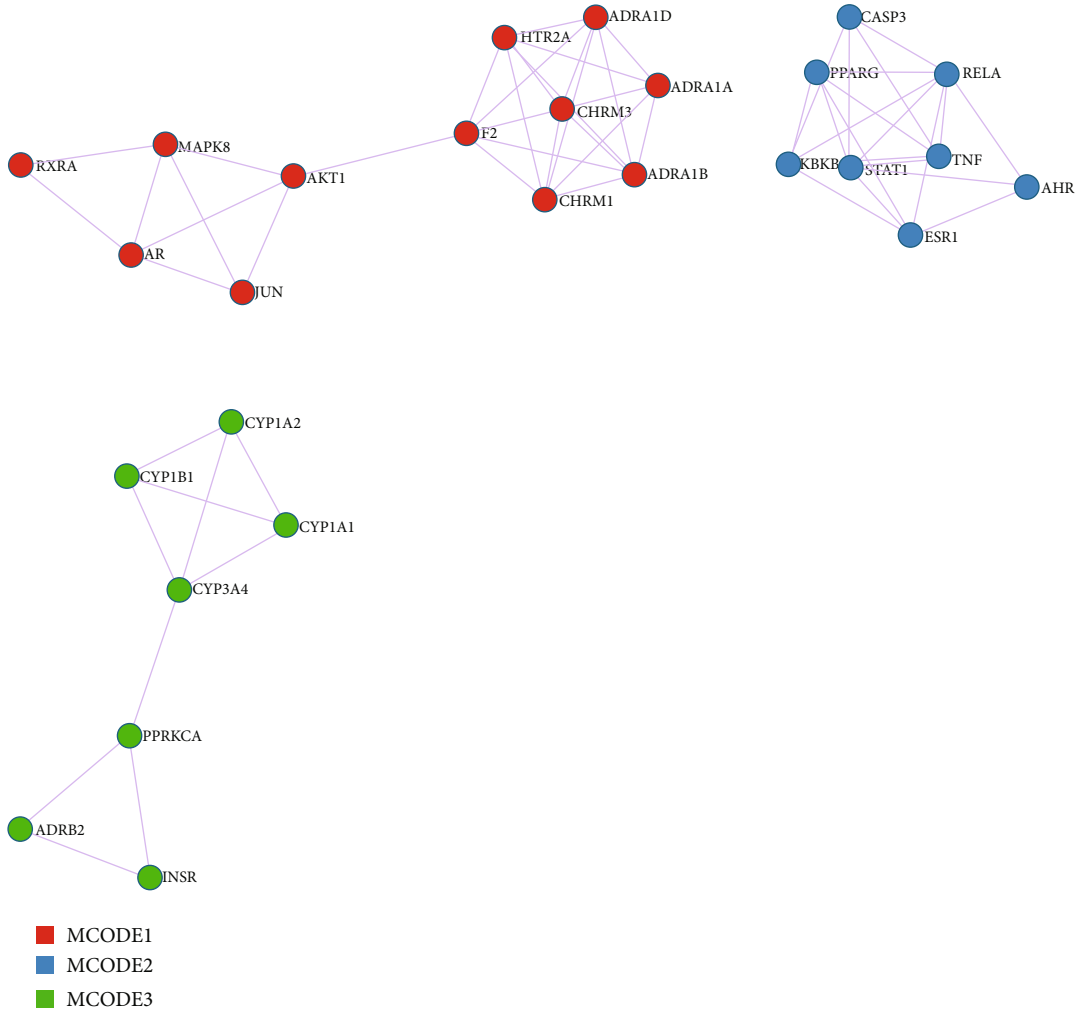

Figure 4: Protein interaction network of active ingredient in PRA.

Table 4: Common target genes of PRA and asthma.

Comment target genes
Arachidonate 5-lipoxygenase (5-LOX)
DNA topoisomerase II (TOP2)
E-selectin (SELE)
Muscarinic acetylcholine receptor M2 (CHRM2)
Muscarinic acetylcholine receptor M3 (CHRM3)
Muscarinic acetylcholine receptor M4 (CHRM4)
Neuronal acetylcholine receptor alpha-7 (CHRNA7)
Nitric-oxide synthase inducible (NOS2)
Prostaglandin G/H synthase (COX/PTGS1)
Prostaglandin G/H synthase 2 (COX-2/PTGS2)
Tumor necrosis factor (TNF)
Heat shock protein 90 (HSP90)

neutrophils to cause degranulation and an increase in respiratory burst activity. TNF-α can promote the adhesion of neutrophils to endothelial cells [12], and it can also promote the activation of monocytes and accelerate the expression of IL-2 receptors [13]. The phagocytic function of alveolar macrophages causes damage, which stimulates the activation of inflammatory mediators and induces the body to produce asthma symptoms. The asthma pathway map of our study indicates that TNF-α is the key target of PRA for the treatment of asthma. Among them, TNF-related active ingredients are kaempferol and paeoniflorin. Kaempferol suppresses eosinophil infiltration and airway inflammation in airway epithelial cells and in mice with allergic asthma through inhibition of TNF-α [14]. Kaempferol can inhibit ceramide signaling pathway, which reduce the release of TNF-α, reduce the transcription of MMP genes, and reduce the expression of MMP. Due to the reduced expression of MMP, it can effectively protect the extracellular membrane (ECM) and basement membrane in the lung from dissolution and avoid asthma symptoms [15]. Paeoniflorin attenuates adipocyte lipolysis and inhibits the phosphorylation of ERK, JNK, and IKK stimulated by TNF-α [16]. Thus, previous work on the compounds correlates with the results of our bioinformatic analysis of network pharmacology exploration of asthma and PRA.

Furthermore, there are many other genes which play roles in the coacting target genes, such as *CHRM*, *COX*,

Table 5: KEGG pathway enrichment analysis of key 13 genes (part).

Term	Input	*P* value
P00003:Alzheimer disease-amyloid secretase pathway	4	$5.76E-09$
hsa04725:cholinergic synapse	4	$5.33E-08$
hsa04080:neuroactive ligand-receptor interaction	5	$6.40E-08$
hsa00590:arachidonic acid metabolism	3	$1.33E-06$
hsa04668:TNF signaling pathway	3	$7.12E-06$
hsa04726:serotonergic synapse	3	$7.69E-06$
hsa05310:asthma	1	0.0107
H00079:asthma	1	0.00368

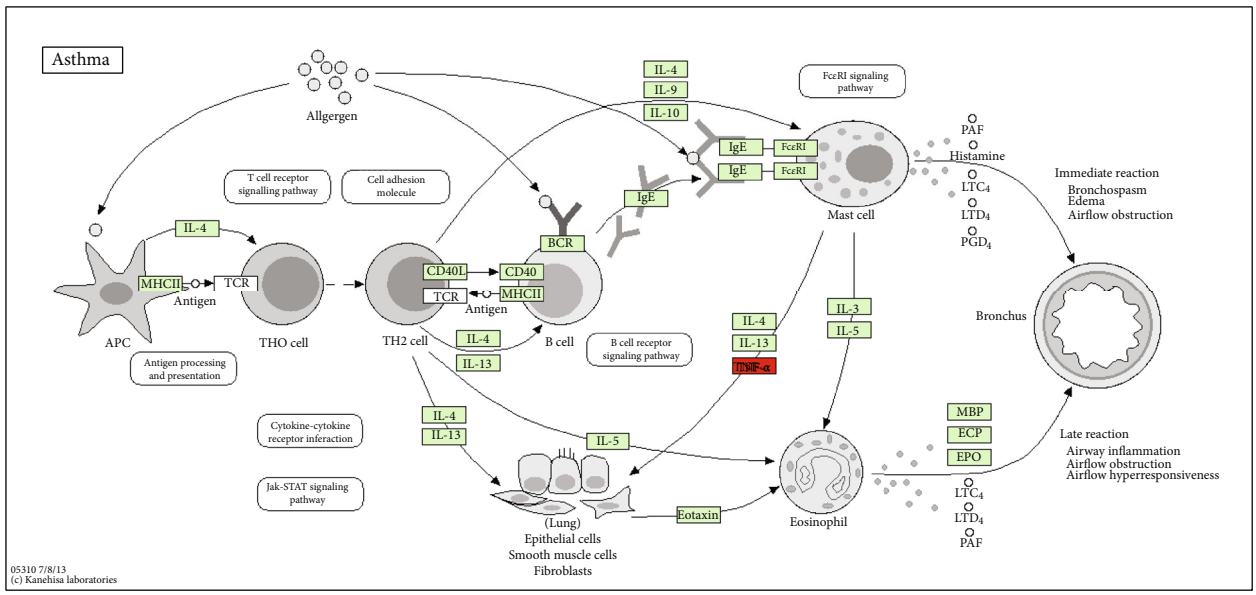

Figure 5: The pathway map of asthma.

and *PTGS2*. Kaempferol has anti-inflammatory effects by inhibiting interleukin-4 (IL-4) kinase and downregulating the NF-κB pathway [17]. By inhibiting IL-4 expression and cyclooxygenase 2 (COX2), kaempferol has a significant inhibitory effect on NADPH oxidase activity. When kaempferol reduces the reactive oxygen species (ROS) through the direct binding of NADPH oxidase, it can promote COX2 induction, thereby inhibiting epithelial thickening, indicating that this component can have a better adjuvant therapeutic effect on respiratory diseases through anti-inflammatory effects [18].

There are many highly sensitive cough receptors in the throat and trachea. When the mucosa of respiratory tract is stimulated by foreign bodies or secretions in the respiratory tract, it will produce a cough response through a series of neural reflexes, with the intention of expelling the secretions in the respiratory tract. A series of mechanical or chemical stimuli, such as the inhalation of harmful gases, the invasion of pathogenic microorganisms, the inflammatory factors produced by airway inflammation, and the contraction of airway smooth muscles, can all be used as inducements to cause the receptors to transmit signals to the cough center after the body is stimulated. Through network pharmacological analysis, it is found that PRA can act on key targets in cough response-related pathways. Beta-sitosterol and sitogluside, the active ingredients in PRA, can regulate the concentration of Ca^{2+} through the calcium ion pathway and inhibit the activation of CHRM2 and CHRM3 on the bronchial smooth muscle, thereby inhibiting the contraction of the bronchial smooth muscle and reducing cough [19]. The stimulus received by the receptors, in turn, plays a role in relieving cough. In addition, the Ca^{2+} produced by this reaction can directly bind to ion channels and can indirectly participate in the process of other signaling pathways related to the cough and asthma reaction [20].

Asthma is mainly related to allergic inflammation and neurological reactions. When the mucous membrane of the respiratory tract tissue is stimulated by allergens, it will promote the production of large amounts of IgE antibodies, triggering type I allergies. IgE high-affinity receptor "FcεRI" is expressed on the surface of a variety of immune cells (mast

cells, B cells, eosinophils, etc.). The massively secreted IgE can trigger allergic inflammation cascades by activating inflammatory cells, leading to airway smooth muscles contract, triggering asthma. Through network pharmacology analysis, it is found that β-sitosterol can bind to key targets on the pathways related to asthma response [21]. Chan et al. found through research that the *PTGS2* gene is closely related to the inflammation of the asthmatic response, and the cyclooxygenase encoded by the *PTGS2* gene has an airway remodeling effect [22]. Kaempferol can slow down the asthma response by breaking down fat or regulating fatty acid metabolism [23]. From the molecular mechanism of our result, it is found that PRA has a strong inhibitory effect on the inflammation of the respiratory system. Further studies are warranted to clarify the role of PRA in the treatment of asthma via the TNF-α signaling pathway.

In summary, this study used network pharmacology to analyze the main active ingredients of PRA. The main active ingredients and their possible molecular mechanisms for the treatment of asthma have been clarified. These results provide a theoretical basis of PRA for the treatment of asthma and provide a scientific basis for its better clinical application.

Data Availability

Source data of this study is derived from the public repositories, as indicated in "Methods" of the manuscript. All data that support the findings of this study is available from the corresponding authors upon reasonable request.

Conflicts of Interest

The authors declare that they have no conflicts of interest.

Authors' Contributions

All authors listed have made a substantial, direct, and intellectual contribution to the work and approved it for publication. Jingwei Wang and Ling Peng contributed equally to this work. Jingwei Wang and Ling Peng are co-first authors.

Acknowledgments

This work was supported by the National Natural Science Foundation of China (Nos. 81573677, 81673645, and 81873047), Opening Project of Zhejiang Provincial First-rate Subject (Traditional Chinese Medicine) of Zhejiang Chinese Medical University (No. Ya2017012), and Scientific Funding of Zhejiang Chinese Medical University (No. 2020ZZ11).

References

[1] A. Papi, C. Brightling, S. Pedersen, and H. Reddel, "Asthma," *The Lancet*, vol. 391, 2018.

[2] T. Boonpiyathad, Z. Sözener, P. Satitsuksanoa, and C. Akdis, "Immunologic mechanisms in asthma," *Seminars in Immunology*, vol. 46, p. 101333, 2019.

[3] S. Kany, J. T. Vollrath, and B. Relja, "Cytokines in inflammatory disease," *International Journal of Molecular Sciences*, vol. 20, no. 23, p. 6008, 2019.

[4] H. Chan and T. Ng, "Traditional Chinese medicine (TCM) and allergic diseases," *Current Allergy and Asthma Reports*, vol. 20, no. 11, 2020.

[5] X.-M. Li and L. Brown, "Efficacy and mechanisms of action of traditional Chinese medicines for treating asthma and allergy," *The Journal of allergy and clinical immunology*, vol. 123, no. 2, pp. 297–306, 2009.

[6] Y. Q. Tan, H. W. Chen, J. Li, and Q. J. Wu, "Efficacy, chemical constituents, and pharmacological actions of Radix Paeoniae Rubra and Radix Paeoniae Alba," *Frontiers in Pharmacology*, vol. 11, p. 1054, 2020.

[7] Q. Shou, J. Lang, L. Jin et al., "Total glucosides of peony improve ovalbumin-induced allergic asthma by inhibiting mast cell degranulation," *Journal of Ethnopharmacology*, vol. 244, p. 112136, 2019.

[8] S. T. Holgate, S. Wenzel, D. S. Postma, S. T. Weiss, H. Renz, and P. D. Sly, "Asthma," *Nature Reviews. Disease Primers*, vol. 1, p. 15025, 2015.

[9] M. E. Kuruvilla, F. E. Lee, and G. B. Lee, "Understanding asthma phenotypes, endotypes, and mechanisms of disease," *Clinical Reviews in Allergy and Immunology*, vol. 56, pp. 219–233, 2019.

[10] S. J. Galli and M. Tsai, "IgE and mast cells in allergic disease," *Nature Medicine*, vol. 18, pp. 693–704, 2012.

[11] M. Krystel-Whittemore, K. N. Dileepan, and J. G. Wood, "Mast cell: a multi-functional master cell," *Frontiers in Immunology*, vol. 6, p. 620, 2015.

[12] W. Y. Sun, S. M. Pitson, and C. S. Bonder, "Tumor necrosis factor-induced neutrophil adhesion occurs via sphingosine kinase-1-dependent activation of endothelial {alpha}5{beta}1 integrin," *The American Journal of Pathology*, vol. 177, pp. 436–446, 2010.

[13] N. Parameswaran and S. Patial, "Tumor necrosis factor-alpha signaling in macrophages," *Critical Reviews in Eukaryotic Gene Expression*, vol. 20, pp. 87–103, 2010.

[14] J. H. Gong, D. Shin, S. Y. Han, J. L. Kim, and Y. H. Kang, "Kaempferol suppresses eosionphil infiltration and airway inflammation in airway epithelial cells and in mice with allergic asthma," *The Journal of Nutrition*, vol. 142, pp. 47–56, 2012.

[15] C. P. Vieira, L. P. de Oliveira, M. B. Da Silva et al., "Role of metalloproteinases and TNF-alpha in obesity-associated asthma in mice," *Life Sciences*, vol. 259, p. 118191, 2020.

[16] P. Kong, R. Chi, L. Zhang, N. Wang, and Y. Lu, "Effects of paeoniflorin on tumor necrosis factor-alpha-induced insulin resistance and changes of adipokines in 3T3-L1 adipocytes," *Fitoterapia*, vol. 91, pp. 44–50, 2013.

[17] B. Li, B. Luo, L. Jiang, and C. Jiang, "Kaempferol nanoparticles achieve strong and selective inhibition of ovarian cancer cell viability," *International Journal of Nanomedicine*, vol. 7, pp. 3951–3959, 2012.

[18] D. Shin, S.-H. Park, Y.-J. Choi et al., "Dietary compound kaempferol inhibits airway thickening induced by allergic reaction in a bovine serum albumin-induced model of asthma," *International Journal of Molecular Sciences*, vol. 16, pp. 29980–29995, 2015.

[19] E. A. Townsend, M. A. Thompson, C. M. Pabelick, and Y. S. Prakash, "Rapid effects of estrogen on intracellular Ca2+

regulation in human airway smooth muscle," *American Journal of Physiology. Lung Cellular and Molecular Physiology*, vol. 298, pp. L521–L530, 2010.

[20] M. A. Valverde, G. Cantero-Recasens, A. Garcia-Elias, C. Jung, A. Carreras-Sureda, and R. Vicente, "Ion channels in asthma," *The Journal of Biological Chemistry*, vol. 286, pp. 32877–32882, 2011.

[21] Y. Sun, L. Gao, W. Hou, and J. Wu, "Beta-sitosterol alleviates inflammatory response via inhibiting the activation of ERK/p38 and NF-kappaB pathways in LPS-exposed BV2 cells," *BioMed Research International*, vol. 2020, Article ID 7532306, 2020.

[22] I. H. S. Chan, N. L. S. Tang, T. F. Leung et al., "Association of prostaglandin-endoperoxide synthase 2 gene polymorphisms with asthma and atopy in Chinese children," *Allergy*, vol. 62, pp. 802–809, 2007.

[23] L. Thors, M. Belghiti, and C. J. Fowler, "Inhibition of fatty acid amide hydrolase by kaempferol and related naturally occurring flavonoids," *British Journal of Pharmacology*, vol. 155, pp. 244–252, 2008.

Hindawi
Journal of Immunology Research
Volume 2021, Article ID 9483433, 11 pages
https://doi.org/10.1155/2021/9483433

Review Article

A Perspective on *Withania somnifera* Modulating Antitumor Immunity in Targeting Prostate Cancer

Seema Dubey,[1] Manohar Singh,[1] Ariel Nelson,[2] and Dev Karan[1]

[1]*Department of Pathology, MCW Cancer Center and Prostate Cancer Center of Excellence, Medical College of Wisconsin, 8701 Watertown Plank Road, Milwaukee, WI 53226, USA*
[2]*Department of Medicine, Division of Hematology and Oncology, Medical College of Wisconsin, 8701 Watertown Plank Road, Milwaukee, WI 53226, USA*

Correspondence should be addressed to Dev Karan; dkaran@mcw.edu

Received 2 July 2021; Accepted 7 August 2021; Published 26 August 2021

Academic Editor: Tomasz Baczek

Medicinal plants serve as a lead source of bioactive compounds and have been an integral part of day-to-day life in treating various disease conditions since ancient times. Withaferin A (WFA), a bioactive ingredient of *Withania somnifera*, has been used for health and medicinal purposes for its adaptogenic, anti-inflammatory, and anticancer properties long before the published literature came into existence. Nearly 25% of pharmaceutical drugs are derived from medicinal plants, classified as dietary supplements. The bioactive compounds in these supplements may serve as chemotherapeutic substances competent to inhibit or reverse the process of carcinogenesis. The role of WFA is appreciated to polarize tumor-suppressive Th1-type immune response inducing natural killer cell activity and may provide an opportunity to manipulate the tumor microenvironment at an early stage to inhibit tumor progression. This article signifies the cumulative information about the role of WFA in modulating antitumor immunity and its potential in targeting prostate cancer.

1. Introduction

Since ancient times, people have used herbal medicines from plants or their extracts derived from flowers, seeds, bark, leaves, or roots to prevent or treat multiple disease types. Despite significant progress in early detection, advancement in understanding the molecular targets, and improved anticancer therapy, prostate cancer remains the second most common male malignancy and the fifth leading cause of cancer deaths among men worldwide [1]. Many useful bioactive compounds, currently in use as chemotherapy drugs, including taxanes, the camptothecin derivatives, the epipodophyllotoxins, and the vinca alkaloids, have been extracted and isolated from plant sources [2]. In addition, epidemiological studies support that dietary modification may substantially reduce a man's risk of developing prostate cancer [3, 4]. Therefore, understanding the role of plant-based therapies in determining the immune mechanisms of prostate cancer prevention and the therapeutic efficacy is crucial.

Withania somnifera, also known as Indian ginseng, is a traditional Ayurvedic medicinal plant that contains diverse bioactive compounds, including alkaloids, withanolides, and saponins. The main phytochemicals are withanolides, which are structurally similar to the ginsenosides of *Panax ginseng* (Asian ginseng), *Panax notoginseng* (Sanchi ginseng), and *Panax quinquefolius* (American ginseng). However, the ginsenoside contents within the *Panax* species vary significantly [5]. The pharmacological activity of *W. somnifera* is assigned to its main withanolide—Withaferin A (WFA) [6]. Although various parts of this plant are used for multiple disease treatments, root extract is a rich source of WFA. Growing evidence has shown that WFA has anti-inflammatory, antimicrobial, and anticancer activities [7–10]. This review highlights the effect of WFA in regulating both the

immunological and nonimmunological targets and its potential as an anticancer agent for prostate carcinoma.

2. Nonimmune Molecular Targets of WFA

Withaferin A is a nontoxic, bioactive compound of *Withania somnifera*, a widely used traditional medicine in Asia and Africa for its anticancer activities and to enhance the immunological response. Numerous studies have described the anticancer effect of WFA in various cancer types, including leukemia, melanoma, prostate cancer, breast cancer, ovarian cancer, head and neck cancer, and colon cancer [11–14]. WFA inhibits cell proliferation, invasion, metastasis, angiogenesis, proteasome, endoplasmic reticulum (ER) stress, protein folding, and maturation in cancer cells and regulates multiple targets by direct interaction or regulation of secondary targets in establishing its anticancer activity. Since several succinct review articles have described the role of WFA in various cancer types [11, 12, 15], we limit our discussion to prostate cancer along with important molecular targets from other cancer types.

2.1. WFA-Mediated Cell Cycle Inhibition. Analysis of cell cycle-related events is a primary mechanism to examine a natural compound's biological effect in targeting cancer cells. WFA inhibits cell proliferation by inducing cell cycle arrest in the G2/M phase in multiple studies [16–20]. Dysregulation in the cell cycle process is associated with prostate cancer development, and currently, several cell cycle inhibitors are being evaluated in clinical trials for prostate cancer treatment [21]. In prostate cancer cell lines PC3 and DU145, WFA showed cell cycle inhibition in the G2/M phase by upregulating p21, phosphorylated wee-1, phosphorylated histone H3, and aurora B and downregulating cyclin (A2, B1, and E2) expression [22]. Interestingly, WFA showed a higher cytotoxic effect in androgen-resistant, androgen receptor (AR) negative cell lines PC3 and DU145 than androgen-sensitive, AR positive LNCaP cells [23]. In addition, WFA increased prostate apoptosis response-4 protein (Par-4) to enhance proapoptotic signaling in prostate cancer cells [14].

Following other targeted mechanisms, WFA decreased cyclin-dependent kinase (Cdk1), cell division cycle (Cdc 25B), and Cdc 25C expression and arresting cell cycle in the G2/M phase in breast cancer [18]. WFA prevents Cdk1/cyclin B1 complex formation, a critical step of cell cycle progression in gastric cancer, by dephosphorylating Cdk1 at Thr161 and p21 upregulation in glioblastome [16]. Additional studies showed that increased oxidative stress is critical in the WFA-mediated cell cycle and cell proliferation inhibition [17]. WFA-directed reticence in cell proliferation and migration is credited to blocking STAT3 transcription activity in colon cancer [24]. More importantly, combined treatment of WFA and liposomal preparation of doxorubicin enhanced cell death in ovarian cancer cells and inhibited the expression of cancer stem cell markers ALDH1 (aldehyde dehydrogenase) and Notch1 [25]. WFA is also known to restore tumor necrosis factor-related apoptosis-inducing ligand (TRAIL) sensitivity inducing apoptosis in human renal and breast cancer cells [26, 27].

2.2. Proteasomal Inhibition by WFA. Ubiquitin proteasome plays a critical role in neoplastic cell growth, survival, and apoptosis by reducing unwanted and misfolded proteins. Proteasome inhibitors showed anticancer activity in cancer cells resistant to conventional chemotherapeutic drugs. Bortezomib was the first proteasome inhibitor approved to treat refractory multiple myeloma [28]. WFA treatment of cancer cells showed an accumulation of ubiquitinated proteins signifying its effect on proteasome inhibition, associated with increased ER stress, reactive oxygen species, and proapoptotic signaling [29, 30]. Ghosh et al. reported WFA-induced cell death in breast cancer cells by introducing impaired autophagy and unfolded protein response [31]. WFA inhibits chymotrypsin-like activity of a 26S proteasome in PC3 xenografts in nude mice and the PC3 cell line, leading to accretion of proteasome target proteins p27, Bax, and IκB-α and increase in PARP cleavage proteins inducing apoptosis in prostate cancer cells [32]. Additional docking studies revealed that WFA blocks the chymotrypsin-like activity of a purified rabbit 20S proteasome activity by blocking the N-terminal threonine (Thr1) function.

2.3. WFA Inhibits Angiogenesis. Angiogenesis is one of the hallmarks of cancer growth, where vascular endothelial growth factor (VEGF) regulates angiogenesis. The utilization of anti-VEGF therapies has been successful in prolonging survival benefits in multiple cancer types. Increased VEGF expression in prostate tissues and plasma levels has been associated with tumor grade and biochemical and clinical recurrence of prostate cancer [33, 34]. Anti-VEGF therapy in phase II clinical trials in prostate cancer showed improved relapse-free survival and disease stabilization [35]. However, the phase III results of antiangiogenic treatment in prostate cancer showed toxicity without improving the overall survival [36]. Plant-based compounds are efficient in preventing the formation of new blood vessels in the tumor microenvironment; hence, several natural compounds such as curcumin, resveratrol, and thymoquinone have been studied as potential antiangiogenic drugs [37–40]. In human umbilical vein endothelial cells (HUVECs), WFA showed an antiangiogenic effect by inhibiting HUVEC sprouting in the three-dimensional collagen-I matrix [41]. Similarly, WFA deters VEGF-mediated tube formation by HUVECs and binds to vimentin and intermediate filament protein to inhibit tumor angiogenesis [42, 43].

2.4. Effect of WFA on Tumor Growth in Mice. In prostate mouse models (TRAMP: transgenic adenocarcinoma of mouse prostate and Pten-knockout) with spontaneous tumor development, oral administration of WFA showed a significant decrease in prostate tumor growth. TRAMP mouse studies revealed that WFA inhibited AKT and pAKT expression and activated Foxo3a-Par-4-induced tumor cell death in mice [44]. Foxo3a works upstream of Par-4 signaling and is essential for apoptosis induction in castration-resistant prostate cancer (CRPC) cells. Deleting the Foxo3a binding site on the Par-4 promoter inhibits Foxo3a-Par-4 interaction and Par-4 activation, suggesting the positive role of Foxo3a in Par-4 stimulation and apoptosis [45]. In Pten-knockout

Table 1: Nonimmune molecular targets of WFA and *Withania somnifera* (WS) root extract in prostate cancer.

Compound type	Model system	Molecular targets
Withaferin A	LNCaP, PC3, and 22RV1 cell lines	Induces cytoprotective autophagy by increasing GABARAPL1 (ATG8L) expression [11]
Withaferin A	PC3 cell line	Induction of prostate apoptosis response-4-(Par-4-) dependent apoptosis [14]
Withaferin A	PC3 and DU145 cell lines	Upregulation of Aurora B, phosphor histone H3, and phospho-Wee-1 expression and downregulation of cyclins (A2, B1, and E2) and phospho-Chk1 (Ser345), Chk2 (Thr68), and Cdc2 (Tyr15) [22]
Withaferin A	Cell lines PC3, DU145, and LNCaP	Disrupt vimentin cytoskeleton by induction of ROS and c-Fos expression and suppression of c-FLIP(L) [23]
Withaferin A	LNCaP cells and PC3 xenografts in nude mice, i.p. injection with 4 or 8 mg/kg/day for 24 days	Target β5 subunit and inhibition of chymotrypsin-like activity in vivo tumors of PC3 xenografts with an accumulation of proteasome target proteins (p27, Bax, and IκB-α) and decreased AR protein in in vitro LNCaP cell line [32]
Withaferin A	TRAMP model, oral gavage of 5 mg/kg	Prevent prostate adenocarcinoma, inhibit AKT signaling, and activate Foxo3a-Par-4-induced cell death and EMT markers (vimentin, β-catenin, and snail and upregulate E-cadherin) [44]
Withaferin A	Pten-KO mice, oral gavage with 3 or 5 mg/kg	Inhibit primary tumor growth and lung metastasis, downregulation of pAKT-mediated EMT markers [46]
Withaferin A and ethanol extract of WS root	LNCaP and 22RV1 cell lines	Inhibits fatty acid synthesis by decreasing fatty acid metabolism enzymes: acetyl-CoA carboxylase 1, ATP citrate lyase, carnitine palmitoyltransferase 1A, and fatty acid synthase with a decrease in c-Myc and pAKT [49]
WS root extract	PC3 cell line	Inhibit expression levels of cyclooxygenase-2 and interleukin-8 [50]

AR: androgen receptor; EMT: epithelial-to-mesenchymal transition; i.p.: intraperitoneal; LPS: lipopolysaccharides; PARP: poly (ADP-ribose) polymerase; ROS: reactive oxygen species; TRAMP: transgenic adenocarcinoma of mouse prostate.

mice, WFA treatment obliterated lung metastasis of prostate cancer and was associated with a decrease in epithelial-to-mesenchymal transition markers (N-cadherin and β-catenin) [46]. A significant reduction in tumor growth with subcutaneous xenografts of ovarian cancer and glioblastoma cells in nude mice also demonstrated the therapeutic efficacy of WFA [47, 48].

Thus, WFA showed pleiotropic functions and exerted its potential anticancer effect via targeting multiple molecular pathways to incapacitate the cancer cell activities. Table 1 summarizes the nonimmune molecular targets of WFA in prostate cancer.

3. Effect of WFA in Targeting Inflammation via Inflammasomes

The association of chronic inflammation in cancer development and progression is well-established [51–54]. Therefore, studies are focused on targeting inflammatory cytokines to understand the immunobiology of prostate cancer [55–58]. Mechanistically, a diverse array of signals such as inflammasomes, toll-like receptors (TLRs), and transcription factors regulate the secretion of inflammatory cytokines. Upregulated inflammasome activity is correlated with various cancer types, including gastric cancer, breast cancer, prostate cancer, and brain tumor [59–61]. TLRs, a family of pattern recognition receptors, drive inflammation via activating NF-κB signaling to promote prostate cancer development [62, 63]. Indeed, the transcriptional activity of NF-κB and associated signaling pathways are implicated in multiple disease types and have been a prime target for pharmacological interventions [64]. Nuclear translocation of NF-κB in prostate cancer cells was associated with biochemical recurrence and bone metastatic prostate cancer development. In a retrospective study using a multi-institutional cohort, Grosset et al. showed that an increased level of nuclear NF-κB p65 might serve as a prognostic marker for prostate cancer [65]. The study performed tissue microarrays of radical prostatectomy specimens from two independent cohorts ($n = 250$ and $n = 1262$) of treatment-naïve prostate cancer patients collected at multiple centers. The association of p65 nuclear expression and prostate cancer outcome was evaluated by immunohistochemistry. Multivariate analysis revealed that p65 nuclear frequency in prostate cancer cells was an independent predictor of biochemical recurrence and may help identify high-risk prostate cancer patients. In another study, a similar analysis of NK-κB p65 in 105 prostate tissue specimens showed nuclear translocation of p65 expression during the

transition of disease from prostatic intraepithelial neoplasia to prostate cancer [66]. Multivariate analysis showed that preoperative PSA level, Gleason score, and nuclear KF-κB p65 translocation were independent predictors of biochemical relapse. Thus, blocking NF-κB activation is a promising target for modifying the cancer-associated inflammation and immune activation signaling.

Dietary agents are considered potent inhibitors of the NF-κB signaling pathway and reduce cancer-associated inflammation [67]. For example, curcumin, a dietary supplement from turmeric spice, and ginger extract showed anticancer and anti-inflammatory effects by inhibiting NF-κB activity [68–71]. Lycopene blocks NF-κB signaling to inhibit prostate cancer cell growth in vitro and reduces in vivo prostate cancer growth in mice [72, 73]. In a chronic prostatitis rat model, the intragastric lycopene administration (20 mg/kg, daily for four weeks) reduces inflammation in the prostate and the serum level of IL-1β, TNF-α, IL-2, and IL-6 cytokines [74]. This anti-inflammatory effect of lycopene was attributed to NF-κB inhibition in the prostate tissues [74]. Resveratrol isolated from grapes is also one of the potent inhibitors of NF-κB and leads to anti-inflammatory and antitumor effects [75]. Likewise, ursolic acid derived from berries, leaves, and fruits is a pentacyclic triterpenoid with anti-inflammatory effects by inhibiting NF-κB signaling through IKKα and p65 phosphorylation [76]. WFA inhibits NF-κB activation by blocking Akt to reduce nitric oxide and inducible nitric oxide synthase expression in RAW 264.7 macrophage cell line regulating inflammatory process [77], suggesting that WFA has alternative pathways to regulate NF-κB activation. Based on protein array analysis, it has been demonstrated that WFA regulates multiple cytokines in LPS-induced THP-1 cells. In silico studies showed that the downregulated cytokines possess a common regulatory factor NF-κB and that WFA blocked the nuclear translocation of NF-κB [78]. The root extract of *W. somnifera* is also known for its antioxidant, anti-inflammatory, and immunomodulatory activities [79, 80]. Culture supernatant from the LPS-primed, *W. somnifera* root extract- (0.05-0.4 mg/ml) treated human PBMCs, and THP-1 cells showed decreased TNF-α, IL-1β, and IL-6 levels as measured by ELISA [79]. However, further discussions are limited in this article since a recent review described a general perspective of WFA in chronic inflammation [81]. These studies suggest that the medicinal plant product regulating NF-κB activity can alter inflammatory profiles to benefit the host, targeting inflammation-associated cancer.

Scientific advancement in understanding the regulation of inflammation also suggests the role of the inflammasome signaling complex in the activation of inflammation-associated responses. The inflammasome consists of a nucleotide-binding domain, leucine-rich repeat, and pyrin domain (NRLP), along with caspase activation and recruitment domain (ASC) and procaspase-1. Microbe-associated molecular patterns (MAMPs), danger-associated molecular patterns (DAMPs), pattern-recognition receptors (PRRs), and various pathogens activate the inflammasome. Once activated, the inflammasome recruits the ASC and procaspase-1 producing an active form of caspase-1, which cleaves the proform of interleukin- (IL-) 1β and IL-18 to release mature IL-1β and IL-18 associated with various biological activities [60, 61].

Although limited information is available on the effect of WFA in regulating inflammasomes, a mouse model of chronic pancreatitis showed that WFA blocks ER stress and the NLRP3 inflammasome to prevent pancreatitis progression [82]. WFA inhibits *Helicobacter pylori*-induced IL-1β and NLRP3 inflammasome signaling molecules in bone marrow-derived dendritic cells and macrophages, indicating the preventive and therapeutic effect of WFA in *H. pylori* infection-associated cancers [83]. Pretreatment of mice with WFA inhibited ovalbumin-induced lung injury and fibrosis progression. This preventive effect was attributed to decreased inflammatory cell infiltration in the lungs and a correspondingly low level of proinflammatory cytokines and reduced NLRP3 inflammasome activation [84]. WFA disintegrates the NLRP3 inflammasome complex reducing downstream signaling products IL-1β and IL-18. WFA blocks the NF-κB activity altering the level of multiple genes associated with NF-κB regulation and inhibits inflammasome activity suppressing inflammatory cytokine network [78]. Growing evidence suggests that the inflammasomes play a key role in inflammation-associated diseases, including cancer, and emerges as a game-changer in understanding how inflammation affects the immunobiology of cancer [61]. Therefore, the mechanism of WFA in the regulation of inflammasome activity warrants further investigation.

4. Effect of WFA on Immune Cell Regulation and Antitumor Immunity

Medicinal herbs have long been recognized as a way to increase immune system activation. However, the mechanism(s) regulating specific immune cells' functional activation by these herbs, including WFA, remains mostly unknown. Barua et al. showed that *W. somnifera* treatment induces natural killer (NK) cell activation [85], an essential component of the innate immune response to tumors, and actively eliminates early neoplastic cells. NK cells kill tumor targets on contact using perforin (a cytolytic protein) and granzyme (protease family member) machinery [86, 87]. Similarly, IFN-γ is a key cytokine produced by NK cells and T lymphocytes and facilitates the antitumor response. Malik et al. showed that herbal formulation of *W. somnifera* induced Th1 immunity in tumor-bearing mice as measured by the secretion of IFN-γ and IL-12 and increased proliferation of $CD4^+$, $CD8^+$ T cells, and NK cells [88]. Following *W. somnifera* supplement, hens susceptible to ovarian cancer displayed a significant reduction in tumor development associated with increased NK cell population [85].

Similarly, oral administration of *W. somnifera* extract (400 mg/kg body weight) once a week for four weeks treating azoxymethane-induced colon cancer in Swiss albino mice increased the number and functional activity of immune cells [89]. NMITLI 101R, a chemotype of *W. somnifera*, generated humoral and cellular immune responses in Balb/c mice as measured by a high number of antibody-producing cells. The cytokine response remained polarized to the Th1 type

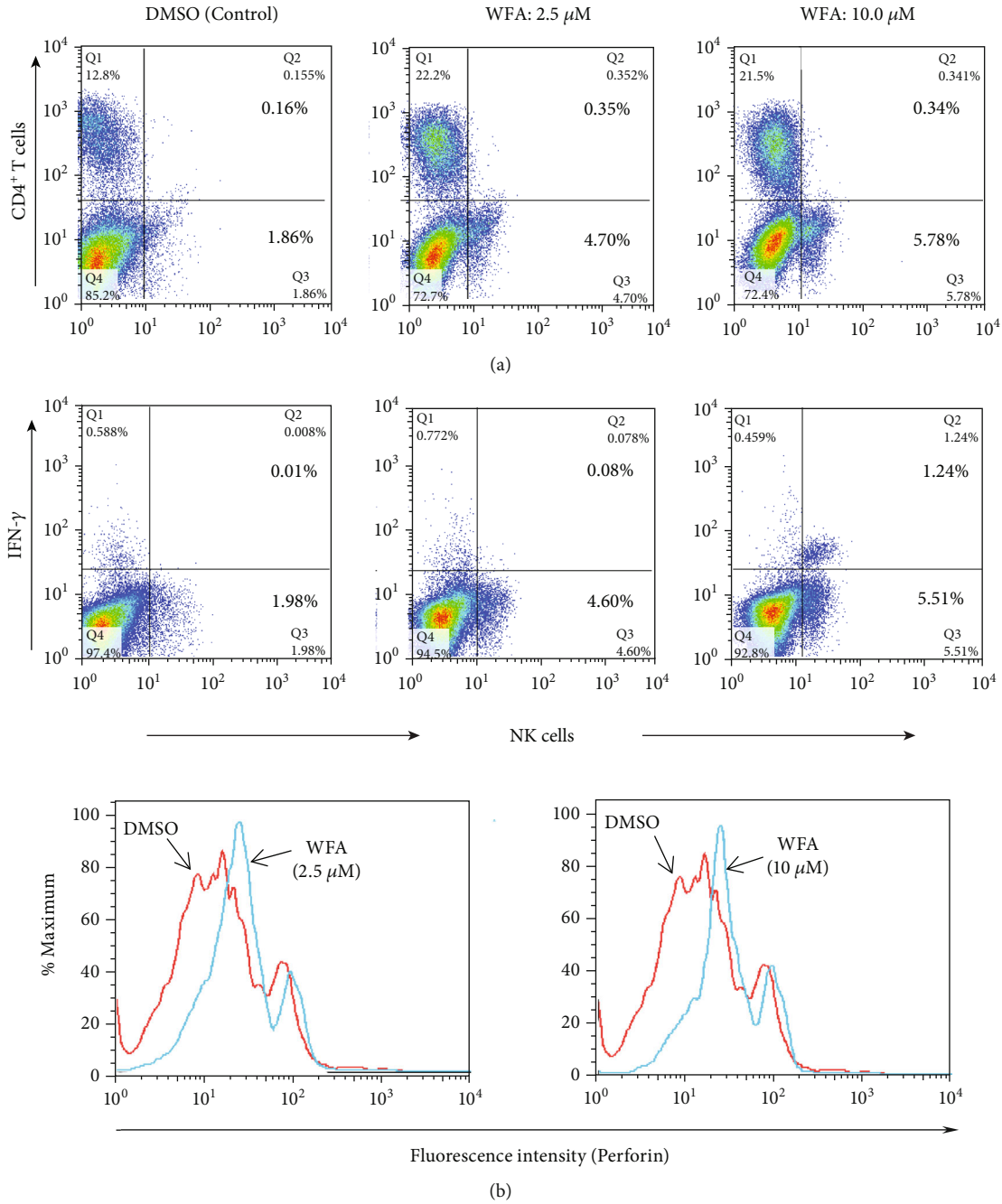

Figure 1: (a) WFA-induced frequency and (b) function (increase in IFN-γ and perforin) of NK cells examined by flow cytometry gated on CD8-negative T cells. Splenocytes from the naïve C57BL/6 mice were homogenized into a single-cell suspension, seeded at a density of 5×10^6 cells/well supplemented with cytokine IL-2 (10 U/ml) in 24-well plates, and incubated overnight in the presence or absence of WFA and DMSO as control.

with increased levels of IFN-γ [90]. In parasite-infected hamsters, the chemotype NMITLI 101R surges antileishmanial drug efficacy by generating strong IFN-γ- and IL-12-mediated immune responses while suppressing the Th2 cytokines (IL-4, IL-10, and TGF-β) [91].

The present team also examined the effect of WFA and found that the WFA augments the quality and quantity of NK cell function measured by intracellular cytokine staining for IFN-γ and perforin. The number of NK cells producing IFN-γ and perforin was significantly higher in WFA-treated splenocytes than in the DMSO control (Figures 1(a) and 1(b)).

To further study the role of WFA-induced NK cells in antitumor immunity, the authors used RM1 mouse prostate tumor cells (syngeneic to C57BL/6 mice). RM1 cells express a low level of MHC I and are sensitive to NK cell killing [92]. Intraperitoneal administration of WFA (8 mg/kg/BW) significantly ($p = 0.04$) inhibited the growth of established prostate tumors (Figures 2(a) and 2(b)). To follow the prolonged therapeutic effect of WFA, these experimental mice

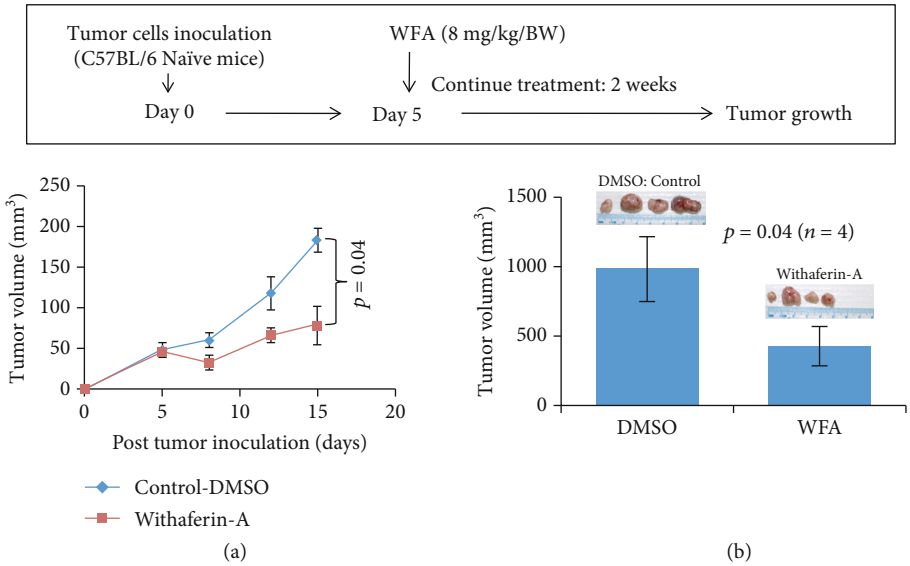

FIGURE 2: (a) WFA-induced activation of anticancer activity inhibiting the growth of established tumors in mice inoculated with RM1 mouse prostate tumor cells; (b) tumor volume on day 29. Six-to-seven-week-old, naive C57BL/6 mice were inoculated subcutaneously with RM1 tumor cells (5×10^5). Starting on day five following tumor inoculations, a group of mice (4 mice/group) received an intraperitoneal (i.p.) injection of WFA (8 mg/kg/BW) five days per week for two weeks. DMSO serves as the control at the same level (*v*/*v*) as for WFA treatment groups.

were left untreated for ten additional days. It appeared that the developed immune response following WFA treatment maintained the reduced tumor growth (Figure 2(b)). These observations indicate that the WFA induces NK cell activation, thereby augmenting antitumor immunity to inhibit the development and progression of prostate tumors; however, these preliminary studies need further validation.

Both mouse and human studies further support the role of WFA in the induction of NK cells. Balb/c mice were given an i.p. injection of *W. somnifera* root extract with 20 mg/dose/mouse for 5 consecutive days [93]. Mouse splenocytes were harvested 24 hours after the last injection, and were used as effectors against NK-sensitive K562 cells in a chromium release assay to measure the cytotoxic activity of NK cells. Splenocytes from WFA-treated mice showed ~53% higher cytotoxicity than splenocytes from vehicle-treated control mice. An observational study in humans also supports WFA-mediated NK cell regulation. Five human subjects consumed 6 ml of *W. somnifera* root extract with cow's milk (8 ounces) twice daily for four days. Peripheral blood sample analysis revealed a significant increase in mean fluorescence intensity of $CD4^+$ T (4.2-fold; $p < 0.05$) cells and NK cell activation (3.2-fold; $p < 0.01$) after four days compared to the baseline [94].

Although therapeutic targeting of prostate cancer has evolved remarkably, one significant challenge remains that prostate tumors are enriched with immune suppressor cells (myeloid-derived suppressor cells (MDSCs), M2 macrophages, and T-regulatory cells), hampering the benefits of therapeutic regimens [95, 96]. Sinha and Ostrand-Rosenberg reported that administration of WFA in tumor-bearing mice with 4T1 cells significantly reduces the tumor burden, decreases the number of MDSCs and reactive oxygen species (ROS), and suppresses the protumor cytokine IL-10 by the MDSCs and macrophages [97]. WFA was orally administered in mice at different doses (1-8 mg/kg body weight) every other day for the study duration and found that 1 mg/kg dose of WFA was efficient in delaying tumor growth and suppressing MDSCs in the circulation. In vitro analysis revealed that 1 μg/ml of WFA reduces ROS (measured by H_2O_2) production by >50% in MDSCs while 1 μg/ml treatment dose of withanolide A and *W. somnifera* root extract was ineffective. The dose of *W. somnifera* root extract was increased to 166.7 μg/ml to achieve a concentration equal to 1 μg/ml of WFA for complete inhibition of H_2O_2 production in MDSCs. Withaferin A also inhibited the secretion of proinflammatory cytokines TNF-α, IL-6, and IL-12 from macrophages suggesting the role of WFA as a potent inhibitor of proinflammatory mediators [97]. This study corroborates with previous annotations that the use of WFA polarized the immunity towards the Th1 type augmenting antitumor immunity [88, 90, 91]. Thus, the stimulation of NK cell activity and decreased immune suppressor cells provide a novel opportunity to test the immunotherapeutics of WFA in prostate cancer studies.

When boosting the body's immune system for the prevention or treatment of cancer, one of the critical components is to activate the antigen-presenting cells (APCs) such as macrophages and dendritic cells (DCs). Induction of Th1-type immune response is associated with tumor suppression, while Th2 immune responses are tumor-promoting. It is noticeable that WFA treatment polarized the immune response towards the Th1 type of immunity, increasing IFN-γ and IL-12 while decreasing Th2 type-associated IL-4, IL-10, and TGF-β cytokines. Thus, WFA injection of mice potentially activates APCs to release IL-12 and TNF-α cytokines activating NK cell functions; however, such a hypothesis needs further validation.

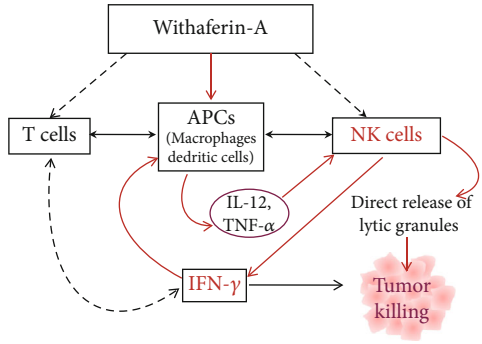

Figure 3: WFA triggers immunostimulatory cascade associated with NK cell regulation and antitumor immunity.

Figure 3 describes a schematic presentation for the potential mechanism of WFA-induced immune cell activation.

5. Clinical Potential of WFA

A PubMed search for clinical trials using the term "*Withania somnifera*" yielded few clinical studies testing the impact of *W. somnifera*. Most of these studies consumed root extracts of *W. somnifera* alone or combined with other therapeutic drugs. The published clinical studies demonstrated the safety profile and efficacy of root preparation in various conditions, including chronic stress and anxiety [98–100], schizophrenia [101, 102], memory and cognitive improvement [103], obsessive-compulsive disorder [104], and subclinical hypothyroidism [105]. However, clinical studies testing the impact of *W. somnifera* directly in cancer patients are minimal. In an open-label prospective nonrandomized comparative trial on 100 breast cancer patients in all stages who received chemotherapy with or without oral *W. somnifera*, the use of *W. somnifera* showed an improvement in the quality-of-life and fatigue scores [106]. A phase I study of WFA in advanced-stage high-grade osteosarcoma patients also demonstrated that WFA was safe and well-tolerated up to 4800 mg per day [107]. Surprisingly, no clinical study has tested the efficacy of WFA for prostate cancer.

6. Conclusions and Future Perspectives

Withania somnifera establishes various health benefits, including antistress, anti-inflammatory, anticancer, and immunostimulatory properties. Indeed, administration of WFA and its impact on tumor growth inhibition in TRAMP and Pten-knockout prostate cancer mouse models with functional immune systems indicate enhanced antitumor immunity. However, to further understand the role of WFA in regulating the immunobiology of prostate cancer, detailed studies are needed to analyze the infiltrating immune cells in these tumors. Many prostate cancers are organ-confined at the time of diagnosis, and some patients prefer to remain under active surveillance. Since WFA-induces Th1-type responses and NK cell activation, the slow-growing nature of some prostate cancers may provide an opportunity for immune manipulation at early prostate cancer stages and may represent a paradigm for the use of WFA for cancer-related or chemotherapy-induced fatigue, cancer prevention, and therapeutic efficacy. WFA usage combined with standard treatment regimens may help induce both innate and adaptive immune system arms to achieve greater therapeutic efficacy to target prostate cancer. The preclinical observations suggest pluripotent functions of WFA targeting prostate cancer; therefore, more extensive randomized clinical studies are needed to establish the safety profile of the WFA compound.

Data Availability

The additional experimental data used to support the findings of this study are included within the article.

Conflicts of Interest

The authors have no financial conflict of interest.

Authors' Contributions

Conceptualization was performed by D.K. and S.D.; writing and original draft preparation were performed by D.K., S.D., M.S., and A.N.; writing, reviewing, and editing were performed by D.K., S.D., M.S., and A.N.; supervision was performed by D.K.; project administration was performed by D.K.; D.K was responsible for funding acquisition. All authors agreed and approved the final manuscript.

Acknowledgments

DK's research is supported by the National Institutes of Health (CA204786). A part of these studies was initiated during the National Institutes of Health (NIH)/NCI funding (CA169453) to DK.

References

[1] M. B. Culp, I. Soerjomataram, J. A. Efstathiou, F. Bray, and A. Jemal, "Recent global patterns in prostate cancer incidence and mortality rates," *European Urology*, vol. 77, no. 1, pp. 38–52, 2020.

[2] D. J. Newman and G. M. Cragg, "Natural products as sources of new drugs over the nearly four decades from 01/1981 to 09/2019," *Journal of Natural Products*, vol. 83, no. 3, pp. 770–803, 2020.

[3] M. Matsushita, K. Fujita, and N. Nonomura, "Influence of diet and nutrition on prostate cancer," *International Journal of Molecular Sciences*, vol. 21, no. 4, p. 1447, 2020.

[4] P. H. Lin, W. Aronson, and S. J. Freedland, "Nutrition, dietary interventions and prostate cancer: the latest evidence," *BMC Medicine*, vol. 13, no. 3, 2015.

[5] E. M. Schlag and M. S. McIntosh, "Ginsenoside content and variation among and within American ginseng (*Panax quinquefolius* L.) populations," *Phytochemistry*, vol. 67, no. 14, pp. 1510–1519, 2006.

[6] M. Elsakka, E. Grigorescu, U. Stanescu, U. Stanescu, and V. Dorneanu, "New data referring to chemistry of Withania somnifera species," *Revista Medico-Chirurgicală a Societății de Medici şi Naturalişti din Iaşi*, vol. 94, no. 2, pp. 385–387, 1990.

[7] E. P. Sabina, S. Chandal, and M. K. Rasool, "Inhibition of monosodium urate crystal-induced inflammation by withaferin a," *Journal of Pharmacy & Pharmaceutical Sciences*, vol. 11, no. 4, pp. 46–55, 2008.

[8] R. Munagala, H. Kausar, C. Munjal, and R. C. Gupta, "Withaferin A induces p53-dependent apoptosis by repression of HPV oncogenes and upregulation of tumor suppressor proteins in human cervical cancer cells," *Carcinogenesis*, vol. 32, no. 11, pp. 1697–1705, 2011.

[9] S. D. Stan, E. R. Hahm, R. Warin, and S. V. Singh, "Withaferin A causes FOXO3a- and Bim-dependent apoptosis and inhibits growth of human breast cancer cells in vivo," *Cancer Research*, vol. 68, no. 18, pp. 7661–7669, 2008.

[10] V. S. Sivasankarapillai, R. Madhu Kumar Nair, A. Rahdar et al., "Overview of the anticancer activity of withaferin A, an active constituent of the Indian ginseng Withania somnifera," *Environmental Science and Pollution Research International*, vol. 27, no. 21, pp. 26025–26035, 2020.

[11] E. R. Hahm, S. H. Kim, K. B. Singh, K. Singh, and S. V. Singh, "A comprehensive review and perspective on anticancer mechanisms of withaferin A in breast cancer," *Cancer Prevention Research (Philadelphia, Pa.)*, vol. 13, no. 9, pp. 721–734, 2020.

[12] B. Hassannia, E. Logie, P. Vandenabeele, T. Vanden Berghe, W. Vanden Berghe, and A. Withaferin, "Withaferin A: from ayurvedic folk medicine to preclinical anti-cancer drug," *Biochemical Pharmacology*, vol. 173, article 113602, 2020.

[13] X. Zhang, A. K. Samadi, K. F. Roby, B. Timmermann, and M. S. Cohen, "Inhibition of cell growth and induction of apoptosis in ovarian carcinoma cell lines CaOV3 and SKOV3 by natural withanolide withaferin A," *Gynecologic Oncology*, vol. 124, no. 3, pp. 606–612, 2012.

[14] S. Srinivasan, R. S. Ranga, R. Burikhanov, S. S. Han, and D. Chendil, "Par-4-dependent apoptosis by the dietary compound withaferin A in prostate cancer cells," *Cancer Research*, vol. 67, no. 1, pp. 246–253, 2007.

[15] T. Behl, A. Sharma, L. Sharma et al., "Exploring the multifaceted therapeutic potential of withaferin A and its derivatives," *Biomedicines*, vol. 8, no. 12, p. 571, 2020.

[16] G. Kim, T. H. Kim, E. H. Hwang, K. T. Chang, J. J. Hong, and J. H. Park, "Withaferin A inhibits the proliferation of gastric cancer cells by inducing G2/M cell cycle arrest and apoptosis," *Oncology Letters*, vol. 14, no. 1, pp. 416–422, 2017.

[17] H.-W. Chang, R.-N. Li, H.-R. Wang et al., "Withaferin A induces oxidative stress-mediated apoptosis and DNA damage in oral cancer cells," *Frontiers in Physiology*, vol. 8, p. 634, 2017.

[18] S. D. Stan, Y. Zeng, and S. V. Singh, "Ayurvedic medicine constituent withaferin a causes G2 and M phase cell cycle arrest in human breast cancer cells," *Nutrition and Cancer*, vol. 60, Supplement 1, pp. 51–60, 2008.

[19] Q. Tang, L. Ren, J. Liu et al., "Withaferin A triggers G2/M arrest and intrinsic apoptosis in glioblastoma cells via ATF4-ATF3-CHOP axis," *Cell Proliferation*, vol. 53, no. 1, article e12706, 2020.

[20] S. Okamoto, T. Tsujioka, S. I. Suemori et al., "Withaferin A suppresses the growth of myelodysplasia and leukemia cell lines by inhibiting cell cycle progression," *Cancer Science*, vol. 107, no. 9, pp. 1302–1314, 2016.

[21] A. Batra and E. Winquist, "Emerging cell cycle inhibitors for treating metastatic castration-resistant prostate cancer," *Expert Opinion on Emerging Drugs*, vol. 23, no. 4, pp. 271–282, 2018.

[22] R. V. Roy, S. Suman, T. P. Das, J. E. Luevano, and C. Damodaran, "Withaferin A, a steroidal lactone from Withania somnifera, induces mitotic catastrophe and growth arrest in prostate cancer cells," *Journal of Natural Products*, vol. 76, no. 10, pp. 1909–1915, 2013.

[23] Y. Nishikawa, D. Okuzaki, K. Fukushima et al., "Withaferin A induces cell death selectively in androgen-independent prostate cancer cells but not in normal fibroblast cells," *PLoS One*, vol. 10, no. 7, article e0134137, 2015.

[24] B. Y. Choi and B.-W. Kim, "Withaferin-A inhibits colon cancer cell growth by blocking STAT3 transcriptional activity," *Journal of Cancer Prevention*, vol. 20, no. 3, pp. 185–192, 2015.

[25] S. S. Kakar, C. A. Worth, Z. Wang, K. Carter, M. Ratajczak, and P. Gunjal, "DOXIL when combined with withaferin A (WFA) targets ALDH1 positive cancer stem cells in ovarian cancer," *Journal of Cancer Stem Cell Research*, vol. 4, no. 2, p. 1, 2016.

[26] T.-J. Lee, H. J. Um, J.-W. Park, K. S. Choi, and T. K. Kwon, "Withaferin A sensitizes TRAIL-induced apoptosis through reactive oxygen species-mediated up-regulation of death receptor 5 and down-regulation of c-FLIP," *Free Radical Biology and Medicine*, vol. 46, no. 12, pp. 1639–1649, 2009.

[27] A. Nagalingam, P. Kuppusamy, S. V. Singh, D. Sharma, and N. K. Saxena, "Mechanistic elucidation of the antitumor properties of withaferin A in breast cancer," *Cancer Research*, vol. 74, no. 9, pp. 2617–2629, 2014.

[28] Q. Ping Dou, "A Zonder J. Overview of proteasome inhibitor-based anti-cancer therapies: perspective on bortezomib and second generation proteasome inhibitors versus future generation inhibitors of ubiquitin-proteasome system," *Current Cancer Drug Targets*, vol. 14, no. 6, pp. 517–536, 2014.

[29] M. Ri, "Endoplasmic-reticulum stress pathway-associated mechanisms of action of proteasome inhibitors in multiple myeloma," *International Journal of Hematology*, vol. 104, no. 3, pp. 273–280, 2016.

[30] M. J. Choi, E. J. Park, K. J. Min, J.-W. Park, and T. K. Kwon, "Endoplasmic reticulum stress mediates withaferin A-induced apoptosis in human renal carcinoma cells," *Toxicology In Vitro*, vol. 25, no. 3, pp. 692–698, 2011.

[31] K. Ghosh, S. De, S. Mukherjee, S. Das, A. N. Ghosh, and S. B. Sengupta, "Withaferin A induced impaired autophagy and unfolded protein response in human breast cancer cell-lines MCF-7 and MDA-MB-231," *Toxicology In Vitro*, vol. 44, pp. 330–338, 2017.

[32] H. Yang, G. Shi, and Q. P. Dou, "The tumor proteasome is a primary target for the natural anticancer compound withaferin A isolated from "Indian winter cherry"," *Molecular Pharmacology*, vol. 71, no. 2, pp. 426–437, 2007.

[33] J. L. Duque, K. R. Loughlin, R. M. Adam, P. Kantoff, E. Mazzucchi, and M. R. Freeman, "Measurement of plasma levels of vascular endothelial growth factor in prostate cancer patients: relationship with clinical stage, Gleason score, prostate volume, and serum prostate-specific antigen," *Clinics (São Paulo, Brazil)*, vol. 61, no. 5, pp. 401–408, 2006.

[34] Y. Nordby, S. Andersen, E. Richardsen et al., "Stromal expression of VEGF-A and VEGFR-2 in prostate tissue is associated with biochemical and clinical recurrence after radical prostatectomy," *The Prostate*, vol. 75, no. 15, pp. 1682–1693, 2015.

[35] R. R. McKay, A. J. Zurita, L. Werner et al., "A randomized phase II trial of short-course androgen deprivation therapy with or without bevacizumab for patients with recurrent prostate cancer after definitive local therapy," *Journal of Clinical Oncology*, vol. 34, no. 16, pp. 1913–1920, 2016.

[36] W. K. Kelly, S. Halabi, M. Carducci et al., "Randomized, double-blind, placebo-controlled phase III trial comparing docetaxel and prednisone with or without bevacizumab in men with metastatic castration-resistant prostate cancer: CALGB 90401," *Journal of Clinical Oncology*, vol. 30, no. 13, pp. 1534–1540, 2012.

[37] Z. Hoseinkhani, F. Norooznezhad, M. Rastegari-Pouyani, and K. Mansouri, "Medicinal plants extracts with antiangiogenic activity: where is the link?," *Advanced Pharmaceutical Bulletin*, vol. 10, no. 3, pp. 370–378, 2020.

[38] T. P. Fan, J. C. Yeh, K. W. Leung, P. Y. Yue, and R. N. Wong, "Angiogenesis: from plants to blood vessels," *Trends in Pharmacological Sciences*, vol. 27, no. 6, pp. 297–309, 2006.

[39] A. E. Gururaj, M. Belakavadi, D. A. Venkatesh, D. Marme, and B. P. Salimath, "Molecular mechanisms of anti-angiogenic effect of curcumin," *Biochemical and Biophysical Research Communications*, vol. 297, no. 4, pp. 934–942, 2002.

[40] W. H. Hu, R. Duan, Y. T. Xia et al., "Binding of resveratrol to vascular endothelial growth factor suppresses angiogenesis by inhibiting the receptor signaling," *Journal of Agricultural and Food Chemistry*, vol. 67, no. 4, pp. 1127–1137, 2019.

[41] R. Mohan, H. Hammers, P. Bargagna-mohan et al., "Withaferin A is a potent inhibitor of angiogenesis," *Angiogenesis*, vol. 7, no. 2, pp. 115–122, 2004.

[42] P. Bargagna-Mohan, A. Hamza, Y. E. Kim et al., "The tumor inhibitor and antiangiogenic agent withaferin A targets the intermediate filament protein vimentin," *Chemistry & Biology*, vol. 14, no. 6, pp. 623–634, 2007.

[43] S. Prasanna Kumar, P. Shilpa, and B. P. Salimath, "Withaferin A suppresses the expression of vascular endothelial growth factor in Ehrlich ascites tumor cells via Sp1 transcription factor," *Current Trends in Biotechnology and Pharmacy*, vol. 3, no. 2, pp. 138–148, 2009.

[44] S. Suman, T. P. Das, J. Moselhy et al., "Oral administration of withaferin A inhibits carcinogenesis of prostate in TRAMP model," *Oncotarget*, vol. 7, no. 33, pp. 53751–53761, 2016.

[45] T. Das, S. Suman, H. Alatassi, M. Ankem, and C. Damodaran, "Inhibition of AKT promotes FOXO3a-dependent apoptosis in prostate cancer," *Cell Death & Disease*, vol. 7, no. 2, pp. e2111–e2111, 2016.

[46] J. Moselhy, S. Suman, M. Alghamdi et al., "Withaferin A inhibits prostate carcinogenesis in a PTEN-deficient mouse model of prostate cancer," *Neoplasia*, vol. 19, no. 6, pp. 451–459, 2017.

[47] E. Chang, C. Pohling, A. Natarajan et al., "AshwaMAX and withaferin A inhibits gliomas in cellular and murine orthotopic models," *Journal of Neuro-Oncology*, vol. 126, no. 2, pp. 253–264, 2016.

[48] A. N. Sari, P. Bhargava, J. K. Dhanjal et al., "Combination of withaferin-A and CAPE provides superior anticancer potency: bioinformatics and experimental evidence to their molecular targets and mechanism of action," *Cancers (Basel)*, vol. 12, no. 5, p. 1160, 2020.

[49] S. H. Kim, K. B. Singh, E. R. Hahm, B. L. Lokeshwar, and S. V. Singh, "*Withania somnifera* root extract inhibits fatty acid synthesis in prostate cancer cells," *Journal of Traditional and Complementary Medicine*, vol. 10, no. 3, pp. 188–197, 2020.

[50] A. Setty Balakrishnan, A. A. Nathan, M. Kumar, S. Ramamoorthy, and S. K. Ramia Mothilal, "*Withania somnifera* targets interleukin-8 and cyclooxygenase-2 in human prostate cancer progression," *Prostate International*, vol. 5, no. 2, pp. 75–83, 2017.

[51] G. Multhoff, M. Molls, and J. Radons, "Chronic inflammation in cancer development," *Frontiers in Immunology*, vol. 2, p. 98, 2011.

[52] F. R. Greten and S. I. Grivennikov, "Inflammation and cancer: triggers, mechanisms, and consequences," *Immunity*, vol. 51, no. 1, pp. 27–41, 2019.

[53] L. M. Coussens and Z. Werb, "Inflammation and cancer," *Nature*, vol. 420, no. 6917, pp. 860–867, 2002.

[54] H. Xu, M.-b. Hu, P.-d. Bai et al., "Proinflammatory cytokines in prostate cancer development and progression promoted by high-fat diet," *BioMed Research International*, vol. 2015, Article ID 249741, 7 pages, 2015.

[55] T. Hayashi, K. Fujita, S. Nojima et al., "High-fat diet-induced inflammation accelerates prostate cancer growth via IL6 signaling," *Clinical Cancer Research*, vol. 24, no. 17, pp. 4309–4318, 2018.

[56] J. S. de Bono, C. Guo, B. Gurel et al., "Prostate carcinogenesis: inflammatory storms," *Nature Reviews. Cancer*, vol. 20, no. 8, pp. 455–469, 2020.

[57] M. Archer, N. Dogra, and N. Kyprianou, "Inflammation as a driver of prostate cancer metastasis and therapeutic resistance," *Cancers (Basel)*, vol. 12, no. 10, p. 2984, 2020.

[58] D. Karan, J. Holzbeierlein, and J. B. Thrasher, "Macrophage inhibitory cytokine-1: possible bridge molecule of inflammation and prostate cancer," *Cancer Research*, vol. 69, no. 1, pp. 2–5, 2009.

[59] M. Terlizzi, V. Casolaro, A. Pinto, and R. Sorrentino, "Inflammasome: cancer's friend or foe?," *Pharmacology & Therapeutics*, vol. 143, no. 1, pp. 24–33, 2014.

[60] L. Zitvogel, O. Kepp, L. Galluzzi, and G. Kroemer, "Inflammasomes in carcinogenesis and anticancer immune responses," *Nature Immunology*, vol. 13, no. 4, pp. 343–351, 2012.

[61] D. Karan, "Inflammasomes: emerging central players in cancer immunology and immunotherapy," *Frontiers in Immunology*, vol. 9, p. 3028, 2018.

[62] S. Zhao, Y. Zhang, Q. Zhang, F. Wang, and D. Zhang, "Toll-like receptors and prostate cancer," *Frontiers in Immunology*, vol. 5, p. 352, 2014.

[63] T. Ou, M. Lilly, and W. Jiang, "The pathologic role of toll-like receptor 4 in prostate cancer," *Frontiers in Immunology*, vol. 9, p. 1188, 2018.

[64] B. Eluard, C. Thieblemont, and V. Baud, "NF-κB in the new era of cancer therapy," *Trends Cancer*, vol. 6, no. 8, pp. 677–687, 2020.

[65] A. A. Grosset, V. Ouellet, C. Caron et al., "Validation of the prognostic value of NF-κB p65 in prostate cancer: a retrospective study using a large multi-institutional cohort of the Canadian Prostate Cancer Biomarker Network," *PLoS Medicine*, vol. 16, no. 7, article e1002847, 2019.

[66] J. Domingo-Domenech, B. Mellado, B. Ferrer et al., "Activation of nuclear factor- κ B in human prostate carcinogenesis

and association to biochemical relapse," *British Journal of Cancer*, vol. 93, no. 11, pp. 1285–1294, 2005.

[67] H. Khan, H. Ullah, P. Castilho et al., "Targeting NF-κB signaling pathway in cancer by dietary polyphenols," *Critical Reviews in Food Science and Nutrition*, vol. 60, no. 16, pp. 2790–2800, 2020.

[68] J. U. Marquardt, L. Gomez-Quiroz, L. O. Arreguin Camacho et al., "Curcumin effectively inhibits oncogenic NF-κB signaling and restrains stemness features in liver cancer," *Journal of Hepatology*, vol. 63, no. 3, pp. 661–669, 2015.

[69] S. Liu, Z. Wang, Z. Hu et al., "Anti-tumor activity of curcumin against androgen-independent prostate cancer cells via inhibition of NF-κB and AP-1 pathway in vitro," *Journal of Huazhong University of Science and Technology. Medical Sciences*, vol. 31, no. 4, pp. 530–534, 2011.

[70] S. H. Habib, S. Makpol, N. A. Abdul Hamid, S. Das, W. Z. Ngah, and Y. A. Yusof, "Ginger extract (Zingiber officinale) has anti-cancer and anti-inflammatory effects on ethionine-induced hepatoma rats," *Clinics (São Paulo, Brazil)*, vol. 63, no. 6, pp. 807–813, 2008.

[71] N. A. Abd Wahab, N. H. Lajis, F. Abas, I. Othman, and R. Naidu, "Mechanism of anti-cancer activity of curcumin on androgen-dependent and androgen-independent prostate cancer," *Nutrients*, vol. 12, no. 3, p. 679, 2020.

[72] L. N. Jiang, Y. B. Liu, and B. H. Li, "Lycopene exerts anti-inflammatory effect to inhibit prostate cancer progression," *Asian Journal of Andrology*, vol. 21, p. 80, 2019.

[73] E. A. Assar, M. C. Vidalle, M. Chopra, and S. Hafizi, "Lycopene acts through inhibition of IκB kinase to suppress NF-κB signaling in human prostate and breast cancer cells," *Tumour Biology*, vol. 37, no. 7, pp. 9375–9385, 2016.

[74] Q. Zhao, F. Yang, L. Meng et al., "Lycopene attenuates chronic prostatitis/chronic pelvic pain syndrome by inhibiting oxidative stress and inflammation via the interaction of NF-κB, MAPKs, and Nrf2 signaling pathways in rats," *Andrology*, vol. 8, no. 3, pp. 747–755, 2020.

[75] S. C. Gupta, J. H. Kim, R. Kannappan, S. Reuter, P. M. Dougherty, and B. B. Aggarwal, "Role of nuclear factor-κB-mediated inflammatory pathways in cancer-related symptoms and their regulation by nutritional agents," *Experimental Biology and Medicine (Maywood, N.J.)*, vol. 236, no. 6, pp. 658–671, 2011.

[76] S. Shishodia, S. Majumdar, S. Banerjee, and B. B. Aggarwal, "Ursolic acid inhibits nuclear factor-kappaB activation induced by carcinogenic agents through suppression of IkappaBalpha kinase and p65 phosphorylation: correlation with down-regulation of cyclooxygenase 2, matrix metalloproteinase 9, and cyclin D1," *Cancer Research*, vol. 63, no. 15, pp. 4375–4383, 2003.

[77] J. H. Oh, T. J. Lee, J. W. Park, T. K. Kwon, and A. Withaferin, "Withaferin A inhibits iNOS expression and nitric oxide production by Akt inactivation and down-regulating LPS-induced activity of NF-κB in RAW 264.7 cells," *European Journal of Pharmacology*, vol. 599, no. 1-3, pp. 11–17, 2008.

[78] S. Dubey, H. Yoon, M. S. Cohen, P. Nagarkatti, M. Nagarkatti, and D. Karan, "Withaferin A associated differential regulation of inflammatory cytokines," *Frontiers in Immunology*, vol. 9, p. 195, 2018.

[79] D. B. Naidoo, A. A. Chuturgoon, A. Phulukdaree, K. P. Guruprasad, K. Satyamoorthy, and V. Sewram, "Withania somnifera modulates cancer cachexia associated inflammatory cytokines and cell death in leukaemic THP-1 cells and peripheral blood mononuclear cells (PBMC's)," *BMC Complementary and Alternative Medicine*, vol. 18, no. 1, p. 126, 2018.

[80] M. Rasool and P. Varalakshmi, "Immunomodulatory role of *Withania somnifera* root powder on experimental induced inflammation: an in vivo and in vitro study," *Vascular Pharmacology*, vol. 44, no. 6, pp. 406–410, 2006.

[81] E. Logie and B. W. Vanden, "Tackling chronic inflammation with withanolide phytochemicals-a withaferin A perspective," *Antioxidants (Basel)*, vol. 9, no. 11, 2020.

[82] M. A. Kanak, R. Shahbazov, G. Yoshimatsu, M. F. Levy, M. C. Lawrence, and B. Naziruddin, "A small molecule inhibitor of NFκB blocks ER stress and the NLRP3 inflammasome and prevents progression of pancreatitis," *Journal of Gastroenterology*, vol. 52, no. 3, pp. 352–365, 2017.

[83] J. E. Kim, J. Y. Lee, M. J. Kang et al., "Withaferin A inhibits Helicobacter pylori-induced production of IL-1β in dendritic cells by regulating NF-κB and NLRP3 inflammasome activation," *Immune Network*, vol. 15, no. 6, pp. 269–277, 2015.

[84] H. M. Zhao, Z. W. Gao, S. X. Xie, X. Han, and Q. S. Sun, "Withaferin A attenuates ovalbumin induced airway inflammation," *Frontiers in Bioscience*, vol. 24, pp. 576–596, 2019.

[85] A. Barua, M. J. Bradaric, P. Bitterman et al., "Dietary supplementation of Ashwagandha (Withania somnifera, Dunal) enhances NK cell function in ovarian tumors in the laying hen model of spontaneous ovarian cancer," *American Journal of Reproductive Immunology*, vol. 70, no. 6, pp. 538–550, 2013.

[86] T. A. Fehniger, S. F. Cai, X. Cao et al., "Acquisition of murine NK cell cytotoxicity requires the translation of a pre- existing pool of granzyme B and perforin mRNAs," *Immunity*, vol. 26, no. 6, pp. 798–811, 2007.

[87] M. J. Smyth, E. Cretney, J. M. Kelly et al., "Activation of NK cell cytotoxicity," *Molecular Immunology*, vol. 42, no. 4, pp. 501–510, 2005.

[88] F. Malik, A. Kumar, S. Bhushan et al., "Immune modulation and apoptosis induction: two sides of antitumoural activity of a standardised herbal formulation of *Withania somnifera*," *European Journal of Cancer*, vol. 45, no. 8, pp. 1494–1509, 2009.

[89] G. Muralikrishnan, A. K. Dinda, and F. Shakeel, "Immunomodulatory effects of Withania somnifera on azoxymethane induced experimental colon cancer in mice," *Immunological Investigations*, vol. 39, no. 7, pp. 688–698, 2010.

[90] S. Kushwaha, S. Roy, R. Maity et al., "Chemotypical variations in *Withania somnifera* lead to differentially modulated immune response in BALB/c mice," *Vaccine*, vol. 30, no. 6, pp. 1083–1093, 2012.

[91] C. D. Tripathi, P. K. Kushawaha, R. S. Sangwan, C. Mandal, S. Misra-Bhattacharya, and A. Dube, "*Withania somnifera* chemotype NMITLI 101R significantly increases the efficacy of antileishmanial drugs by generating strong IFN- γ and IL-12 mediated immune responses in *Leishmania donovani* infected hamsters," *Phytomedicine*, vol. 24, pp. 87–95, 2017.

[92] T. S. Griffith, M. Kawakita, J. Tian et al., "Inhibition of murine prostate tumor growth and activation of immunoregulatory cells with recombinant canarypox viruses," *Journal of the National Cancer Institute*, vol. 93, no. 13, pp. 998–1007, 2001.

[93] L. Davis and G. Kuttan, "Effect of Withania somnifera on cell mediated immune responses in mice," *Journal of*

Experimental & Clinical Cancer Research, vol. 21, no. 4, pp. 585–590, 2002.

[94] J. Mikolai, A. Erlandsen, A. Murison et al., "In vivo effects of Ashwagandha (Withania somnifera) extract on the activation of lymphocytes," *Journal of Alternative and Complementary Medicine*, vol. 15, no. 4, pp. 423–430, 2009.

[95] N. Chi, Z. Tan, K. Ma, L. Bao, and Z. Yun, "Increased circulating myeloid-derived suppressor cells correlate with cancer stages, interleukin-8 and -6 in prostate cancer," *International Journal of Clinical and Experimental Medicine*, vol. 7, no. 10, pp. 3181–3192, 2014.

[96] A. Erlandsson, J. Carlsson, M. Lundholm et al., "M2 macrophages and regulatory T cells in lethal prostate cancer," *The Prostate*, vol. 79, no. 4, pp. 363–369, 2019.

[97] P. Sinha and S. Ostrand-Rosenberg, "Myeloid-derived suppressor cell function is reduced by withaferin A, a potent and abundant component of Withania somnifera root extract," *Cancer Immunology, Immunotherapy*, vol. 62, no. 11, pp. 1663–1673, 2013.

[98] S. Fuladi, S. A. Emami, A. H. Mohammadpour, A. Karimani, A. A. Manteghi, and A. Sahebkar, "Assessment of Withania somnifera root extract efficacy in patients with generalized anxiety disorder: a randomized double-blind placebo-controlled trial," *Current Clinical Pharmacology*, vol. 15, 2020.

[99] A. L. Lopresti, P. D. Drummond, and S. J. Smith, "A randomized, double-blind, placebo-controlled, crossover study examining the hormonal and vitality effects of Ashwagandha (Withania somnifera) in aging, overweight males," *American Journal of Men's Health*, vol. 13, no. 2, 2019.

[100] A. L. Lopresti, S. J. Smith, H. Malvi, and R. Kodgule, "An investigation into the stress-relieving and pharmacological actions of an Ashwagandha (Withania somnifera) extract: a randomized, double-blind, placebo-controlled study," *Medicine (Baltimore)*, vol. 98, no. 37, article e17186, 2019.

[101] K. N. R. Chengappa, J. S. Brar, J. M. Gannon, and P. J. Schlicht, "Adjunctive use of a standardized extract of *Withania somnifera* (Ashwagandha) to treat symptom exacerbation in schizophrenia: a randomized, double-blind, placebo-controlled study," *The Journal of Clinical Psychiatry*, vol. 79, no. 5, 2018.

[102] J. M. Gannon, J. Brar, A. Rai, and K. N. R. Chengappa, "Effects of a standardized extract of Withania somnifera (Ashwagandha) on depression and anxiety symptoms in persons with schizophrenia participating in a randomized, placebo-controlled clinical trial," *Annals of Clinical Psychiatry*, vol. 31, no. 2, pp. 123–129, 2019.

[103] D. Choudhary, S. Bhattacharyya, and S. Bose, "Efficacy and safety of Ashwagandha (Withania somnifera (L.) Dunal) root extract in improving memory and cognitive functions," *Journal of Dietary Supplements*, vol. 14, no. 6, pp. 599–612, 2017.

[104] S. P. Jahanbakhsh, A. A. Manteghi, S. A. Emami et al., "Evaluation of the efficacy of *Withania somnifera* (Ashwagandha) root extract in patients with obsessive-compulsive disorder: a randomized double-blind placebo-controlled trial," *Complementary Therapies in Medicine*, vol. 27, pp. 25–29, 2016.

[105] A. K. Sharma, I. Basu, and S. Singh, "Efficacy and safety of Ashwagandha root extract in subclinical hypothyroid patients: a double-blind, randomized placebo-controlled trial," *Journal of Alternative and Complementary Medicine*, vol. 24, no. 3, pp. 243–248, 2018.

[106] B. M. Biswal, S. A. Sulaiman, H. C. Ismail, H. Zakaria, and K. I. Musa, "Effect of Withania somnifera (Ashwagandha) on the development of chemotherapy-induced fatigue and quality of life in breast cancer patients," *Integrative Cancer Therapies*, vol. 12, no. 4, pp. 312–322, 2013.

[107] N. Pires, V. Gota, A. Gulia, L. Hingorani, M. Agarwal, and A. Puri, "Safety and pharmacokinetics of withaferin-A in advanced stage high grade osteosarcoma: a phase I trial," *Journal of Ayurveda and Integrative Medicine*, vol. 11, no. 1, pp. 68–72, 2020.

Hindawi
Journal of Immunology Research
Volume 2021, Article ID 8030297, 11 pages
https://doi.org/10.1155/2021/8030297

Review Article

Bifidobacterium Longum: Protection against Inflammatory Bowel Disease

Shunyu Yao, Zixi Zhao, Weijun Wang, and Xiaolu Liu

School of Chemistry and Biological Engineering, University of Science and Technology Beijing, Beijing 100083, China

Correspondence should be addressed to Xiaolu Liu; xiaoluliu@ustb.edu.cn

Received 22 April 2021; Accepted 10 July 2021; Published 23 July 2021

Academic Editor: Kai Wang

The prevalence of inflammatory bowel disease (IBD), which includes ulcerative colitis (UC) and Crohn's disease (CD), increases gradually worldwide in the past decades. IBD is generally associated with the change of the immune system and gut microbiota, and the conventional treatments usually result in some side effects. Bifidobacterium longum, as colonizing bacteria in the intestine, has been demonstrated to be capable of relieving colitis in mice and can be employed as an alternative or auxiliary way for treating IBD. Here, the mechanisms of the Bifidobacterium longum in the treatment of IBD were summarized based on previous cell and animal studies and clinical trials testing bacterial therapies. This review will be served as a basis for future research on IBD treatment.

1. Introduction

Inflammatory bowel disease (IBD) is mainly manifested as chronic and recurrent inflammation in the gastrointestinal tract. It includes ulcerative colitis (UC) and Crohn's disease (CD) [1]. Although traditionally regarded as a disease prevalent in Western countries, the incidence of IBD is gradually increasing globally, especially in newly industrialized countries [2]. In the past decade, IBD has become a global public health challenge [3]. Its main symptoms include diarrhea, abdominal cramps, weight loss, fatigue, anemia, and extraintestinal symptoms (especially joint pain or arthritis). These will cause serious obstacles and troubles to human's normal life [4]. Most patients with IBD suffer from fecal incontinence and also face the risk of a weakened immune system and bowel cancer [5]. The occurrence of IBD is closely related to genetic susceptibility, environment, immune regulation dysfunction, gut microbiota, nutrition, and lifestyle [6]. However, the exact cause of IBD has yet to be determined, which makes it difficult to develop targeted treatments [4, 7].

At present, the commonly used drugs for the treatment of IBD include immunosuppressive drugs, biological agents, and antibiotics [8]. Among them, 5-aminosalicylic acid (5-ASA) is widely used in the treatment of IBD due to its good clinical efficacy [9]. However, taking this medicine will cause adverse reactions such as diarrhea, abdominal pain, headache, and nasopharyngitis, making the patient uncomfortable [8]. Monoclonal cytokines such as anti-TNF-α and IL-6 can also treat IBD, but the high production cost of this method makes it unacceptable for some patients [6]. Recently, studies have found that Bifidobacterium longum can be used as an adjuvant treatment for IBD [10]. Bifidobacterium longum belongs to the genera Actinomyces and Bifidobacterium. It is a gram-positive bacterium that performs anaerobic respiration [11]. The genus Bifidobacterium inhabits intestinal tracts of humans and animals. It is one of the first microorganisms to colonize the host gut [12]. It has more than 50 different species, of which, Bifidobacterium longum is one of the most abundant microorganisms in the intestines of infants and adults [8, 9]. It can be separated from a variety of animals, including intestines of babies and long-lived elderly [13]. Diseases inside and outside the intestine are closely related to the changes in the abundance of Bifidobacterium longum. Compared with healthy people, the abundance of Bifidobacterium longum

flora in the stool of patients with intestinal diseases is much lower [14]. Bifidobacterium can be stably colonized in the human intestine. It has immune tolerance to the human body and will not cause rejection [15]. A large number of animal experiments and clinical studies have shown that Bifidobacterium longum can reduce the symptoms of colitis and relieve chronic inflammation [16]. However, the mechanisms of Bifidobacterium longum to treat IBD and regulate the intestinal immune system are still unclear. In this review, we will focus on the cell and animal experiments and clinical trials to summarize the mechanisms of Bifidobacterium longum on the prevention and treatment of IBD, which would provide a basis for subsequent therapeutic applications.

2. Interaction between Bifidobacterium longum and the Host

The human gastrointestinal environment can be regarded as a complex ecosystem. It contains trillions of microbes, which are usually called gut microbiota [17, 18]. Scientists have discovered that the composition of the gut microbiota and its metabolites plays an important role in protecting the intestinal barrier and regulating the immune balance [19]. Disturbances of the gut microbiota often occur in patients with intestinal diseases, such as irritable bowel syndrome, idiopathic chronic diarrhea, colorectal cancer, and IBD [20]. Some studies have shown that IBD usually causes general changes in the structure of the gut microbiota of patients, resulting in a decrease in the diversity and species abundance [21, 22]. The anaerobic species and short-chain fatty acid producers depleted, and the facultative anaerobic bacteria increased in the gut of patients [23]. Changes in gut microbiota will affect the normal operation of the mucosal immune system, leading to functional degradation [24]. Probiotics that promote the balance of gut microbiota play an important role in the treatment of IBD [25].

It is reported that the intervention of probiotics improved the gut microbiota and has an effective protective effect on the immune health of the host [26, 27]. The results of animal and clinical studies showed that products containing probiotics or prebiotics improved IBD by regulating proinflammatory signaling pathways and downregulating proinflammatory cytokines [7]. Bifidobacterium longum, as one of the most abundant members in the gut, can protect the intestinal epithelial barrier and tissue structure and balance the gut microbiota to alleviate the symptoms of colitis [28]. Moreover, Bifidobacterium can secrete a variety of active metabolites [29]. They influence the interaction between digestion, endocrine, cardiovascular, immune, and nervous systems to maintain the host in a healthy state [30, 31]. Bifidobacterium longum inhibits inflammation by regulating the balance of the immune system, improving the intestinal barrier function, and increasing acetate production [32]. This species has been widely used as a probiotic because of its beneficial effects on host health and has been recognized as safe by the United States Food and Drug Administration and the European Food Safety Authority [15].

3. Mechanisms of Bifidobacterium longum in Improvement of IBD

3.1. Bifidobacterium Longum and Antioxidant Activity. Oxidative stress has been regarded as one of the major mechanisms involved in the pathophysiology of IBD [33]. It is characterized by the inability of the organism to detoxify reactive oxygen species (ROS) caused by a disequilibrium in the balance between their production and accumulation in cells and tissues [34]. The infiltration of immune cells occurred in active IBD as the prominent feature. More extensive recruitment of neutrophils and less of monocytes are the typical characteristics in lesion location. Myeloperoxidase (MPO), an abundant granule heme enzyme, is unique to both neutrophils and monocytes [35]. Through the halogenation or peroxidase cycle, MPO could generate reactive oxygen species (ROS) effectively [36]. ROS mainly includes the oxygen-containing ions, molecules, or groups with high activity. The abnormal accumulation of ROS will cause serious damage to normal physiological metabolic activity [37]. They induce fatty acid side-chain reactions to create lipid malondialdehyde and hydroperoxides, which results in the damage of biological macromolecules and causes the impairment of cell structure and function [37]. Substantial evidence shows that the imbalance between the accumulation of ROS and antioxidant activity is closely related to the incidence and severity of IBD. For IBD patients, oxidative stress occurs with the raise of ROS levels and decline of antioxidant levels, which leads to chronic tissue damage continuously [38, 39] (Figure 1).

Studies in cell and animal experiments have shown that Bifidobacterium longum strains regulate oxidative stress by enhancing the body's antioxidant activity and regulating the production and accumulation of ROS, thereby reducing the symptoms of IBD. B. longum 5(1A) administration in the dextran sulfate sodium- (DSS-) induced colitis in mice abated severe lesions in the colon with the decreased level of eosinophil peroxidase [40] (Figure 1). In addition, oral Bifidobacterium longum is also an effective treatment of ethanol-induced gastritis injury. Application of microbial inoculum downregulates the tumor necrosis factor (TNF) expression, myeloperoxidase activity, and hemorrhagic ulcerative lesions area [41]. Moreover, similar antioxidant effects have been found for the fermented products or metabolites of B. longum YS108R [24]. Without altering cell viability, B. longum CCFM752 supernatants increased intracellular antioxidative capacity with enhanced intracellular catalase activity and reduced NADPH oxidase activation [42].

Many anaerobic microorganisms remove ROS mainly by secreting and producing enzymes, such as NADH oxidase, NADH peroxidase, catalase and superoxide dismutase [43]. Currently, there are few studies concerning oxygen resistance and free radical scavenging genes or enzymes of B. longum, and there have been reports only about the strains NCC2705 [44], BBMN68 [43], and LTBL16 [45]. It has been found that B. longum LTBL16 had three peroxide oxidoreductase coding genes (LTBL16-000027, LTBL16-000028, LTBL16-000976) and one NADH oxidase coding

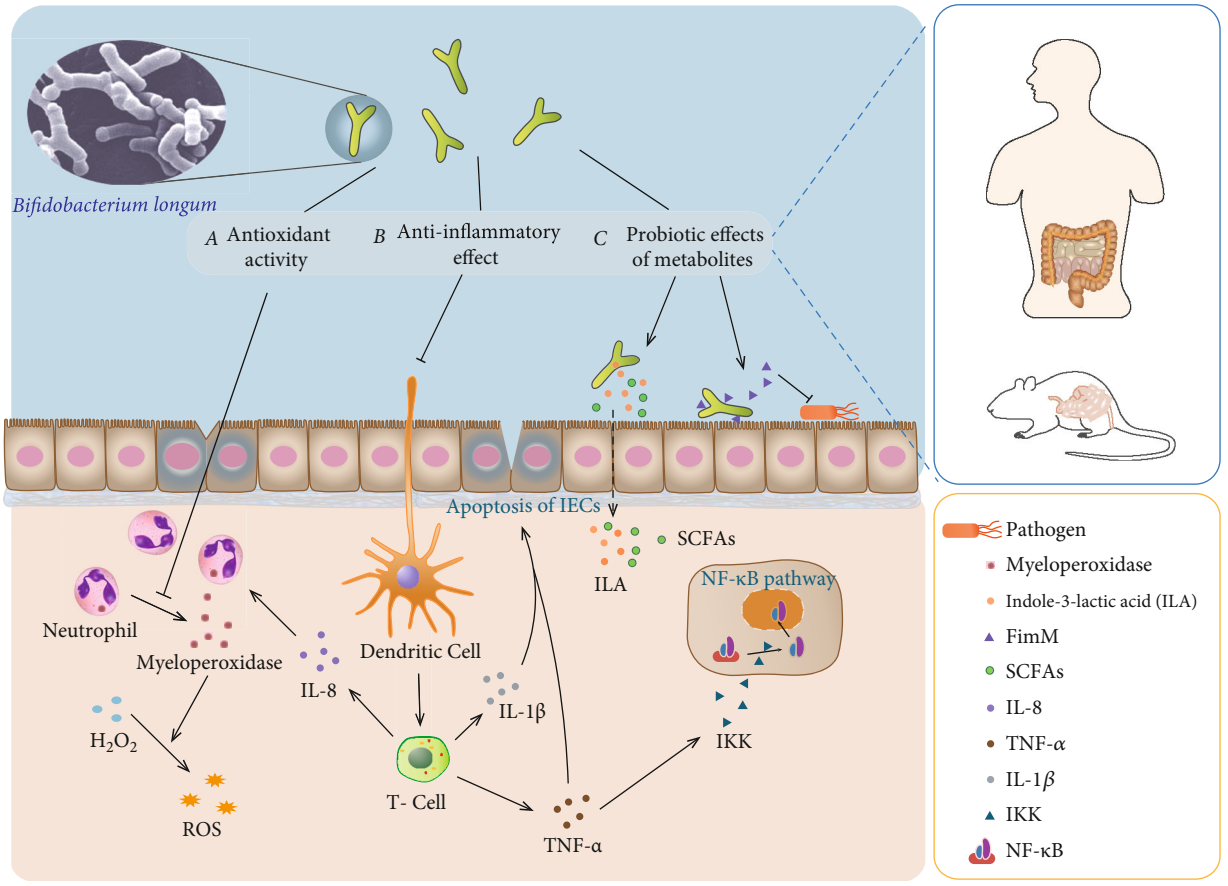

Figure 1: Protective mechanism of Bifidobacterium longum against intestinal inflammation.

gene (LTBL-001911), which can effectively remove ROS in bifidobacteria and improve oxygen resistance [45]. Recent studies have found that Bifidobacterium longum BBMN68 had an incomplete glutredoxin system. Thioredoxin and glutaredoxin make up the thioredoxin- and glutaredoxin-dependent reduction systems in Escherichia coli and many other bacteria and are responsible for maintaining a reduced environment in the cell cytosol [46]. Under oxidative stress, the genes *grxC1*- (BBMN68_125-) and *grxC2*- (BBMN68_1397-) encoding glutaredoxin, *trxB1*- (BBMN68_1345-) encoding thioredoxin reductase, and BBMN68_991-encoding thioredoxin are all upregulated [43]. Studies have found that when Bifidobacterium is under oxidative stress, thioredoxin reductase can respond positively to its transcription and translation [47]. In addition, the thioredoxin-dependent reduction system can reduce perredoxin and H2O2, scavenging free radicals, quenching singlet oxygen, and then maintaining the intracellular thioldisulfide balance [48]. Thus, the thioredoxin-dependent antioxidant system might be the major redox homeostasis system in strain BBMN68.

In mammals, several longevity proteins of the sirtuin family have been shown to play an antioxidant role by deacetylation activity. The cytosolic isoform SIRT2 is capable of deacetylating forkhead box protein FOXO1a and FOXO3a, thereby increasing FOXO-dependent transcription of antioxidant enzymes and reducing the cellular ROS level [49]. The probiotic (B. longum NCC2705) has the *Sir2* gene family and has antioxidant activity in the human body. BL-Sir2 regulated FOXO3a mediated antioxidant genes, deacetylated σH, and increased the activity of manganese superoxide dismutase and catalase and reduced ROS [44]. In addition, a *Sir2*-encoding gene (LTBL16-002010) was also found in B. longum LTBL16, which could improve FOXO-dependent transcription of antioxidant enzymes encoding genes and reduce ROS levels in cells [45]. Therefore, Bifidobacterium longum can suppress oxidative stress and stimulate the production of antioxidants, thereby reducing the oxidative damage of intestinal tract of IBD (Figure 1).

Bifidobacterium longum can protect intestinal epithelial cells by different mechanisms. These include (a) Bifidobacterium longum can decline myeloperothe xidase activity and the production of ROS, suppress oxidative stress, and reduce the damage of the tintestinal tract. (b) Bifidobacterium longum can downregulate inflammatory cytokines and inhibit NF-κB pathway to regulate the intestinal immune system and protect intestinal epithelial cells. (c) Bifidobacterium longum can produce various metabolites to enhance adhesion to the intestinal tract and inhibit harmful bacteria. It can also participate in immune regulation. Bifidobacterium longum was photographed by Mark Schell, University of Georgia, Athens, GA [50].

3.2. Bifidobacterium longum Reduces the Inflammatory Cytokine Expression in the Intestine. In vitro experiments

Table 1: Effects of B. longum strains in modulating inflammation based on in vitro and ex vivo studies.

Strains	Dose	Cell	Effect	Ref.
B. longum CECT-7347	2×10^9 cells/mL	HT-29 cell	IL-8 ↓	[62]
B. longum Bif10 and Bif16	1×10^{10} CFU/mL	RAW264.7 cell	TNF-α, IL-1β, IL-6 ↓ SCFA ↑	[59]
B. longum BB536	5×10^8 cells/mL	PIE cell	TNF-α↓	[60]
B. longum KACC 91563	1×10^6, 10^7, 10^8 CFU/well	Splenocytes macrophages	TNF-α ↓, IgE ↓ IL-2, 4, 6, 10, IFN-γ ↓	[51]
B. longum R0033	100 : 1 for bacteria to cell ratio	HT-29 cell	TNF-α, IL-8 ↓	[61]
B. longum 5^{1A}	1×10^3, 10^5 CFU/well	Keratinocyte fibroblast cell	IL-6, IL-8 ↓	[73]
B. longum BL05	5×10^4, 10^5, 10^6 CFU/well	HT-29 cell THP-1 cell	IL-10 ↑ IL-1β, IL-6 ↓	[67]
B. longum LC67	1×10^3, 10^5 CFU/mL	KATO III cells	NF-κB ↓ IL-8 ↓	[41]
B. longum LC67	1×10^4, 10^6 CFU/mL	Caco-2 cells	NF-κB ↓	[28, 74]

and animal models indicate that Bifidobacterium longum has anti-inflammatory effects on intestinal diseases (Table 1 and Table 2). Bifidobacterium longum can reduce spontaneous and chemically induced colitis by regulating cytokines or inducing immune regulation mechanisms in a specific way [51]. The intestine is an important immune organ. Goblet cells in the intestine produce mucus to fight off invading pathogens. Under the mucus, intestinal epithelial cells and various immune cells form another defense barrier to prevent the invasion of pathogenic microorganisms [52]. These cells can specifically secrete various cytokines to regulate the immune system. For example, Th1 cells can secrete tumor necrosis factor α (TNF-α) to initiate a variety of proinflammatory responses [53]. Th17 cells are involved in the activation and recruitment of neutrophils [54]. Treg cells can express the transcription factor forkhead box P3 (FOXP3) and secrete the anti-inflammatory cytokine IL-10, thereby inhibiting a strong inflammatory response [55].

Under normal circumstances, the mucosal cells of the intestine can keep the proinflammatory and anti-inflammatory cytokines in a relatively balanced state [51]. In the intestines of patients with IBD, this balance is disrupted. The increase in the number and activity of proinflammatory cytokines in the mucosa leads to damage and inflammation of the intestinal tissues [56]. In the process of IBD, immune cells are activated after receiving a stimulating signal. A large number of inflammatory cytokines are secreted, including tumor necrosis factor (TNF-α), interleukin (IL-1β), IL-6, and ROS [57] (Figure 1). An increase in intestinal epithelial cell (IEC) apoptosis is a major characteristic of IBD. Studies have shown that excessive TNF-α can destroy the integrity of the intestinal epithelium and induce apoptosis of IECs [58] (Figure 1). The study of T cell metastasis showed that the content of TNF-α in the intestinal tract of colitis increased significantly [59]. In the study of various strains of Bifidobacterium longum, it was found that after incubating cells with probiotics, the level of TNF-α was significantly reduced. The disease can be alleviated by the neutralizing effect of TNF-α [51, 60, 61].

Furthermore, TNF-α induces inflammatory responses with the expression of proinflammatory cytokines, including IL-1β, IL-6, and IL-8 [62]. The IL-1β is produced by IECs in a paracrine manner. It could disrupt the maturation and function of IECs resulting in exerting major epithelial barrier alterations [63]. As a pleiotropic cytokine, IL-6 plays a central role in immunoregulation, inflammation response, and oncogenesis. Anti-IL-6 monoclonal antibody effectively suppresses chronic intestinal inflammation in mouse models [64]. A previous research demonstrates that proinflammatory molecules like IL-8 could be induced by enteropathogenic bacteria colonizing in the gut. As a consequence, neutrophils and other inflammatory cells will be recruited [65]. Infiltration of neutrophils may perpetuate inflammation and result in cell damage, epithelial barrier dysfunction, and diarrhea [66]. Marzia et al. used B. longum and macrophages to conduct a simulation study of the intestinal epithelial barrier function. It was found that IL-10 was induced by probiotics significantly. On the contrary, the production of IL-1β and IL-6 was downregulated by 70% and 80%, respectively [67]. Similarly, after coincubation with B. longum HT-CECT-7347, HT29 cells stimulated by TNF-α displayed a drastic dose-dependent decline in IL-8 production [62]. In addition, it was found that after treatment with Bifidobacterium longum, colitis mice alleviated inflammation, and the content of short-chain fatty acids in the intestinal tract also increased. The regulation of immunity by short-chain fatty acids (SCFAs) is mainly mediated by activation of free fatty acid receptor 2 (FFA2) or inhibition of histone deacetylase (HDAC) [68]. As the main receptor of SCFA, FFA2 is expressed on immune cells and inhibits the NF-κB signaling pathway to produce anti-inflammatory effects [69]. HDACs are generally expressed in immune, endothelial, and vascular smooth muscle cells [70]. Inhibition of HDAC activity causes an open structure of DNA/chromatin, which facilitates the regulation of the expression of transcription factors, such as NF-κB and FOXP3 [68]. Therefore, B. longum can regulate intracellular signaling pathways and decrease the level of IL-1β, IL-6, and IL-8, reduce the alterations of the in vitro

Table 2: Animal studies of B. longum strain effects in modulating inflammation.

Strains	Dose	Model	Effect	Ref.
B. longum Bif10 and Bif16	5×10^9 CFU/mouse/day	DSS-induced colitis in mice	SCFA ↑ TNF-α, IL-1β, IL-6 ↓	[59]
B. longum 5 (1A)	1×10^8 CFU/mouse/day	DSS-induced colitis in mice	IL-1 ↓ MPO ↓	[40]
B. longum YS108R	1×10^9 CFU/mouse/day	DSS-induced colitis in mice	IL-10 ↑ TNF-α, MPO, IL-1β, IL-6, IL-17A ↓	[24, 72]
B. longum ATCC 15707	1×10^7 CFU/kg/day	DSS-induced colitis in mice	SCFA ↑ TNF-α, IL-6, TGF-β ↓	[71]
B. longum HB5502	4×10^9 CFU/day	TNBS-induced colitis in mice	HMGB1 ↓	[84]
B. Longum LC67	1×10^9 CFU/mouse/day	Ethanol-induced gastritis in mice	NF-κB, CXCL4, TNF ↓	[41]
B. longum LC67	1×10^9 CFU/mouse/day	High-fat diet-induced colitis in mice	AMPK ↑ NF-κB ↓	[74]
B. longum LC67	1×10^9 CFU/mouse/day	TNBS-induced colitis in mice	NF-κB, MPO ↓	[79]

epithelial barrier induced by DSS, and regulate the inflammatory response [59, 71, 72] (Figure 1).

NF-κB plays a crucial role in a variety of immune and inflammatory reactions in the intestine. It can participate in the induction and regulation of the related gene expression [75]. Studies have found that TNF-α acts through the activation of TNF receptors. This activation triggers a series of intracellular events that result in the activation of the transcription factor NF-κB [76]. Its activation level is closely related to the severity of intestinal inflammation. Upon receipt of a proinflammatory stimulus, IKK phosphorylates inhibitory kB (IkB) molecules, releases NF-κBp50-p65 heterodimeric protein, migrates to the cell nucleus, and binds to specific kB sites (Figure 1). Genes encoding cytokines and chemokines, cell adhesion molecules, and immune receptors will be activated and transcribed to produce important mediators of inflammation [77, 78]. In an ethanol-induced gastroenteritis study, the oral administration of B. longum LC67 in mice was found to suppress the TNF-α expression and NF-κB activation in mucosal cells, restore the gut microbiota disturbance, and alleviate ethanol-induced GI inflammation [28]. For the mice with high-fat diet- (HFD-) induced obesity, B. longum alleviated colitis by regulating NF-κB activation through the inhibition of the production of harmful substances in the gut microbiota [74]. Further research showed that Bifidobacterium longum could prevent the nuclear localization of NF-κB-p65 in the damaged intestine to a certain extent and increase the expression of NF-κB-p65 in the cytoplasm [62, 79].

Besides, probiotics can secrete tryptophan metabolites to maintain the healthy homeostasis of the host [80]. It has previously been reported that a number of colonizing intestinal bacteria, particularly Gram-negative organisms, can metabolize the amino acid tryptophan to improve health and provide immune protection [81]. Bifidobacterium longum subsp. infantis can produce indole-3-lactic acid (ILA) in its culture medium as an anti-inflammatory molecule (Figure 1). This molecule reduces the IL-8 response after IL-1β stimulus. It interacts with the transcription factor aryl hydrocarbon receptor (AHR) and prevents transcription of the inflammatory cytokine IL-8 [82]. In addition, it could significantly attenuate lipopolysaccharide- (LPS-) induced activation of NF-κB in macrophages and significantly attenuate TNF-alpha and IL-8 in intestinal epithelial cells to protects gut epithelial cells [82, 83]. ILA increased the mRNA expression of the aryl hydrogen receptor- (AhR-) target gene *CYP1A1* and nuclear factor erythroid 2-related factor 2- (Nrf2-) targeted genes glutathione reductase 2 (*GPX2*), superoxide dismutase 2 (*SOD2*), and NADPH dehydrogenase (*NQO1*) and protects gut epithelial cells in culture via activation of the AhR and Nrf2 pathway [83]. Therefore, Bifidobacterium longum can reduce the production of proinflammatory cytokines, inhibit the activation of NF-κB induced by TNF-α, and improve the symptoms of IBD (Figure 1).

3.3. Bifidobacterium longum Enhances the Intestinal Barrier Function. Intact intestinal epithelial cells can ensure the normal intestinal function. It can resist pathogenic microorganisms and harmful substances in the intestinal environment to avoid damage [85]. Good intestinal barrier function requires tight junctions between intestinal epithelial cells [86]. In IBD, the intestinal permeability of the patient's intestinal mucosa increases, and the expression of the tight junction protein (TJP) decreases, which affects the protective function of the intestine and causes inflammation [87]. Inflammation of the intestinal epithelial mucosa will exacerbate this phenomenon, leading to a further decrease in TJP and forming a vicious circle [88]. Studies have shown that feeding mice with B. longum YS108R can improve the mucosal barrier damage induced by DSS and increase the expression of TJP and mucin2 to alleviate colitis [24]. In a similar experiment on 2,4,6-trinitrobenzenesulfonic acid- (TNBS-) induced colitis mice, it was found that the expression of tight junction proteins ZO-1, occluding, and claudin-1 in the colon was significantly reduced, but this phenomenon was alleviated after feeding with B. longum HB5502 [84].

Moreover, some studies have shown that IBD patients were accompanied with weight loss, inflammatory cell infiltration, anemia, decrease of colon length, and damage of

the mucosal layer [89]. Mice with colitis induced by chemical reagents are often used as models to obtain symptoms similar to IBD for research on the treatment of related diseases [90]. Feeding mice with Bifidobacterium longum strains Bif10 and Bif16 could reduce their crypt deformation, diarrhea, etc. The decrease in colon length was alleviated, and the survival rate was improved [59]. Compared to the control group, the infiltration of inflammatory cells in the colon tissue of the B. longum ATCC 1570 treatment group was improved. Crypt alterations and ulceration areas were not observed in the epithelium [71]. Similarly, Bifidobacterium longum LC67 can alleviate TNBS-induced colon shortening in mice. Myeloperoxidase activity is also reduced. At the same time, the edema and destruction of colonic epithelial cells have been relieved, and the expression of the colonic tight junction protein has been restored [79]. In addition, the study found that after treatment with Bifidobacterium longum, the content of SCFAs in the intestinal tract of colitis mice also increased. SCFAs, as metabolites of the gut bacteria, are used by epithelial cells as their primary energy source to promote the health of the GI system [91]. SCFAs improves the expression of connexin in intestinal epithelial cells by enhancing the expression of the *MUC2* gene and activating the AMP-activated protein kinase (AMPK) pathway [92]. Moreover, SCFA has an impact on the population and function of innate immune cells through G-protein coupled receptor signaling and HDAC inhibition and plays an important role in maintaining the intestinal barrier function [91, 93].

3.4. Bifidobacterium longum Regulates Gut Microbiota. In normal individuals, symbiosis exists between the gut microbiota and the host. This harmonious and stable symbiotic relationship can regulate mucosal immunity and prevent the colonization of pathogens in the intestine [94] (Figure 1). Recently, studies have revealed that gut microbiota imbalance played a vital role in the causation of various diseases including IBD [95]. The improvement of gut microbiota composition has been proposed as an effective auxiliary method for the treatment of certain intestinal inflammatory diseases [96]. A previous research has revealed that the gut flora of DSS-treated mice changed significantly in comparison with the control group. The abundance of gut microbiota was reduced, and the bifidobacteria supplementation alleviated the changes of gut microbiota induced by DSS [72]. B. longum YS108R can produce abundant extracellular polymeric substances (EPS). After feeding the fermented milk to DDS-induced colitis mice, it was found that the gut microbiota was adjusted, and pathogenic bacteria such as Enterobacteriaceae were also suppressed [24].

Probiotics in the intestine can release many biologically active peptides, bringing countless benefits to the health of the host [97]. Adhesion to the gastrointestinal tract is considered to be important for bifidobacteria to colonize the human gut and exert their probiotic effects. FimM is a novel surface adhesin that is mainly present in B. longum strains. Under normal circumstances, FimM may block pathogen access to the mucus layer by binding to mucins. Under pathogen invasion, FimM could competitively inhibit pathogen adhesion by binding to fibronectin and fibrinogen [98]. In addition, Bifidobacterium supplementation increased the level of intestinal SCFAs and inhibited the abundances of pathobionts at the genus level. Bacterial components of B. longum fed mice were slightly different from those of healthy mice [59]. As the final products of anaerobic intestinal microbiota fermentation, SCFAs have beneficial effects in accelerating intestinal movement and modulating the body immune system. They can also increase the risk of metabolic syndrome and reduce plasma cholesterol levels [99, 100] (Figure 1). Another study stated that B. longum KACC 91563 exists favorable impacts on increase of the SCFA content in feces of normal dogs and improves the gut microbiota structure [101]. The study found that B. longum BB536 had a synergistic effect with gut microbiota, which is helpful to maintain body homeostasis, and reduce the probability of gastrointestinal and allergic diseases [18]. These results indicated that Bifidobacterium longum had active influences on host healthy through restoring the gut microbiota balance.

4. Application of Bifidobacterium longum in Clinical Trials

Many clinical trials have shown that using Bifidobacterium longum can effectively improve the symptoms of IBD (Table 3). In comparison with placebo-treated subjects, B. longum 536 can improve the clinical symptoms of patients with mild to moderately active UC. 8 weeks after treatment, disease activity and clinical scores are greatly reduced [102]. 12 weeks after treatment with Bifidobacterium longum in patients with IBS-D, proinflammatory cytokines (IL-6, IL-8, and tumor necrosis factor TNF-α) were decreased, and intestinal permeability and gastrointestinal symptoms were improved [103]. Besides, Bifidobacterium longum is also used together with other ingredients to achieve better results. For example, when it was used together with the prebiotic synergy 1, the CD activity and histological score were reduced [104]. Bifidobacterium longum and inulin-oligofructose were provided to UC patients. 4 weeks after treatment, it was found that the expression of β-defensin, IL-1α, and TNF-α genes was decreased. At the same time, rectal biopsy was improved, inflammation was reduced, and epithelial tissue was regenerated [105].

When the probiotic product VSL#3 embodying Bifidobacterium longum was administered to patients with active UC, the symptoms of enteritis were effectively relieved 6 weeks after treatment, and there was no adverse reactions [79]. In 2009, similar results were obtained in experiments on patients with mild to moderate UC, and the disease activity index was also reduced [106]. Fedorak et al. assessed the preventive effect of VSL#3 against postoperative CD recurrence and found that the reduction of the proinflammatory cytokines in the patient's intestinal mucosa was owed to VSL#3, and the postoperative recurrence rate was also remained at a low level [107]. Similarly, the use of VSL#3 was found to be able to alleviate the pain of IBD patients to varying degrees and has great potential for disease treatment [108–111]. Therefore, the results of clinical trials prove that the use of Bifidobacterium longum alone or in combination

Table 3: Clinical evidence for B. longum with IBD.

Strains	Number of patients (age)	Length of treatment	Dose	Effect	Ref.
B. longum 536	56 (31-58 years old)	8 weeks	$2-3\times10^{11}$ CFU/day	Clinical remission UC disease activity index ↓	[102]
B. longum ES1	16 (16-65 years old)	12 weeks	1×10^{9} CFU/day	Proinflammatory cytokines ↓ Improved intestinal permeability	[103]
B. longum and synergy 1	35 (18-79 years old)	6 months	4×10^{11} CFU/day	CD activity ↓ TNF-α ↓	[104]
B. longum and inuli	18 (24-67 years old)	4 weeks	4×10^{11} CFU/day	Inflammatory parameters ↓	[105]
VSL #3	147 (26-52 years old)	12 weeks	7.2×10^{12} CFU/day	Induction of remission in mild-to-moderate UC	[106]
VSL #3	119 (25-49 years old)	9 months	1.8×10^{10} CFU/day	Inflammatory cytokine levels ↓	[107]
VSL #3	131 (33-62 years old)	8 weeks	3.6×10^{9} CFU/day	Clinical scores in UC ↓	[109]
B. longum 536	12 (28-45 years old)	1 months	4×10^{9} CFU/day	Improvement of gut microbiota	[112]

with other probiotics can effectively improve the symptoms of IBD patients. Bifidobacterium longum can be used as an effective preventive or auxiliary treatment for IBD.

5. Future Perspectives of Bifidobacterium longum-Associated Therapy in IBD

In the past decades, the use of genetic engineering and biological engineering to express proteins or polypeptides with specific functions using bifidobacteria as vectors has become a new therapeutic method [113, 114]. Bifidobacterium is an excellent candidate for the development of living vectors for the production and delivery of heterologous proteins on mucosal surfaces. Bifidobacterium longum, which is a probiotic, can be colonized in the intestine for a long time, and it is immune tolerant to the human body. In the case of long-term use, it will not cause rejection by the human body [115]. However, compared to the use of a single bacterial agent, the effect of using a composite bacterial agent is more significant. The optimal dose and treatment time of the bacterial agent in the course of use and its molecular mechanism of action have not yet been determined. In addition, probiotic preparations take a long time to be effective [116]. In the treatment of severe acute inflammatory bowel disease, chemical drugs and surgical treatment are still the first choice [117]. Therefore, the above issues will be the focus of future research.

6. Conclusions

Bifidobacterium longum is a symbiotic bacterium existed in the human gastrointestinal tract. Both animal and clinical trials have found and demonstrated that Bifidobacterium longum had preventive and protective impacts on IBD. Bifidobacterium longum can change the structure of the gut microbiota, induce and regulate immune responses, and reduce the expression of inflammatory cytokines and ROS in the intestine. Besides, it can also maintain the normal intestinal barrier function by increasing the expression of the TJP protein. Therefore, Bifidobacterium longum has great potential and can be used as a prevention, replacement, or adjuvant treatment for IBD.

Conflicts of Interest

The authors declare that there is no conflict of interest to report.

Acknowledgments

This study was supported by the Fundamental Research Funds for the Central Universities (Project No. FRF-BR-19-003B and FRF-BR-20-03B).

References

[1] A. N. Ananthakrishnan, "Epidemiology and risk factors for IBD," *Nature Reviews. Gastroenterology & Hepatology*, vol. 12, no. 4, pp. 205–217, 2015.

[2] S. C. Ng, H. Y. Shi, N. Hamidi et al., "Worldwide incidence and prevalence of inflammatory bowel disease in the 21st century: a systematic review of population-based studies," *The Lancet*, vol. 390, no. 10114, pp. 2769–2778, 2017.

[3] G. G. Kaplan, "The global burden of IBD: from 2015 to 2025," *Nature Reviews Gastroenterology & Hepatology*, vol. 12, no. 12, pp. 720–727, 2015.

[4] D. Parada Venegas, M. K. de la Fuente, G. Landskron et al., "Short chain fatty acids (SCFAs)-mediated gut epithelial and immune regulation and its relevance for inflammatory bowel diseases," *Frontiers in Immunology*, vol. 10, 2019.

[5] S. Fourie, D. Jackson, and H. Aveyard, "Living with Inflammatory Bowel Disease: A review of qualitative research studies," *International Journal of Nursing Studies*, vol. 87, pp. 149–156, 2018.

[6] W. J. Sandborn, B. G. Feagan, C. Marano et al., "Subcutaneous golimumab induces clinical response and remission in patients with moderate-to-severe ulcerative colitis," *Gastroenterology*, vol. 146, no. 1, pp. 85–95, 2014.

[7] M. A. Mijan and B. O. Lim, "Diets, functional foods, and nutraceuticals as alternative therapies for inflammatory bowel disease: present status and future trends," *World Journal of Gastroenterology*, vol. 24, no. 25, pp. 2673–2685, 2018.

[8] Y. Wang, C. E. Parker, B. G. Feagan, and J. K. Macdonald, "Oral 5-aminosalicylic acid for maintenance of remission in ulcerative colitis," *Cochrane Database of Systematic Reviews*, vol. 5, 2016.

[9] C. Rousseaux, B. Lefebvre, L. Dubuquoy et al., "Intestinal antiinflammatory effect of 5-aminosalicylic acid is dependent on peroxisome proliferator-activated receptor-γ," *Journal of Experimental Medicine*, vol. 201, no. 8, pp. 1205–1215, 2005.

[10] J. Plaza-Díaz, F. J. Ruiz-Ojeda, L. M. Vilchez-Padial, and A. Gil, "Evidence of the anti-inflammatory effects of probiotics and synbiotics ini chronic diseases," *Nutrients*, vol. 9, no. 6, p. 555, 2017.

[11] F. Bottacini, D. van Sinderen, and M. Ventura, "Omics of bifidobacteria: research and insights into their health-promoting activities," *Biochemical Journal*, vol. 474, no. 24, pp. 4137–4152, 2017.

[12] A. O'Callaghan and D. van Sinderen, "Bifidobacteria and their role as members of the human gut microbiota," *Frontiers in Microbiology*, vol. 7, 2016.

[13] F. Turroni, S. Duranti, C. Milani, G. A. Lugli, D. van Sinderen, and M. Ventura, "Bifidobacterium bifidum: a key member of the early human hut microbiota," *Microorganisms*, vol. 7, no. 11, p. 544, 2019.

[14] S. Arboleya, C. Watkins, C. Stanton, and R. P. Ross, "Gut bifidobacteria populations in human health and aging," *Frontiers in Microbiology*, vol. 7, no. 1204, 2016.

[15] C. C. Zhang, Z. M. Yu, J. X. Zhao, H. Zhang, Q. X. Zhai, and W. Chen, "Colonization and probiotic function of *Bifidobacterium longum*," *Journal of Functional Foods*, vol. 53, pp. 157–165, 2019.

[16] M. Zhang, L. Zhou, S. Zhang et al., "*Bifidobacterium longum* affects the methylation level of forkhead box P3 promoter in 2, 4, 6-trinitrobenzenesulphonic acid induced colitis in rats," *Microbial Pathogenesis*, vol. 110, pp. 426–430, 2017.

[17] E. Thursby and N. Juge, "Introduction to the human gut microbiota," *Biochemical Journal*, vol. 474, no. 11, pp. 1823–1836, 2017.

[18] C. B. Wong, T. Odamaki, and J.-z. Xiao, "Beneficial effects of *Bifidobacterium longum* subsp. *longum* BB536 on human health: Modulation of gut microbiome as the principal action," *Journal of Functional Foods*, vol. 54, pp. 506–519, 2019.

[19] D. Liang, R. K.-K. Leung, W. Guan, and W. W. Au, "Involvement of gut microbiome in human health and disease: brief overview, knowledge gaps and research opportunities," *Gut Pathogens*, vol. 10, no. 1, p. 3, 2018.

[20] Y. Gu, G. Zhou, X. Qin, S. Huang, B. Wang, and H. Cao, "The potential role of gut mycobiome in irritable bowel syndrome," *Frontiers in Microbiology*, vol. 10, 2019.

[21] T. Zuo and S. C. Ng, "The gut microbiota in the pathogenesis and therapeutics of inflammatory bowel disease," *Frontiers in Microbiology*, vol. 9, 2018.

[22] K. Wang, Z. Wan, A. Ou et al., "Monofloral honey from a medical plant,Prunella Vulgaris, protected against dextran sulfate sodium-induced ulcerative colitisviamodulating gut microbial populations in rats," *Food & Function*, vol. 10, no. 7, pp. 3828–3838, 2019.

[23] A. Vich Vila, F. Imhann, V. Collij et al., "Gut microbiota composition and functional changes in inflammatory bowel disease and irritable bowel syndrome," *Science Translational Medicine*, vol. 10, no. 472, article eaap8914, 2018.

[24] S. Yan, B. Yang, R. P. Ross et al., "*Bifidobacterium longum* subsp. *longum* YS108R fermented milk alleviates DSS induced colitis via anti-inflammation, mucosal barrier maintenance and gut microbiota modulation," *Journal of Functional Foods*, vol. 73, p. 104153, 2020.

[25] B. Sanchez, S. Delgado, A. Blanco-Miguez, A. Lourenco, M. Gueimonde, and A. Margolles, "Probiotics, gut microbiota, and their influence on host health and disease," *Molecular Nutrition & Food Research*, vol. 61, no. 1, 2017.

[26] A. Sarkar, S. M. Lehto, S. Harty, T. G. Dinan, J. F. Cryan, and P. W. J. Burnet, "Psychobiotics and the manipulation of bacteria-gut-brain signals," *Trends in Neurosciences*, vol. 39, no. 11, pp. 763–781, 2016.

[27] T. Ma, H. Jin, L.-Y. Kwok, Z. Sun, M.-T. Liong, and H. Zhang, "Probiotic consumption relieved human stress and anxiety symptoms possibly via modulating the neuroactive potential of the gut microbiota," *Neurobiology of Stress*, vol. 14, article 100294, 2021.

[28] W. G. Kim, H. I. Kim, E. K. Kwon, M. J. Han, and D. H. Kim, "Lactobacillus plantarumLC27 andBifidobacterium longumLC67 mitigate alcoholic steatosis in mice by inhibiting LPS-mediated NF-κB activation through restoration of the disturbed gut microbiota," *Food & Function*, vol. 9, no. 8, pp. 4255–4265, 2018.

[29] B. Chugh and A. Kamal-Eldin, "Bioactive compounds produced by probiotics in food products," *Current Opinion in Food Science*, vol. 32, pp. 76–82, 2020.

[30] S. Chen, G. Huang, W. Liao et al., "Discovery of the bioactive peptides secreted by *Bifidobacterium* using integrated MCX coupled with LC -MS and feature-based molecular networking," *Food Chemistry*, vol. 347, article 129008, 2021.

[31] A. Sánchez and A. Vázquez, "Bioactive peptides: a review," *Food Quality and Safety*, vol. 1, no. 1, pp. 29–46, 2017.

[32] M. Chichlowski, N. Shah, J. L. Wampler, S. S. Wu, and J. A. Vanderhoof, "Bifidobacterium longum subspecies infantis (B. infantis) in pediatric nutrition: current state of knowledge," *Nutrients*, vol. 12, no. 6, p. 1581, 2020.

[33] J. L. Zhao, X. J. Cai, W. Gao et al., "Prussian blue nanozyme with multienzyme activity reduces colitis in mice," *ACS Applied Materials & Interfaces*, vol. 10, no. 31, pp. 26108–26117, 2018.

[34] G. Pizzino, N. Irrera, M. Cucinotta et al., "Oxidative stress: harms and benefits for human health," *Oxidative Medicine and Cellular Longevity*, vol. 2017, Article ID 8416763, 13 pages, 2017.

[35] D. D. Eichele and K. K. Kharbanda, "Dextran sodium sulfate colitis murine model: an indispensable tool for advancing our understanding of inflammatory bowel diseases pathogenesis," *World Journal of Gastroenterology*, vol. 23, no. 33, pp. 6016–6029, 2017.

[36] B. Chami, N. J. J. Martin, J. M. Dennis, and P. K. Witting, "Myeloperoxidase in the inflamed colon: a novel target for treating inflammatory bowel disease," *Archives of Biochemistry and Biophysics*, vol. 645, pp. 61–71, 2018.

[37] Z. Gu, Y. Liu, S. Hu et al., "Probiotics for alleviating alcoholic liver injury," *Gastroenterology Research and Practice*, vol. 2019, Article ID 9097276, 8 pages, 2019.

[38] S. V. Rana, S. Sharma, K. K. Prasad, S. K. Sinha, and K. Singh, "Role of oxidative stress & antioxidant defence in ulcerative colitis patients from North India," *Indian Journal of Medical Research*, vol. 139, pp. 568–571, 2014.

[39] Z. W. Liu, Z. P. Ren, J. Zhang et al., "Role of ROS and nutritional antioxidants in human diseases," *Frontiers in Physiology*, vol. 9, 2018.

[40] F. A. Abrantes, B. B. Nascimento, M. E. R. Andrade et al., "Treatment withBifidobacterium longum51A attenuates intestinal damage and inflammatory response in experimental colitis," *Beneficial Microbes*, vol. 11, no. 1, pp. 47–57, 2020.

[41] E. K. Kwon, G. D. Kang, W. K. Kim, M. J. Han, and D. H. Kim, "*Lactobacillus plantarum* LC27 and *Bifidobacterium longum* LC67 simultaneously alleviate ethanol-induced gastritis and hepatic injury in mice," *Journal of Functional Foods*, vol. 38, pp. 389–398, 2017.

[42] Y. S. Wang, Z. F. Fang, Q. X. Zhai et al., "Supernatants of Bifidobacterium longum and Lactobacillus plantarum strains exhibited antioxidative effects on A7R5 cells," *Microorganisms*, vol. 9, no. 2, p. 452, 2021.

[43] F. Zuo, R. Yu, M. Xiao et al., "Transcriptomic analysis of *Bifidobacterium longum* subsp. *longum* BBMN68 in response to oxidative shock," *Scientific Reports*, vol. 8, no. 1, article 17085, 2018.

[44] Q. Guo, S. Li, Y. Xie et al., "The NAD^+-dependent deacetylase, *Bifidobacterium longum* Sir2 in response to oxidative stress by deacetylating SigH (σ^H) and FOXO3a in *Bifidobacterium longum* and HEK293T cell respectively," *Free Radical Biology and Medicine*, vol. 108, pp. 929–939, 2017.

[45] G. Huang, H. Pan, Z. Zhu, and Q. Li, "The complete genome sequence of *Bifidobacterium longum* LTBL16, a potential probiotic strain from healthy centenarians with strong antioxidant activity," *Genomics*, vol. 112, no. 1, pp. 769–773, 2020.

[46] O. Carmel-Harel and G. Storz, "Roles of the glutathione- and thioredoxin-dependent reduction systems in the Escherichia coli and Saccharomyces cerevisiae responses to oxidative stress," *Annual Review of Microbiology*, vol. 54, no. 1, pp. 439–461, 2000.

[47] M. Xiao, P. Xu, J. Y. Zhao et al., "Oxidative stress-related responses of Bifidobacterium longum subsp. longum BBMN68 at the proteomic level after exposure to oxygen," *Microbiology*, vol. 157, no. 6, pp. 1573–1588, 2011.

[48] T. Zeller and G. Klug, "Thioredoxins in bacteria: functions in oxidative stress response and regulation of thioredoxin genes," *Naturwissenschaften*, vol. 93, no. 6, pp. 259–266, 2006.

[49] M. Kitade, Y. Ogura, I. Monno, and D. Koya, "Sirtuins and type 2 diabetes: role in inflammation, oxidative stress, and mitochondrial function," *Frontiers in Endocrinology*, vol. 10, 2019.

[50] B. Reinert, *Friendly tenants in the human gut: The genome of B. longum*, Genome News Network, 2002, 2021, http://www.genomenewsnetwork.org/articles/10_02/bifido.shtml.

[51] M. Choi, Y. Lee, N. K. Lee et al., "Immunomodulatory effects by Bifidobacterium longum KACC 91563 in mouse splenocytes and macrophages," *Journal of Microbiology and Biotechnology*, vol. 29, no. 11, pp. 1739–1744, 2019.

[52] C. Tang, R. X. Ding, J. Sun, J. Liu, J. Kan, and C. H. Jin, "The impacts of natural polysaccharides on intestinal microbiota and immune responses - a review," *Food & Function*, vol. 10, no. 5, pp. 2290–2312, 2019.

[53] D. I. Jang, A. H. Lee, H. Y. Shin et al., "The role of tumor necrosis factor alpha (TNF-α) in autoimmune disease and current TNF-α inhibitors in therapeutics," *International Journal of Molecular Sciences*, vol. 22, no. 5, p. 2719, 2021.

[54] K. Passelli, O. Billion, and F. Tacchini-Cottier, "The impact of neutrophil recruitment to the skin on the pathology induced by Leishmania infection," *Frontiers in Immunology*, vol. 12, no. 446, 2021.

[55] S. G. Tangye, C. S. Ma, R. Brink, and E. K. Deenick, "The good, the bad and the ugly – T_{FH} cells in human health and disease," *Nature Reviews. Immunology*, vol. 13, no. 6, pp. 412–426, 2013.

[56] L. Zhao, H. Wu, A. Zhao et al., "The in vivo and in vitro study of polysaccharides from a two-herb formula on ulcerative colitis and potential mechanism of action," *Journal of Ethnopharmacology*, vol. 153, no. 1, pp. 151–159, 2014.

[57] T. Zhang, J. Jiang, J. Liu et al., "MK2 is required for neutrophil-derived ROS production and inflammatory bowel disease," *Frontiers in Medicine*, vol. 7, 2020.

[58] J. Pott, A. M. Kabat, and K. J. Maloy, "Intestinal epithelial cell autophagy is required to protect against TNF- induced apoptosis during chronic colitis in mice," *Cell Host & Microbe*, vol. 23, no. 2, pp. 191–202.e4, 2018.

[59] S. Singh, R. Bhatia, P. Khare et al., "Anti-inflammatory *Bifidobacterium strains* prevent dextran sodium sulfate induced colitis and associated gut microbial dysbiosis in mice," *Scientific Reports*, vol. 10, no. 1, 2020.

[60] N. Sato, M. Yuzawa, M. I. Aminul et al., "Evaluation of porcine intestinal epitheliocytes as an in vitro immunoassay system for the selection of probiotic bifidobacteria to alleviate inflammatory bowel disease," *Probiotics and Antimicrobial Proteins*, vol. 13, no. 3, pp. 824–836, 2021.

[61] C. W. MacPherson, P. Shastri, O. Mathieu, T. A. Tompkins, and P. Burguiere, "Genome-wide immune modulation of TLR3-mediated inflammation in intestinal epithelial clls differs between single and multi-strain probiotic combination," *Plos One*, vol. 12, no. 1, article e0169847, 2017.

[62] P. Martorell, B. Alvarez, S. Llopis et al., "Heat-treated Bifidobacterium longum CECT-7347: a whole-cell postbiotic with antioxidant, anti-inflammatory, and gut-barrier protection properties," *Antioxidants*, vol. 10, no. 4, p. 536, 2021.

[63] R. Nowarski, R. Jackson, N. Gagliani et al., "Epithelial IL-18 equilibrium controls barrier function in colitis," *Cell*, vol. 163, no. 6, pp. 1444–1456, 2015.

[64] G. Bevivino and G. Monteleone, "Advances in understanding the role of cytokines in inflammatory bowel disease," *Expert Review of Gastroenterology & Hepatology*, vol. 12, no. 9, pp. 907–915, 2018.

[65] A. Saxena, F. Lopes, and D. M. McKay, "Reduced intestinal epithelial mitochondrial function enhances in vitro interleukin-8 production in response to commensal Escherichia coli," *Inflammation Research*, vol. 67, no. 10, pp. 829–837, 2018.

[66] V. Lohrasbi, M. Abdi, A. Asadi et al., "The effect of improved formulation of chitosan-alginate microcapsules of *Bifidobacteria* on serum lipid profiles in mice," *Microbial Pathogenesis*, vol. 149, article 104585, 2020.

[67] M. Sichetti, S. De Marco, R. Pagiotti, G. Traina, and D. Pietrella, "Anti-inflammatory effect of multistrain probiotic formulation (*L. rhamnosus*, *B. lactis* and *B. longum*)," *Nutrition*, vol. 53, pp. 95–102, 2018.

[68] M. Li, B. van Esch, G. T. M. Wagenaar, J. Garssen, G. Folkerts, and P. A. J. Henricks, "Pro- and anti-inflammatory effects of short chain fatty acids on immune and endothelial cells," *European Journal of Pharmacology*, vol. 831, pp. 52–59, 2018.

[69] T. Ulven, "Short-chain free fatty acid receptors FFA2/GPR43 and FFA3/GPR41 as new potential therapeutic targets," *Front Endocrinol*, vol. 3, 2012.

[70] S. A. Amin, N. Adhikari, and T. Jha, "Structure-activity relationships of HDAC8 inhibitors: non-hydroxamates as anticancer agents," *Pharmacological Research*, vol. 131, pp. 128–142, 2018.

[71] L. S. Celiberto, R. Bedani, N. N. Dejani et al., "Effect of a probiotic beverage consumption (Enterococcus faecium CRL 183 and Bifidobacterium longum ATCC 15707) in rats with chemically induced colitis," *Plos One*, vol. 12, no. 4, p. e0175935, 2017.

[72] S. Yan, B. Yang, J. C. Zhao et al., "A ropy exopolysaccharide producing strainBifidobacterium longumsubsp.longumYS108R alleviates DSS-induced colitis by maintenance of the mucosal barrier and gut microbiota modulation," *Food & Function*, vol. 10, no. 3, pp. 1595–1608, 2019.

[73] A. K. S. Silva, T. R. N. Silva, J. R. Nicoli, L. M. C. Vasquez-Pinto, and F. S. Martins, "In vitroevaluation of antagonism, modulation of cytokines and extracellular matrix proteins byBifidobacteriumstrains," *Letters in Applied Microbiology*, vol. 67, no. 5, pp. 497–505, 2018.

[74] H. in Kim, J. K. Kim, J. Y. Kim, S. E. Jang, M. J. Han, and D. H. Kim, "*Lactobacillus plantarum* LC27 and *Bifidobacterium longum* LC67 simultaneously alleviate high-fat diet-induced colitis, endotoxemia, liver steatosis, and obesity in mice," *Nutrition Research*, vol. 67, pp. 78–89, 2019.

[75] T. Liu, L. Zhang, D. Joo, and S.-C. Sun, "NF-κB signaling in inflammation," *Signal Transduction and Targeted Therapy*, vol. 2, no. 1, article 17023, 2017.

[76] D. C. de Oliveira, A. A. Hastreiter, A. S. Mello et al., "The effects of protein malnutrition on the TNF-RI and NF-κB expression via the TNF-α signaling pathway," *Cytokine*, vol. 69, no. 2, pp. 218–225, 2014.

[77] M. F. Neurath, C. Becker, and K. Barbulescu, "Role of NF-κB in immune and inflammatory responses in the gut," *Gut*, vol. 43, no. 6, pp. 856–860, 1998.

[78] P. Viatour, M. P. Merville, V. Bours, and A. Chariot, "Phosphorylation of NF-κB and IκB proteins: implications in cancer and inflammation," *Trends in Biochemical Sciences*, vol. 30, no. 1, pp. 43–52, 2005.

[79] S. E. Jang, J. J. Jeong, J. K. Kim, M. J. Han, and D. H. Kim, "Simultaneous amelioratation of colitis and liver injury in mice by *Bifidobacterium longum* LC67 and *Lactobacillus plantarum* LC27," *Scientific Reports*, vol. 8, no. 1, p. 7500, 2018.

[80] T. Sakurai, T. Odamaki, and J. Z. Xiao, "Production of indole-3-lactic acid by bifidobacterium strains isolated fromhuman infants," *Microorganisms*, vol. 7, no. 9, p. 340, 2019.

[81] H. M. Roager and T. R. Licht, "Microbial tryptophan catabolites in health and disease," *Nature Communications*, vol. 9, no. 1, p. 3294, 2018.

[82] D. Meng, E. Sommella, E. Salviati et al., "Indole-3-lactic acid, a metabolite of tryptophan, secreted by *Bifidobacterium longum* subspecies *infantis* is anti-inflammatory in the immature intestine," *Pediatric Research*, vol. 88, no. 2, pp. 209–217, 2020.

[83] A. M. Ehrlich, A. R. Pacheco, B. M. Henrick et al., "Indole-3-lactic acid associated with Bifidobacterium-dominated microbiota significantly decreases inflammation in intestinal epithelial cells," *BMC Microbiology*, vol. 20, no. 1, p. 357, 2020.

[84] X. H. Chen, Y. Fu, L. L. Wang, W. Qian, F. Zheng, and X. H. Hou, "Bifidobacterium longum and VSL3 ® amelioration of TNBS-induced colitis associated with reduced HMGB1 and epithelial barrier impairment," *Developmental and Comparative Immunology*, vol. 92, pp. 77–86, 2019.

[85] W. Strober, I. Fuss, and P. Mannon, "The fundamental basis of inflammatory bowel disease," *The Journal of Clinical Investigation*, vol. 117, no. 3, pp. 514–521, 2007.

[86] C. Vanderpool, F. Yan, and B. D. Polk, "Mechanisms of probiotic action: implications for therapeutic applications in inflammatory bowel diseases," *Inflammatory Bowel Diseases*, vol. 14, no. 11, pp. 1585–1596, 2008.

[87] A. Buckley and J. R. Turner, "Cell biology of tight junction barrier regulation and mucosal disease," *Cold Spring Harbor Perspectives in Biology*, vol. 10, no. 1, 2018.

[88] L.-M. Weber, A. Fischer, S. Scholz, D. Metzke, and D. C. Baumgart, "Impact of proinflammatory cytokines and mesalamine on the expression of the tight junction protein claudin-1 in intestinal epithelial cells," *Gastroenterology*, vol. 152, no. 5, p. S740, 2017.

[89] I. Schoultz and Å. Keita, "Cellular and molecular therapeutic targets in inflammatory bowel disease-focusing on intestinal barrier function," *Cells*, vol. 8, no. 2, p. 193, 2019.

[90] S. Wirtz, V. Popp, M. Kindermann et al., "Chemically induced mouse models of acute and chronic intestinal inflammation," *Nature Protocols*, vol. 12, no. 7, pp. 1295–1309, 2017.

[91] Y. Fattahi, H. R. Heidari, and A. Y. Khosroushahi, "Review of short-chain fatty acids effects on the immune system and cancer," *Food Bioscience*, vol. 38, 2020.

[92] S. Ghosh, C. S. Whitley, B. Haribabu, and V. R. Jala, "Regulation of intestinal barrier function by microbial metabolites," *Cellular and Molecular Gastroenterology and Hepatology*, vol. 11, no. 5, pp. 1463–1482, 2021.

[93] E. S. Chambers, T. Preston, G. Frost, and D. J. Morrison, "Role of gut microbiota-generated short-chain fatty acids in metabolic and cardiovascular health," *Current Nutrition Reports*, vol. 7, no. 4, pp. 198–206, 2018.

[94] K. Wang, X. Jin, Q. Li et al., "Propolis from different geographic origins decreases intestinal inflammation and bacteroidesspp. Populations in a model of DSS-induced colitis," *Molecular Nutrition & Food Research*, vol. 62, no. 17, article 1800080, 2018.

[95] I. Khan, N. Ullah, L. J. Zha et al., "Alteration of gut microbiota in inflammatory bowel disease (IBD): cause or consequence? IBD treatment targeting the gut microbiome," *Pathogens*, vol. 8, no. 3, p. 126, 2019.

[96] C. C. Evans, K. J. LePard, J. W. Kwak et al., "Exercise prevents weight gain and alters the gut microbiota in a mouse model of high fat diet-induced obesity," *Plos One*, vol. 9, no. 3, p. e92193, 2014.

[97] M. E. Sanders, D. J. Merenstein, G. Reid, G. R. Gibson, and R. A. Rastall, "Probiotics and prebiotics in intestinal health and disease: from biology to the clinic," *Nature Reviews Gastroenterology & Hepatology*, vol. 16, no. 10, pp. 605–616, 2019.

[98] Y. Xiong, Z. Y. Zhai, Y. Q. Lei, B. B. Xiao, and Y. L. Hao, "A novel major pilin subunit protein FimM is involved in adhesion of Bifidobacterium longum BBMN68 to intestinal epithelial cells," *Frontiers in Microbiology*, vol. 11, 2020.

[99] R. Hemalatha, A. C. Ouwehand, M. T. Saarinen, U. V. Prasad, K. Swetha, and V. Bhaskar, "Effect of probiotic supplementation on total lactobacilli, bifidobacteria and short chain fatty acids in 2–5-year-old children," *Microbial Ecology in Health and Disease*, vol. 28, no. 1, article 1298340, 2017.

[100] W. S. Song, H. G. Park, S. M. Kim et al., "Chemical derivatization-based LC-MS/MS method for quantitation of gut microbial short-chain fatty acids," *Journal of Industrial and Engineering Chemistry*, vol. 83, pp. 297–302, 2020.

[101] H. E. Park, Y. J. Kim, M. Kim et al., "Effects of Queso Blanco cheese containing *Bifidobacterium longum* KACC 91563 on fecal microbiota, metabolite and serum cytokine in healthy beagle dogs," *Anaerobe*, vol. 64, p. 102234, 2020.

[102] H. Tamaki, H. Nakase, S. Inoue et al., "Efficacy of probiotic treatment withBifidobacterium longum 536for induction of remission in active ulcerative colitis: a randomized, double-blinded, placebo-controlled multicenter trial," *Digestive Endoscopy*, vol. 28, no. 1, pp. 67–74, 2016.

[103] G. P. Caviglia, A. Tucci, R. Pellicano et al., "Clinical response and changes of cytokines and zonulin levels in patients with diarrhoea-predominant irritable bowel syndrome treated with Bifidobacterium Longum ES1 for 8 or 12 weeks: a preliminary report," *Journal of Clinical Medicine*, vol. 9, no. 8, p. 2353, 2020.

[104] H. Steed, G. T. Macfarlane, K. L. Blackett et al., "Clinical trial: the microbiological and immunological effects of synbiotic consumption - a randomized double-blind placebo-controlled study in active Crohn's disease," *Alimentary Pharmacology & Therapeutics*, vol. 32, no. 7, pp. 872–883, 2010.

[105] E. Furrie, S. Macfarlane, A. Kennedy et al., "Synbiotic therapy (Bifidobacterium longum/synergy 1) initiates resolution of inflammation in patients with active ulcerative colitis: a randomised controlled pilot trial," *Gut*, vol. 54, no. 2, pp. 242–249, 2005.

[106] A. Sood, V. Midha, G. K. Makharia et al., "The probiotic preparation, VSL3 induces remission in patients with mild-to- moderately active ulcerative colitis," *Clinical Gastroenterology and Hepatology*, vol. 7, no. 11, pp. 1202–1209.e1, 2009.

[107] R. N. Fedorak, B. G. Feagan, N. Hotte et al., "The probiotic VSL3 has anti-inflammatory effects and could reduce endoscopic recurrence after surgery for Crohn's disease," *Clinical Gastroenterology and Hepatology*, vol. 13, no. 5, pp. 928–935.e2, 2015.

[108] E. Miele, F. Pascarella, E. Giannetti, L. Quaglietta, R. N. Baldassano, and A. Staiano, "Effect of a probiotic preparation (VSL#3) on induction and maintenance of remission in children with ulcerative colitis," *The American Journal of Gastroenterology*, vol. 104, no. 2, pp. 437–443, 2009.

[109] A. Tursi, G. Brandimarte, A. Papa et al., "Treatment of relapsing mild-to-moderate ulcerative colitis with the probiotic VSL#3 as adjunctive to a standard pharmaceutical treatment: a double-blind, randomized, placebo-controlled study," *The American Journal of Gastroenterology*, vol. 105, no. 10, pp. 2218–2227, 2010.

[110] A. Tursi, G. Brandimarte, G. M. Giorgetti, G. Forti, M. E. Modeo, and A. Gigliobianco, "Low-dose balsalazide plus a high-potency probiotic preparation is more effective than balsalazide alone or mesalazine in the treatment of acute mild-to-moderate ulcerative colitis," *Medical Science Monitor*, vol. 10, no. 11, pp. PI126–PI131, 2004.

[111] R. Bibiloni, R. N. Fedorak, G. W. Tannock et al., "VSL#3 probiotic-mixture induces remission in patients with active ulcerative colitis," *The American Journal of Gastroenterology*, vol. 100, no. 7, pp. 1539–1546, 2005.

[112] M. Toscano, R. De Grandi, L. Stronati, E. De Vecchi, and L. Drago, "Effect ofLactobacillus rhamnosusHN001 and *Bifidobacterium longum* BB536 on the healthy gut microbiota composition at phyla and species level: a preliminary study," *World Journal of Gastroenterology*, vol. 23, no. 15, pp. 2696–2704, 2017.

[113] A. Mauras, F. Chain, A. Faucheux et al., "A new Bifidobacteria Expression SysTem (BEST) to produce and deliver interleukin-10 in Bifidobacterium bifidum," *Frontiers in Microbiology*, vol. 9, 2018.

[114] N. S. Dosoky, L. S. May-Zhang, and S. S. Davies, "Engineering the gut microbiota to treat chronic diseases," *Applied Microbiology and Biotechnology*, vol. 104, no. 18, pp. 7657–7671, 2020.

[115] M. Ventura, F. Turroni, and D. van Sinderen, "Chapter 4 - Bifidobacteria of the Human Gut: Our Special Friends," in *Diet-Microbe Interactions in the Gut*, K. Tuohy and D. Rio, Eds., pp. 41–51, Academic Press, San Diego, 2015.

[116] R. Y. Gao, X. H. Zhang, L. S. Huang, R. R. Shen, and H. L. Qin, "Gut microbiota alteration after long-term consumption of probiotics in the elderly," *Probiotics and Antimicrobial Proteins*, vol. 11, no. 2, pp. 655–666, 2019.

[117] M. Kaur, R. L. Dalal, S. Shaffer, D. A. Schwartz, and D. T. Rubin, "Inpatient management of inflammatory bowel disease-related complications," *Clinical Gastroenterology and Hepatology*, vol. 18, no. 6, pp. 1346–1355, 2020.

Hindawi
Journal of Immunology Research
Volume 2021, Article ID 8286189, 13 pages
https://doi.org/10.1155/2021/8286189

Research Article

RNA-seq and *In Vitro* Experiments Reveal the Protective Effect of Curcumin against 5-Fluorouracil-Induced Intestinal Mucositis via IL-6/STAT3 Signaling Pathway

Xuan-ying Wang,[1] Bo Zhang,[2] Yi Lu,[3] Lu Xu,[2] Yi-jie Wang,[1] Bi-yu Cai,[1] and Qing-hua Yao [2]

[1]*Second Clinical Medical College, Zhejiang Chinese Medical University, Hangzhou, Zhejiang Province 310053, China*
[2]*Department of Integrated Traditional Chinese and Western Medicine, The Cancer Hospital of the University of Chinese Academy of Sciences (Zhejiang Cancer Hospital), Institute of Basic Medicine and Cancer (IBMC), Chinese Academy of Sciences, Hangzhou, Zhejiang Province 310022, China*
[3]*Department of Clinical Nutrition, The Cancer Hospital of the University of Chinese Academy of Sciences (Zhejiang Cancer Hospital), Institute of Basic Medicine and Cancer (IBMC), Chinese Academy of Sciences, Hangzhou, Zhejiang Province 310022, China*

Correspondence should be addressed to Qing-hua Yao; yaoqh@zjcc.org.cn

Received 23 April 2021; Accepted 10 July 2021; Published 21 July 2021

Academic Editor: Kai Wang

Although first-line chemotherapy drugs, including 5-fluorouracil (5-FU), remain one of the major choice for cancer treatment, the clinical use is also accompanied with dose-depending toxicities, such as intestinal mucositis (IM), in cancer patients undergoing treatment. IM-induced gastrointestinal adverse reactions become frequent reason to postpone chemotherapy and have negative impacts on therapeutic outcomes and prognosis. Various studies have evidenced the anticancer role of curcumin in many cancers; except for this effect, studies also indicated a protective role of curcumin in intestinal diseases. Therefore, in this study, we investigated the effect of curcumin on inflammation, intestinal epithelial cell damage in an IM model. 5-FU was used to induce the model of IM in intestinal epithelial cells, and curcumin at different concentrations was administrated. The results showed that curcumin efficiently attenuated 5-FU-induced damage to IEC-6 cells, inhibited the levels of inflammatory cytokines, attenuated the 5-FU-induced inhibition on cell viability, and displayed antiapoptosis effect on IEC-6 cells. Further RNA-sequencing analysis and experiment validation found that curcumin displays its protective effect against 5-FU-induced IM in intestinal epithelial cells by the inhibition of IL-6/STAT3 signaling pathway. Taken together, these findings suggested that curcumin may be provided as a therapeutic agent in prevention and treatment of chemotherapy-induced IM.

1. Introduction

Chemotherapy remains one of the major strategies for cancer treatment, with the ability of inhibiting cancer cell growth and metastasis to a certain extent. But there are also some unavoidable problems occurring during the treatment [1]. Intestinal mucositis (IM) is a major adverse effect induced by chemotherapeutic agents, such as 5-fluorouracil (5-FU), in cancer patients undergoing treatment [2]. 5-FU is a commonest first-line systemic chemotherapy drug used to fight against numerous types of cancers, particularly colorectal cancer [3–5]. But the use of 5-FU in colorectal cancer patients is often accompanied by alimentary system injury through the activation of inflammation response and toxicity to intestinal mucosa and intestinal epithelial cell, thus resulting in IM [6, 7]. A series of gastrointestinal reactions, including vomiting, diarrhea, indigestion, ulceration, and loss of appetite, are the main clinical manifestations of IM [8]. Approximately 5 ~ 15% of the patients suffered from IM worldwide, which is a frequent reason to postpone chemotherapy and a cause of mortality in chemotherapy patients [2]. Current management options for IM mainly focused

on supportive care. Thus, curative or preventative medicines are unmet in order to reduce or eliminate the severity of IM symptoms induced by chemotherapy.

Chemotherapy-induced IM is mainly characterized by destruction of the intestinal mucosal barrier. The intestinal epithelial cell is a critical part to maintain the homeostasis of the intestinal mucosal barrier. 5-FU acts anticancer effect by its cytotoxicity, inhibiting DNA synthesis of not only tumor cells but also normal cells, especially the sensitive intestinal epithelial cell of the intestinal mucosal barrier [9]. In addition, 5-FU activates a diverse range of proinflammatory pathways to excessive release proinflammatory cytokines, such as TNF-α and IL-6, culminating in histopathological damages in the intestinal mucosa [10]. Therefore, inflammation is a key event in IM, and many studies also focus on preventing 5-FU-induced IM through the regulation of inflammation and related signals.

Curcumin is a well-known dietary polyphenol found from *Curcuma longa L.* (turmeric), a perennial herb belonging to the family Zingiberaceae. It has been used as a traditional medicine for over 2,000 years in China and India [11]. Abundant studies have indicated the beneficial role of curcumin against various chronic diseases, including various types of cancers, diabetes, cardiovascular, pulmonary, neurological, and autoimmune diseases [12]. Particularly, the ability of curcumin to target multiple pathways makes its effect on cancer have been studied mostly [13]. Except for its anticancer effect, studies also indicated a protective role of curcumin in alimentary system. Curcumin can protect human intestinal epithelial cell from inflammatory damage and cell apoptosis induced by IFN-γ, indicated the preventive role of curcumin in intestinal damage [14]. Zhang et al. also report that curcumin displays a protective role in intestinal inflamed rat, and this effect is realized by inhibiting cell apoptosis and JAK/STAT pathways [15].

However, up to date, reports about the protective effects and under mechanism of curcumin against 5-FU-induced IM are less known. Therefore, in this study, we investigated the effect of curcumin on intestinal epithelial cell damage and inflammation induced by 5-FU. The discovered protective properties of curcumin in this study may provide a possible option in prevention and treatment 5-FU-induced IM.

2. Material and Methods

2.1. Cell Culture. The rat intestinal epithelial cell line IEC-6 was obtained from the iCell Bioscience Inc. (Shanghai, China). Cells were cultured in Dulbecco's modified eagle media (DMEM) supplemented with 10% fetal bovine serum (FBS), 100 U/mL penicillin, and 100 μg/mL streptomycin. Cells were maintained at 37°C in a humidified incubator with 5% CO2. The culture medium was changed twice a week.

2.2. Plasmid Construction and Cell Transfection. STAT3 overexpressed plasmid and IL-6 overexpressed plasmid were obtained from Shanghai Genchem Co., LTD (China). IEC-6 cells were transfected with these plasmids following the manufacturer's instructions of Lipofectamine 2000 (Invitrogen, USA), and pcDNA vector was transfected as matched negative control (NC).

2.3. Cell Treatment. IEC-6 cells were divided into the following groups in this study: 5-FU group: IEC-6 cells were incubated with 5-FU at a concentration of 50 mg/mL for 24 h; 5-FU + curcumin group: cells were incubated with 5-FU at a concentration of 50 mg/mL for 24 h and then further incubated with curcumin at different concentrations (5, 10, and 20 μmol/L); 5-FU + curcumin + STAT3 group: STAT3 overexpressed plasmid transfected IEC-6 cells were incubated with 5-FU for 24 h, with curcumin at 10 μmol/L for another 24 h; and 5-FU + curcumin + IL-6 group: IEC-6 cells firstly transfected with IL-6 overexpressed plasmid, and then, cells were incubated with 5-FU and curcumin at 10 μmol/L for another 24 h. Control group IEC-6 cells were incubated with PBS instead.

2.4. CCK-8 Cell Viability Assessment. Briefly, IEC-6 cells were seeded into 96 plates and allowed to adhere for 24 h. Then, the medium was substituted with 5-FU diluted in DMEM or a new medium as control alone for 24 h. Afterwards, curcumin at different concentrations was added into the medium and coincubated with IEC-6 cells for another 24 or 48 h. Subsequently, CCK-8 solution (10 μL) was added into each well, and the optical density (OD) value was then measured using a microplate reader (Molecular Devices, USA).

2.5. Colony Formation Assay. After adhesion, IEC-6 cells were treated with 5-FU plus curcumin; cells were trypsinised and plated into 6 well plates for routinely incubation for 14 days. After that, the colonies were fixed with 4% paraformaldehyde and further stained with 0.1% crystal violet. Then, the colonies in each group were counted.

2.6. Flow Cytometry Assay. The Annexin-V-FITC/Propidium Iodide (PI) Apoptosis Detection Kit (CoWin Biosciences, China) was used to detect the cell apoptosis. Treated IEC-6 cells were seeded into 6 well plates. The cells were allowed to adhere and washed by PBS twice. Then, they were collected at a density of 1×10^6 cells per well and ringed with 500 μL of binding buffer. After removed, the supernatant and resuspended in binding buffer (200 μL), 5 μL Annexin V-FITC, and 10 μL PI solution were added into the plates and incubated for 15 min in the dark. Followed by the readdition of binding buffer (300 μL), the cell apoptosis was assessed by a flow cytometer (Beckman coulter, USA).

2.7. TUNEL Staining Assay. TUNEL staining assay was performed to stain apoptotic cells and detect cell apoptosis. The staining of the treated IEC-6 cells was performed using a TUNEL cell death detection kit (Sangon Biotech, China) according to the manufacturer's instructions. After staining and washing with PBS, cell nuclei were further stained with DAPI solution. The TUNEL positive cells were photographed using an inverted fluorescence microscope (Nikon, Japan), and the TUNEL positive cells were analyzed.

2.8. Wound Healing for Cellular Migration. Migration ability of IEC-6 cells was analyzed using wound healing assay. The

IEC-6 cells were seeded in a 6-well plate, allowed to adherent, and then treated with the indicated regent. A pipette tip was allowed to draw a line along the ruler at the bottom of the plate. Then, cells were allowed to recover in next 24 h under routine incubation. Pictures of the scratches were photographed at 0 h and 24 h, and the cell migration distance was also detected.

2.9. qRT-PCR. Total RNA was isolated according to the instructions of Trizol regent. And the isolated RNA was reversely transcribed into cDNA using a cDNA synthesis kit (CoWin Biosciences, China). The RT-PCR procedure was performed using a SYBR Green qPCR kit (CoWin Biosciences, China) according to the manufacturer's instructions. And the PCR reaction condition was 95°C for 10 min, 95°C for 15 s, and 60°C for 60 s for 40 cycles. The primer sequences of the detected genes were as follows: IL-6, forward primer: 5′-CCAGTTGCCTGGGACT-3′, reverse primer: 5′-TGCCATTGCAACTTTTC-3′; STAT3, forward primer: 5′-GAGCTTGGGGTTCCGACG-3′, reverse primer: 5′-AGGGGTGACCACTGTCTCT-3′; and GAPDH, forward primer: 5′-ATGATTCTACCCACGGCAAG-3′, reverse primer: 5′-CTGGAAGATGGTGATGGGTT-3′.

GAPDH was used as the internal reference, and the mRNA levels was calculated using the $2^{-\triangle\triangle Ct}$ method.

2.10. Western Blotting. The total protein of each group cells was extracted with radio-immunoprecipitation assay (RIPA) lysis buffer, and the extracted protein concentration was detected using a Bradford protein assay (BCA) method (Solarbio, China). Then, the protein samples were separated on 10% sodium dodecyl sulfate-polyacrylamide gel electrophoresis (SDS-PAGE) gels and transferred onto the membranes of nitrocellulose. It was blocked with 5% skim milk at room temperature for 2 h, and then, the membranes were incubated with primary antibody anti-IL-6, anti-Phospho-Stat3, anti-E-cadherin, anti-vimentin, anti-N-cadherin, and anti-β-actin (CST, USA) at 4°C overnight. Subsequently, the membranes were further incubated with the secondary antibody (HRP-conjugated) for 2 h at room temperature. The blots were visualised using an enhanced chemiluminescence (ECL) kit and were photographed. The blot density was quantified, and the densitometry was analyzed using the ImageJ software.

2.11. RNA-Sequencing. The IEC-6 cells from the control, 5-FU, and 5-FU + curcumin (10 μmol/L) groups were harvested for RNA-sequencing analysis. Generally, total RNA from the cells was isolated and purified using TRIzol reagent (Invitrogen, USA). The RNA purity was quantified using NanoDrop ND-1000 (NanoDrop, USA); the RNA integrity was assessed by Bioanalyzer 2100 (Agilent, USA) and confirmed by denaturing agarose gel electrophoresis. Poly (A) RNA was purified from 1 μg total RNA using Dynabeads Oligo (dT)25-61005 (Thermo Fisher, USA). Then, the obtained poly (A) RNA was fragmented into small pieces using Magnesium RNA Fragmentation Module (NEB, cat. e6150, USA) under 94°C for 5-7 min. Then, the RNA fragments were reverse-transcribed for cDNA library preparation and RNA-sequencing following the manufacturer's protocol. The 2 × 150 bp paired-end sequencing (PE150) was performed on an Illumina Novaseq™ 6000 (LC-Bio Technology CO., Ltd., China) following the vendor's recommended protocol.

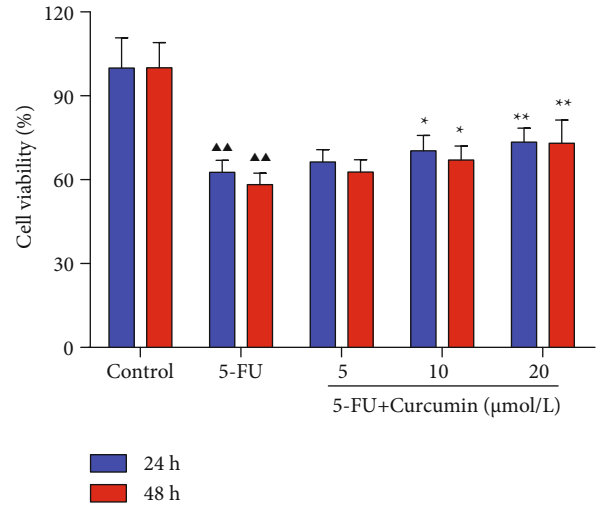

Figure 1: Effect of curcumin on the cell viability of the 5-FU-stimulated IEC-6 cells. IEC-6 cells were stimulated with 5-FU for 24 h and then further treated with curcumin at 5, 10, and 20 μmol/L for 24 h or 48 h. CCK-8 assays were performed to detect the cell viability of each group cells. Data were expressed as mean ± standard error mean (SEM), $^{\blacktriangle\blacktriangle}p$ value < 0.01 vs. control group; $^{*}p$ value < 0.05 vs. 5-FU group; $^{**}p$ value < 0.01 vs. 5-FU group. 5-FU: 5-fluorouracil.

2.12. RNA-Sequencing Data Analysis. The raw reads that contained adaptor contamination were firstly removed using the Cutadapt software (https://cutadapt.readthedocs.io/en/stable/,version:cutadapt-1.9).Then, the HISAT2 software (https://daehwankimlab.github.io/hisat2/,version:hisat2-2.0.4) was used to map reads to the genome, and the mapped reads of each sample were assembled using StringTie (http://ccb.jhu.edu/software/stringtie/,version:stringtie-1.3.4d.Linux_x86_64) with default parameters. After that, transcriptomes from all the samples were merged to reconstruct a comprehensive transcriptome using the gffcompare software (http://ccb.jhu.edu/software/stringtie/gffcompare.shtml,version:gffcompare-0.9.8.Linux_x86_64). After the final transcriptome was generated, StringTie and ballgown (http://www.bioconductor.org/packages/release/bioc/html/ballgown.html) were used to estimate the expression levels of all transcripts and calculate FPKM for mRNAs. The thresholds of differentially expressed genes (DEGs) were |log fold change (FC)| >1 and p value < 0.05 analyzed by R package edgeR (https://bioconductor.org/packages/release/bioc/html/edgeR.html) or DESeq2 (http://www.bioconductor.org/packages/release/bioc/html/DESeq2.html). The analysis of protein-protein intersection (PPI), Gene Ontology (GO) enrichment, and Kyoto Encyclopedia of Genes and Genomes (KEGG) enrichment of the differentially expressed mRNAs was also performed using online tool STRING (https://string.embl.de/) and R package.

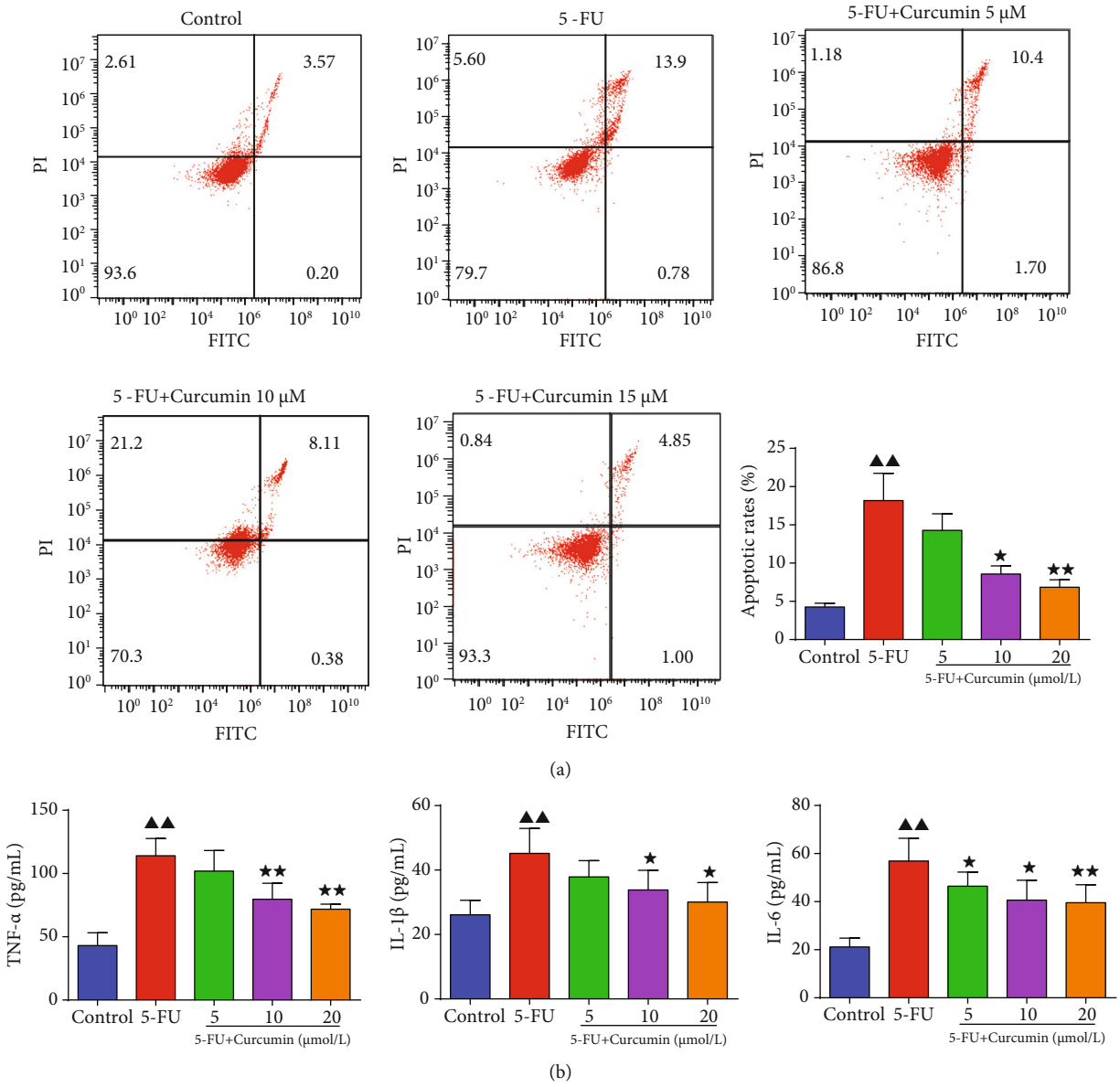

Figure 2: Effect of curcumin on the apoptosis and inflammation of the 5-FU-stimulated IEC-6 cells. IEC-6 cells were stimulated with 5-FU for 24 h and then further treated with curcumin at 5, 10, and 20 μmol/L for 24 h. (a) Flow cytometry assay was performed to detect the cell apoptosis of each group cells. (b) The levels of TNF-α, IL-1β, and IL-6 were detected using ELISA kits. Data were expressed as mean ± standard error mean (SEM), $^{\blacktriangle\blacktriangle}p$ value < 0.01 vs. control group; $^{*}p$ value < 0.05 vs. 5-FU group; $^{**}p$ value < 0.01 vs. 5-FU group. 5-FU: 5-fluorouracil.

2.13. Statistical Analysis. All *in vitro* experiments were repeated 3 times. All data were expressed as mean ± standard error mean (SEM). The statistical analysis was performed using the SPSS software. Differences between unpaired comparisons between two groups were analyzed using the Student's *t*-test. One-way ANOVA followed by Student Newman-Keuls was used for multiple group comparisons.

3. Results

3.1. Effect of Curcumin on the Viability of the 5-FU-Stimulated IEC-6 Cells. As presented in Figure 1, 5-FU stimulation significantly inhibited the viability of intestinal epithelial IEC-6 cells compared to the untreated cells; the cell viability in the 5-FU group was reduced to approximately 60% after exposed to 5-FU for 24 h and 48 h. In the curcumin-treated groups, it could be observed that the coincubation with curcumin at 10 and 20 μmol/L for 24 h and 48 h significantly improved the IEC-6 cell viability, compared with the 5-FU group. And there was no significant difference of the cell viability between 24 h and 48 h of treatment; thus, 24 h of incubation with curcumin was used for subsequent experiments.

3.2. Effect of Curcumin on the Apoptosis of the 5-FU-Stimulated IEC-6 Cells. After stimulated with 5-FU and

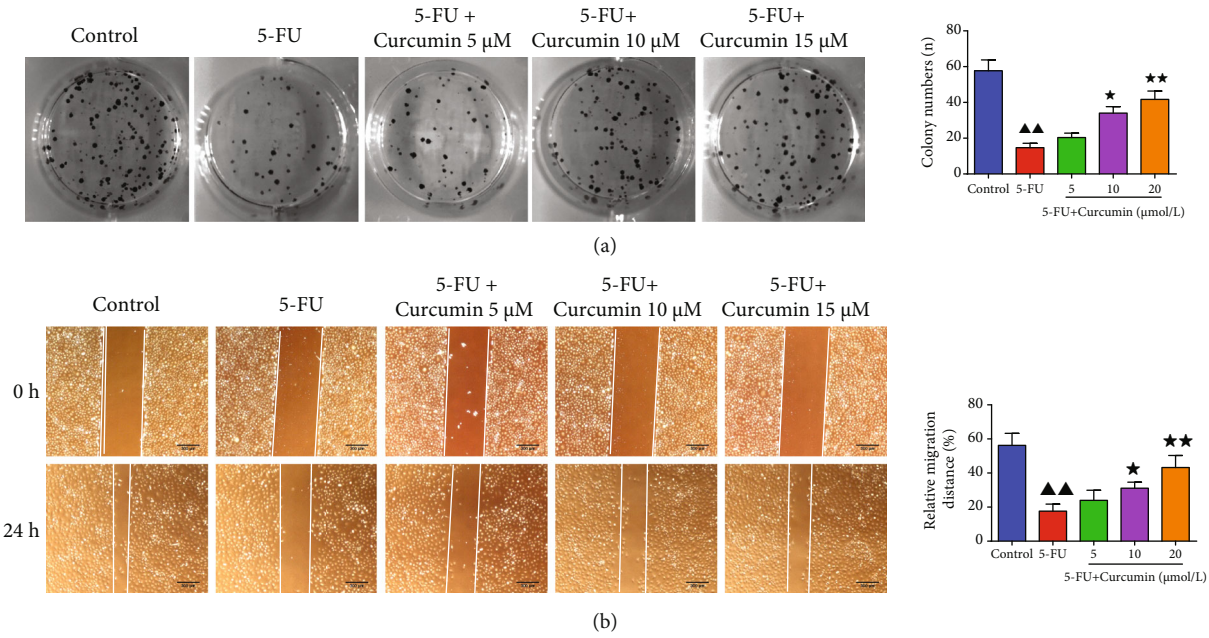

FIGURE 3: Effect of curcumin on the cloning ability and migration of the 5-FU-stimulated IEC-6 cells. IEC-6 cells were stimulated with 5-FU for 24 h and then further treated with curcumin at 5, 10, and 20 μmol/L for 24 h. (a) Colony formation assay was performed to detect the cell colony ability of each group cells. (b) Wound healing assay was performed to detect the cell migration distance from 0 h to 24 h of each group cells. Data were expressed as mean ± standard error mean (SEM), $^{\blacktriangle\blacktriangle}p$ value < 0.01 vs. control group; $^{*}p$ value < 0.05 vs. 5-FU group; $^{**}p$ value < 0.01 vs. 5-FU group. 5-FU: 5-fluorouracil.

treated with curcumin, the cell apoptosis was assessed. Relative results indicated that 5-FU stimulation significantly induced the apoptosis of IEC-6 cells, and the cell apoptotic rates were increased to approximately 18% in 5-FU group cells (Figure 2(a)). However, this proapoptosis effect on IEC-6 cells was reserved after curcumin treatment. It showed that in IEC-6 cells coincubated with curcumin, the cell apoptotic rates were decreased. And the cell apoptotic rates in curcumin 10 and 20 μmol/L groups were below 10%, which also had statistical differences compared to the 5-FU group.

3.3. Effect of Curcumin on the Proinflammatory Cytokine Levels in the 5-FU-Stimulated IEC-6 Cells. The results in Figure 2(b) showed that the levels of TNF-α, IL-1β, and IL-6 were significantly increased in the 5-FU-stimulated IEC-6 cell group compared to the control group. In the curcumin-treated groups, it could be found that the levels of these proinflammatory cytokines were reduced, especially in curcumin 10 and 20 μmol/L group cells.

3.4. Effect of Curcumin on the Cloning Ability and Migration of the 5-FU-Stimulated IEC-6 Cells. Colony formation result in Figure 3(a) showed that the cloning ability of IEC-6 cells was reduced with the pretreatment of 5-FU, displayed by significantly decreased colony numbers in plate. In the curcumin treatment groups, it showed that the colony numbers were increased compared to the 5-FU group, especially in 10 and 20 μmol/L concentrations. Cell migration assessment by wound healing assay (Figure 3(b)) showed that the cell migration viability inhibited by 5-FU was alleviated by curcumin treatment, from 0 h to 24 h. The relative cell migration distance in the curcumin groups was increased compared to the 5-FU group, but the control group cells still had the longest migration distance. Western blotting also detected the migration-related factors, including E-cadherin, vimentin, and N-cadherin. Results in Figure 4 showed that their relative protein levels were changed after 5-FU stimulation, and E-cadherin was decreased, while vimentin and N-cadherin were increased significantly, and after treated with curcumin, their changed expression levels were recovered in a certain extent.

3.5. Effect of Curcumin on the IL-6/STAT3 Signaling in the 5-FU-Stimulated IEC-6 Cells. As previous study indicated that curcumin has regulation effect on IL-6/STAT3 signaling, we also detected the protein expression levels of genes in IL-6/STAT3 signaling pathway. As shown in Figure 4, it could be found that 5-FU exposure activated the expression levels of IL-6 and p-STAT3 in IEC-6 cells. And after curcumin treatment, the expression levels of IL-6 and p-STAT3 were reduced in 5, 10, and 20 μmol/L group cells, indicating the inhibition effect of curcumin on the IL-6/STAT3 signaling in 5-FU-stimulated IEC-6 cells.

3.6. Identification of DEGs in Curcumin-Treated IEC-6 Cells. The IEC-6 cells from the control, 5-FU, and 5-FU + curcumin (10 μmol/L) groups were further collected for RNA-sequencing analysis to identify curcumin-associated genes. According to the thresholds of $p < 0.05$ and $|\log FC| > 1$, a total of 1247 DEGs were selected between the 5-FU and 5-FU + curcumin groups, including 393 upregulated DEGs and 854 downregulated DEGs (Figure 5(a)). The volcano plot

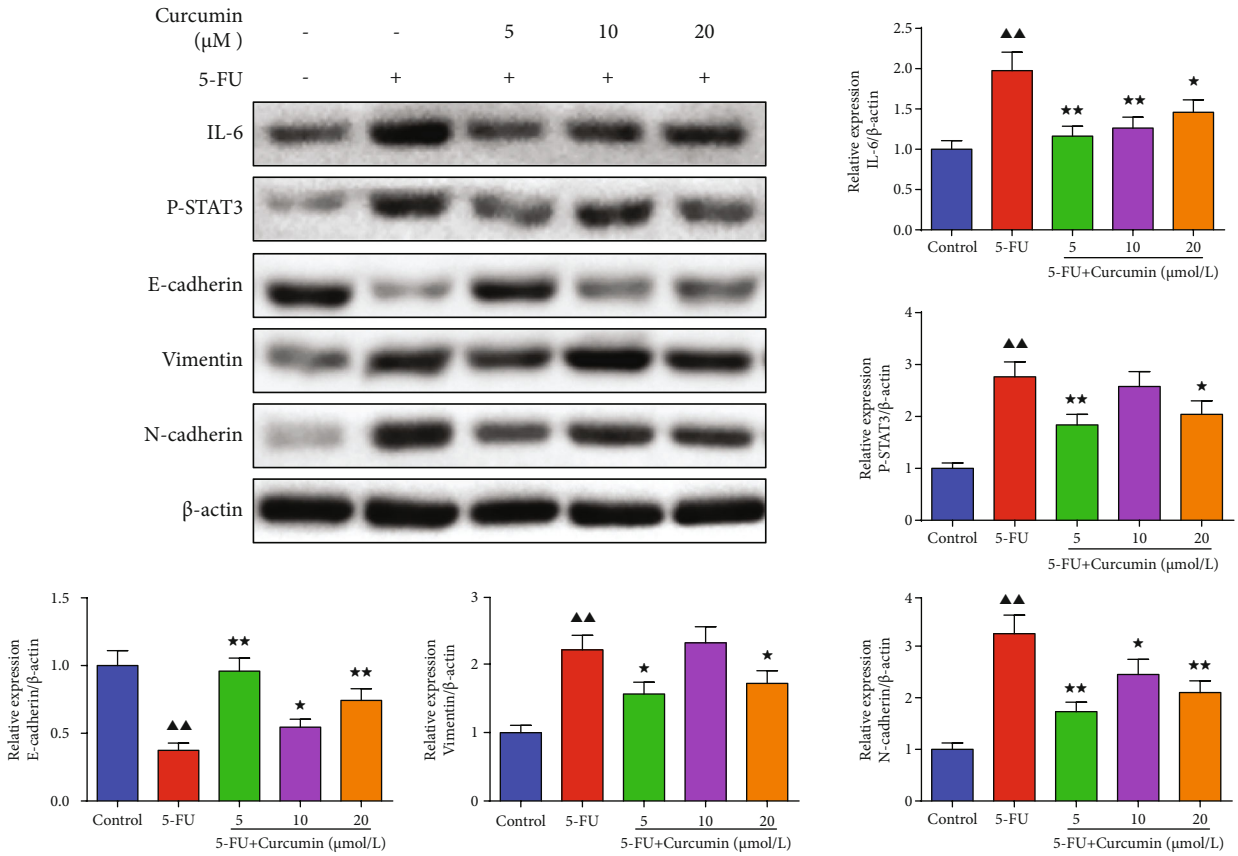

Figure 4: Effect of curcumin on the IL-6/STAT3 signaling in the 5-FU-stimulated IEC-6 cells. Western blotting assay was performed to detect the protein expression levels of E-cadherin, vimentin, N-cadherin, IL-6, and p-STAT3 in each group cells. Data were expressed as mean ± standard error mean (SEM), $^{▲▲}p$ value < 0.01 vs. control group; $^{*}p$ value < 0.05 vs. 5-FU group; $^{**}p$ value <0.01 vs. 5-FU group. 5-FU: 5-fluorouracil.

of the identified DEGs is presented in Figure 5(b). Cluster analysis of the top 100 DEGs in Figure 5(c) showed that these DEGs had significant clustering between the 5-FU and curcumin group cell samples.

3.7. PPI Network Analysis of the DEGs. PPI networks of the upregulated and downregulated DEGs were constructed by the STRING database (Figure 6). A total of 1059 edges and 217 nodes were included in the upregulated DEGs' PPI network (Figure 6(a)). The CXCL10 (degree = 54), IL10 (degree = 51), IRF7 (degree = 49), ISG15 (degree = 43), and MX1 (degree = 43) were selected as key upregulated DEGs in the network because of their high node degree. For the downregulated DEGs' PPI network, there were 675 DEGs mapped into the network, forming 675 nodes and 5112 edges in the network (Figure 6(b)). Also, CDK1 (degree = 111), CCNB1 (degree = 98), IL6 (degree = 98), and CDC20 (degree = 96) were selected as key downregulated DEGs in the network because of their high node degree.

3.8. Functional Enrichment Analysis of the DEGs. GO functional enrichment analysis of the DEGs showed that these DEGs were significantly enriched in biological process terms of regulation of transcription by RNA polymerase II, positive regulation of cell population proliferation, protein phosphorylation, and cell adhesion; in molecular function terms of protein binding, metal ion binding, ATP binding, nucleotide binding, and identical protein binding; and in cellular component terms of cytoplasm, cytosol, extracellular space, extracellular region, endoplasmic reticulum, etc. (Figures 7(a) and 7(b)). KEGG pathway enrichment analysis of the DEGs showed that these DEGs were enriched in pathways including IL-6/STAT3 signaling pathway, pathways in cancer, human papillomavirus infection, herpes simplex virus 1 infection, human immunodeficiency virus 1 infection, human cytomegalovirus, and human T-cell leukemia virus 1 infection (Figure 7(c)).

3.9. Validation of IL-6 and STAT3 Levels in Transfected IEC-6 Cells. After IEC-6 cells were transfected with STAT3 overexpressed plasmid or IL-6 overexpressed plasmid, respectively, the expressions of IL-6 and STAT3 in transfected IEC-6 cells were validated. As shown in Figures 8(a) and 8(b), the mRNA and protein expressions of IL-6 and STAT3 were all significantly higher in transfected cells compared to the control group or vector NC group cells.

3.10. Overexpression of IL-6 and STAT3 Reserved the Effect of Curcumin on 5-FU-Stimulated IEC-6 Cells. Based on the above results, we assumed that curcumin displayed the

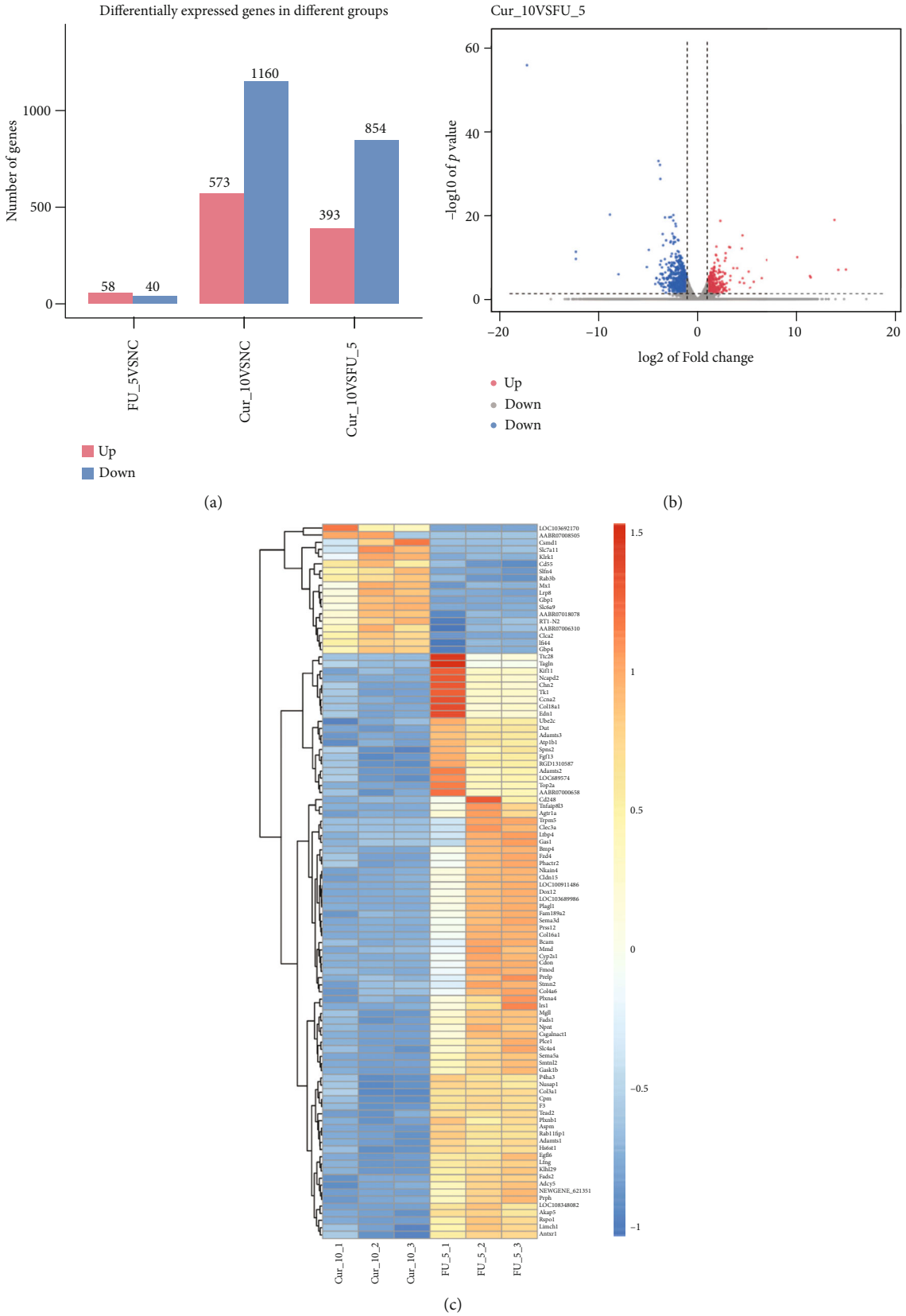

Figure 5: RNA-sequencing and identification of DEGs in curcumin-treated IEC-6 cells. (a) Identification of DEGs between the tested groups according to the thresholds of $p < 0.05$ and $|\log FC| > 1$. (b) Volcano plot of the identified DEGs between the 5-FU and 5-FU + curcumin groups. Blue plot represented downregulated DEGs; red plot represented upregulated DEGs. (c) Cluster analysis of the top 100 DEGs. 5-FU: 5-fluorouracil; Cur: curcumin; DEGs: differentially expressed genes.

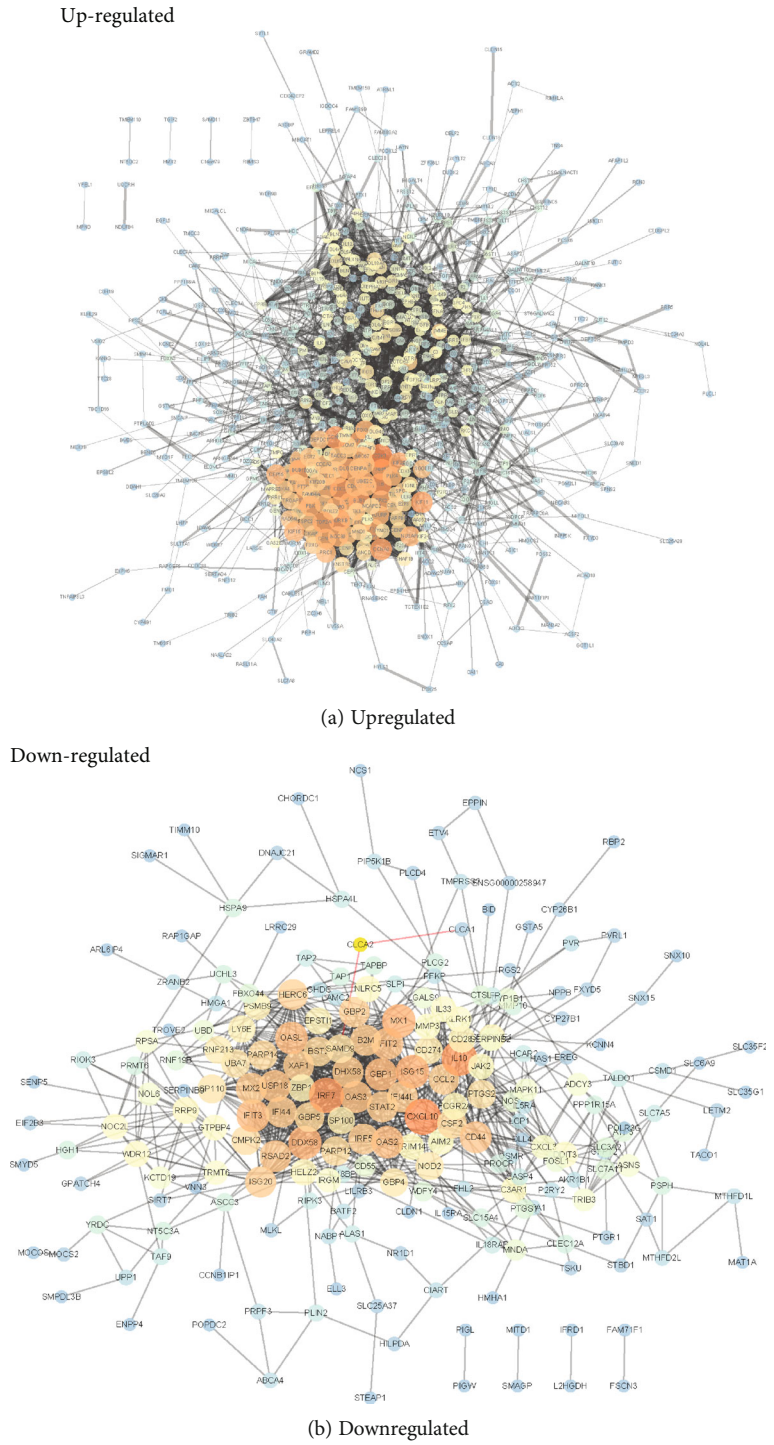

(a) Upregulated

(b) Downregulated

Figure 6: PPI network analysis of the DEGs: (a) PPI network of the upregulated DEGs; (b) PPI network of the downregulated DEGs.

protective effects on IEC-6 cells against 5-FU by IL-6/STAT3 signaling. Then, the influence of IL-6/STAT3 signaling on curcumin in 5-FU-stimulated IEC-6 cells was evaluated. As displayed in Figure 9, the results showed that compared to the 5-FU + curcumin group cells, the protective effects of curcumin on 5-FU-stimuted IEC-6 cells were overturned in IL-6 and STAT3 overexpression transfected cells. Compared to those in the 5-FU + curcumin group cells, overexpression of IL-6 and STAT3 inhibited the colony numbers, increased TUNEL positive cells, and decreased the migration distance. Taken together, these data manifested that curcumin protects against 5-FU-induced intestinal epithelial cell damage via downregulating of IL-6/STAT3 signaling.

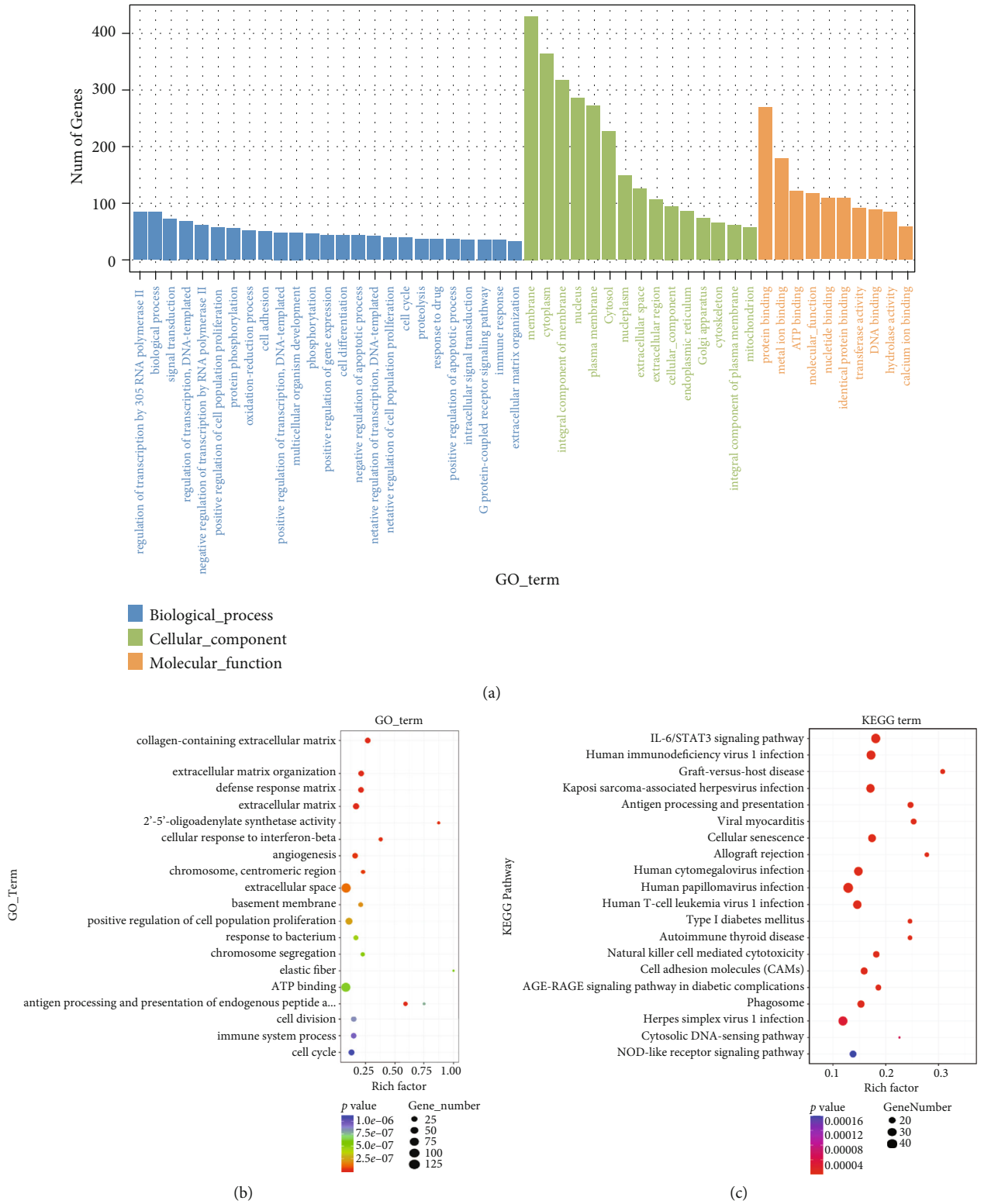

Figure 7: Functional enrichment analysis of the DEGs: (a, b) GO functional enrichment analysis of the DEGs; (c) KEGG pathway enrichment analysis of the DEGs. GO: Gene Ontology; KEGG: Kyoto Encyclopedia of Genes and Genomes.

4. Discussion

5-FU, served as an antimetabolite chemotherapy drug, displays its effect through interrupting DNA synthesis, leading to cell death by proapoptosis. However, the clinical use of 5-FU for the treatment of cancers, including colorectal cancer, is also accompanied with dose-dependent toxicities, such as IM [2, 3]. This adverse effect negatively impacts on

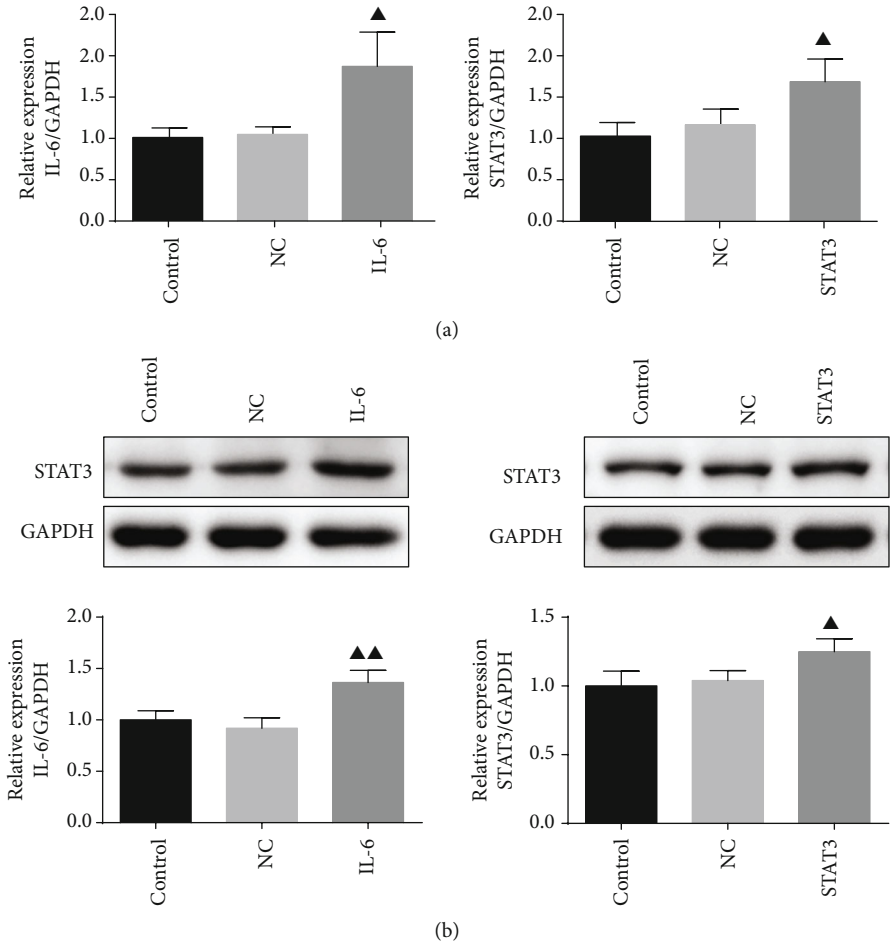

Figure 8: Validation of IL-6 and STAT3 levels in transfected IEC-6 cells. IEC-6 cells were transfected with STAT3 overexpressed plasmid and IL-6 overexpressed plasmid, respectively; the expression of IL-6 and STAT3 in transfected IEC-6 cells was validated by qRT-PCR analysis (a) and western blot assay (b). Data were expressed as mean ± standard error mean (SEM), $^{\blacktriangle}p$ value < 0.05 vs. control group.

therapeutic outcomes and prognosis of cancer patients. In present study, in an *in vitro* model of IM, we demonstrated that curcumin efficiently attenuated cell damage of intestinal epithelial cells exposed to 5-FU. 5-FU caused inhibition on IEC-6 cell viability, colony formation and migration ability, and induced cell apoptosis, which were restored by curcumin treatment.

As a natural product with a wide range properties, curcumin also displays potential on the gastrointestinal system disorders. It is reported to have the ability to suppress the inflammation and improve intestinal barrier function in inflammatory bowel disease [16, 17]. This therapeutic effect may contribute to its anti-inflammatory, antimicrobial, immunomodulatory properties, the modulation of signaling mediators, and tight junctions. Based on abundant preclinical findings, clinical trials assessed the therapy efficacy of curcumin in multiple types of diseases also yielded beneficial data [18]. Moreover, poor bioavailability of curcumin is overcame by in combination with other compounds or as a nanocarrier formulation [19, 20]. In cancer treatment, curcumin is capable of reserving the toxicity induced by chemotherapy drugs, including IM. Sakai et al. reported that curcumin administered can prevent the symptoms of diarrhea induced by 5-FU in mice [21]. In this study, in IEC-6 cells stimulated with 5-FU, our results showed that curcumin efficiently attenuated 5-FU-induced intestinal epithelial cell damage, attenuated 5-FU-induced inhibition on cell viability, and displayed antiapoptosis effect on IEC-6 cells. This antiapoptosis effect on IEC-6 cells was also reported in Ouyang et al.'s study [22]. In the irinotecan-induced intestinal mucosal injury model in nude mice, curcumin was found to attenuate the development of diarrhea and intestinal mucosa damage effectively and also improved cell morphology, inhibited apoptosis, and suppressed oxidative stress in irinotecan-treated IEC-6 cells.

When we further investigated the impact of 5-FU on IEC-6 cells and protective effect of curcumin, relative experiments showed that 5-FU stimulation induced inflammation and damage, while curcumin displayed its protective effect against cell damage through inflammation-related mediators and signaling. Inflammation is a major event in IM; the pathogenesis of IM involves in the interfere of inflammatory mediators, which are mainly over produced by 5-FU or other drug stimulation [2, 23]. In Dark Agouti rat injected with 5-FU, there is a markedly increase of NF-κB, TNF-α, IL-1β, and IL-6 expression in oral mucosa, jejunum, and colon

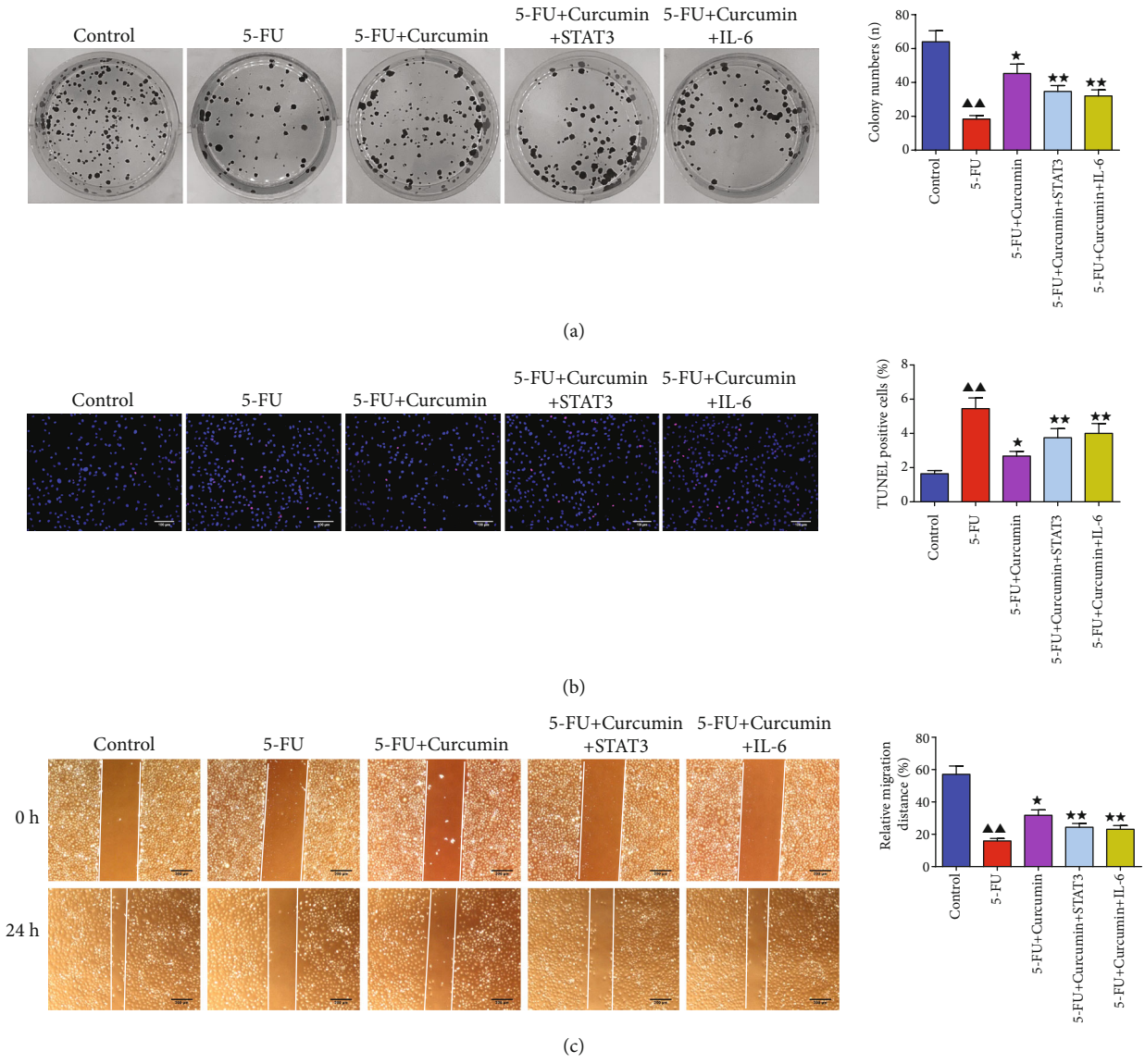

FIGURE 9: Overexpression of IL-6 and STAT3 reserved the effect of curcumin on 5-FU-stimulated IEC-6 cells. (a) Colony formation assay. (b) TUNEL staining. (c) Wound healing assay. Data were expressed as mean ± standard error mean (SEM), ▲▲p value < 0.01 vs. control group; $^{*}p$ value < 0.05 vs. 5-FU group; $^{**}p$ value < 0.01 vs. 5-FU group. 5-FU: 5-fluorouracil.

tissues [10]. A study investigating the impact of 5-FU chemotherapy on gut inflammation showed that in AOM/DSS-induced colorectal cancer model mouse treated with 5FU, significantly elevated expression of intestinal inflammatory genes was found, including TNF-α, MCP-1, NOS2, IL6, IL1-β, and FOXP3 [24]. In this study, ELISA assay and Western blotting results showed that in 5-FU-suppressed IEC-6 cells, the expression levels of TNF-α, IL1-β, IL-6, and STAT3 were increased, indicated the presence of inflammation in intestinal epithelial cells with 5-FU, which contributed to the development of IM. In addition, curcumin treatment suppressed the expression of these mediators.

More importantly, RNA-sequencing analysis in this study identified 393 upregulated DEGs and 854 downregulated DEGs in curcumin-treated IEC-6 cells. KEGG pathway analysis also found that these DEGs were enriched in IL-6/STAT3 signaling. Further experimental validation of IEC-6 cells transfected with IL-6 overexpressed plasmid or STAT3 overexpressed plasmid showed that curcumin protected against intestinal epithelial cell damage via the downregulation of IL-6/STAT3 signaling. IL-6 is a critical mediator stimulated by a variety of cells, including T lymphocytes, epithelial cells, monocytes, macrophages, and tumor cells. Elevated levels of IL-6 are often observed in chemotherapy-induced IM, which closely correlate with intestinal pathophysiological condition and gut homeostasis, including inflammation promoting [25, 26]. And studies focused on reducing symptoms of various intestinal diseases, such as IM, are always accompanied by lower IL-6 level [27–29]. STAT3 is a molecular in STAT family with crucial effects

on cell proliferation, differentiation, migration, and angiogenesis in cancer progression; persistent STAT3 activation is found to promote chronic inflammation, which increases susceptibility of healthy cells to carcinogenesis [30, 31]. When the intestinal mucosa is stimulated, elevated IL-6 can activate the phosphorylation of STAT3 and response to NF-κB, a central mediator of intestinal inflammation, to promote the injury of inflammatory factors to intestinal epithelial cells [32]. Several genome-wide studies on intestinal disorder patients identified variants of STAT3 as a risk factor for diseases development, and the activated expression of STAT3 in intestinal cells, including intestinal epithelial cells, was also detected in inflamed intestinal regions [33, 34]. Therefore, IL-6/STAT3 signaling pathway is important for intestinal homeostasis maintenance, and regulation of this signaling is an approach in treatment of intestinal disorders.

Previous studies also proved the regulation ability of curcumin on IL-6/STAT3 signaling pathway. Curcumin is reported as an inhibitor of p-STAT3, to abrogate the IL-6-induced phosphorylation of STAT3, and inhibits the proliferation and survival of multiple myeloma cells [35]. In psoriasis mice induced by imiquimod, curcumin could improve the pathological injuries of the mouse skin, reduced the expressions of IL-6, p-STAT3, and its downstream proteins. In intestinal disorders including IM, curcumin exerts its anti-inflammatory effects not only by inhibiting NF-κB activation but also contributes to its ability to regulate IL-6/STAT3 signaling. Curcumin is reported to exert therapeutic effects in experimental colitis induced by dextran sulfate sodium (DSS) through blocking STAT3 signaling pathway [36]. Curcumin can alleviate the severity of colitis by suppressing the expression of STAT3, NF-κB, COX-2, and iNOS [37]. Except for the anti-inflammation effect by curcumin in IM, the protective role of curcumin also attributed to maintain intestinal mucosal barrier function and intestinal microbe homeostasis.

In conclusion, the present study used a chemotherapy drug, 5-FU, to induce a model of IM in intestinal epithelial cells; the results showed that curcumin efficiently attenuated 5-FU-induced IEC-6 cell damage and inflammation, attenuated the 5-FU-induced inhibition on cell viability, and displayed antiapoptosis effect on IEC-6 cells. Further RNA-sequencing analysis and experiments also found that curcumin displayed its protective effect against 5-FU-induced IM in intestinal epithelial cells by the inhibition of IL-6/STAT3 signaling pathway. Taken together, these findings suggested that curcumin may be provided as an adjunctive agent in alleviation of chemotherapy-induced IM.

Data Availability

The data used to support the findings of this study are included in this manuscript.

Conflicts of Interest

The authors have declared no conflicts of interest.

Acknowledgments

This work was supported by the National Nature Science Foundation of China (No. 81673813), the Chinese Medicine Research Program of Zhejiang Province (No. 2020ZA018), and the Natural Science Foundation of Zhejiang Province (No. 2021KY569).

References

[1] E. Levy, P. Piedbois, M. Buyse et al., "Toxicity of fluorouracil in patients with advanced colorectal cancer: effect of administration schedule and prognostic factors. Meta-Analysis Group In Cancer," *Journal of Clinical Oncology*, vol. 16, no. 11, pp. 3537–3541, 1998.

[2] R. A. Ribeiro, C. W. Wanderley, D. V. T. Wong et al., "Irinotecan- and 5-fluorouracil-induced intestinal mucositis: insights into pathogenesis and therapeutic perspectives," *Cancer Chemotherapy and Pharmacology*, vol. 78, no. 5, pp. 881–893, 2016.

[3] S. Vodenkova, T. Buchler, K. Cervena, V. Veskrnova, P. Vodicka, and V. Vymetalkova, "5-fluorouracil and other fluoropyrimidines in colorectal cancer: past, present and future," *Pharmacology & Therapeutics*, vol. 206, p. 107447, 2020.

[4] S. E. al-Batran, N. Homann, C. Pauligk et al., "Perioperative chemotherapy with fluorouracil plus leucovorin, oxaliplatin, and docetaxel versus fluorouracil or capecitabine plus cisplatin and epirubicin for locally advanced, resectable gastric or gastro-oesophageal junction adenocarcinoma (FLOT4): a randomised, phase 2/3 trial," *The Lancet*, vol. 393, no. 10184, pp. 1948–1957, 2019.

[5] J. B. Vermorken, E. Remenar, C. van Herpen et al., "Cisplatin, fluorouracil, and docetaxel in unresectable head and neck cancer," *The New England Journal of Medicine*, vol. 357, no. 17, pp. 1695–1704, 2007.

[6] S. Zhang, Y. Liu, D. Xiang et al., "Assessment of dose-response relationship of 5-fluorouracil to murine intestinal injury," *Biomedicine & Pharmacotherapy*, vol. 106, pp. 910–916, 2018.

[7] N. J. Spencer, "Motility patterns in mouse colon: gastrointestinal dysfunction induced by anticancer chemotherapy," *Neurogastroenterology and Motility*, vol. 28, no. 12, pp. 1759–1764, 2016.

[8] Y. Gan, G. Ai, J. Wu et al., "Patchouli oil ameliorates 5-fluorouracil-induced intestinal mucositis in rats via protecting intestinal barrier and regulating water transport," *Journal of Ethnopharmacology*, vol. 250, p. 112519, 2020.

[9] G. Pepe, S. F. Rapa, E. Salviati et al., "Bioactive polyphenols from pomegranate juice reduce 5-fluorouracil-induced intestinal mucositis in intestinal epithelial cells," *Antioxidants*, vol. 9, no. 8, p. 699, 2020.

[10] C. S. Lee, E. J. Ryan, and G. A. Doherty, "Gastro-intestinal toxicity of chemotherapeutics in colorectal cancer: the role of inflammation," *World Journal of Gastroenterology*, vol. 20, no. 14, pp. 3751–3761, 2014.

[11] H. P. Ammon and M. A. Wahl, "Pharmacology of Curcuma longa," *Planta Medica*, vol. 57, no. 1, pp. 1–7, 1991.

[12] Y. Hong, Y. Q. Han, Y. Z. Wang et al., "Paridis Rhizoma Saponins attenuates liver fibrosis in rats by regulating the expression of RASAL1/ERK1/2 signal pathway," *Journal of Ethnopharmacology*, vol. 192, pp. 114–122, 2016.

[13] J. G. Devassy, I. D. Nwachukwu, and P. J. Jones, "Curcumin and cancer: barriers to obtaining a health claim," *Nutrition Reviews*, vol. 73, no. 3, pp. 155–165, 2015.

[14] C. Loganes, S. Lega, M. Bramuzzo et al., "Curcumin anti-apoptotic action in a model of intestinal epithelial inflammatory damage," *Nutrients*, vol. 9, no. 6, p. 578, 2017.

[15] X. Zhang, J. Wu, B. Ye, Q. Wang, X. Xie, and H. Shen, "Protective effect of curcumin on TNBS-induced intestinal inflammation is mediated through the JAK/STAT pathway," *BMC Complementary and Alternative Medicine*, vol. 16, no. 1, p. 299, 2016.

[16] K. Burge, A. Gunasekaran, J. Eckert, and H. Chaaban, "Curcumin and intestinal inflammatory diseases: molecular mechanisms of protection," *International Journal of Molecular Sciences*, vol. 20, no. 8, p. 1912, 2019.

[17] J. Wang, S. S. Ghosh, and S. Ghosh, "Curcumin improves intestinal barrier function: modulation of intracellular signaling, and organization of tight junctions," *American Journal of Physiology. Cell Physiology*, vol. 312, no. 4, pp. C438–C445, 2017.

[18] F. Fallahi, S. Borran, M. Ashrafizadeh et al., "Curcumin and inflammatory bowel diseases: from in vitro studies to clinical trials," *Molecular Immunology*, vol. 130, pp. 20–30, 2021.

[19] M. Moballegh Nasery, B. Abadi, D. Poormoghadam et al., "Curcumin delivery mediated by bio-based nanoparticles: a review," *Molecules*, vol. 25, no. 3, p. 689, 2020.

[20] A. B. Kunnumakkara, C. Harsha, K. Banik et al., "Is curcumin bioavailability a problem in humans: lessons from clinical trials," *Expert Opinion on Drug Metabolism & Toxicology*, vol. 15, no. 9, pp. 705–733, 2019.

[21] H. Sakai, Y. Kai, A. Oguchi et al., "Curcumin inhibits 5-fluorouracil-induced up-regulation of CXCL1 and CXCL2 of the colon associated with attenuation of diarrhoea development," *Basic & Clinical Pharmacology & Toxicology*, vol. 119, no. 6, pp. 540–547, 2016.

[22] M. Ouyang, Z. Luo, W. Zhang et al., "Protective effect of curcumin against irinotecan-induced intestinal mucosal injury via attenuation of NF-κB activation, oxidative stress and endoplasmic reticulum stress," *International Journal of Oncology*, vol. 54, no. 4, pp. 1376–1386, 2019.

[23] R. M. Logan, A. M. Stringer, J. M. Bowen, R. J. Gibson, S. T. Sonis, and D. M. K. Keefe, "Is the pathobiology of chemotherapy-induced alimentary tract mucositis influenced by the type of mucotoxic drug administered?," *Cancer Chemotherapy and Pharmacology*, vol. 63, no. 2, pp. 239–251, 2009.

[24] A. T. Sougiannis, B. N. VanderVeen, R. T. Enos et al., "Impact of 5 fluorouracil chemotherapy on gut inflammation, functional parameters, and gut microbiota," *Brain, Behavior, and Immunity*, vol. 80, pp. 44–55, 2019.

[25] Y. Guo, B. Wang, T. Wang et al., "Biological characteristics of IL-6 and related intestinal diseases," *International Journal of Biological Sciences*, vol. 17, no. 1, pp. 204–219, 2021.

[26] V. Jeffery, A. J. Goldson, J. R. Dainty, M. Chieppa, and A. Sobolewski, "IL-6 signaling regulates small intestinal crypt homeostasis," *Journal of Immunology*, vol. 199, no. 1, pp. 304–311, 2017.

[27] C. B. Polakowski, M. Kato, V. B. Preti, M. E. M. Schieferdecker, and A. C. Ligocki Campos, "Impact of the preoperative use of synbiotics in colorectal cancer patients: a prospective, randomized, double-blind, placebo-controlled study," *Nutrition*, vol. 58, pp. 40–46, 2019.

[28] J. Wang, Y. Pan, Y. Cao, W. Zhou, and J. Lu, "Salidroside regulates the expressions of IL-6 and defensins in LPS-activated intestinal epithelial cells through NF-κB/MAPK and STAT3 pathways," *Iranian Journal of Basic Medical Sciences*, vol. 22, no. 1, pp. 31–37, 2019.

[29] J. Ali, A. U. Khan, F. A. Shah et al., "Mucoprotective effects of Saikosaponin-A in 5-fluorouracil-induced intestinal mucositis in mice model," *Life Sciences*, vol. 239, p. 116888, 2019.

[30] J. H. Lee, C. D. Mohan, S. Basappa et al., "The IκB kinase inhibitor ACHP targets the STAT3 signaling pathway in human non-small cell lung carcinoma cells," *Biomolecules*, vol. 9, no. 12, p. 875, 2019.

[31] C. Y. Loh, A. Arya, A. F. Naema, W. F. Wong, G. Sethi, and C. Y. Looi, "Signal transducer and activator of transcription (STATs) proteins in cancer and inflammation: functions and therapeutic implication," *Frontiers in Oncology*, vol. 9, p. 48, 2019.

[32] B. Dou, W. Hu, M. Song, R. J. Lee, X. Zhang, and D. Wang, "Anti-inflammation of Erianin in dextran sulphate sodium-induced ulcerative colitis mice model via collaborative regulation of TLR4 and STAT3," *Chemico-Biological Interactions*, vol. 324, p. 109089, 2020.

[33] K. Sato, M. Shiota, S. Fukuda et al., "Strong evidence of a combination polymorphism of the tyrosine kinase 2 gene and the signal transducer and activator of transcription 3 gene as a DNA-based biomarker for susceptibility to Crohn's disease in the Japanese population," *Journal of Clinical Immunology*, vol. 29, no. 6, pp. 815–825, 2009.

[34] J. Mudter, B. Weigmann, B. Bartsch et al., "Activation pattern of signal transducers and activators of transcription (STAT) factors in inflammatory bowel diseases," *The American Journal of Gastroenterology*, vol. 100, no. 1, pp. 64–72, 2005.

[35] A. C. Bharti, N. Donato, and B. B. Aggarwal, "Curcumin (diferuloylmethane) inhibits constitutive and IL-6-inducible STAT3 phosphorylation in human multiple myeloma cells," *Journal of Immunology*, vol. 171, no. 7, pp. 3863–3871, 2003.

[36] L. Liu, Y. L. Liu, G. X. Liu et al., "Curcumin ameliorates dextran sulfate sodium-induced experimental colitis by blocking STAT3 signaling pathway," *International Immunopharmacology*, vol. 17, no. 2, pp. 314–320, 2013.

[37] J. Y. Yang, X. Zhong, S. J. Kim et al., "Comparative effects of curcumin and tetrahydrocurcumin on dextran sulfate sodium-induced colitis and inflammatory signaling in mice," *Journal of Cancer Prevention*, vol. 23, no. 1, pp. 18–24, 2018.

Hindawi
Journal of Immunology Research
Volume 2021, Article ID 9957451, 13 pages
https://doi.org/10.1155/2021/9957451

Research Article

Anti-Inflammatory and Healing Activity of the Hydroalcoholic Fruit Extract of Solanum diploconos (Mart.) Bohs

Larissa Benvenutti,[1] Roberta Nunes,[1] Ivonilce Venturi,[1] Silvia Aparecida Ramos,[1] Milena Fronza Broering,[1] Fernanda Capitanio Goldoni,[2] Sarah Eskelsen Pavan,[2] Maria Verônica Dávila Pastor,[2] Angela Malheiros,[1,2] Nara Lins Meira Quintão,[1,2] Elizabeth Soares Fernandes ,[3,4] and José Roberto Santin [1,2]

[1]*Postgraduate Program in Pharmaceutical Science, Universidade do Vale do Itajaí, Rua Uruguai, 458, Itajaí, SC 88302-202, Brazil*
[2]*School of Health Sciences, Biomedicine Course, Universidade do Vale do Itajaí, Rua Uruguai, 458, Itajaí, SC 88302-202, Brazil*
[3]*Programa de Pós-graduação em Biotecnologia Aplicada à Saúde da Criança e do Adolescente, Faculdades Pequeno Príncipe, Av. Iguaçu, 333, Curitiba, PR 80230-020, Brazil*
[4]*Instituto de Pesquisa Pelé Pequeno Príncipe, Av. Silva Jardim, 1632, Curitiba, PR 80250-060, Brazil*

Correspondence should be addressed to Elizabeth Soares Fernandes; elizabeth.fernandes@pelepequenoprincipe.org.br and José Roberto Santin; jrs.santin@univali.br

Received 22 March 2021; Revised 15 June 2021; Accepted 6 July 2021; Published 20 July 2021

Academic Editor: Michael Conlon

Background. *Solanum diploconos* (Mart.) Bohs is a native Brazilian plant belonging to the Solanaceae family, popularly known as "tomatinho do mato" and poorly investigated. Herein, we presented for the first time evidence for the anti-inflammatory and wound healing activities of *S. diploconos* fruit hydroalcoholic extract. *Material and Methods*. *In vitro* fMLP-induced chemotaxis, LPS-induced inflammatory mediator levels (cytokines by ELISA and NO release by Griess reaction), and adhesion molecule expression (CD62L, CD49d, and CD18, by flow-cytometry) were assessed in neutrophils treated with different concentrations of the extract. Inflammation resolution was measured by the efferocytosis assay and the healing activity by *in vivo* and *in vitro* assays. The air pouch model of carrageenan-induced inflammation in Swiss mice was used to investigate the *in vivo* anti-inflammatory effects of the extract. Leukocyte influx (by optical microscopy) and cytokine release were quantified in the pouch exudates. Additionally, the acute and subacute toxic and genotoxic effects of the extract were evaluated. *Results*. *In vitro*, the extract impaired neutrophil chemotaxis and its ability to produce and/or release cytokines (TNFα, IL-1β, and IL-6) and NO upon LPS stimuli ($p < 0.01$). LPS-treated neutrophils incubated with the extract presented increased CD62L expression ($p < 0.01$), indicating a reduced activation. An enhanced efferocytosis of apoptotic neutrophils by macrophages was observed and accompanied by higher IL-10 and decreased TNFα secretion ($p < 0.01$). *In vivo*, similar results were noted, including reduction of neutrophil migration, protein exudation, and cytokine release ($p < 0.01$). Also, the extract increased fibroblast proliferation and promoted skin wound healing ($p < 0.01$). No signs of toxicity or genotoxicity were observed for the extract. *Conclusion*. *S. diploconos* fruit extract is anti-inflammatory by modulating neutrophil migration/activation as well macrophage-dependent efferocytosis and inflammatory mediator release. It also indicates its potential use as a healing agent. Finally, the absence of acute toxic and genotoxic effects reinforces its possible use as medicinal product.

1. Introduction

Inflammation is a physiological response to injury characterized by complex processes which are aimed at restoring tissue homeostasis. Its first stage comprises the quick activation and migration of immune cells to the injury site to prevent the invasion of microorganisms and damage by hazardous substances in the absence of tissue integrity [1]. In this context, neutrophils play an important role, arriving at the site of inflammation in a multistep controlled process which

encompasses marginalization, slow rolling, adhesion, and transendothelial or abluminal migration [2, 3]. All these processes are dependent on the specific interactions between proteins expressed on endothelial cells and leukocytes, such as integrins and selectins [2, 4]. The CD62L selectin is expressed on the neutrophil membrane and mediates its binding to endothelial cell adhesion molecules (P and E-selectins and integrins); it is also responsible for the neutrophil rolling behaviour [3, 5]. On the other hand, integrins such as CD18 and CD49a, are involved in the neutrophil adhesion to the endothelium, allowing its transmigration to the injury site [6].

Once at the injury site, neutrophils carry out an efficient local response, marked by the production of nitric oxide (NO), reactive oxygen species (ROS), and cytokines; release of cytotoxic granular contents; formation of neutrophil extracellular traps; and phagocytosis. Neutrophil migration can become continuous in some cases, contributing to an uncontrolled inflammation, thus, leading to tissue damage and/or loss of function and chronification of the injury [1].

In this context, neutrophil clearance is an important step of the resolution of inflammation and ultimate tissue repair [7]. This process comprises the limitation of neutrophil migration, downregulation of proinflammatory mediators, induction of neutrophil apoptosis, and its subsequent phagocytosis (efferocytosis) by resident macrophages [7, 8]. Following efferocytosis, the macrophages switch from the inflammatory to the anti-inflammatory phenotype, characterized by the release of anti-inflammatory cytokines and growth factors. In turn, these changes contribute towards angiogenesis, wound healing, tissue repair, and homeostasis [7].

Natural products have been used as sources of biological active substances and even of new drugs [9]. The *Solanum* genus comprises approximately 1500 species, making this genus the largest and most complex of the Solanaceae family. It is distributed in temperate and tropical regions, and it presents several classes of compounds such as alkaloids, triterpenes, flavonoids, and saponins [10]. Some compounds found in this genus have toxic effects; therefore, toxicological studies are needed to ensure safe usage [11].

S. diploconos (Mart.) Bohs is a poorly investigated Brazilian native plant, popularly known as "tomatinho-do-mato" which belongs to the same genus of important food crops such as tomato (*S. lycorpersicum*) and potato (*S. tuberosum*). Its fruits are edible and slightly acidic, consumed either *in natura* or as a juice [12]. Despite its consumption as food, the biological activities of *S. diploconos* fruits remain unclear. Phenolic compounds, carotenoids, tocopherols, and ascorbic acid were the main classes of secondary metabolites found in the freeze-dried pulp and peel and in the extract obtained from the whole fruit of *S. diploconos*. Furthermore, the whole fruit extract presented antioxidant actions when assessed *in vitro* against ROS and reactive nitrogen intermediates [13].

Data from the literature indicate a great therapeutic potential for the *Solanum* genus, highlighting the anti-inflammatory activity of extracts [14, 15] and some of the compounds also identified in *S. diploconos* [16], including wound healing activity [17]. In this context, this study was aimed at investigating the anti-inflammatory effects, wound healing activity, and the acute toxicity profile of the hydroalcoholic extract obtained from *S. diploconos* fruits using *in vivo* and *in vitro* protocols.

2. Material and Methods

2.1. Plant Material and Phytochemical Analysis. *S. diploconos* (Mart) Bohs fruits were harvested from Itaiópolis, SC, Brazil (latitude 60° 66′ 27″ S and longitude 70° 68′ 53″ W, elevation: 800.33 m; SisGen protocol A478BBA) in April 2014, and voucher specimens were deposited in the Herbarium Barbosa Rodrigues (HBR55276) and the Herbarium Dr. Roberto Miguel Klein (FURB49359). Whole fresh ripe fruits (peel and pulp with seeds) were ground and subjected to extraction by dynamic maceration with 95% ethanol in the proportion 1 : 10 (*m*/*v*), for 6 h at room temperature (24-28°C). The extract was concentrated and dried under reduced pressure on a rotary evaporator with temperature below 50°C.

The chromatographic analysis was carried out on a HPLC Shimadzu® LC 20-AT system, consisting of a quaternary pump and a Shimadzu SPD-M20A photodiode array detector. A SIL-20A HT autosampler with a Shimadzu CTO-10AS VT column oven equilibrated at 35°C and software LC Solution were used. The chromatographic column used was Phenomenex® C18 (250 × 4.6 mm) with particles of 5 μm. For the method development, different solvent systems were assayed in gradient conditions using acetonitrile (A) and ultrapure water acidified with acetic acid (pH 2.5; B). The chosen gradient was (A : B): 05 : 95 at 0-10 min, 15 : 85 at 10-20 min, 30 : 70 at 20-30 min, 40 : 60 at 30-40 min, 55 : 45 at 40-45 min, and 05 : 95 at 4550 min. The flow rate was 1.0 mL/min. The detection of the compounds was carried out at 320 nm. This method was chosen for the analysis of phenolic compounds as previously established by Ribeiro et al. [13].

2.2. Animals. Experiments were performed in male Swiss mice and female Wistar rats (exclusively for the toxicological evaluation). All animals were obtained from the Central Animal Facility of the Universidade do Vale do Itajaí (UNIVALI) and kept in a climate-controlled room at 22 ± 2°C, under light/dark (12 : 12 h) cycle, with water and food *ad libitum*. All experiments were approved by the local ethics committee (CEUA/UNIVALI: 028/16 and 019/18).

2.3. In Vitro Anti-Inflammatory Effects

2.3.1. Neutrophil Isolation. For this, male Swiss mice received an intraperitoneal (i.p.) injection of 1% sterile oyster glycogen in phosphate-buffered saline (PBS; 3 mL). After 4 h, the animals were culled with an overdose of ketamine (80 mg/kg, i.p.) and xylazine (8 mg/kg, i.p.), and their peritoneal cells were collected by washing the peritoneal cavity with 3 mL of sterile PBS. The number of viable cells (98%) was counted in a Neubauer chamber using a light microscope (Nikon, Japan) by the trypan blue exclusion test.

2.3.2. Lipopolysaccharide-Stimulated Neutrophils. Neutrophils (1×10^6 cells per well) were incubated with RPMI medium (10% foetal bovine serum (FBS)) in the presence or absence of lipopolysaccharide (LPS; 5 μg/mL) and simultaneously treated with *S. diploconos* extract (1, 10, or 100 μg/mL) for 18 h, at 37°C in a 5% CO_2 atmosphere. Then, the supernatant was collected for the subsequent analysis of cytokine and nitrite (NO_2^-) levels. Neutrophil viability was assessed by the trypan blue exclusion test. None of the tested extract concentrations produced cell toxicity (data not shown).

2.3.3. Expression of Adhesion Molecules on Neutrophils. Neutrophils (1×10^6 cells per well) stimulated or not with LPS (5 μg/mL) were coincubated with either vehicle (cell culture medium) or the extract (1, 10, or 100 μg/mL). After 1 h, the cells were collected and incubated with monoclonal anti-CD62L (FITC), anti-CD18 (PE), or anti-CD49d (APC) antibodies in the dark for 20 minutes, at 4°C. Cells were then analysed on an Accuri C6 Flow Cytometer (BD Bioscience), and data from 10,000 events was obtained. The results are expressed as mean fluorescence intensity (MFI) [18].

2.3.4. In Vitro Neutrophil Chemotaxis. Neutrophil chemotaxis was evaluated as described by Nelson et al. [19]. Briefly, neutrophils (1×10^7 cells/mL) treated or not with *S. diploconos* extract (1, 10, or 100 μg/mL, for 1 h) were placed into peripheral wells (10 μL) made in an agarose gel solidified in a Petri dish. The chemotactic factor (N-Formyl-Met-Leu-Phe (fMLP); 0.1 μM, 10 μL) was added to the central well, and the plates were incubated for 4 h, at 37°C and 5% CO_2. After incubation, the number of cells that migrated towards the central well containing fMLP was counted.

2.3.5. Efferocytosis Assay. Macrophages were obtained by washing the mouse medullary cavity with sterile PBS. The cell suspension (1×10^6 cells/well) was incubated in a 24-well plate onto a round glass coverslip at 37°C and 5% CO_2 for up to 2 h to allow macrophage adherence. After this period, the wells were washed three times with sterile PBS to remove nonadherent cells and then, the remaining ones were incubated with *S. diploconos* extract diluted in DMEM (1, 10, or 100 μg/mL). After 1 h, senescent mouse neutrophils (1×10^6 cells) were added to each well and 20 min later, the supernatant was collected for cytokine analysis. The remaining cells on the slides were analysed by microscopy with immersion objective (100x). One hundred macrophages were observed, and the phagocytosis of senescent neutrophils was expressed as the percentage (%) of macrophages containing neutrophils [20].

2.3.6. Cytokine and Nitrite Analysis. The levels of IL-1β, TNFα, IL-6, and IL-10 were analysed in the supernatants obtained from the cell cultures, including those from the efferocytosis assay, or in exudate samples from the air pouch model. One hundred μL of each sample was used for the assays performed in accordance to the manufacturer's instructions (DuoSet R&D Systems, Minneapolis, MN, USA). NO levels were indirectly quantified by the detection of nitrite (NO_2^-) using the Griess reaction [21]. For this, samples (100 μL/well) were incubated for 10 min at 37°C, with 100 μL of Griess reagent (1% sulfanilamide, 0.1% naphthylethylenediamine dihydrochloride in 5% phosphoric acid). The absorbances were then determined at 550 nm. All cytokine results are expressed in picograms per milliliter, and NO levels as micromolar of NO_2^-.

2.4. In Vivo Anti-Inflammatory Effects

2.4.1. In Vivo Leukocyte Migration: Air Pouch Model. Air pouches were produced on the back of the mice as previously described [22, 23]. Briefly, the animals were fasted for 4 h and then orally treated by gavage with *S. diploconos* extract (100 mg/kg, $n = 6$), indomethacin (30 mg/kg, positive control, $n = 6$), or vehicle (PBS; 10 mL/kg; $n = 6$). After 1 h, carrageenan (1%; 3 mL/cavity) was injected directly into the air pouch chamber. Four hours later, a small incision was made in the air pouch. The cavity was washed with 5 mL of PBS, and the inflammatory infiltrate collected for analysis. Total and differential cell counts were performed, and the rest of the exudate was kept for the further quantification of cytokines.

The air pouch lining tissue was collected for histological analysis and preserved in formaldehyde solution until the blades were made. The preparation consisted of the insertion of the tissue fragment into a cassette. The sample then underwent a 1 h dehydration process in increasing concentrations of ethanol (70%, 96%, and absolute ethanol). Subsequently, each sample was placed in xylol followed by paraffin bath. Then, the cassettes containing samples were placed in a microtome where serial sections of 3 or 4 μm were made. The sections were placed onto slides and stained with haematoxylin and eosin. Samples were analysed by microscopy under the 4, 10, and 40x objectives.

2.5. Wound Healing Assessment

2.5.1. In Vitro Scratch Assay. Murine L929 cells were obtained from the Bank of Cells of Rio de Janeiro (Rio de Janeiro, RJ, Brazil) and maintained in DMEM supplemented with 10% FBS, 100 μg/L streptomycin, and 100 IU/mL penicillin, at 37°C in a 5% CO_2 atmosphere. Briefly, L929 cells (5×10^4 cells/mL) were seeded into each well of a 24-well plate and incubated at 37°C with 5% CO_2. After cell confluence, the culture medium was removed and a continuous scratch was made in the medial surface of each well with a 200 μL tip. Then, the wells were washed with PBS to remove cell debris. The remaining cells were incubated with DMEM containing *S. diploconos* fruit extract (1, 10, or 100 μg/mL). The analysis was performed by measuring the scratched area in square millimeter at 0 (immediately after mechanical trauma) and 24 h after incubation with the extract, by microscopy (Olympus CKX 41), using ImageJ1.46r software. The results are expressed as the percent of the coverage area at 24 h in relation to time 0 [24].

2.5.2. In Vivo Wound Healing Assay. For topical application, a semisolid formulation of the *S. diploconos* extract was made. An oil in water (O/W) emulsion-based cream was

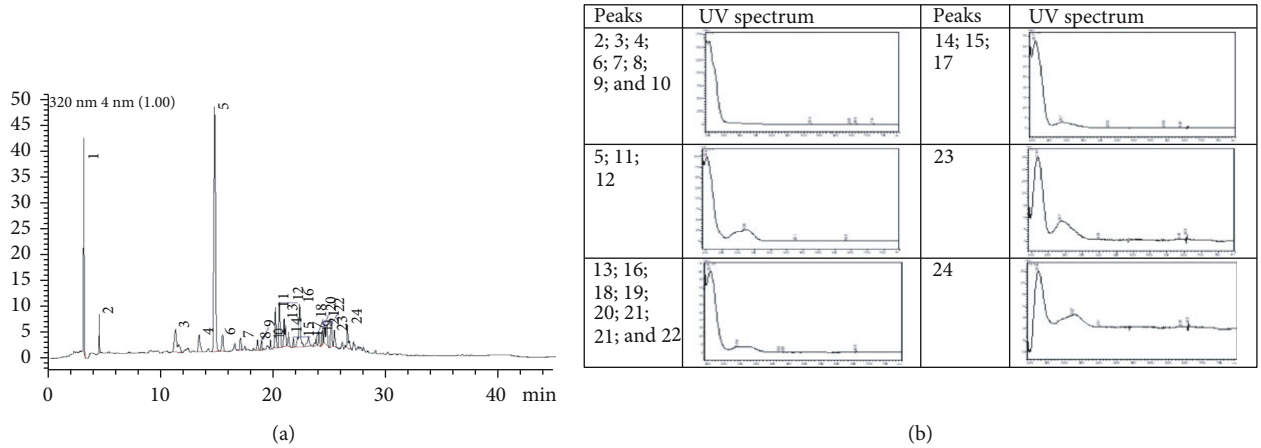

(a) (b)

Figure 1: Chromatogram of the *S. diploconos* fruit extract at $\lambda = 320$ nm (a) and respective UV absorption spectra (b).

prepared by mixing Sepigel 305, vaseline, crodalan, isopropyl myristate, BHT, cetostearyl alcohol, Phenonip®, EDTA, and water with slight warming. The oil-soluble components were dissolved in the oil phase and heated to 75°C. The water-soluble components were dissolved in the aqueous phase and heated to 75°C. After heating, the aqueous phase was added in portions to the oil phase with continuous stirring until cooling took place. Then, the hydroalcoholic extract obtained from *S. diploconos* fruits (1%) was incorporated to the base cream. The formulation was packed in aluminium tubes, with a seal and polypropylene cover.

Mice were divided in two groups: group I (base cream, $n = 6$) and group II (1% *S. diploconos*, $n = 6$). The animals were anaesthetized, and their backs were shaved with an electric clipper. Then, a surgical excision of the skin (1.5 cm of diameter) was made on the dorsal area of each mouse, as previously described by Tonin et al. [25]. The extract was topically applied to each wound (once a day, for 7 days). The wounds were photographed daily with a scale, and the wounded areas were measured and calculated in square millimeter by using the ImageJ1.46r software.

2.6. Toxicity Evaluation

2.6.1. Cytotoxicity Assays. Possible toxic effects of the extract were investigated in L929 cells. For this, the cells were cultured in DMEM (containing 10% FBS, 100 μg/L streptomycin, and 100 IU/mL penicillin) at 37°C in a 5% CO_2 atmosphere and incubated with either *S. diploconos* extract (0.1, 1, 10, or 100 μg/mL) or vehicle (RPMI medium). After 24 h, the cell viability was evaluated by the MTT method [26]. The results are expressed as percent of viable cells in relation to the control (vehicle-treated wells).

2.6.2. Pathophysiological Analysis. In the acute toxicity assay, rats ($n = 5$/group) received either *S. diploconos* extract (2 g/kg) or vehicle (distilled water, 10 mL/kg) by oral route (gavage). The animals were then observed at every 30 min during the first 4 h followed by a daily observation for 14 days. The cumulative weight change was calculated as percent to baseline. At the end of the observation period, all survivors were autopsied. The blood was collected for biochemical (aspartate aminotransferase (AST), alanine aminotransferase (ALT), alkaline phosphatase (ALP), urea, and creatinine) and hematological (total and differential cell, erythrogram, and platelet counts) analysis [27].

In the repeated dose 28-day oral toxicity (subacute) study, female Wistar rats were divided into different groups ($n = 5$/group) and orally treated by gavage with *S. diploconos* extract (30, 100, or 300 mg/kg) or vehicle (distilled water, 10 mL/kg). The extract and vehicle were administered once a day, for 28 days. At the end of the observation period, the macroscopic characteristics of the lungs, kidneys, liver, spleen, and heart were observed. In addition, the blood was collected for analysis of biochemical and hematological parameters.

2.6.3. Micronucleus Test. The micronucleus test was performed 24 h after *S. diploconos* extract (2 g/kg, by gavage) administration to the mice. Vehicle- (10 mL/kg) and methyl methanesulfonate- (MMS; 50 mg/kg, i.p.) treated animals were used as negative and positive controls, respectively. After treatments, the mouse right femurs were collected, and the epiphyses cut. The medullary cavity of each femur was washed using a syringe containing FBS (3 mL). The lavage fluid was centrifuged at $1000 \times g$, for 10 min at 5°C; the cells were obtained; and their viability was assessed by using 0.4% trypan blue dye. Then, 50 μL of the cell suspensions was placed onto glass slides, fixed with cold methanol, and stained with Giemsa for 10 min. The slides were washed and dried for examination under a light microscope (1000x). One thousand polychromatic cells were assessed per slide. The ratio between monochromatic and polychromatic erythrocytes was established and analysed [28].

2.7. Statistics. Data is expressed as mean ± standard error of the mean (SEM). The percentages of inhibition were individually calculated and expressed as mean ± SEM%. Statistical differences between groups were assessed by Student's t-test or one-way analysis of variance (ANOVA) followed by Tukey's post hoc test, as appropriate. Values of $p < 0.05$ were considered as significant.

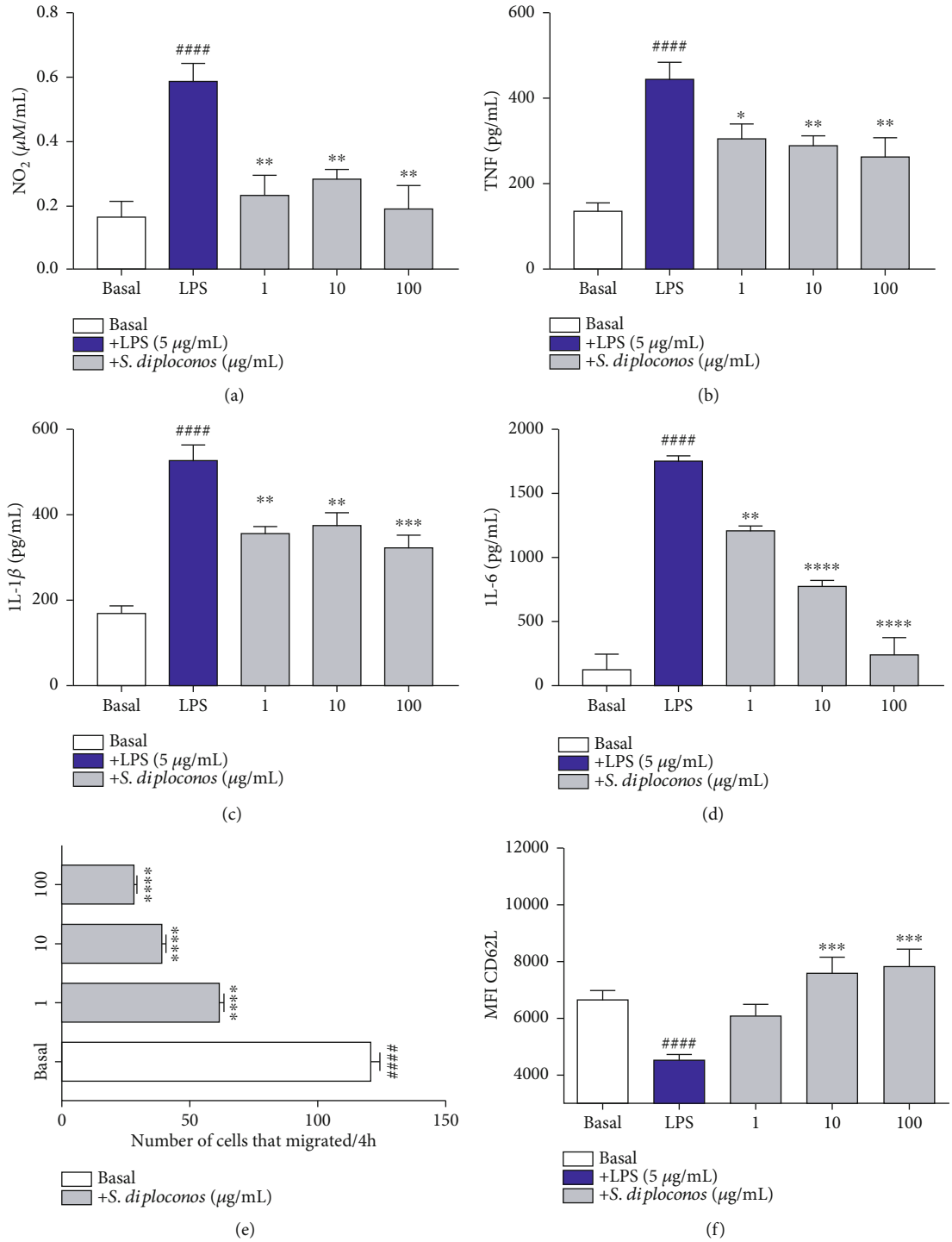

Figure 2: Continued.

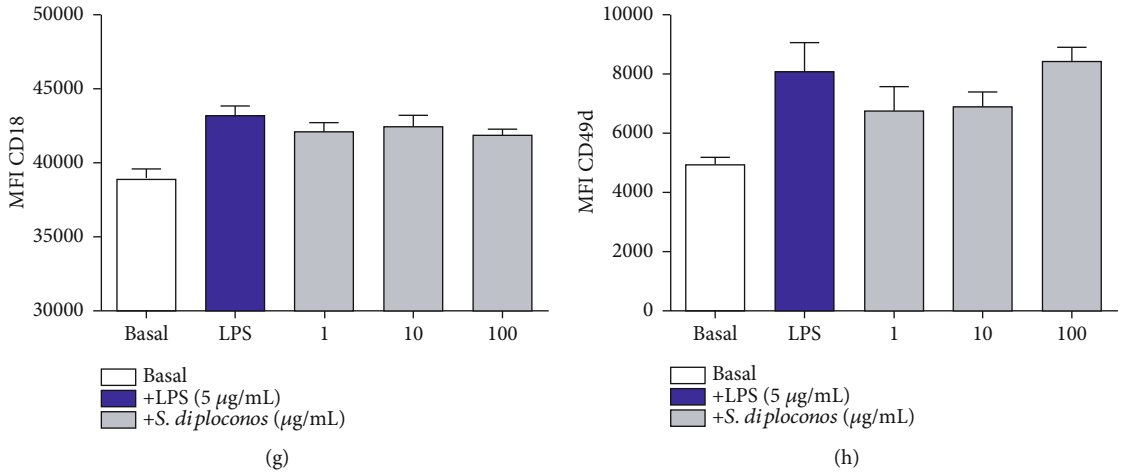

Figure 2: Effects of the *S. diploconos* fruit extract on neutrophils. Neutrophils obtained from the peritoneal cavity of Swiss mice (1% oyster glycogen) were incubated in the presence or absence of LPS (5 μg/mL) and with S. diploconos (1, 10, or 100 μg/mL). Nitrite levels were measured by the Griess reaction (a). The levels of (b) TNFα, (c) IL-1β, and (d) IL-6 were determined by ELISA. For the chemotaxis assay (e), a neutrophil suspension (1×10^7) was incubated with different concentrations of S. diploconos (1, 10, or 100 μg/mL) for 15 minutes and placed in front of the fMLP (1 μM) on an agarose plate. Quantification was made from the margin of the peripheral perforations towards the chemotactic agent (central perforation). Neutrophils (1×10^6) were incubated in the presence or absence of LPS (5 μg/mL) along with S. diploconos (1, 10, or 100 μg/mL) for evaluation of the neutrophil adhesion molecules. Adhesion molecule expression was assessed by labeling with (f) CD62L, (g) CD18, and (h) CD49 detection antibodies by flow cytometry. Values express the mean ± SEM of tests performed with cells obtained from 8 animals per group. $^{*}p < 0.05$; $^{**}p < 0.01$; $^{***}p < 0.001$; and $^{****}p < 0.0001$ vs. the LPS group significantly different from the basal group $^{\#\#\#\#}p < 0.0001$ (one-way ANOVA followed by Turkey's post hoc test).

3. Results

3.1. Chemical Profile of Solanum diploconos Fruit Extract. The yield of the whole fresh ripe fruit hydroalcoholic extract was 11.49%. Its chemical composition (main classes of metabolites) was analysed by HPLC with a photodiode detector. The HPLC/UV profiles of the extract are shown in Figure 1. Six distinct absorption profiles were detected. The first profile demonstrates a band with a maximum absorption at 210 nm (peaks 2-4 and 6-10) which indicates compounds with chromophore groups that present $\pi - \pi *$ electronic transition such as those with olefinic groups. Many classes of compounds are absorbed in this region; making it difficult to determine the major one. Other five profiles indicate bands with a maximum absorption between 270 and 330 nm (other peaks). This is a region in which $n - \pi *$ transitions are observed. Of note, carbonyl compounds as well as aromatic groups present this transition (Figure 1).

3.2. S. diploconos Fruit Extract Affects the Secretion of Proinflammatory Cytokines and Nitric Oxide by Neutrophils. In order to evaluate the direct effects of the fruit extract on inflammatory mediator production (TNFα, IL-6, IL-1β, and NO_2^- levels), the supernatants from the neutrophil culture were assessed. Data depicted in Figures 2(a)–2(d) demonstrate that LPS induces the production of inflammatory mediators by neutrophils. Treatment with *S. diploconos* extract significantly reduced NO_2^- (maximum inhibition of 63.5 ± 7.3%), TNFα (maximum inhibition of 54.2 ± 2.1%), IL-1β (maximum inhibition of 68.9 ± 3.1%), and IL-6 (maximum inhibition of 73.6 ± 0.9%) levels in comparison with LPS-treated neutrophils (Figures 2(a)–2(d)).

3.3. S. diploconos Fruit Extract Impairs Neutrophil Migration. Figure 2 also shows the effect of *S. diploconos* extract on neutrophil migration. Vehicle-treated neutrophils presented a significant migration towards fMLP, whilst those treated with *S. diploconos* exhibited impaired chemotaxis (maximum inhibition of 78.1 ± 1.2%; Figure 2(e)).

Once leukocyte migration is mediated by adhesion molecules, the expression of L-selectin (CD62L), β2-integrin (CD18), and CD49d on neutrophils was evaluated by flow cytometry. LPS triggered the activation of neutrophils as they presented shedding of CD62L and increased expression of CD18 and CD49b on their surface. Incubation of LPS-treated neutrophils with *S. diploconos* extract impaired neutrophil activation, denoted by increased expression of CD62L (1.7-fold increase for the concentrations of 10 and 100 μg/mL), i.e., increased MFI in comparison with LPS controls (Figures 2(f) and 2(g)).

3.4. S. diploconos Fruit Extract Induces Efferocytosis of Apoptotic Neutrophils. All tested concentrations of the *S. diploconos* fruit extract (1, 10, or 100 μg/mL) were able to significantly increase the efferocytosis process (maximum increase of 2.0-fold; Figure 3(a)). The extract was also able to reduce TNFα (maximum inhibition of 80.7 ± 1.2%; Figure 3(b)) and increase IL-10 (maximum increase of 11.5-fold; Figure 3(c)) levels in the supernatant samples obtained from the efferocytosis assay.

3.5. S. diploconos Fruit Extract Presents In Vivo Anti-Inflammatory Activity. The *in vivo* effects of *S. diploconos* fruit extract on neutrophil migration were evaluated in the air pouch model, using carrageenan as a phlogistic agent.

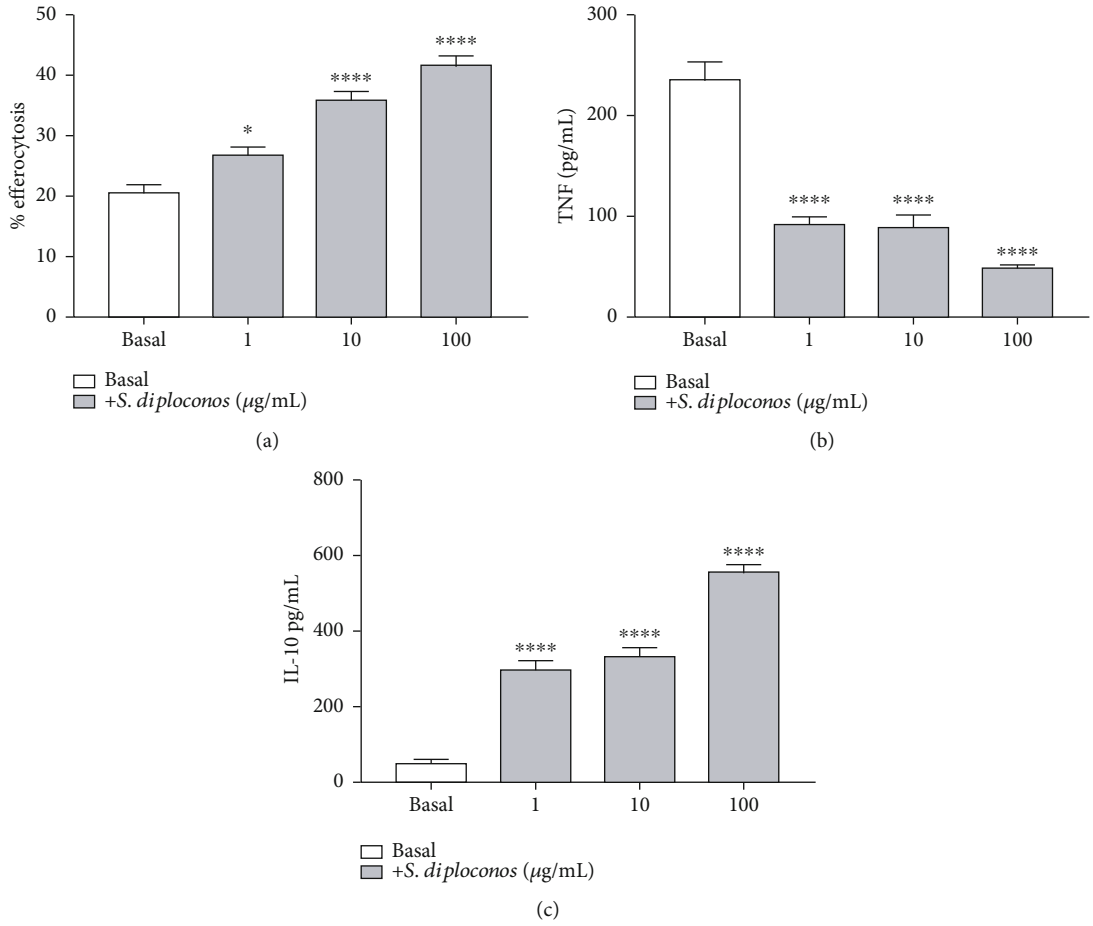

Figure 3: Effects of *S. diploconos* on efferocytosis. Quantification of efferocytosis (a) and supernatant levels of TNFα (b) and IL-10 (c). Data is expressed as a mean ± SEM of cells obtained from four animals. Statistical analysis was performed using one-way ANOVA followed by Tukey's test. $^{*}p < 0.05$; $^{**}p < 0.01$; $^{***}p < 0.001$, and $^{****}p < 0.0001$ vs. basal.

The histological analysis (Figure 4) of air pouch tissue sections from *naive* animals indicated that they present an air pouch wall with connective tissue, rich in blood vessels, and with relatively low cellular content (Figures 4(a) and 4(b)). Their cell lining was primarily formed by fibroblasts, and, in some areas, scarce macrophages were observed within the air pouch walls (Figures 4(b) and 4(c)).

Vehicle-treated animals challenged with carrageenan exhibited typical morphological changes of inflammation including increased thickness of the air pouch membrane and intense oedema, with fibrin-haemorrhagic exudate, leukocyte accumulation, and tissue injury (Figures 4(d) and 4(e)). Most of the inflammatory cells were neutrophils, as identified by their lobulated nuclei. These cells were extensively infiltrated in the damaged tissue and distributed within the adjacent muscular fibres. Macrophages with a foamy appearance were also observed, possibly due to the phagocytosis of carrageenan (Figures 4(e) and 4(f)).

Indomethacin treatment reduced the thickness of carrageenan-challenged air pouch membranes in comparison with vehicle-injected mice (Figures 4(g) and 4(h)). Oedema was restricted to limited areas, and there was also an evident reduction of the neutrophil infiltrate. Few normal and foamy macrophages were seen in the pouch membrane, along with fibroblasts and neutrophils (Figures 4(h) and 4(i)).

In the *S. diploconos*-treated group, the thickness of the air pouches challenged with carrageenan was visibly reduced, and the walls were formed by loose connective tissue with newly formed blood vessels. No signs of oedema were observed (Figures 4(j) and 4(k)). Neutrophil and macrophage numbers were largely diminished in comparison with the negative control group, and a lining of fibroblast-like cells with no directional orientation was observed. Additionally, under the hair follicles, there was a layer of fibroblasts on an augmented deposit of collagen (Figures 4(k) and 4(l)). These histological findings suggest that the acute inflammatory response caused by carrageenan in the pouch wall is significantly suppressed by the treatment with *S. diploconos* fruit extract.

The data presented in Figure 4(m) demonstrate that similarly to indomethacin, the fruit extract at 100 mg/kg was able to reduce cell counts in the exudate in comparison with the control group. Inhibitions were of 73.5 ± 2.9 and $95.4 \pm 0.8\%$ for *S. diploconos* and indomethacin, respectively. Differential cell analysis indicates that both *S. diploconos* fruit extract and indomethacin affect mainly neutrophils (Figure 4(n)).

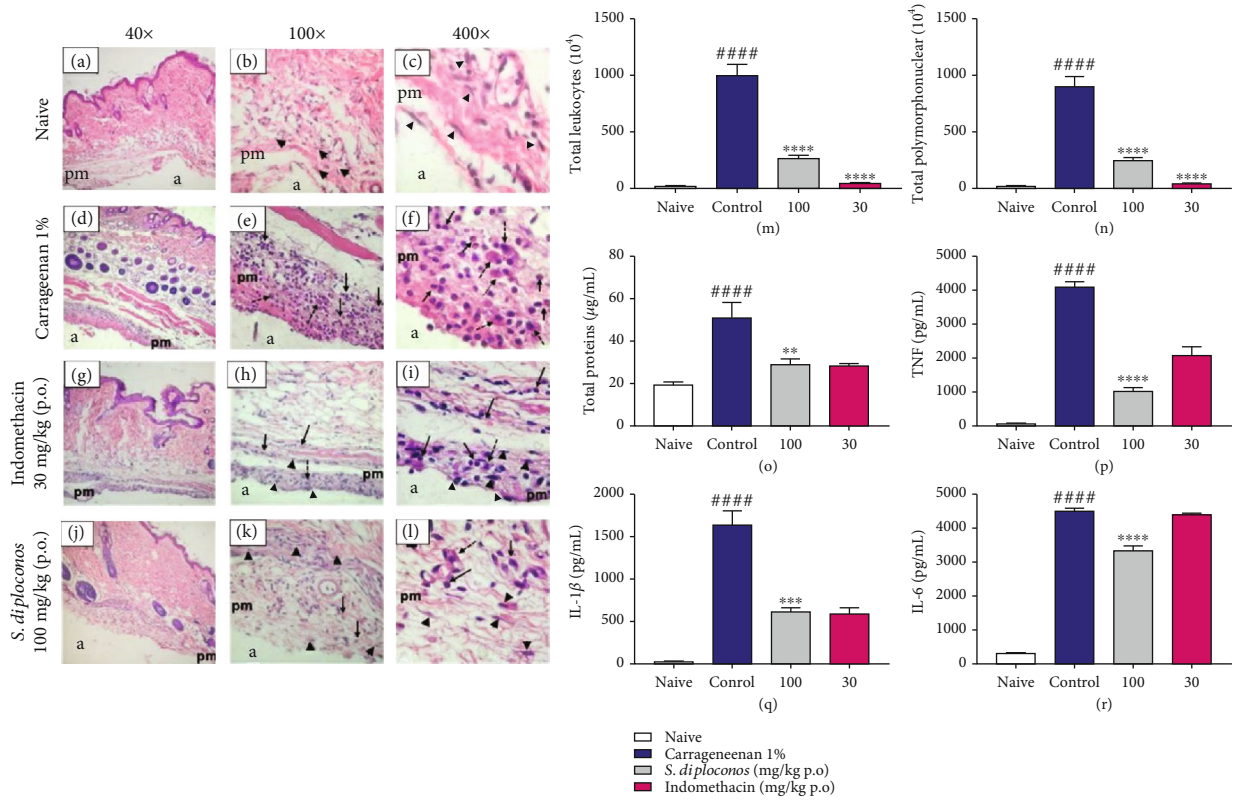

FIGURE 4: *S. diploconos* actions in mouse air pouches challenged with carrageenan. Air pouch was induced in the dorsal subcutaneous tissue of Swiss mice. The animals were treated orally one hour before the injection of 2 mL of carrageenan (1%). Representative H.E. histological sections of skin biopsies obtained from mice with air pouches (40, 100, and 400x). Black arrows indicate PMN leukocytes, dashed black arrows indicate macrophages, and arrowheads indicate fibroblasts (a-l). Air space pouch "a"; pouch membrane "pm." The lavage of the inflammatory infiltrate was collected 4 hours after the injection of carrageenan into the air pouch. The determination of the (m) total number of exudate cells was performed on a Neubauer chamber, and the (n) differential value was performed. (o) The protein concentration was measured in a spectrophotometer at 590 nm using the Bradford reagent. The levels of (P) TNFα, (q) IL-1β, and (r) IL-6 were determined by the ELISA method. Values express the mean ± SEM of tests performed with the inflammatory exudate obtained from 6 animals per group. $^{*}p < 0.05$, $^{**}p < 0.01$, and $^{****}p < 0.0001$, vs. the control group significantly different from the naïve group $^{\#\#\#\#}p < 0.0001$ (one-way ANOVA followed by Tukey's post hoc test).

The fruit extract also reduced by nearly half the exudate protein concentration (Figure 4(o)). Additionally, carrageenan-challenged mice treated with *S. diploconos* exhibited lower levels of TNFα (Figure 4(p), 76.0 ± 2.7%), IL-1β (Figure 4(q), 63.3 ± 2.6%), and IL-6 (Figure 4(r), 25.3 ± 3.1%) in comparison with vehicle controls. Indomethacin-treated animals presented similar results; however, this compound did not affect IL-6 production (Figure 4(r)). Indomethacin diminished TNFα and IL-1β concentrations by 50.4 ± 6.2% and 63.8 ± 3.3%, respectively.

3.6. S. diploconos Fruit Extract Presents Wound Healing Activity. Data obtained from the *in vitro* scratch model using L929 cells show that *S. diploconos* fruit extract is able to promote an increase of fibroblast migration at all tested concentrations (maximum increase of 2.6-fold) in comparison with the control group (Figures 5(a) and 5(b)). Additionally, when assessed *in vivo* as a semisolid cream, *S. diploconos* extract (1%) promoted a faster healing of skin wounds in comparison with the control group (base cream). This is denoted by a significant reduction (~35%) of the wounded area as demonstrated in Figures 5(c) and 5(d).

3.7. S. diploconos Fruit Extract Does Not Present Acute or Subacute Toxicity. The fruit extract did not present genotoxic effects since no significant differences in the ratio of polychromatic and monochromatic erythrocytes were observed. On the other hand, MMS induced a significant increase in the ratio of polychromatic to monochromatic erythrocytes (36.0-fold increase, Table 1). Additionally, the extract did not promote cell cytotoxicity in the MTT assay.

In the acute toxicity test, animals received a single administration of *S. diploconos* fruit extract at the dose of 2 g/kg. The extract did not induce animal death or alterations in the following parameters: vocalization, behaviour, grip, body tonus, and twisting. Ataxia, tremors, convulsions, tail Straub sign, hypnosis, anaesthesia, ptosis, lacrimation, piloerection, alterations of the respiratory rate, and cyanosis were not observed. The characteristics of the skin, fur, and eyes remained normal and unchanged during the observation

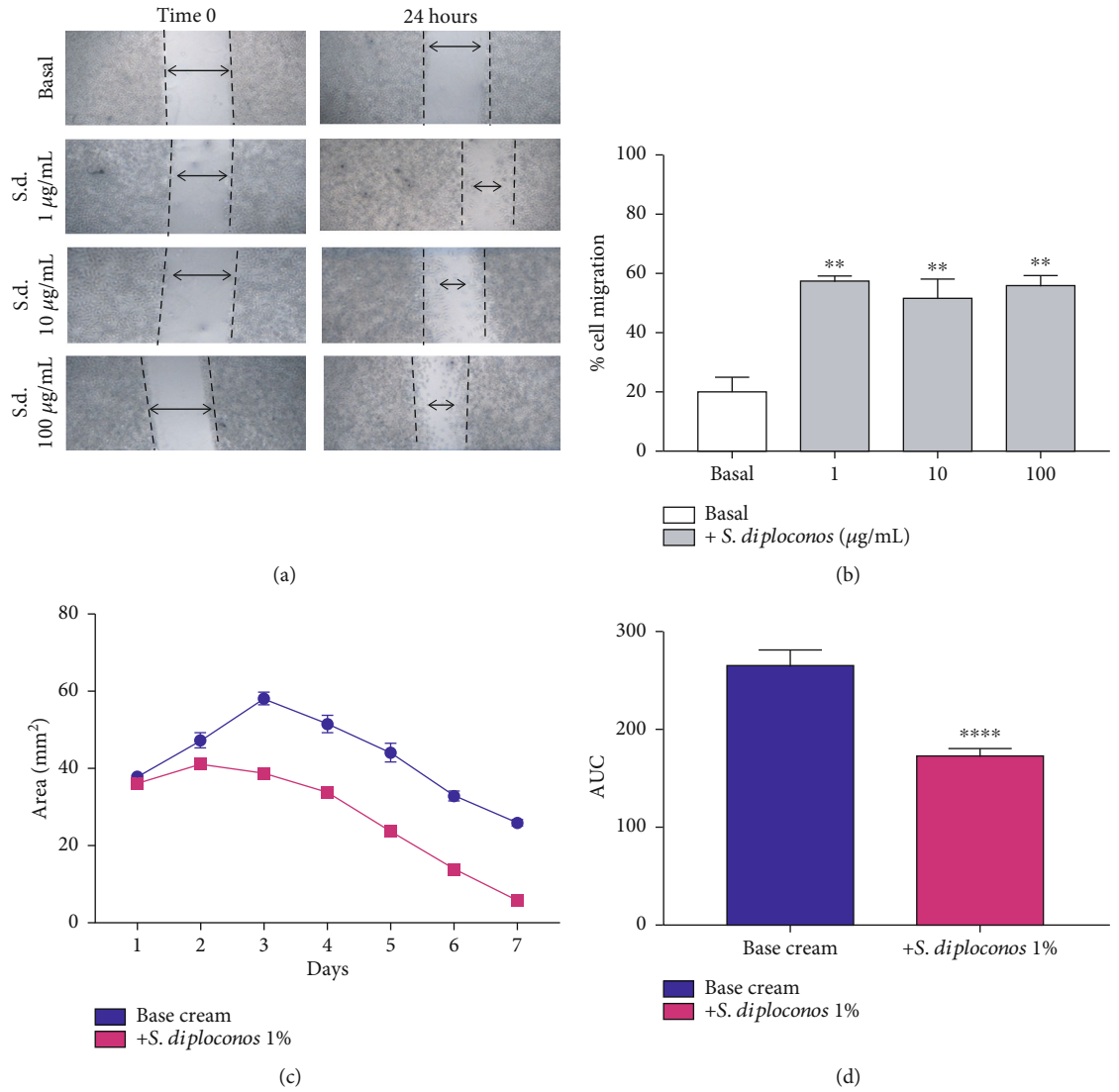

Figure 5: Analysis of the effects of the *S. diploconos* fruit extract in fibroblast migration and wound healing. (a) Representative image of the *in vitro* scratch migration assay in fibroblasts (L929) and (b) percentage of fibroblast migration. Skin ulcers were treated individually with *S. diploconos* 1% cream or vehicle (base cream). Progression of wound healing area over time after extract treatment (c) and area under the curve (AUC) (d). Values express the mean ± SEM from 6 animals per group. Statistical analysis was performed using one-way ANOVA followed by Tukey's test (cell migration assay) with $^{**}p < 0.01$ vs. basal and *t*-test (AUC assessment) $^{****}p < 0.0001$ vs. base cream.

Table 1: Percentage of polychromatic erythrocyte (PCE) micronuclei (PCEMN) in animals treated with *S. diploconos* fruit extract. Percentage of polychromatic erythrocyte (PCE) micronuclei (PCEMN) in the micronucleus assay performed in erythrocytes obtained from the bone marrow (the values are expressed as mean ± SEM ($n = 5$). $^{***}p < 0.001$ vs. the vehicle group).

Group	Dose (mg/kg)	PCEMN/2000 PCE (%)
Vehicle	—	0.33 ± 0.33
MMS	50	11.90 ± 1.09***
S. diploconos	2000	1.75 ± 0.52

period (12 h). Accordingly, no alterations were seen in the food/water intake or body weight of *S. diploconos*-treated animals in comparison with vehicle-treated rats.

Similarly, *S. diploconos* administration did not cause any alterations to internal organs (Table 2). Additionally, the histological analysis of the liver and kidney demonstrated normal and conserved architecture, without degenerative or inflammatory lesions in *S. diploconos* and vehicle groups.

No significant hematological parameter changes were found. In the platelet count, the high SEM presented for the extract-treated group refers to just one animal. Biochemical analysis indicated that the extract promotes a decrease of 39.8% in glucose and an increase of 1.3-fold in urea levels when compared with the vehicle group (Table 3).

Table 2: Effects of *Solanum diploconos* extract treatment on the organ weights of mice following the acute oral toxicity experiments (values expressed as mean ± SEM ($n = 5$)).

Organ		Acute toxicity		Subacute toxicity			
		Vehicle	2000 (mg/kg)	Vehicle	30 (mg/kg)	100 (mg/kg)	300 (mg/kg)
Heart	Absolute (g)	0.853 ± 0.071	0.763 ± 0.053	0.676 ± 0.027	0.625 ± 0.012	0.623 ± 0.031	0.679 ± 0.039
	Relative (%)	0.326 ± 0.013	0.307 ± 0.017	0.351 ± 0.008	0.319 ± 0.008	0.335 ± 0.015	0.352 ± 0.020
Lung	Absolute (g)	1.191 ± 0.097	1.098 ± 0.124	0.975 ± 0.023	0.936 ± 0.032	0.941 ± 0.020	0.962 ± 0.024
	Relative (%)	0.455 ± 0.029	0.442 ± 0.041	0.506 ± 0.007	0.477 ± 0.016	0.506 ± 0.012	0.499 ± 0.017
Liver	Absolute (g)	9.182 ± 0.522	8.123 ± 0.840	5.300 ± 0.248	5.364 ± 0.141	5.071 ± 0.155	5.202 ± 0.122
	Relative (%)	3.515 ± 0.256	3.273 ± 0.316	2.751 ± 0.098	2.734 ± 0.058	2.725 ± 0.741	2,699 ± 0.070
Spleen	Absolute (g)	0.635 ± 0.047	0.593 ± 0.056	0.542 ± 0.038	0.554 ± 0.033	0.480 ± 0.008	0.496 ± 0.022
	Relative (%)	0.242 ± 0.012	0.238 ± 0.014	0.280 ± 0.015	0.282 ± 0.017	0.258 ± 0.003	0.257 ± 0.012
Left kidney	Absolute (g)	0.998 ± 0.076	0.914 ± 0.057	0.765 ± 0.034	0.862 ± 0.038	0.737 ± 0.017	0.779 ± 0.024
	Relative (%)	0.381 ± 0.024	0.368 ± 0.013	0.397 ± 0.012	0.439 ± 0.017	0.396 ± 0.008	0.404 ± 0.014
Right kidney	Absolute (g)	1.021 ± 0.071	0.910 ± 0.100	0.802 ± 0.034	0.836 ± 0.043	0.753 ± 0.012	0.756 ± 0.029
	Relative (%)	0.391 ± 0.038	0.366 ± 0.030	0.416 ± 0.013	0.426 ± 0.019	0.405 ± 0.007	0.392 ± 0.015

Table 3: Biochemical markers and hematological parameters following the acute administration of the *S. diploconos* fruit extract (values expressed as mean ± SEM ($n = 5$)). $^*p < 0.05$ vs. the vehicle group.

Parameters	Acute toxicity		Subacute toxicity			
	Vehicle	2000 (mg/kg)	Vehicle	30 (mg/kg)	100 (mg/kg)	300 (mg/kg)
Biochemical parameters						
Glucose (mg/dL)	261.60 ± 16.93*	157.30 ± 16.23	131.6 ± 6.30	148.20 ± 11.10	125.20 ± 10.54	125.80 ± 3.48
AST (U/L)	91.60 ± 5.97	128.81 ± 14.45	108.21 ± 10.79	100.69 ± 7.02	104.23 ± 6.16	89.22 ± 7.97
ALT (U/L)	56.40 ± 5.14	38.61 ± 9.69	39.89 ± 4.39	37.86 ± 2.11	37.36 ± 1.89	33.07 ± 2.09
ALP (U/L)	61.20 ± 7.94	73.80 ± 15.65	53.12 ± 4.30	60.59 ± 6.01	56.68 ± 2.06	56.30 ± 6.25
Urea (mg/dL)	41.60 ± 1.21	53.50 ± 3.03*	35.00 ± 1.70	32.60 ± 1.50	36.80 ± 2.78	36.80 ± 1.39
Creatinine (mg/dL)	0.53 ± 0.02	0.39 ± 0.053	0.30 ± 0.01	0.28 ± 0.01	0.25 ± 0.01	0.29 ± 0.02
Hematological parameters						
Leukocyte (mil/mm^3)	1.120 ± 0.149	0.800 ± 0.152	3.425 ± 0.118	2.900 ± 0.207	4.020 ± 0.497	2.520 ± 0.323
Neutrophil (%)	10.600 ± 1.805	13.333 ± 2.333	2.750 ± 0.250	2.400 ± 0.245	2.400 ± 0.245	3.600 ± 0.678
Lymphocyte (%)	87.400 ± 2.014	84.667 ± 2.403	95.500 ± 0.288	95.800 ± 0.374	96.200 ± 0.374	94.400 ± 1.886
Monocytes (%)	2.000 ± 0.707	1.333 ± 0.333	1.750 ± 0.250	1.800 ± 0.374	1.400 ± 0.245	2.000 ± 1.265
Eosinophil (%)	0.000 ± 0.000	0.666 ± 0.333	0.000 ± 0.000	0.000 ± 0.000	0.000 ± 0.000	0.000 ± 0.000
Basophil (%)	0.000 ± 0.000	0.000 ± 0.000	0.000 ± 0.000	0.000 ± 0.000	0.000 ± 0.000	0.000 ± 0.000
Erythrocyte (millions/mm^3)	5.562 ± 0.067	4.960 ± 0.496	7.050 ± 0.131	7.000 ± 0.092	7.146 ± 0.129	6.698 ± 0.113
Hemoglobin (g/dL)	11.540 ± 0.153	10.266 ± 1.185	14.050 ± 0.342	13.940 ± 0.150	13.960 ± 0.265	13.220 ± 0.587
Hematocrit (%)	31.100 ± 0.389	27.533 ± 2.936	40.600 ± 0.849	40.220 ± 0.414	40.560 ± 0.867	38.120 ± 0.587
Platelets (10^3/mm^3)	408.400 ± 34.993	293.000 ± 142.815	702.250 ± 46.424	657.400 ± 44.800	651.800 ± 39.328	715.600 ± 69.974

The data obtained in the subacute toxicity test demonstrate that *S. diploconos* extract does not induce any alteration in the biochemical and hematological parameters at the highest evaluated dose (300 mg/kg). In this case, a no observed adverse effect level (NOAEL) was established at 300 mg/kg.

4. Discussion

Neutrophils are cells with multiple functions which modulate inflammation from its initial phase to tissue repair. Neutrophils interact with other immune cells, directly or via

inflammatory mediator production, affecting the course of both innate and adaptive immune responses [29]. We showed for the first time that *S. diploconos* fruit extract is able to modulate neutrophil functions by reducing chemotaxis, cytokine, and NO release and also promotes resolution of inflammation and wound healing. Additionally, the assays performed indicate that the extract may directly affect intracellular neutrophil pathways.

Several inflammatory mediators are synthesized and secreted during an inflammatory response with neutrophils responding directly to these signals and producing different inflammatory mediators such as cytokines that, in turn, modulate inflammation and drive the immune response [29, 30]. In this context, it is well known that cytokines such as TNFα and IL-6 are increased in inflammation and may contribute to excessive neutrophil accumulation and subsequent tissue damage [31]. Previous studies demonstrated that some *Solanum* species are able to reduce inflammatory mediator secretion by immune cells; however, their effects on neutrophils were unknown [18, 32]. In this context, our data clearly show the direct inhibitory actions of *S. diploconos* fruit extract on LPS-induced neutrophil-mediated secretion of cytokines and NO.

Herein, the obtained phytochemical profile was compared to that presented by Ribeiro et al. [13]. The authors identified derivatives of caffeic, ferulic and coumaric acids in the freeze-dried pulp and peel of *S. diploconos* fruits, as well as in an extract obtained from its whole fruit using HPLC-DAD-ESI-MS/MS [13]. Some phenolic compounds detected by the authors presented a similar UV absorption profile also observed in this study for the peaks 5, 11-13, and 18-24.

The anti-inflammatory effect observed for *S. diploconos* may be due to the content of caffeic acid, lutein, and β-carotene present in the extract [13], which were previously shown to reduce the translocation of the transcription factor NF-κB [16, 33, 34] necessary for the transcription of inflammatory mediators such as cytokines [35].

We also found that *S. diploconos* fruit extract markedly reduces fMLP-induced neutrophil chemotaxis *in vitro*. Interestingly, *S. diploconos* extract increased the expression of CD62L on LPS-stimulated neutrophils without altering CD18 and CD49d profiles. It is important to highlight that CD62L mediates neutrophil rolling [36], whilst CD49d and CD18 mediate adhesion to the endothelium [6, 37]. CD62L becomes highly expressed on the cell membrane of leukocytes when haemodynamic changes or production of inflammatory mediators occurs [3]. After the activation process, however, CD62L is cleaved by the action of membrane metalloproteinases, allowing the activation of CD18 which is responsible for the strong adhesion of inflammatory cells to endothelial cells [6, 36]. It is possible, thus, that the extract prevents L-selectin from being cleaved, allowing leukocytes to remain in rolling behaviour instead of adhering to the endothelium and migrating to the inflammatory focus.

S. diploconos inhibitory effects on neutrophil migration were confirmed *in vivo*. Our data demonstrate that the oral treatment with *S. diploconos* decreases the production of inflammatory mediators (TNFα, IL-6, and IL-1β) which may explain the reduced leukocyte recruitment and protein levels in the air pouch exudates obtained from mice challenged with carrageenan. A similar effect on neutrophils was also observed in the skin tissue.

Neutrophils can indirectly contribute to tissue restoration by modulating the functions of other cells. In this context, macrophages are moved to a state of tissue remodelling by performing efferocytosis (phagocytosis of apoptotic neutrophils). Indeed, when neutrophils become apoptotic, they trigger a phagocytic activity in macrophages and stimulate their differentiation into M2 macrophages which are involved in tissue repair [38, 39]. The increased production of TGF-β and IL-10 is suggested to underlie these responses [7, 38, 40]. Herein, macrophages treated with *S. diploconos* presented increased efferocytosis, paralleled to decreased TNFα and enhanced IL-10 production.

These data indicate that *S. diploconos* may favour the resolution of inflammation. In order to confirm this evidence, we assessed the effects of the extract in a scratch assay with L929 cells and *in vivo*, in animals with skin wounds. *S. diploconos* induced *in vitro* fibroblast proliferation and accelerated the healing of skin wounds in mice. Similar proliferative and healing actions were previously observed for other *Solanum* species, such as *S. incanum* and *S. xanthocarpum*, which presented healing activities in burn models and in the treatment of diabetic skin ulcers [32, 41].

Both the anti-inflammatory and healing activities of *S. diploconos* may be correlated to the presence of caffeic, ferulic, and coumaric acids in its extract. It is known that caffeic acid presents anti-inflammatory and wound healing effects in different experimental models [42, 43], and the same was observed for ferulic acid [44, 45].

Finally, an analysis of the possible toxic effects of the extract was performed. No important toxic effects were observed *in vitro* (in L929 cells) or *in vivo*, apart from a reduction of glucose and an increase in urea levels in the acute but not in the subacute toxicity assay. Normal urea levels indicate that the metabolism of ammoniac to urea by the liver is not altered and that the detoxification and excretion liver functions are preserved [45]. Despite observing increased urea levels, the histopathological analysis showed no alterations in the renal tissue. These data indicate that the acute and subacute oral treatments with *S. diploconos* fruit extract may be safe. Nonetheless, further studies are necessary to address possible toxic effects of this extract when administered repeatedly.

5. Conclusion

Taken together, the data demonstrate the anti-inflammatory and prohealing activities of the *S. diploconos* fruit extract. These effects were linked to its ability to modulate neutrophil functions including the production of inflammatory mediators and chemotaxis, in addition to promoting efferocytosis and the resolution of acute inflammation. The absence of important acute and subacute toxic effects suggests the promising application of the extract as a therapeutic aid for acute inflammatory reactions and wound healing.

Data Availability

The datasets used to support this study will be made available upon request. Requests should be sent to JRS.

Conflicts of Interest

The authors declare no conflicts of interest.

Authors' Contributions

JRS and NLMQ conceived and designed research. LB, RN, IV, SAP, MFB, FCG, and SEP conducted experiments. AM contributed with analytical tools. JRS, MVDP, and NLMQ analysed the data. ESF, JRS, LB, and NLMQ drafted, critically revised, and wrote the final manuscript. All authors read and approved the manuscript.

Acknowledgments

This study was supported by grants from the Conselho Nacional de Desenvolvimento Científico e Tecnológico (CNPq, grant numbers 429505/2018-3 to JRS, 305676/2019-9 to ESF, and 305550/2018-7 to NLMQ) and the Coordenação de Aperfeiçoamento de Pessoal de Nível Superior (CAPES) (Finance Code 001).

References

[1] M. Phillipson and P. Kubes, "The healing power of neutrophils," *Trends in Immunology*, vol. 40, no. 7, pp. 635–647, 2019.

[2] S. Thome, D. Begandt, R. Pick, M. Salvermoser, and B. Walzog, "Intracellular β_2 integrin (CD11/CD18) interacting partners in neutrophil trafficking," *European Journal of Clinical Investigation*, vol. 48, article e12966, 2018.

[3] A. Dabrowski, J. Osada, M. I. Dabrowska, U. Wereszczynska-Siemiatkowska, and A. Siemiatkowski, "Increased expression of the intercellular adhesion molecule-1 (ICAM-1) on peripheral blood neutrophils in acute pancreatitis," *Advances in Medical Sciences*, vol. 59, no. 1, pp. 102–107, 2014.

[4] S. Schmidt, M. Moser, and M. Sperandio, "The molecular basis of leukocyte recruitment and its deficiencies," *Molecular Immunology*, vol. 55, no. 1, pp. 49–58, 2013.

[5] D. N. Granger and E. Senchenkova, "Inflammation and the microcirculation," *Colloquium Series on Integrated Systems Physiology: From Molecule to Function*, vol. 2, no. 1, pp. 1–87, 2010.

[6] K. Mastej and R. Adamiec, "Neutrophil surface expression of CD11b and CD62L in diabetic microangiopathy," *Acta Diabetologica*, vol. 45, no. 3, pp. 183–190, 2008.

[7] S. E. Headland and L. V. Norling, "The resolution of inflammation: principles and challenges," *Seminars in Immunology*, vol. 27, no. 3, pp. 149–160, 2015.

[8] M. A. Sugimoto, L. P. Sousa, V. Pinho, M. Perretti, and M. M. Teixeira, "Resolution of inflammation: what controls its onset?," *Frontiers in Immunology*, vol. 7, p. 160, 2016.

[9] A. G. Atanasov, B. Waltenberger, E. M. Pferschy-Wenzig et al., "Discovery and resupply of pharmacologically active plant-derived natural products: a review," *Biotechnology Advances*, vol. 33, no. 8, pp. 1582–1614, 2015.

[10] R. M. Hernández-Herrera, F. Santacruz-Ruvalcaba, M. A. Ruiz-López, J. Norrie, and G. Hernández-Carmona, "Effect of liquid seaweed extracts on growth of tomato seedlings (*Solanum lycopersicum* L.)," *Journal of Applied Phycology*, vol. 26, no. 1, pp. 619–628, 2014.

[11] C. C. J. Almança, S. V. Saldanha, D. R. Sousa et al., "Toxicological evaluation of acute and sub-chronic ingestion of hydroalcoholic extract of *Solanum cernuum* Vell. in mice," *Journal of Ethnopharmacology*, vol. 138, no. 2, pp. 508–512, 2011.

[12] S. R. I. JR, L. A. Mentz, M. F. Agra, M. Vignoli-Silva, and L. Giacomin, *Solanaceae*, Lista de Espécies da Flora do Brasil, 2015.

[13] A. B. Ribeiro, R. C. Chisté, J. L. F. C. Lima, and E. Fernandes, "Solanum diploconos fruits: profile of bioactive compounds and in vitro antioxidant capacity of different parts of the fruit," *Food & Function*, vol. 7, no. 5, pp. 2249–2257, 2016.

[14] L. C. Lopes, J. E. de Carvalho, M. Kakimore et al., "Pharmacological characterization of Solanum cernuum Vell.: 31-norcycloartanones with analgesic and anti-inflammatory properties," *Inflammopharmacology*, vol. 22, pp. 179–185, 2013.

[15] L. Zhao, L. Wang, S. Di et al., "Steroidal alkaloid solanine A from *Solanum nigrum* Linn. exhibits anti- inflammatory activity in lipopolysaccharide/interferon γ-activated murine macrophages and animal models of inflammation," *Biomedicine & Pharmacotherapy*, vol. 105, pp. 606–615, 2018.

[16] L. C. Wang, K. H. Chu, Y. C. Liang, Y. L. Lin, and B. L. Chiang, "Caffeic acid phenethyl ester inhibits nuclear factor-κB and protein kinase B signalling pathways and induces caspase-3 expression in primary human CD4+ T cells," *Clinical and Experimental Immunology*, vol. 160, no. 2, pp. 223–232, 2010.

[17] H. O. Kazancioglu, M. C. Bereket, S. Ezirganli, M. S. Aydin, and S. Aksakalli, "Effects of caffeic acid phenethyl ester on wound healing in calvarial defects," *Acta Odontologica Scandinavica*, vol. 73, no. 1, pp. 21–27, 2015.

[18] R. Nunes, M. F. Broering, R. De Faveri et al., "Effect of the metanolic extract from the leaves of *Garcinia humilis* Vahl (Clusiaceae) on acute inflammation," *Inflammopharmacology*, vol. 29, pp. 423–438, 2021.

[19] R. D. Nelson, P. G. Quie, and R. L. Simmons, "Chemotaxis under agarose: a new and simple method for measuring chemotaxis and spontaneous migration of human polymorphonuclear leukocytes and monocytes," *Journal of Immunology*, vol. 115, pp. 1650–1656, 1975.

[20] M. F. Broering, R. Nunes, R. De Faveri et al., "Effects of Tithonia diversifolia (Asteraceae) extract on innate inflammatory responses," *Journal of Ethnopharmacology*, vol. 242, article 112041, 2019.

[21] L. C. Green, D. A. Wagner, J. Glogowski, P. L. Skipper, J. S. Wishnok, and S. R. Tannenbaum, "Analysis of nitrate, nitrite, and [^{15}N] nitrate in biological fluids," *Analytical Biochemistry*, vol. 126, pp. 131–138, 1982.

[22] A. D. Sedgwick and P. Lees, "Studies of eicosanoid production in the air pouch model of synovial inflammation," *Agents and Actions*, vol. 18, no. 3-4, pp. 429–438, 1986.

[23] M. Jain and H. S. Parmar, "Evaluation of antioxidative and anti-inflammatory potential of hesperidin and naringin on the rat air pouch model of inflammation," *Inflammation Research*, vol. 60, no. 5, pp. 483–491, 2011.

[24] P. Y. K. Yue, E. P. Y. Leung, N. K. Mak, and R. N. S. Wong, "A simplified method for quantifying cell migration/wound

healing in 96-well plates," *Journal of Biomolecular Screening*, vol. 15, no. 4, pp. 427–433, 2010.

[25] T. D. Tonin, L. C. Thiesen, M. L. de Oliveira Nunes et al., "Rubus imperialis (Rosaceae) extract and pure compound niga-ichigoside F1: wound healing and anti-inflammatory effects," *Naunyn-Schmiedeberg's Archives of Pharmacology*, vol. 389, no. 11, pp. 1235–1244, 2016.

[26] F. Denizot and R. Lang, "Rapid colorimetric assay for cell growth and survival: modifications to the tetrazolium dye procedure giving improved sensitivity and reliability," *Journal of Immunological Methods*, vol. 89, pp. 271–277, 1986.

[27] Organization For Economic Cooperation And Development, "Test No. 420: acute oral toxicity–fixed dose procedure," in *OECD Guidel. Test*, p. 14, OECD, Chem, 2002.

[28] Organization For Economic Cooperation And Development, "Test No. 487: in vitro mammalian cell micronucleus test," in *Guidel. Test*, OECD, Ed., p. 23, Chem, 2010.

[29] C. Rosales, "Neutrophil: a cell with many roles in inflammation or several cell types?," *Frontiers in Physiology*, vol. 9, p. 113, 2018.

[30] A. Azab, A. Nassar, and A. N. Azab, "Anti-inflammatory activity of natural products," *Molecules*, vol. 21, no. 10, p. 1321, 2016.

[31] M. Fronza, C. Muhr, D. S. C. da Silveira et al., "Hyaluronidase decreases neutrophils infiltration to the inflammatory site," *Inflammation Research*, vol. 65, no. 7, pp. 533–542, 2016.

[32] Z. Qureshi, T. Khan, A. J. Shah, and F. Wahid, "Solanum incanum extract enhances wound healing and tissue regeneration in burn mice model," *Bangladesh Journal of Pharmacology*, vol. 14, no. 2, pp. 101–106, 2019.

[33] J. H. Kim, H. J. Na, C. K. Kim et al., "The non-provitamin A carotenoid, lutein, inhibits NF-κB-dependent gene expression through redox-based regulation of the phosphatidylinositol 3-kinase/PTEN/Akt and NF-κB-inducing kinase pathways: role of H2O2 in NF-κB activation," *Free Radical Biology & Medicine*, vol. 45, no. 6, pp. 885–896, 2008.

[34] S. O. Cho, M.-H. Kim, and H. Kim, "β-Carotene inhibits activation of NF-κB, activator protein-1, and STAT3 and regulates abnormal expression of some adipokines in 3T3-L1 adipocytes," *Journal of Cancer Prevention*, vol. 23, no. 1, pp. 37–43, 2018.

[35] R. P. Kumar and A. Abraham, "Inhibition of LPS induced pro-inflammatory responses in RAW 264.7 macrophage cells by PVP-coated naringenin nanoparticle *via* down regulation of NF-κB/P38MAPK mediated stress signaling," *Pharmacological Reports*, vol. 69, no. 5, pp. 908–915, 2017.

[36] K. Uchimura and S. D. Rosen, "Sulfated L-selectin ligands as a therapeutic target in chronic inflammation," *Trends in Immunology*, vol. 27, no. 12, pp. 559–565, 2006.

[37] V. C. Ridger, B. E. Wagner, W. A. Wallace, and P. G. Hellewell, "Differential effects of CD18, CD29, and CD49 integrin subunit inhibition on neutrophil migration in pulmonary inflammation," *Journal of Immunology*, vol. 166, no. 5, pp. 3484–3490, 2001.

[38] J. Bystrom, I. Evans, J. Newson et al., "Resolution-phase macrophages possess a unique inflammatory phenotype that is controlled by cAMP," *Blood*, vol. 112, no. 10, pp. 4117–4127, 2008.

[39] W. K. E. Ip, N. Hoshi, D. S. Shouval, S. Snapper, and R. Medzhitov, "Anti-inflammatory effect of IL-10 mediated by metabolic reprogramming of macrophages," *Science*, vol. 356, no. 6337, pp. 513–519, 2017.

[40] J. A. Marwick, R. Mills, O. Kay et al., "Neutrophils induce macrophage anti-inflammatory reprogramming by suppressing NF-κB activation," *Cell Death & Disease*, vol. 9, no. 6, p. 665, 2018.

[41] K. M. Parmar, P. R. Shende, N. Katare, M. Dhobi, and S. K. Prasad, "Wound healing potential of Solanum xanthocarpum in streptozotocin-induced diabetic rats," *The Journal of Pharmacy and Pharmacology*, vol. 70, no. 10, pp. 1389–1400, 2018.

[42] F. M. Da Cunha, D. Duma, J. Assreuy et al., "Caffeic acid derivatives: in vitro and in vivo anti-inflammatory properties," *Free Radical Research*, vol. 38, no. 11, pp. 1241–1253, 2004.

[43] B. Romana-Souza, J. S. dos Santos, and A. Monte-Alto-Costa, "Caffeic acid phenethyl ester promotes wound healing of mice pressure ulcers affecting NF-κB, NOS2 and NRF2 expression," *Life Sciences*, vol. 207, pp. 158–165, 2018.

[44] K. Zduńska, A. Dana, A. Kolodziejczak, and H. Rotsztejn, "Antioxidant properties of ferulic acid and its possible application," *Skin Pharmacology and Physiology*, vol. 31, no. 6, pp. 332–336, 2018.

[45] Z. N. Yin, W. J. Wu, C. Z. Sun et al., "Antioxidant and anti-inflammatory capacity of ferulic acid released from wheat bran by solid-state fermentation of Aspergillus niger," *Biomedical and Environmental Sciences*, vol. 32, no. 1, pp. 11–21, 2019.

Hindawi
Journal of Immunology Research
Volume 2021, Article ID 8100298, 13 pages
https://doi.org/10.1155/2021/8100298

Research Article

Exosomes Derived from Nerve Stem Cells Loaded with FTY720 Promote the Recovery after Spinal Cord Injury in Rats by PTEN/AKT Signal Pathway

Jianbin Chen,[1] Can Zhang,[2] Shouye Li,[3] Zheming Li,[3] Xiaojing Lai,[4,5] and Qingqing Xia[6]

[1]*Department of Neurosurgery, Tongji Hospital, Tongji Medical College, Huazhong University of Science and Technology, Wuhan, Hubei 430030, China*
[2]*Department of Biomedical Engineering, College of Biology, Hunan University, Changsha 410082, China*
[3]*College of Pharmacy, Hangzhou Medical College, Hangzhou, 310022 Zhejiang, China*
[4]*The Cancer Hospital of the University of Chinese Academy of Sciences (Zhejiang Cancer Hospital), Hangzhou, 310022 Zhejiang, China*
[5]*Institute of Basic Medicine and Cancer (IBMC), Chinese Academy of Sciences, Banshan East Road 1, Gongshu District, Hangzhou, 310022 Zhejiang, China*
[6]*Department of Laboratory Medicine, Huangyan Hospital of Wenzhou Medical University (Taizhou First People's Hospital), Hengjie Road 218, Huangyan District, Taizhou, 318020 Zhejiang, China*

Correspondence should be addressed to Xiaojing Lai; czz20160127@163.com and Qingqing Xia; 418714257@qq.com

Received 7 April 2021; Revised 8 June 2021; Accepted 1 July 2021; Published 14 July 2021

Academic Editor: Kai Wang

Background. Spinal cord injury (SCI) remains a challenge owing to limited therapies. The exosome of neural stem cells (NSCs-Exos) and FTY720 transplantation could improve SCI effectively. However, the effect and mechanism of NSCs-Exos combined with FTY720 (FTY720-NSCs-Exos) transplantation in the treatment of SCI are not fully understood. *Methods*. Sprague Dawley rats (8-week-old) were used to establish the SCI model, followed by the treatment of NSCs-Exos, FTY720, and FTY720-NSCs-Exos. The effect of FTY720, NSCs-Exos, and FTY720-NSCs-Exos combination treatment on hindlimb function, pathological changes, apoptosis activity, and the expression of spinal edema-related proteins and apoptosis-related proteins in SCI models were investigated by BBB scoring, HE staining, TUNEL staining and immunohistochemistry, and Western blotting. Meanwhile, the effect of these treatments on spinal cord microvascular endothelial cells (SCMECs) was detected under hypoxic circumstance. *Results*. Our results found that FTY720-NSCs-Exos could alleviate pathological alterations and ameliorate the hindlimb function and oxygen insufficiency in model mice after SCI. In addition, exosomes could ameliorate the morphology of neurons, reduce inflammatory infiltration and edema, decrease the expression of Bax and AQP-4, upregulate the expression of claudin-5 and Bcl-2, and inhibit cell apoptosis. At the same time, *in vitro* experiments showed that FTY720-NSCs-Exos could protect the barrier of SCMECs under hypoxic circumstance, and the mechanism is related to PTEN/AKT pathway. *Conclusion*. FTY720-NSCs-Exos therapy displayed a positive therapeutic effect on SCI by regulating PTEN/AKT pathway and offered a new therapy for SCI.

1. Introduction

Spinal cord injury (SCI) is a common and harmful injury in spinal surgery with 0.6–0.9 million new patients worldwide every year [1]. Symptoms of SCI range from minimal dysfunction to quadriplegia and consist entirely of sensory, motor, and autonomic dysfunction [2]. Usually, after the primary traumatic mechanical destruction of the spinal cord tissues, secondary damage was rapidly triggered, such as inflammation, hypoxia, ischemia, and neuronal apoptosis [3]. Over time, SCI will eventually lead to motor and sensory dysfunction [4]. However, improving the recovery of neurological function after SCI is still the biggest challenge.

Nowadays, stem cell transplantation is increasingly used for SCI therapy. This may be due to its pluripotency and can be induced into a variety of cells [5]. Several studies have showed that transplantation of neural stem cells (NSCs) can ameliorate the function of motor nerve, sensory, and/or autonomic nerve in SCI [6–8]. However, stem cell transplantation has lots of disadvantages, such as low survival rate, immune rejection, dedifferentiation, and malignant tumor formation according to previous studies [9, 10]. At present, studies have shown that the efficacy of NSCs is mainly due to the role of their secreted exosomes [11, 12]. As the crucial paracrine factors of stem cells, the diameter of exosomes was between 20 and 150 nm and composed of a lipid bilayer that encapsulates RNA, DNA, and soluble proteins [13, 14]. Several studies have shown that exosomes of NSCs can protect neuronal function, promote neurocognitive impairment, and SCI repair [8, 15, 16]. It is used to treat liver, cardiovascular, and kidney injuries.

FTY720 is a functional antagonist of sphingosine 1-phosphate receptor-1 (S1P1), has a longer half-life *in vivo*, and can play an immunomodulatory function [17]. It has been proved that the systemic application of FTY720 has a positive effect on the recovery of SCI [18, 19]. However, it may cause serious adverse effects by systemic administration of FTY720. The locally released FTY720 is more conducive to remodel microvascular and regenerate bone tissue [20]. Therefore, we used the exosomes of NSCs (NSCs-Exos) as the carrier of FTY720 to detect the repairment of SCI, including behavioral assessment, inflammatory response, neuronal apoptosis, and spinal cord edema. Meanwhile, the improvement of FTY720-NSCs-Exos on SCMECs under hypoxic condition and its potential mechanism were also discussed. This study showed that localized delivery of FTY720 can ameliorate the injury of SCI through PTEN/AKT signaling pathway and offer a new therapeutic method for SCI.

2. Materials and Methods

2.1. NSCs-Exos Generation and Collection. Rat Fetal NSCs (N7744100, USA) were purchased from Thermo Fisher Scientific. Before NSC culturing, fetal bovine serum was centrifuged at 110000 g for 6 h to remove FBS's own exosomes. Then, the NSCs were cultured in a medium which contained FBS for 48 h when it reached 60–80% confluence. Then, the supernatant of the medium was collected, and separated exosomes by multistep centrifugation according to the previous studies [21, 22]. In brief, the supernatant was centrifuged at 300 g for 10 min, 1000 g for 20 min, and 10000 g for 30 min to remove the debris and dead cells. After filtering with a 0.22 μm filter membrane, the supernatant was centrifugated at 110000 g for 70 min to remove contaminated proteins. After filtering with a 0.22 μm filter membrane, the exosomes were saved at -80°C. Meanwhile, CD9 and CD81 were detected by Western blotting.

2.2. Characterization of NSCs-Exos. NSCs-Exos were fixed with 2% paraformaldehyde (PFA) and loaded to 200-mesh copper grids. After fixing with 1% (w/v) glutaraldehyde, the grids were stained with 4% uranyl acetate, then washed and dried in darkness at room temperature. After that, the grids were observed by Transmission Electron Microscopy (TEM, HT-7700,120 KV) to detect the morphology of NSCs-Exos.

The size of NSCs-Exos was detected by nanoparticle-tracking analysis (NTA) according to previous studies [23, 24]. The NSCs-Exos were diluted in PBS (1 : 10) and recorded via videos (30 s for each time, three times). Then, NTA software (N30E, NanoFCM) was performed to analyze the particle size.

2.3. Exosome Labeling with FTY720. The purifed NSCs-Exos (3 mg) was dispersed in PBS solution (0.9 mL). Then, 0.1 mL FTY720 DMSO solution was added and sonicated 15 cycles (2 seconds per cycle, stop for 2 seconds) in an ultrasonic cell pulverizer. After that, the mixture was incubated at 37°C for 60 minutes. Centrifugation (12000 g, 30 minutes) was performed to get rid of unbound FTY720. After that, the FTY720-NSC-Exos pellet was washed 3 times and resuspended in PBS to an extent concentration. After passed through 0.22 μm syringe filter, FTY720-NSC-Exos was used for further study.

2.4. Detected the Concentration of FTY720 in FTY720-NSC-Exos. The content of FTY720 in NSC-Exos was determined by HPLC (Agilent 1200, Agilent Technologies). To evaporate solvent, FTY720-NSC-Exos (0.3 mL, contained 20 mg FTY720-NSC-Exos) was heated at 70°C. Then, the same volume of acetonitrile was added, after ultrasound, centrifuging at 24000 g for 10 minutes. The supernatant was filtered with a 0.22 μm syringe filter, and 20 μL aliquots were transferred into HPLC autosampler vials. To measure FTY720 concentration, standard curve of FTY720 was established. Samples were taken at different time points and analyzed using HPLC.

2.5. In Vivo

2.5.1. Animals and the SCI Model Establishment. 65 Sprague-Dawley (SD) rats (8-week-old, male) were purchased from the Shanghai SLAC Laboratory Animal Co., Ltd. (Shanghai, China). All the rats were allowed to access food and water free and living in standard condition (humidity: 55~70%; room temperature: 23 ± 2°C; light cycle: 12-h light/dark). All animal assays were performed according to the National Institutes of Health Guide for the Care and Use of Laboratory Animals. The animal experiments were in accordance with the guidelines of laboratory animal care and were approved by the Hangzhou Eyong Biotechnological Co., Ltd. Animal Experiment Center (Hangzhou, China).

After 1 week of adaptive feeding, according to previous study, the rats were anesthetized by inhaling 1.5% isoflurane and fixed in the prone position on the heating pad to perform thoracic grade 10 (T10) laminectomy [25]. The spinous procedures of T8 and T11 were clamped to fix the spine, and a laminectomy was performed at the T10 level by Horizons Impactor, causing 50 kd spinal contusion injury to the rats. Rats that only experienced laminectomy and without damage were used as the sham group. After the operation, all rats were placed in an environment of about 38.5°C until they woke up, and the bladder was emptied manually every

8 hours. At the same time, on the first day, all rats were administered with buprenorphine (0.05 mg/kg, ip) every 6 hours to relieve pain.

2.5.2. Experimental Groups. After surgery, 60 rats were divided into 5 groups ($n = 12$/group): sham, model, FTY720 (3 mg/kg) + model, NSC-Exos + model, and FTY720-NSC-Exos + model. After SCI within an hour, rats were treated with NSC-Exos or FTY720-NSC-Exos by tail vein injection (20 μg of NSC-Exos or FTY720-NSC-Exos in 0.3 mL PBS). The FTY720 (3 mg/kg) was administered by gavage, while the sham and model rats were administered 0.3 mL PBS by tail vein injection.

After 48 hours of surgery, the spinal cord was removed from each group of rats ($n = 6$) for immunohistochemistry, HE and TUNEL staining. Three rats were performed to evaluate the spinal cord edema in each group, and the remaining three rats in each group were performed behavioral studies 4 weeks after the surgery.

2.5.3. Rehabilitation of Spinal Cord Function. The Basso, Beattie and Bresnahan (BBB) exercise scale was used to estimate the recovery of hindlimb function after 1, 2, 3, and 4 weeks after injury. Briefly, electromyography was used to detect motor-evoked potentials and evaluate muscle response. After anesthesia, the stimulating electrode was used to stimulate the motor potential on the sciatic nerve and placed the recording electrode into gastrocnemius muscle to record the response of the induced motor potential.

2.5.4. Detection of Spinal Cord Edema. After being anesthetized (100 mg/kg body weight, sodium pentobarbital), T9, T10, and T11 (all about 2 mm) segments were removed from each rat immediately to evaluate the formation of edema. All samples were quantified and placed in a 90°C oven for 72 hours to acquire the dry weight. Edema was calculated as follows: Edema (%) = (wet weight − dry weight)/wet weight ∗ 100 [26].

2.5.5. Tissue Collection. After SCI for 48 hours, rats were anesthetized and perfused with 0.9% saline (containing 50 U/mL heparin) through the endocardium and then perfused with phosphate buffer (containing 4% PFA). A spinal cord segment (10 mm) was cut at the injured site and fixed in 4% PFA for 48 hours at room temperature. Then, the tissues were embedded in paraffin.

2.5.6. Histological Examination. Pathological damages of spinal cord segment tissues were investigated by hematoxylin and eosin (HE) in each group. The spinal cord segment tissues were postfixed and embedded in paraffin, then sectioned into about 4 μm thickness and stained with HE.

2.5.7. Apoptosis Assay. Terminal deoxynucleotidyl transferase dUTP nick end labeling (TUNEL) staining was used to detect the apoptosis during injury by In Situ Cell Death Detection Kit. The sections were deparaffinization and rehydration, then stained in accordance to the instructions of TUNEL kit. The apoptotic activity was detected by optical microscope.

2.5.8. Immunohistochemistry. After embedding in paraffin wax, the tissues were sliced to 4 μm thickness, then incubated in 0.3% H_2O_2 for 30 minutes and incubated in 0.1% Triton X-100 for 20 minutes. Next, the sections were incubated with primary antibodies, including anti-Aquaporin-4 (AQP4) antibody (1 : 50; AF5164; Affinity) and anti-claudin-5 antibody (1 : 50; AF5216; Affinity) overnight at 4°C and secondary antibody for 60 min at 37°C. Lastly, the sections were stained with DAB to develop the color and counterstained with hematoxylin.

2.5.9. Western Blotting Assay. The proteins of spinal cord (epicenter ±5 mm) were extracted by radioimmunoprecipitation assay (RIPA) cold lysis buffer. After loaded onto a SDS-PAGE gel, the proteins were separated by electrophoresis and transferred to a polyvinylidene difluoride (PVDF) membrane (GE Healthcare Life, USA). Then, 5% dried skim milk was added to block the nonspecific binding sites of membranes at 37°C for 1.5 hours. After that, the membranes were incubated with dilute solution of antibodies at 4°C overnight. After being washed, secondary antibody were added and incubated with the membranes at 37°C for 1 hour. The protein expression was then tested by enhanced chemiluminescence (ECL) (Solarbio, Beijing, China). The primary antibodies including β-actin (1 : 1000; 3700S; CST), anti-Bax antibody (1 : 1000; ab32503; Abcam), and anti-Bcl-2 antibody (1 : 2000; ab182858; Abcam).

2.6. In Vitro

2.6.1. Culture and Identification of Spinal Cord Microvascular Endothelial Cells (SCMECs). Five rats were anesthetized, and the spinal cords were removed. Then, the microvessel fragments were isolated according to previous study [27] and cultured in DMEM medium which contain 10% FBS, 100 μg/mL streptomycin, 100 U/mL penicillin, and 4 μg/mL puromycin. The medium was replaced by the same medium without puromycin after being incubated for 48 hours, then changed the medium every 2 days. When cells reached 80-90% confluence, they were used for the further experiments. Von Willebrand Factor (vWF, 1 : 250; ab154193; Abcam) was performed to detect the contamination of endothelial cell by immunocytochemistry [28].

2.6.2. Establishment of Cell Hypoxic Model. SCMECs were transferred into 6-well plates. When the cells reached 90%, the mediums were changed. SCMECs were divided into five groups: (1) control: SCMECs were cultured in a normal incubator. (2) Hypoxic: SCMECs were incubated in a hypoxic incubator. (3) Hypoxic+FTY720: SCMECs were cultured in the medium which contained 1 mM FTY720 in hypoxia incubator. (4) Hypoxic+NSC-Exos: SCMECs were cultured in the medium which contained 20 μg/mL NSC-Exos. (5) Hypoxic +FTY720-NSC-Exos: SCMECs were cultured in the medium which contained 20 μg/mL FTY720-NSC-Exos (NSC-Exos containing 1 mM FTY720) in hypoxia incubator. Each group was cultured for 6 h [29].

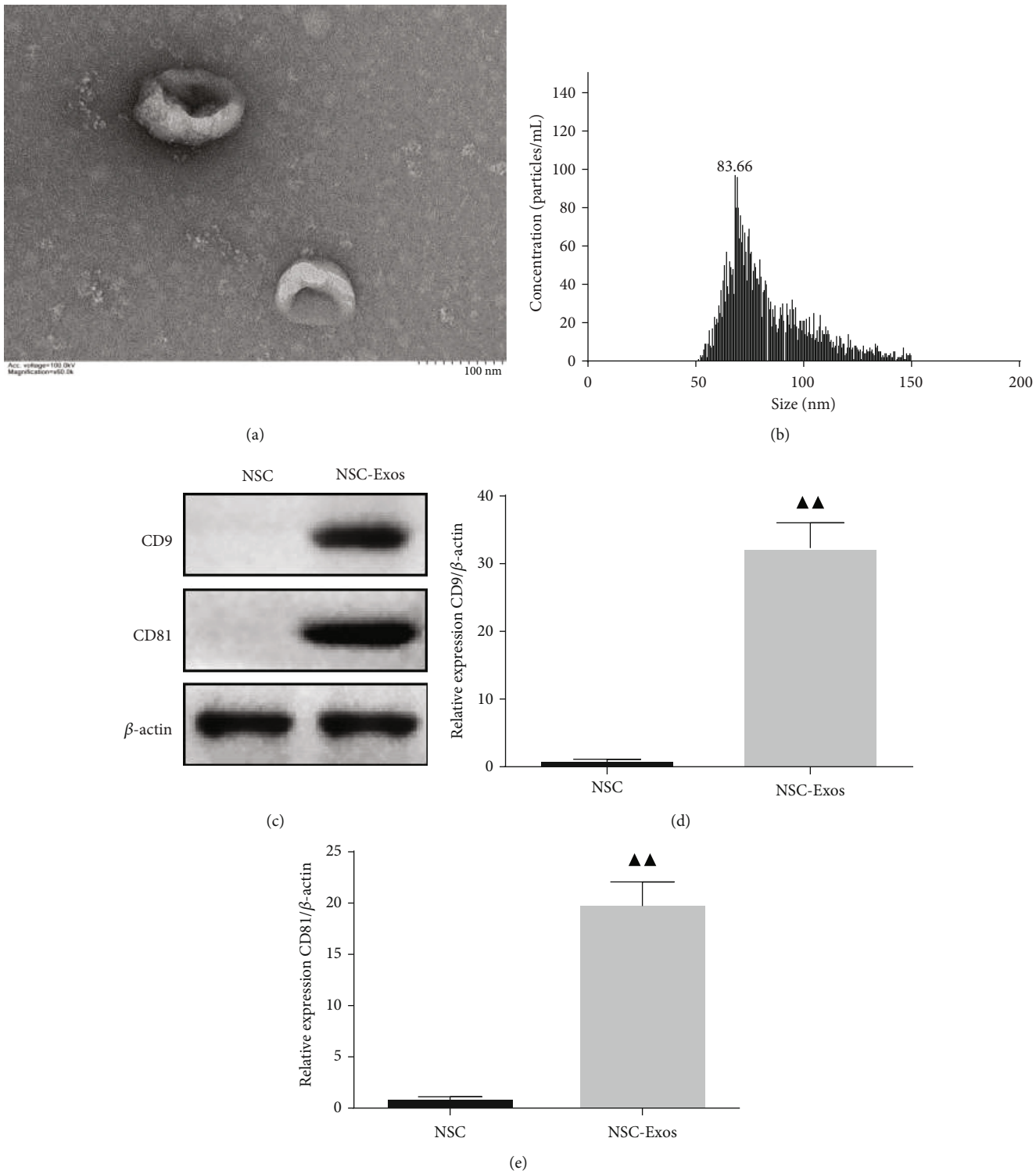

Figure 1: Identification of the neural stem cell exosomes (NSCs-Exos). (a) Morphology of NSCs-Exos was observed by TEM. (b) Nanoparticle size distribution was analyzed by nanoparticle-tracking analysis (NTA). (c) Representative immunoblots of exosomes CD9 and CD81 in different treatment groups. (d, e) Quantitative densitometric analysis of CD9 and CD81 on the exosomes. $^{\blacktriangle}P < 0.05$, $^{\blacktriangle\blacktriangle}P < 0.01$ vs. NSC.

2.6.3. Endothelial Permeability Measurement. The flux of FITC-dextran across the endothelial monolayer was measured by Transwell system to assess the paracellular permeability. Briefly, we put FITC-conjugated dextran in the upper chamber of the Transwell system. Then, aliquots (10 μL) got out from the lower chamber, and the medium was changed at 0, 5, 15, 30, 60, or 90 min, respectively. Finally, the fluorescence of each group was measured.

2.6.4. Western Blotting. The proteins of SCMECs in each group were also extracted using radioimmunoprecipitation assay (RIPA) cold lysis buffer. Specific operational procedures and primary antibodies were in accordance with that described above. The primary antibodies include β-actin (1 : 1000; 3700S; CST), anti-PTEN antibody (1 : 1000; ab267787; Abcam), phospho-pan-AKT1/2/3 (Ser473) antibody (1 : 500; ab38449; Affinity), and anti-ZO1 tight junction protein antibody (1 : 1000; ab96587; Abcam).

2.7. Statistical Analysis. The statistical analyses of all the data in this study were detected by SPSS 16.0 (IBM, USA). The results are expressed as $\bar{\chi} \pm s$. Group comparisons were investigated by Student's t-test or the Kruskal-Wallis H test according to variance homogeneity and inconsistency. In each experiment, $P < 0.05$ was seen as statistical significance.

3. Results

3.1. Characterization of NSC-Exos. NSCs-Exos were investigated by TEM, NTA, and Western blotting. There were spherical vesicles in NSCs-Exos, which were typically cup-shaped (Figure 1(a)). According to the NTA result, the distribution of NSCs-Exos diameter size were ranged from 30 to 150 nm and showed a relatively normal distribution (Figure 1(b)). Western blotting results showed that CD9 and CD81 were positive in NSCs-Exos and further confirmed the exosomes (Figures 1(c) and 1(d)).

3.2. The Concentration of FTY720 in FTY720-NSC-Exos. According to HPLC result, with the time of culturing increased, the concentration of FTY720 was increased. When FTY720 and NSC-Exos cocultured for 60 min, the concentration of FTY720 reached maximum (2.91 ± 0.11 mg) and no longer increased over time (Figure 2). Then, the FTY720-NSC-Exos was used for further study.

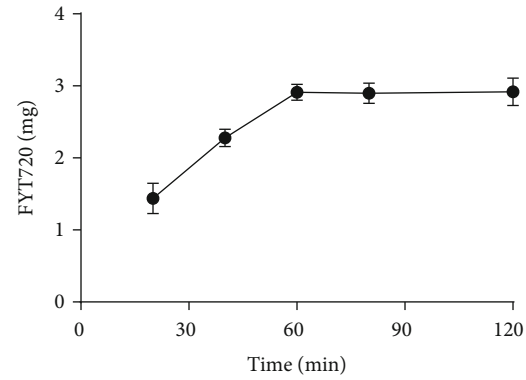

Figure 2: Concentration of FTY720 in FTY720-NSC-Exos with the development of cocultured time.

3.3. In Vivo

3.3.1. FTY720-NSC-Exos Ameliorated Motor Function of SCI Rats. In order to detect the ameliorated effect of FTY720-NSC-Exos on locomotion of SCI rats, the BBB experiment was performed every week and last 4 weeks in all groups. Compared with the model rats, FTY720-NSC-Exos treatment markedly ameliorated the locomotor function of the hind limbs after SCI 4 weeks ($P < 0.01$). At the same time, the improvement of FTY720-NSC-Exos was better than FTY720 and NSC-Exos ($P < 0.01$). These results revealed that FTY720-NSC-Exos can ameliorate the movement of SCI rats (Figure 3(a)).

3.3.2. FTY720-NSC-Exos Prevented the Formation of Edema. The effect of FTY720-NSC-Exos on the edema formation was evaluated. As shown in Figure 3(b), after SCI, the edema formation was significantly increased compared with sham group. FTY720, NSC-Exos, and FTY720-NSC-Exos significantly inhibited the accumulation of water on the injury site. Similarly, the inhibition of FTY720-NSC-Exos on the edema formation was better than other groups. These results suggested that FTY720-NSC-Exos could protect against edema formation.

3.3.3. FTY720-NSC-Exos Reduced SCI Lesion. HE assay result implied the structure of spinal cord in sham group rats was complete, neural cell morphology was normal, and no inflammatory cell infiltration was found. However, the morphology and tissue structure of spinal cord was incomplete and disordered, and the cell nuclear was split or even disappeared in SCI group. Meanwhile, a large number of inflammatory cell infiltration was observed and the interspace of cells and vascular was enlarged. After treated with FTY720, NSC-Exos, and FTY720-NSC-Exos, the inflammatory cell infiltration was less, and the tissue structure was more complete. The ameliorate effect on inflammation between the FTY720 and NSC-Exos had no significant differences. Particularly, rats which received FTY720-NSC-Exos showed a lower level of SCI lesion than other rats (Figures 4(a) and 4(b)).

3.3.4. FTY720-NSC-Exos Attenuated Cell Apoptosis. The number of apoptosis neuronal cells in the injury site of the spinal cord was assessed by TUNEL assay (Figures 4(a) and 4(c)). Compared with the model rats, the number of TUNEL-positive cells decreased obviously after treated with FTY720, NSC-Exos, and FTY720-NSC-Exos ($P < 0.01$). Meanwhile, the apoptotic index in the FTY720-NSC-Exos groups was markedly lower than that of the other two groups ($P < 0.01$).

3.3.5. The Effect of FTY720-NSC-Exos on the Edema-Related Proteins. Aquaporins acts as a key role in keeping the spinal cord water balance. The effect of exosomes on the expression of AQP4 and claudin-5 was detected by immunohistochemistry. The expression of claudin-5 was markedly decreased, while AQP4 was increased ($P < 0.01$). However, FTY720, NSC-Exos, and FTY720-NSC-Exos increased the expression of claudin-5. Meanwhile, the expression of AQP4 was decreased obviously ($P < 0.01$, Figure 5).

3.3.6. The Effect of FTY720-NSC-Exos on the Apoptosis-Related Proteins. In order to detect the effect of FTY720-NSC-Exos on the apoptosis-related proteins, Western blotting

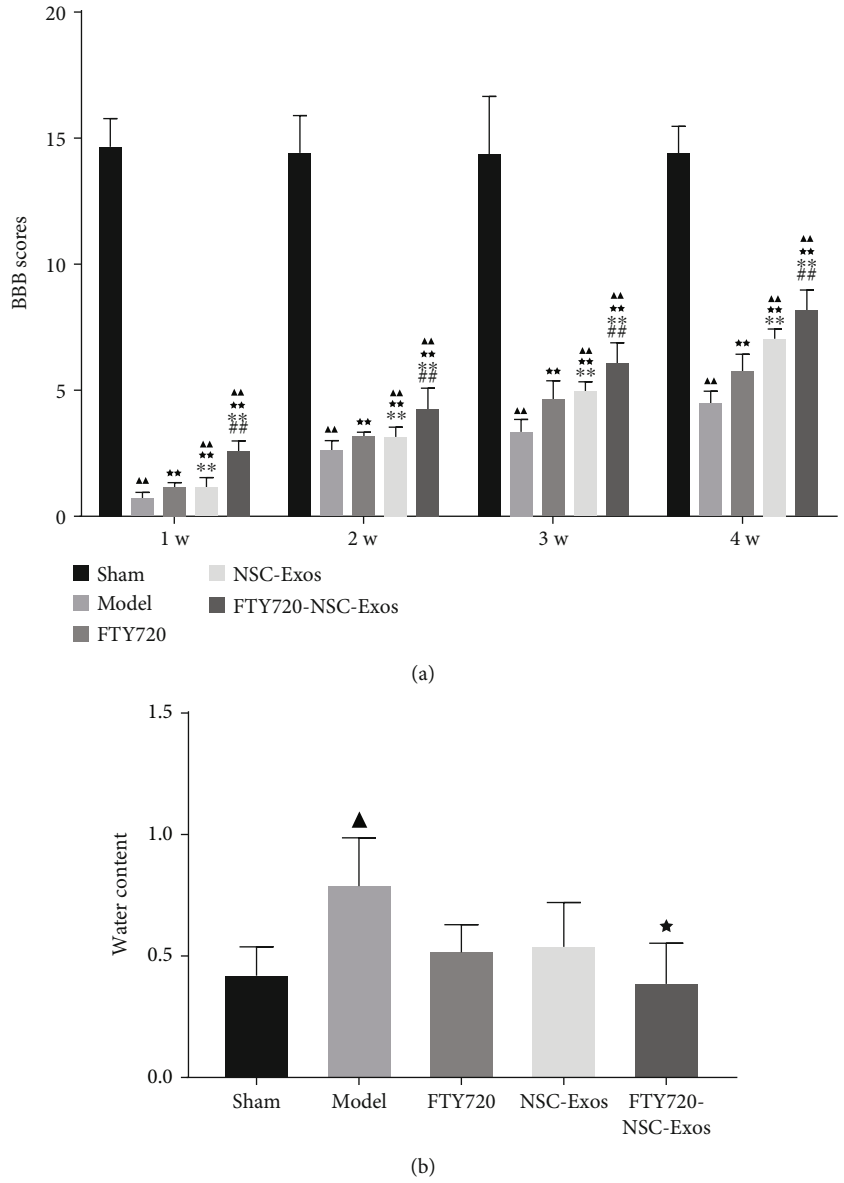

Figure 3: FTY720-NSC-Exos repaired the hindlimb dysfunction and reduced edema in SCI model rats. (a) Basso, Beattie, and Bresnahan (BBB) scores was performed to access the function of hindlimb recovery from 1 to 4 weeks in each group ($\bar{\chi} \pm s$, $n = 3$). $^{\blacktriangle}P < 0.05$, $^{\blacktriangle\blacktriangle}P < 0.01$ vs. sham, $^{\bigstar}P < 0.05$, $^{\bigstar\bigstar}P < 0.01$ vs. model, $^{*}P < 0.05$, $^{**}P < 0.01$ vs. FTY720, $^{\#}P < 0.05$, $^{\#\#}P < 0.01$ vs. NSCs-Exos.

was performed. The protein expression of Bax was markedly downregulated, and the protein expression of Bcl-2 was markedly upregulated. However, compared to the model group, FTY720, NSC-Exos, and FTY720-NSC-Exos attenuated the expression of Bax and upregulated the expression of Bcl-2 ($P < 0.01$). What is more, the inhibitory effect of FTY720-NSC-Exos on apoptosis was better than FTY720 and NSC-Exos ($P < 0.01$) (Figure 6).

3.4. In Vitro

3.4.1. Identification of SCMECs. The morphology of microvessel segments were typically beaded or branched, and SCMECs crawled out of the microvessel segments after 48 hours. Then, the SCMECs are with a typical "pebble" shape and adherent growth. After 72 hours, the cells gradually increased and were identified by labeled with vWF (Figure 7(a)). Figure 5(b) showed that vWF had a high expression in SCMECs.

3.4.2. FTY720-NSC-Exos Protected SCMECs under Hypoxic Conditions. Transwell experiment was performed to detect the permeability of SCMECs. The permeability of the SCMECs was highly improved under hypoxic circumstance. Interestingly, the permeability induced by hypoxia was decreased after treated with FTY720, NSC-Exos, and FTY720-NSC-Exos ($P < 0.05$). These results were consistent with Western blotting results; FTY720, NSC-Exos, and

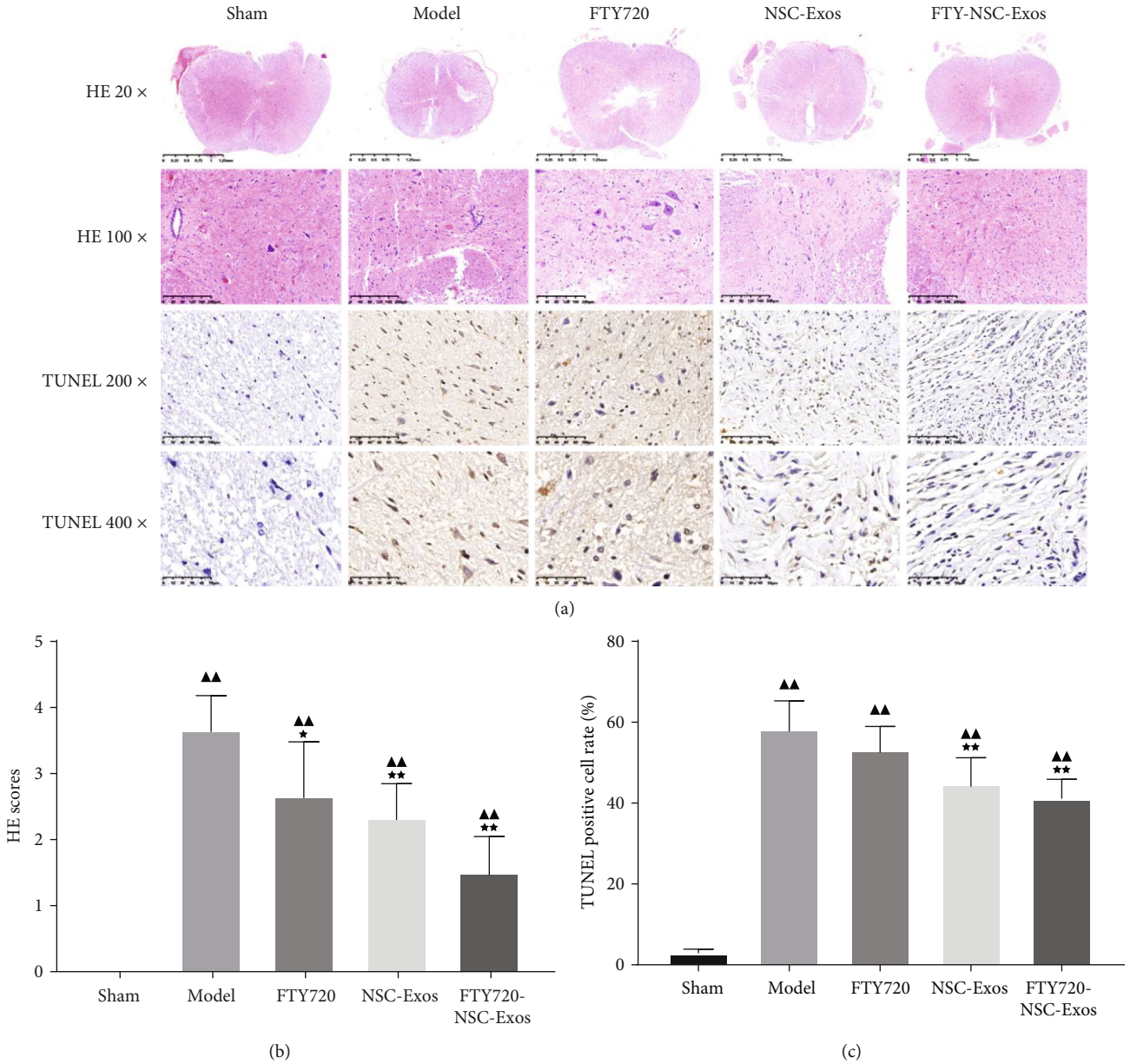

Figure 4: FTY720-NSC-Exos restored histological abnormalities and alleviated damages in spinal cord. (a) Representative microphotographs of HE (original magnification 20x, 100x) and TUNEL staining in each group (original magnification 200x, 400x). (b) Semiquantitative estimate of the histological lesions. (c) Quantitative analysis of the neuronal apoptosis in the lesions site of the spinal cord ($\bar{\chi} \pm s$, $n = 6$), $^{\blacktriangle}P < 0.05$, $^{\blacktriangle\blacktriangle}P < 0.01$ vs. sham, $^{\star}P < 0.05$, $^{\star\star}P < 0.01$ vs. model.

FTY720-NSC-Exos can downregulate the expression of PTEN and upregulate the expression of p-Akt and ZO-1 in SCMECs under hypoxic circumstance (Figure 8). Moreover, the improvement of FTY720-NSC-Exos on the permeability was better than others, which indicates that FTY720-NSC-Exos treatment can protect SCMECs under hypoxic conditions.

4. Discussion

We investigated the improvement of FTY720-NSC-Exos on locomotors in SCI rats and the mechanism of FTY720-NSC-Exos in improving secondary degeneration after SCI. FTY720 is the nonselective S1P ($S1P_1$, $S1P_3$, $S1P_4$, and $S1P_5$) receptor agonist and is phosphorylated by sphingosine kinase [30]. At present, S1P1 receptor-mediated immunosuppression is the common systemic effect of FTY720 administration [31]. The positive effectivity of FTY720 has been demonstrated in multifarious autoimmune disorders and allograft survival animal models [32–34]. It was believed that immunity is the main biological activity of these diseases, but our study demonstrated the nonimmunity impact of FTY720 in the SCI treatment.

At the same time, stem cell transplantation has shown a good application prospect in the treatment of SCI [35]. In the past, homing, differentiation, and replacement of injured

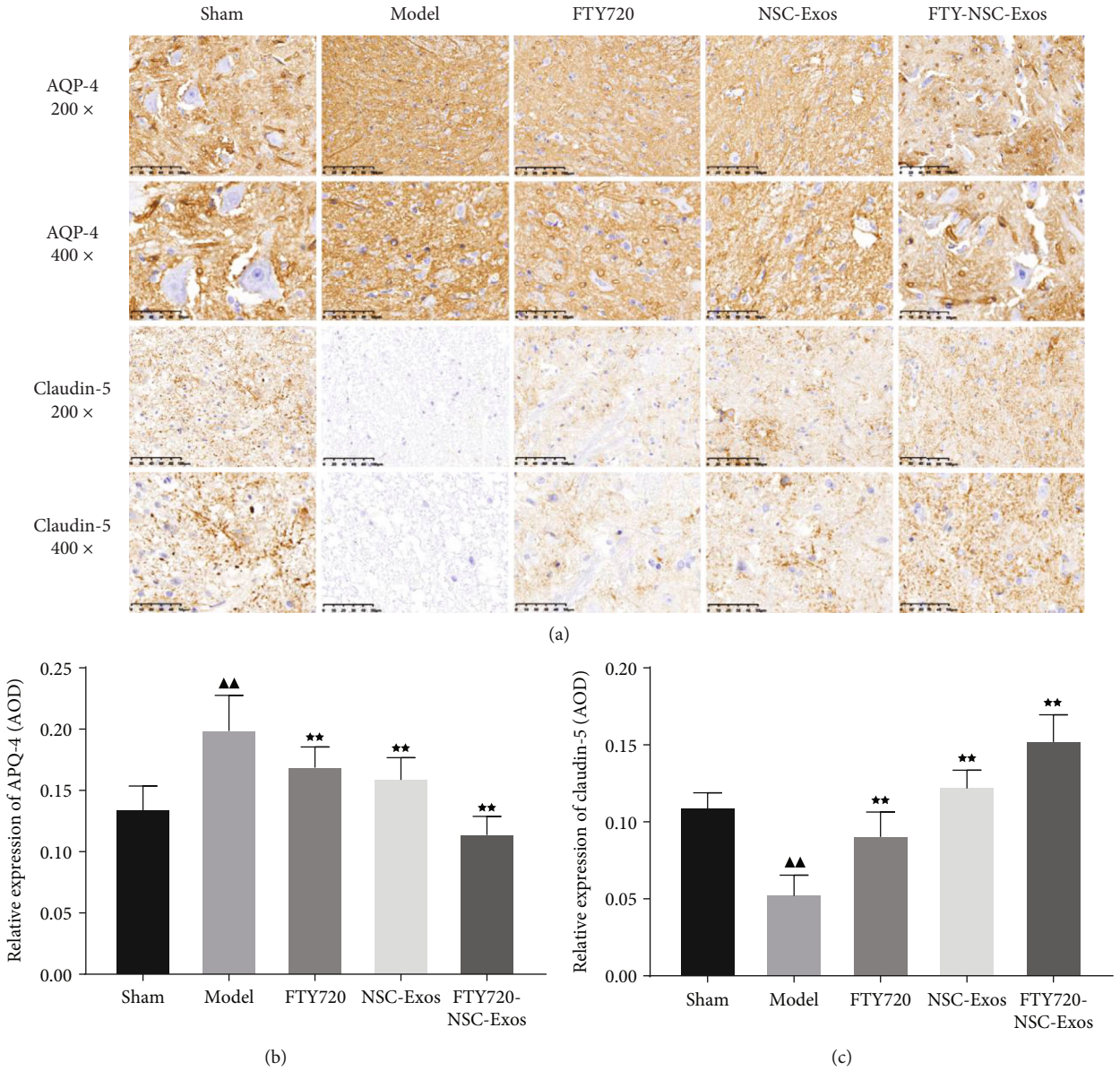

Figure 5: The expression level of AQP-4 and claudin-5 was investigated by immunohistochemical in each group rats. (a) Representative microphotographs of AQP-4 and claudin-5 (original magnification 200x, 400x). (b) Quantitative analysis of AQP-4 and claudin-5 protein expression ($\bar{\chi} \pm s$, $n = 6$), $^{\blacktriangle}P < 0.05$, $^{\blacktriangle\blacktriangle}P < 0.01$ vs. sham, $^{\star}P < 0.05$, $^{\star\star}P < 0.01$ vs. model, $^{*}P < 0.05$, $^{**}P < 0.01$ vs. FTY720, $^{\#}P < 0.05$, $^{\#\#}P < 0.01$ vs. NSCs-Exos.

cells were seen as the repair mechanism of stem cells [36]. However, the repairment of extracellular vesicles secreted by transplanted cells to SCI was attracted more attention nowadays [37]. The exosomes of NSCs play a consistent effect with NSC transplantation and avoid the limitations of direct stem cell transplantation. Firstly, the NSCs-Exos were derived from NSCs and with a diameter range from 30 to 150 nm by using NTA analysis in this study. At the same time, surface markers CD9 and CD81 were expressed on the surface of NSCs-Exos. And the morphology of NSCs-Exos was confirmed by TEM. After that, we prepared NSCs-Exos containing FTY720 and conducted a series of experiments to investigate the therapeutic effect in the SCI model *in vivo* and *in vitro*.

A range of complex pathophysiological changes, such as hemorrhage, ischemia, edema, damage of the blood-spinal barrier, and obstacles to microhemodynamics were caused by SCI [38]. These changes further promote cell apoptosis, necrosis, inflammatory cells infiltration, and the reconstruction of inhibitory functional synapses, which in turn affect functional recovery [39]. Tissue edema is a common symptom in SCI and caused by raised permeability of the blood spinal cord barrier (BSCB) [40]. The permeability changes of BSCB increased the exchange of harmful factors in tissue and blood and further induced cell death and permanent neurological dysfunction [41]. Claudin-5 is mainly expressed of endothelial cells and acts a key role in BSCB [42]. During SCI, alterations of its distribution and expression affect the

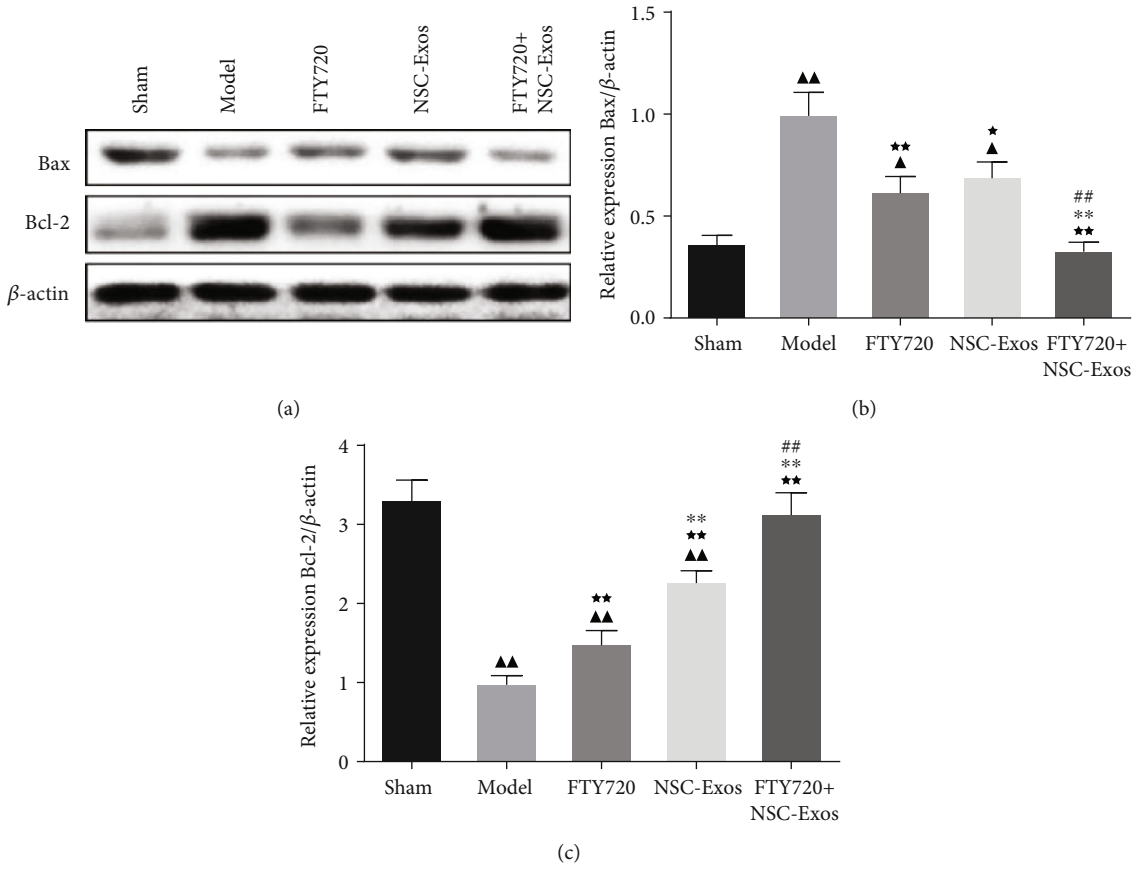

Figure 6: (a–c) The expressions of apoptotic-related proteins in each groups were determined by WB ($\bar{\chi} \pm s$, $n = 6$), $^{\blacktriangle}P < 0.05$, $^{\blacktriangle\blacktriangle}P < 0.01$ vs. sham, $^{\bigstar}P < 0.05$, $^{\bigstar\bigstar}P < 0.01$ vs. model, $^{*}P < 0.05$, $^{**}P < 0.01$ vs. FTY720, $^{\#}P < 0.05$, $^{\#\#}P < 0.01$ vs. NSCs-Exos.

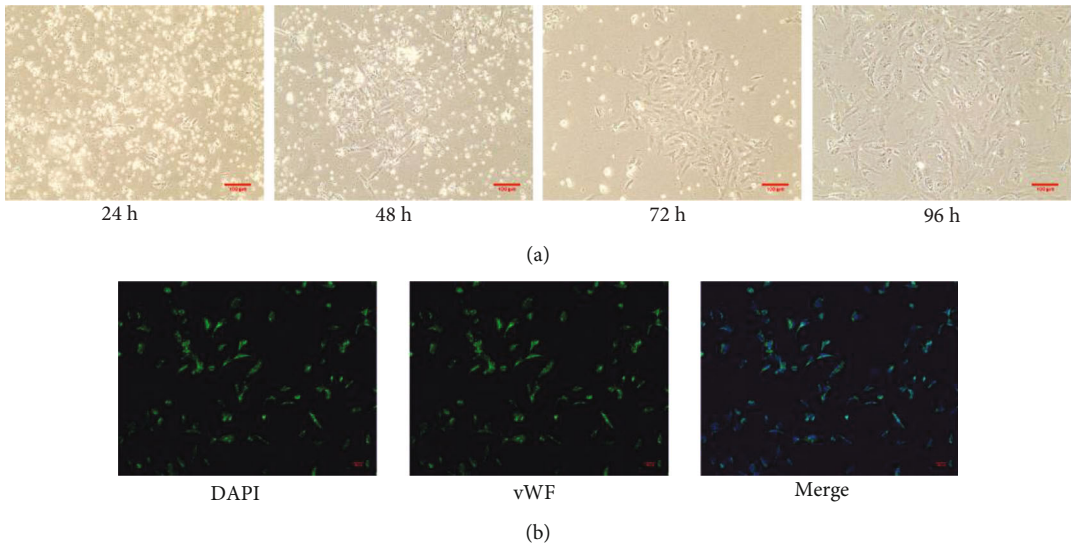

Figure 7: Identification of SCMECs. (a) Morphology photographs of SCMECs (original magnification 100x). (b) Expression of vWF antibodies in SCMECs (original magnification 200x) ($\bar{\chi} \pm s$, $n = 6$).

changes of BSCB permeability [43]. Reducing the formation of edema after traumatic SCI is beneficial to the functional recovery of acute and chronic stage after damage [44]. In this study, we observed that FYT720-NSCS-Exos markedly reduced the formation of edema and increased the expression of Claudin-5 after SCI. Meanwhile, AQP4 acts a key role in angioedema and cytotoxic edema and is essential for the removal of angioedema [45]. When the expression of AQP4

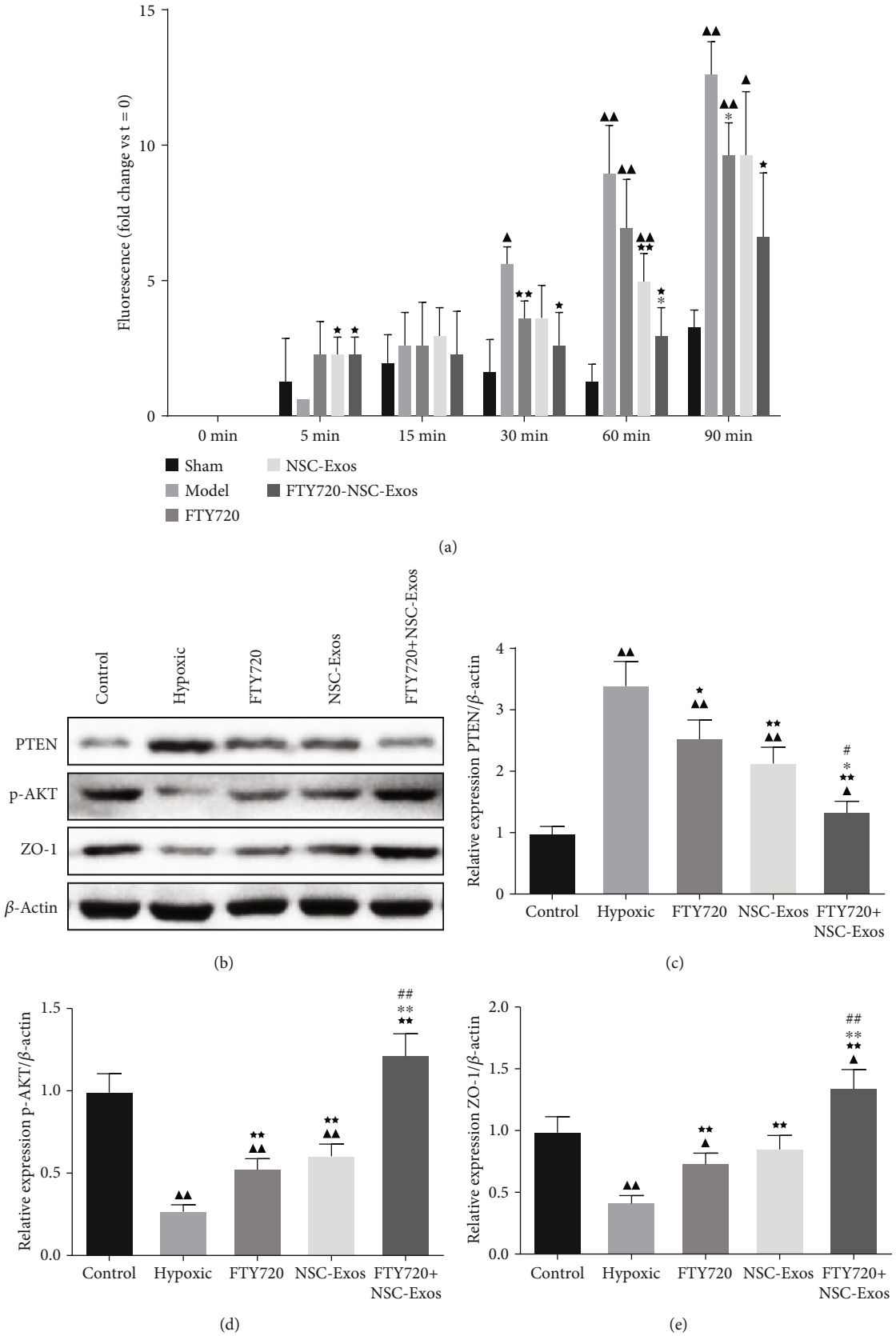

Figure 8: FTY720-NSC-Exos protected SCMECs under hypoxic conditions. (a) The permeability of the SCMECs was detected by Transwell experiment. (b–e) The protein level of PTEN, p-AKT, and ZO-1 in each groups ($\bar{\chi} \pm s$, $n = 6$), $^{\blacktriangle}P < 0.05$, $^{\blacktriangle\blacktriangle}P < 0.01$ vs. control, $^{\bigstar}P < 0.05$, $^{\bigstar\bigstar}P < 0.01$ vs. hypoxic, $^{*}P < 0.05$, $^{**}P < 0.01$ vs. FTY720, $^{\#}P < 0.05$, $^{\#\#}P < 0.01$ vs. NSCs-Exos.

was high, the liquid was entered into cells and caused cytotoxic edema. Here, the expression of AQP4 in the damage location was raised. It might be the increased expression of AQP4 promotes water entered into spinal cord parenchyma from the vasculature and increases the spinal cord swelling after injury. After treated with FYT720-NSCS-Exos, the expression of AQP4 was significantly reduced. This suggested that FYT720-NSCS-Exos can alleviate spinal cord edema by regulating the expression of claudin-5 and AQP4 proteins during SCI.

Apoptosis is related to many central nervous system diseases and affects the functional recovery after SCI [46]. Meanwhile, Bax and Bcl-2 are key cell apoptosis-related components. TUNEL assay showed that FYT720-NSCS-Exos treatment can reduce the apoptosis of neuronal cells, which was consistent with Western blotting assay. The protein level of Bax was markedly decreased, while the level of Bcl-2 was increased. These assays all implied that FYT720-NSCS-Exos treatment could protect neuronal cells from apoptosis induced by SCI. In addition, the administration of FYT720-NSCS-Exos also improved the morphology of neuronal cells, reduced inflammatory infiltration, and further improved motor behaviour of the hind limbs.

In order to further estimate the mechanism of barrier protection, the permeability of endothelial cells was evaluated by the Transwell assay in an *in vitro* hypoxia model. The result showed that FYT720-NSCS-Exos can availably protect the endothelial barrier and promote the expression of ZO-1 under the hypoxic circumstance. PI3K/AKT pathway is a regulator of apoptosis and survival, and PTEN is considered to be a negative regulator of the PI3K/AKT pathway [47]. p-Akt is a key protein in PI3K/AKT pathway and could inhibit cell apoptosis and improve cell survival [48]. Here, we confirmed that FYT720-NSCS-Exos downregulated the expression of PTEN and promoted the expression of p-Akt in SCMECs. It is suggested that FYT720-NSCS-Exos could reduce cell apoptosis by regulating the PTEN/AKT signal pathway.

In conclusion, we demonstrated that FTY720-NSCs-Exos treatment after SCI can promote the morphological of neurons, thereby improving hindlimb motor behavior. At the same time, FTY720-NSCs-Exos treatment could improve endothelial function and alleviate cell apoptotic and spinal cord edema, thereby ameliorating functional and behavioral after SCI by regulating the PTEN/AKT signal pathway. Meanwhile, the protection of the endothelial cells under hypoxia circumstance might be one of its potential mechanisms. These findings indicated that FTY720-NSCs-Exos is a promising therapy for SCI.

Data Availability

All data generated or analyzed during this study are included in this article.

Conflicts of Interest

The authors declare that there are no conflicts of interest.

Acknowledgments

The work was supported by the Basic Public Welfare Research Project of Zhejiang Province (No. LGF19H060001).

References

[1] R. Kumar, J. Lim, R. A. Mekary et al., "Traumatic spinal injury: global epidemiology and worldwide volume," *World Neurosurgery*, vol. 113, pp. e345–e363, 2018.

[2] A. Lattard, G. Poulen, S. Bartolami, Y. N. Gerber, and F. E. Perrin, "Negative impact of sigma-1 receptor agonist treatment on tissue integrity and motor function following spinal cord injury," *Frontiers in Pharmacology.*, vol. 12, 2021.

[3] X. Yuan, Q. Wu, P. Wang et al., "Exosomes derived from pericytes improve microcirculation and protect blood-spinal cord barrier after spinal cord injury in mice," *Frontiers in Neuroscience*, vol. 13, 2019.

[4] X. Zhang, X. D. Liu, Y. F. Xian, F. Zhang, and Z. X. Lin, "Berberine enhances survival and axonal regeneration of motoneurons following spinal root avulsion and re-implantation in rats," *Free Radical Biology and Medicine*, vol. 143, no. 11, pp. 454–470, 2019.

[5] J. Penney and L. H. Tsai, "JAKMIP1: translating the message for social behavior," *Neuron*, vol. 88, no. 6, pp. 1070–1072, 2015.

[6] T. Fukuoka, A. Kato, M. Hirano, and A. Natsume, "Neurod4 converts endogenous neural stem cells to neurons with synaptic formation after spinal cord injury," *IScience*, vol. 24, no. 2, p. 102074, 2021.

[7] M. Deng, P. Xie, Z. Chen et al., "Mash-1 modified neural stem cells transplantation promotes neural stem cells differentiation into neurons to further improve locomotor functional recovery in spinal cord injury rats," *Gene*, vol. 22, 2021.

[8] L. Zhang, C. Fan, W. Hao et al., "Nscs migration promoted and drug delivered exosomes-collagen scaffold via a bio-specific peptide for one-step spinal cord injury repair," *Advanced Healthcare Materials*, vol. 10, 2021.

[9] J. O. Jeong, J. W. Han, J. M. Kim et al., "Malignant tumor formation after transplantation of short-term cultured bone marrow mesenchymal stem cells in experimental myocardial infarction and diabetic neuropathy," *Circulation Research*, vol. 108, no. 11, pp. 1340–1347, 2011.

[10] S. Koprivec, M. Novak, S. Bernik, and G. Majdič, "Treatment of cranial cruciate ligament injuries in dogs using a combination of tibial tuberosity advancement procedure and autologous mesenchymal stem cells/multipotent mesenchymal stromal cells - a pilot study," *Acta Veterinaria Hungarica*, vol. 68, 2021.

[11] A. A. Nargesi, L. O. Lerman, and A. Eirin, "Mesenchymal stem cell-derived extracellular vesicles for kidney repair: current status and looming challenges," *Stem Cell Research & Therapy*, vol. 8, no. 1, p. 273, 2017.

[12] S. Keshtkar, N. Azarpira, and M. H. Ghahremani, "Mesenchymal stem cell-derived extracellular vesicles: novel frontiers in regenerative medicine," *Stem Cell Research & Therapy.*, vol. 9, no. 1, p. 63, 2018.

[13] A. S. Azmi, B. Bao, and F. H. Sarkar, "Exosomes in cancer development, metastasis, and drug resistance: a comprehensive review," *Cancer Metastasis Reviews*, vol. 32, no. 3–4, pp. 623–642, 2013.

[14] G. K. Tofaris, "A critical assessment of exosomes in the pathogenesis and stratification of Parkinson's disease," *Journal of Parkinson's Disease*, vol. 7, no. 4, pp. 569–576, 2017.

[15] W. Y. Li, Q. B. Zhu, L. Y. Jin, and X. Y. Hu, "Exosomes derived from human induced pluripotent stem cell-derived neural progenitor cells protect neuronal function under ischemic conditions," *Neural Regeneration Research*, vol. 16, no. 10, pp. 2064–2070, 2021.

[16] C. R. Harrell, A. Volarevic, V. Djonov, and V. Volarevic, "Mesenchymal stem cell-derived exosomes as new remedy for the treatment of neurocognitive disorders," *International Journal of Molecular Sciences.*, vol. 22, no. 3, p. 1433, 2021.

[17] D. T. Bowers, C. E. Olingy, P. Chhabra et al., "An engineered macroencapsulation membrane releasing fty720 to precondition pancreatic islet transplantation," *Journal of Biomedical Materials Research. Part B, Applied Biomaterials*, vol. 106, no. 2, pp. 555–568, 2018.

[18] Y. Norimatsu, T. Ohmori, A. Kimura et al., "FTY720 improves functional recovery after spinal cord injury by primarily non-immunomodulatory mechanisms," *The American Journal of Pathology*, vol. 180, no. 4, pp. 1625–1635, 2012.

[19] K. Yamazaki, M. Kawabori, T. Seki et al., "Fty720 attenuates neuropathic pain after spinal cord injury by decreasing systemic and local inflammation in a rat spinal cord compression model," *Journal of Neurotrauma*, vol. 37, no. 15, pp. 1720–1728, 2020.

[20] L. J. Sim-Selley, J. L. Wilkerson, J. J. Burston et al., "Differential tolerance to fty720-induced antinociception in acute thermal and nerve injury mouse pain models: role of sphingosine-1-phosphate receptor adaptation," *Journal of Pharmacology & Experimental Therapeutics*, vol. 366, no. 3, pp. 509–518, 2018.

[21] H. Xin, Y. Li, B. Buller et al., "Exosome-mediated transfer of miR-133b from multipotent mesenchymal stromal cells to neural cells contributes to neurite outgrowth," *Stem Cells*, vol. 30, no. 7, pp. 1556–1564, 2012.

[22] C. Villarroya-Beltri, C. Gutiérrez-Vázquez, F. Sánchez-Madrid, and M. Mittelbrunn, "Analysis of microRNA and protein transfer by exosomes during an immune synapse," *Methods in Molecular Biology*, vol. 1024, pp. 41–51, 2013.

[23] K. Dissanayake, G. Midekessa, F. Lttekivi, and A. Fazeli, "Measurement of the size and concentration and zeta potential of extracellular vesicles using nanoparticle tracking analyzer," *Methods in Molecular Biology*, vol. 2273, pp. 207–218, 2021.

[24] P. Carnell-Morris, D. Tannetta, A. Siupa, P. Hole, and R. Dragovic, "Analysis of extracellular vesicles using fuorescence nanoparticle tracking analysis," *Methods in Molecular Biology*, vol. 1660, pp. 153–173, 2017.

[25] X. C. Yuan, P. Wang, H. W. Li et al., "Effects of melatonin on spinal cord injury-induced oxidative damage in mice testis," *Andrologia*, vol. 49, no. 7, article e12692, 2017.

[26] T. Winkler, H. S. Sharma, E. Stlberg, and R. D. Badgaiyan, "Neurotrophic factors attenuate alterations in spinal cord evoked potentials and edema formation following trauma to the rat spinal cord," *Acta Neurochirurgica. Supplement*, vol. 76, pp. 291–296, 2000.

[27] X. Yuan, Q. Wu, X. Liu, H. Zhang, and R. Xiu, "Transcriptomic profile analysis of brain microvascular pericytes in spontaneously hypertensive rats by RNA-Seq," *American Journal of Translational Research*, vol. 10, no. 8, pp. 2372–2386, 2018.

[28] Q. Wu, Y. Jing, X. Yuan et al., "The distinct abilities of tube-formation and migration between brain and spinal cord microvascular pericytes in rats," *Clinical Hemorheology and Microcirculation*, vol. 60, no. 2, pp. 231–240, 2015.

[29] K. Nohda, T. Nakatsuka, D. Takeda et al., "Selective vulnerability to ischemia in the rat spinal cord: a comparison between ventral and dorsal horn neurons," *Spine*, vol. 32, no. 10, pp. 1060–1066, 2007.

[30] V. Brinkmann, J. G. Cyster, and T. Hla, "FTY720: sphingosine 1-phosphate receptor-1 in the control of lymphocyte egress and endothelial barrier function," *American Journal of Transplantation*, vol. 4, no. 7, pp. 1019–1025, 2004.

[31] S. Mandala, R. Hajdu, J. Bergstrom et al., "Alteration of lymphocyte trafficking by sphingosine-1-phosphate receptor agonists," *Science*, vol. 296, no. 5566, pp. 346–349, 2002.

[32] M. Aoki, A. Kondo, N. Matsunaga, A. Honda, and R. Ogawa, "The immunosuppressant fingolimod (FTY720) for the treatment of mechanical force-induced abnormal scars," *Journal of Immunology Research*, vol. 2020, 11 pages, 2020.

[33] X. D. Guo, J. Ji, T. F. Xue, Y. Q. Sun, and X. L. Sun, "Fty720 exerts anti-glioma effects by regulating the glioma microenvironment through increased cxcr4 internalization by glioma-associated microglia," *Frontiers in Immunology*, vol. 11, p. 178, 2020.

[34] A. S. Perla, L. Fratini, P. S. Cardoso, F. CBD, and R. Roesler, "Fingolimod (fty720) reduces viability and survival and increases histone h3 acetylation in medulloblastoma cells," *Pediatric Hematology and Oncology*, vol. 37, no. 2, 2019.

[35] I. Jones, L. N. Novikova, M. Wiberg, and L. N. Novikov, "Human embryonic stem cell-derived neural crest cells promote sprouting and motor recovery following spinal cord injury in adult rats," *Cell Transplantation*, vol. 30, article 096368972098824, 2021.

[36] M. Sadat-Ali, D. A. Al-Dakheel, A. Ahmed, and M. I. Al-Bayat, "Spinal cord injury regeneration using autologous bone marrow-derived neurocytes and rat embryonic stem cells: a comparative study in rats," *World Journal of Stem Cells*, vol. 12, no. 12, pp. 1591–1602, 2020.

[37] M. Z. Ratajczak, T. Jadczyk, D. Pêdziwiatr, and W. Wojakowski, "New advances in stem cell research: practical implications for regenerative medicine," *Polskie Archiwum Medycyny Wewnętrznej*, vol. 124, no. 7-8, pp. 417–426, 2014.

[38] J. Wang, W. Zhao, X. Wang, and J. Yan, "Enhanced store-operated calcium entry (SOCE) exacerbates motor neurons apoptosis following spinal cord injury," *Gen Physiol Biophys*, vol. 40, no. 1, pp. 61–69, 2021.

[39] W. J. Alilain, K. P. Horn, H. Hu, T. E. Dick, and J. J. N. Silver, "Functional regeneration of respiratory pathways after spinal cord injury," *Nature*, vol. 475, no. 7355, pp. 196–200, 2011.

[40] X. Ying, Q. Xie, S. Li, and S. Jiang, "Water treadmill training attenuates blood-spinal cord barrier disruption in rats by promoting angiogenesis and inhibiting matrix metalloproteinase-2/9 expression following spinal cord injury," *Fluids Barriers CNS*, vol. 17, no. 1, p. 70, 2020.

[41] Z. K. Fan, Y. Cao, G. Lv, Y. S. Wang, and Z. P. Guo, "The effect of cigarette smoke exposure on spinal cord injury in rats," *Journal of Neurotrauma*, vol. 30, no. 6, pp. 473–479, 2013.

[42] Y. Kong, Y. Yang, Q. B. Guan, L. Guo, and C. Y. Han, "Study on the effect of bfgf combined with antrodia camphorate polysaccharide on the repair of neural function after mechanical spinal cord injury," *Chin J Mod Appl Pharm*, vol. 36, no. 1, pp. 85–89, 2019.

[43] S. Liebner, C. J. Czupalla, and H. Wolburg, "Current concepts of bloodbrain barrier development," *The International Journal of Developmental Biology*, vol. 55, no. 4-5, pp. 467–476, 2011.

[44] A. M. Fukuda, A. Adami, V. Pop et al., "Posttraumatic reduction of edema with aquaporin-4 RNA interference improves acute and chronic functional recovery," *Journal of Cerebral Blood Flow and Metabolism*, vol. 33, no. 10, pp. 1621–1632, 2013.

[45] J. A. Hubbard, J. I. Szu, J. M. Yonan, and D. K. Binder, "Regulation of astrocyte glutamate transporter-1 (GLT1) and aquaporin-4 (AQP4) expression in a model of epilepsy," *Experimental Neurology*, vol. 283, no. Part A, pp. 85–96, 2016.

[46] J. Zhang, Z. Cui, G. Feng et al., "RBM5 and p53 expression after rat spinal cord injury: implications for neuronal apoptosis," *The International Journal of Biochemistry & Cell Biology*, vol. 60, pp. 43–52, 2015.

[47] S. Shen, M. Zhang, M. Ma, and J. Qu, "Potential neuroprotective mechanisms of methamphetamine treatment in traumatic brain injury defined by large-scale ionstar-based quantitative proteomics," *International Journal of Molecular Sciences*, vol. 22, no. 5, p. 2246, 2021.

[48] B. Saurav and P. M. Abdul-Muneer, "Pten blocking stimulates corticospinal and raphespinal axonal regeneration and promotes functional recovery after spinal cord injury," *Journal of Neuropathology & Experimental Neurology*, vol. 80, no. 2, pp. 169–181, 2020.

Hindawi
Journal of Immunology Research
Volume 2021, Article ID 5707242, 14 pages
https://doi.org/10.1155/2021/5707242

Research Article

Curculigoside Protects against Titanium Particle-Induced Osteolysis through the Enhancement of Osteoblast Differentiation and Reduction of Osteoclast Formation

Fangbing Zhu,[1] Jianyue Wang,[2,3] Yueming Ni,[2,3] Wei Yin,[4] Qiao Hou,[2,3] Yingliang Zhang,[2,3] Shigui Yan ,[1] and Renfu Quan [2,3]

[1]*Department of Orthopaedic Surgery, Second Affiliated Hospital, School of Medicine, Zhejiang University, Hangzhou, 310009 Zhejiang Province, China*
[2]*Department of Orthopaedics, Xiaoshan Traditional Chinese Medical Hospital, Hangzhou, 311201 Zhejiang Province, China*
[3]*Department of Orthopedics, Affiliated Jiangnan Hospital of Zhejiang Chinese Medical University, Hangzhou, 311201 Zhejiang Province, China*
[4]*School of Medicine, Zhejiang University, Hangzhou, 310058 Zhejiang Province, China*

Correspondence should be addressed to Shigui Yan; zrjwsj@zju.edu.cn and Renfu Quan; quanrenfu@126.com

Received 21 April 2021; Accepted 15 June 2021; Published 5 July 2021

Academic Editor: Kai Wang

Wear particle-induced periprosthetic osteolysis is mainly responsible for joint replacement failure and revision surgery. Curculigoside is reported to have bone-protective potential, but whether curculigoside attenuates wear particle-induced osteolysis remains unclear. In this study, titanium particles (Ti) were used to stimulate osteoblastic MC3T3-E1 cells in the presence or absence of curculigoside, to determine their effect on osteoblast differentiation. Rat osteoclastic bone marrow stromal cells (BMSCs) were cocultured with Ti in the presence or absence of curculigoside, to evaluate its effect on osteoclast formation *in vitro*. Ti was also used to stimulate mouse calvaria to induce an osteolysis model, and curculigoside was administrated to evaluate its effect in the osteolysis model by micro-CT imaging and histopathological analyses. As the results indicated, in MC3T3-E1 cells, curculigoside treatment attenuated the Ti-induced inhibition on cell differentiation and apoptosis, increased alkaline phosphatase activity (ALP) and cell mineralization, and inhibited TNF-α, IL-1β, and IL-6 production and ROS generation. In BMSCs, curculigoside treatment suppressed the Ti-induced cell formation and suppressed the TNF-α, IL-1β, and IL-6 production and F-actin ring formation. *In vivo*, curculigoside attenuated Ti-induced bone loss and histological damage in murine calvaria. Curculigoside treatment also reversed the RANK/RANKL/OPG and NF-κB signaling pathways, by suppressing the RANKL and NF-κB expression, while activating the OPG expression. Our study demonstrated that curculigoside treatment was able to attenuate wear particle-induced periprosthetic osteolysis in *in vivo* and *in vitro* experiments, promoted osteoblastic MC3T3-E1 cell differentiation, and inhibited osteoclast BMSC formation. It suggests that curculigoside may be a potential pharmaceutical agent for wear particle-stimulated osteolysis therapy.

1. Introduction

It is no doubt that total joint arthroplasty (TJA) is a landmark of orthopedic surgery in the 20th century, with the notable advantages of joint pain relief and joint function restoration in patients with bone and articular maladies [1]. A follow-up study of more than 15 years reported that approximately 82% of total knee replacements (TKRs) last 25 years and 70% of unicondylar knee replacements (UKRs) last 25 years; the 25-year pooled survival rate of hip replacements and joint replacement was 77.6% and 57.9%, respectively, indicating generally excellent outcomes of TJA [2, 3]. However, all TJA will eventually fail because of the gradually emerged issues, such as infection, fracture, or loosening and wear. And these factors are the most prevalent reasons for TJA revision. Among them, the ratio of aseptic

loosening (38%) is higher than the sum of deep infection and periprosthetic fractures, and most of the aseptic loosening is caused by particle wear and thereby induced osteolysis [4, 5]. Thus, osteolysis has become a key challenge restricting the life of artificial joint and is also the main cause of TJA renovation.

In an artificial joint, wear particles accumulate around the prosthesis over the years, aggravate local friction between the bone and implant, and further increase wear particle accumulation [6]. On the other hand, the accumulated wear particles could stimulate the secretion of inflammatory mediators, like NF-κB, IL-1β, TNF-α, and IL-6, to induce chronic inflammation and periprosthetic osteolysis. During this process, RANKL/RANK/OPG and NF-κB signaling pathways play an important role. NF-κB could be activated by macrophages due to the phagocytosis of wear-produced particles, which then regulates the expression of other mediators, such as TNF-α, IL-1β, and IL-6 [7]. These mediators are particularly involved in the activation and differentiation of osteoclasts, to mediate osteoclastic bone resorption and lead to osteolysis [6, 8]. RANKL (receptor activator of nuclear factor κB ligand), a critical osteoclast differentiation factor, is massively secreted by periprosthetic fibroblasts, osteoblasts, and stromal cells. It combines with RANK and cooperates with NF-κB, to promote osteoclast differentiation and survival, as well as osteoclastic bone resorption [9]. However, OPG, an osteoclast differentiation inhibitor, usually competes with RANK to integrate RANKL and blocks the promotion effect of RANKL/RANK on osteoclast and osteoclastic bone resorption, to inhibit osteolysis. As a result, the imbalance between osteoblastic bone formation and osteoclastic bone resorption ultimately induces osteolysis of the periprosthesis. Hence, a therapeutic agent focusing on promoting osteogenesis and preventing osteolysis could be a promising strategy for osteolysis of the periprosthesis.

Curculigo orchioides Gaertn. is a medicinal herb used for the treatment of lumbar and knee joint arthritis for a long history in traditional Chinese medicine [10, 11]. As a major compound of *Curculigo orchioides*, curculigoside also proves profound bone-protective activity. *In vivo* and *in vitro* studies reported that curculigoside exhibits antiarthritic effects in a rat model of arthritis and rheumatoid arthritis-derived MH7A cells [12]. Ding et al. reported that curculigoside significantly relieved the hind paw swelling and arthritis index to protect against adjuvant arthritis in model rats [13]. Curculigoside was also found to alleviate excess iron overload-induced bone loss in Zhang et al.'s study [14]. These findings indicated that curculigoside is beneficial for osteogenesis and plays a protective role in bone and articular maladies. Therefore, we hypothesized the inhibition potential of curculigoside on osteolysis induced by wear particles in TJA. In this study, titanium particles (Ti) were chosen to mimic periprosthetic osteolysis in *in vivo* and *in vitro* studies; then, the effect of curculigoside on osteolysis was investigated. Taken together, our results hope to provide curculigoside as a potential therapeutic agent for the prevention and treatment of osteolysis induced by wear particles.

2. Materials and Methods

2.1. Titanium Particle Preparation. In this study, osteolysis was stimulated using titanium particles (Ti), which were purchased from ALFA. Over 95% of the Ti diameters were ≤ 4 μm. Then, titanium particles underwent the following procedures to remove endotoxin. Ti were calcined at 180°C for 6 h and further soaked in concentrated hydrochloric acid for 5 h. After centrifugation to remove concentrated hydrochloric acid, Ti were rinsed in 75% ethanol for 48 h. The concentration of endotoxins was detected using a chromogenic endpoint TAL on a diazo coupling detection kit, and endotoxin concentration < 0.1 EU/ml was qualified. Then, DMEM was added to obtain Ti suspension at a concentration of 0.1 mg/ml for subsequent experiments [15].

2.2. Osteoblast Culture and Differentiation Induction. The mouse osteoblast cell line MC3T3-E1 was purchased from iCell Bioscience Inc. (Shanghai, China) and maintained in Alpha-Minimum Essential Medium (α-MEM) containing 10% FBS in a humidified atmosphere of 5% CO_2 at 37°C. The cell differentiation was induced by using cultured DMEM supplemented with 10% FBS, 1% penicillin/streptomycin, 100 nM dexamethasone, 10 mM β-glycerophosphate, and 50 mM vitamin C [16]. And Ti (0.1 mg/ml) were added into the cells to stimulate periprosthetic osteolysis and inhibit osteoblast differentiation in MC3T3-E1 cells. Then, MC3T3-E1 cells were treated with curculigoside (HPLC purity $\geq$ 98%, EY-B0626, Shanghai Yiyan Biotechnology Co. Ltd., China) at 25, 50, and 100 μg/ml in the presence of Ti.

2.3. Bone Marrow Stromal Cell (BMSC) Isolation and Treatment. Healthy C57/BL6 mice aged 4-6 weeks were obtained from Shanghai Slack Animal Co., Ltd. (Shanghai, China) and housed in a temperature of 22~26°C, humidity of 70%, and 12 h light/dark cycle, with free access to water and feeding. All animal procedures were approved by the Animal Research Committee of Zhejiang Traditional Chinese Medical University (Hangzhou, China). The BMSCs were isolated from the tibias and femurs of mice and incubated with α-MEM containing 30 ng/ml M-CSF, 10% FBS, and 1% penicillin/streptomycin to induce mature osteoclast. The medium was changed every three days. Then, 5×10^5 BMSCs were seeded in 12-well plates containing α-MEM supplemented with 0.1 mg/mL Ti. And curculigoside at increasing concentrations (25, 50, and 100 μg/ml) was added into the cells with the presence of Ti.

2.4. Cell Viability Assay. MC3T3-E1 cells or BMSCs in the logarithmic phase were seeded in 96-well plates and coincubated with curculigoside for 24 h, 48 h, or 72 h. After that, the CCK-8 reagent (10 μl, MCE) was added into each well for incubation for another 2 h. Then, the optical density was measured using a microplate reader (CMaxPlus, MD) at a wavelength of 450 nm to evaluate cell viability.

2.5. Cell Apoptosis Assay. Cell apoptosis in each group was assessed using flow cytometry (FCM). Briefly, logarithmic phase MC3T3-E1 cells were seeded in 6-well plates, and binding buffer was added into the plates and centrifuged to

remove the supernatants. After being remixed with 100 μl binding buffer, cells were maintained with annexin V-FITC (5 μl, CoWin Biosciences, China) and PI (10 μl, CoWin Biosciences, China) for reaction in the dark room for 15 min. Afterwards, binding buffer (400 μl) was added into the plates, and cell apoptosis was assessed by FCM (C6, BD Biosciences, USA).

2.6. Alkaline Phosphatase (ALP) Assay. The ALP assay was performed to evaluate the osteogenic function of MC3T3-E1 cells. After cells were treated with curculigoside (25, 50, and 100 μg/ml) in the presence of Ti, cells were further maintained in osteogenic induction medium for 7 days. Then, an ALP kit (Beyotime, China) was used for ALP staining according to the manufacturer's protocol, and p-nitrophenyl phosphate (pNPP) (Sigma, USA) served as a substrate. Afterwards, cells were observed under light microscopy (AE2000, Motic, China) at 405 nm.

2.7. Alizarin Red Staining. Cell mineralization was evaluated using Alizarin Red S staining. After being stimulated with the indicated agents (curculigoside, Ti), MC3T3-E1 cells were fixed in 4% paraformaldehyde for 15 min. Next, cells were stained with 500 μl/well Alizarin Red solution (Solarbio, China) for 20 min at room temperature. Finally, cells were ringed 3 times with ddH2O and imaged under an inverted fluorescence microscope (Ts2-FC, Nikon, Japan).

2.8. Mitochondrial Membrane Potential Assay. The mitochondrial membrane potential was analyzed using a 5,5,6,6-tetrachloro-1,1,3,3-tetraethyl-imidacarbocyanine iodide (JC-1) probe. Briefly, MC3T3-E1 cells were seeded in 6-well plates with 3×10^5 cells/well and intervened with curculigoside and Ti. Then, cells were added with 1 ml of JC-1 staining solution (Beyotime, China) per well for incubation for 20 min at 37°C under dark. At the end of incubation, the fluorescence density of the stained cells was monitored under FCM (C6, BD Biosciences, USA).

2.9. Intracellular ROS Measurement. After MC3T3-E1 cells were intervened with curculigoside and Ti, cell culture medium was replaced with a ROS indicator, 2′,7′-dichlorodihydrofluoresceindiacetate (DCF-DA), for 30 min at 37°C. After incubation, the fluorescence was detected by FCM (C6, BD Biosciences, USA).

2.10. Enzyme-Linked Immunosorbent Assay (ELISA). After MC3T3-E1 cells or BMSCs were intervened with curculigoside and Ti, cells were added into 96-well plates and maintained at 37°C for 48 h. After that, cells were centrifuged to obtain the supernatants. Then, the cell supernatants were filtered through a 0.22 μm filter and detected with the corresponding ELISA kits including TNF-α, IL-1β, IL-6, RANKL, and OPG (MEIMIAN, China) according to the manufacturer's protocol. Finally, the optical density was detected by using a microplate reader (CMaxPlus, Molecular Devices, USA) at 450 nm.

2.11. Immunofluorescence Assay of F-actin Ring Formation. BMSCs were grown on cover glasses and treated with curculigoside and Ti. After that, 1 ml of 0.5% Triton X-100 was added into each well for cell permeabilization. And 3% BSA was used to block the reaction; then, BMSCs were incubated with the primary antibody against F-actin (Abcam, USA) overnight at 4°C and further incubated with the secondary antibody (Abcam, USA). After incubation and washing with PBS, the cell nuclei were stained with DAPI. Cells were observed under an inverted fluorescence microscope (Ts2-FC, Nikon, Japan).

2.12. RT-qPCR. The total RNA of MC3T3-E1 cells or BMSCs was extracted using a TRIzol reagent (Sangon Biotech, China) and reverse transcribed into cDNA with the cDNA Synthesis kit (CW Bioscience, China) following the manufacturer's protocol. RT-qPCR analysis was performed using a Roche LightCycler® 96 real-time PCR system. The following conditions were used: 95°C, 10 min; 95°C, 15 s; 60°C, 60s; and 40 cycles. The primers used are listed in Table 1, and GAPDH was used as an internal control. The gene expression was analyzed using the comparative $2^{-\Delta\Delta Cq}$ method.

2.13. Western Blot Assay. The total proteins of MC3T3-E1 cells or BMSCs were extracted and lysed with RIPA buffer (Beyotime, China), and protein concentration was detected using a BCA protein assay kit (Solarbio, China). Then, a 20 μg total protein sample was loaded onto 10% sodium dodecyl sulfate polyacrylamide gel electrophoresis (SDS-PAGE) for separation and transferred to a PVDF membrane. After being blocked with 5% skimmed milk, the membrane was incubated at 37°C with the primary antibodies against caspase-3 (ab13847, Abcam), caspase-9 (ab32539, Abcam), SIRT1 (ab110304, Abcam), BMP-2 (ab214821, Abcam), RANKL (ab45039, Abcam), OPG (ab73400, Abcam), IκBα (ab32518, Abcam), p-IκBα (AF2002, Affinity), p65 (ab207297, Abcam), p-p65 (AF2006, Affinity), IKKα (ab32041, Abcam), p-IKKα (AF3013, Affinity), NFATc1 (ab2796, Abcam), and cathepsin K (ab19027, Abcam) at 4°C overnight. After that, the membrane was further incubated with the secondary antibody at room temperature for 1 h. Then, the enhanced chemiluminescence (ECL) reagent (Solarbio, China) was used to visualize the protein bands, and the relative band density was semiquantified with the ImageJ software.

2.14. Animal Experiments and Drug Administration. Male C57/BL6 mice were randomly divided into four groups with 8 rats per group: sham group, Ti group, curculigoside 20 mg/kg group, and curculigoside 40 mg/kg group. A Ti-induced osteolysis model in mouse calvaria was prepared as previously described [14, 16]. After the mice were anesthetized and fixed on a sterile operating table, the skin of the head was disinfected with skin disinfectant; then, in the middle of the calvaria, an incision was made. And 20 mg Ti containing PBS was gently injected to the anterior fontanelle of the skull [16]. The sham group was injected with the same volume of PBS without Ti. After the incision was stitched up with 4-0 surgical sutures, mice were turned back into the cages with conventional feeding. On 2 days, mice in the curculigoside group were injected (i.p.) with curculigoside at a dosage of 20 mg/kg/d and 40 mg/kg/d, respectively. Sham

Table 1: Primer sequences of the gene.

Gene	Forward primer	Reverse primer
Mouse Runx2	5′-TGGCCGGGAATGATGAGAAC-3′	5′-TGAAACTCTTGCCTCGTCCG-3′
Mouse osterix	5′-GTGGGAACAAGAGTGAGCTGG-3′	5′-CCATAGTGAGCTTCTTCCTGGGTA-3′
Mouse OCN	5′-CCTGAGTCTGACAAAGCCTTCA-3′	5′-AGATGCGTTTGTAGGCGGTC-3′
Mouse cath-K	5′-TTCCCGCAGTAATGACACCC-3′	5′-GGAACCACACTGACCCTGAT-3′
Mouse TRAP	5′-CTGCTGGTCATTCCTGTCGT-3′	5′-GCAGGGGGTAAGATCTCATT-3′
Mouse NFATc1	5′-TGGAGAAGGCTCCAGATGGC-3′	5′-CTGGTTGCGGAAAGGTGGTA-3′
Mouse MMP-9	5′-TTGAGTCCGGCAGACAATCC-3′	5′-ACTTCCAGTACCAACCGTCC-3′
Mouse GAPDH	5′-TGTCAAGCTCATTTCCTGGTATG-3′	5′-TTATGGGGGTCTGGGATGGA-3′

and Ti groups were injected with saline instead. After 14-day administration, mice in each group were sacrificed, and the calvaria tissues were collected for further experiments.

2.15. Micro-CT Analysis. A micro-CT (MCT-III, ZKKS) was applied to detect the surface erosion in the calvaria of each group of mice before sacrifice. The scanning parameters were set as follows: voltage 45 keV, current 555 μA, power 25 W, exposed time 48 ms, resolution 35 μm, scanning angle 180°, and scanning thickness 9 μm with continuous scanning. Volume of interest (VOI) was determined in the center of each calvaria. The CTvox software was used for 3D reconstruction and data processing. Bone mineral density (BMD), bone volume (BV), ratio of bone volume to tissue volume (BV/TV), and trabecular thickness (Tb.Th) were determined.

2.16. HE Staining and TRAP Staining. The obtained calvaria tissues were fixed and embedded in molten paraffin. Then, tissues were sectioned into 4 μm pieces and stained with hematoxylin and eosin (H&E) and tartrate-resistant acid phosphatase (TRAP) according to the manufacturer's protocols. Images were obtained with a light microscope (DM3000, Leica, Germany).

2.17. Immunohistochemical (IHC) Analysis. The calvaria tissue sections were dewaxed with xylene and subjected to gradient hydration and antigen retrieval with citric acid solution. Sections were added with corresponding primary antibodies against RANKL, OPG, TNF-α, IL-1β, and IL-6 and incubated overnight at 4°C. Then, IHC-positive stained cells were stained using a DAB Horseradish Peroxidase Color Development Kit and photographed using a light microscope (DM3000, Leica, Germany).

2.18. Statistical Analysis. Data were expressed as means ± standard deviation (SD). Statistical significance among multiple comparisons was analyzed by one-way ANOVA with the SNK test. A value of $P < 0.05$ was considered statistically significant.

3. Results

3.1. Curculigoside Attenuated the Ti-Induced Inhibition of Osteoblastic Differentiation in MC3T3-E1 Cells. After osteoblast MC3T3-E1 cells were intervened with Ti and treated with curculigoside at different concentrations (25, 50, and 100 μg/ml) for 24 h, 48 h, and 72 h, cell viability was detected by the CCK-8 assay. As displayed in Figure 1(a), compared to the Con group, the cell viability of Ti group cells was significantly inhibited in 24 h, 48 h, and 72 h. While being compared to the Ti group, the cell viability in curculigoside-treated groups was increased, with significant differences in curculigoside 50 and 100 μg/ml groups in 24 h, 48 h, and 72 h treatment and curculigoside 25 μg/ml groups in 48 h and 72 h treatment. FCM results in Figures 1(b) and 1(d) showed that after Ti intervention, the MC3T3-E1 cell apoptosis rate was significantly increased compared to the Con group, while in curculigoside-treated groups at different concentrations, cell apoptosis was decreased.

3.2. Curculigoside Treatment Alleviated Ti-Induced Mitochondrial Damage in MC3T3-E1 Cells. As shown in Figures 1(c) and 1(e), the FCM results showed that after being intervened with Ti, the mitochondrial membrane potential was reduced in MC3T3-E1 cells. However, curculigoside treatment offset the decrease in the mitochondrial membrane potential, especially in curculigoside 50 and 100 μg/ml groups.

3.3. Curculigoside Treatment Alleviated Ti-Induced Osteogenic Reduction and Osteoblastic Mineralization Inhibition in MC3T3-E1 Cells. ALP results demonstrated that Ti intervention significantly inhibited ALP activity compared to the Con group, which indicated an inhibitory effect of Ti on osteoblastic differentiation (Figure 2(a)). However, this osteogenic inhibition effect was reversed by curculigoside treatment; it recovered the ALP activity in MC3T3-E1 cells. Consistent with this, Alizarin Red staining showed that curculigoside treatment effectively stimulated cell mineralization (Figures 2(b) and 2(d)). And the number of mineralized tubes was also significantly increased in curculigoside-treated cells.

3.4. Curculigoside Treatment Inhibited the ROS Generation in Ti-Intervened MC3T3-E1 Cells. Intracellular ROS generation results in Figures 2(c) and 2(e) showed that compared with the Con group, the ROS generation was significantly

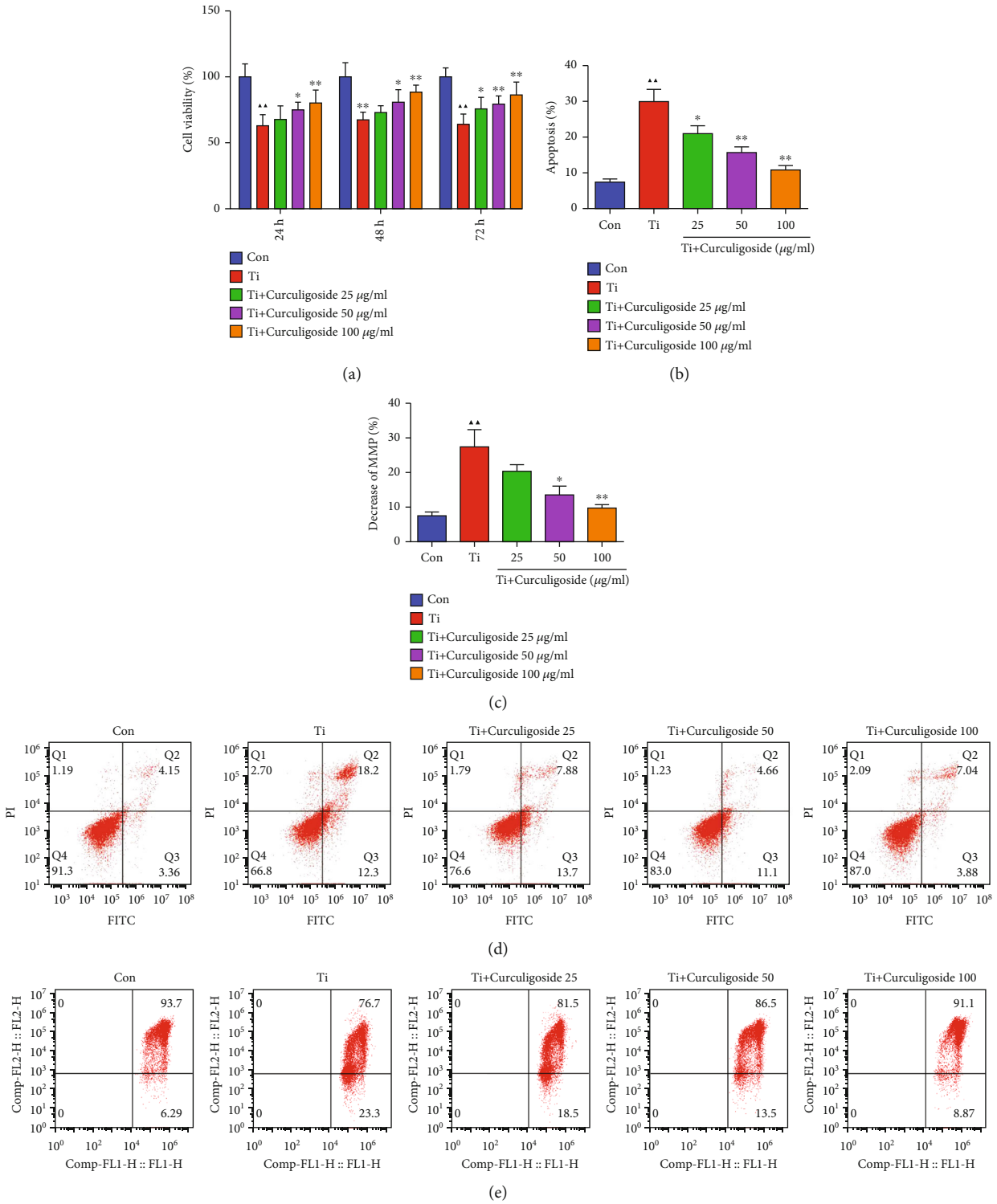

Figure 1: Curculigoside treatment attenuated Ti-induced inhibition of osteoblastic differentiation in MC3T3-E1 cells. (a) After being intervened with Ti and treated with curculigoside at different concentrations (25, 50, and 100 μg/ml) for 24 h, 48 h, and 72 h, MC3T3-E1 cell viability was detected by the CCK-8 assay ($n = 6$). (b, d) After being intervened with Ti and treated with curculigoside, cell apoptosis was detected by flow cytometry ($n = 3$). (c, e) Mitochondrial membrane potential of MC3T3-E1 cells cultured under Ti and different concentrations of curculigoside was assayed by flow cytometry using JC-1 assay kits, and the decrease in the MMP index in each group cell was quantified ($n = 3$). Results are represented as the mean ± SD. $^{\blacktriangle}P < 0.05$, compared to the Con group; $^{\blacktriangle\blacktriangle}P < 0.01$, compared to the Con group; $^{*}P < 0.05$, compared to the Ti group; $^{**}P < 0.01$, compared to the Ti group. Ti: titanium particle; Con: control; MMP: mitochondrial membrane potential.

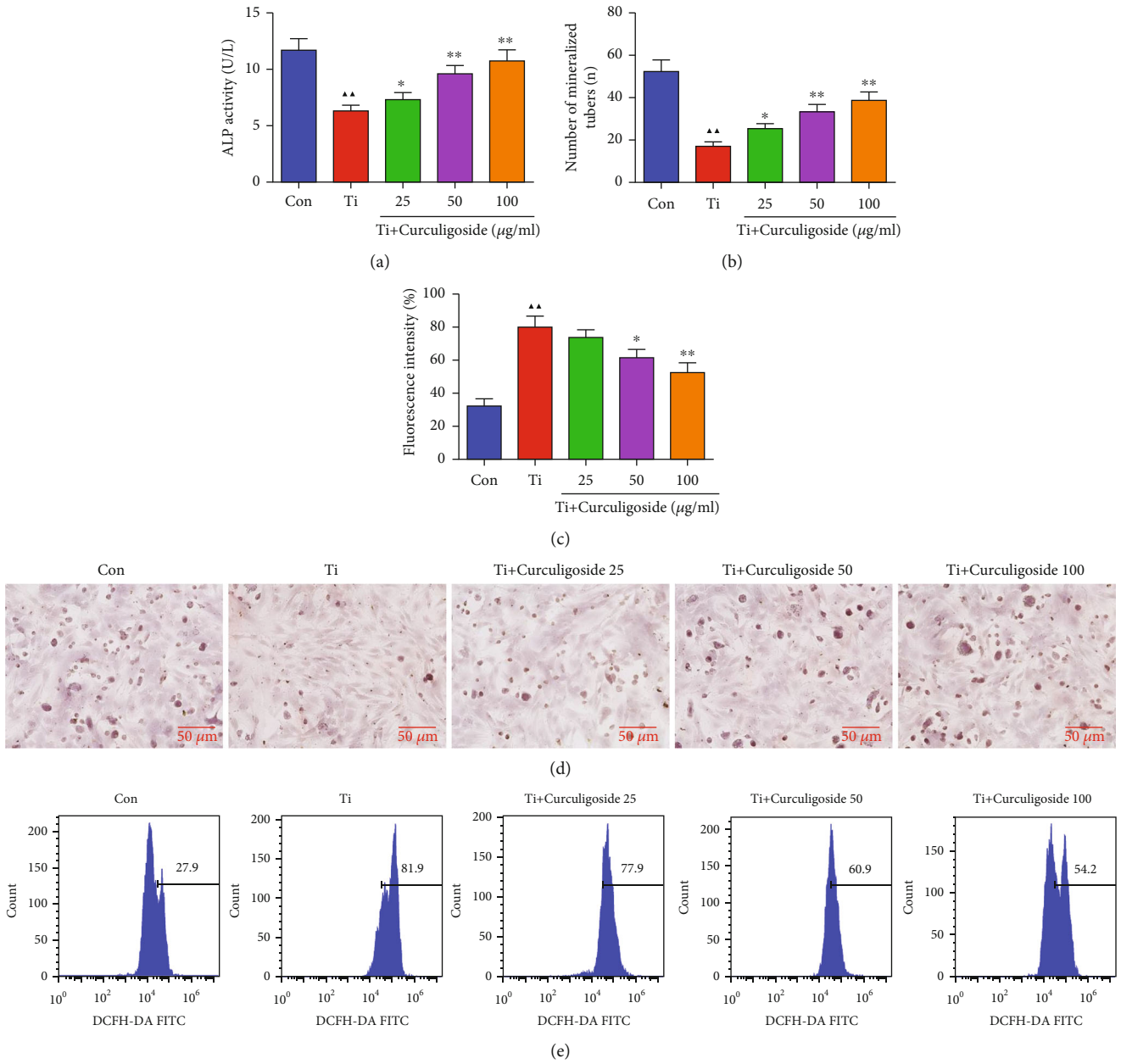

FIGURE 2: Curculigoside treatment alleviated Ti-induced inhibition on ALP activity, mineralization, and ROS generation in MC3T3-E1 cells. (a) MC3T3-E1 cells were detected with ALP staining, and ALP activity was quantified. (b, d) MC3T3-E1 cells were assayed by Alizarin Red staining, and the mineralization in each group cell was quantified. (c, e) Intracellular ROS level of MC3T3-E1 cells after Ti intervention and curculigoside treatment was assayed by flow cytometry, and ROS production in each group cell was quantified ($n = 3$); results are represented as the mean ± SD. $^{\blacktriangle}P < 0.05$, compared to the Con group; $^{\blacktriangle\blacktriangle}P < 0.01$, compared to the Con group; $^{*}P < 0.05$, compared to the Ti group; $^{**}P < 0.01$, compared to the Ti group. Ti: titanium particle; Con: control; ALP: alkaline phosphatase.

increased after Ti intervention. However, in curculigoside-treated cells, the increased ROS generation induced by Ti was decreased, which indicated an oxidative stress inhibition effect of curculigoside in MC3T3-E1 cells.

3.5. Osteoblast-Associated Factors and Proinflammatory Cytokine Levels in MC3T3-E1 Cells. The levels of TNF-α, IL-1β, IL-6, RANKL, and OPG in MC3T3-E1 cells were detected (Figure 3). It could be observed that compared to the Con group, the levels of proinflammatory cytokines in MC3T3-E1 cells, including TNF-α, IL-1β, and IL-6, were significantly increased with Ti intervention. However, in curculigoside-treated groups, these increased levels were restored and decreased significantly compared to the Ti group. As a differentiation factor of osteoclasts, the increased level of RANKL in Ti-intervened cells was significantly decreased with curculigoside treatment. Corresponding to this, the decreased level of OPG, an osteoclast differentiation suppressor, in Ti-intervened cells was significantly increased with curculigoside treatment.

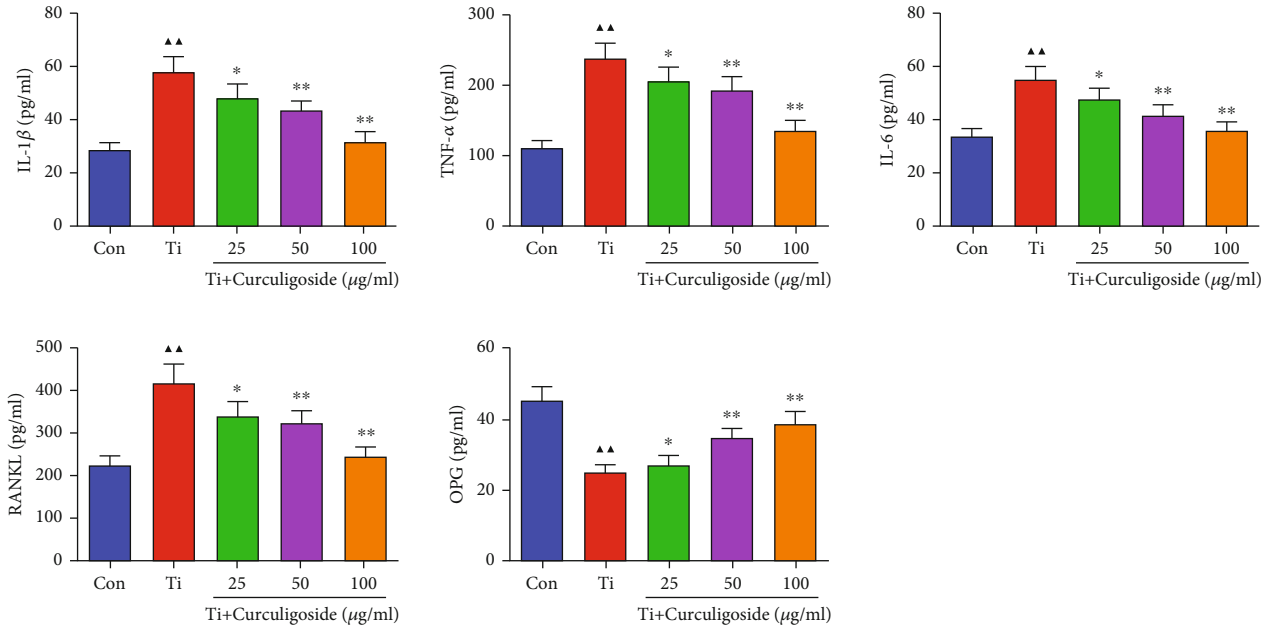

Figure 3: The levels of TNF-α, IL-1β, IL-6, RANKL, and OPG in MC3T3-E1 cells were detected using ELISA kits ($n = 3$); results are represented as the mean ± SD. $^{\blacktriangle}P < 0.05$, compared to the Con group; $^{\blacktriangle\blacktriangle}P < 0.01$, compared to the Con group; $^{*}P < 0.05$, compared to the Ti group; $^{**}P < 0.01$, compared to the Ti group. Ti: titanium particle; Con: control.

3.6. Curculigoside Treatment Promoted the Osteoblast- and Apoptosis-Associated Gene Expression in Ti-Induced MC3T3-E1 Cells. qRT-PCR results demonstrated that Ti intervention in MC3T3-E1 cells induced a significant inhibition on the expression levels of osteoblastic differentiation-related genes, including Runx2, OCN, and osterix (Figure 4(a)). Curculigoside treatment resulted in a significant increase in the expression levels of Runx2, OCN, and osterix. As shown in Figure 4(b), the relative protein levels of caspase-3, caspase-9, and RANKL were significantly increased in Ti group cells compared with the untreated Con group; SIRT 1, BMP-2, and OPG were significantly decreased in Ti group cells, while curculigoside treatment offset the protein expression of these genes.

3.7. Curculigoside Treatment Inhibited the Ti-Induced Activation of Osteoclast Activity in BMSCs. BMSCs were also intervened with Ti to induce osteoclast activity, and CCK-8 results in Figure 5(a) showed that cell viability in Ti group BMSCs was significantly increased compared to that in the Con group. However, in curculigoside 50 and 100 μg/ml group BMSCs, the cell viability was decreased significantly compared to the Ti group. Ti treatment also significantly increased the levels of TNF-α, IL-1β, and IL-6 in BMSCs, and curculigoside treatment restored the elevated levels of these procytokines (Figure 5(b)). And for bone resorption-related prerequisite, F-actin, its expression intensity enhanced by Ti was diminished by curculigoside administration (Figure 5(c)).

3.8. Curculigoside Treatment Alleviated Osteoclast-Associated Gene Expression in Ti-Induced BMSCs. qRT-PCR results in Figure 6(a) showed that the mRNA expressions of cath-K, TRAP, NFATc1, and MMP-9 were significantly increased in BMSCs with Ti intervention. And in Ti-intervened BMSCs incubated with curculigoside, the expressions of these genes were restrained. Ti also induced the increased protein expressions of p-IκBα, p-p65, p-IKKα, NFATc1, and cathepsin K in BMSCs (Figure 6(b)). And in curculigoside-treated groups, the protein expressions of p-IκBα/IκBα, p-p65/p65, p-IKKα/IKKα, NFATc1, and cathepsin K were all decreased.

3.9. Curculigoside Treatment Attenuated Ti-Induced Osteolysis and Enhanced Bone Formation in Model Mice. In *in vivo* experiments of the Ti-induced osteolysis mouse model, micro-CT results (Figure 7) illustrated that Ti injection induced osteolysis and bone loss in mouse calvaria. The osteolysis-related parameters, including BMC, BMD, BV/TV, and Tb.Th, in the Ti group were also significantly changed compared to those in the sham group. While curculigoside treatment attenuated the morphological alteration and osteolysis of calvaria in Ti model mice, the relative parameters were also attenuated.

3.10. Curculigoside Treatment Restored Histological Damage of the Calvaria. HE and TRAP staining was performed to analyze the histological changes of the calvaria in Ti model mice upon curculigoside treatment. HE staining results (Figure 8(a)) showed that the calvaria in Ti group mice showed osteolysis characteristics, with eroded bone surface observed. TRAP staining (Figure 8(b)) also showed that the TRAP-positive cells were increased in Ti model group mouse calvaria. In curculigoside treatment groups, the degree of Ti-induced osteolysis and TRAP-positive cells were attenuated.

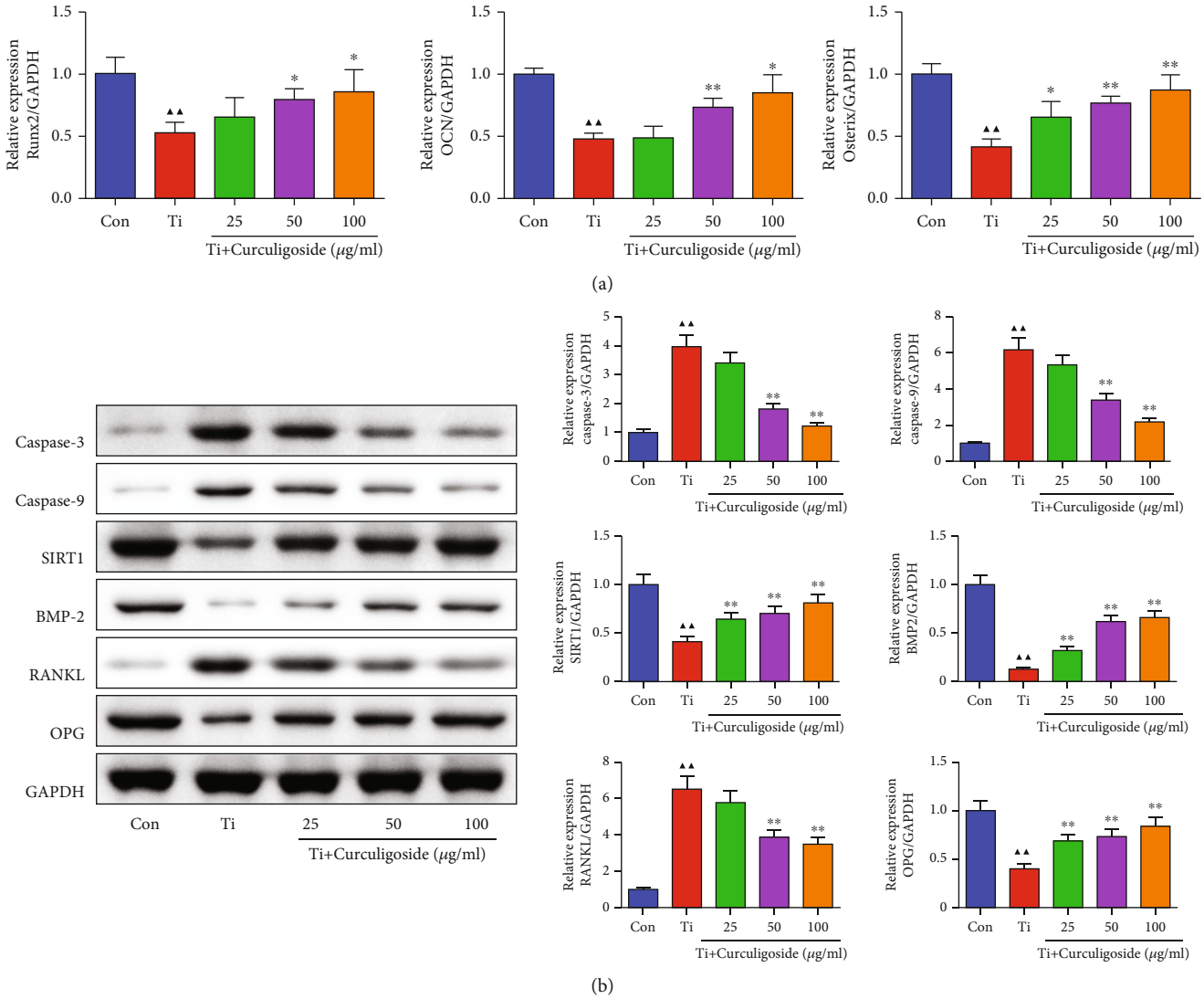

Figure 4: Curculigoside treatment promoted the osteogenic-associated gene expression in Ti-induced in MC3T3-E1 cells. (a) qRT-PCR analysis was performed to detect the relative mRNA expression of Runx2, osterix, and OCN in MC3T3-E1 cells. (b) Western blot analysis was performed to detect the relative protein expression of casepase-3, casepase-9, SIRT1, BMP-2, RANKL, and OPG in MC3T3-E1 cells ($n = 3$); results are represented as the mean ± SD. $^{▲}P < 0.05$, compared to the Con group; $^{▲▲}P < 0.01$, compared to the Con group; $^{*}P < 0.05$, compared to the Ti group; $^{**}P < 0.01$, compared to the Ti group. Ti: titanium particle; Con: control.

3.11. Curculigoside Treatment Attenuated Ti-Induced Osteolysis by Enhancing Osteogenesis. The IHC results in Figure 9 demonstrated that Ti injection increased the expression of IL-1β, IL-6, RANKL, and TNF-α and inhibited OPG expression in the calvaria of mice, to increase the proinflammatory cytokine production and the RANKL/OPG ratio. While after curculigoside treatment, the expressions of IL-1β, IL-6, RANKL, and TNF-α were inhibited, OPG was increased, thus restoring the RANKL/OPG ratio and inhibiting inflammation.

4. Discussion

Joint prosthesis longevity and function are largely dependent on the degree of interface wear between the bone and implant, as well as the formation pace of wear particles. Against this, many strategies, including new types of prosthesis, wear-resistant materials, surgical methods, fixation techniques, and rehabilitation management improvements, have been developed and applied in TJA [17–21]. These strategies greatly avoid joint prosthesis loosening and wear, but wear still cannot be solved completely. Wear particles came to be an unavoidable problem that leads to periprosthetic osteolysis and TJA failure. As mentioned before, wear particles could induce macrophages and osteoclasts to secrete proinflammatory and osteoclastogenic cytokines and break the balance between the bone formation by osteoblasts and the bones resorption by osteoclasts, thus resulting in periprosthetic osteolysis.

Osteoblastic bone formation and osteoclastic bone resorption are critically responsible for the maintenance of bone homeostasis [22]. Osteoblast serves as a functional cell

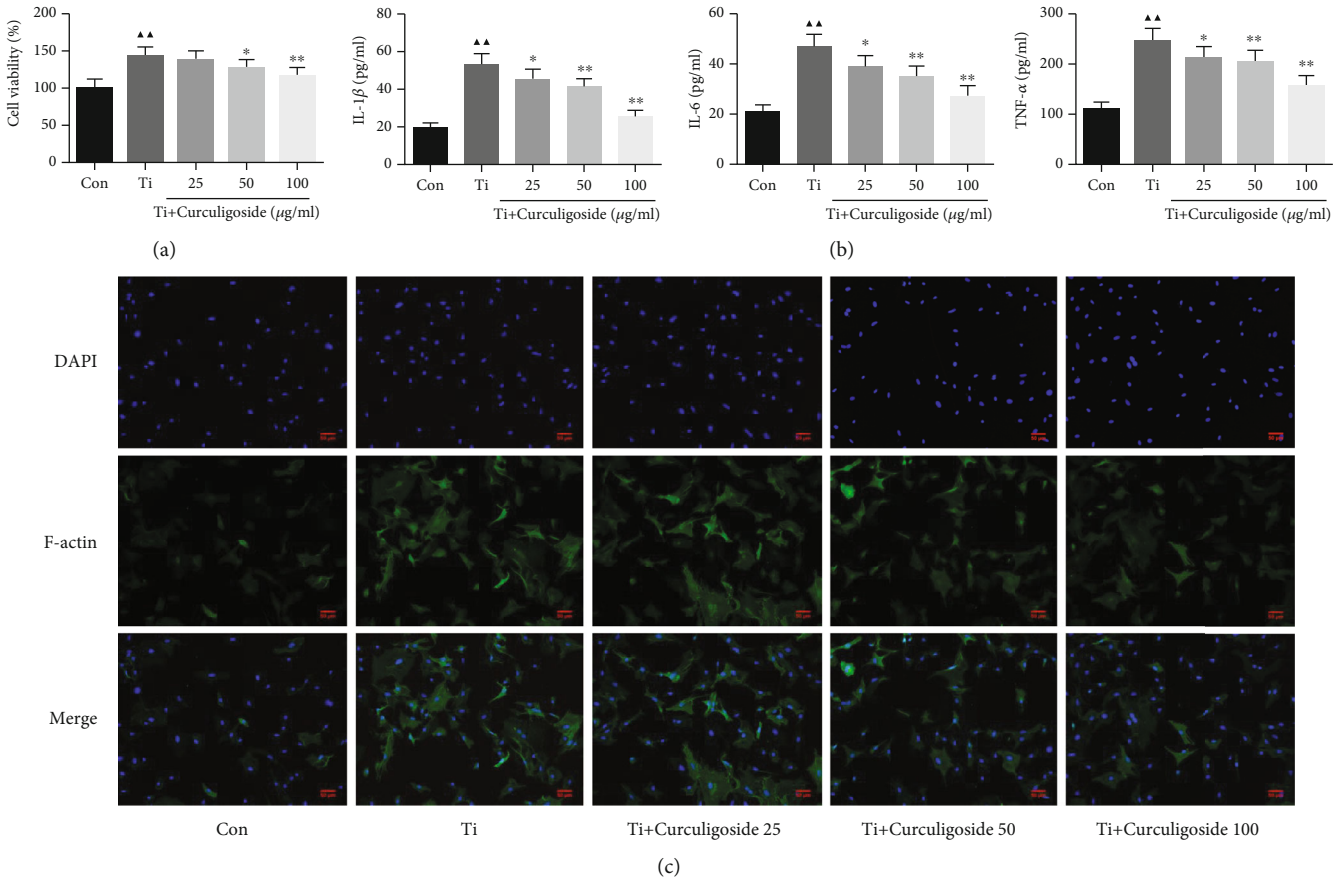

Figure 5: Curculigoside treatment inhibited Ti-induced activation of osteoclast activity in BMSCs. (a) After being intervened with Ti and treated with curculigoside at different concentrations (25, 50, and 100 μg/ml) for 48 h, BMSC viability was detected by the CCK-8 assay ($n = 6$). (b) The levels of TNF-α, IL-1β, and IL-6 in BMSCs were detected using ELISA kits. (c) Cellular immunofluorescence of F-actin in BMSCs ($n = 3$); results are represented as the mean ± SD. $^{\blacktriangle}P < 0.05$, compared to the Con group; $^{\blacktriangle\blacktriangle}P < 0.01$, compared to the Con group; $^{*}P < 0.05$, compared to the Ti group; $^{**}P < 0.01$, compared to the Ti group. BMSCs: bone marrow stromal cells; Ti: titanium particles; Con: control.

for bone formation and participates in the synthesis, secretion, and mineralization of the bone matrix. Thus, the proliferation and differentiation of osteoblasts directly affect osteogenesis, and abnormalities of these physiologies could lead to bone diseases, including osteoporosis, osteoarthritis, and primary bone tumors [23, 24]. Increasing evidences show that wear particles significantly affect osteoblastic physiologies and suppress bone formation, to induce osteolysis. Particles inhibit the osteoblast's proliferation, and inhibiting calcium deposition and ALP activity suppressed the osteoblast's ability to produce a mineralized bone matrix [25]. In addition, the particles are capable of stimulating osteoblasts to secrete proinflammatory cytokines. A study about Ti-stressed murine MC3T3-E1 cells reported that Ti reduced osteoblast differentiation by inhibiting ALP activity, matrix mineralization, and osteogenesis-related gene expression, as well as increasing the RANKL/OPG ratio in cells [26]. In this study, our results also indicated an inhibition role of Ti in osteoblast differentiation and osteogenesis. Results showed that Ti intervention significantly decreased MC3T3-E1 cell viability and promoted the production of TNF-α, IL-1β, and IL-6, cell apoptosis, and apoptotic gene expression, including caspase-3 and caspase-9. More importantly, ALP staining showed that the activity of ALP, a marker of osteoblast differentiation, was inhibited; Alizarin Red staining showed that cell mineralization was inhibited with Ti treatment. Osteogenic-associated gene expression was also changed in Ti-intervened MC3T3-E1 cells, including RANKL, OPG, Runx2, osterix, and OCN.

Osteoclast is a significant functional cell for bone resorption and also has a critical role in wear particle-induced periprosthetic osteolysis. *In vivo*, these wear particles have the ability to activate the proinflammatory cells, gather at the periprosthetic area, and activate osteoclasts for bone resorption; *in vitro*, these particles also activate osteoclast formation and differentiation, to stimulate bone resorption [27–29]. In this study, we isolated BMSCs from rats to investigate the effect of Ti on osteoclasts. Corresponding with published studies, our results showed that Ti stimulated osteoclast viability and the production of TNF-α, IL-1β, and IL-6 and increased F-actin ring formation, a cytoskeleton structure of osteoclasts. In addition, NF-κB and related NFATc1 pathway

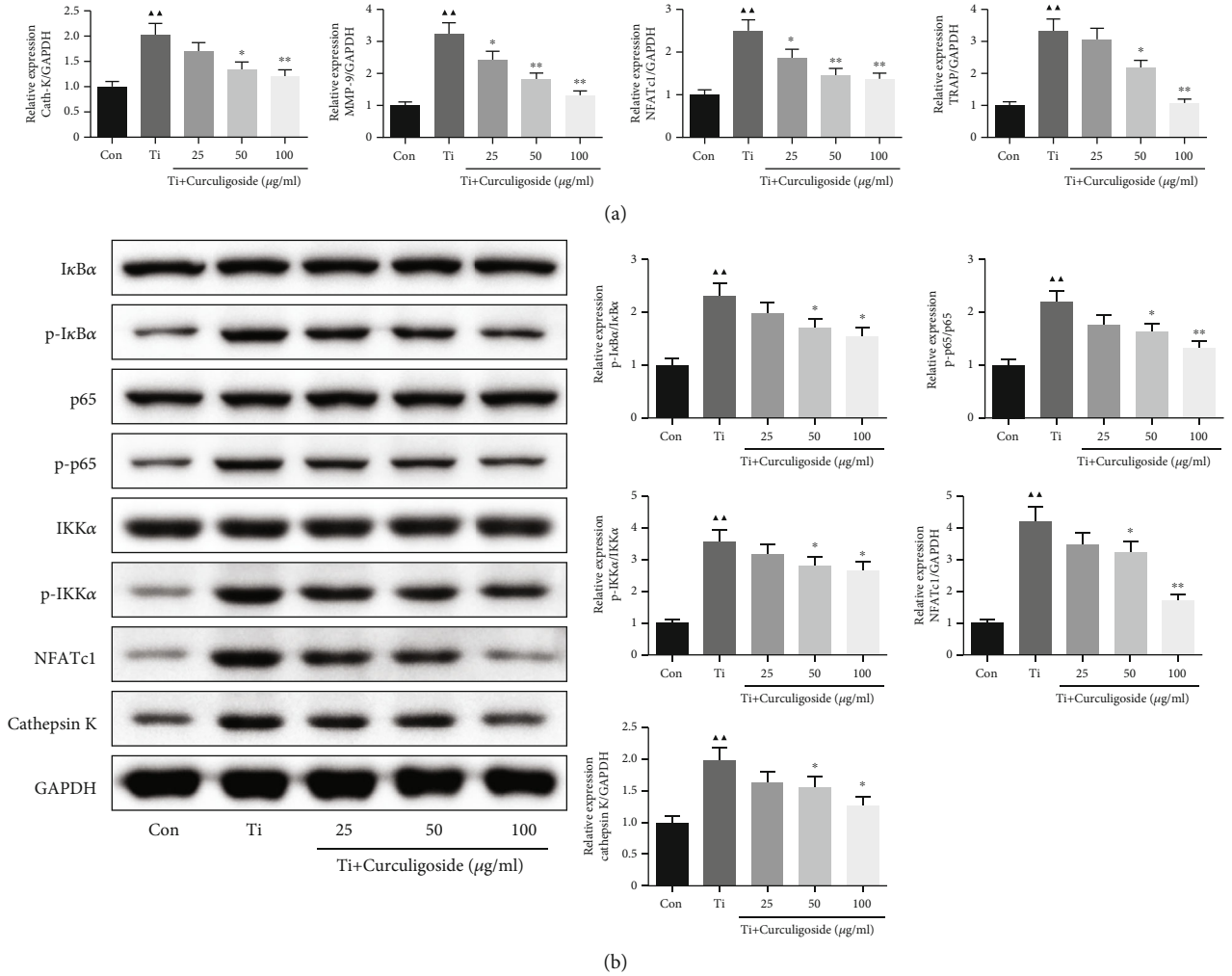

Figure 6: Curculigoside treatment alleviated osteoclast-associated gene expression in Ti-induced BMSCs. (a) qRT-PCR analysis was performed to detect the relative mRNA expression of cathepsin K, TRAP, NFATc1, and MMP-9 in BMSCs. (b) Western blot analysis was performed to detect the relative protein expression of IκBα, p-IκBα, p65, p-p65, IKKα, p-IKKα, NFATc1, and cathepsin K in BMSCs ($n = 3$); results are represented as the mean ± SD. $^{\blacktriangle}P < 0.05$, compared to the Con group; $^{\blacktriangle\blacktriangle}P < 0.01$, compared to the Con group; $^{*}P < 0.05$, compared to the Ti group; $^{**}P < 0.01$, compared to the Ti group. BMSCs: bone marrow stromal cells; Ti: titanium particles; Con: control.

are also involved in osteoclast formation effect of Ti, and the expression of NF-κB p65, IκBα, cathepsin K, TRAP, NFATc1, and MMP-9 was changed in Ti-intervened BMSCs.

In this study, *in vitro* experiments showed that curculigoside reversed the Ti-induced inhibition of osteoblast-associated bone formation in MC3T3-E1 cells and activation of osteoclast-associated bone resorption in BMSCs, to inhibit osteolysis. In MC3T3-E1 cells, curculigoside treatment reversed the Ti-induced inhibition of cell differentiation, increased ALP activity and cell mineralization, and inhibited apoptosis, inflammation, and ROS generation. In BMSCs, curculigoside treatment suppressed the Ti-induced cell activity and suppressed the inflammatory cytokines and F-actin ring formation. The expressions of osteoblast- and osteoclast-associated genes were also restored by curculigoside. The osteogenic induction effect of curculigoside was also found in normal BMSCs, represented by increased ALP activity, cell mineralization, and expression of osteogenic genes (ALP, Col I, OCN, OPG, and Runx2) [30]. And curculigoside's major metabolite in rat plasma, M2, was also found to exhibit antiosteoporotic activity in osteoblastic MC3T3-E1 cells [14]. In Ti-induced osteolysis in mouse calvaria, relative results also showed that curculigoside treatment was able to attenuate bone loss, suggesting its potential for the treatment of wear particle-induced periprosthetic osteolysis. In Wang et al.'s study [31], they also demonstrated that curculigoside was able to alleviate bone loss in mice and MC3T3-E1 cells, the biochemical parameters related to bone metabolism and the expression of Runx2 and OCN were improved by curculigoside, and the bone-mineralized nodule formation was also increased *in vitro*, which were consistent with our findings. In arthritic rats, a study also proved that curculigoside treatment decreases serum levels of TNF-α, IL-1β, IL-6, IL-10, IL-12, and IL-17A and regulated the expression of NF-κB p65 and IκB, to exhibit significant antiarthritic effects [11]. Therefore,

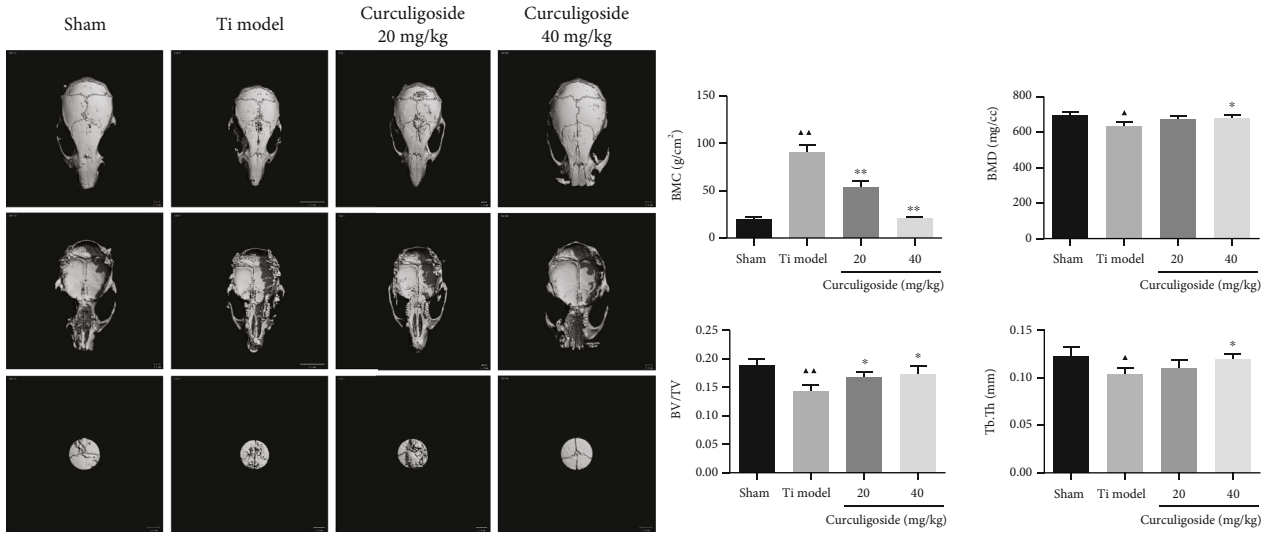

Figure 7: Curculigoside treatment attenuated Ti-induced osteolysis in a mouse calvaria model. (a) Micro-CT reconstruction images of the calvaria in each group of mice. (b) BMC, BMD, BV/TV, and Tb.Th were determined ($n = 3$); results are represented as the mean ± SD. ▲$P < 0.05$, compared to the sham group; ▲▲$P < 0.01$, compared to the sham group; *$P < 0.05$, compared to the Ti group; **$P < 0.01$, compared to the Ti group. Ti: titanium particle; BMC: bone mineral content; BMD: bone mineral density; BV/TV: bone volume to tissue volume; Tb.Th: trabecular thickness.

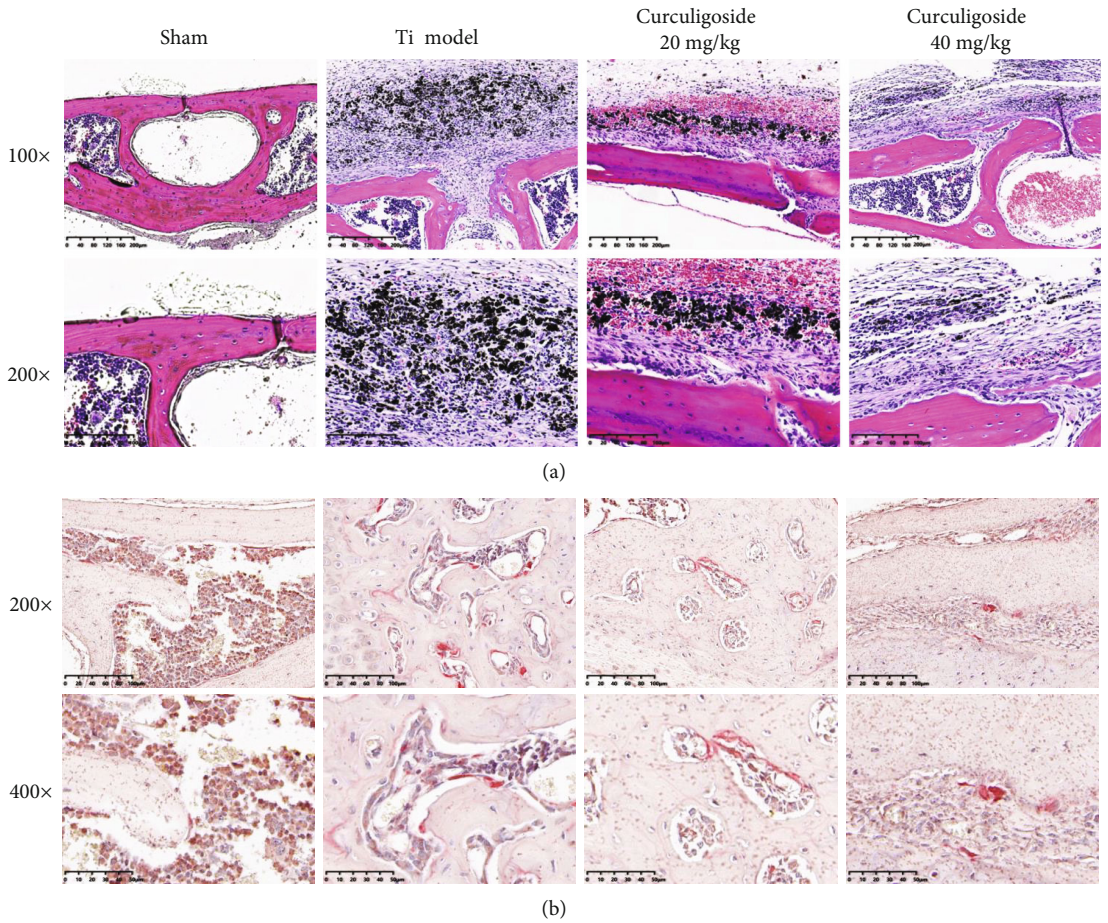

Figure 8: Curculigoside treatment attenuated Ti-induced osteolysis in histological analysis of calvaria sections: (a) HE staining; (b) TRAP staining. Ti: titanium particle.

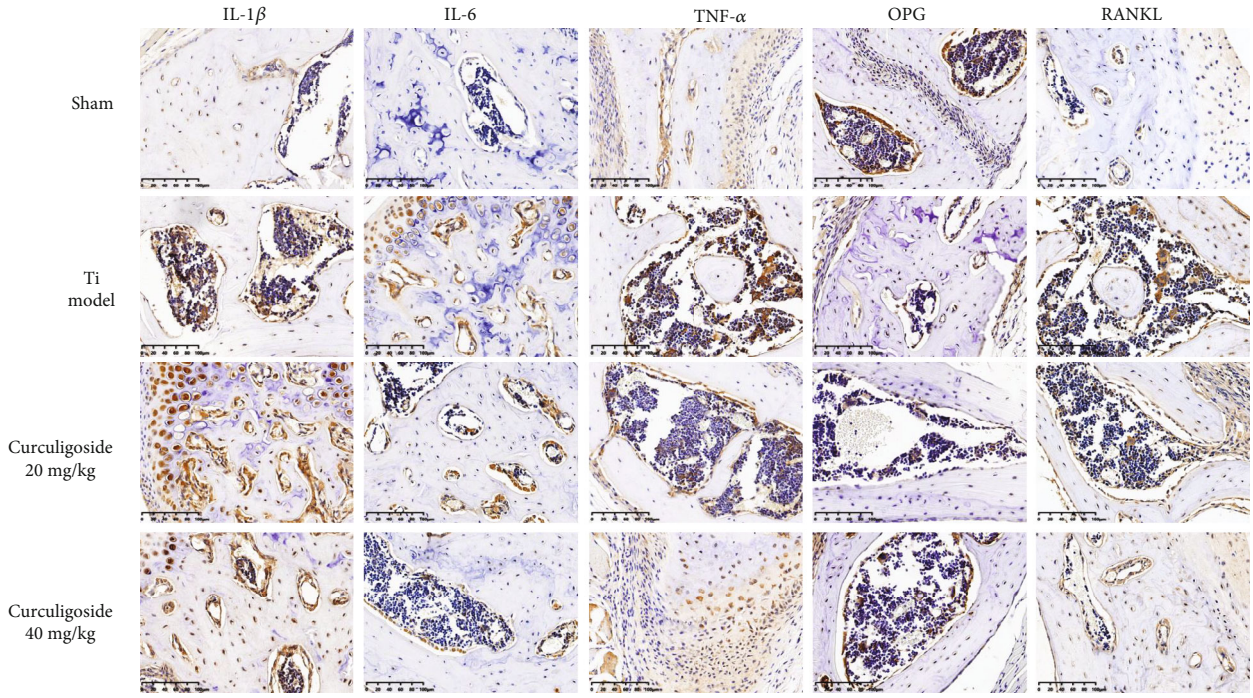

FIGURE 9: Immunohistochemical analysis for RANKL, OPG, TNF-α, IL-1β, and IL-6 in calvaria sections of each group of mice. Ti: titanium particle. Magnification, ×200.

combined with these studies, we suggested the inhibition potential of curculigoside on osteolysis induced by wear particles.

Furthermore, we explored the potential molecular mechanism of curculigoside's positive impact on osteogenesis. To our knowledge, many cytokines, hormones, genes, and signaling pathways are involved in bone remodeling [21]. The RANK/RANKL/OPG signal is critically correlated with periprosthetic osteolysis [32]. OPG, an osteoclastogenesis inhibitory factor, can bind to RANKL to block RANKL/RANK, and this further affects the main signaling pathways of osteoclast differentiation and activation. RANK/RANKL/OPG signaling also regulates osteoclast formation, activation, and survival via modulating different signaling pathways, including IκKα/NF-κB and calcineurin/NFATc1 [33, 34]. Researches focus on these signals also providing clues for developing therapeutic approaches for bone diseases, including osteolysis [35–37]. As mentioned earlier, previous studies also demonstrated the regulation potential of curculigoside on RANK/RANKL/OPG and NF-κB signaling pathways [11, 13, 14]. And in this study, the results showed that curculigoside reversed the RANK/RANKL/OPG and NF-κB signaling pathway-associated gene expression in Ti-induced osteolysis *in vitro* and *in vivo*, by inhibiting RANKL, NF-κB p-p65/p65, p-IκBα/IκBα, and p-IKKα/IKKα and increasing OPG.

5. Conclusion

In summary, based on *in vitro* and *in vivo* experiments, the present study demonstrated that curculigoside treatment was able to attenuate Ti-induced periprosthetic osteolysis, activate osteoblastic MC3T3-E1 cell differentiation, inhibit osteoclast BMSC formation, and enhance bone formation in the mouse model. And this protective effect was involved in the regulation of RANK/RANKL/OPG and NF-κB signaling pathways. We propose that curculigoside may be a potential pharmaceutical agent used for the prevention and treatment of wear particle-stimulated osteolysis.

Data Availability

All data generated or analyzed during this study are included in this article.

Conflicts of Interest

The authors declare that there are no conflicts of interest.

Authors' Contributions

Fangbing Zhu, Jianyue Wang, and Yueming Ni contributed equally to this work.

Acknowledgments

The work was supported by the Zhejiang Medicine and Health Science and Technology Plan (No. 2019320455) and Hangzhou Medical and Health Technology Project (Nos. 0020190358 and 0020190844).

References

[1] I. D. Learmonth, C. Young, and C. Rorabeck, "The operation of the century: total hip replacement," *The Lancet*, vol. 370, no. 9597, pp. 1508–1519, 2007.

[2] J. T. Evans, J. P. Evans, R. W. Walker, A. W. Blom, M. R. Whitehouse, and A. Sayers, "How long does a knee replacement last? A systematic review and meta-analysis of case series and national registry reports with more than 15 years of follow-up," *The Lancet*, vol. 393, no. 10172, pp. 655–663, 2019.

[3] J. T. Evans, J. P. Evans, R. W. Walker, A. W. Blom, M. R. Whitehouse, and A. Sayers, "How long does a hip replacement last? A systematic review and meta-analysis of case series and national registry reports with more than 15 years of follow-up," *The Lancet*, vol. 393, no. 10172, pp. 647–654, 2019.

[4] A. Prkic, C. Welsink, The B, M. P. J. van den Bekerom, and D. Eygendaal, "Why does total elbow arthroplasty fail today? A systematic review of recent literature," *Archives of Orthopaedic and Trauma Surgery*, vol. 137, no. 6, pp. 761–769, 2017.

[5] M. Dobzyniak, T. K. Fehring, and S. Odum, "Early failure in total hip arthroplasty," *Clinical Orthopaedics and Related Research*, vol. 447, pp. 76–78, 2006.

[6] O. N. Schipper, S. L. Haddad, P. Pytel, and Y. Zhou, "Histological analysis of early osteolysis in total ankle arthroplasty," *Foot & Ankle International*, vol. 38, no. 4, pp. 351–359, 2017.

[7] T. H. Lin, Y. Tamaki, J. Pajarinen et al., "Chronic inflammation in biomaterial-induced periprosthetic osteolysis: NF-κB as a therapeutic target," *Acta Biomaterialia*, vol. 10, no. 1, pp. 1–10, 2014.

[8] N. A. Athanasou, "The pathobiology and pathology of aseptic implant failure," *Bone & Joint Research*, vol. 5, no. 5, pp. 162–168, 2016.

[9] Y. Wittrant, S. Théoleyre, C. Chipoy et al., "RANKL/RANK/OPG: new therapeutic targets in bone tumours and associated osteolysis," *Biochimica et Biophysica Acta (BBA) - Reviews on Cancer*, vol. 1704, no. 2, pp. 49–57, 2004.

[10] Y. Nie, X. Dong, Y. He et al., "Medicinal plants of genus Curculigo: traditional uses and a phytochemical and ethnopharmacological review," *Journal of Ethnopharmacology*, vol. 147, no. 3, pp. 547–563, 2013.

[11] W. Yingjun, H. Xuan, K. Xu, and J. Yiwei, "Clinical research progress and therapeutic mechanisms of traditional Chinese medicine compound in treating damp-heat gouty arthritis[J]," *The Chinese Journal of Modern Applied Pharmacy*, vol. 37, no. 18, pp. 2299–2304, 2020.

[12] S. Tan, J. Xu, A. Lai et al., "Curculigoside exerts significant anti-arthritic effects in vivo and in vitro via regulation of the JAK/STAT/NF-κB signaling pathway," *Molecular Medicine Reports*, vol. 19, no. 3, pp. 2057–2064, 2019.

[13] H. Ding, G. Gao, L. Zhang et al., "The protective effects of curculigoside A on adjuvant-induced arthritis by inhibiting NF-κB/NLRP3 activation in rats," *International Immunopharmacology*, vol. 30, pp. 43–49, 2016.

[14] Q. Zhang, L. Zhao, Y. Shen et al., "Curculigoside protects against excess-iron-induced bone loss by attenuating Akt-FoxO1-dependent oxidative damage to mice and osteoblastic MC3T3-E1 cells," *Oxidative Medicine and Cellular Longevity*, vol. 2019, Article ID 9281481, 14 pages, 2019.

[15] Y. W. Ge, Z. Q. Liu, Z. Y. Sun et al., "Titanium particle-mediated osteoclastogenesis may be attenuated via bidirectional ephrin-B2/eph-B4 signaling in vitro," *International Journal of Molecular Medicine*, vol. 42, no. 4, pp. 2031–2041, 2018.

[16] L. Xiong, Y. Liu, F. Zhu et al., "Acetyl-11-keto-β-boswellic acid attenuates titanium particle-induced osteogenic inhibition via activation of the GSK-3β/β-catenin signaling pathway," *Theranostics*, vol. 9, no. 24, pp. 7140–7155, 2019.

[17] A. I. Viswanath, C. M. Frampton, and P. C. Poon, "A review of the New Zealand National Joint Registry to compare the outcomes of Coonrad-Morrey and latitude total elbow arthroplasty," *Journal of Shoulder and Elbow Surgery*, vol. 29, no. 4, pp. 838–844, 2020.

[18] C. J. Vertullo, R. N. de Steiger, P. L. Lewis, M. Lorimer, Y. Peng, and S. E. Graves, "The effect of prosthetic design and polyethylene type on the risk of revision for infection in total knee replacement," *The Journal of Bone and Joint Surgery. American Volume*, vol. 100, no. 23, pp. 2033–2040, 2018.

[19] R. Thorkildsen, O. Reigstad, and M. Røkkum, "Chrome nitride coating reduces wear of small, spherical CrCoMo metal-on-metal articulations in a joint simulator," *The Journal of Hand Surgery, European Volume*, vol. 42, no. 3, pp. 310–315, 2017.

[20] S. J. Fitzgerald, T. C. Palmer, and M. J. Kraay, "Improved perioperative care of elective joint replacement patients: the impact of an orthopedic perioperative hospitalist," *The Journal of Arthroplasty*, vol. 33, no. 8, pp. 2387–2391, 2018.

[21] J. A. López-López, R. L. Humphriss, A. D. Beswick et al., "Choice of implant combinations in total hip replacement: systematic review and network meta-analysis," *BMJ*, vol. 359, p. j4651, 2017.

[22] X. Chen, Z. Wang, N. Duan, G. Zhu, E. M. Schwarz, and C. Xie, "Osteoblast-osteoclast interactions," *Connective Tissue Research*, vol. 59, no. 2, pp. 99–107, 2018.

[23] A. Neve, A. Corrado, and F. P. Cantatore, "Osteoblast physiology in normal and pathological conditions," *Cell and Tissue Research*, vol. 343, no. 2, pp. 289–302, 2011.

[24] P. J. Marie, "Osteoblast dysfunctions in bone diseases: from cellular and molecular mechanisms to therapeutic strategies," *Cellular and Molecular Life Sciences*, vol. 72, no. 7, pp. 1347–1361, 2015.

[25] S. C. O'Neill, J. M. Queally, B. M. Devitt, P. P. Doran, and J. M. O'Byrne, "The role of osteoblasts in peri-prosthetic osteolysis," *The Bone & Joint Journal*, vol. 95-B, no. 8, pp. 1022–1026, 2013.

[26] Y. Gu, Z. Wang, J. Shi et al., "Titanium particle-induced osteogenic inhibition and bone destruction are mediated by the GSK-3β/β-catenin signal pathway," *Cell Death & Disease*, vol. 8, no. 6, article e2878, 2017.

[27] H. Xu, C. C. Guo, Z. Y. Gao et al., "Micrometer-sized titanium particles induce aseptic loosening in rabbit knee," *BioMed Research International*, vol. 2018, Article ID 5410875, 11 pages, 2018.

[28] Z. Wang, Z. Deng, J. Gan et al., "$TiAl_6V_4$ particles promote osteoclast formation via autophagy-mediated downregulation of interferon-beta in osteocytes," *Acta Biomaterialia*, vol. 48, pp. 489–498, 2017.

[29] Y. Jiang, T. Jia, W. Gong, P. H. Wooley, and S. Y. Yang, "Titanium particle-challenged osteoblasts promote osteoclastogenesis and osteolysis in a murine model of periprosthestic osteolysis," *Acta Biomaterialia*, vol. 9, no. 7, pp. 7564–7572, 2013.

[30] Q. Shen, D. Zeng, Y. Zhou et al., "Curculigoside promotes osteogenic differentiation of bone marrow stromal cells from ovariectomized rats," *Journal of Pharmacy and Pharmacology*, vol. 65, no. 7, pp. 1005–1013, 2013.

[31] L. Wang, Y. J. He, T. Han et al., "Metabolites of curculigoside in rats and their antiosteoporotic activities in osteoblastic MC3T3-E1 cells," *Fitoterapia*, vol. 117, pp. 109–117, 2017.

[32] L. Wang, Z. Dai, J. Xie, H. Liao, C. Lv, and Y. Hu, "Alteration of the RANKL/RANK/OPG system in periprosthetic osteolysis with septic loosening," *Inflammation*, vol. 39, no. 1, pp. 218–227, 2016.

[33] T. Yamashita, Z. Yao, F. Li et al., "Osteoclast differentiation and activation," *Clinical Calcium*, vol. 17, no. 4, pp. 484–492, 2007.

[34] W. J. Boyle, W. S. Simonet, and D. L. Lacey, "NF-kappaB p50 and p52 regulate receptor activator of NF-kappaB ligand (RANKL) and tumor necrosis factor-induced osteoclast precursor differentiation by activating c-Fos and NFATc1," *The Journal of Biological Chemistry*, vol. 282, no. 25, pp. 18245–18253, 2007.

[35] H. Yasuda, "Discovery of the RANKL/RANK/OPG system," *Journal of Bone and Mineral Metabolism*, vol. 39, no. 1, pp. 2–11, 2021.

[36] B. Meng, D. Wu, Y. Cheng et al., "Interleukin-20 differentially regulates bone mesenchymal stem cell activities in RANKL-induced osteoclastogenesis through the OPG/RANKL/RANK axis and the NF-κB, MAPK and AKT signalling pathways," *Scandinavian Journal of Immunology*, vol. 91, no. 5, article e12874, 2020.

[37] C. H. Zhou, Z. L. Shi, J. H. Meng et al., "Sophocarpine attenuates wear particle-induced implant loosening by inhibiting osteoclastogenesis and bone resorption via suppression of the NF-κB signalling pathway in a rat model," *British Journal of Pharmacology*, vol. 175, no. 6, pp. 859–876, 2018.

Hindawi
Journal of Immunology Research
Volume 2021, Article ID 2183427, 10 pages
https://doi.org/10.1155/2021/2183427

Research Article

The Potential Role of Korean Mistletoe Extract as an Anti-Inflammatory Supplementation

Soo-Min Ha,[1] **Ji-Hyeon Kim**,[2] **Jong-Won Kim**,[3] **Do-Yeon Kim**,[1] **and Min-Seong Ha**[4]

[1]*Laboratory of Exercise Physiology, Department of Physical Education, Pusan National University, 2 Busandaehak-ro 63beon-gil, Geumjeong-gu, Busan 46241, Republic of Korea*
[2]*Department of Liberal Arts, Mokpo National Maritime University, 91 Haeyangdaehak-ro, Mokpo-si, Jeollanam-do 58628, Republic of Korea*
[3]*Department of Physical Education, Busan National University of Education, 33 Gyodae-ro, Yeonje-gu, Busan 47503, Republic of Korea*
[4]*Department of Sports Culture, College of the Arts, Dongguk University-Seoul, 30 Pildong-ro 1-gil, Jung-gu, Seoul 04620, Republic of Korea*

Correspondence should be addressed to Do-Yeon Kim; kdy4955@pusan.ac.kr and Min-Seong Ha; haminseong@dgu.ac.kr

Received 28 April 2021; Accepted 20 June 2021; Published 30 June 2021

Academic Editor: Tomasz Baczek

Korean *mistletoe* has anti-inflammatory and antioxidant functions and may be a useful training supplement. We investigated the effect of Korean *mistletoe* extract (KME) on inflammatory markers after high-intensity exercise by 20 university male rowers (KME group vs. CON group) consuming 110 mL KME/dose (2 times a day over 8 weeks). Blood samples were collected for measurement of serum cytokine levels at baseline, immediately after exercise, and following 30 minutes of recovery. Interleukin-6 (IL-6), tumor necrosis factor-alpha (TNF-α), and C-reactive protein (CRP) were used as markers for inflammation. After supplementation, IL-6 and TNF-α levels were significantly lowered in the KME group than in the CON group at baseline, immediately after exercise, and following 30 minutes of recovery. KME can reduce high-strength exercise-induced increases in the levels of serum inflammatory cytokines in active individuals and improve anti-inflammatory functions.

1. Introduction

Exercise promotes health, prevents disease, increases life expectancy, and is considered to some to be a medicine. However, elite athletes are a paradox that should be emphasized [1]. For athletes to achieve a higher rank or exceptional results in competitive sport, tolerance for strenuous exercise is necessary.

Strenuous exercise may serve as a physical stressor and can thus create a state similar to an inflammatory response [2]. Inflammation is a tissue's immune response to various stimuli [3], and during inflammatory processes by macrophages and inflammatory cells, inflammatory mediators including nitric oxide, cytokines, and chemokines are released [4]. As such, arduous conditions during exercise activate neutrophils, monocytes, and macrophages. It can also increase levels of proinflammatory cytokines including interleukin-1 beta (IL-1β), tumor necrosis factor-alpha (TNF-α), and interleukin-6 (IL-6) and amplify different aspects of inflammation through cytokine action [5]. These factors impede exercise performance and increase interactions between serum inflammatory cytokines and other organ systems, resulting in signs and symptoms of inflammation [1, 6]. TNF-α is the major active cytokine during an acute inflammatory response and sends a stimulatory signal to leukocytes at sites of inflammation to eliminate microorganisms and decrease inflammation [7]. Activation of nuclear factor kappa-light-chain-enhancer of activated B cells (NF-κB), in combination with the TNF receptor 1, exerts a negative effect on induction of intracellular gene expression in response to oxidative stress [8]. IL-6 is a

cytokine that is essential to the transport of proteins that regulate immunity. IL-6 levels change significantly in response to exercise. It is mostly activated during skeletal muscle contraction and plays crucial roles in the control of immune and metabolic functions [9]. IL-6 simultaneously regulates both inflammatory and anti-inflammatory functions [10, 11]. Inflammatory proteins, enzymes, and C-reactive protein (CRP) have been used as biomarkers in medicine to assess levels of inflammation, infection, and injury [12].

Nutrition planning may be useful to counteract inflammatory responses after strenuous exercise, and dietary supplements are able to inhibit inflammatory response and specific immune functions [13]. Thus, many studies have attempted to establish the importance of nutrition that enhances immunity during athlete training and during competition [14]. Dietary supplements with anti-inflammatory and antioxidant functions may aid athlete recovery after repetitive intense exercise [15]. To characterize the effects of such dietary supplements on exercise physiology, future studies should be planned carefully and with precision. It is important to determine the effect of specific supplements on exercise physiology, as opposed to having performance as the sole consideration [16]. Vegetable polyphenols are known to have various biological effects, and administration of polyphenols can reduce oxidative stress and levels of proinflammatory cytokines [17].

Mistletoe (*Viscum album* var. *coloratum*) is an angiosperm that survives by absorbing moisture, minerals, and organic materials from several host trees. As it retains photosynthetic function, this makes it a hemiparasite that is not entirely dependent on its host. *Mistletoe* is chemically composed of viscotoxins, lectins, flavonoids, phenolic acids, terpenoids, sterols, phenylpropanoids, and alkaloids [18]. It has been reported to be effective not only as an antitumor [19] and anti-inflammatory agent [20] but also for immune enhancement and regulation [21] and treatment of atherosclerosis and hypotension [22]. *Mistletoe* also promotes antioxidant functions [23], increases endurance through increased mitochondrial activity [24], and has an antidiabetic effect through insulin secretion [25]. As such, *mistletoe* is used as a supplement to ameliorate symptoms of the above illnesses.

Excessive long-term training and intense exertion during exercise can cause expression of inflammatory cytokines. Various measures have been explored to minimize this response, and dietary supplements with anti-inflammatory and antioxidant effects may help athletes to recover from repetitive intense exercise and thus prevent reductions in performance. To address this, we conducted this study to determine the effects of *mistletoe* extract supplementation on levels of inflammatory markers in university-aged male rowing athletes during an 8-week training period. The performance measure for high-intensity aerobic and anaerobic sport involved rowing a 2,000 m distance on an ergometer.

2. Methods

2.1. Subjects. Study subjects included 20 university-aged male rowing athletes (means ± SD: age = 20.37 ± 1.20 year, height = 179.96 ± 4.33 cm, weight = 80.57 ± 8.73 kg) at H University, Busan, Republic of Korea. Subjects individually had more than 5 years of rowing experience and were national-level athletes who won at national competitions. This study was conducted in accordance with protocols approved by the institutional review board at Pusan National University (PNU IRB/2016_24_HR). The subjects were fully informed about the study and understood its objective and intent prior to participation. Only those who gave voluntary written consent were included in this study. All subjects were athletes without a prior record of musculoskeletal or other injuries and had not been treated with medication in the 6 months prior to the study. The subjects were prohibited from taking other nutritional supplements or drugs for a month before commencement of the study and for its duration.

2.2. Study Design. Subjects were randomly divided into two groups: the experimental group that was administered the Korean *mistletoe* extract (KME) supplement ($n = 10$) and the control (CON) group ($n = 10$). All subjects undertook preseason training for 8 weeks (January to February), and the KME group were administered *mistletoe* extract during this period. All of the following parameters were measured using the same protocol and under the same conditions: 2,000 m rowing ergometer performance was assessed and serum IL-6, TNF-α, and CRP levels were measured before (0 week) and after (8 weeks) the training period. They were measured at baseline, immediately after the 2,000 m rowing exercise, and following 30 min of recovery. We set the recovery time of inflammation markers through mistletoe extract intake to 30 minutes based on previous recovery studies after 2,000 m rowing ergometer performance of rowers [26, 27]. The KME group was also administered *mistletoe* extract (110 mL) and had 30 min of recovery after the rowing test. The study design is shown in Figure 1.

2.3. Supplementation. The KME group was administered 220 mL of *mistletoe* extract (*mistletoe* juice, Jinheong Food Ltd., Uljin, South Korea) daily during the 8-week training period, divided into two doses. A 110 mL dose was administered once every morning and again 1 h after the evening meal [28]. The KME group was administered an additional 110 mL of *mistletoe* extract before and immediately following the 2,000 m rowing exercise, prior to blood collection. *Mistletoe* extract was prepared according to a method validated in previous studies on natural plants [28, 29]. The specific manufacturing process is as follows. Oak mistletoe (*Viscum album* var. *coloratum*) grown at an altitude of 800 m or higher in Uljin (Mt. Tonggo and Mt. Baekam) in Gyeongsangbuk-do, Republic of Korea, was harvested and dried naturally for 1 month. After that, it was cut into pieces of 5 cm each and roasted, 1,650 g of mistletoe and 22,000 mL of water were added to the extractor, and the pressure was 0.15 kgf/cm^2 at 110°C, and extraction was performed for 3 hours. After extraction, it was pasteurized for 40 minutes. The mistletoe extract was provided by sealing and refrigeration in a plastic pack of 110 mL (content of mistletoe, 13 g/pack).

Analysis by the Korea Advanced Food Research Institute (2016) found that the main chemical components of *mistletoe* extract were water (97%), crude ash (0.2%), crude fat

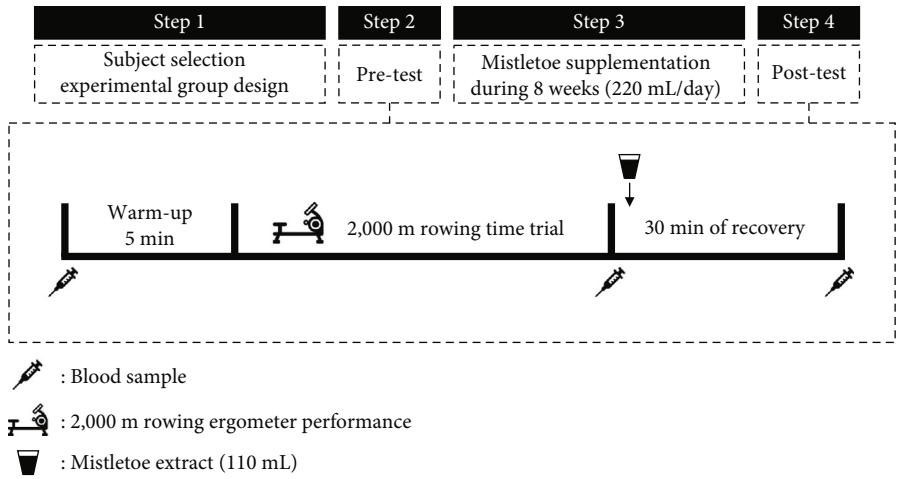

Figure 1: Overview of intervention study design. The pre- and postsupplementation was performed in the experiment in the same condition and methods. Rowing performance measures (2,000 m rowing ergometer race simulation) were completed before and after each supplementation period (the mistletoe supplement group and the control group). Venous blood samples at the baseline were assessed before the subjects underwent rowing ergometer test. After the exercise, venous blood measures were assessed immediately and after 30 minutes. The KME group took 110 mL of mistletoe extract immediately after the exercise.

Table 1: Physical characteristics of subjects in both groups.

Variables Group	Age (yr)	Height (cm)	Weight (kg)	BMI (kg/m^2)	Career (yr)
KME ($n = 10$)	20.44 ± 0.99	180.87 ± 5.03	81.73 ± 8.52	24.99 ± 1.56	5.70 ± 1.34
CON ($n = 10$)	20.30 ± 1.42	179.05 ± 3.53	79.41 ± 9.24	24.76 ± 3.03	5.20 ± 1.55

Values are means ± SD. KME: Korean mistletoe extract intake group; CON: control group.

(0.5%), crude protein (0.3%), carbohydrate (2.0%), sodium (3.9 mg/100 g), and flavonoids (32.0 mg/100 g).

2.4. Rowing Performance Test. An indoor rowing ergometer (Concept2 Inc., VT, USA) that is typically used for physical or technical training of rowing athletes was used to assess exercise performance. Performance in a 2,000 m rowing test was measured. This was a physically demanding task that required maximum effort from the subjects. During the rowing performance test, heart rate was maintained at ≥80% heart rate reserve, and changes in heart rate were measured every 5 s using a wireless heart rate meter (Polar RS400sd, Polar Electro Inc., NY, USA). Prior to the test, all subjects freely performed a warm-up on the rowing ergometer for 5 min.

2.5. Biochemical Analysis. Prior to blood collection, subjects were required to fast from 8:00 pm of the previous day. To measure cytokine levels at baseline, immediately after the 2,000 m rowing exercise, and following 30 min of recovery, 10 mL of blood was drawn from the forearm vein using a vacuum collection tube. The blood samples obtained were then centrifuged (Combi-514R, Hanil, Korea) for 10 min at 3,000 rpm. Serum was separated from blood cells, transferred to a microfuge tube, and was then stored at −80°C until analysis. Enzyme-linked immunosorbent assay (ELISA) was performed to determine serum concentration of IL-6 and TNF-α using CymaxTM Human IL-6 and TNF-α ELISA Kits (AB Frontier, Korea), respectively, and OD at 450 nm was measured using GENios (TECAN, Switzerland). An immunoturbidimetric assay with CRPL3 (Roche, Germany) and a Modular Analytics (Roche, Germany) analyzer was used to measure levels of CRP.

2.6. Statistical Analysis. Sample size was determined using a G-power version 3.1 Windows program (Kiel University, Kiel, Germany), based on a 0.25-point effect size (default), an alpha level of $p < 0.05$, and 60% power [30]. The mean value (M) and standard deviation (SD) of the measured parameters were calculated using the Statistical Package for the Social Sciences (SPSS) version 23.0 for Windows (SPSS Inc., Chicago, IL). To analyze interaction of differences between the groups (KME vs. CON, 2) and between periods (before vs. after, 2), a two-way repeated measures analysis of variance analysis was performed. To assess changes within each group before and after supplementation, a paired t-test was performed. An independent t-test was also used to analyze the delta (Δ) change. The level of statistical significance was set at $p < 0.05$.

3. Results

3.1. Subject Characteristics. The physical characteristics of study subjects are summarized in Table 1. There was no significant difference in mean age, height, weight, body mass

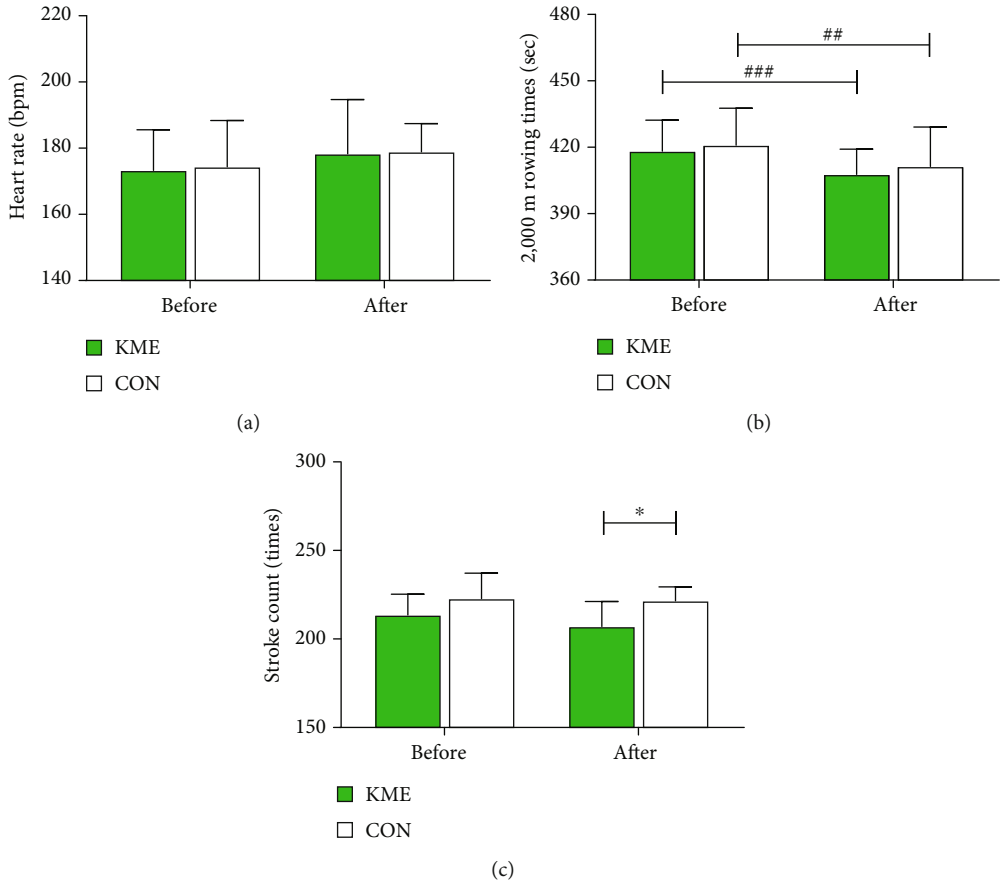

Figure 2: Before and after supplementation of 2,000 m rowing ergometer performance: (a) heart rate during the 2,000 m rowing test; (b) 2,000 m rowing time trial; (c) total stroke count during the 2,000 m rowing test. Data are shown as means ± SD. $^{\#\#}p < 0.01$ and $^{\#\#\#}p < 0.001$ before vs. after; $^{*}p < 0.05$ KME vs. CON.

index, and career achievements of the rowers in the KME and CON groups.

3.2. 2,000 m Rowing Ergometer Test. During the 2,000 m rowing ergometer trial test, there was no difference in heart rate between groups and periods (KME group before: 173.33 ± 12.26 bpm, after: 178.29 ± 16.43 bpm, $t = -1.032$, $p = 0.329$; CON group before: 174.39 ± 13.95 bpm, after: 178.91 ± 8.52 bpm, $t = -1.514$, $p = 0.164$). There was no significant difference in performance for the 2,000 m rowing test between the KME group (418.25 ± 14.03 s) and the CON group (420.98 ± 16.64 s) prior to the experiment ($t = -.397$, $p = 0.696$). The 2,000 m rowing test times significantly decreased in both the KME group (407.77 ± 11.39 s, $t = 6.676$, $p < 0.001$) and the CON group (411.33 ± 17.82 s, $t = 3.770$, $p < 0.01$) at after 8 weeks. Total rowing stroke count also did not differ significantly for the 2,000 m rowing test in both groups prior to supplementation. The KME group had a rowing stroke count of 213.60 ± 11.5, and the CON group had a count of 222.80 ± 14.40 ($t = -1.566$, $p = 0.135$). Following supplementation, total rowing stroke count was significantly different between the groups. The KME group (207.10 ± 14.11) had a lower rowing stroke count than the CON group (221.60 ± 7.82), as shown in Figure 2 ($t = -2.843$, $p < 0.05$).

3.3. Serum Inflammation Markers

3.3.1. Interleukin-6 (IL-6). After the 8 weeks, baseline levels of serum IL-6 decreased from 4.13 ± 1.16 pg/mL to 3.57 ± 0.55 pg/mL in the KME group and increased from 4.62 ± 1.41 pg/mL to 5.46 ± 0.54 pg/mL in the CON group. The main effect of the two groups ($F = 5.745$, $p < 0.05$) after the 8 weeks was different at baseline ($t = -7.760$, $p < 0.001$). Immediately following exercise, the concentration of serum IL-6 in the KME group was 9.95 ± 1.79 pg/mL before and 10.22 ± 1.49 pg/mL after supplementation. In the CON group, the concentration of serum IL-6 increased from 11.07 ± 2.38 pg/mL to 13.99 ± 3.21 pg/mL after the 8 weeks. An interaction effect ($F = 6.596$, $p < 0.05$) and the main effect of the groups ($F = 12.117$, $p < 0.01$) were observed immediately following exercise. Serum IL-6 significantly increased immediately after exercise in the CON group ($t = -2.443$, $p < 0.05$). There were significant differences between the groups after the 8 weeks ($t = -3.373$, $p < 0.01$). The concentration of serum IL-6 in the KME group after 30 min of recovery was 5.86 ± 1.98 pg/mL before supplementation and 5.45 ± 1.49 pg/mL after supplementation. In the CON group, the concentration of serum IL-6 was 7.59 ± 1.43 pg/mL before and 8.78 ± 2.70 pg/mL after the 8 weeks. The main effect of the groups

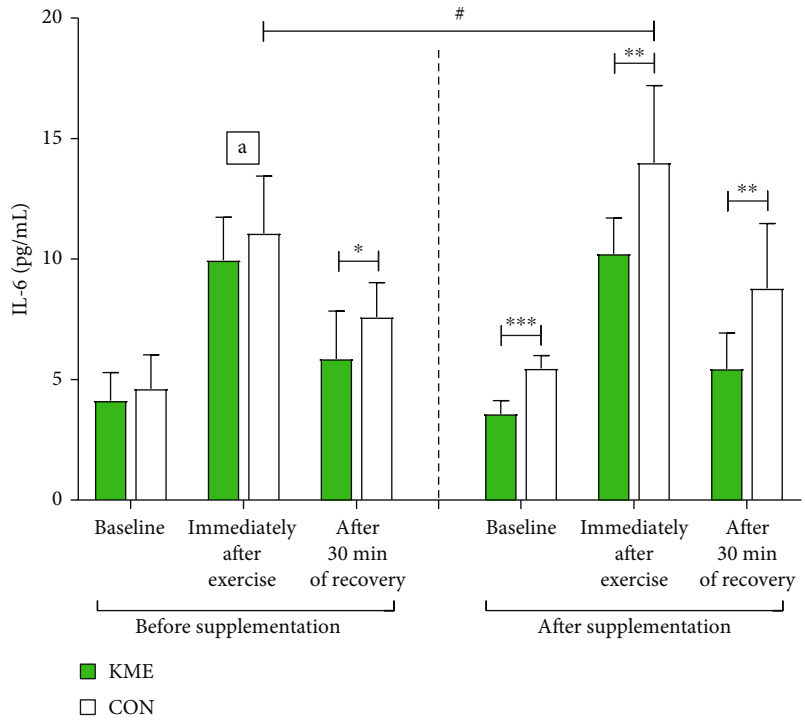

Figure 3: Changes in interleukin-6 levels during the 2,000 m rowing ergometer exercise trials performed before and after supplementation (means ± SD). [a]Interaction effects immediately after exercise. $^{\#}p < 0.05$ before vs. after; $^{*}p < 0.05$, $^{**}p < 0.01$, and $^{***}p < 0.001$ KME vs. CON.

($F = 7.748$, $p < 0.05$) and comparison of differences between the two groups revealed that they were significantly different before ($F = -2.229$, $p < 0.05$) and after the 8-week period ($F = -3.425$, $p < 0.01$), as seen in Figure 3.

Differences (Δ) between serum levels of IL-6 before and after the 8 weeks are represented in Figure 4(a). Briefly, the baseline of Δ-IL-6 was -0.56 ± 0.90 pg/mL in the KME group and 0.84 ± 1.54 pg/mL in the CON group. This was significantly different ($t = -2.493$, $p < 0.05$). Immediately following exercise, the Δ-IL-6 was 0.27 ± 1.91 pg/mL in the KME group and 2.92 ± 3.79 pg/mL in the CON group ($t = -1.978$, $p = 0.063$). After 30 min of recovery, the Δ-IL-6 was -0.42 ± 0.88 pg/mL in the KME group and 1.19 ± 2.22 pg/mL in the CON group. This was again significantly different ($t = -2.136$, $p < 0.05$).

3.3.2. Tumor Necrosis Factor-Alpha (TNF-α). An interaction effect ($F = 8.678$, $p < 0.05$) was observed for baseline levels of serum TNF-α; there was a significant main effect of group ($F = 7.612$, $p < 0.05$). Concentration of serum TNF-α decreased from 54.05 ± 16.75 pg/mL to 41.51 ± 3.68 pg/mL after supplementation in the KME group. In contrast, in the CON group, concentration of serum TNF-α was 56.57 ± 13.90 pg/mL prior to and 64.89 ± 10.06 after the 8 weeks. This demonstrated that the KME group had significantly lower TNF-α levels ($t = 2.360$, $p < 0.05$). Significant differences were observed between the two groups after the 8 weeks ($F = -6.900$, $p < 0.001$). Immediately following exercise, concentration of serum TNF-α in the KME group decreased from 140.04 ± 34.17 pg/mL to 93.27 ± 5.10 pg/mL after supplementation. In the CON group, concentration of serum TNF-α was 134.28 ± 23.27 pg/mL before and 138.46 ± 25.59 pg/mL after the 8 weeks. There was an interaction effect ($F = 8.201$, $p < 0.05$), a main effect of group ($F = 6.169$, $p < 0.05$), and main effect of time ($F = 10.827$, $p < 0.01$). The decrease observed in the KME group was statistically significant ($t = 4.092$, $p < 0.01$). After the 8-week period, the difference between the two groups was also statistically significant ($t = -5.477$, $p < 0.001$). After 30 min of recovery, serum concentration of TNF-α in the KME group was 65.31 ± 32.71 pg/mL prior to supplementation and 66.14 ± 19.05 pg/mL after supplementation. In the CON group, serum concentration of TNF-α was 91.68 ± 20.32 pg /mL prior to and 94.22 ± 20.64 pg/mL after the 8 weeks. There was no statistically significant interaction. We observed significant differences between the two groups prior to ($t = -2.165$, $p < 0.05$) and after supplementation ($t = -3.161$, $p < 0.01$), as shown in Figure 5.

Differences (Δ) in levels of TNF-α before and after the 8-week period are presented in Figure 4(b). The baseline Δ-TNF-α was -12.54 ± 16.81 pg/mL in the KME group and 8.32 ± 16.23 pg/mL in the CON group. This difference was significant ($t = -2.823$, $p < 0.05$). Immediately following exercise, Δ-TNF-α was -46.77 ± 36.14 in the KME group and 4.18 ± 33.38 pg/mL in the CON group ($t = -3.275$, $p < 0.01$). After 30 min of recovery, Δ-TNF-α was 0.83 ± 21.26 pg/mL in the KME group and 2.54 ± 18.43 in the CON group ($t = -0.192$, $p = 0.850$).

3.3.3. C-Reactive Protein (CRP). Baseline concentration of serum CRP in the KME group was 0.21 ± 0.16 mg/L prior to and 0.22 ± 0.15 mg/L after supplementation. In the CON group, it was 0.33 ± 0.20 mg/L before and 0.35 ± 0.31 mg/L after the 8-week period. Immediately following exercise,

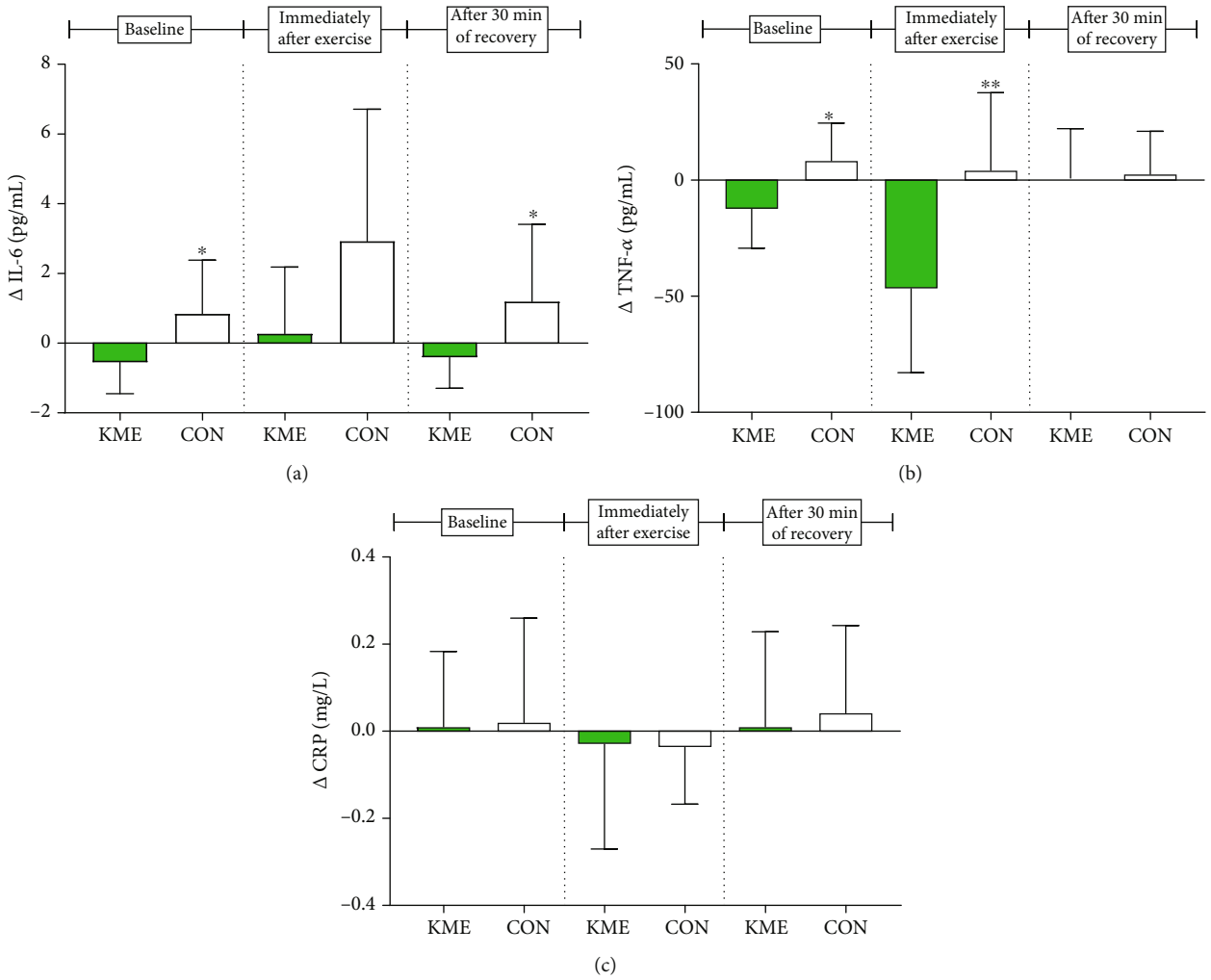

Figure 4: Change in inflammation biomarkers. (a) Significant differences were observed at baseline and after 30 min of recovery in the delta (Δ) values of IL-6 ($^{*}p < 0.05$, $^{*}p < 0.05$). (b) Significant differences were observed at baseline and immediately after exercise in the delta (Δ) values of TNF-α ($^{*}p < 0.05$, $^{**}p < 0.01$). (c) Δ values of CRP, no significant differences were observed. Data are shown as means ± SD.

concentration of serum CRP in the KME group was 0.27 ± 0.23 mg/L prior to and 0.24 ± 0.15 mg/L after supplementation. In the CON group, it was 0.36 ± 0.24 mg/L before and 0.32 ± 0.28 after the 8-week period. After 30 min of recovery, the concentration of serum CRP in the KME group was 0.21 ± 0.17 mg/L prior to and 0.22 ± 0.19 mg/L after supplementation. In the CON group, the concentration was 0.30 ± 0.18 mg/L before and 0.34 ± 0.26 mg/L after the 8-week period. No interaction effect was observed, and there were no significant differences between the two groups (Figure 6).

Differences (Δ) in concentration of serum CRP before and after the 8-week period are represented in Figure 4(c). There were no significant differences observed for all time points. The baseline for Δ-CRP in the KME group was 0.01 ± 0.17 mg/L and was 0.02 ± 0.24 mg/L in the CON group ($t = -0.107$, $p = 0.916$). Immediately following exercise, Δ-CRP was −0.03 ± 30.24 mg/L in the KME group and −0.04 ± 0.13 mg/L in the CON group ($t = 0.081$, $p = 0.936$). After 30 min of recovery, Δ-CRP was 0.01 ± 0.22 mg/L in the KME group and 0.04 ± 0.21 mg/L in the CON group ($t = -0.341$, $p = 0.737$).

4. Discussion

This study demonstrated the effect of *mistletoe* supplementation on the release of proinflammatory cytokines induced by strenuous exercise. Immediately following a bout of strenuous exercise (a 2,000 m rowing ergometer trial), there was a rapid increase in serum inflammatory cytokines such as IL-6 and TNF-α. Supplementation with *mistletoe* extract after exercise for the purposes of quick recovery dampened the increase in IL-6 and TNF-α from baseline levels. Daily administration of the *mistletoe* extract supplement for 8 weeks prevented possible increases in the levels of IL-6 and TNF-α induced by long training periods. Immediately following a break after strenuous exercise, levels of serum IL-6 and TNF-α decreased. Our data suggest that *mistletoe* extract decreases levels of inflammation in elite athletes. This is the first study to investigate the effects of such an antioxidant treatment on exercise-induced oxidative stress.

Training protocols include long training times and high-intensity training for the purposes of reinforcing skills and improving performance. In this study, the subjects

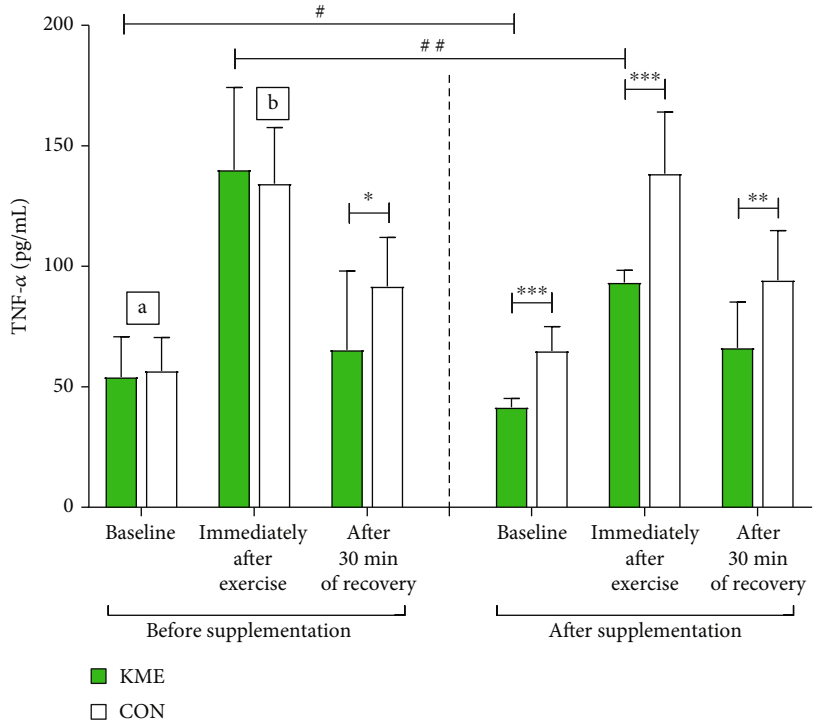

Figure 5: Changes in tumor necrosis factor alpha levels during the 2,000 m rowing ergometer exercise trials before and after supplementation (means ± SD). [a]Interaction effects at the baseline level. [b]Interaction effects immediately after exercise. $^{\#}p < 0.05$ and $^{\#\#}p < 0.01$ before vs. after; $^{*}p < 0.05$, $^{**}p < 0.01$, and $^{***}p < 0.001$ KME vs. CON.

performed high-intensity training for 8 weeks. During the off-season period, performance of rowing athletes in a 2,000 m rowing ergometer trial was compared pre- and postsupplementation with *mistletoe* extract. Our results demonstrated that the time taken to row 2,000 m on the rowing ergometer significantly decreased in each group. As both groups had undertaken 8 weeks of training, the time for the trial decreased compared to the baseline level in both groups. In particular, the KME group reduced the record of 2,000 m rowing performance. Furthermore, the total number of strokes was significantly lower in the KME group compared to the CON group.

Mistletoe extract stimulates the release of peroxisome proliferator-activated receptor gamma coactivator 1-alpha and sirtuin 1 in myoblasts, resulting in improved endurance by upregulating mRNA expression of genes associated with mitochondrial creation and function [24]. It has also been shown to increase expression of mitochondrial uncoupling protein-3 in a myoblast cell line, which activates adenosine monophosphate-activated protein kinase (AMPK) [31]. Another animal study on *mistletoe* extract supplement enhancement of endurance reported that administration of *mistletoe* extract for 12 weeks extended time to exhaustion on the treadmill by 2.5 times and swimming time by 212% and reduced postexercise lactate levels in the experimental group compared to the control group [24]. Administration of *mistletoe* extract during treadmill exercise also increased distance and duration of exercise till exhaustion compared to control [31]. This suggests that rowing performance improvements in the KME group that was administered *mistletoe* extract may be due to increased capacity in the electron transport chain system through increased oxygen consumption by mitochondria [24]. Alternatively, improvements may be due to changes in muscle function and muscle differentiation index [32].

Several mechanisms are involved in inflammatory responses: (1) detection of harmful stimuli *via* binding to the cell surface receptor, (2) revitalizing inflammatory channels, (3) release of inflammatory molecules, and (4) recruitment of inflammatory cells [12]. Cytokines regulate inflammation through a complex network of interactions and calibrate immune response to infection or inflammation. However, excessive inflammatory cytokine production can cause damage including tissue injury, hemodynamic changes, and organ insufficiency that ultimately results in death [33, 34]. An appropriate level of IL-6 maintains glucose homeostasis in muscle tissue and activates the production of AMPK in skeletal muscles to stimulate absorption of glucose and fat oxidation [35]. IL-6 plays a major role in anti-inflammation by blocking the IL-1 receptor and directly inhibiting the expression of TNF-α and IL-1β and is therefore classified as both a pro- and anti-inflammatory cytokine [36]. However, a rapid increase in IL-6 causes cytokine imbalance and induces a critical inflammation state. Athletes who engage in intensive strength-based exercise for long periods are vulnerable to chronic inflammatory conditions [14], and this form of physical exertion results in increased levels of inflammatory cytokines in the blood [37].

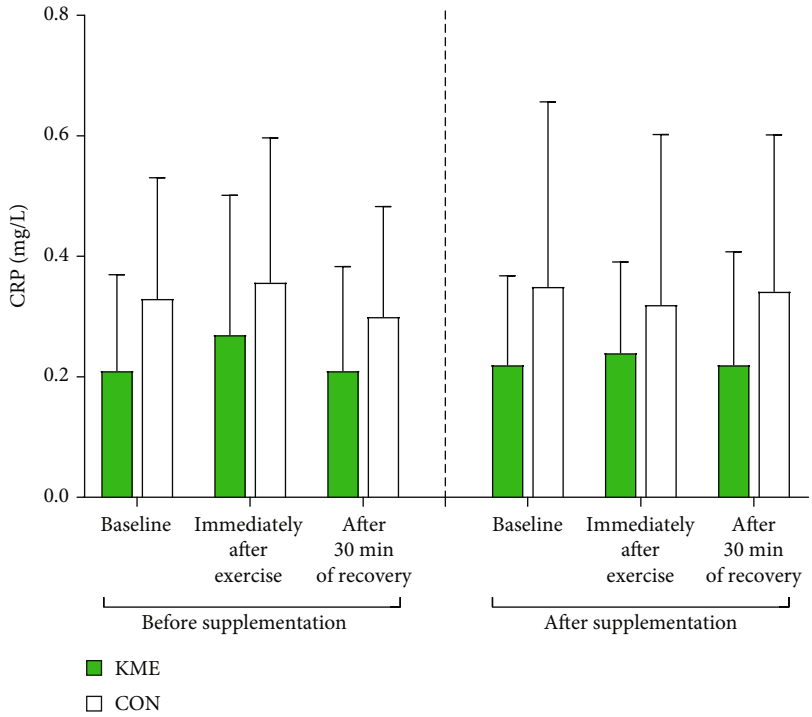

Figure 6: Changes in C-reactive protein levels during the 2,000 m rowing ergometer exercise trials before and after supplementation (means ± SD). There was no difference.

Inflammation is accompanied by muscle pain and discomfort, which increases risk of injury and reduces performance of athletes [38].

Korean *mistletoe* has higher inhibition of lipid peroxidation than an equivalent concentration (10 mg) of vitamin C and demonstrates high antioxidative properties [39]. Oak tree *mistletoe* plays a role as a natural antioxidant as it contains polyphenols, has a superior ability to donate electrons, and increases activity of superoxide dismutase [40]. In particular, homoflavoyadorinin-B, a bioactive flavonoid found exclusively in *mistletoe*, shows potential in preventing and treating diseases associated with the generation of reactive oxygen species [41]. *Mistletoe*'s anti-inflammatory effects also include inhibition of cytokines induced by prostaglandin E2 biosynthesis through selective inhibition of cyclooxygenase-2 (COX-2) [20]. It has also recently been suggested that Korean *mistletoe* may exert anti-inflammatory effects *via* activating transcription factor 3 and mitogen-activated protein kinase (MAPK) and inhibiting NF-κB signal transduction, decreasing inflammatory effectors such as inducible nitric oxide synthases (iNOS), COX-2, TNF-α, and interleukin-1 beta (IL-1β) [42].

Serum TNF-α was elevated after the 2,000 m rowing trial and induced IL-6 expression. The KME group had a lower concentration of IL-6 and TNF-α compared to the CON group after 30 min of recovery, both before and after postexercise supplementation. This indicated that supplementation with *mistletoe* extract was effective in treating acute exercise-induced inflammation when coupled with 30 min of recovery. The KME group also had a lower concentration of serum inflammatory cytokines compared to the CON group at baseline, immediately after exercise, and after 30 min of recovery postsupplementation. This finding implies that supplementation with *mistletoe* ameliorates inflammatory responses induced by long-term intensive training.

However, despite the rapid increase in serum inflammatory cytokines after the 2,000 m rowing trial, there was no significant change in the level of CRP and no interaction effect. Acute phase proteins including CRP also increased after excessive exercise, but it was confirmed that the increase was delayed compared to IL-6 and TNF-α. Because CRP increases dramatically during the inflammatory process and remains elevated for long periods of time, it is thought to be considered in future studies of chronic inflammation levels in athletes.

5. Conclusions

Supplementation with *mistletoe* extract had anti-inflammatory and positive effects on performance during long-term high-intensity training and extreme exertion (a 2,000 m rowing trial). Thus, we propose that *mistletoe* extract may be a valuable anti-inflammatory supplement that protects against exercise-induced oxidative damage in athletes who have increased inflammation due to high-intensity training.

Abbreviations

KME: Korean *mistletoe* extract
IL-6: Interleukin-6
TNF-α: Tumor necrosis factor-alpha

CRP: C-reactive protein
NF-κB: Nuclear factor kappa-light-chain-enhancer of activated B cells
COX-2: Cyclooxygenase-2
MAPK: Mitogen-activated protein kinase
iNOS: Inducible nitric oxide synthases
IL-1β: Interleukin-1 beta.

Data Availability

The data used to support the findings of this study are available from the corresponding author upon request.

Additional Points

Highlights. (i) Korean *mistletoe* extract (KME) has shown functional foods for anti-inflammation. (ii) Inflammatory cytokine expression increased dramatically after strenuous exercise. (iii) KME supplementation prevented increases in IL-6 and TNF-α levels induced by high-intensity training. (iv) KME was consequently helpful in recovery.

Conflicts of Interest

The authors declare that they have no competing interests.

Authors' Contributions

S-M.H. and D-Y.K. contributed in conceptualization; S-M.H., J-H.K., J-W.K., and D.Y.K. contributed in methodology; S-M.H. and M-S.H. contributed in data analysis; S-M.H., M-S.H., and J-H.K. contributed in investigation; S-M.H., M-S.H., and D-Y.K. contributed in original draft preparation; M-S.H. and D-Y.K. contributed in manuscript review and editing; S-M.H. contributed in visualization; D-Y.K. contributed in supervision; S-M.H. and J-H.K. contributed in project administration. All authors have read and approved the final version of the manuscript and agree with the order of presentation of the authors.

References

[1] A. L. da Rocha, A. P. Pinto, E. B. Kohama et al., "The proinflammatory effects of chronic excessive exercise," *Cytokine*, vol. 119, pp. 57–61, 2019.

[2] F. C. Mooren, A. Lechtermann, and K. Volker, "Exercise-induced apoptosis of lymphocytes depends on training status," *Medicine and Science in Sports and Exercise*, vol. 36, no. 9, pp. 1476–1483, 2004.

[3] F. L. Fontes, D. M. Pinheiro, A. H. Oliveira, R. K. Oliveira, T. B. Lajus, and L. F. Agnez-Lima, "Role of DNA repair in host immune response and inflammation," *Mutation Research, Reviews in Mutation Research*, vol. 763, pp. 246–257, 2015.

[4] H. de la Fuente, D. Cibrian, and F. Sanchez-Madrid, "Immunoregulatory molecules are master regulators of inflammation during the immune response," *FEBS Letters*, vol. 586, no. 18, pp. 2897–2905, 2012.

[5] L. L. Smith, "Cytokine hypothesis of overtraining: a physiological adaptation to excessive stress?," *Medicine and Science in Sports and Exercise*, vol. 32, no. 2, pp. 317–331, 2000.

[6] N. T. Vargas and F. Marino, "A neuroinflammatory model for acute fatigue during exercise," *Sports Medicine*, vol. 44, no. 11, pp. 1479–1487, 2014.

[7] L. A. Macedo Santiago, L. G. L. Neto, G. Borges Pereira et al., "Effects of resistance training on immunoinflammatory response, TNF-alpha gene expression, and body composition in elderly women," *Journal of Aging Research*, vol. 2018, Article ID 1467025, 10 pages, 2018.

[8] S. Vallabhapurapu and M. Karin, "Regulation and function of NF-κB transcription factors in the immune system," *Annual Review of Immunology*, vol. 27, no. 1, pp. 693–733, 2009.

[9] S. Glund, A. Deshmukh, Y. C. Long et al., "Interleukin-6 directly increases glucose metabolism in resting human skeletal muscle," *Diabetes*, vol. 56, no. 6, pp. 1630–1637, 2007.

[10] I. J. Elenkov, G. P. Chrousos, and R. L. Wilder, "Neuroendocrine regulation of IL-12 and TNF-alpha/IL-10 balance. Clinical implications," *Annals of the New York Academy of Sciences*, vol. 917, pp. 94–105, 2000.

[11] A. M. Petersen and B. K. Pedersen, "The anti-inflammatory effect of exercise," *Journal of Applied Physiology (Bethesda, MD: 1985)*, vol. 98, no. 4, pp. 1154–1162, 2005.

[12] L. Chen, H. Deng, H. Cui et al., "Inflammatory responses and inflammation-associated diseases in organs," *Oncotarget*, vol. 9, no. 6, pp. 7204–7218, 2018.

[13] S. Bermon, L. M. Castell, P. C. Calder et al., "Consensus statement immunonutrition and exercise," *Exercise Immunology Review*, vol. 23, pp. 8–50, 2017.

[14] J. Scherr, D. C. Nieman, T. Schuster et al., "Nonalcoholic beer reduces inflammation and incidence of respiratory tract illness," *Medicine and Science in Sports and Exercise*, vol. 44, no. 1, pp. 18–26, 2012.

[15] L. C. R. Lima, C. O. Assumpcao, J. Prestes, and B. S. Denadai, "Consumption of cherries as a strategy to attenuate exercise-induced muscle damage and inflammation in humans," *Nutrición Hospitalaria*, vol. 32, no. 5, pp. 1885–1893, 2015.

[16] K. H. Myburgh, "Polyphenol supplementation: benefits for exercise performance or oxidative stress?," *Sports Medicine*, vol. 44, Supplement 1, pp. S57–S70, 2014.

[17] L. Funes, L. Carrera-Quintanar, M. Cerdan-Calero et al., "Effect of lemon verbena supplementation on muscular damage markers, proinflammatory cytokines release and neutrophils' oxidative stress in chronic exercise," *European Journal of Applied Physiology*, vol. 111, no. 4, pp. 695–705, 2011.

[18] A. Szurpnicka, J. K. Zjawiony, and A. Szterk, "Therapeutic potential of mistletoe in CNS-related neurological disorders and the chemical composition of Viscum species," *Journal of Ethnopharmacology*, vol. 231, pp. 241–252, 2019.

[19] G. S. Kienle and H. Kiene, "Complementary cancer therapy: a systematic review of prospective clinical trials on anthroposophic mistletoe extracts," *European Journal of Medical Research*, vol. 12, no. 3, pp. 103–119, 2007.

[20] P. Hegde, M. S. Maddur, A. Friboulet, J. Bayry, and S. V. Kaveri, "*Viscum album* exerts anti-inflammatory effect by selectively inhibiting cytokine-induced expression of cyclooxygenase-2," *PLoS One*, vol. 6, no. 10, article e26312, 2011.

[21] I. Fidan, S. Ozkan, I. Gurbuz et al., "The efficiency of *Viscum album* ssp. album and Hypericum perforatum on human immune cells in vitro," *Immunopharmacology and Immunotoxicology*, vol. 30, no. 3, pp. 519–528, 2008.

[22] J. A. Ojewole and S. O. Adewole, "Hypoglycaemic and hypotensive effects of Globimetula cupulata (DC) Van Tieghem

(Loranthaceae) aqueous leaf extract in rats," *Cardiovascular Journal of South Africa*, vol. 18, no. 1, pp. 9–15, 2007.

[23] B. K. Kim, M. J. Choi, K. Y. Park, and E. J. Cho, "Protective effects of Korean mistletoe lectin on radical-induced oxidative stress," *Biological & Pharmaceutical Bulletin*, vol. 33, no. 7, pp. 1152–1158, 2010.

[24] H. Y. Jung, A. N. Lee, T. J. Song et al., "Korean mistletoe (*Viscum album* coloratum) extract improves endurance capacity in mice by stimulating mitochondrial activity," *Journal of Medicinal Food*, vol. 15, no. 7, pp. 621–628, 2012.

[25] K. W. Kim, S. H. Yang, and J. B. Kim, "Protein fractions from Korean mistletoe (*Viscum album* coloratum) extract induce insulin secretion from pancreatic beta cells," *Evidence-based Complementary and Alternative Medicine*, vol. 2014, Article ID 703624, 8 pages, 2014.

[26] J. H. Kim, D. Y. Kim, J. A. Lee, and H. D. Ha, "Effects of aquatic dynamic recovery on blood lactate, ammonia, LDH and CK after performing rowing ergometer in rowers," *Journal of Coach Develop*, vol. 17, no. 3, pp. 141–149, 2015.

[27] Y. H. Lee, K. O. Shin, K. S. Kim, Y. I. Kim, and J. H. Woo, "The effects of D-ribose supplementation on the production of blood fatigue factors after maximal intensity exercise," *Journal of Life Science*, vol. 21, no. 5, pp. 729–733, 2011.

[28] M. S. Ha, J. H. Kim, S. M. Ha, Y. S. Kim, and D. Y. Kim, "Positive influence of aqua exercise and burdock extract intake on fitness factors and vascular regulation substances in elderly," *Journal of Clinical Biochemistry and Nutrition*, vol. 64, no. 1, pp. 73–78, 2019.

[29] J. J. Kwak, J. S. Yook, and M. S. Ha, "Potential biomarkers of peripheral and central fatigue in high-intensity trained athletes at high-temperature: a pilot study with *Momordica charantia* (bitter melon)," *Journal of Immunology Research*, vol. 2020, Article ID 4768390, 11 pages, 2020.

[30] F. Faul, E. Erdfelder, A. G. Lang, and A. Buchner, "G∗Power 3: a flexible statistical power analysis program for the social, behavioral, and biomedical sciences," *Behavior Research Methods*, vol. 39, no. 2, pp. 175–191, 2007.

[31] S.-H. Lee, I.-B. Kim, J.-B. Kim, D.-H. Park, and K.-J. Min, "The effects of Korean mistletoe extract on endurance during exercise in mice," *Animal Cells and Systems*, vol. 18, no. 1, pp. 34–40, 2014.

[32] N. J. Lim, J. H. Shin, H. J. Kim et al., "A combination of Korean mistletoe extract and resistance exercise retarded the decline in muscle mass and strength in the elderly: a randomized controlled trial," *Experimental Gerontology*, vol. 87, Part A, pp. 48–56, 2017.

[33] A. J. Czaja, "Review article: chemokines as orchestrators of autoimmune hepatitis and potential therapeutic targets," *Alimentary Pharmacology & Therapeutics*, vol. 40, no. 3, pp. 261–279, 2014.

[34] Z. Liu, Y. Wang, Y. Wang et al., "Dexmedetomidine attenuates inflammatory reaction in the lung tissues of septic mice by activating cholinergic anti-inflammatory pathway," *International Immunopharmacology*, vol. 35, pp. 210–216, 2016.

[35] B. B. Kahn, T. Alquier, D. Carling, and D. G. Hardie, "AMP-activated protein kinase: ancient energy gauge provides clues to modern understanding of metabolism," *Cell Metabolism*, vol. 1, no. 1, pp. 15–25, 2005.

[36] B. K. Pedersen, A. Steensberg, and P. Schjerling, "Exercise and interleukin-6," *Current Opinion in Hematology*, vol. 8, no. 3, pp. 137–141, 2001.

[37] H. Bruunsgaard, "Physical activity and modulation of systemic low-level inflammation," *Journal of Leukocyte Biology*, vol. 78, no. 4, pp. 819–835, 2005.

[38] A. Moreira, R. A. Kekkonen, L. Delgado, J. Fonseca, R. Korpela, and T. Haahtela, "Nutritional modulation of exercise-induced immunodepression in athletes: a systematic review and meta-analysis," *European Journal of Clinical Nutrition*, vol. 61, no. 4, pp. 443–460, 2007.

[39] H.-S. Song, Y.-H. Park, S.-K. Kim, W.-K. Moon, D.-W. Kim, and K.-Y. Moon, "Downregulatory effect of extracts from mistletoe (*Viscum album*) and pueraria root (*Pueraria radix*) on cellular NF-κB activation and heir antioxidant activity," *Journal of the Korean Society of Food Science and Nutrition*, vol. 33, no. 10, pp. 1594–1600, 2004.

[40] H.-J. Lee, J.-R. Do, J.-H. Kwon, and H.-K. Kim, "Physiological properties of oak mistletoe (*Loranthus yadoriki*) extracts by microwave extraction condition," *Korean Journal of Food Preservation*, vol. 18, no. 1, pp. 72–78, 2011.

[41] S.-Y. Choi, S.-K. Chung, S.-K. Kim et al., "An antioxidant homo-flavoyadorinin-B from Korean mistletoe (*Viscum album* var. coloratum)," *Journal of Applied Biological Chemistry*, vol. 47, no. 2, pp. 279–282, 2004.

[42] S. B. Park, G. H. Park, H. N. Kim et al., "Anti-inflammatory effect of the extracts from the branch of *Taxillus yadoriki* being parasitic in *Neolitsea sericea* in LPS-stimulated RAW264.7 cells," *Biomedicine & Pharmacotherapy*, vol. 104, pp. 1–7, 2018.

Hindawi
Journal of Immunology Research
Volume 2021, Article ID 8029963, 13 pages
https://doi.org/10.1155/2021/8029963

Research Article

Schisandrin B Attenuates Airway Inflammation by Regulating the NF-κB/Nrf2 Signaling Pathway in Mouse Models of Asthma

Yaqin Chen,[1] Yu Kong,[2] Qili Wang,[1] Jian Chen,[3] Hua Chen,[3] Huihui Xie,[1] and Lan Li[1]

[1]*Department of Pediatrics, The First Affiliated Hospital of Zhejiang Chinese Medical University, Hangzhou, Zhejiang 310006, China*
[2]*The First Clinical Medical School, Zhejiang Chinese Medical University, Hangzhou, Zhejiang 310006, China*
[3]*Tricare Management Activity, Zhejiang Chinese Medical University, Hangzhou, Zhejiang 310006, China*

Correspondence should be addressed to Lan Li; lilan99@zcmu.edu.cn

Received 15 April 2021; Revised 10 June 2021; Accepted 16 June 2021; Published 29 June 2021

Academic Editor: Kai Wang

Background. Asthma is a complex inflammatory disorder that plagues a large number of people. Schisandrin B is an active ingredient of the traditional Chinese herbal medicine Schisandra with various proven physiological activities such as anti-inflammatory and antioxidant activities. In this study, we explored the anti-inflammatory and antioxidant effects and provided the mechanistic insights into the activity of schisandrin B in a mouse model of ovalbumin- (OVA-) induced allergic asthma. *Methods*. Male BALB/c mice were sensitized and challenged with OVA to induce asthma and treated with various doses (15 mg/kg, 30 mg/kg, and 60 mg/kg) of SCH to alleviate the features of allergic asthma, airway hyperresponsiveness, inflammatory response, OVA-specific immunoglobulin (Ig)E level, and pathological injury. *Results*. Schisandrin B significantly attenuated the airway hyperresponsiveness induced by OVA. Moreover, schisandrin B administration suppressed inflammatory responses, reduced the level of IgE, and attenuated pathological injury. Mechanistically, schisandrin B treatment promoted the activation of nuclear erythroid 2-related factor 2 (Nrf2), but suppressed the stimulation of the NF-κB pathway caused by OVA. *Conclusion*. Taken together, our study suggests that schisandrin B attenuates the features of asthmatic lungs by inhibiting the NF-κB pathway and activating the Nrf2 signaling pathway.

1. Introduction

Asthma is a chronic and complicated airway disease that has become a global health problem in recent years. Approximately one-fifth of the current total global population has been diagnosed with asthma, and the prevalence, morbidity, and mortality have rapidly increased in the past few years [1, 2]. Although several patients are well controlled by therapy such as corticosteroid inhalation, severe symptoms are difficult to control. Therefore, an understanding of the precise pathology and the search for perfect treatment methods are important to achieve a better management of asthma.

The classic manifestation of bronchial asthma is chronic airway inflammation, which is distinguished by airway inflammation dominated by eosinophils, increased mucus production, and airway hyperresponsiveness (AHR) [3]. Interleukin-4 (IL-4), IL-13, and IL-5 are type 2 (Th2) cytokines that support the vital role of Th2 lymphocytes in asthma pathogenesis by reducing the release of immunoglobulin (Ig)E and eosinophil infiltration into lung tissues, which accelerate the process of allergic asthma [4, 5]. Meanwhile, the production of reactive oxygen species (ROS), catalase (CAT), glutathione peroxidase (GSH-Px), superoxide dismutase (SOD), nitric oxide (NO), and malondialdehyde (MDA) imbalanced in an asthma model compared with a normal model [6]. Moreover, a large number of signaling pathways are involved in the pathophysiology of asthma. Both nuclear factor kappa-light-chain-enhancer of activated B cells (NF-κB) and nuclear erythroid 2-related factor 2 (Nrf2) pathways are strongly linked to airway inflammation and remodeling in asthma [7]. Overstimulation of the NF-κB pathway regulates the expression of airway inflammatory factors and their excessive secretion from inflammatory cells in allergic asthma [5]. Nrf2 is a main regulator of oxidative stress responses. Specific activation of the Nrf2 pathway enhances the inhibition of the airway inflammatory response

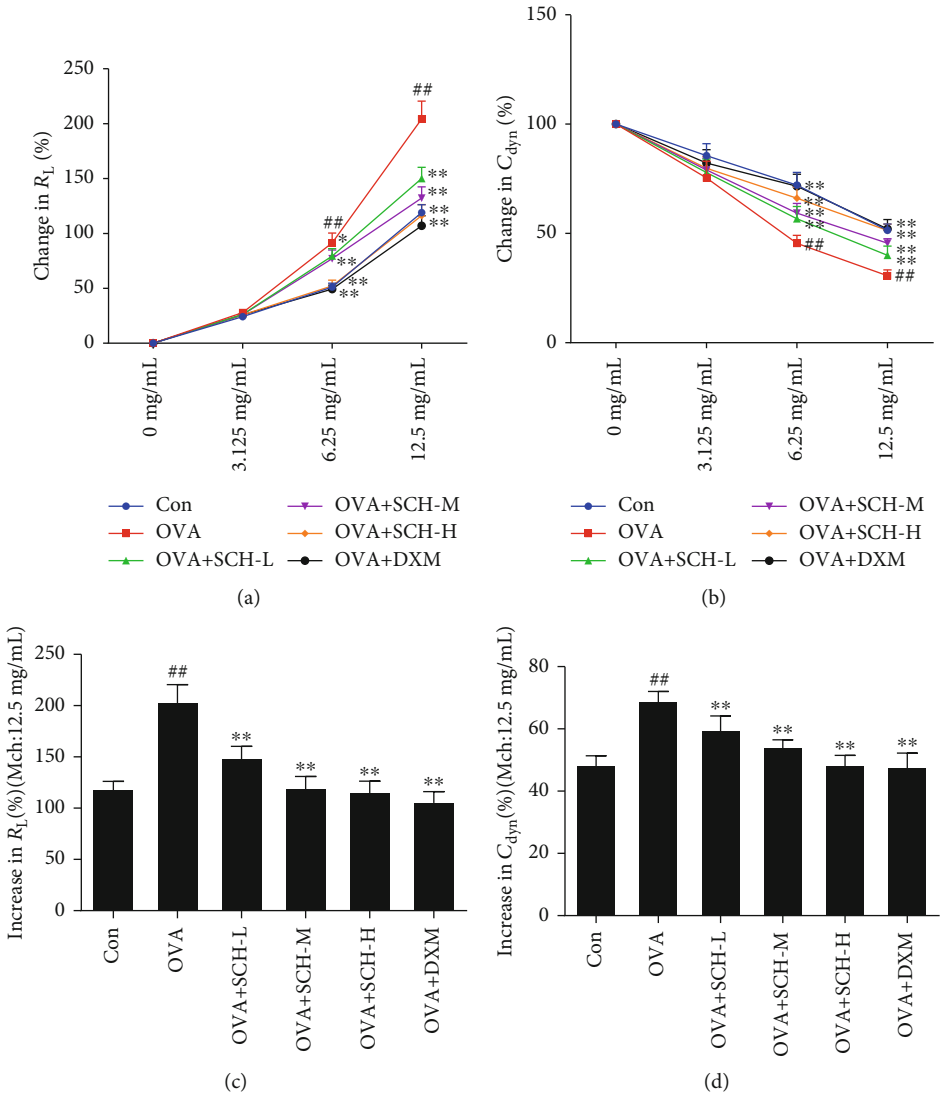

FIGURE 1: Effect of SCH on AHR. (a, b) R_L (%) and C_{dyn} (%) were evaluated. (c, d) R_L (%) and C_{dyn} (%) were again assessed separately after the administration of an Mch dose of 12.5 mg/mL. Data are reported as the means ± SD; $n = 6$. $^{###}p < 0.001$ and $^{##}p < 0.01$ compared with the control group; $^{**}p < 0.01$ and $^{*}p < 0.05$ compared with the OVA group.

and significantly reduces allergen-induced AHR, secretion of mucus, and discharge of Th2 cytokines (IL-13, IL-5, and IL-4) [8].

Schisandrin B (SCH), a lignan active ingredient, was extracted from Schisandra, a traditional Chinese herbal medicine. In addition, it exerts a wide range of effects on physiological activities, such as anti-inflammatory, antioxidant, and antitumor effects and liver toxicity [9]. A previous study reported that the water extract of Schisandra has a certain role in protecting against lung injury, which may be related to improving oxidative stress and airway inflammation, mainly manifesting as the inhibition of the infiltration of neutrophils and macrophages in lung tissues, the production of NO, and the secretion of IL-8 and MCP-1 [10]. SCH restrains the LPS-induced excessive inflammatory response in human umbilical vein endothelial cells by activating the Nrf2 pathway [11]. Moreover, SCH also attenuates airway damage and inflammation-induced lung injury caused by the inhalation of cigarettes by restricting the NF-κB pathway and activating the Nrf2 pathway [11]. Nevertheless, the protective effect and potential mechanism of SCH in asthma remain unclear. This study focused on the antiasthmatic effect of SCH and its theoretical foundation in asthmatic models. We aimed to explore the potential protective role of SCH in asthma through the activation of Nrf2 and inhibition of the NF-κB pathway.

2. Materials and Methods

2.1. Animals. Specific pathogen-free (SPF) inbred BALB/c mice aged approximately 6–8 weeks were purchased from Zhejiang Chinese Medical University Animal Experiment Center (Certificate No. SYXK (Zhe) 2018-0012) and under standard laboratory conditions at a constant temperature of 25°C and a 12-12 h day/night cycle for 7 days before the start

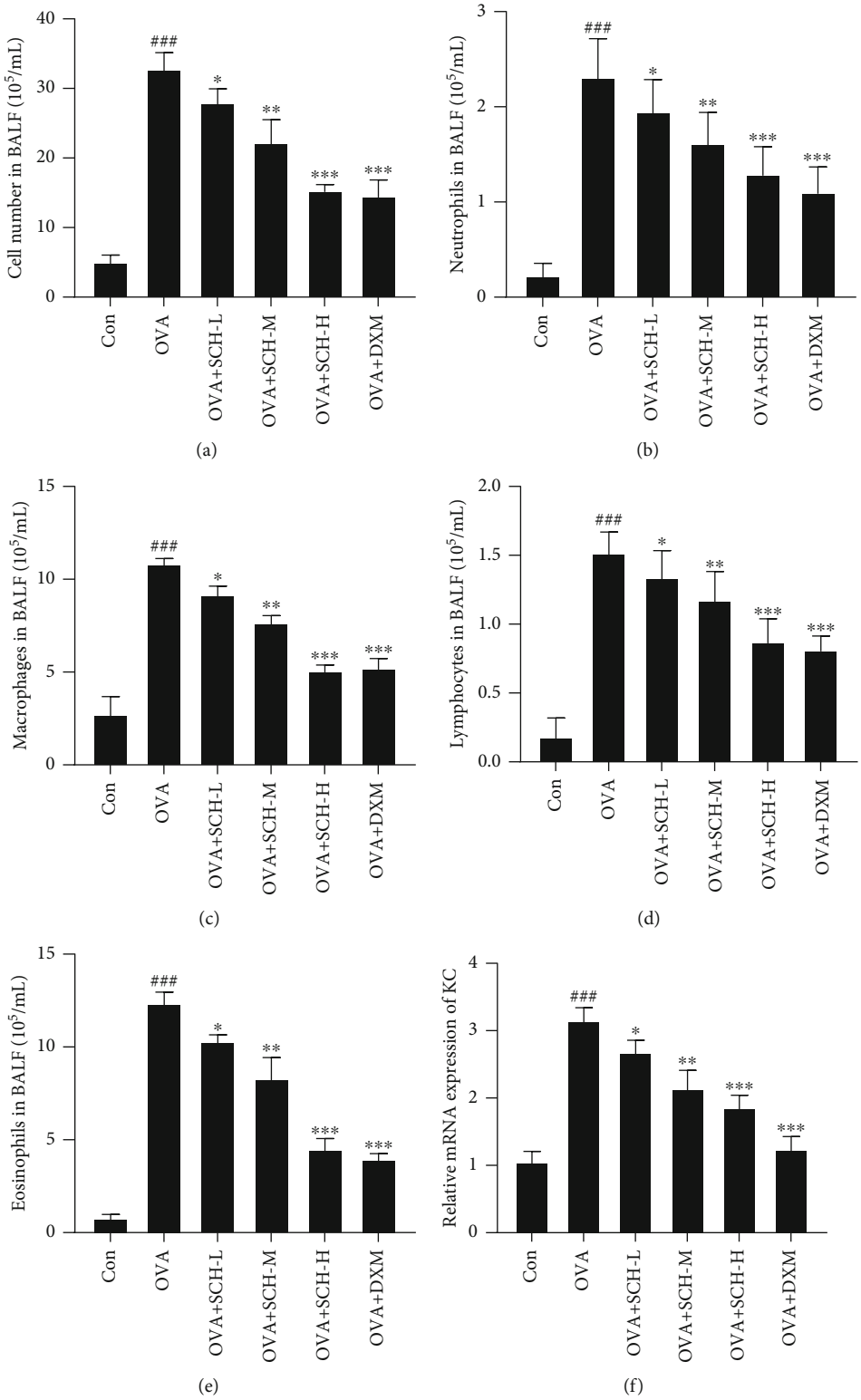

Figure 2: Effect of SCH on the number of inflammatory cells in BALF. The BALF was collected to determine the number of (a) total cells, (b) neutrophils, (c) lymphocytes, (d) macrophages, and (e) eosinophils and the (f) expression of the keratinocyte-derived protein chemokine (KC). Data are presented as the means ± SD; $n = 6$. $^{###}p < 0.001$ compared with the control group; $^{***}p < 0.001$, $^{**}p < 0.01$, and $^{*}p < 0.05$ compared with the OVA group.

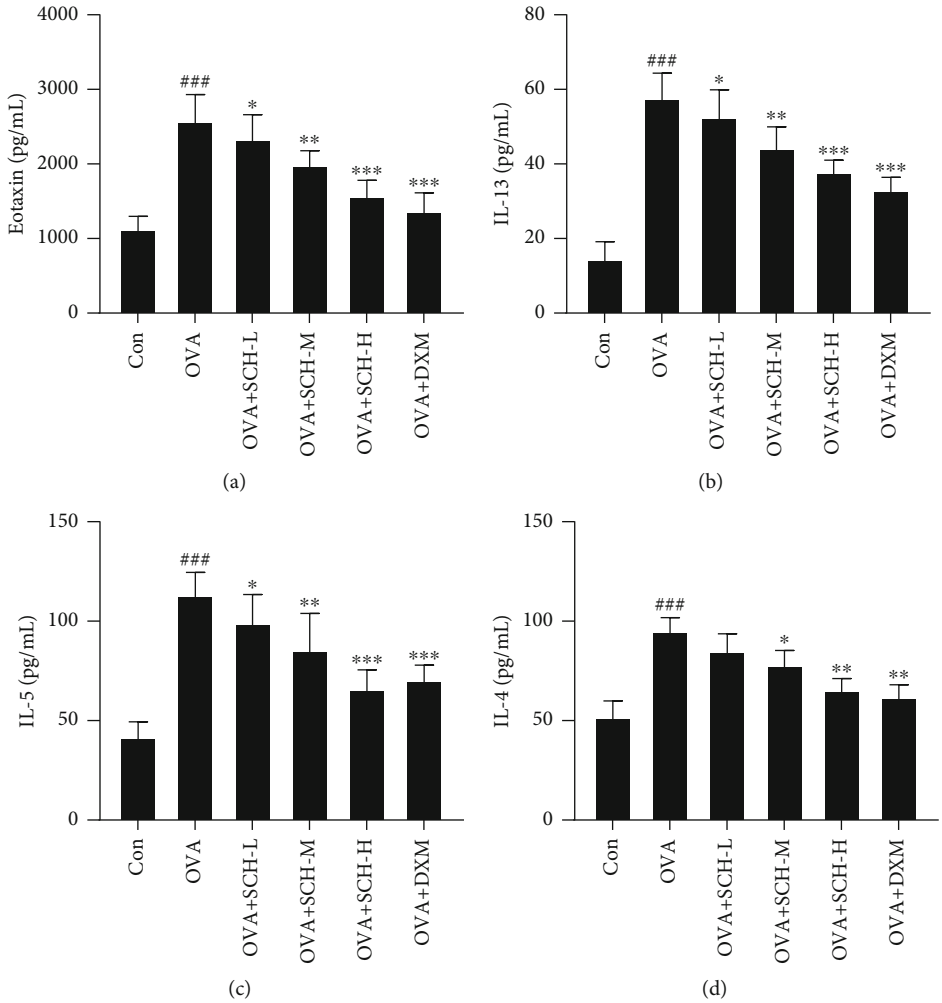

Figure 3: Effect of SCH on the airway levels of inflammatory factors. Samples of BALF were collected to detect the levels of (a) eotaxin, (b) IL-15, (c) IL-5, and (d) IL-4 via using ELISA. Data are reported as the means ± SD; $n = 6$. $^{###}p < 0.001$ and $^{##}p < 0.01$ compared with the control group; $^{***}p < 0.001$, $^{**}p < 0.01$, and $^{*}p < 0.05$ compared with the OVA group.

of the experiments. The mice were freely provided water and standard food.

This study was authorized by the Animal Ethics Committee of Hangzhou Eyong Biotechnological Co., Ltd., and all experiments were conducted according to the Guidelines for the Care and Use of Laboratory Animals.

2.2. Experimental Mouse Model of Allergic Asthma. Sixty BALB/c male mice weighing 18-20 g were stochastically distributed into 6 groups (equal distribution): normal group (control), ovalbumin- (OVA-) induced asthma model group (OVA), SCH (Sigma-Aldrich, China) low-dose group (15 mg/kg, OVA+SCH-L), SCH middle-dose group (30 mg/kg, OVA+SCH-M), SCH megadose group (60 mg/kg, OVA +SCH-H), and positive control group (0.5 mg/kg, dexamethasone, OVA+DXM). Mice were sensitized several times by injecting a 2 mg/mL ovalbumin (OVA, Grade V) solution with 4% aluminum hydroxide gel (Sigma-Aldrich, China) to establish an asthma model. On the first day, 0.5 mL of the OVA solution was injected into the hind feet, groin, subcutaneous, cervical subcutaneous area, and abdominal cavity

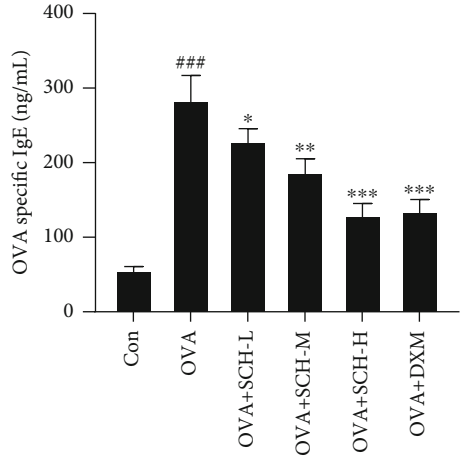

Figure 4: Effect of SCH on the level of OVA-specific IgE. BAL fluids were collected to detect OVA-specific IgE. Data are presented as the means ± SD; $n = 6$. $^{###}p < 0.001$ compared with the control group; $^{***}p < 0.001$, $^{**}p < 0.01$, and $^{*}p < 0.05$ compared with the OVA group.

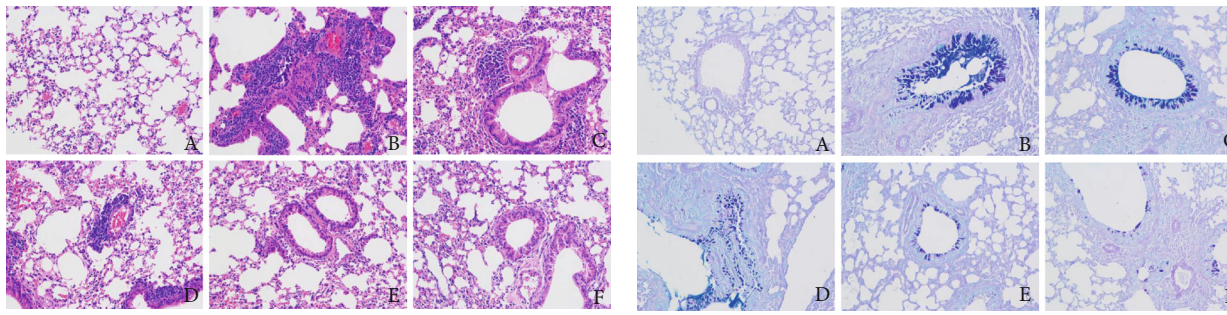

Figure 5: Effect of SCH on lung cell histology. (a) The lung tissues were combined to visualize the pathological condition using H&E staining. (b) Goblet cell hyperplasia in different groups was detected using AB-PAS staining. Magnification, ×200. Group notations: A: control group; B: OVA group; C: OVA+SCH-L group; D: OVA+SCH-M group; E: OVA+SCH-H group; F: OVA+DXM group.

of each mouse [12]. Then, on the 14th day, 0.2 mL of the OVA solution was injected into the abdominal cavity to strengthen the allergic response. Finally, on the 23rd day, an aerosolized physiological saline solution with 10 mg/mL ovalbumin was inhaled by mice for 30 min, at a frequency of 3 times a week for 2 months. Along with OVA physiological saline, all mice were administrated SCH or normal saline by oral gavage 1 h before OVA challenge once a day for 2 months. Dexamethasone (Sigma-Aldrich, China) was administered to mice in the positive control group 3 times a week for 2 months.

2.3. The Evaluation of AHR. One day after the final OVA treatment, conscious mice were placed into the plethysmography chamber (EMKA, Germany) to record baseline readings for an evaluation of lung function. Then, the mice sequentially inhaled 50 μL of normal saline and 0.0625, 0.125, 0.25, 0.5, 1.0, and 2.0 mg/mL aerosolized methacholine (Mch). Lung resistance (R_L) and dynamic compliance (C_{dyn}) were recorded at every stage.

2.4. Enzyme-Linked Immunosorbent Assay (ELISA). ELISA kits (R&D Systems, USA) were employed to detect the level of the inflammatory factors eotaxin, IL-13, IL-5, and IL-4 in BALF according to the manufacturer's instructions. Moreover, OVA-specific IgE in the blood samples was also detected by using ELISA kits (BioLegend, USA) according to the manufacturer's instructions. The antibodies used were purchased from Abcam.

2.5. Analysis of Inflammatory Cells in Bronchoalveolar Lavage Fluid (BALF). One day after the final OVA stimulation, the mice were sacrificed by anesthesia using a 0.75% pentobarbital solution. Then, the trachea was cannulated with a deeply inserted catheter and the left upper lobe was ligated. The lungs were lavaged for three times to collect bronchoalveolar lavage fluid using 700 μL of cold PBS, and the lung tissues were collected. BALF cells were centrifuged with the cytospin technique and stained with Swiss Giemsa dye to count the total cells, lymphocytes, neutrophils, eosinophils, and macrophages.

2.6. Histopathological Analysis of the Lung. A 4% paraformaldehyde solution was used to fix the converged lung tissues of mice for 24 h. After embedding in paraffin, 4 μm slices were cut and a light microscopy examination was performed after hematoxylin-eosin (H&E) and Alcian blue-periodic acid–Schiff (AB-PAS) staining. Inflammation of the airway was observed by assessing morphological changes in the lung tissue using H&E staining, while AB-PAS staining was carried out to determine goblet cell hyperplasia. The detailed methods are described in a previous study [13].

2.7. Immunohistochemistry. Lung slices with a thickness of 4 μm were placed in a 60°C oven for 2 h. The slices were dewaxed with xylene, dehydrated with graded concentrations of alcohol, incubated in an extraction buffer, and incubated with a high-power microwave for 15 minutes. The slices were then cooled, washed with washing buffer, and sequentially incubated with a primary antibody against NF-κB p65 (1 : 1000, Santa Cruz, CA, USA), Nrf2 (1 : 200, CST, USA), iNOS (1 : 200, Abcam, Cambridge, UK), or HO-1 (1 : 200, CST, USA) and secondary antibody (1 : 2000, CST, USA). Finally, the sections were stained with diaminobenzidine (DAB), counterstained with hematoxylin, cleared with xylene, and fixed. Five different microscope fields were randomly selected under a 200x magnification lens.

2.8. Western Blot. The levels of p-IKKα, IKKα, p-NF-κB, NF-κB, p-IκBα, IκBα, Nrf2, and HO-1 were determined to detect the levels of proteins related to the NF-κB and Nrf2 pathways, with GAPDH serving as the internal standard. First, proteins were extracted from the collected lung tissues, and then, the total protein content was quantified using a bicinchoninic acid (BCA) protein detection kit (Beyotime, Hangzhou, China). Protein samples with the same concentrations were separated on 10% SDS-PAGE gels, and the proteins were transferred onto porous nitrocellulose (NC) membranes (Thermo Fisher Scientific, USA). Afterwards, the membranes were blocked with nonfat milk and incubated with the primary antibodies at 4°C for 24 h. The blots were incubated with the secondary goat anti-rabbit antibody at room temperature for 1 h. Blots were incubated with the ECL reagents (Beyotime Biotechnology, Shanghai, China) and analyzed using ImageJ software. All the antibodies used in this study were purchased from CST.

2.9. Real-Time Quantitative RT-PCR. Total RNA was isolated from the lungs using TRIzol reagent (Invitrogen, Carlsbad, CA, USA). The expression of the KC and GAPDH mRNAs

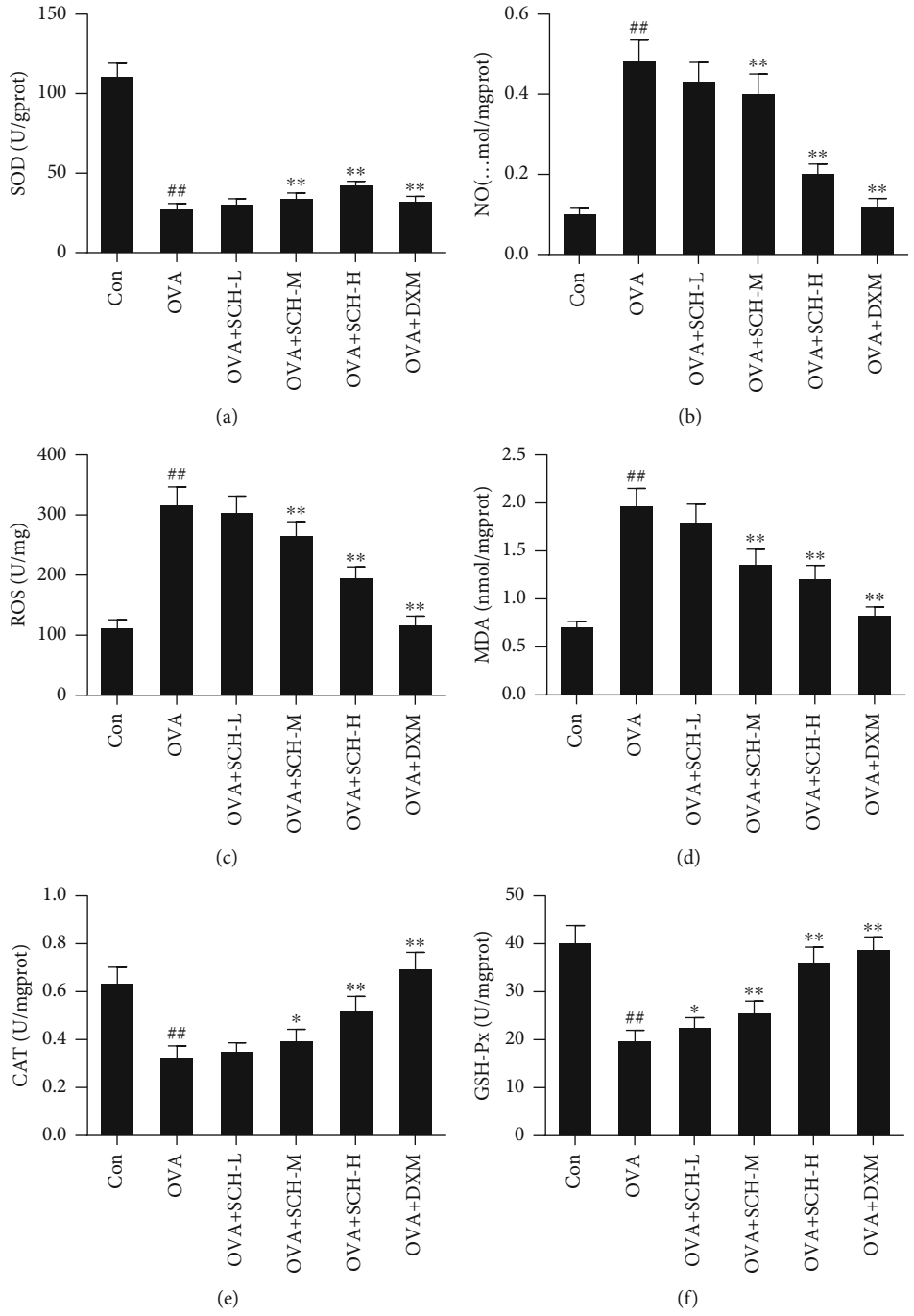

Figure 6: Antioxidant effects of SCH on the lung. The levels of (a) SOD, (b) NO, (c) ROS, (d) MDA, (e) CAT, and (f) GSH-Px in lung tissues were investigated to evaluate the antioxidant function of SCH. Data are presented as the means ± SD; $n = 6$. $^{\#\#}p < 0.01$ compared with the control group; $^{**}p < 0.01$ and $^{*}p < 0.05$ compared with the OVA group. MDA: malondialdehyde; SOD: superoxide dismutase; ROS: reactive oxygen species; NO: nitric oxide; GSH-Px: glutathione peroxidase; CAT: catalase.

was detected with real-time PCR using SYBR green (Takara), an ABI StepOnePlus real-time PCR system, and the following primers: KC forward 5′-CAATGAGCTGCGCTGTCAGTG-3′ and reverse 5′-CTTGGGGACACCTTTTAGCATC-3′; GAPDH forward 5′-GGGAAACCCATCACCATCTT-3′ and reverse 5′-CCAGTAGACTCCACGACATACT-3′. The thermocycling protocol was as follows: 95°C predenaturation for 10 min, followed by 40 cycles of 95°C for 5 s and 60°C for 1 min. GAPDH was chosen as the reference gene, and the formula ($2^{-\Delta\Delta Ct}$) was used to the relative expression level of the tested genes.

2.10. Detection of Oxidative Stress in the Lung. Homogenates of the lung tissues with the same weight were prepared in 0.05 M Tris-HCl buffer (pH 7.4). The homogenate supernatant was collected to measure CAT, ROS, SOD, GSH-Px,

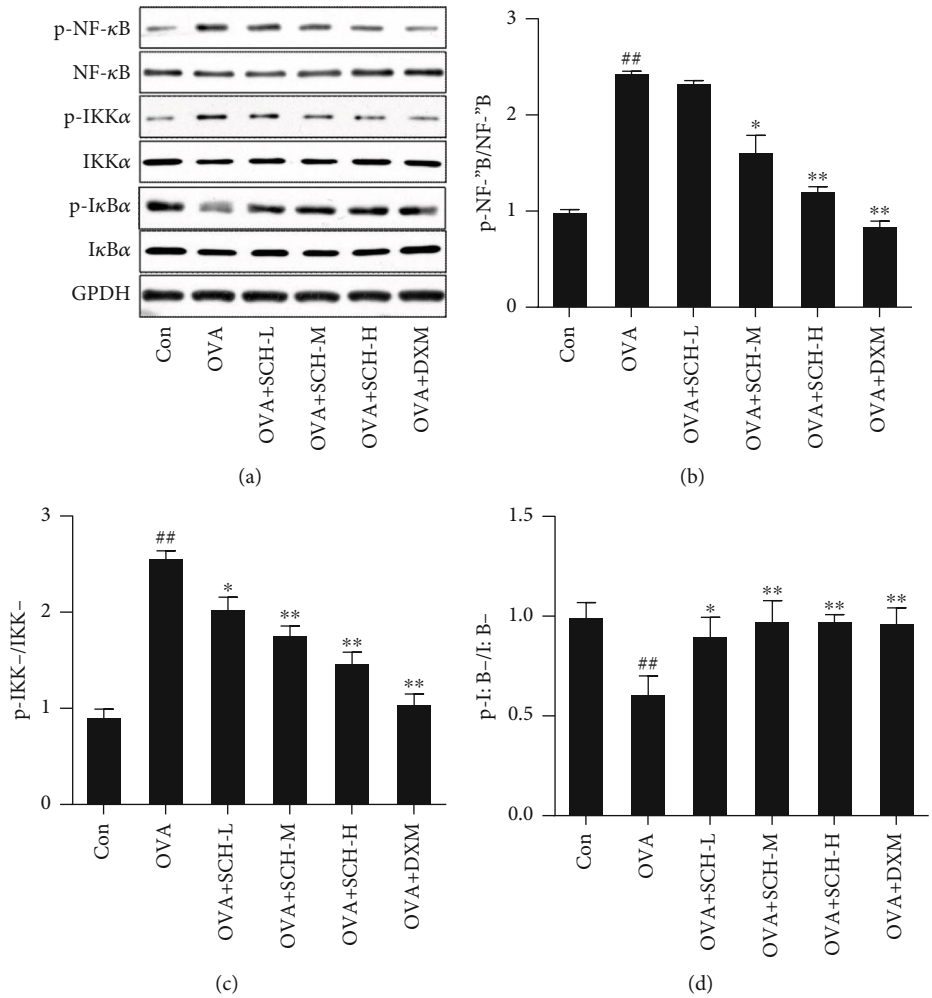

Figure 7: Effect of SCH on NF-κB pathways. (a) The levels of p-NF-κB, NF-κB, p-IKKα, IKKα, p-IκBα, and IκBα were analyzed using Western blotting. (b–d) Quantification of the relative density of p-NF-κB/NF-κB, p-IKKα/IKKα, and p-IκBα/IκBα. Data are reported as the means ± SD; $n = 4$. $^{\#\#}p < 0.01$ compared with the control group; $^{**}p < 0.01$ and $^{*}p < 0.05$ compared with the OVA group.

MDA, and NO levels with commercial kits (Jiancheng, Nanjing, China) according to the manufacturer's protocol.

2.11. Statistical Analysis. Data are presented as the means ± standard deviations (SD). Values of $p < 0.05$ were accepted as statistically significant among different comparisons. One-way ANOVA and Tukey's multiple-comparison test were used to compare multiple groups.

3. Results

3.1. SCH Ameliorates AHR. Airway reactivity is evaluated by calculating the percentage of C_{dyn} [14], which is interpreted as the change in lung volume in response to pressure, and R_L, which is the compression force driving breathing divided by flow [13]. OVA-induced mice received a series of doses of SCH to further determine the effect of SCH on asthmatic AHR. As shown in Figures 1(a) and 1(c), compared with the control, C_{dyn} of the asthma model mice was significantly reduced. However, this reduction was actually reversed by SCH treatment, and high concentrations of SCH produced better results. In addition, compared with the control, the lung resistance (R_L) of the asthma model mice was significantly increased. As expected, the administration of dexamethasone decreased R_L in a dose-dependent manner (Figures 1(b) and 1(d)).

3.2. SCH Suppresses Inflammatory Cell Infiltrations in BALF. Inflammatory cells in the BALF were counted to determine the effectiveness of SCH at inhibiting the infiltration of inflammatory cells from the circulation into the lung space (BALF). The total cell number (Figure 2(a)) and counts of neutrophils (Figure 2(b)), lymphocytes (Figure 2(c)), macrophages (Figure 2(d)), and eosinophils (Figure 2(e)) in BALF were dramatically increased in asthmatic mice, while the increases were restrained by SCH in a dose-dependent manner. We also observed increased expression of the KC mRNA in asthmatic mice following the OVA intervention using qPCR, while this increase was inhibited by SCH in a dose-dependent manner (Figure 2(f)).

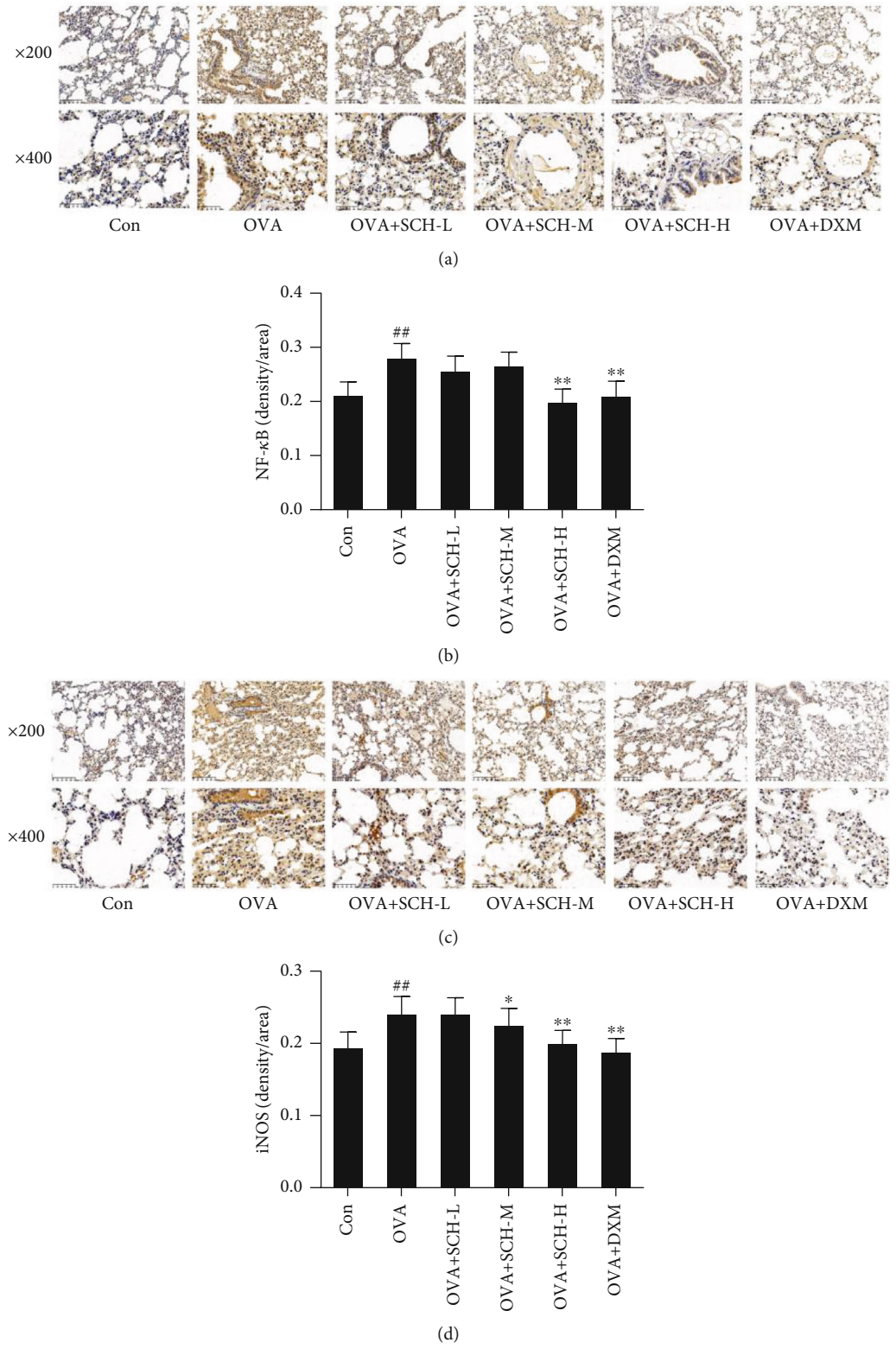

Figure 8: Effect of SCH on the levels of NF-κB and iNOS. (a and c) The levels of NF-κB and iNOS in lung tissues were detected using immunohistochemistry. (b and d) Quantification of the average density of NF-κB and iNOS. At ×200 magnification, scale bars represent 100 μm. At ×400 magnification, scale bars represent 50 μm. Data are presented as the means ± SD; $n = 6$. $^{\#\#}p < 0.01$ compared with the control group; $^{**}p < 0.01$ and $^{*}p < 0.05$ compared with the OVA group.

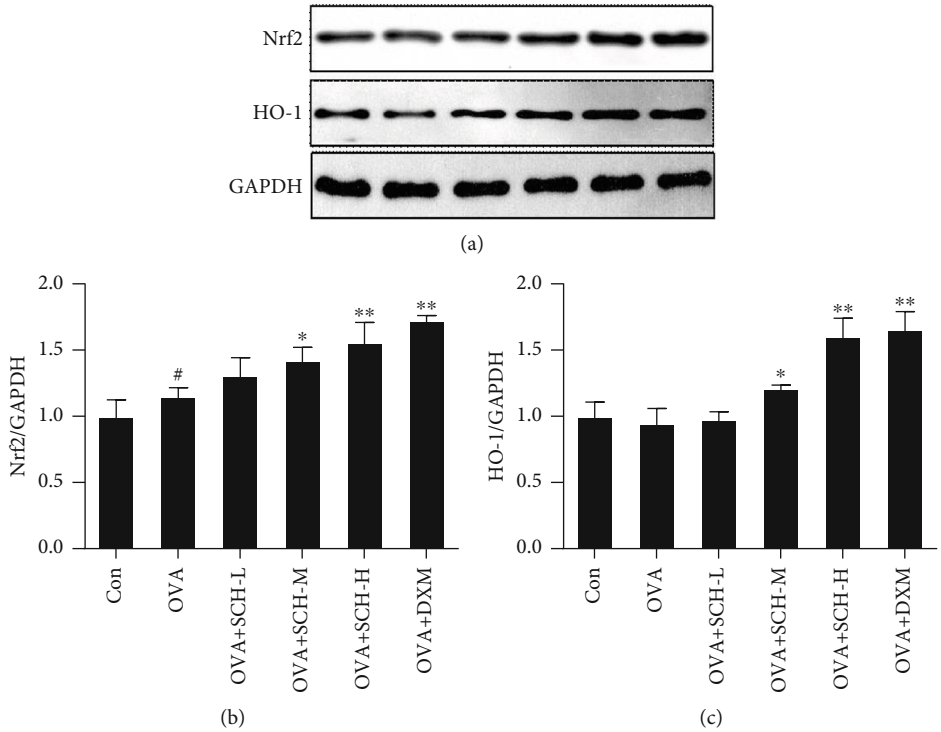

Figure 9: Effect of SCH on the activation of the Nrf2 pathway. (a) The expression of the HO-1 and Nrf2 proteins was analyzed using Western blotting. (b and c) Quantification of the relative density of HO-1 and Nrf2. Data are presented as the means ± SD; $n = 4$. $^{\#}p < 0.05$ compared with the control group; $^{**}p < 0.01$ and $^{*}p < 0.05$ compared with the OVA group.

3.3. SCH Reduces the Airway Levels of Inflammatory Factors. Levels of the inflammatory factors eotaxin, IL-13, IL-5, and IL-4 were assessed using ELISAs to investigate whether SCH regulated the OVA-induced airway inflammatory response. As anticipated, SCH administration significantly reduced the OVA-induced increases in the levels of eotaxin (Figure 3(a)), IL-13 (Figure 3(b)), IL-5 (Figure 3(c)), and IL-4 (Figure 3(d)), and the high dosage of SCH exerted an obvious effect.

3.4. SCH Reduces the Blood Level of OVA-Specific IgE. Next, OVA-induced asthmatic mice received a large dosage of SCH to determine whether the level of OVA-specific IgE was affected by SCH. As shown in Figure 4, the level of OVA-specific IgE was markedly higher in the asthmatic group than in the control group, while SCH reduced this level in a dose-dependent manner (Figure 4).

3.5. SCH Attenuates Histological Lung Injury. Lung tissues were collected from different groups of mice for a histopathological study. Consistent with the results for the inflammatory response, H&E staining of lung tissues clearly indicated a significantly increased quantity of inflammatory cells in the asthma model group, while the SCH treatment reduced inflammatory cell infiltration in a dose-dependent manner (Figure 5(a)). AB-PAS staining was conducted on lung sections to assess the beneficial effects of SCH on cell hyperplasia. SCH administration significantly alleviated the OVA-induced secretion of mucus by goblet cells, and high dose of SCH exerted a better effect (Figure 5(b)).

3.6. SCH Alleviates Oxidative Stress in the Lung. The expression of SOD, NO, ROS, MDA, CAT, and GSH-Px was detected to evaluate antioxidant activity in the lung. As shown in Figure 6(a), SOD levels were substantially decreased in the OVA group compared with the control group. In the OVA+SCH-M, OVA+SCH-H, and OVA +DXM groups, SOD levels were substantially increased compared with those in the OVA group. In contrast, the levels of ROS, NO, and MDA were substantially increased in the OVA group compared with the control group but greatly decreased in the OVA+SCH-M, OVA+SCH-H, and OVA+DXM groups compared with the OVA group (Figures 6(b)–6(d)). CAT and GSH-Px levels were substantially decreased by OVA-induced injury but noticeably increased by SCH and DXM compared with the OVA group (Figures 6(e) and 6(f)).

3.7. SCH Inhibits NF-κB Pathways. The effect on the NF-κB pathway was explored in this study to further determine the underlying mechanism by which SCH eases asthma. OVA-induced injury resulted in an increase in p-NF-κB and p-IKKα levels compared to the control group (Figures 7(b) and 7(c)). Intervention with DXM and SCH reversed these changes in NF-κB and IKKα phosphorylation. The phosphorylation of IκBα was also remarkably decreased in response to OVA-induced injury, and this decrease was reversed by SCH intervention (Figure 7(d)). IHC showed increased nuclear translocation of p65 and iNOS in the OVA+SCH-M, OVA+SCH-H, and OVA+DXM groups (Figures 8(b) and 8(d)).

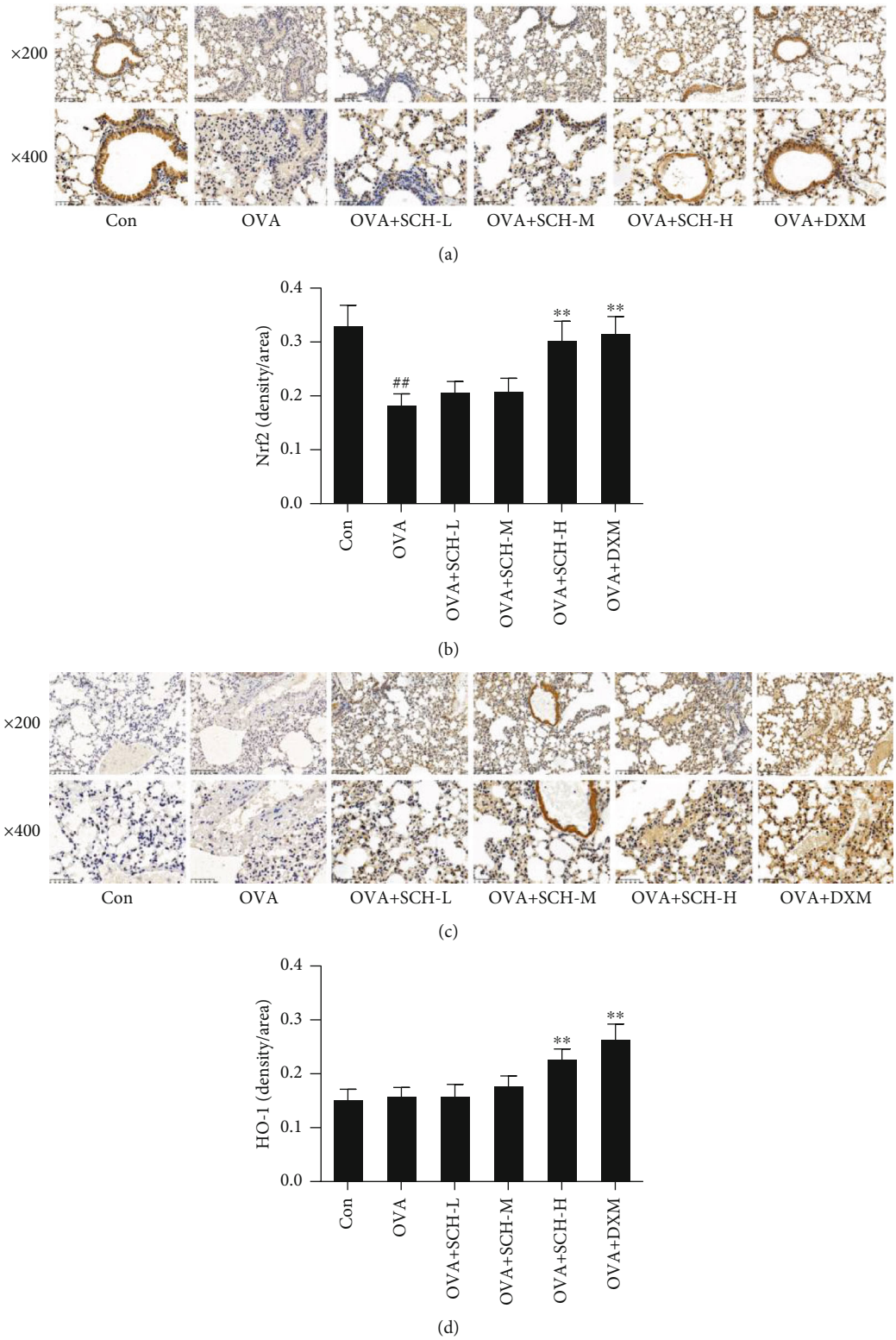

Figure 10: Effect of SCH on the expression of Nrf2 and HO-1. (a and c) The levels of Nrf2 and HO-1 were determined using IHC. (b and d) Quantification of the average density of Nrf2 and HO-1. Data are reported as the means ± SD; $n = 6$. $^{\#\#}p < 0.01$ compared with the control group; $^{**}p < 0.01$ compared with the OVA group.

3.8. SCH Activates Nrf2 Pathways. The OVA challenge decreased the expression of Nrf2, whereas this inhibitory effect was successfully reversed in the OVA+SCH-M, OVA+SCH-H, and OVA+DXM groups (Figures 9(a) and 9(b)). DXM and SCH treatments increased the expression of Nrf2 compared to animals with OVA-induced injury. Likewise,

the level of HO-1 was slightly increased in response to OVA application and additionally increased by SCH and DXM treatments (Figures 9(a) and 9(c)). These consequences were highly consistent with the outcome of IHC. OVA-induced injury remarkably increased the level of HO-1 compared to that in the controls, and an even larger increase was observed in animals treated with SCH and DXM (Figure 10).

4. Discussion

Asthma is a chronic and complicated airway inflammatory disease that simultaneously affects many people worldwide [5]. Asthma can cause severe morbidity and even mortality. More importantly, bronchodilators (such as β-agonists), steroids, and leukotriene inhibitors are the main treatment strategies for asthma. However, potential targeted mechanisms and interventions for asthma require further research [15]. Numerous studies have identified a critical role for the inflammatory response in the process of asthma, and asthma is always accompanied by airway inflammation, which is mainly characterized by inflammatory cell infiltration and increased mucus secretion [16–18].

In recent years, natural products and extracts from natural herbaceous plants have been investigated in the pharmaceutical industry due to their prominent biological activities, and herbal drugs have attracted increasing attention as effective treatments for many chronic diseases. For example, ripe hawthorn fruit provided better beneficial remediation of the cardiopulmonary circulation system due to its abundant proanthocyanidins and flavan-3-ol (-)-epicatechin levels correlated with (-)-epicatechin levels [19]. Meadowsweet likewise protects the digestive tract mucosa by reducing excess acidity and relieving nausea [20]. In the present study, SCH extracted from Schisandra appeared to contribute to ameliorating the airway inflammatory response in OVA-induced asthmatic mice, indicating its potential role in clinical asthma treatment.

The anti-inflammatory activity of extracts from natural herbaceous plants toward asthma has been widely studied. For example, forsythiaside A decreases allergic airway inflammation caused by OVA by activating the Nrf2 pathway [16]. Aloperine attenuates the inflammatory reaction in the asthmatic lung by decreasing inflammatory cell infiltration and preventing the accumulation of inflammatory factors in the airways [3], and SCH reduces allergic airway inflammation caused by OVA through the activation of the Nrf2 pathway [21]. In this study, we suggested the phylactic effect of SCH on an allergic airway inflammation model induced by OVA, which was mediated by its anti-inflammatory and antioxidant effect.

Asthma is characterized by the activation of Th2 cell activity, and the production of Th2-type cytokines results in the Th2-dominated immune response. IL-13, IL-5, and IL-4 are the primary cytokines released by Th2 cells. Therefore, increased levels of IL-13, IL-5, and IL-4 mediate the development of asthma [21]. The production of IgE is related to allergic reactions, such as allergic asthma. The production of allergen-specific IgE is mediated by activating the inflammatory response and mast cells [22]. In the present study, SCH specifically reduced the numbers of neutrophils, lymphocytes, macrophages, and eosinophils during allergic airway inflammation caused by OVA, accompanied by a decrease in the levels of proinflammatory factors, such as AHR and IgE, and lower expression of KC. These helpful effects of SCH are consistent with the results of the histopathological examination, indicating a decrease in airway inflammation and mucus production. All these results revealed the anti-asthmatic effects of SCH.

As the vital calibrator of cytobeneficial proteins, the transcription factor Nrf2 decreases AHR, airway inflammation, secretion of Th2 cytokines, and mucus teratogenesis [23]. Moreover, Nrf2 signaling is a key factor determining susceptibility to allergic asthma, and Nrf2 reduces the wheezing phenotypes of asthma model mice [8]. In addition, HO-1 effectively reduces the airway inflammatory reaction and the secretion of mucus in individuals with asthma [8]. The effect of SCH on the Nrf2 signaling pathway was detected to further study its protective mechanism. Based on our results, SCH reduced allergic airway inflammation caused by OVA by activating the Nrf2 pathway. Oxidative stress is a vital characteristic of the etiopathogenesis of asthma. ROS are mainly generated by neutrophil alkaline phosphatase [24]. Furthermore, ROS may cause DNA damage and lipid peroxidation. In contrast, GSH-Px is a crucial marker of oxidative stress that plays a vital role in maintaining the integrity of the epithelium. In the present study, SCH meaningfully restrained oxidative stress caused by OVA, which was verified by the reduced MDA content and increased CAT, GSH-Px, and SOD contents. All of these consequences indicate that SCH protects against OVA-induced asthma by eliminating inflammation and oxidation.

Activation of the NF-κB pathway in individuals with asthma effectively enhances inflammatory damage around the airway induced by antigens, which is an effective contributor to the adaptive immune response [25]. Specifically, when inflammatory cytokines generate activating effects, IκBα bound to NF-κB is rapidly phosphorylated by IκBα kinase, and then, p-IκBα is degraded by the proteasome. The independent dimer of NF-κB released by the degradation of IκBα is transported to the cell nucleus and causes the transcription of miscellaneous target genes encoding a variety of inflammatory factors, which is related to the etiopathogenesis of asthma [26]. In particular, the upregulation of iNOS, a downstream target of NF-κB, facilitates inflammation by increasing the generation of inflammatory transmitters, including inflammatory cytokines, chemokines, and oxidative stress-related factors [27]. The level of iNOS is increased in patients with asthma, along with the upregulation of NF-κB [28]. The production of iNOS during the development of asthma results in NO generation, which further exacerbates asthma lesions because NO represents a destructive factor related to oxidative stress [29]. Hence, inhibiting the NF-κB/iNOS pathway is considered an important treatment of asthma. According to our experimental data, SCH dramatically inhibited the expression of NF-κB and iNOS in asthmatic mice in a dose-dependent manner. Moreover, SCH inhibited the degradation of p-IκBα, which is essential for NF-κB activation, in a dose-dependent manner.

Our results suggested that SCH may alleviate allergic airway inflammation by inhibiting the NF-κB pathway, similar to a previous study [30].

Taken together, we found that SCH obviously reduced the infiltration of inflammatory cells in asthmatic mice. In terms of the mechanism, SCH alleviates asthma by promoting the production of Nrf2 and HO-1, while reducing the levels of NF-κB and IKKα and increasing the level of IκBα, indicating that SCH inhibits airway inflammation by restraining NF-κB but promoting the activation of the Nrf2 pathway. The present study will provide new strategies for the further clinical treatment of asthma.

Data Availability

All data generated or analyzed during this study are included in this article.

Conflicts of Interest

The authors declare that there are no financial and commercial conflicts of interest.

Authors' Contributions

Yaqin Chen and Yu Kong contributed to this work equally.

Acknowledgments

The work was supported by the National Natural Science Foundation of China (No. 81973905) and Construction Project of Inheritance Studio for Famous TCM Doctors (Jingmao Yu) in Zhejiang Province (No. GZS2020003).

References

[1] G. Jordakieva, J. Wallmann, R. Schmutz et al., "Peripheral erythrocytes decrease upon specific respiratory challenge with grass pollen allergen in sensitized mice and in human subjects," *PLoS One*, vol. 9, no. 1, article e86701, 2014.

[2] L. A. Bilaver, A. S. Chadha, P. Doshi, L. O'Dwyer, and R. S. Gupta, "Economic burden of food allergy: a systematic review," *Annals of Allergy, Asthma & Immunology*, vol. 122, no. 4, pp. 373–380.e1, 2019, e371.

[3] C. Wang, Y. H. Choi, Z. Xian, M. Zheng, H. Piao, and G. Yan, "Aloperine suppresses allergic airway inflammation through NF-κB, MAPK, and Nrf2/HO-1 signaling pathways in mice," *International Immunopharmacology*, vol. 65, pp. 571–579, 2018.

[4] B. D. Medoff, S. Y. Thomas, and A. D. Luster, "T cell trafficking in allergic asthma: the ins and outs," *Annual Review of Immunology*, vol. 26, no. 1, pp. 205–232, 2008.

[5] Q. Zhang, L. Wang, B. Chen, Q. Zhuo, C. Bao, and L. Lin, "Propofol inhibits NF-κB activation to ameliorate airway inflammation in ovalbumin (OVA)-induced allergic asthma mice," *International Immunopharmacology*, vol. 51, pp. 158–164, 2017.

[6] S. Gong, X. Ji, J. Su et al., "Yeast fermentate prebiotic ameliorates allergic asthma, associating with inhibiting inflammation and reducing oxidative stress level through suppressing autophagy," *Mediators of Inflammation*, vol. 2021, Article ID 4080935, 13 pages, 2021.

[7] P. Huang, S. Wei, W. Huang et al., "Hydrogen gas inhalation enhances alveolar macrophage phagocytosis in an ovalbumin-induced asthma model," *International Immunopharmacology*, vol. 74, p. 105646, 2019.

[8] T. E. Sussan, S. Gajghate, S. Chatterjee et al., "Nrf2 reduces allergic asthma in mice through enhanced airway epithelial cytoprotective function," *American Journal of Physiology. Lung Cellular and Molecular Physiology*, vol. 309, no. 1, pp. L27–L36, 2015.

[9] P. K. Leong, N. Chen, and K. M. Ko, "Mitochondrial decay in ageing: 'qi-invigorating' schisandrin B as a hormetic agent for mitigating age-related diseases," *Clinical and Experimental Pharmacology & Physiology*, vol. 39, no. 3, pp. 256–264, 2012.

[10] H. Bae, R. Kim, Y. Kim et al., "Effects of _Schisandra chinensis_ Baillon (Schizandraceae) on lipopolysaccharide induced lung inflammation in mice," *Journal of Ethnopharmacology*, vol. 142, no. 1, pp. 41–47, 2012.

[11] Q. Lin, X. Qin, M. Shi et al., "Schisandrin B inhibits LPS-induced inflammatory response in human umbilical vein endothelial cells by activating Nrf2," *International Immunopharmacology*, vol. 49, pp. 142–147, 2017.

[12] G. S. Zhang, R. R. Qiu, J. Pan et al., "Effect of moxibustion on respiratory function and cutaneous histamine and neuropeptide contents of "Feishu" (BL13) in asthmatic rats," *Zhen Ci Yan Jiu*, vol. 45, no. 2, pp. 117–121, 2020.

[13] X. Yang, Y. Li, Y. He et al., "Cordycepin alleviates airway hyperreactivity in a murine model of asthma by attenuating the inflammatory process," *International Immunopharmacology*, vol. 26, no. 2, pp. 401–408, 2015.

[14] W. C. Lenox and C. A. Hirshman, "Amrinone attenuates airway constriction during halothane anesthesia," *Anesthesiology*, vol. 79, no. 4, pp. 789–794, 1993.

[15] M. Chen, Z. Lv, W. Zhang et al., "Triptolide suppresses airway goblet cell hyperplasia and Muc5ac expression _via_ NF-κB in a murine model of asthma," *Molecular Immunology*, vol. 64, no. 1, pp. 99–105, 2015.

[16] J. Qian, X. Ma, Y. Xun, and L. Pan, "Protective effect of forsythiaside A on OVA-induced asthma in mice," *European Journal of Pharmacology*, vol. 812, pp. 250–255, 2017.

[17] J. V. Cerqueira, C. S. Meira, E. S. Santos et al., "Anti-inflammatory activity of SintMed65, an _N_ -acylhydrazone derivative, in a mouse model of allergic airway inflammation," *International Immunopharmacology*, vol. 75, p. 105735, 2019.

[18] A. Cardenas, J. E. Sordillo, S. L. Rifas-Shiman et al., "The nasal methylome as a biomarker of asthma and airway inflammation in children," *Nature Communications*, vol. 10, no. 1, p. 3095, 2019.

[19] E. Haslam, "Natural polyphenols (vegetable tannins) as drugs: possible modes of action," *Journal of Natural Products*, vol. 59, no. 2, pp. 205–215, 1996.

[20] M. Rohner Machler, T. M. Glaus, and C. E. Reusch, "Life threatening intestinal bleeding in a Bearded Collie associated with a food supplement for horses," *Schweizer Archiv für Tierheilkunde*, vol. 146, no. 10, pp. 479–482, 2004.

[21] P. Ye, X. L. Yang, X. Chen, and C. Shi, "Hyperoside attenuates OVA-induced allergic airway inflammation by activating Nrf2," *International Immunopharmacology*, vol. 44, pp. 168–173, 2017.

[22] A. O. Antwi, D. D. Obiri, and N. Osafo, "Stigmasterol modulates allergic airway inflammation in guinea pig model of

ovalbumin-induced asthma," *Mediators of Inflammation*, vol. 2017, Article ID 2953930, 11 pages, 2017.

[23] T. Rangasamy, J. Guo, W. A. Mitzner et al., "Disruption of Nrf2 enhances susceptibility to severe airway inflammation and asthma in mice," *The Journal of Experimental Medicine*, vol. 202, no. 1, pp. 47–59, 2005.

[24] H. N. Li, W. Li, J. Yang, C. Y. Zhang, and H. Y. Wu, "Effects of neutrophils alkaline phosphatase on functions of neutrophils in vitro," *Zhonghua Xue Ye Xue Za Zhi*, vol. 37, no. 5, pp. 405–411, 2016.

[25] J. Duan, J. Kang, W. Qin et al., "Exposure to formaldehyde and diisononyl phthalate exacerbate neuroinflammation through NF-κB activation in a mouse asthma model," *Ecotoxicology and Environmental Safety*, vol. 163, pp. 356–364, 2018.

[26] W. Huang, M. L. Li, M. Y. Xia, and J. Y. Shao, "Fisetin-treatment alleviates airway inflammation through inhbition of MyD88/NF-κB signaling pathway," *International Journal of Molecular Medicine*, vol. 42, no. 1, pp. 208–218, 2018.

[27] J. L. Lowry, V. Brovkovych, Y. Zhang, and R. A. Skidgel, "Endothelial nitric-oxide synthase activation generates an inducible nitric-oxide synthase-like output of nitric oxide in inflamed endothelium," *The Journal of Biological Chemistry*, vol. 288, no. 6, pp. 4174–4193, 2013.

[28] M. C. de Andres, A. Takahashi, and R. O. Oreffo, "Demethylation of an NF-κB enhancer element orchestrates _iNOS_ induction in osteoarthritis and is associated with altered chondrocyte cell cycle," *Osteoarthritis and Cartilage*, vol. 24, no. 11, pp. 1951–1960, 2016.

[29] J. C. Lim, F. Y. Goh, S. R. Sagineedu et al., "A semisynthetic diterpenoid lactone inhibits NF-κB signalling to ameliorate inflammation and airway hyperresponsiveness in a mouse asthma model," *Toxicology and Applied Pharmacology*, vol. 302, pp. 10–22, 2016.

[30] J. Hou, M. Hu, L. Zhang, Y. Gao, L. Ma, and Q. Xu, "Dietary taxifolin protects against dextran sulfate sodium-induced colitis via NF-kappaB signaling, enhancing intestinal barrier and modulating gut microbiota," *Frontiers in Immunology*, vol. 11, p. 631809, 2020.

Hindawi
Journal of Immunology Research
Volume 2021, Article ID 9920416, 18 pages
https://doi.org/10.1155/2021/9920416

Review Article

Natural Formulations: Novel Viewpoint for Scleroderma Adjunct Treatment

Shirin Assar,[1] **Hosna Khazaei**,[2] **Maryam Naseri**,[2] **Fardous El-Senduny**,[3] **Saeideh Momtaz**,[4,5,6] **Mohammad Hosein Farzaei**,[2] **and Javier Echeverría**[7]

[1]*Clinical Research Development Center, Imam Reza Hospital, Kermanshah University of Medical Sciences, Kermanshah, Iran*
[2]*Pharmaceutical Sciences Research Center, Health Institute, Kermanshah University of Medical Sciences, Kermanshah 6734667149, Iran*
[3]*Biochemistry Division, Chemistry Department, Faculty of Science, Mansoura University, Mansoura 35516, Egypt*
[4]*Medicinal Plants Research Center, Institute of Medicinal Plants, ACECR, Karaj, Iran*
[5]*Toxicology and Diseases Group (TDG), Pharmaceutical Sciences Research Center (PSRC), The Institute of Pharmaceutical Sciences (TIPS), and Department of Toxicology and Pharmacology, School of Pharmacy, Tehran University of Medical Sciences, Tehran 1417614411, Iran*
[6]*Gastrointestinal Pharmacology Interest Group (GPIG), Universal Scientific Education and Research Network (USERN), Tehran, Iran*
[7]*Departamento de Ciencias del Ambiente, Facultad de Química y Biología, Universidad de Santiago de Chile, Santiago, Chile*

Correspondence should be addressed to Mohammad Hosein Farzaei; mh.farzaei@gmail.com

Received 29 March 2021; Revised 27 May 2021; Accepted 8 June 2021; Published 25 June 2021

Academic Editor: Kai Wang

Background. Scleroderma is a complex disease involving autoimmune, vascular, and connective tissues, with unknown etiology that can progress through any organ systems. *Objective*. Yet, no cure is available; the thorough treatment of scleroderma and current treatments are based on controlling inflammation. Nowadays, medicinal plants/natural-based formulations are emerging as important regulators of many diseases, including autoimmune diseases. Here, we provided an overview of scleroderma, also focused on recent studies on medicinal plants/natural-based formulations that are beneficial in scleroderma treatment/prevention. *Methods*. This study is the result of a search in PubMed, Scopus, and Cochrane Library with "scleroderma", "systemic sclerosis", "plant", "herb", and "phytochemical" keywords. Finally, 22 articles were selected from a total of 1513 results entered in this study. *Results*. Natural products can modulate the inflammatory and/or oxidative mediators, regulate the production or function of the immune cells, and control the collagen synthesis, thereby attenuating the experimental and clinical manifestation of the disease. *Conclusion*. Natural compounds can be considered an adjunct treatment for scleroderma to improve the quality of life of patients suffering from this disease.

1. Introduction

Within the human body, the immune system is considered one of the most complex biological systems [1], playing a fundamental role in protecting the body against detrimental effects of microbial pathogens and malignant tumor by various mechanisms such as engulfing, modulating, and moderating [2–4]. As a result, infectious diseases are prevented, and tissue or organ damages are abrogated. Aberrant immune responses may lead to autoimmune diseases [5] and destroy body cells [6]. Up to date, a broad range of chemical medications with well-known side effects are prescribed to manage the immune responses in immune pathology associated with infections, graft versus host disease, and hypersensitivity immune reactions (immediate or delayed-type) and especially for the treatment of autoimmune diseases [7]. Besides that, plant species with a broad spectrum of phytochemicals, fewer side effects, better compatibility, greater accuracy, low cost, and easy availability are frequently used to manage a wide range of diseases [8, 9]. Herbal formulations and their

bioactive metabolites were found effective to mediate the proper functionality of the immune system through both immunosuppressive and immunomodulatory activities [2, 10–12], making them remarkable candidates for the treatment of immune-mediated disorders including autoimmune diseases and organ transplant rejection [13]. It was reported that several pure bioactive compounds of *Ganoderma lucidum* (Curt.: Fr.) P. Karst. (Aphyllophoromycetideae), *Panax ginseng* C.A. Mey. (Araliaceae), and *Zingiber officinale* Roscoe (Zingiberaceae) possessed immune cell-stimulating activity [3]. The immunosuppressive properties of isogarcinol, a natural compound from *Garcinia mangostana* L. (Clusiaceae), could serve as a new oral immunomodulatory drug for preventing transplant rejection and for long-term medication in autoimmune diseases [14]. It was proposed that herbal immune-stimulator compounds were able to modulate the innate immune response in fish and shellfish diseases [9]. The significant effect of *Salvia miltiorrhiza* Bunge (Lamiaceae) on the reduction of the inflammatory cytokines and mediators was proven against acute graft rejection and autoimmunity diseases [13]. This review tries to highlight the efficacy of medicinal plants on scleroderma treatment. Besides, we provided a brief introduction to autoimmune diseases and beneficial herbal plants for the treatment of such disorders.

1.1. Autoimmune Diseases. Although autoimmune diseases are rare, approximately 7.6–9.4% of the world population is affected by autoimmune inflammatory diseases. However, the incidence and prevalence of various autoimmune diseases are rising in women [6]. In addition to being a cause of mortality all around the world, autoimmune diseases are accompanied by severe chronic morbidity in patients' life including pain, inflammation, and tissue damage [15, 16]. Intense lifestyle and constant medical services for patients with autoimmune diseases are a huge burden for public health and the economy [17]. The description of autoimmune diseases requires a brief explanation of the immune system.

1.2. Current Treatment for Autoimmune Disease. Traditional medications for autoimmune inflammatory diseases include nonsteroidal anti-inflammatory drugs (NSAIDs), glucocorticoids, and disease-modifying antirheumatic drugs (DMARDs). NSAIDs are often prescribed for the treatment of arthritis and headaches because they possess analgesic, antipyretic, and anti-inflammatory effects [18] and can reduce pain through blocking cyclooxygenase (COX) enzymes [19]. NSAIDs are including traditional nonselective NSAIDs and selective COX-2 inhibitors [20]. Despite the diversity in their chemical structures, NSAIDs can inhibit autoimmune inflammatory responses [18]; however, they suffer from adverse effects (i.e., on the cardiovascular system) [21, 22]. Glucocorticoids such as prednisone/prednisolone, methylprednisolone, and fluorinated glucocorticoids such as dexamethasone and betamethasone are more frequently used for the treatment of severe rheumatoid arthritis since 1940 [23–25]. Glucocorticoids suppress cellular signaling pathways such as activator protein 1 (AP-1) and nuclear factor kappa-light-chain-enhancer of activated B cells (NF-κB), as they can bind to specific receptors, and ultimately regulate the expression of cytokines and chemokines [26]. Furthermore, it has been reported that glucocorticoids can inhibit the proliferation of effector T cells [27]. Despite the high efficiency of glucocorticoids in the treatment of chronic diseases, their undesirable effects including gastrointestinal ulcers and bleeding, infection, immunosuppression, and bone damage are undeniable [28]. To alleviate inflammation in autoimmune diseases, several medications with diverse chemical structures were developed as DMARDs, which include methotrexate, leflunomide, gold compounds, sulfasalazine, azathioprine, cyclophosphamide, antimalarials, D-penicillamine, and cyclosporine [29]. Antitumor necrosis factor (anti-TNF) biologics or combination therapy of conventional disease-modifying antirheumatic drugs (cDMARDs) [16, 30], corticosteroids, anticytokine therapies, physical therapy, inhibition of intracellular signaling pathways, costimulation inhibition, biological inhibitors of T cells, B cell energy and depletion, regulatory T cells, and stem cell transplantation are other current treatments for patients with autoimmune diseases [31]. Considering their adverse effects, the introduction of novel strategies with fewer or no life-threatening adverse effects and lower toxicity with high efficacy seems essential [5]. To this notion, two different approaches were assumed: behavioral modification, which is an impact factor to suppress the onset of some autoimmune diseases or reduce their frequency, and the discovery of new drugs to inhibit the autoimmune diseases at early stages, rather than just controlling the symptoms [15]. Thus, usage of plant origin active substances in human diet might be an effective approach to regulate immune diseases and to maintain the body health [4].

1.3. Scleroderma. Scleroderma is an autoimmune disease. The name comes from SCLERO (hardness) and DERMA (skin). Scleroderma is characterized by typical changes in the skin (becomes hard locally or all over the body) and may affect visceral organs including kidneys, lung, heart, gastrointestinal tract, and skeletal muscles. It involves the accumulation of collagen leading to skin fibrosis. It can be classified into local or systemic (affects not only the skin but also other organs such as the lung) [32]. In the North American population, around 443 cases/10^6 are diagnosed with scleroderma [33]. The prevalence, incidence, and clinical features of the disease change per the geographic place, where the severity and complication of scleroderma were higher in African-Americans in comparison with Caucasians due to the difference in the autoantibodies that were detected [34–39]. An Asian-Indian study demonstrated that the disease is more prevalent in younger ages [39]. Women are more susceptible to scleroderma than men (in the range of 3 : 1 to 14 : 1), indicating probable involvement of sex hormones (i.e., estrogen) in the development of scleroderma [40]. Estrogen has been found to regulate the extracellular matrix (ECM) components and the cell adhesion molecules in fibrosis [41, 42]. Considering the speed of progression, severity of skin hardening, and involvement of visceral organs, there are two main subdivisions of systemic sclerosis: limited cutaneous (lc-SSc)

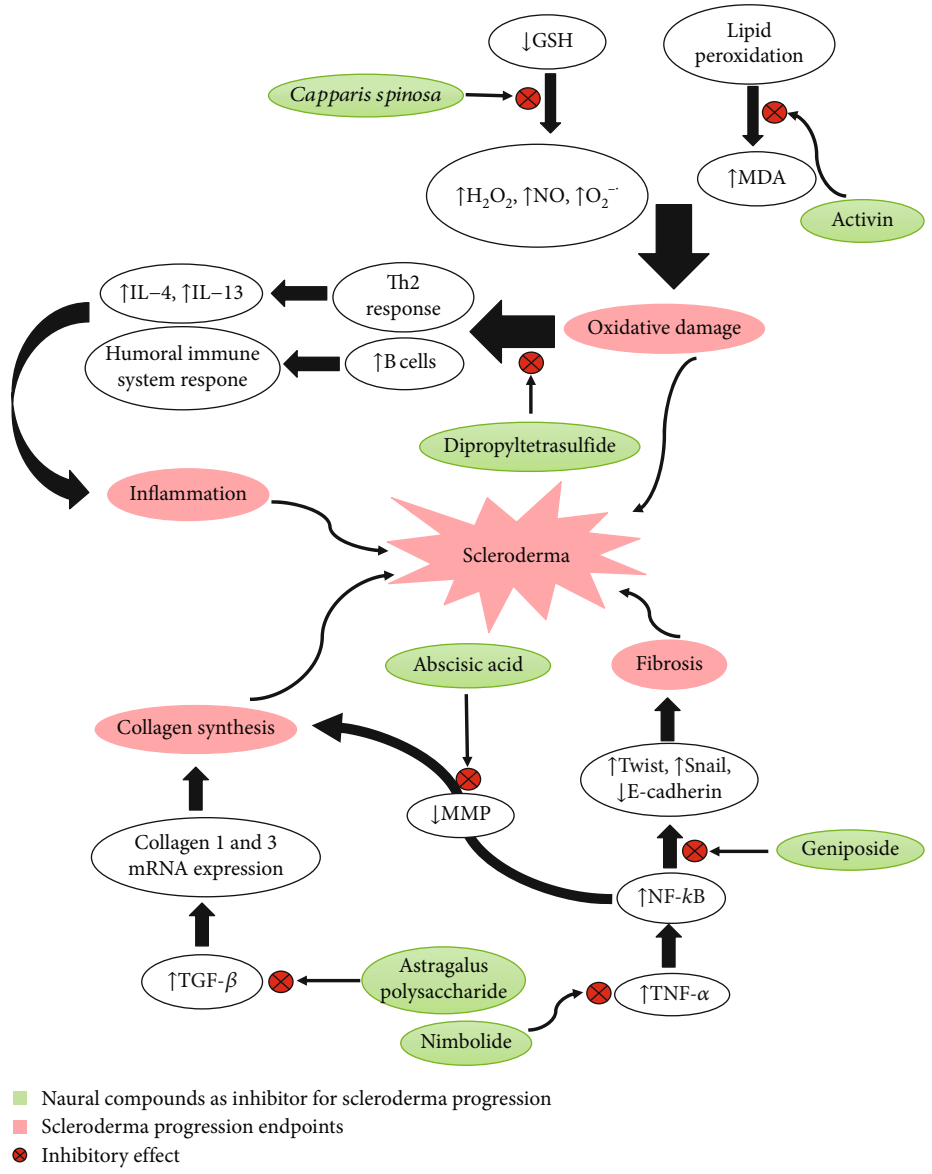

Figure 1: Pathogenesis of scleroderma; some natural compounds can inhibit its progression.

and diffuse cutaneous (dc-SSc). In lc-SSc, the fibrosis is limited to the arms, hands, and face, whereas in dc-SSc, the fibrosis could reach the heart, lung, and kidney [43, 44].

1.4. Pathogenesis of Scleroderma. Different factors have been reported to play roles in scleroderma onset or progression, in which alterations in the immune components, exposure to toxins, genetic mutations, and oxidative stress are the most important participants (Figure 1).

1.5. Immune System and Scleroderma. B cells produce autoantibodies against different cellular organs such as anti-centromere, anti-topoisomerase-1, and anti-RNA polymerase III, which may progress skin fibrosis and tighten. The interplay between major histocompatibility complex (MHC) in dendritic cells and T cell receptors leads to the expression of anti-inflammatory cytokines (interleukins 4 and 13 (IL-4 and IL-13)) and the activation of B cells to secrete vascular epidermal growth factor (VEGF) [45]. Patients with scleroderma were shown to have higher levels of rheumatoid factors (RF), cryoglobulins, and γ-globulin autoantibodies [46]. Upregulation of coreceptor cluster of differentiation-19 (CD19), CD21, CD86, and CD95 on memory B cells elevates the autoantibody production against endothelial and fibroblast cells. The binding of endothelial and fibroblast autoantibodies with their antigen induces the production of reactive oxygen species (ROS) and apoptosis [47, 48]. The most dominant type of T cells is $CD4^+$ type over $CD8^+$ one [49]. The T cell receptor type is $\gamma{:}\delta$ showing $V\delta1$ chains [50]. The skin is composed of three layers: the outermost layer of skin is called the epidermis, the layer beneath it is called the dermis, and the deeper layer is called subcutaneous or hypodermis. The infiltration of T cell subsets is different between the layers of the skin. The avian model of systemic

sclerosis showed infiltration of the γ:δ T cell, while the dermis and subcutaneous were infiltrated with the other subtypes of T cells (α:β T cell) [51]. Infiltration of $CD14^+$ monocytes/macrophages was detected in early diagnosed patients with systemic sclerosis [52]. In addition to that, the degranulated mast cells increased in scleroderma patients at early stages [53]. The imbalance in the level of cytokines has been implicated with the pathogenesis of scleroderma. Higher levels of the inflammatory cytokines such as interferon gamma (INF-γ), colony-stimulating factors (CSF), IL-1, IL-4, IL-17A, IL-6, IL-13, IL-12 [54], IL-23 [55], IL-27 [56], transforming growth factor beta 1 (TGF-β1), T helper 2 (Th2) cytokine, and the chemotaxis monocyte chemoattractant protein 1 (MCP-1) were detected in scleroderma patients. An increase of Th2 cytokines leads to collagen synthesis, differentiation of fibroblasts to myofibroblast phenotype, and production of TGF-β, inducing the ECM remodeling [57]. Additionally, the infiltration of $CD8^+$ and $CD4^+$ T cells, activated macrophages, and human leukocyte antigen-DR isotype (HLA-DR) has been manifested in scleroderma patients [58]. Usually, this infiltration is observed in the early stages of the disease, which are diminished later. However, some patients with a longstanding history of the disease showed infiltration of immune cells in skin lesions. Most of these cytokines are associated with fibrosis of the skin and lung as well as with a higher level of autoantibody production against topoisomerase I [58].

1.6. Signaling Pathways in Scleroderma

1.6.1. Platelet-Derived Growth Factor Pathway. The predominant manifestation of scleroderma is associated with dysregulation of the immune system, cytokine production, and production of collagen and its deposition. The growth and proliferation of connective tissue cells are regulated by the level of growth factors such as platelet-derived growth factor (PDGF) and its receptor (PDGFR). The binding of PDGF with its receptor induces the expression of extracellular matrix components such as collagen [59, 60]. Immunostaining of skin biopsy from scleroderma patients showed that there is a high level of PDGF-beta receptor in their skin [59]. This was correlated with a previous finding for the higher serum level of β-thromboglobulin. It has been reported that β-thromboglobulin is colocalized with PDGF in the granules of platelets, which may contribute to the higher level of PDGF in scleroderma patients [60–62]. An early pathological alteration in the scleroderma is vascular damage, where the function of endothelial cells and the ultrastructure of microvessels are altered [48, 63].

1.6.2. Transforming Growth Factor Pathway. TGF-β is a key regulator for the signaling pathway that secrete the components of the extracellular matrix. The correlation between the severity of the scleroderma and the level of TGF-β is controversial. A low level of TGF-β1 was detected at the early stages of scleroderma; however, higher levels of TGF-β1 are responsible for the disease prognosis [64, 65]. Moreover, Wakhlu et al. correlated interstitial lung fibrosis with an elevated level of TGF-β1 and other cytokines [58]. Upon binding of TGF-β1 to its receptor, the intracellular cytoplasmic Smad3 is phosphorylated and translocated to the nucleus, leading to the transcriptional activation of genes involved in ECM remodeling [66]. It was reported that fibroblasts derived from systemic sclerosis contain a high level of pSmad3 and more DNA-binding affinity [67, 68]. Targeting the TGF-β1 signaling may provide a reliable therapeutic approach for the treatment of skin fibrosis in scleroderma patients. It was shown that inhibition of TGF-β1 by Repsox attenuated skin fibrosis *in vitro* and *in vivo* (bleomycin-treated mice) through downregulation of the connective tissue growth factor [68].

1.6.3. NOTCH Pathway. The NOTCH proteins are required for cell proliferation, fate, differentiation, and death. NOTCH is a unique pathway, since both the ligand and the receptor are transmembrane molecules (called juxtacrine). The ligands for the NOTCH receptor (signal-receiving cell) are expressed on neighboring cells (signal-emitting cell) and known as Delta (called Delta-like in humans) and Serrate (called jagged in humans) [69]. The binding of the ligand with the extracellular domain of NOTCH leads to the activation of endocytosis by signal-emitting cells causing the proteolytic cleavage of the extraocular domain by the α-secretase enzyme (called 1^{st} cleavage). After that, a second cleavage occurs in the intracellular domain by γ-secretase to release the NOTCH intracellular domain (NICD). NICD then is translocated to the nucleus to release transcriptional repressors and to activate the gene transcription [70, 71]. There is evidence that NOTCH proteins are involved in the regulation of fibrosis and physiology and function of the vascular system [72, 73]. The polymorphism in *NOTCH4* (rs443198 and rs9296015) gene has been associated with systemic sclerosis [74]. Moreover, a missense mutation in the *NOTCH4* gene (chromosome 6p21 locus, c.4245G > A: p.Met1415Ile) was identified by a family-based whole exosome sequencing study and was linked to the pathogenesis and development of systemic sclerosis in this family [75, 76]. Strong immunostaining of NICD and overexpression of the HES-1 gene were detected in dermal fibroblasts of systemic sclerosis patients. Additionally, infiltrated lesions in the same skin biopsies represented a selective staining pattern against the ligand jagged canonical notch ligand 1 (JAG1) on T cells. This may indicate the possible interaction between T cells and the dermal fibroblasts, which leads to the overexpression of type 1 collagen and differentiation of fibroblast into myofibroblast (higher level of alpha-smooth muscle actin (α-SMA)) [77, 78]. Targeting the NOTCH pathway could be a valuable therapy for systemic and local sclerosis.

1.6.4. JAK/Signal Transducer Activator of Transcription. Janus kinases (JAKs) are known as nonreceptor tyrosine kinases. They play a key role in the response to cytokines (such as IL-6) and growth factors. Upon binding of IL-6 to its receptor, JAK becomes activated and phosphorylates the cytoplasmic domain of the IL-6R at tyrosine residues. Signal transducer activator of transcription (STAT) is recruited at the phosphorylated tyrosine residue and dimerized upon

phosphorylation. The dimer of STAT is translocated to the nucleus for activation of gene transcription [79]. Although dermal fibroblasts do not express IL-6R, a high level of soluble IL-6R can interact with IL-6, allowing the complex to bind to the fibroblast surface via glycoprotein 130 (gp-130) protein. Such binding activates the downstream STAT3 proteins and allows fibroblasts to differentiate to myofibroblasts, thus increasing the expression of type 1 collagen [66]. It was stated that the expression of STAT4 (rs7574685) changes in pulmonary fibrosis [74, 76]. Moreover, the knockdown of STAT4 protected the bleomycin-injected mice from the development of systemic sclerosis via reducing the T cell infiltration and the cytokine levels of tumor necrosis factor-alpha (TNF-α), IL-6, IL-2, and INF-γ [80]. Targeting IL-6 in systemic sclerosis patients showed moderate clinical improvement, while selective targeting of its downstream kinases such as JAK could be a potential therapeutic approach [81, 82]. A recent finding by Wang et al. revealed that JAK1 and 3 and selective inhibitor tofacitinib [83] were able to inhibit skin and lung fibrosis in bleomycin-treated and noninflammatory fibrosis (tight skin 1 (TSK-1)) mouse model [84].

1.6.5. Akt/PI3K/mTOR/HIF-1α Pathway. Akt or protein kinase B is involved in metabolism, proliferation, and cell survival. It is activated by insulin and growth factors via the activation of phosphoinositide-3-kinase (PI3K). The activation of Akt/PI3K leads to the activation of mammalian target of rapamycin (mTOR), which further increases the synthesis of proteins such as hypoxia-inducing factor-1α (HIF-1α) [85]. In normoxia, there is a low level of HIF-1α within cells, while it is rapidly degraded after translation. On the other hand, in hypoxic conditions, HIF-1α is activated. HIF-1α plays the main role in response to a hypoxic condition, resulting in ECM remodeling, and cytokine and growth factor secretions [86]. The skin of naïve scleroderma patients showed a high level of HIF-1α associated with the overexpression of VEGF [87].

1.6.6. Mitogen-Activated Protein Kinase (MAPK) Pathway. The Ras/Raf/MEK/ERK pathway transfers the extracellular signal to the nucleus via a tyrosine kinase receptor. The output signal depends on the cell type [88]. Chen et al. revealed that in systemic sclerosis patients constitutive ERK is activated, which is characterized by the overexpression of profibrotic genes (CGGF) and syndecan 2 and 4 (heparan sulfate proteoglycans) [89]. The constitutive ERK activation was reported in lung fibroblast, and its inhibition by PD98059 reduced collagen production [90].

1.7. Extracellular Matrix and Scleroderma. The cells connect with each other from the same type (homophilic interaction) or with different cell types (heterophilic interaction). The interaction is controlled by different cell adhesion molecules (CAMs) such as the immunoglobulin-like superfamily, integrins, cadherin, and selectins. The trafficking of lymphocytes and immune cells in general is regulated by the extracellular matrix components [91]. In systemic sclerosis patients, the level of surface CAMs is reduced in comparison with an elevated level of soluble forms (circulating) such as the intercellular adhesion molecule 1 (ICAM-1), endothelial leukocyte adhesion molecule 1 (ELAM-1), vascular cell adhesion molecule 1 (VCAM-l), P-selectin, and E-selectin [92–94]. The higher level of CAMs and expression of procollagen led to fibrosis in systemic scleroderma patients (90.9%) [95], indicating the key role of CAMs in the induction of inflammation and infiltration of immune cells at the skin and internal organs.

1.8. Fibroblast and Scleroderma. Within the body, fibroblasts are the main producer of collagen. Fibroblasts are activated upon engagement with endothelial cells and the infiltrated immune cells. It has been reported that activated fibroblasts produce type I and II collagens in the microvasculature and the perivascular [96]. *In vitro* studies exhibited that fibroblasts from systemic sclerosis patients express high levels of α-SMA and CAMs ($\alpha v\beta 3$ and $\alpha v\beta 5$ integrin) that leads to sustained activation of the TGF-β pathway [97], as well as proinflammatory and chemotaxis cytokines such as IL-6, TNF-α, IL-1α, IL-1β, and MCP-1 [98–100]. Additionally, these fibroblasts resist Fas-mediated apoptosis [101]. Later, Samuel et al. showed that this apoptosis resistance might be due to a deficiency in acid sphingomyelinase [102]. Based on this information, activated fibroblasts are potential targets for treatment or attenuation of the complications of scleroderma.

1.9. Oxidative Stress and Scleroderma. Oxidative stress is a term used when there is an imbalance between antioxidants and reactive oxygen and nitrogen. Reactive oxygen species (ROS) include superoxide anion ($O_2^{\cdot}$), hydrogen peroxide (H_2O_2), and hydroxyl radicals ($^{\cdot}OH$). Reactive nitrogen species (RNOS) include nitric oxide ($^{\cdot}NO$) and peroxynitrite ($ONOO^{-}$). In addition to that, the hypochlorous acid (HOCl) is produced by neutrophil by the action of myeloperoxidase [103, 104]. When the level of ROS, RNOS, and HOCl is higher than the capacity of the antioxidant system in the cells, oxidative stress happens. Oxidative stress attacks different cellular targets including lipids, proteins, DNA, and other biomolecules. There are enzymatic and nonenzymatic antioxidants that scavenge the radicals and inhibit cellular damage. Enzymatic antioxidants include superoxide dismutase, glutathione peroxidase, GSSG (oxidized glutathione) reductase, glutathione-*S*-transferase, and catalase. Nonenzymatic antioxidants include α-tocopherol and carotenoids [105]. Antioxidants quench free radicals and prevent deleterious damage to cellular molecules.

The link between oxidative stress and the pathogenesis of scleroderma was explained by Murrell for the first time [106]. It has been reported that ROS can activate the secretion of proinflammatory and profibrotic cytokines such as PDGF and TGF-β. In turn, these cytokines induce fibroblast differentiation into myofibroblasts, enhance the expression of type I collagen, and cause vascular damage [107–109]. Increased ROS in the serum of systemic sclerosis patients with pulmonary arterial hypertension could induce collagen type I promoter in vascular smooth muscle cells [110]. Application of mesenchymal stem cells overexpressing thioredoxin-1

restored skin morphology, endothelial cell function, and tubular formation in a bleomycin-induced mouse model via reduction of oxidative damage and inhibition of TGF-β and hypoxia-inducing apoptosis [111]. The administration of N-acetyl-L-cysteine (NAC) *in vitro* showed promising results in alleviating the symptoms of systemic sclerosis and idiopathic pulmonary fibrosis by removal of superoxide anions and peroxynitrite [112–115]. ROS was found to maintain the phosphorylated form of PDGFR and ERK via the inhibition of protein tyrosine phosphatase 1B (PTP1B) phosphatase activity through oxidation of cystine residue at the active site [116]. Probable benefits of antioxidants should be considered in systemic sclerosis treatment.

1.10. Apoptosis and Scleroderma. As mentioned, apoptosis is highly regulated by different genes such as Fas. Pathogenesis of scleroderma is somehow correlated with dysregulation in the apoptosis process. High percentages of apoptotic endothelial cells were found in the dermis of systemic sclerosis patients and local cutaneous sclerosis biopsies. An excessive level of antiendothelial cell antibodies (AECA) was detected in these cells, a piece of evidence that indicated apoptosis may be involved in the development of scleroderma [117]. In another study, bleomycin induced scleroderma via the overexpression of Fas and Fas ligand and by subsequent activation of caspase 3 and apoptosis in a mouse model [118]. The $CD8^+$ T cell apoptotic rate was higher than that of $CD4^+$ T cells in the systemic sclerosis patients due to a low level of NF-κB transcription factor and increase of $CD4^+$:$CD8^+$ T cells [119].

1.11. MicroRNA and Scleroderma. MicroRNAs (miRNAs) are noncoding RNAs 15-22 nucleotides in length. They bind to the 3′-untranslated region of mRNA (3′-UTR), leading to repression of protein translation [120]. Under certain conditions, miRNAs can activate gene expression [121]. It has been reported that miRNAs shuttle between cellular compartments and can be excreted to the extracellular matrix [122]. miRNAs play an important role in animal development, and their dysregulations have been reported in different diseases [123, 124]. Alteration in the miRNA level is correlated with the pathogenesis of scleroderma [125]. Honda et al. showed that dermal fibroblasts express a low level of miR-196a, which leads to the overexpression of type I collagen [126], and this downregulation was mediated via the TGF-β pathway [126]. Furthermore, downregulation of let-7a miRNA induced fibrosis by excessive production of type 1 collagen [127]. The serum level and dermal fibroblast level of miR-92a were found to be high in systemic sclerosis patients, leading to downregulation of metalloprotease-1 and collagen accumulation [128]. Suppression of miR-150 was correlated with the clinical manifestation of systemic sclerosis patients. A low level of miR-150 led to the overexpression of β3 integrin, Smad3 phosphorylation, and upregulation of type 1 collagen [129]. Recent work by Nakayama et al. revealed that a balance between miR-4458 and miR-18a is required for collagen synthesis downregulation. Both miR-4458 and miR-18a are downstream targets of IL-23 cytokine [130]. This may indicate the potential use of anti-IL-23 in scleroderma treatment.

2. Methods

2.1. Search Strategy. Data were collected by searching databases including PubMed, Scopus, and Cochrane Library, using search terms as "scleroderma" OR "systemic sclerosis" keywords in the title/abstract and "plant" OR "herb" OR "herbal preparation" OR "phytochemicals" keywords in the whole text. Search results were entered into the study regardless of time limitation; however, the final papers used in the study were from 1964 to 2020. Two researchers separately assessed the studies, and non-English, review, and duplicate articles were excluded from the study (Figure 2).

3. Results

From a total of 1513 studies, 390 studies were deleted based on their title and abstract, 538 studies were excluded due to duplication, and 460 reviews and 97 non-English studies were omitted. 28 studies remained for checking of the full text; therefore, 6 studies were deleted based on their full text. 34 other studies were further deleted due to irrelevancy to the criteria for the present study. Figure 2 represents the method of the study and criteria for article selection.

3.1. Medicinal Plants/Herbal Formulations for Scleroderma Treatment. Here, we introduce some herbal formulations and their relevant mechanism of action that are beneficial for scleroderma treatment (Figure 3).

3.1.1. Capparis spinosa L. Capparis spinosa L. (Capparidaceae), common name caper, contains active compounds such as alkaloids, flavonoids, polyphenols, and sterols that are responsible for therapeutic properties of this plant-like anti-inflammatory, antioxidant, antiallergic, and antidiabetic [131]. *In vitro* investigation on systemic sclerosis and dermal fibroblasts showed that treatment with the ethanolic extract of *C.spinosa* reduced H_2O_2 and O_2^- production, ROS level, and Ha-Ras expression and inhibited the phosphorylation of ERK/2. It was stated that the ROS-ERK1/2-Ha-Ras loop plays an important role in the pathogenicity of systemic sclerosis; therefore, *C.spinosa* can modulate systemic sclerosis by reducing oxidative stress and modulating the ROS-ERK1/2-Ha-Ras pathway [132] (Table 1).

3.1.2. Ginkgo biloba L. Ginkgo biloba L. (Ginkgoaceae), common name ginkgo, is a historical medicinal plant with a broad set of therapeutic actions [133, 134]. A high percentage of flavonoids and terpenoids is implicated in the pharmacological activities of *G. biloba* [135]. In a clinical trial on systemic sclerosis patients, consumption of *G. biloba* pills (120 mg/kg/day) for 3 months improved Raynaud's phenomenon such as reduction of attack duration and Raynaud's condition score. Raynaud's phenomenon is a complication of systemic sclerosis [136] (Table 1).

3.1.3. Gui-Zhi-Fu-Ling-Wan (Keishi-Bukuryo-Gan). Gui-Zhi-Fu-Ling-Wan (Keishi-bukuryo-gan) (GFW) is a herbal mixture consisting of 5 herbs including *Cinnamomum cassia* (L.) J. Presl (Lauraceae), *Wolfiporia extensa* (Pecks) Ginns (Polyporaceae), *Paeonia* × *suffruticosa* Andrews, *Paeonia lactiflora*

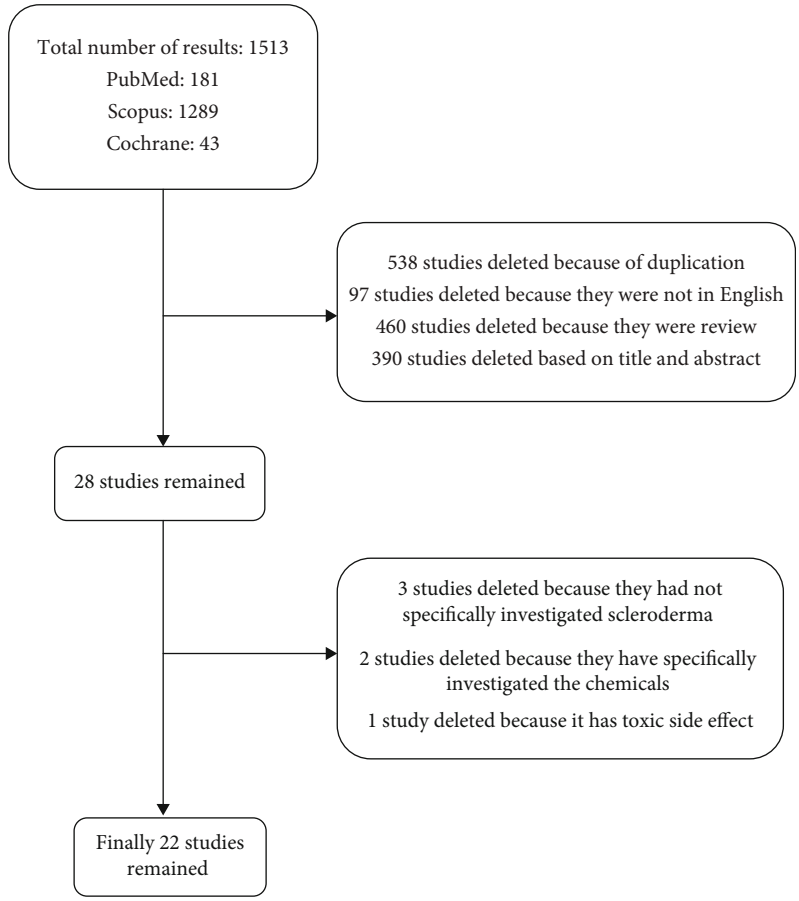

Figure 2: Study design diagram.

Pall. or *Paeonia veitchii* Lynch (Paeoniaceae), and *Prunus persica* (L.) Batsch or *Prunus davidiana* (Carrière) Franch (Rosaceae). This mixture has many pharmacological applications in Chinese traditional medicine such as anti-inflammation, antioxidant, enhancement of the blood circulation, and improvement of scleroderma [137]. Coculture of fibroblast MRC-5 cells with GFW downregulated TNF-α, macrophage inflammatory protein 2 (MIP-2), and IL-6 mRNA expression and inhibited the proliferation of the fibroblasts [138]. Administration of GFW inhibited proliferation of human fibroblast cells and collagen synthesis *in vitro*, resulting in improvement of sclerosis of skin and internal organs. This treatment did not affect mRNA expression of collagen, so probably this inhibitory effect on collagen synthesis is in the posttranscriptional level [139] (Table 1).

3.1.4. Oenothera biennis L. Oenothera biennis L. (Onagraceae), commonly called evening primrose, is a plant used in herbal medicine because its oil has a high content of gamma-linolenic acid, a precursor to prostaglandin E1. Prostaglandin E1 increases blood flow and reduces inflammation, thus improving Raynaud's phenomenon and other defects associated with scleroderma [140]. In patients suffering from scleroderma, *O. biennis* oil treatment improved Raynaud's phenomenon, pain in hands and feet, ulcers, skin texture, and telangiectasia [141, 142] (Table 1).

3.1.5. Persea americana Mill. (Avocado) and Glycine max (L.) Merr. (Soybean) Unsaponifiables. Avocado and soybean unsaponifiables are natural compounds made from one-third of avocado oil and two-thirds of soybean oil. Phytosterols, β-sitosterol, campesterol, stigmasterol, some vitamins, strolls, and terpenes are among the active components of this mixture. The therapeutic potential of this formulation was associated with the anti-inflammatory and antioxidant properties of its bioactive content. The mixture was found beneficial for osteoarthritis and another inflammatory disease [143]. It was reported that avocado and soybean unsaponifiables can restrain osteoarthritis through inhibition of proinflammatory cytokines such as IL-1β, IL-3, IL-6, IL-8, IL-13, and TGF-β; also, they can modulate oxidative damages by repression of ROS production [144–146].

In a study on 100 patients suffering from scleroderma, administration of 300 mg/kg/day of avocado and soybean unsaponifiables during 6 months reduced disability and deformity of these patients and improved the symptoms of the disease. It has been suggested that this herbal mixture can suppress the inflammatory mediators, inflammation, and cutaneous fibrosis, while enhancing collagen solubility and connective tissue regeneration, probably due to its rich antioxidant content [147]. Therefore, based on these studies, avocado and soybean unsaponifiables may be a candidate to alleviate scleroderma (Table 1).

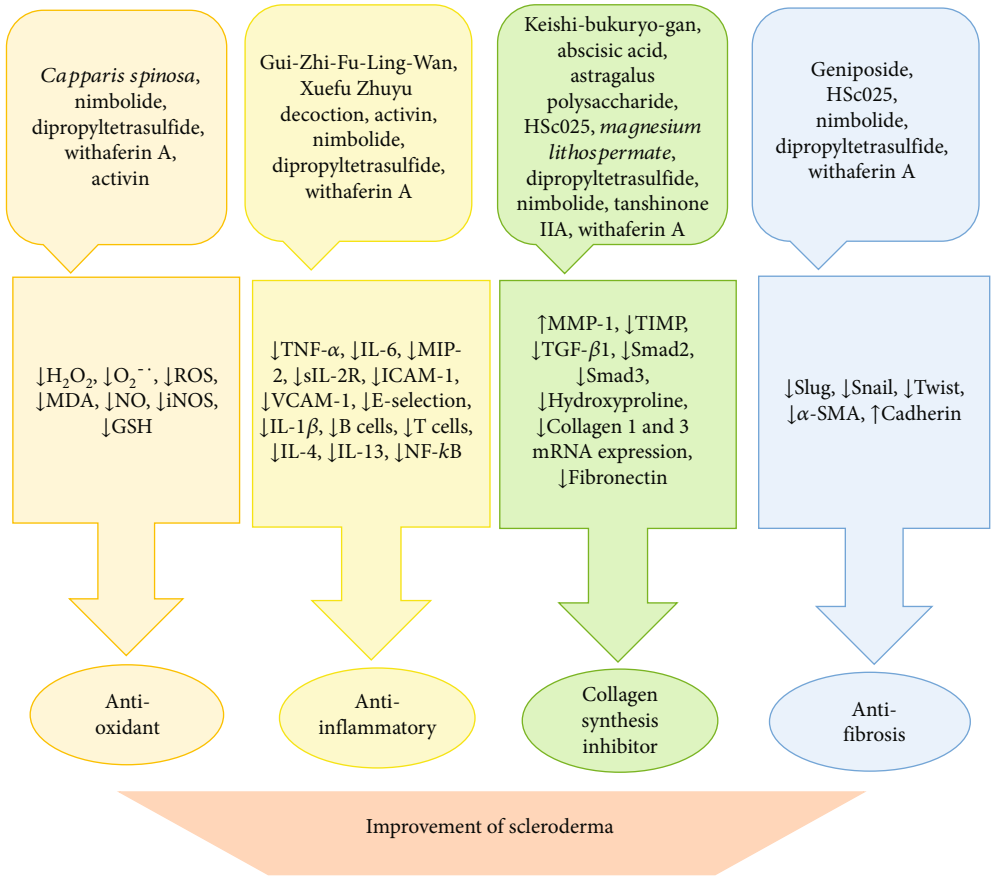

Figure 3: Mechanisms of action of herbal formulations and natural product for scleroderma treatment.

Table 1: *In vitro*, *in vivo*, and clinical interventions of medicinal plants for scleroderma treatment.

Herbal species and/or formulation	Type of study	Outcomes	Reference
Capparis spinosa L.	*In vitro*/systemic sclerosis dermal fibroblasts	↓H_2O_2, ↓$O_2^{\cdot-}$, ↓ROS, ↓cell death, ↓Ha-Ras, ↓ERK1/2	[132]
Ginkgo biloba L.	*In vivo*/clinical trial	↓Attack duration, ↓Raynaud's score	[136]
Gui-Zhi-Fu-Ling-Wan: *Cinnamomum cassia* (L.) J. Presl, *Wolfiporia extensa* Ginns, *Paeonia* × *suffruticosa* Andrews, *Paeonia lactiflora* Pall. or *Paeonia veitchii* Lynch, and *Prunus persica* (L.) Batsch or *Prunus davidiana* (Carrière) Franch.	*In vitro*/MRC-5 cells	↓TNF-α, ↓MIP-2, ↓IL-6	[138]
	In vitro/human fibroblasts	↓Proliferation, ↓collagen	[139]
Oenothera biennis L.	*In vivo*/clinical trial	↓Raynaud's score, ↓ulcers, ↓pain, ↓telangiectasia	[141, 142]
Persea americana Mill. (avocado) and *Glycine max* (L.) Merr. (soybean) unsaponifiables	*In vivo*/clinical trial	↓Deformity, ↓disability	[147]
Tripterygium wilfordii Hook f.	*In vivo*/clinical trial	↑FVC, ↑FVC pred%	[150]
Xuefu Zhuyu decoction *Bupleurum chinense* DC., *Paeonia lactiflora* Pall., *Cyathula officinalis* K.C. Kuan, *Conioselinumanthriscoides* "Chuanxiong," *Angelica sinensis* (Oliv) Diels., *Prunus persica* (L.) Batsch, *Glycyrrhiza uralensis* Fisch. ex DC., *Carthamus tinctorius* L., *Platycodon grandiflorum* (Jacq.) A. DC., *Rehmannia glutinosa* (Gaertn.) DC., and *Citrus* × *aurantium* L. plus vitamin B6	*In vivo*/clinical trial	↓TNF-α, ↓sIL-2R	[152]

Table 2: *In vitro*, *in vivo*, and clinical interventions of natural therapeutics for scleroderma treatment.

Samples	Inducer	Type of study	Outcome	Ref.
Abscisic acid	—	*In vitro*/dermal fibroblast	↓Collagen, ↑MMP-1, ↑TIMP-1, ↓migration	[154]
Activin	—	*In vivo*/clinical trial	↓ICAM-1, ↓VCAM-1, ↓E-selectin, ↓MDA	[156]
Astragalus polysaccharide	BLM	*In vivo*/mice	↓Collagen, ↓TGF-β1, ↓MCP-1, ↓Smad2, ↓Smad3	[158]
Bee venom	—	*In vivo*/clinical trial	↓NRS for itch intensity, ↓NRS for sleep disturbance	[160]
Bromelain	—	*In vivo*/clinical trial	↓Depigmentation area, ↑food intake, ↑improvement of hand and foot activity	[172]
Curcumin	BLM	*In vivo*/mice *In vitro*/SLF	↑SLF apoptosis	[161]
Dipropyltetrasulfide	—	*In vivo*/mice *In vitro*/mouse dermal fibroblast	↓α-SMA, ↓AOPP, ↓pSmad2/3, ↓B cells, ↓T cells, ↓IL-4, ↓IL-13, ↑GSH	[163]
Geniposide	BLM	*In vivo*/mice *In vitro*/HUVECs	↓End MT, ↓α-SMA, ↓phospho-mTOR, ↓phospho-S6, ↓Slug, ↓Snail, ↓Twist, ↑CD31, ↑E-cadherin	[165]
HSc025	BLM	*In vivo*/mice *In vitro*/human dermal fibroblasts	↓Collagen, ↓hypodermal thickness, ↓hydroxyproline, ↓α-SMA, ↓fibrosis	[166]
Magnesium lithospermate	—	*In vitro*/human dermal fibroblast	↓Collagen	[168]
Nimbolide	BLM	*In vivo*/mice	↓Skin thickness, ↓NO, ↓TNF-α, ↓IL-1β, ↓p-NF-κB, ↓TGF-β1, ↓Smad2/3, ↓α-SMA, ↓N-cadherin, ↑GSH	[170]
Tanshinone IIA	IL-17A	*In vitro*/DVSMCs	↓Proliferation, ↓collagen 1 and 3, ↓migration, ↓ERK phosphorylation	[175]
Withaferin A	BLM	*In vivo*/mice	↓Skin thickness, ↓E-cadherin, ↓α-SMA, ↓fibronectin, ↓hydroxyproline, ↓collagen, ↓p-Akt, ↓TGF-β1, ↓Smad2/3, ↓p-NF-κB, ↓p65, ↓IKKβ, ↓TNF-α, ↓IL-1β, ↓NO, ↓iNOS, ↑FOXO3a, ↑GSH	[177]

Abbreviations: AOPP = advanced oxidation protein products; BLM = bleomycin; HUVECs = human umbilical vein endothelial cells.

3.1.6. Tripterygium wilfordii Hook f. *Tripterygium wilfordii* Hook f. (Celastraceae), Chinese name Lei Gong Teng, is a plant used in Chinese traditional medicine for many aims such as treatment of RA, systemic lupus, and systemic sclerosis. The plant contains more than 300 active compounds, of which diterpenoids, triptolide, tripdiolide, and triptomide were found effective in the treatment of autoimmune disease [148, 149]. Treatment with *T. wilfordii* improved forced vital capacity (FVC) and FVC percentages of predicted values (pred%) that are indicators of improvement of pulmonary function in systemic sclerosis patients [150] (Table 1).

3.1.7. Xuefu Zhuyu Decoction. Xuefu Zhuyu decoction is a herbal decoction used in traditional Chinese medicine for enhancing blood circulation and treatment of atherosclerosis and neurodegenerative disease. Xuefu Zhuyu includes *Bupleurum chinense* DC. (Apiaceae), *Paeonia lactiflora* Pall. (Paeoniaceae), *Cyathula officinalis* K.C. Kuan (Amaranthaceae), *Conioselinumanthriscoides* "Chuanxiong" (Apiaceae), *Angelica sinensis* (Oliv) Diels. (Apiaceae), *Prunus persica* (L.) Batsch (Rosaceae), *Glycyrrhiza uralensis* Fisch. ex DC. (Fabaceae), *Carthamus tinctorius* L. (Asteraceae), *Platycodon grandiflorum* (Jacq.) A. DC. (Campanulaceae), *Rehmannia glutinosa* (Gaertn.) DC. (Orobanchaceae), and *Citrus* × *aurantium* L. (Rutaceae) [151]. Treatment of patients with localized scleroderma with vitamin B6 and Xuefu Zhuyu decoction reduced TNF-α and soluble interleukin 2 receptor (sIL-2R) levels in serum, possibly through the improvement of blood circulation and decrease of inflammation [152] (Table 1).

3.2. Natural Therapeutics for Scleroderma. Here, we introduce some natural therapeutics and their relevant mechanism of action that are beneficial for scleroderma treatment (Figure 3).

3.2.1. Abscisic Acid. Abscisic acid is a phytohormone and also is an endogenous human hormone involved in many inflammatory processes of the body including the increase of the production of proinflammatory cytokines like TNF-α, MCP-1, matrix metalloproteinase 9 (MMP-9), and prostaglandin E2 (PGE2) and cell migration [153]. Abscisic acid treatment of Bruzzone et al. in human dermal fibroblasts enhanced proliferation of fibroblasts and decreased their migration, reduced the collagen level, and increased the MMP-1 and tissue inhibitor of metalloproteinase 1 (TIMP-1) levels. It is known that the expression of MMP-1 and TIMP-1 (MMP-1 inhibitor) reduces during the systemic sclerosis progression. Also, the plasma level of abscisic acid is lower in systemic sclerosis patients compared with normal people [154] (Table 2).

3.2.2. Activin. Activin is a phytochemical derived from grape seed proanthocyanidins with strong antioxidant activity. The compound is used to improve cardiovascular disease associated with oxidative damage [155]. Treatment of activin (100 mg/kg/day) in systemic sclerosis patients for 30 days reduced soluble adhesion molecules (i.e., ICAM-1, VCAM-1, E-selectin) and malondialdehyde (MDA) levels in serum. E-selectin is a type of selectin molecule that plays an

important role in the inflammation process and is activated by cytokines. Also, VCAM-1 and ICAM-1 are involved in inflammatory pathways. Therefore, this compound can modulate systemic sclerosis through attenuation of oxidative stress and reduction of adhesion molecules involved in inflammation [156] (Table 2).

3.2.3. Astragalus Polysaccharides. Astragalus polysaccharide is a phytochemical derived from *Astragalus mongholicus* Bunge (Fabaceae) with great pharmacological activities, particularly in the treatment of cancer and modulation of inflammatory responses [157]. Administration of *Astragalus* polysaccharide in bleomycin-induced systemic sclerosis mice reduced the collagen production in skin tissue, also downregulating the TGF-β1, MCP-1, Smad2, and Smad3 mRNA expressions. As mentioned, activation of the TGF-β1/Smad2/3 pathway leads to an increase of the mRNA expression of collagen 1. Therefore, Astragalus polysaccharides can modulate systemic sclerosis by inhibiting collagen production [158] (Table 2).

3.2.4. Bee Venom. Bee venom is used in traditional Chinese medicine for 3000 years with various health-promoting actions such as anti-inflammatory, antioxidant, antifibrotic, antiapoptotic, and antiatherosclerosis activities [159]. Bee venom modulated the number of itches and improved sleep index in scleroderma patients. The sleep index is defined as the numeric scale (NRS) score for itch and sleep [160] (Table 2).

3.2.5. Curcumin. Curcumin treatment increased apoptosis in scleroderma lung fibroblast (SLF) but not in normal lung fibroblast (NLF), because protein kinase C (PKC) and heme oxygenase 1 (HO-1) and glutathione-*S*-transferase P1 (GST P1) are not active in SLF. Interestingly, the apoptotic effect of curcumin is specific to SLF, due to the activity of PKC in healthy cells and its inactivity in damaged cells. Overall, curcumin can modulate systemic sclerosis by increasing apoptosis in damaged cells [161] (Table 2).

3.2.6. Dipropyltetrasulfide. Dipropyltetrasulfide is a natural compound derived from *Allium* spp. with high antioxidant, antiproliferative, and antibacterial activities and is used in folk medicine for the treatment of many diseases such as diabetes, cancer, and cardiovascular disease [162]. Administration of dipropyltetrasulfide in HOCl-induced systemic sclerosis mice reduced the expressions of α-SMA and pSmad2/3 in the skin tissue. Besides, dipropyltetrasulfide declined the count and proliferation of B and T cells in the spleen and the IL-4 and IL-13 levels in the serum of treated mice. *In vitro*, dipropyltetrasulfide reduced the proliferation of dermal fibroblasts and raised glutathione (GSH) levels. Modulation of the immune system, suppression of oxidative stress, and antifibrotic activity are the main mechanisms underlying the therapeutic property of dipropyltetrasulfide against systemic sclerosis [163] (Table 2).

3.2.7. Geniposide. Geniposide is a phytochemical derived from *Gardenia jasminoides* J. Ellis (Rubiaceae) with a variety of pharmacological and biological activities such as antioxidant, anti-inflammatory, antidiabetic, antiproliferative, and neuroprotective actions [164]. In bleomycin-induced scleroderma mice, treatment of geniposide inhibited endothelial to mesenchymal transition (EndMT) process activity. In addition, geniposide increased the E-cadherin levels and Slug, Snail, and Twist protein expressions *in vivo*, while reducing α-SMA, phospho-mTOR, and phosphor S6 and enhancing cluster of differentiation 31 (CD31) in fibroblast cells *in vitro*. Slug, Snail, and Twist are transcriptional factors that regulate the expression of E-cadherin. Geniposide can attenuate systemic sclerosis via endothelial cell protection and inhibition of the mTOR pathway [165] (Table 2).

3.2.8. HSc025. HSc025 is a novel small compound of trihydroxy-α-sanshool. Trihydroxy-α-sanshool is a compound derived from *Zanthoxylum piperitum* (L.) DC. (Rutaceae). Previous studies showed that the extract of this herb can inhibit collagen gene expression [166]. Hasegawa et al. demonstrated that treatment with HSc025 in human dermal fibroblasts reduced collagen expression. *In vivo*, HSc025 decreased the hypodermal thickness, hydroxyproline content, and the frequency of α-SMA-positive myofibroblasts in the skin of scleroderma mice. Moreover, HSc025 reduced lung fibrosis in these animals as measured by the Ashcroft score. HSc025 can be considered a treatment for systemic sclerosis by inhibiting TGF-β/Smad signaling and improving pulmonary fibrosis [166] (Table 2).

3.2.9. Magnesium Lithospermate. Magnesium lithospermate is a compound derived from *Salvia miltiorrhiza* Bunge (Lamiaceae) with antioxidant, vasodilator, antifibrotic, improvement of blood circulation, and neuro- and cardiovascular-protective effects [167]. Shigematsu et al. demonstrated that treatment of human dermal fibroblasts from scleroderma patients with magnesium lithospermate reduced collagen synthesis by inhibition of prolyl and lysyl hydroxylase activities, indicating that magnesium lithospermate may be an antifibrotic drug for systemic sclerosis treatment [168] (Table 2).

3.2.10. Nimbolide. Nimbolide is a phytochemical derived from *Azadirachta indica* A. Juss. (Meliaceae) and is used in Indian traditional medicine for the treatment of many diseases. It has a wide range of biological activities such as anticancer, antiarthritic, antifungal, antifibrotic, anti-inflammatory, antioxidant, and antigastric ulcer [169]. Treatment of nimbolide reduced skin thickness and oxidative stress in bleomycin-induced scleroderma mice. Nimbolide attenuated the progression of scleroderma by controlling inflammatory factors such as TNF-α, IL-1β, and p-NF-κB and by downregulating the TGF-β/Smad signaling axis (inhibition of TGF-β expression and Smad2/3 protein phosphorylation). In addition, nimbolide inhibited the expressions of α-SMA and N-cadherin, indicators of epithelial to mesenchymal transition [170] (Table 2).

3.2.11. Bromelain. Bromelain is a protein-digesting enzyme mixture derived from the stem, fruit, and juice of the pineapple, *Ananas comosus* (L.) Merr. (Bromeliaceae). It has been used for the treatment of inflammatory disease, pain, and muscle soreness in America [171]. In a case report study, it

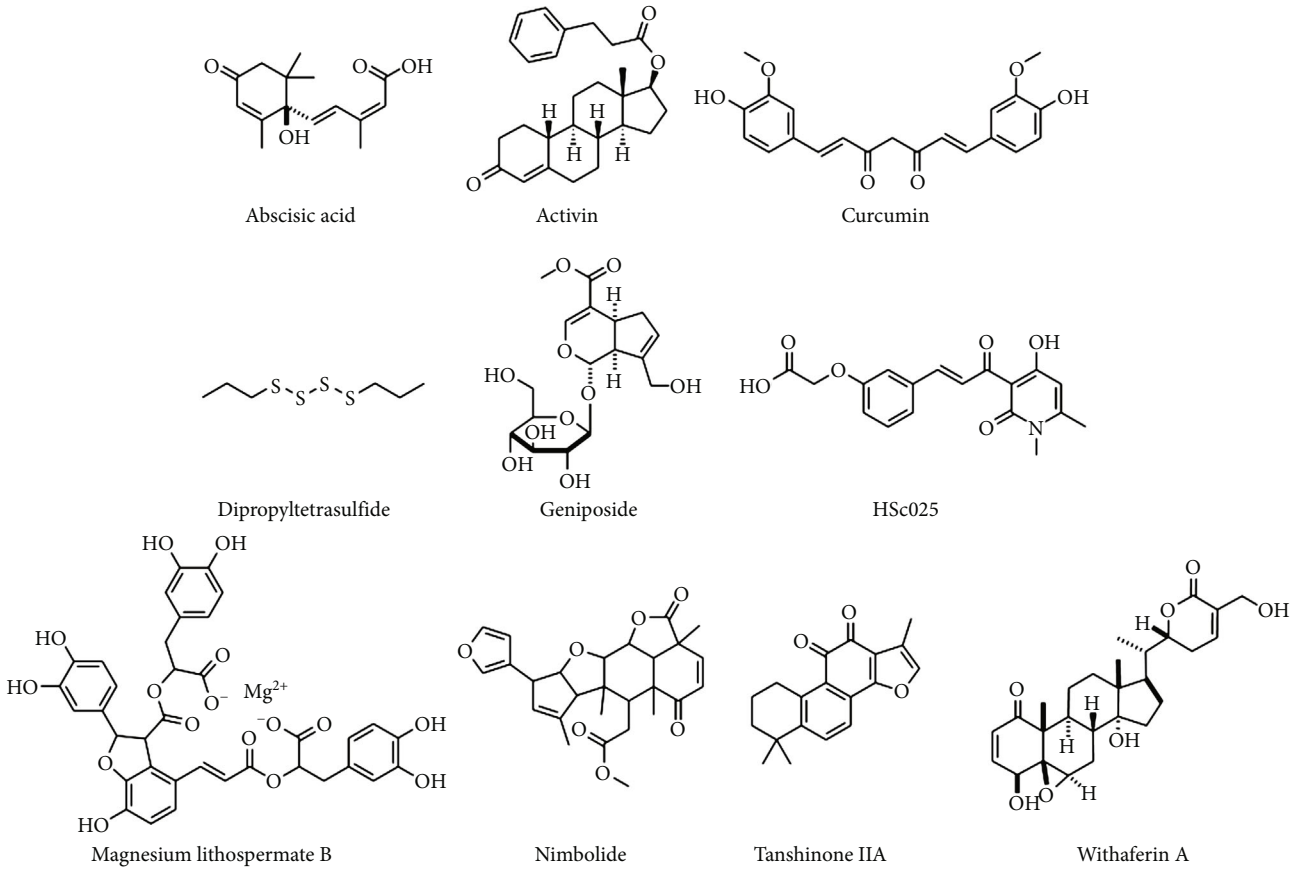

Figure 4: Chemical structures of selected natural product compounds with potential for scleroderma treatment.

was shown that treatment of a systemic sclerosis patient with bromelain improved the patient condition by reducing depigmentation areas of the forehead and scalp, improving eating food, and improving hand and foot activities [172] (Table 2).

3.2.12. Tanshinone IIA. Tanshinone IIA is a phytochemical derived from *S. miltiorrhiza*, which is used in traditional Chinese medicine for the treatment of oxidative damages, connective tissue diseases, cardiovascular diseases, systemic lupus erythematosus, systemic sclerosis, and inflammatory diseases like RA and pulmonary hypertension [173, 174]. Liu et al. demonstrated that treatment with tanshinone IIA in human dermal vascular smooth muscle cells (DVSMCs) reduced cell proliferation, collagen 1 and 3 expressions, migration, and ERK phosphorylation. The ERK/MAPK signaling pathway is an important pathway for systemic sclerosis progression, and tanshinone IIA can block this pathway [175] (Table 2).

3.2.13. Withaferin A. Withaferin A is one of the active compounds derived from *Withania somnifera* (L.) Dunal (Solanaceae) and used in Indian traditional medicine with known applications for the treatment of immunological and inflammatory diseases [176]. Withaferin A reduced skin thickness and modulated the antioxidant parameters (reduced nitric oxide (NO) and inducible nitric oxide synthase (iNOS) and raised GSH levels) in supernatants of skin in bleomycin-induced systemic sclerosis mice. Withaferin A alleviated the E-cadherin, collagen, and hydroxyproline levels and the α-SMA and fibronectin expressions. Withaferin A treatment repressed the TGF-β1/Smad signaling pathway by inhibiting the expression of TGF-β1 and the phosphorylation of Smad2/3 protein. Besides, withaferin A downregulated the p-Akt, p-NF-κB, p65, inhibitor of nuclear factor kappa-B (IKKβ), TNF-α, and IL-1β expressions, while promoting the FOXO3a expression. Beneficial properties of withaferin A might be correlated with inhibition of inflammation, collagen synthesis, and oxidative stress in systemic sclerosis damaged tissue [177] (Table 2).

Figure 4 shows the chemical structures of selected natural product compounds with potential for scleroderma treatment.

4. Discussion

Sclerodermas are rare autoimmune diseases, virtually affecting all the body tissues. Molecular analyses suggest that environmental and genetic factors may trigger the disease in vulnerable subjects. It was shown that both the innate and the adaptive immune systems are involved. Upon such condition, the number of autoreactive B cells producing autoantibodies and secretion of proinflammatory and profibrotic cytokines such as TGF-β, platelet-derived growth factor,

connective tissue growth factor, IL-6, IL-4, and IL-1α by the immune, endothelial, and fibroblast cells increases, while T regulator cells are suppressed [178]. Yet, there is no definite cure; the lack of a uniform clinical-epidemiological approach, the necessity of long-term management in affected individuals, and adverse effects of current medications indicate an urgent need for new strategies for early diagnosis and to minimize the development of serious morbidity and to improve the quality of life for these patients. In this regard, natural products are a reliable source of new medicines, providing versatile lead structures to stimulate or prevent many pharmacological targets and activities. We provided evidence showing that natural preparations can improve systemic fibrosis mainly through suppressing inflammatory activities, inhibiting mitogen-induced lymphocyte proliferation, inducing cellular apoptosis targeting the mediators and signaling pathways of apoptosis, and eliciting T regulatory cells. However, these results are mainly based on research outcomes from Chinese pharmaceutical formulations, and to achieve a comprehensive conclusion, more evaluations and long-term clinical trials have to be conducted worldwide. Caution regarding the use of natural products/herbal formulations is still warranted since potential long-term consequences have not been evaluated.

Conflicts of Interest

There is not any conflict of interest.

References

[1] U. Patil, A. Jaydeokar, and D. Bandawane, "Immunomodulators: a pharmacological review," *International Journal of Pharmacy and Pharmaceutical Sciences*, vol. 4, no. 1, pp. 30–36, 2012.

[2] M. T. Sultan, M. S. Buttxs, M. M. N. Qayyum, and H. A. R. Suleria, "Immunity: plants as effective mediators," *Critical Reviews in Food Science and Nutrition*, vol. 54, no. 10, pp. 1298–1308, 2014.

[3] B. K. Tan and J. Vanitha, "Immunomodulatory and antimicrobial effects of some traditional Chinese medicinal herbs: a review," *Current Medicinal Chemistry*, vol. 11, no. 11, pp. 1423–1430, 2004.

[4] J. J. Bright, "Targeting autoimmune diseases through nutraceuticals," *Nutrition*, vol. 20, no. 1, pp. 39–43, 2004.

[5] H.-D. Ma, Y. R. Deng, Z. Tian, and Z. X. Lian, "Traditional Chinese medicine and immune regulation," *Clinical Reviews in Allergy & Immunology*, vol. 44, no. 3, pp. 229–241, 2013.

[6] K. R. Rengasamy, H. Khan, S. Gowrishankar et al., "The role of flavonoids in autoimmune diseases: therapeutic updates," *Pharmacology & Therapeutics*, vol. 194, pp. 107–131, 2019.

[7] N. Singh, M. Tailang, and S. Mehta, "A review on herbal plants as immunomodulators," *International Journal of Pharmaceutical Sciences and Research*, vol. 7, no. 9, p. 3602, 2016.

[8] A. Karim, M. Nouman Soh, S. Munir, and S. Sattar, "Pharmacology and phytochemistry of Pakistani herbs and herbal drugs used for treatment of diabetes," *International Journal of Pharmacology*, vol. 7, no. 4, pp. 419–439, 2011.

[9] R. Harikrishnan, C. Balasundaram, and M.-S. Heo, "Impact of plant products on innate and adaptive immune system of cultured finfish and shellfish," *Aquaculture*, vol. 317, no. 1-4, pp. 1–15, 2011.

[10] P. K. Mukherjee, N. K. Nema, S. Bhadra, D. Mukherjee, F. C. Braga, and M. G. Matsabisa, "Immunomodulatory leads from medicinal plants," NISCAIR-CSIR, India, 2014, http://nopr.niscair.res.in/handle/123456789/27905.

[11] H. Wagner, "Immunostimulants of plant origin," *Croatica Chemica Acta*, vol. 68, no. 3, pp. 615–626, 1995.

[12] R. Sharma, A. Rohilla, and V. Arya, "A short review on pharmacology of plant immunomodulators," *International Journal of Pharmaceutical Sciences Review and Research*, vol. 9, pp. 126–131, 2011.

[13] Z. Amirghofran, "Herbal medicines for immunosuppression," *Iranian Journal of Allergy, Asthma and Immunology*, vol. 11, pp. 111–119, 2012.

[14] J. Cen, M. Shi, Y. Yang et al., "Isogarcinol is a new immunosuppressant," *PLoS One*, vol. 8, no. 6, p. e66503, 2013.

[15] I. E. Cock and M. Cheesman, "The potential of plants of the genus Syzygium (Myrtaceae) for the prevention and treatment of arthritic and autoimmune diseases," in *Bioactive Food as Dietary Interventions for Arthritis and Related Inflammatory Diseases*, pp. 401–424, Elsevier, 2019.

[16] P. Li, Y. Zheng, and X. Chen, "Drugs for autoimmune inflammatory diseases: from small molecule compounds to anti-TNF biologics," *Frontiers in Pharmacology*, vol. 8, p. 460, 2017.

[17] N. L. Bragazzi, A. Watad, F. Brigo, M. Adawi, H. Amital, and Y. Shoenfeld, "Public health awareness of autoimmune diseases after the death of a celebrity," *Clinical Rheumatology*, vol. 36, no. 8, pp. 1911–1917, 2017.

[18] K. Rainsford, "Anti-inflammatory drugs in the 21st century," in *Inflammation in the pathogenesis of chronic diseases*, pp. 3–27, Springer, 2007.

[19] D. Simmons, R. M. Botting, and T. Hla, "Cyclooxygenase isozymes: the biology of prostaglandin synthesis and inhibition," *Pharmacological Reviews*, vol. 56, no. 3, pp. 387–437, 2004.

[20] E. M. Antman, J. S. Bennett, A. Daugherty et al., "Use of nonsteroidal antiinflammatory drugs: an update for clinicians: a scientific statement from the American Heart Association," *Circulation*, vol. 115, no. 12, pp. 1634–1642, 2007.

[21] W. A. Ray, C. M. Stein, J. R. Daugherty, K. Hall, P. G. Arbogast, and M. R. Griffin, "COX-2 selective non-steroidal anti-inflammatory drugs and risk of serious coronary heart disease," *The Lancet*, vol. 360, no. 9339, pp. 1071–1073, 2002.

[22] M. Hermann and F. Ruschitzka, "Coxibs, non-steroidal anti-inflammatory drugs and cardiovascular risk," *Internal Medicine Journal*, vol. 36, no. 5, pp. 308–319, 2006.

[23] J. Glyn, "The discovery and early use of cortisone," *Journal of the Royal Society of Medicine*, vol. 91, no. 10, pp. 513–517, 1998.

[24] F. Joana, A. Alaa, and E. Paul, "Glucocorticoids and rhematoid arthritis," *Rheumatic Diseases Clinics of North America*, vol. 42, pp. 33–46, 2016.

[25] F. Buttgereit, G. R. Burmester, R. H. Straub, M. J. Seibel, and H. Zhou, "Exogenous and endogenous glucocorticoids in rheumatic diseases," *Arthritis and Rheumatism*, vol. 63, no. 1, pp. 1–9, 2011.

[26] P. J. Barnes, "Anti-inflammatory actions of glucocorticoids: molecular mechanisms," *Clinical Science*, vol. 94, no. 6, pp. 557–572, 1998.

[27] X. Chen, J. . J. Oppenheim, R. . T. Winkler-Pickett, J. . R. Ortaldo, and O. . M. . Z. Howard, "Glucocorticoid amplifies IL-2-dependent expansion of functional FoxP3+ CD4+ CD25+ T regulatory cells in vivo and enhances their capacity to suppress EAE," *European Journal of Immunology*, vol. 36, no. 8, pp. 2139–2149, 2006.

[28] O. Ethgen, F. de Lemos Esteves, O. Bruyere, and J. Y. Reginster, "What do we know about the safety of corticosteroids in rheumatoid arthritis?," *Current Medical Research and Opinion*, vol. 29, no. 9, pp. 1147–1160, 2013.

[29] S. E. Gabriel, D. Coyle, and L. W. Moreland, "A clinical and economic review of disease-modifying antirheumatic drugs," *PharmacoEconomics*, vol. 19, no. 7, pp. 715–728, 2001.

[30] R. F. van Vollenhoven, P. Geborek, K. Forslind et al., "Conventional combination treatment versus biological treatment in methotrexate-refractory early rheumatoid arthritis: 2 year follow-up of the randomised, non-blinded, parallel-group Swefot trial," *The Lancet*, vol. 379, no. 9827, pp. 1712–1720, 2012.

[31] E. Rosato, S. Pisarri, and F. Salsano, "Current strategies for the treatment of autoimmune diseases," *Journal of Biological Regulators and Homeostatic Agents*, vol. 24, no. 3, pp. 251–259, 2010.

[32] A. U. Wells, "Interstitial lung disease in systemic sclerosis," *La Presse Médicale*, vol. 43, no. 10, pp. e329–e343, 2014.

[33] S. Bernatsky, L. Joseph, C. A. Pineau, P. Belisle, M. Hudson, and A. E. Clarke, "Scleroderma prevalence: demographic variations in a population-based sample," *Arthritis Care & Research*, vol. 61, no. 3, pp. 400–404, 2009.

[34] K. Nishioka, I. Katayama, H. Kondo et al., "Epidemiological analysis of prognosis of 496 Japanese patients with progressive systemic sclerosis (SSc)," *The Journal of Dermatology*, vol. 23, no. 10, pp. 677–682, 1996.

[35] T. Tamaki, S. Mori, and K. Takehara, "Epidemiological study of patients with systemic sclerosis in Tokyo," *Archives of Dermatological Research*, vol. 283, no. 6, pp. 366–371, 1991.

[36] F. M. Meier, K. W. Frommer, R. Dinser et al., "Update on the profile of the EUSTAR cohort: an analysis of the EULAR Scleroderma Trials and Research group database," *Annals of the Rheumatic Diseases*, vol. 71, no. 8, pp. 1355–1360, 2012.

[37] V. Steen, R. T. Domsic, M. Lucas, N. Fertig, and T. A. Medsger Jr., "A clinical and serologic comparison of African American and Caucasian patients with systemic sclerosis," *Arthritis and Rheumatism*, vol. 64, no. 9, pp. 2986–2994, 2012.

[38] T. L. Skare, A. E. Fonseca, A. C. Luciano, and P. M. Azevedo, "Autoantibodies in scleroderma and their association with the clinical profile of the disease. A study of 66 patients from southern Brazil," *Anais Brasileiros de Dermatologia*, vol. 86, no. 6, pp. 1075–1081, 2011.

[39] R. Janardana, A. M. Nair, A. K. Surin, J. A. J. Prakash, M. Gowri, and D. Danda, "Unique clinical and autoantibody profile of a large Asian Indian cohort of scleroderma—do South Asians have a more aggressive disease?," *Clinical Rheumatology*, vol. 38, no. 11, pp. 3179–3187, 2019.

[40] C. R. Pasarikovski, J. T. Granton, A. M. Roos et al., "Sex disparities in systemic sclerosis-associated pulmonary arterial hypertension: a cohort study," *Arthritis Research & Therapy*, vol. 18, no. 1, p. 30, 2016.

[41] A. Gabrielli, E. V. Avvedimento, and T. Krieg, "Scleroderma," *New England Journal of Medicine*, vol. 360, no. 19, pp. 1989–2003, 2009.

[42] S. Soldano, P. Montagna, R. Brizzolara et al., "Effects of estrogens on extracellular matrix synthesis in cultures of human normal and scleroderma skin fibroblasts," *Annals of the New York Academy of Sciences*, vol. 1193, no. 1, pp. 25–29, 2010.

[43] E. C. LeRoy, C. Black, R. Fleischmajer et al., "Scleroderma (systemic sclerosis): classification, subsets and pathogenesis," *The Journal of Rheumatology*, vol. 15, no. 2, pp. 202–205, 1988.

[44] P. Sobolewski, M. Maślińska, M. Wieczorek et al., "Systemic sclerosis - multidisciplinary disease: clinical features and treatment," *Reumatologia*, vol. 57, no. 4, pp. 221–233, 2019.

[45] J. Folkman, "Angiogenesis in cancer, vascular, rheumatoid and other disease," *Nature Medicine*, vol. 1, no. 1, pp. 27–30, 1995.

[46] V. Calvaruso and A. Craxì, "Immunological alterations in hepatitis C virus infection," *World journal of gastroenterology: WJG*, vol. 19, no. 47, pp. 8916–8923, 2013.

[47] Y. S. Gu, J. Kong, G. S. Cheema, C. L. Keen, G. Wick, and M. E. Gershwin, "The immunobiology of systemic sclerosis," *Seminars in Arthritis and Rheumatism*, vol. 38, no. 2, pp. 132–160, 2008.

[48] R. Sgonc, M. S. Gruschwitz, G. Boeck, N. Sepp, J. Gruber, and G. Wick, "Endothelial cell apoptosis in systemic sclerosis is induced by antibody-dependent cell-mediated cytotoxicity via CD95," *Arthritis & Rheumatism*, vol. 43, no. 11, pp. 2550–2562, 2000.

[49] C. Mavalia, C. Scaletti, P. Romagnani et al., "Type 2 helper T-cell predominance and high CD30 expression in systemic sclerosis," *The American Journal of Pathology*, vol. 151, no. 6, pp. 1751–1758, 1997.

[50] R. Giacomelli, M. Matucci-Cerinic, P. Cipriani et al., "Circulating Vδ1 + T cells are activated and accumulate in the skin of systemic sclerosis patients," *Arthritis & Rheumatism*, vol. 41, no. 2, pp. 327–334, 1998.

[51] A. Kalogerou, E. Gelou, S. Mountantonakis, L. Settas, E. Zafiriou, and L. Sakkas, "Early T cell activation in the skin from patients with systemic sclerosis," *Annals of the Rheumatic Diseases*, vol. 64, no. 8, pp. 1233–1235, 2005.

[52] B. M. Kräling, G. G. Maul, and S. A. Jimenez, "Mononuclear cellular infiltrates in clinically involved skin from patients with systemic sclerosis of recent onset predominantly consist of monocytes/macrophages," *Pathobiology*, vol. 63, no. 1, pp. 48–56, 1995.

[53] J. R. Seibold, R. C. Giorno, and H. N. Claman, "Dermal mast cell degranulation in systemic sclerosis," *Arthritis & Rheumatism*, vol. 33, no. 11, pp. 1702–1709, 1990.

[54] S. Sato, H. Hanakawa, M. Hasegawa et al., "Levels of interleukin 12, a cytokine of type 1 helper T cells, are elevated in sera from patients with systemic sclerosis," *The Journal of Rheumatology*, vol. 27, no. 12, pp. 2838–2842, 2000.

[55] K. Komura, M. Fujimoto, M. Hasegawa et al., "Increased serum interleukin 23 in patients with systemic sclerosis," *The Journal of Rheumatology*, vol. 35, no. 1, pp. 120–125, 2008.

[56] A. Yoshizaki, K. Yanaba, Y. Iwata et al., "Elevated serum interleukin-27 levels in patients with systemic sclerosis: association with T cell, B cell and fibroblast activation," *Annals of the Rheumatic Diseases*, vol. 70, no. 1, pp. 194–200, 2011.

[57] J. Varga and C. P. Denton, "Scleroderma, inflammatory myopathies, and overlap syndromes," in *Kelley's Textbook of Rheumatology*, pp. 1311–1351, Saunders Elsevier, USA, 8th edition, 2009.

[58] A. Wakhlu, R. R. Sahoo, J. R. Parida et al., "Serum interleukin-6, interleukin-17A, and transforming growth factor beta are raised in systemic sclerosis with interstitial lung disease," *Indian Journal of Rheumatology*, vol. 13, no. 2, pp. 107–112, 2018.

[59] L. Klareskog, R. Gustafsson, A. Scheynius, and R. Hällgren, "Increased expression of platelet-derived growth factor type B receptors in the skin of patients with systemic sclerosis," *Arthritis & Rheumatism*, vol. 33, no. 10, pp. 1534–1541, 1990.

[60] S. Gay, R. E. Jones Jr., G. Q. Huang, and R. E. Gay, "Immunohistologic demonstration of platelet-derived growth factor (PDGF) and sis-oncogene expression in scleroderma," *Journal of Investigative Dermatology*, vol. 92, no. 2, pp. 301–303, 1989.

[61] K. L. Kaplan, M. J. Broekman, A. Chernoff, G. R. Lesznik, and M. Drillings, "Platelet alpha-granule proteins: studies on release and subcellular localization," *Blood*, vol. 53, no. 4, pp. 604–618, 1979.

[62] C.-H. Heldin and B. Westermark, "Mechanism of action and in vivo role of platelet-derived growth factor," *Physiological Reviews*, vol. 79, no. 4, pp. 1283–1316, 1999.

[63] R. J. Prescott, A. J. Freemont, C. J. P. Jones, J. Hoyland, and P. Fielding, "Sequential dermal microvascular and perivascular changes in the development of scleroderma," *The Journal of Pathology*, vol. 166, no. 3, pp. 255–263, 1992.

[64] M. Dziadzio, R. E. Smith, D. J. Abraham, C. M. Black, and C. P. Denton, "Circulating levels of active transforming growth factor β1 are reduced in diffuse cutaneous systemic sclerosis and correlate inversely with the modified Rodnan skin score," *Rheumatology*, vol. 44, no. 12, pp. 1518–1524, 2005.

[65] H. Higley, K. Persichitte, S. Chu, W. Waegell, R. Vancheeswaran, and C. Black, "Immunocytochemical localization and serologic detection of transforming growth factor β1," *Arthritis & Rheumatism*, vol. 37, no. 2, pp. 278–288, 1994.

[66] S. O'Reilly, M. Ciechomska, R. Cant, and J. M. van Laar, "IL-6 trans signalling drives a STAT3 dependant pathway that leads to hyperactive TGF-β signalling promoting SMAD3 activation and fibrosis via gremlin," *Journal of Biological Chemistry*, vol. 289, no. 14, 2014.

[67] Y. Asano, H. Ihn, K. Yamane, M. Kubo, and K. Tamaki, "Impaired Smad7-Smurf–mediated negative regulation of TGF-β signaling in scleroderma fibroblasts," *The Journal of Clinical Investigation*, vol. 113, no. 2, pp. 253–264, 2004.

[68] M. Ide, M. Jinnin, Y. Tomizawa et al., "Transforming growth factor β-inhibitor Repsox downregulates collagen expression of scleroderma dermal fibroblasts and prevents bleomycin-induced mice skin fibrosis," *Experimental Dermatology*, vol. 26, no. 11, pp. 1139–1143, 2017.

[69] H. Komatsu, M. Y. Chao, J. Larkins-Ford et al., "OSM-11 facilitates LIN-12 Notch signaling during Caenorhabditis elegans vulval development," *PLoS Biology*, vol. 6, no. 8, article e196, 2008.

[70] R. Kopan and M. X. G. Ilagan, "The canonical Notch signaling pathway: unfolding the activation mechanism," *Cell*, vol. 137, no. 2, pp. 216–233, 2009.

[71] F. Logeat, C. Bessia, C. Brou et al., "The Notch1 receptor is cleaved constitutively by a furin-like convertase," *Proceedings of the National Academy of Sciences*, vol. 95, no. 14, pp. 8108–8112, 1998.

[72] T. Gridley, "Notch signaling in vascular development and physiology," *Development*, vol. 134, no. 15, pp. 2709–2718, 2007.

[73] B. Hu and S. H. Phan, "Notch in fibrosis and as a target of anti-fibrotic therapy," *Pharmacological Research*, vol. 108, pp. 57–64, 2016.

[74] O. Gorlova, J. E. Martin, B. Rueda et al., "Correction: identification of novel genetic markers associated with clinical phenotypes of systemic sclerosis through a genome-wide association strategy," *PLoS Genetics*, vol. 7, no. 8, 2011.

[75] C. J. Cardinale, D. Li, L. Tian et al., "Association of a rare NOTCH4 coding variant with systemic sclerosis: a family-based whole exome sequencing study," *BMC Musculoskeletal Disorders*, vol. 17, no. 1, p. 462, 2016.

[76] P. S. Tsou and A. H. Sawalha, "Unfolding the pathogenesis of scleroderma through genomics and epigenomics," *Journal of Autoimmunity*, vol. 83, pp. 73–94, 2017.

[77] N. Warde, "Notch signaling: an important player in SSc fibrosis," *Nature Reviews Rheumatology*, vol. 7, no. 6, pp. 312–312, 2011.

[78] C. Dees, M. Tomcik, P. Zerr et al., "Notch signalling regulates fibroblast activation and collagen release in systemic sclerosis," *Annals of the Rheumatic Diseases*, vol. 70, no. 7, pp. 1304–1310, 2011.

[79] D. M. Schwartz, Y. Kanno, A. Villarino, M. Ward, M. Gadina, and J. J. O'Shea, "JAK inhibition as a therapeutic strategy for immune and inflammatory diseases," *Nature Reviews Drug Discovery*, vol. 16, no. 12, pp. 843–862, 2017.

[80] J. Avouac, B. G. Fürnrohr, M. Tomcik et al., "Inactivation of the transcription factor STAT-4 prevents inflammation-driven fibrosis in animal models of systemic sclerosis," *Arthritis and Rheumatism*, vol. 63, no. 3, pp. 800–809, 2011.

[81] D. Khanna, C. P. Denton, C. J. F. Lin et al., "Safety and efficacy of subcutaneous tocilizumab in systemic sclerosis: results from the open-label period of a phase II randomised controlled trial (faSScinate)," *Annals of the Rheumatic Diseases*, vol. 77, no. 2, pp. 212–220, 2018.

[82] C. P. Denton, V. H. Ong, S. Xu et al., "Therapeutic interleukin-6 blockade reverses transforming growth factor-beta pathway activation in dermal fibroblasts: insights from the faSScinate clinical trial in systemic sclerosis," *Annals of the Rheumatic Diseases*, vol. 77, no. 9, pp. 1362–1371, 2018.

[83] A. Berekmeri, F. Mahmood, M. Wittmann, and P. Helliwell, "Tofacitinib for the treatment of psoriasis and psoriatic arthritis," *Expert Review of Clinical Immunology*, vol. 14, no. 9, pp. 719–730, 2018.

[84] W. Wang, S. Bhattacharyya, R. G. Marangoni et al., "The JAK/STAT pathway is activated in systemic sclerosis and is effectively targeted by tofacitinib," *Journal of Scleroderma and Related Disorders*, vol. 5, pp. 40–50, 2019.

[85] B. A. Hemmings and D. F. Restuccia, "PI3K-PKB/Akt pathway," *Cold Spring Harbor Perspectives in Biology*, vol. 4, no. 9, article a011189, 2012.

[86] I. A. Darby and T. D. Hewitson, "Hypoxia in tissue repair and fibrosis," *Cell and Tissue Research*, vol. 365, no. 3, pp. 553–562, 2016.

[87] M. Ioannou, A. Pyrpasopoulou, G. Simos et al., "Upregulation of VEGF expression is associated with accumulation of HIF-1α in the skin of naïve scleroderma patients," *Modern Rheumatology*, vol. 23, no. 6, pp. 1245–1248, 2013.

[88] F. Chang, L. S. Steelman, J. T. Lee et al., "Signal transduction mediated by the Ras/Raf/MEK/ERK pathway from cytokine receptors to transcription factors: potential targeting for therapeutic intervention," *Leukemia*, vol. 17, no. 7, pp. 1263–1293, 2003.

[89] Y. Chen, X. Shi-wen, J. van Beek et al., "Matrix contraction by dermal fibroblasts requires transforming growth factor-β/activin-linked kinase 5, heparan sulfate-containing proteoglycans, and MEK/ERK: insights into pathological scarring in chronic fibrotic disease," *The American Journal of Pathology*, vol. 167, no. 6, pp. 1699–1711, 2005.

[90] X. Shi-wen, S. L. Howat, E. A. Renzoni et al., "Endothelin-1 induces expression of matrix-associated genes in lung fibroblasts through MEK/ERK," *Journal of Biological Chemistry*, vol. 279, no. 22, pp. 23098–23103, 2004.

[91] B. N. Cronstein and G. Weissmann, "The adhesion molecules of inflammation," *Arthritis and Rheumatism*, vol. 36, no. 2, pp. 147–157, 1993.

[92] H. Ihn, M. Fujimoto, S. Sato et al., "Increased levels of circulating intercellular adhesion molecule-1 in patients with localized scleroderma," *Journal of the American Academy of Dermatology*, vol. 31, no. 4, pp. 591–595, 1994.

[93] C. Carson, L. D. Beall, G. G. Hunder, C. M. Johnson, and W. Newman, "Serum ELAM-1 is increased in vasculitis, scleroderma, and systemic lupus erythematosus," *The Journal of Rheumatology*, vol. 20, no. 5, pp. 809–814, 1993.

[94] M. S. Gruschwitz, O. P. Hornstein, and P. V. D. Driesch, "Correlation of soluble adhesion molecules in the peripheral blood of scleroderma patients with their in situ expression and with disease activity," *Arthritis & Rheumatism*, vol. 38, no. 2, pp. 184–189, 1995.

[95] H. N. Claman, R. C. Giorno, and J. R. Seibold, "Endothelial and fibroblastic activation in scleroderma: the myth of the "uninvolved skin"," *Arthritis and Rheumatism*, vol. 34, no. 12, pp. 1495–1501, 1991.

[96] O. Distler, T. Pap, O. Kowal-Bielecka et al., "Overexpression of monocyte chemoattractant protein 1 in systemic sclerosis: role of platelet-derived growth factor and effects on monocyte chemotaxis and collagen synthesis," *Arthritis and Rheumatism*, vol. 44, no. 11, pp. 2665–2678, 2001.

[97] Y. Asano, H. Ihn, K. Yamane, M. Jinnin, Y. Mimura, and K. Tamaki, "Increased expression of integrin $\alpha v\beta 3$contributes to the establishment of autocrine TGF-β signaling in scleroderma fibroblasts," *The Journal of Immunology*, vol. 175, no. 11, pp. 7708–7718, 2005.

[98] M. Gruschwitz, M. Albrecht, G. Vieth, and U. F. Haustein, "In situ expression and serum levels of tumor necrosis factor-alpha receptors in patients with early stages of systemic sclerosis," *The Journal of Rheumatology*, vol. 24, no. 10, pp. 1936–1943, 1997.

[99] Y. Kawaguchi, "IL-1 alpha gene expression and protein production by fibroblasts from patients with systemic sclerosis," *Clinical & Experimental Immunology*, vol. 97, no. 3, pp. 445–450, 1994.

[100] Y. Kawaguchi, M. Harigai, K. Suzuki et al., "Interleukin 1 receptor on fibroblasts from systemic sclerosis patients induces excessive functional responses to interleukin 1β," *Biochemical and Biophysical Research Communications*, vol. 190, no. 1, pp. 154–161, 1993.

[101] A. Jelaska and J. H. Korn, "Role of apoptosis and transforming growth factor β1 in fibroblast selection and activation in systemic sclerosis," *Arthritis & Rheumatism*, vol. 43, no. 10, pp. 2230–2239, 2000.

[102] G. H. Samuel, S. Lenna, A. M. Bujor, R. Lafyatis, and M. Trojanowska, "Acid sphingomyelinase deficiency contributes to resistance of scleroderma fibroblasts to Fas-mediated apoptosis," *Journal of Dermatological Science*, vol. 67, no. 3, pp. 166–172, 2012.

[103] K. SJ and H. CB, "Role of myeloperoxidase-mediated antimicrobial systems in intact leukocytes," 1972, http://pascal-francis.inist.fr/vibad/index.php?action=getRecordDetail&idt=PASCAL7334010484.

[104] J. M. Pullar, M. C. Vissers, and C. C. Winterbourn, "Living with a killer: the effects of hypochlorous acid on mammalian cells," *IUBMB Life*, vol. 50, no. 4, pp. 259–266, 2000.

[105] H. Sies, "Oxidative stress: oxidants and antioxidants," *Experimental Physiology*, vol. 82, no. 2, pp. 291–295, 1997.

[106] D. F. Murrell, "A radical proposal for the pathogenesis of scleroderma," *Journal of the American Academy of Dermatology*, vol. 28, no. 1, pp. 78–85, 1993.

[107] A. Gabrielli, S. Svegliati, G. Moroncini, G. Pomponio, M. Santillo, and E. V. Avvedimento, "Oxidative stress and the pathogenesis of scleroderma: the Murrell's hypothesis revisited," *Seminars in Immunopathology*, vol. 30, no. 3, pp. 329–337, 2008.

[108] A. Gabrielli, S. Svegliati, G. Moroncini, and D. Amico, "New insights into the role of oxidative stress in scleroderma fibrosis," *Open Rheumatol J*, vol. 6, no. 1, pp. 87–95, 2012.

[109] B. Grygiel-Górniak and M. Puszczewicz, "Oxidative damage and antioxidative therapy in systemic sclerosis," *Mediators of Inflammation*, vol. 2014, Article ID 389582, 11 pages, 2014.

[110] F. Boin, G. L. Erre, A. M. Posadino et al., "Oxidative stress-dependent activation of collagen synthesis is induced in human pulmonary smooth muscle cells by sera from patients with scleroderma-associated pulmonary hypertension," *Orphanet Journal of Rare Diseases*, vol. 9, no. 1, p. 123, 2014.

[111] M. Jiang, Y. Yu, J. Luo et al., "Bone marrow-derived mesenchymal stem cells expressing thioredoxin 1 attenuate bleomycin-induced skin fibrosis and oxidative stress in scleroderma," *The Journal of Investigative Dermatology*, vol. 137, no. 6, pp. 1223–1233, 2017.

[112] P. Sambo, D. Amico, R. Giacomelli et al., "Intravenous N-acetylcysteine for treatment of Raynaud's phenomenon secondary to systemic sclerosis: a pilot study," *The Journal of Rheumatology*, vol. 28, no. 10, pp. 2257–2262, 2001.

[113] P. Failli, L. Palmieri, C. D'Alfonso et al., "Effect of N-acetyl-L-cysteine on peroxynitrite and superoxide anion production of lung alveolar macrophages in systemic sclerosis," *Nitric Oxide*, vol. 7, no. 4, pp. 277–282, 2002.

[114] M. Demedts, J. Behr, R. Buhl et al., "High-dose acetylcysteine in idiopathic pulmonary fibrosis," *New England Journal of Medicine*, vol. 353, no. 21, pp. 2229–2242, 2005.

[115] C. F. Zhou, J. F. Yu, J. X. Zhang et al., "N-acetylcysteine attenuates subcutaneous administration of bleomycin-induced skin fibrosis and oxidative stress in a mouse model of scleroderma," *Clinical and Experimental Dermatology*, vol. 38, no. 4, pp. 403–409, 2013.

[116] P. S. Tsou, N. N. Talia, A. J. Pinney et al., "Effect of oxidative stress on protein tyrosine phosphatase 1B in scleroderma dermal fibroblasts," *Arthritis and Rheumatism*, vol. 64, no. 6, pp. 1978–1989, 2012.

[117] R. Sgonc, M. S. Gruschwitz, H. Dietrich, H. Recheis, M. E. Gershwin, and G. Wick, "Endothelial cell apoptosis is a primary pathogenetic event underlying skin lesions in avian and human scleroderma," *The Journal of Clinical Investigation*, vol. 98, no. 3, pp. 785–792, 1996.

[118] T. Yamamoto and K. Nishioka, "Possible role of apoptosis in the pathogenesis of bleomycin-induced scleroderma," *The Journal of Investigative Dermatology*, vol. 122, no. 1, pp. 44–50, 2004.

[119] A. Kessel, I. Rosner, M. Rozenbaum et al., "Increased CD8+ T cell apoptosis in scleroderma is associated with low levels of NF-kappa B," *Journal of Clinical Immunology*, vol. 24, no. 1, pp. 30–36, 2004.

[120] M. Ha and V. N. Kim, "Regulation of microRNA biogenesis," *Nature Reviews Molecular Cell Biology*, vol. 15, no. 8, pp. 509–524, 2014.

[121] S. Vasudevan, "Posttranscriptional upregulation by microRNAs," *Wiley Interdisciplinary Reviews: RNA*, vol. 3, no. 3, pp. 311–330, 2012.

[122] J. A. Makarova, M. U. Shkurnikov, D. Wicklein et al., "Intracellular and extracellular microRNA: an update on localization and biological role," *Progress in Histochemistry and Cytochemistry*, vol. 51, no. 3-4, pp. 33–49, 2016.

[123] G. Fu, J. Brkić, H. Hayder, and C. Peng, "MicroRNAs in human placental development and pregnancy complications," *International Journal of Molecular Sciences*, vol. 14, no. 3, pp. 5519–5544, 2013.

[124] Y. Peng and C. M. Croce, "The role of microRNAs in human cancer," *Signal Transduction and Targeted Therapy*, vol. 1, no. 1, pp. 1–9, 2016.

[125] S. Koba, M. Jinnin, K. Inoue et al., "Expression analysis of multiple microRNAs in each patient with scleroderma," *Experimental Dermatology*, vol. 22, no. 7, pp. 489–491, 2013.

[126] N. Honda, M. Jinnin, I. Kajihara et al., "TGF-β–mediated downregulation of microRNA-196a contributes to the constitutive upregulated type I collagen expression in scleroderma dermal fibroblasts," *The Journal of Immunology*, vol. 188, no. 7, pp. 3323–3331, 2012.

[127] K. Makino, M. Jinnin, A. Hirano et al., "The downregulation of microRNA let-7a contributes to the excessive expression of type I collagen in systemic and localized scleroderma," *The Journal of Immunology*, vol. 190, no. 8, pp. 3905–3915, 2013.

[128] T. Sing, M. Jinnin, K. Yamane et al., "MicroRNA-92a expression in the sera and dermal fibroblasts increases in patients with scleroderma," *Rheumatology*, vol. 51, no. 9, pp. 1550–1556, 2012.

[129] N. Honda, M. Jinnin, T. Kira-Etoh et al., "miR-150 downregulation contributes to the constitutive type I collagen overexpression in scleroderma dermal fibroblasts via the induction of integrin β3," *The American Journal of Pathology*, vol. 182, no. 1, pp. 206–216, 2013.

[130] W. Nakayama, M. Jinnin, Y. Tomizawa et al., "Dysregulated interleukin-23 signalling contributes to the increased collagen production in scleroderma fibroblasts via balancing microRNA expression," *Rheumatology (Oxford)*, vol. 56, no. 1, pp. 145–155, 2017.

[131] M. Eddouks, A. Lemhadri, and J.-B. Michel, "Caraway and caper: potential anti-hyperglycaemic plants in diabetic rats," *Journal of Ethnopharmacology*, vol. 94, no. 1, pp. 143–148, 2004.

[132] Y.-l. Cao, X. Li, and M. Zheng, "Capparis spinosa protects against oxidative stress in systemic sclerosis dermal fibroblasts," *Archives of Dermatological Research*, vol. 302, no. 5, pp. 349–355, 2010.

[133] L. Dong, L. Fan, G. F. Li, Y. Guo, J. Pan, and Z. W. Chen, "Anti-aging action of the total lactones of ginkgo on aging mice," *Acta Pharmaceutica Sinica*, vol. 39, no. 3, pp. 176–179, 2004.

[134] M.-S. Tan, J. T. Yu, C. C. Tan et al., "Efficacy and adverse effects of ginkgo biloba for cognitive impairment and dementia: a systematic review and meta-analysis," *Journal of Alzheimer's Disease*, vol. 43, no. 2, pp. 589–603, 2015.

[135] J. Smith and Y. Luo, "Studies on molecular mechanisms of Ginkgo biloba extract," *Applied Microbiology and Biotechnology*, vol. 64, no. 4, pp. 465–472, 2004.

[136] Z. Mirfeizi, M. Jokar, and M. Mirfeizi, "Ginkgo biloba reduces the duration and severity of Raynaud's attacks of patients with systemic sclerosis," *Clinical and Experimental Rheumatology*, vol. 32, no. 2, pp. S72–S72, 2014.

[137] Y. Nagata, H. Goto, H. Hikiami et al., "Effect of keishibukuryogan on endothelial function in patients with at least one component of the diagnostic criteria for metabolic syndrome: a controlled clinical trial with crossover design," *Evidence-based Complementary and Alternative Medicine*, vol. 2012, Article ID 359282, 10 pages, 2012.

[138] Q. Wang, G. Shi, Y. Zhang et al., "Deciphering the potential pharmaceutical mechanism of GUI-ZHI-FU-LING-WAN on systemic sclerosis based on systems biology approaches," *Scientific Reports*, vol. 9, no. 1, pp. 1–13, 2019.

[139] F. Y. Sheng, A. Ohta, and M. Yamaguchi, "Inhibition of collagen production by traditional Chinese herbal medicine in scleroderma fibroblast cultures," *Internal Medicine*, vol. 33, no. 8, pp. 466–471, 1994.

[140] M. Martin and J. Tooke, "Effects of prostaglandin E1 on microvascular haemodynamics in progressive systemic sclerosis," *British Medical Journal (Clinical Research Ed.)*, vol. 285, no. 6356, pp. 1688–1690, 1982.

[141] J. J. F. Belch, B. Shaw, A. O'Dowd et al., "Evening primrose oil (Efamol) in the treatment of Raynaud's phenomenon: a double blind study," *Thrombosis and Haemostasis*, vol. 53, no. 2, pp. 490–494, 1985.

[142] A. Strong, A. Campbell, and J. Thomson, "The effect of oral linoleic acid and gamma-linolenic acid (Efamol [G])," *The British Journal of Clinical Practice*, vol. 39, no. 11-12, pp. 444-445, 1985.

[143] B. A. Christiansen, S. Bhatti, R. Goudarzi, and S. Emami, "Management of osteoarthritis with avocado/soybean unsaponifiables," *Cartilage*, vol. 6, no. 1, pp. 30–44, 2015.

[144] L. Altinel, Z. K. Saritas, K. C. Kose, K. Pamuk, Y. Aksoy, and M. Serteser, "Treatment with unsaponifiable extracts of avocado and soybean increases TGF-.BETA.1 and TGF-.BETA.2 levels in canine joint fluid," *The Tohoku Journal of Experimental Medicine*, vol. 211, no. 2, pp. 181–186, 2007.

[145] F.-J. He and J.-Q. Chen, "Consumption of soybean, soy foods, soy isoflavones and breast cancer incidence: differences between Chinese women and women in Western countries

and possible mechanisms," *Food Science and Human Wellness*, vol. 2, no. 3-4, pp. 146–161, 2013.

[146] S. L. Ownby, L. V. Fortuno, A. Y. Au, M. W. Grzanna, A. M. Rashmir-Raven, and C. G. Frondoza, "Expression of pro-inflammatory mediators is inhibited by an avocado/soybean unsaponifiables and epigallocatechin gallate combination," *Journal of Inflammation*, vol. 11, no. 1, p. 8, 2014.

[147] S. Jablonska, "Avocado/soybean unsaponifiables in the treatment of scleroderma: comment on the article by Maheu et al.," *Arthritis & Rheumatism*, vol. 41, no. 9, pp. 1705–1705, 1998.

[148] M. Lv, J. Deng, N. Tang, Y. Zeng, and C. Lu, "Efficacy and safety of Tripterygium wilfordii Hook F on psoriasis vulgaris: a systematic review and meta-analysis of randomized controlled trials," *Evidence-based Complementary and Alternative Medicine*, vol. 2018, Article ID 2623085, 10 pages, 2018.

[149] Q. W. Lv, W. Zhang, Q. Shi et al., "Comparison of Tripterygium wilfordii Hook F with methotrexate in the treatment of active rheumatoid arthritis (TRIFRA): a randomised, controlled clinical trial," *Annals of the Rheumatic Diseases*, vol. 74, no. 6, pp. 1078–1086, 2015.

[150] L. Yang, Q. Wang, Y. Hou et al., "The Chinese herb Tripterygium wilfordii Hook F for the treatment of systemic sclerosis-associated interstitial lung disease: data from a Chinese EUSTAR Center," *Clinical Rheumatology*, vol. 39, no. 3, pp. 813–821, 2020.

[151] X. Song, J. Wang, P. Wang, N. Tian, M. Yang, and L. Kong, "^{1}H NMR-based metabolomics approach to evaluate the effect of Xue-Fu-Zhu-Yu decoction on hyperlipidemia rats induced by high-fat diet," *Journal of Pharmaceutical and Biomedical Analysis*, vol. 78-79, pp. 202–210, 2013.

[152] W. Wen-ling, S. You-ming, Y. Rong-ya, Z. Jie, and X. Yang, "Follow-up efficacy of integrative Chinese and Western drugs on localized scleroderma with vitamine B 6 and Xuefu Zhuyu decoction," *Chinese Journal of Integrative Medicine*, vol. 11, no. 1, pp. 34–36, 2005.

[153] M. Magnone, S. Bruzzone, L. Guida et al., "Abscisic acid released by human monocytes activates monocytes and vascular smooth muscle cell responses involved in atherogenesis," *Journal of Biological Chemistry*, vol. 284, no. 26, pp. 17808–17818, 2009.

[154] S. Bruzzone, F. Battaglia, E. Mannino et al., "Abscisic acid ameliorates the systemic sclerosis fibroblast phenotype in vitro," *Biochemical and Biophysical Research Communications*, vol. 422, no. 1, pp. 70–74, 2012.

[155] T. Pataki, I. Bak, P. Kovacs, D. Bagchi, D. K. Das, and A. Tosaki, "Grape seed proanthocyanidins improved cardiac recovery during reperfusion after ischemia in isolated rat hearts," *The American Journal of Clinical Nutrition*, vol. 75, no. 5, pp. 894–899, 2002.

[156] R. Kalfin, A. Righi, A. del Rosso et al., "Activin, a grape seed-derived proanthocyanidin extract, reduces plasma levels of oxidative stress and adhesion molecules (ICAM-1, VCAM-1 and E-selectin) in systemic sclerosis," *Free Radical Research*, vol. 36, no. 8, pp. 819–825, 2002.

[157] I.-S. Shin, J. Hong, C. M. Jeon et al., "Diallyl-disulfide, an organosulfur compound of garlic, attenuates airway inflammation via activation of the Nrf-2/HO-1 pathway and NF-kappaB suppression," *Food and Chemical Toxicology*, vol. 62, pp. 506–513, 2013.

[158] J. Zhou, Z. Qu, S. Yan et al., "Differential roles of STAT3 in the initiation and growth of lung cancer," *Oncogene*, vol. 34, no. 29, pp. 3804–3814, 2015.

[159] S. Zhang, Y. Liu, Y. Ye et al., "Bee venom therapy: potential mechanisms and therapeutic applications," *Toxicon*, vol. 148, pp. 64–73, 2018.

[160] J. H. Hwang and K.-H. Kim, "Bee venom acupuncture for circumscribed morphea in a patient with systemic sclerosis: a case report," *Medicine*, vol. 97, no. 49, p. e13404, 2018.

[161] E. Tourkina, P. Gooz, J. C. Oates, A. Ludwicka-Bradley, R. M. Silver, and S. Hoffman, "Curcumin-induced apoptosis in scleroderma lung fibroblasts," *American Journal of Respiratory Cell and Molecular Biology*, vol. 31, no. 1, pp. 28–35, 2004.

[162] C. Busch, C. Jacob, A. Anwar et al., "Diallylpolysulfides induce growth arrest and apoptosis," *International Journal of Oncology*, vol. 36, no. 3, pp. 743–749, 2010.

[163] W. Marut, V. Jamier, N. Kavian et al., "The natural organosulfur compound dipropyltetrasulfide prevents HOCl-induced systemic sclerosis in the mouse," *Arthritis Research & Therapy*, vol. 15, no. 5, p. R167, 2013.

[164] J. Liu, F. Yin, X. Zheng, J. Jing, and Y. Hu, "Geniposide, a novel agonist for GLP-1 receptor, prevents PC12 cells from oxidative damage via MAP kinase pathway," *Neurochemistry International*, vol. 51, no. 6-7, pp. 361–369, 2007.

[165] Q. Qi, Y. Mao, Y. Tian et al., "Geniposide inhibited endothelial-mesenchymal transition via the mTOR signaling pathway in a bleomycin-induced scleroderma mouse model," *American Journal of Translational Research*, vol. 9, no. 3, pp. 1025–1036, 2017.

[166] M. Hasegawa, Y. Matsushita, M. Horikawa et al., "A novel inhibitor of Smad-dependent transcriptional activation suppresses tissue fibrosis in mouse models of systemic sclerosis," *Arthritis & Rheumatism*, vol. 60, no. 11, pp. 3465–3475, 2009.

[167] J. T. C. Tzen, T. R. Jinn, Y. C. Chen et al., "Magnesium lithospermate B possesses inhibitory activity on Na^+,K^+-ATPase and neuroprotective effects against ischemic stroke," *Acta Pharmacologica Sinica*, vol. 28, no. 5, pp. 609–615, 2007.

[168] T. Shigematsu, S. Tajima, T. Nishikawa, S. Murad, S. R. Pinnell, and I. Nishioka, "Inhibition of collagen hydroxylation by lithospermic acid magnesium salt, a novel compound isolated from *Salviae miltiorrhizae* Radix," *Biochimica et Biophysica Acta (BBA)-General Subjects*, vol. 1200, no. 1, pp. 79–83, 1994.

[169] M. A. Alzohairy, "Therapeutics role of Azadirachta indica (Neem) and their active constituents in diseases prevention and treatment," *Evidence-based Complementary and Alternative Medicine*, vol. 2016, Article ID 7382506, 11 pages, 2016.

[170] S. Diddi, S. Bale, G. Pulivendala, and C. Godugu, "Nimbolide ameliorates fibrosis and inflammation in experimental murine model of bleomycin-induced scleroderma," *Inflammopharmacology*, vol. 27, no. 1, pp. 139–149, 2019.

[171] K. I. Izaka, M. Yamada, T. Kawano, and T. Suyama, "Gastrointestinal absorption and anti-inflammatory effect of bromelain," *Japanese Journal of Pharmacology*, vol. 22, no. 4, pp. 519–534, 1972.

[172] H. E. Pierce Jr., "Pineapple proteases in the treatment of scleroderma: a case report," *Journal of the National Medical Association*, vol. 56, no. 3, p. 272, 1964.

[173] W. Chen, F. Tang, B. Xie, S. Chen, H. Huang, and P. Liu, "Amelioration of atherosclerosis by tanshinone IIA in

hyperlipidemic rabbits through attenuation of oxidative stress," *European Journal of Pharmacology*, vol. 674, no. 2-3, pp. 359–364, 2012.

[174] Q.-S. Liu, X. C. Zhu, J. A. Li et al., "Effects of danshen injection on the proliferation of rheumatoid arthritis fibroblast-like synoviocytes cultured with human serum," *Zhongguo Zhong xi yi Jie he za Zhi Zhongguo Zhongxiyi Jiehe Zazhi= Chinese Journal of Integrated Traditional and Western Medicine*, vol. 33, no. 5, pp. 674–678, 2013.

[175] M. Liu, J. Yang, and M. Li, "Tanshinone IIA attenuates interleukin-17A-induced systemic sclerosis patient-derived dermal vascular smooth muscle cell activation via inhibition of the extracellular signal-regulated kinase signaling pathway," *Clinics*, vol. 70, no. 4, pp. 250–256, 2015.

[176] G. Singh, P. K. Sharma, R. Dudhe, and S. Singh, "Biological activities of Withania somnifera," *Annals of Biological Research*, vol. 1, no. 3, pp. 56–63, 2010.

[177] S. Bale, G. Pulivendala, and C. Godugu, "Withaferin a attenuates bleomycin-induced scleroderma by targeting FoxO3a and NF-$\kappa\beta$ signaling: connecting fibrosis and inflammation," *BioFactors*, vol. 44, no. 6, pp. 507–517, 2018.

[178] E. P. Stern and C. P. Denton, "The pathogenesis of systemic sclerosis," *Rheumatic Disease Clinics of North America*, vol. 41, no. 3, pp. 367–382, 2015.

Hindawi
Journal of Immunology Research
Volume 2021, Article ID 8167283, 9 pages
https://doi.org/10.1155/2021/8167283

Review Article

Role of Intestinal Microbiota on Gut Homeostasis and Rheumatoid Arthritis

Mingxin Li[1] **and Fang Wang**[2]

[1]*Department of Traumatic Orthopaedics, Tianjin Hospital, 406 Jiefangnan Road 406, Tianjin 300210, China*
[2]*College of Mechanical Engineering, Tianjin University of Science and Technology, The Key Laboratory of Integrated Design and On-Line Monitoring of Light Industrial and Food Engineering Machinery and Equipment in Tianjin, Tianjin 300222, China*

Correspondence should be addressed to Fang Wang; fwang@tust.edu.cn

Received 16 April 2021; Accepted 29 May 2021; Published 7 June 2021

Academic Editor: Wen-Kai Ren

Rheumatoid arthritis (RA) is a chronic inflammatory disease that is immune mediated. Patients typically present with synovial inflammation, which gradually deteriorates to investigate severe cartilage and bone damage, affecting an individual's ability to perform basic tasks and impairing the quality of life. When evaluated against healthy controls, patients with RA have notable variations within the constituents of the gut microbiota. The human gastrointestinal tract mucosa is colonized by trillions of commensal microbacteria, which are key actors in the initiation, upkeep, and operation of the host immune system. Gut microbiota dysbiosis can adversely influence the immune system both locally and throughout the host, thus predisposing the host to a number of pathologies, including RA. Proximal intestinal immunomodulatory cells, situated in specific locales within the intestine, are a promising intermediary through which the gastrointestinal microbiota can influence the pathogenesis and progression of RA. In the early stages of the disease, the microbiota appear to differ from those present in healthy controls. This difference may reflect potential autoimmune mechanisms. Research studies evaluating intestinal microbiota have demonstrated that RA is associated with a bacterial population growth or with a decline when judged against control groups. The aim of this review is to examine the studies that connect intestinal dysbiosis with the autoimmune pathways implicated in the pathogenesis of RA.

1. Introduction

Rheumatoid arthritis (RA) is a chronic, immune-mediated disease with an inflammatory pathology. Clinical features include joint swelling, joint tenderness, synovial joint damage, and manifestations of systemic inflammation. RA typically leads to marked disability and an early demise [1, 2]. Premature death results predominantly from excess cardiovascular phenomena that occur autonomously from conventional cardiovascular risk factors and that are linked with augmented systemic inflammation [3]. The exact cause of RA is incompletely elucidated. The contemporary perspective is that, in individuals who have a genetic predisposition to RA, environmental agents provoke a pathological triggering of the immune system that ultimately leads to the clinical syndrome [3].

The European League Against Rheumatism has suggested certain nomenclature for the distinct preclinical stages of RA progression, which do not automatically fall in series and are not incongruous [4]. The risk of RA is heightened by the interplay between the genetic and environmental elements, together with the existence of autoantibodies.

In terms of environmental contributors, the gut microbiota has been shown in mice to participate in the development of arthritis [4, 5]. Increasing numbers of publications have recognized aberrations in gut microbiota constituents as major players in multiple pathological processes, the most notable being chronic inflammatory conditions [6, 7]. Recent work has indicated that some change in the constituents of the gut microbiota leads to a dysbiotic state that impacts the governance of immune function and fosters a proinflammatory phenotype [8]. Consequences include enhanced

vulnerability to autoimmune disorders (e.g., inflammatory bowel disease, systemic inflammatory arthritis, and connective tissue pathologies), dysmetabolic syndromes, and malignancies [7].

It has recently been demonstrated in humans that immunoglobulin A (IgA) anticitrullinated protein antibodies (ACPAs) can be identified for many years before the clinical presentation of arthritis [9]. This finding implies that RA is derived from mucosal areas, such as the intestine and the mouth. The clinical efficacy of antibacterial agents (e.g., minocycline or salazosulfapyridine) in some patients with RA supports the theory that the gut and oral microbial populations are associated with RA [10].

The purpose of this review is to evaluate studies that have demonstrated changes in the constituents of gut microbiota in patients with RA. Furthermore, the presented evidence connects intestinal dysbiosis with the autoimmune pathways implicated in the pathogenesis of RA.

2. Immunopathogenesis of RA

Elucidation of the complicated molecular pathways that contribute to the development of RA remains fraught with difficulty. A range of environmental elements may silently trigger a pathological stimulation of the immune system in individuals who have a genetic predisposition [11]. This untoward immune system galvanization may lead to the synthesis of clinically silent autoantibodies, such as rheumatoid factor (RF) or ACPA. There may then be a period of minimal symptomatology or a preclinical stage, which generally heralds the clinically evident presentation of features that represent typical RA [12].

Earlier work has proposed that immune irregularities, such as immunomodulatory cell (IC) stimulation or suppression, that occur at regional and then systemic levels exist in individuals who are predisposed toward RA [13]. Populations of T and B lymphocyte subsets, in terms of both number and activity, are linked with the mechanisms underlying RA onset [3]. Potential antigens include type II collagen, proteoglycans, and cartilage protein gp39 [14, 15].

The joints of people with RA are complex structures in which intrinsic and adaptive immune cell populations, together with local cell types (i.e., synoviocytes and chondrocytes), participate in the disease process [16]. Autoantibodies and autoreactive T cells identified within the joints reflect the dysregulatory state of the immune system. The manufacture of autoreactive B cells is the most evident change in the immune system of an individual with RA, and this process develops well before the onset of clinical disease. Essential for the pathogenesis of RA, autoreactive B cells generate ACPAs and RFs. Within lymphoid regions, heightened T cell stimulation is associated with the perseverance of switched memory B cells [17]. Fc receptor-like protein 4 is a subset of memory B cells that expresses IgA. It is involved in the regional autoimmune response that promotes joint damage in individuals with RA via receptor stimulation of nuclear factor-κB ligand expression [18].

Many immune system aberrations in RA develop at the level of the mucosa. During RA onset, the immune response within the intestinal mucosa is notably amplified, antigen-presenting cells (APCs) display aberrant stimulation, and immune tolerance is disrupted [19]. Diminished immunity in the mucosa to citrullinated proteins or peptides together with novel B cell conscription is an essential element of antirheumatic treatment responses in individuals at a premature stage of the disease [20].

Many cell types participate in the disease process of RA. Within the synovium, dendritic cells are located predominantly within lymphocytic clusters and the peripheral vasculature, implying that they are derived from the circulation. APCs express major histocompatibility complex alleles that associate extracellular peptides with $CD4^+$ T cells, thus impelling the liberation of proinflammatory cytokines that trigger the manufacture of antibodies from B cells [21].

In rats with collagen-induced arthritis (CIA), $CD8^+$ and $CD4^+$ cell populations were elevated in Peyer's patches compared with the levels in control animals [22]. In mice with CIA, Sundstrom et al. [23] demonstrated that $CD4^+$ T cells in the lamina propria were stimulated before the clinical development of arthritis. This change developed after notable upregulation of interleukin-17A (IL-17A), tumor necrosis factor-alpha (TNF-α), and granulocyte-macrophage colony-stimulating factor. The clinical gravity of the arthritis was notably diminished in the absence of Th17 [23]. Th17 differentiation is bolstered by an environment that contains macrophage-derived and dendritic cell-derived transforming growth factor-β and interleukin-1β, IL-6, IL-21, and IL-23. These factors also inhibit the differentiation of regulatory T cells, thus causing T cell homeostasis to incline toward the inflammatory process [24].

Posttranslational modifications (PTMs) are vital for protein function and antigenicity. Citrullination involves the modification of arginine into citrulline, a reaction catalyzed by peptidyl arginine deiminases; this reaction forms the principal PTM linked with self-antigen identification in RA [21]. Citrulline may change protein configuration and produce novel epitopes linked with the manufacture of ACPAs. Repertoire sequencing before clinical presentation in individuals with RA has demonstrated that this immune phenomenon commences in a highly limited fashion and then magnifies during a time period of several months to possibly years. Epitope dissemination, from the first identified epitope, expands to trigger reactivity to a range of epitopes before RA is diagnosed [25, 26].

The distribution of epitopes trends toward more citrullinated moieties, which is in keeping with the theory that an individual antigen, although not necessarily the identical antigen, initiates the immune response [12]. The levels of ACPAs increase, and the variation in epitopes increases before clinical presentation. ACPAs may encompass the isotypes IgG, IgA, and IgM, and a changed glycosylation condition bestows an augmented binding affinity for the Fc receptor and citrullinated antigens [27]. ACPAs can then act as pathogens per se by stimulating either macrophages or osteoclasts, a reaction mediated by the manufacture of immune complexes and Fc receptor association or, potentially, through an attachment to citrullinated vimentin in the cell membrane, which exacerbates bone loss [27].

Blood analysis of individuals with early RA who have been prescribed antirheumatic treatment has demonstrated that the titers of ACPA, IgA, and IgM swiftly decline, a change associated with reduced pathological activity [11]. The first recognition of antibodies in a subcohort of patients with RA was in the form of citrullinated antigens, but studies now suggest that citrullinated epitopes of numerous autoantigens and antigens originating from microorganisms can be identified by antibodies that are extremely specific for RA [11].

Genetic elements alone are clearly not solely responsible for RA [28], and the contribution of additional risk factors requires deeper investigation. It has been postulated that, during the preclinical stage of RA, an interplay among microbes, other candidate environmental elements (e.g., diet, physical or emotional pressures), and host factors arises at the mucosa, precipitating mucosal inflammation and the disruption of immune tolerance. Mucosal inflammation may then itself promote local and ultimately systemic immune dysregulation. Involved mechanisms may encompass molecular imitation or may enable immediate autoimmunity to the host's own antigens [29, 30].

Additional studies have indicated that the gut microbiota may represent a substantial experimental element in the pathogenesis of RA [31]. Changes in certain mucosal territories imply that microbial factors may influence the local mucosal immune response, thus also contributing to the early phase of RA development [32].

Variations in the microbiota constituent populations and their frequency (i.e., dysbiosis) can stimulate a number of autoimmune and inflammatory pathologies through a loss of equilibrium in the T cell subpopulation (e.g., Th1, Th2, Th17, and Treg cells) [16]. At the mucosal level, citrullinated microbial antigens and molecular mimicry, Toll-like receptor (TLR) signals, and additional intrinsic immune stimulators and hazard signals may be present [32]. Microbiological organisms linked with the mucosa influence members of the immune system (i.e., neutrophils, dendritic cells, and macrophages), viewing them as pathogenic and inflicting injury. This response leads to inflammation, the liberation of cytokines, an increase in chemokine levels, and autoantigen synthesis. Thus, potential engagement occurs among the gut microbiota, ICs, and the pathogenesis and progression of RA—a situation that has gained much attention recently.

3. General Introduction to Intestinal Microbiota

The most sizeable population of colonized bacteria within the human body is situated in the gastrointestinal tract. Each individual contains several hundred species [33], of which more than 90% are members of the *Bacteroidetes* and *Firmicutes* phyla. However, additional phyla (i.e., *Proteobacteria*, *Actinobacteria*, *Fusobacteria*, *Verrucomicrobia*, and *Cyanobacteria*) are also integral players in the upkeep of governance of microbiota homeostasis [30]. The microbiota perform many activities, but a key contribution is that of maintaining host immune system homeostasis. As a consequence, homeostasis may be influenced by any change in the microbiota population [34].

The adult configuration of the microbiota is formed immediately after birth [31]. Within the bacterial population, a number of advantageous symbiotic organisms contribute to homeostasis in a benign and mutually beneficial fashion. Also present are sensitive bacteria that are adversely impacted in the presence of pathologies, pathogenic members of the population that may induce disease, and therapeutic organisms that can assist in restoring the status quo after change [31].

The population of bacteria in the gut can be affected by diet, probiotics, prebiotics, antibiotics, exogenous enzymes, fecal microbiota transplantation (FMT), and additional environmental elements [35]. The microbiota work in concert with the intestinal interface to perform essential activities relating to the safeguarding of the immune homeostasis. Two key elements that may fluctuate and affect barrier robustness and its operation, with consequences on the governance of intestinal permeability, are diet and intestinal microbiota. These elements may permit external antigens to traverse the interface from the gut cavity into the host [33, 36]. These factors are both a consequence of lifestyle, which implies that environmental elements can affect the integrity of the intestinal interface's operations and therefore affect the immune response and the development of conditions such as RA [33].

The gut microbiota have been implicated in the pathogenesis of numerous intestinal and extraintestinal disorders [37]. Furthermore, dysbiosis of the microorganisms within the gut is tightly linked to the intestinal mucosal immune system, which has been associated with autoimmune conditions, including RA. Indeed, changes within the types (i.e., taxa, phyla, or genera) and prevalence of organisms exist; variations within this bacterial population develop at a premature stage of the disease [38], although the pathways underlying the pathogenesis of the changes remain unclear at both the cellular and molecular levels.

4. Evidence from Animal Models

Several rodent models of arthritis, including models of SKG, IL-1ra$^{-/-}$, K/BxN, and CIA, have demonstrated the significance of the intestinal microbiota in the pathogenesis of RA [39, 40]. If mice are raised in a germ-free environment or administered antimicrobials, arthritis does not develop [39]. In germ-free-reared mice, the injection of certain microorganisms can precipitate arthritis [40], implying that the gut microbiota are instrumental in disease development. Specifically, some studies have demonstrated an exacerbation of RA in microbiota-colonized SKG mice [39, 41]. Another report in germ-free SKG mice monocolonized with *Prevotella copri* showed that arthritis could be triggered by a fungal injection [39]. Despite some research reporting an association of *Prevotella* species with the pathogenesis of arthritis, other publications have postulated that *Prevotella* is actually an advantageous, rather than a disease-inducing, species [42, 43].

One study compared bacterial types and proposed that immunological features cannot be determined by the phylum to which the bacterium belongs; this study emphasized the

need to delineate traits at the level of the individual species [44]. Marietta et al. [44] assessed two species of *Prevotella* in relation to arthritis prophylaxis and therapy in HLA-DA8 mice. The capacity to influence the immune response was inconstant between the two strains. *Prevotella histicola* repressed the onset of arthritis by influencing the immune response (i.e., the governance of dendritic cells and the production of Treg cells), leading to suppression of the Th17 response and a decrease in inflammatory cytokines (i.e., IL-2, IL-17, and TNF). Conversely, *Prevotella melaninogenica* induced no alterations in cytokine titers and failed to inhibit the onset of arthritis. *P. histicola* was evaluated in a DBA/1 murine model, which showed that animals receiving this strain acquired less severe arthritis than the animals in the control cohort. These results clarify the fact that an individual *Prevotella* strain can behave in either a positive or an adverse fashion, according to the setting. This variation may be a reason that *Prevotella* species are plentiful in healthy microbiota, and it implies that only some strains have disease-inducing traits.

Segmented filamentous bacteria, which are gut commensals, are able to provoke robust gastrointestinal and systemic follicular helper T (TFH) cell responses, which lead to a surge in autoantibody manufacturing in K/BxN mice [45]. In SKG mice that have received curdlan, an IL-23-dependent decrease in intestinal goblet cells leads to impaired epithelial barrier operation. Furthermore, naïve SKG mice display fecal dysbiosis that also relies on IL-23. IL-23a is intrinsically expressed within the small intestine of naïve SKG animals but is lacking in the gut of naïve BALB/c or germ-free SKG mice [40]. In SKG mice, IL-23 prefers the outgrowth of spondyloarthritis-linked pathobionts, such as *Bacteroidaceae*, *Porphyromonadaceae*, and *Prevotellaceae*, and diminishes the reinforcement for homeostatic-generating microbiota, including *Clostridiaceae* and *Lachnospiraceae* [46]. In mice, the host mucosal-microbial boundary likely contributes substantially to IL-23-dependent mechanisms in the development of arthritis.

IL-1 receptor antagonist knockout (IL-1rn$^{-/-}$) mice spontaneously acquire T cell-mediated arthritis under certain pathogen-free circumstances, forming another experimental murine model [47]. These animals fail to present with arthritis in a germ-free habitat. If the mice are monocolonized with *Lactobacillus bifidus*, arthritis is precipitated.

A study by Rogier et al. [48] demonstrated that the changed microbiota in RA is typified by a large prevalence of *Helicobacter* species and a modest presence of *Ruminococcus* species. Therapy with tobramycin diminished the quantity of commensal microorganisms, including *Helicobacter* species, and inhibited the development of arthritis in IL-1ra -/-$^{-/-}$ rodents. In addition, when IL-1ra and TLR4 double-knockout mice were examined, dysbiosis in IL-1ra$^{-/-}$ mice was demonstrated to be TLR4 dependent in nature [48].

A T cell receptor transgenic murine model of inflammatory arthritis, the K/BxN scenario, offers straightforward discernment between the initiation and effector phases [49]. K/BxN T cell receptor transgenic mice present with inflammatory joint disease associated with elevated autoantibodies toward glucose-6-phosphate isomerase [50]. When established in a germ-free setting, the mice fail to develop arthritis; diminished Th17 cell populations can be observed within the small intestine and spleen [51]. The addition of a monocolony of segmented filamentous organisms is enough to generate Th17 cell-dependent arthritis in these mice.

CIA models are frequently used to explore the mechanisms underlying RA. In this setting, alterations in the gut microbiota develop in the early, immune-priming phase, before clinical presentation of disease [4]. In one study, *Firmicutes* and *Proteobacteria* phyla formed the key actors within the intestinal microbiota; the prevalence of *Bacteroides* was diminished in mice with RA compared with levels in naïve DBA/1 mice [52].

Additional work has explored the microbiome of DBA/1 mice in those developing resistance or already resistant to CIA after immunization with type II collagen. Compared with the controls, mice with arthritis had a notably reduced spectrum of bacterial types; this reduction did not occur in the mice showing resistance to arthritis. The mice vulnerable to CIA had the greatest diversity of phyla before the clinical presentation of disease; the most prevalent phyla were *Firmicutes*, *Bacteroidetes*, and *Proteobacteria*. *Lactobacillaceae* were also more prevalent in the animals susceptible to CIA; the genus *Lactobacillus* was markedly more plentiful after the generation of arthritis in the CIA-susceptible versus the CIA-resistant animals [53]. Jubair et al. [54] also documented that CIA can be stimulated by intestinal dysbiosis through mucosal immune responses. In that study, dysbiosis and inflammatory mucosal reactions developed before CIA onset [54]. Jubair et al. [54] also decreased the microbiota using broad-spectrum antimicrobials in a time-dependent fashion. This reduction in microbiota had a maximal effect on the gravity of arthritis when implemented late after the booster injection, whereas microbiota depletion before the immunization had a more modest influence on the disease. The two antimicrobial prescriptions both resulted in the late synthesis of anti-type II collagen antibodies. However, only late administration decreased the glycosylation and complement-fixing capacity of anti-type II collagen antibodies [54].

The results of this study reinforce the conclusion that the host mucosal-microbial boundary is a major participant in enhancing inflammation in concert with the actions of the microbiota, thus triggering autoantibody glycosylation and provoking antigen-antibody-mediated joint disease. Therapy with antimicrobials mitigated disease gravity and diminished anti-type II collagen antibody and serum inflammatory cytokine titers. Thus, some commensal microbiota from the gastrointestinal tract are adequate to precipitate arthritis in murine models, although more detailed evaluations are required to pinpoint effects that may be implicated in arthritis for specific organisms.

5. Dysbiosis and Intestinal Microbiota in Humans with RA

Studies from the final 30 years of the 20th century have indicated quantitative alterations in certain species of microorganisms, including *Clostridium perfringens*, *Bacteroides*, *Prevotella*, and *Porphyromonas*, in individuals with RA [55]. More recent research reinforces the theory that the

Table 1: Altered composition of the gut microbiota in humans with RA.

Author (year)	Increased bacteria	Decreased bacteria	Technology	Reference
Alpizar-Rodriguez et al. (2019)	*Prevotellaceae*, *Prevotella* spp.		16S rRNA sequencing	[56]
Chen et al. (2016)	*Collinsella aerofaciens* and *Eggerthella lenta*	*Faecalibacterium*	16S ribosomal DNA	[57]
Chiang et al. (2019)	*Verrucomicrobia*, *Akkermansia*		16S rRNA sequencing	[58]
Eerola et al. (1994)		Anaerobic bacteria: *Bacteroides*, *Prevotella*, and *Porphyromonas*	Gas-liquid chromatography of bacterial CFAs	[59]
Kishikawa et al. (2019)	*Prevotella*		Whole-genome shotgun	[60]
Liu et al. (2013)	*Lactobacillus*		Quantitative real-time PCR	[61]
Lee et al. (2019)	*Lactobacilli*, *Prevotella*	*Bacteroides*, *Bifidobacterium*, *Bacteroidetes*/*Firmicutes*	16S rRNA sequencing	[62]
Muñiz Pedrogo et al. (2019)	*Clostridiaceae*		Metagenomic shotgun sequencing	[63]
Maeda et al. (2016)	*Prevotella* (*Prevotella copri*)	*Bacteroides*	16S rRNA sequencing	[39]
Rodrigues et al. (2019)	*Bacteroides*, *Prevotella*	*Clostridium leptum*	qPCR	[64]
Shinebaum et al. (1987)	*Clostridium perfringens*, coliform		Estimation of bacterial counts in fecal culture	[65]
Sun et al. (2019)	*Bacteroides*, *Escherichia-Shigella*	*Lactobacillus*, *Alloprevotella*, *Enterobacter*, *Odoribacter*	16S rRNA sequencing	[66]
Scher et al. (2013)	*Prevotella* (*Prevotella copri*)	*Bacteroides*	16S rRNA sequencing	[67]
Vaahtovuo et al. (2008)		*Bacteroides-Porphyromonas-Prevotella*, *Bacteroides fragilis*, *Eubacterium rectale-Clostridium coccoides*	Flow cytometry,16S rRNA hybridization, and DNA staining	[68]
Zhang et al. (2015)	*Lactobacillus salivarius*	*Haemophilus* spp.	Metagenomic shotgun sequencing	[69]

microorganism population within the gastrointestinal tract is a key actor in the pathogenesis of joint disease in humans. The mechanisms underlying bacterial involvement are almost certainly numerous, and proposals have encompassed stimulation of APCs by influencing TLRs or NOD-like receptors (NLRs), enzymatic initiation of peptide citrullination, mimicry of antigens, changes in the permeability of the gut mucosa, governance of the host immune system (e.g., activating T cell differentiation), and augmentation of mucosal inflammation via Th17-mediated pathways. Many case-control studies have demonstrated that the constituents of the intestinal microbiota in individuals with RA are varied (Table 1).

Using 16S RNA/DNA sequencing techniques, some studies have shown relatively enhanced numbers of *P. copri* in individuals, compared with healthy controls [56, 67]. Curiously, this relative increase was seldom identified in patients with RA who were well into the course of the disease or receiving long-term treatment; it was also rare in patients with a psoriatic form of arthritis [67]. The relative plentitude of *P. copri* was inversely associated with the existence of common epitope risk alleles, implying that the contents of the human gut microbiota could, to some extent, rely on the host's genetic material and reflecting the presence of a dysbiosis before the manifestation of the clinical phenotype [67]. An additional study reported that Japanese individuals early in RA harbored an augmented quantity of *Prevotella*, particularly *P. copri*, together with a reduced prevalence of intestinal *Bacteroides* [39]. This study recognized that *P. copri* itself had a notable ability to stimulate the production of Th17 cell-related cytokines, specifically IL-6 and IL-23. Excess amounts of *Prevotella* species have also been linked to heightened mucosal inflammation, which is mediated by Th17 pathways. This finding is in keeping with the notable propensity for *Prevotella* species to steer Th17 immune responses *in vitro* [39].

Another study has documented the increased intestinal prevalence of *Prevotella* species, encompassing *P. copri*, in patients with preclinical RA in European nations, also implying that dysbiosis predates the onset of arthritis [47]. Transplantation of a human microbiota from patients with RA in whom *Prevotella* was overwhelmingly prevalent into an animal model of arthritis led to severe disease; this disease transition failed to occur after transplantation of the microbiota from healthy controls [39]. Thus, an epitope bestowing cross-reactivity to antigens associated with arthritis may be transferred by *P. copri*. Moreover, a prophylactic influence of the *Prevotella* species (e.g., *P. histicola*) has been demonstrated in murine models [44].

However, additional genera may contribute to the generation of inflammatory pathology. Vaahtovuo et al. [68] reviewed the microbiota contents from patients with untreated premature RA or fibromyalgia using flow cytometry, 16S rRNA hybridization, and DNA staining. In the patients with

RA, the genera *Bifidobacterium* and *Eubacterium rectale-Clostridium coccoides* from the *Bacteroides fragilis* subgroup were decreased, which is consistent with earlier reports about individuals with Crohn's disease [70]. Work in China, founded on metagenomic shotgun sequencing, reported increased quantities of *Lactobacillus salivarius* in the intestine, on the teeth, and in the saliva of patients with RA [69]. However, *Haemophilus* species were decreased at all three locations. The prevalence of intestinal *P. copri* was greater in the initial year after clinical presentation, and notably, the dysbiosis detected in individuals with RA was incompletely resolved after therapy with disease-modifying agents [69]. Moreover, Liu et al. [61] documented that fecal *Lactobacillus* species were more plentiful in patients with RA in China compared with healthy controls [61]. Additional microorganisms (e.g., *Collinsella aerofaciens*) have exacerbated arthritis in murine models [57]. Chen et al. [57] noted that, in contrast to healthy controls, individuals with RA demonstrated reduced microbial variation within the gut, which was associated with autoantibody titers and length of disease [57]. Notably, methotrexate increased the number and variation of microbial species in patients with RA [57].

The main gut microbiota implicated in early RA and in its pathogenesis include *P. copri*, *L. salivarius*, and *Collinsella*. A relative increase of *Collinsella* was identified in patients with RA. One way in which *Collinsella* causes the disease is by enhancing gut permeability, as seen by decreased tight junction protein expression. The bacteria also affect the epithelial release of IL-17A [57].

In patients with de novo RA, the increased prevalence of *Prevotella* within the gastrointestinal tract has replaced *B. fragilis*, bacteria with notable Treg activity [67]. Increased counts of *P. copri* and analogous species are associated with poor titers of advantageous organisms, and this change may inhibit the immune system and the breakdown of vitamins into components absorbed into the circulation [71].

When exploring the effect of diet on RA, the influence of the intestinal bacteria should be taken into account [72]. *Bacteroides* species are linked with a diet containing substantial quantities of protein and animal fat; high-carbohydrate diets are related to the prevalence of *Prevotella* species [73]. Research has indicated that Mediterranean or vegan styles of eating diminish inflammation and enhance physical function and energy [74], although studies have not assessed parameters that quantify disease activity [75]. These studies also failed to establish whether the alteration in intestinal bacterial content ameliorated RA. The underlying rationale for the various potential arthritogenic organisms involves the host's genetic predisposition and environmental factors (e.g., diet). Additional studies are required to elucidate the role of intestinal dysbiosis and specifically changes in individual species in autoimmunity. Eventually, research must assess whether targeting intestinal microbiota abnormalities in those considered to be high risk for RA is successful in safeguarding against clinical disease presentation.

6. Future Directions

The results of studies evaluating the contribution of microbiota vary among the early disease course, disease before the use of immunosuppressive treatment, and mature disease with long-term treatment [69]. The 16S profiling technique identifies the relative plentitude of the range of species, thus providing a ratio, although the results may be vulnerable to prejudices from a number of intrinsic elements (e.g., bowel habits) [55]. A need exists for a more quantitative assessment of the microbiome and for detailed temporal metagenome-wide association research to investigate the operational ability of the microbiota within the host. This type of assessment will help resolve issues that require meticulous appraisal, including the directionality of dysbiosis. Additional microbiome studies should emphasize strain-level recognition of organisms and surmount the restrictions of analytical methods founded on 16S, which may lack accuracy [76].

To date, several dysbioses have been documented in the microbiota of patients with RA compared with healthy controls [39, 47, 67]. Microbiota from the intestine of individuals with RA has stimulated or worsened pathological phenotypes in RA [39]. Numerous questions must be addressed before a definite causal association between the human microbiome and the pathogenesis of RA can be confirmed. Comprehending these pathways is essential to improve the effectiveness of therapy and to guide patient-centric care. The flexibility of the biome may permit local or systemic maneuvering of specific gut microbiota linked with host pathologies [77]; this possibility engenders the conjecture that such interventions could alter treatment approaches in patients with RA. If the results from this area of research are valid, then transference into the clinical arena would generate de novo prophylactic or therapeutic initiatives.

Data Availability

The data of this manuscript are available from the corresponding author upon reasonable request.

Conflicts of Interest

The authors declared that they have no conflicts of interest in this work.

Authors' Contributions

Mingxin Li wrote the original draft, and Fang Wang reviewed and edited the manuscript. Both the authors contributed to manuscript revision and approved the final version of the manuscript.

Acknowledgments

This study was supported by funds from the National Natural Science Foundation of China (NSFC) Research Grants (31871212), and it was also supported by the Tianjin Natural Science Foundation (18JCTPJC57600) and the Tianjin Education Commission Research Project (2017KDYB21).

References

[1] J. van den Hoek, H. C. Boshuizen, L. D. Roorda et al., "Mortality in patients with rheumatoid arthritis: a 15-year prospective

cohort study," *Rheumatology International*, vol. 37, no. 4, pp. 487–493, 2017.

[2] J. Listing, J. Kekow, B. Manger et al., "Mortality in rheumatoid arthritis: the impact of disease activity, treatment with glucocorticoids, TNFα inhibitors and rituximab," *Annals of the Rheumatic Diseases*, vol. 74, no. 2, pp. 415–421, 2015.

[3] K. Mankia and P. Emery, "Preclinical rheumatoid arthritis: progress toward prevention," *Arthritis & Rhematology*, vol. 68, no. 4, pp. 779–788, 2016.

[4] H. Evans-Marin, R. Rogier, S. B. Koralov et al., "Microbiota-dependent involvement of Th17 cells in murine models of inflammatory arthritis," *Arthritis & Rhematology*, vol. 70, no. 12, pp. 1971–1983, 2018.

[5] G. Horta-Baas, M. D. S. Romero-Figueroa, A. J. Montiel-Jarquin, M. L. Pizano-Zarate, J. Garcia-Mena, and N. Ramirez-Duran, "Intestinal dysbiosis and rheumatoid arthritis: a link between gut microbiota and the pathogenesis of rheumatoid arthritis," *Journal of Immunology Research*, vol. 2017, Article ID 4835189, 13 pages, 2017.

[6] E. L. Zechner, "Inflammatory disease caused by intestinal pathobionts," *Current Opinion in Microbiology*, vol. 35, pp. 64–69, 2017.

[7] S. V. Lynch and O. Pedersen, "The human intestinal microbiome in health and disease," *The New England Journal of Medicine*, vol. 375, no. 24, pp. 2369–2379, 2016.

[8] I. Bartolini, M. Risaliti, M. N. Ringressi et al., "Role of gut microbiota-immunity axis in patients undergoing surgery for colorectal cancer: focus on short and long-term outcomes," *World Journal of Gastroenterology*, vol. 26, no. 20, pp. 2498–2513, 2020.

[9] M. M. Nielen, D. van Schaardenburg, H. W. Reesink et al., "Specific autoantibodies precede the symptoms of rheumatoid arthritis: a study of serial measurements in blood donors," *Arthritis and Rheumatism*, vol. 50, no. 2, pp. 380–386, 2004.

[10] J. R. O'Dell, K. W. Blakely, J. A. Mallek et al., "Treatment of early seropositive rheumatoid arthritis: a two-year, double-blind comparison of minocycline and hydroxychloroquine," *Arthritis and Rheumatism*, vol. 44, no. 10, pp. 2235–2241, 2001.

[11] L. Klareskog, K. Amara, and V. Malmstrom, "Adaptive immunity in rheumatoid arthritis: anticitrulline and other antibodies in the pathogenesis of rheumatoid arthritis," *Current Opinion in Rheumatology*, vol. 26, no. 1, pp. 72–79, 2014.

[12] L. A. van de Stadt, M. H. de Koning, R. J. van de Stadt et al., "Development of the anti-citrullinated protein antibody repertoire prior to the onset of rheumatoid arthritis," *Arthritis and Rheumatism*, vol. 63, no. 11, pp. 3226–3233, 2011.

[13] A. J. Svendsen, N. V. Holm, K. Kyvik, P. H. Petersen, and P. Junker, "Relative importance of genetic effects in rheumatoid arthritis: historical cohort study of Danish nationwide twin population," *BMJ*, vol. 324, no. 7332, pp. 264–266, 2002.

[14] G. F. Verheijden, A. W. Rijnders, E. Bos et al., "Human cartilage glycoprotein-39 as a candidate autoantigen in rheumatoid arthritis," *Arthritis and Rheumatism*, vol. 40, no. 6, pp. 1115–1125, 1997.

[15] M. E. Bauer, "Accelerated immunosenescence in rheumatoid arthritis: impact on clinical progression," *Immunity & Ageing*, vol. 17, no. 1, p. 6, 2020.

[16] N. Lee and W. U. Kim, "Microbiota in T-cell homeostasis and inflammatory diseases," *Experimental & Molecular Medicine*, vol. 49, no. 5, article e340, 2017.

[17] B. Lu, L. T. Hiraki, J. A. Sparks et al., "Being overweight or obese and risk of developing rheumatoid arthritis among women: a prospective cohort study," *Annals of the Rheumatic Diseases*, vol. 73, no. 11, pp. 1914–1922, 2014.

[18] H. Källberg, S. Jacobsen, C. Bengtsson et al., "Alcohol consumption is associated with decreased risk of rheumatoid arthritis: results from two Scandinavian case-control studies," *Annals of the Rheumatic Diseases*, vol. 68, no. 2, pp. 222–227, 2009.

[19] W. Lin, P. Shen, Y. Song, Y. Huang, and S. Tu, "Reactive oxygen species in autoimmune cells: function, differentiation, and metabolism," *Frontiers in Immunology*, vol. 12, article 635021, 2021.

[20] X. Jiang, B. Sundstrom, L. Alfredsson, L. Klareskog, S. Rantapaa-Dahlqvist, and C. Bengtsson, "High sodium chloride consumption enhances the effects of smoking but does not interact with SGK1 polymorphisms in the development of ACPA-positive status in patients with RA," *Annals of the Rheumatic Diseases*, vol. 75, no. 5, pp. 943–946, 2016.

[21] L. Lourido, F. J. Blanco, and C. Ruiz-Romero, "Defining the proteomic landscape of rheumatoid arthritis: progress and prospective clinical applications," *Expert Review of Proteomics*, vol. 14, no. 5, pp. 431–444, 2017.

[22] I. C. Scott, R. Tan, D. Stahl, S. Steer, C. M. Lewis, and A. P. Cope, "The protective effect of alcohol on developing rheumatoid arthritis: a systematic review and meta-analysis," *Rheumatology*, vol. 52, no. 5, pp. 856–867, 2013.

[23] B. Sundstrom, I. Johansson, and S. Rantapaa-Dahlqvist, "Interaction between dietary sodium and smoking increases the risk for rheumatoid arthritis: results from a nested case-control study," *Rheumatology*, vol. 54, no. 3, pp. 487–493, 2015.

[24] I. B. McInnes and G. Schett, "The pathogenesis of rheumatoid arthritis," *The New England Journal of Medicine*, vol. 365, no. 23, pp. 2205–2219, 2011.

[25] K. D. Deane and H. El-Gabalawy, "Pathogenesis and prevention of rheumatic disease: focus on preclinical RA and SLE," *Nature Reviews Rheumatology*, vol. 10, no. 4, pp. 212–228, 2014.

[26] F. Pratesi, E. Petit Teixeira, J. Sidney et al., "HLA shared epitope and ACPA: just a marker or an active player?," *Autoimmunity Reviews*, vol. 12, no. 12, pp. 1182–1187, 2013.

[27] J. S. Smolen, D. Aletaha, and I. B. McInnes, "Rheumatoid arthritis," *The Lancet*, vol. 388, no. 10055, pp. 2023–2038, 2016.

[28] E. Salgado, M. Bes-Rastrollo, J. de Irala, L. Carmona, and J. J. Gomez-Reino, "High sodium intake is associated with self-reported rheumatoid arthritis: a cross sectional and case control analysis within the SUN cohort," *Medicine*, vol. 94, no. 37, article e0924, 2015.

[29] H. van Spaendonk, H. Ceuleers, L. Witters et al., "Regulation of intestinal permeability: the role of proteases," *World Journal of Gastroenterology*, vol. 23, no. 12, pp. 2106–2123, 2017.

[30] Q. Mu, J. Kirby, C. M. Reilly, and X. M. Luo, "Leaky gut as a danger signal for autoimmune diseases," *Frontiers in Immunology*, vol. 8, p. 598, 2017.

[31] Y. Hu, K. H. Costenbader, X. Gao, F. B. Hu, E. W. Karlson, and B. Lu, "Mediterranean diet and incidence of rheumatoid arthritis in women," *Arthritis Care and Research*, vol. 67, no. 5, pp. 597–606, 2015.

[32] V. M. Holers, "Autoimmunity to citrullinated proteins and the initiation of rheumatoid arthritis," *Current Opinion in Immunology*, vol. 25, no. 6, pp. 728–735, 2013.

[33] S. C. Bischoff, G. Barbara, W. Buurman et al., "Intestinal permeability–a new target for disease prevention and therapy," *BMC Gastroenterology*, vol. 14, no. 1, p. 189, 2014.

[34] S. De Santis, E. Cavalcanti, M. Mastronardi, E. Jirillo, and M. Chieppa, "Nutritional keys for intestinal barrier modulation," *Frontiers in Immunology*, vol. 6, p. 612, 2015.

[35] J. Kjeldsen-Kragh, C. F. Borchgrevink, E. Laerum et al., "Controlled trial of fasting and one-year vegetarian diet in rheumatoid arthritis," *The Lancet*, vol. 338, no. 8772, pp. 899–902, 1991.

[36] G. D. Wu, J. Chen, C. Hoffmann et al., "Linking long-term dietary patterns with gut microbial enterotypes," *Science*, vol. 334, no. 6052, pp. 105–108, 2011.

[37] N. L. Bragazzi, A. Watad, S. G. Neumann et al., "Vitamin D and rheumatoid arthritis: an ongoing mystery," *Current Opinion in Rheumatology*, vol. 29, no. 4, pp. 378–388, 2017.

[38] A. Raczkiewicz, B. Kisiel, M. Kulig, and W. Tlustochowicz, "Vitamin D status and its association with quality of life, physical activity, and disease activity in rheumatoid arthritis patients," *Journal of Clinical Rheumatology*, vol. 21, no. 3, pp. 126–130, 2015.

[39] Y. Maeda, T. Kurakawa, E. Umemoto et al., "Dysbiosis contributes to arthritis development via activation of autoreactive T cells in the intestine," *Arthritis & Rhematology*, vol. 68, no. 11, pp. 2646–2661, 2016.

[40] L. M. Rehaume, S. Mondot, D. Aguirre de Cárcer et al., "ZAP-70 genotype disrupts the relationship between microbiota and host, leading to spondyloarthritis and ileitis in SKG mice," *Arthritis & Rhematology*, vol. 66, no. 10, pp. 2780–2792, 2014.

[41] N. Sakaguchi, T. Takahashi, H. Hata et al., "Altered thymic T-cell selection due to a mutation of the ZAP-70 gene causes autoimmune arthritis in mice," *Nature*, vol. 426, no. 6965, pp. 454–460, 2003.

[42] D. Kim and W. U. Kim, "Editorial: can Prevotella copri be a causative pathobiont in rheumatoid arthritis?," *Arthritis & Rhematology*, vol. 68, no. 11, pp. 2565–2567, 2016.

[43] R. E. Ley, "*Prevotella* in the gut: choose carefully," *Nature Reviews Gastroenterology & Hepatology*, vol. 13, no. 2, pp. 69-70, 2016.

[44] E. V. Marietta, J. A. Murray, D. H. Luckey et al., "Suppression of inflammatory arthritis by human gut-derived Prevotella histicola in humanized mice," *Arthritis & Rhematology*, vol. 68, no. 12, pp. 2878–2888, 2016.

[45] F. Teng, C. N. Klinger, K. M. Felix et al., "Gut microbiota drive autoimmune arthritis by promoting differentiation and migration of Peyer's patch T follicular helper cells," *Immunity*, vol. 44, no. 4, pp. 875–888, 2016.

[46] L. M. Rehaume, N. Matigian, A. M. Mehdi et al., "IL-23 favours outgrowth of spondyloarthritis-associated pathobionts and suppresses host support for homeostatic microbiota," *Annals of the Rheumatic Diseases*, vol. 78, no. 4, pp. 494–503, 2019.

[47] S. Abdollahi-Roodsaz, L. A. Joosten, M. I. Koenders et al., "Stimulation of TLR2 and TLR4 differentially skews the balance of T cells in a mouse model of arthritis," *The Journal of Clinical Investigation*, vol. 118, no. 1, pp. 205–216, 2008.

[48] R. Rogier, T. H. A. Ederveen, J. Boekhorst et al., "Aberrant intestinal microbiota due to IL-1 receptor antagonist deficiency promotes IL-17- and TLR4-dependent arthritis," *Microbiome*, vol. 5, no. 1, p. 63, 2017.

[49] A. S. Bergot, R. Giri, and R. Thomas, "The microbiome and rheumatoid arthritis," *Best Practice & Research. Clinical Rheumatology*, vol. 33, no. 6, article 101497, 2019.

[50] I. Matsumoto, A. Staub, C. Benoist, and D. Mathis, "Arthritis provoked by linked T and B cell recognition of a glycolytic enzyme," *Science*, vol. 286, no. 5445, pp. 1732–1735, 1999.

[51] H. J. Wu, I. I. Ivanov, J. Darce et al., "Gut-residing segmented filamentous bacteria drive autoimmune arthritis via T helper 17 cells," *Immunity*, vol. 32, no. 6, pp. 815–827, 2010.

[52] R. Rogier, H. Evans-Marin, J. Manasson et al., "Alteration of the intestinal microbiome characterizes preclinical inflammatory arthritis in mice and its modulation attenuates established arthritis," *Scientific Reports*, vol. 7, no. 1, article 15613, 2017.

[53] X. Liu, B. Zeng, J. Zhang et al., "Role of the gut microbiome in modulating arthritis progression in mice," *Scientific Reports*, vol. 6, no. 1, article 30594, 2016.

[54] W. K. Jubair, J. D. Hendrickson, E. L. Severs et al., "Modulation of inflammatory arthritis in mice by gut microbiota through mucosal inflammation and autoantibody generation," *Arthritis & Rhematology*, vol. 70, no. 8, pp. 1220–1233, 2018.

[55] D. Vandeputte, G. Kathagen, K. D'hoe et al., "Quantitative microbiome profiling links gut community variation to microbial load," *Nature*, vol. 551, no. 7681, pp. 507–511, 2017.

[56] D. Alpizar-Rodriguez, T. R. Lesker, A. Gronow et al., "Prevotella copri in individuals at risk for rheumatoid arthritis," *Annals of the Rheumatic Diseases*, vol. 78, no. 5, pp. 590–593, 2019.

[57] J. Chen, K. Wright, J. M. Davis et al., "An expansion of rare lineage intestinal microbes characterizes rheumatoid arthritis," *Genome Medicine*, vol. 8, no. 1, p. 43, 2016.

[58] H. I. Chiang, J. R. Li, C. C. Liu et al., "An association of gut microbiota with different phenotypes in Chinese patients with rheumatoid arthritis," *Journal of Clinical Medicine*, vol. 8, no. 11, p. 1770, 2019.

[59] E. Eerola, T. Möttönen, P. Hannonen et al., "Intestinal flora in early rheumatoid arthritis," *British Journal of Rheumatology*, vol. 33, no. 11, pp. 1030–1038, 1994.

[60] T. Kishikawa, Y. Maeda, T. Nii et al., "Metagenome-wide association study of gut microbiome revealed novel aetiology of rheumatoid arthritis in the Japanese population," *Annals of the Rheumatic Diseases*, vol. 79, no. 1, pp. 103–111, 2020.

[61] X. Liu, Q. Zou, B. Zeng, Y. Fang, and H. Wei, "Analysis of fecal Lactobacillus community structure in patients with early rheumatoid arthritis," *Current Microbiology*, vol. 67, no. 2, pp. 170–176, 2013.

[62] J. Y. Lee, M. Mannaa, Y. Kim, J. Kim, G. T. Kim, and Y. S. Seo, "Comparative analysis of fecal microbiota composition between rheumatoid arthritis and osteoarthritis patients," *Genes*, vol. 10, no. 10, p. 748, 2019.

[63] D. A. Muñiz Pedrogo, J. Chen, B. Hillmann et al., "An increased abundance of Clostridiaceae characterizes arthritis in inflammatory bowel disease and rheumatoid arthritis: a cross-sectional study," *Inflammatory Bowel Diseases*, vol. 25, no. 5, pp. 902–913, 2019.

[64] G. S. P. Rodrigues, L. C. F. Cayres, F. P. Gonçalves et al., "Detection of increased relative expression units of Bacteroides and Prevotella, and decreased Clostridium leptum in stool samples from Brazilian rheumatoid arthritis patients: a pilot study," *Microorganisms*, vol. 7, no. 10, p. 413, 2019.

[65] R. Shinebaum, V. C. Neumann, E. M. Cooke, and V. Wright, "Comparison of faecal florae in patients with rheumatoid arthritis and controls," *British Journal of Rheumatology*, vol. 26, no. 5, pp. 329–333, 1987.

[66] Y. Sun, Q. Chen, P. Lin et al., "Characteristics of gut microbiota in patients with rheumatoid arthritis in Shanghai, China,"

Frontiers in Cellular and Infection Microbiology, vol. 9, p. 369, 2019.

[67] J. U. Scher, A. Sczesnak, R. S. Longman et al., "Expansion of intestinal Prevotella copri correlates with enhanced susceptibility to arthritis," *eLife*, vol. 2, article e01202, 2013.

[68] J. Vaahtovuo, E. Munukka, M. Korkeamaki, R. Luukkainen, and P. Toivanen, "Fecal microbiota in early rheumatoid arthritis," *The Journal of Rheumatology*, vol. 35, no. 8, pp. 1500–1505, 2008.

[69] X. Zhang, D. Zhang, H. Jia et al., "The oral and gut microbiomes are perturbed in rheumatoid arthritis and partly normalized after treatment," *Nature Medicine*, vol. 21, no. 8, pp. 895–905, 2015.

[70] P. Seksik, L. Rigottier-Gois, G. Gramet et al., "Alterations of the dominant faecal bacterial groups in patients with Crohn's disease of the colon," *Gut*, vol. 52, no. 2, pp. 237–242, 2003.

[71] N. J. Bernard, "*Prevotella copri* associated with new-onset untreated RA," *Nature Reviews Rheumatology*, vol. 10, no. 1, p. 2, 2014.

[72] J. Zimmer, B. Lange, J. S. Frick et al., "A vegan or vegetarian diet substantially alters the human colonic faecal microbiota," *European Journal of Clinical Nutrition*, vol. 66, no. 1, pp. 53–60, 2012.

[73] S. Bengmark, "Gut microbiota, immune development and function," *Pharmacological Research*, vol. 69, no. 1, pp. 87–113, 2013.

[74] L. Skoldstam, L. Hagfors, and G. Johansson, "An experimental study of a Mediterranean diet intervention for patients with rheumatoid arthritis," *Annals of the Rheumatic Diseases*, vol. 62, no. 3, pp. 208–214, 2003.

[75] K. M. Maslowski and C. R. Mackay, "Diet, gut microbiota and immune responses," *Nature Immunology*, vol. 12, no. 1, pp. 5–9, 2011.

[76] N. W. Palm, M. R. de Zoete, T. W. Cullen et al., "Immunoglobulin A coating identifies colitogenic bacteria in inflammatory bowel disease," *Cell*, vol. 158, no. 5, pp. 1000–1010, 2014.

[77] W. Jia, H. Li, L. Zhao, and J. K. Nicholson, "Gut microbiota: a potential new territory for drug targeting," *Nature Reviews Drug Discovery*, vol. 7, no. 2, pp. 123–129, 2008.

Hindawi
Journal of Immunology Research
Volume 2021, Article ID 5569354, 16 pages
https://doi.org/10.1155/2021/5569354

Research Article

Ethanol Extracts of *Solanum lyratum Thunb* Regulate Ovarian Cancer Cell Proliferation, Apoptosis, and Epithelial-to-Mesenchymal Transition (EMT) via the ROS-Mediated p53 Pathway

Chen Zhang,[1] Zheming Li,[2] Jie Wang,[1] Xuelu Jiang,[1] Mengting Xia,[1] Jianfen Wang,[1] Shenyi Lu,[3] Shouye Li,[2] and Hanmei Wang[4]

[1]*Department of Obstetrics and Gynecology, The First Affiliated Hospital of Zhejiang Chinese Medical University (Zhejiang Provincial Hospital of Traditional Chinese Medicine), Hangzhou City 310001, China*
[2]*College of Pharmacy, Hangzhou Medical College, Hangzhou City 310053, China*
[3]*Department of Obstetrics and Gynecology, Zhejiang Chinese Medical University, Hangzhou City 310001, China*
[4]*Department of Obstetrics and Gynecology, Zhuji Hospital Affiliated to Shaoxing University, Zhuji City 311800, China*

Correspondence should be addressed to Hanmei Wang; whm87306102@163.com

Received 6 January 2021; Revised 22 February 2021; Accepted 12 March 2021; Published 2 April 2021

Academic Editor: Kai Wang

Ovarian cancer is a type of common gynecological tumors with high incidence and poor survival. The anticancer effects of the traditional Chinese medicine *Solanum lyratum Thunb* (SLT) have been intensively investigated in various cancers but in ovarian cancer is rare. The current study is aimed at investigating the effect of SLT on ovarian cancer cells. Lactate dehydrogenase (LDH) and MTT assays indicated that SLT concentrations of 0.25 and 0.5 μg/mL were not cytotoxic and had significant inhibitory effects on the cell viabilities of A2780 and SKOV3 cells, hence were used for subsequent experiments. Flow cytometric and western blot analysis revealed that SLT effectively suppressed ovarian cancer cell proliferation via inducing cell cycle arrest and increasing apoptosis. Cell cycle and apoptosis-related protein expressions were also regulated in SLT-treated cells. Moreover, DCFH-DA and western blot assays demonstrated that SLT enhanced ROS accumulation and subsequently activated the p53 signaling pathway. However, SLT-regulated ovarian cancer cell proliferation, apoptosis, migration, invasion, and EMT were significantly reversed by an ROS inhibitor (NAC, N-acetyl-L-cysteine). Furthermore, A2780 and SKOV3 cells cocultured with M0 macrophages showed that SLT activated the polarization of M0 macrophages to M1 macrophages and inhibited the polarization to M2 macrophages, with the increased percentage of CD86+ cells and decreased percentage of CD206+ cells were detected. In summary, this study illustrated the anticancer effects of SLT on ovarian cancer cells, suggesting that SLT may have the potential to provide basic evidence for the discovery of antiovarian cancer agents.

1. Introduction

Human ovarian cancer is the most fatal cancer in the female reproductive system [1–3]. The traditional treatment process is to remove the tumor to the maximum and then combine the paclitaxel and platinum chemotherapy [4]. Although 70% of the patients initially respond well to the chemotherapy, while the emergence of drug resistance and side effects curb the benefits of currently available chemotherapy drugs [5], and the 5-year survival is still unsatisfactory [6–8]. Since few of these strategies can completely protect patients with ovarian cancer from recurrence and metastasis, new drugs are urgently needed. One way to solve this problem is to develop new drugs that are used in combination with existing chemotherapy drugs to produce better results than simple chemotherapy.

In terms of adjuvant therapy, the efficacy and safety of traditional Chinese medicine (TCM) in the management of

cancers have gained increasing acceptance worldwide; TCM were also usually served as rich resources for drug discovery of pharmaceutical companies [9, 10]. In addition to the price advantage, TCM treatment has been reported to have the advantages of chemotherapy efficacy strengthening, toxicity reduction, survival time prolongation, and improving the quality of life and immune function [11, 12]. There are increasing evidences that many natural products, including extracts and isolated chemicals, may interact with multiple targets in signaling pathways that regulate cancer progression [9]. Therefore, it is necessary to study the natural products systematically, clarify their antitumor effects, and understand their mechanism, so as to develop new therapeutic methods.

Solanum lyratum Thunb (SLT) is a common TCM, which is widely used in China to treat malaria, jaundice, cholecystitis, gonorrhea, rheumatoid arthritis, leucorrhea, and cancer [13]. Since the 20th century, a variety of active compounds have been identified in SLT, including saponins, lignans, alkaloids, polyphenols, flavonoids, and polysaccharides [14, 15]. A series of evidences have shown that SLT has antitumor activity, thus attracting much attention. In lung carcinoma-bearing mouse model, study of SLT showed antitumor effect and can improve immune function and survival rate of mice [16]. SLT extracts can induce cell cycle arrest and apoptosis in human osteosarcoma U-2 OS cells, and this worked through the ROS-promoted and mitochondria- and caspase-dependent apoptotic pathways [17]. Another study indicated that the extract of SLT induced cytotoxicity and apoptosis of human colon cancer cell line Colo 205, which may be associated with CDK1, p27, p53, cyclin B1, cyclin E, and apoptosis-related proteins, as well as the activity of cytochrome C [18]. Solasodine, an alkaloid compound extracted from SLT, has been reported to regulate cell apoptosis and autophagy and reduce the metastasis of ovarian cancer cells [19]. These researches suggest that SLT has the potential to be an adjuvant drug for the treatment of cancers. However, the effects of SLT extract on ovarian cancer and its mechanism remain unclear. In the present study, the effects of SLT on the proliferation, apoptosis, epithelial-to-mesenchymal transformation (EMT), and immunomodulatory potential of ovarian cancer cells were detected, and hypothesis of the antiovarian cancer effect was possibly through the regulation of the p53 pathway mediated by ROS.

2. Materials and Methods

2.1. Cell Culture. Human ovarian cancer cell lines, A2780 and SKOV3 cells, were obtained from American Type Culture Collection (ATCC, Rockville, MD, USA) and cultured in Dulbecco's modified Eagle medium (DMEM, Invitrogen, Carlsbad, CA, USA) supplemented with 10% fetal bovine serum (FBS, Sigma, St. Louis, MO, USA) and 100 U/mL penicillin and 100 μg/mL streptomycin (Invitrogen) in 5% CO_2 at 37°C. Human monocytes such as THP-1 were obtained from the Cellular Library of the National Collection of Authenticated Cell Cultures (Shanghai, China) and cultured in RPMI 1640 medium supplemented with 10% FBS in 5% CO_2 at 37°C.

2.2. Preparation of SLT Extract. 50 g SLT was crushed and immersed in 75% ethanol for 3 h, and then soaked and filtered again for three times. The SLT extract was then obtained by mixing the filtrate and drying it with a rotary evaporator. Different concentrations of SLT preparation using dimethyl sulfoxide (DMSO, Sigma-Aldrich, Saint Louis, MO, USA) dissolve SLT extract in preparation of the drug solution concentration of 10 mg/mL, and then diluted with cell culture medium to obtain the concentrations of 0, 0.1, 0.25, 0.5, 1.0, 2.5, 5, and 10 μg/mL SLT extract solution. Taxol (Sigma-Aldrich) dissolved in DMSO and diluted with cell culture medium to a final concentration of 1 μM was used as the positive control.

2.3. MTT Assay. Cells were seeded into 96-well plates at a cell density of 4×10^3 cells per well, cultured overnight, and treated with different concentrations of SLT extract solution or taxol solution for 24 or 48 h. 20 μL of 5 mg/mL MTT solution (5 mg/mL, Sigma) was added into each well for another 4 h of incubation; thereafter, the suspension was removed, and the precipitate was dissolved in 100 μL DMSO. Absorbance levels were measured at 570 nm using a SpectraMax M5 microplate reader (Molecular Devices, Sunnyvale, CA, USA). The experiments were performed in triplicate.

2.4. Lactate Dehydrogenase (LDH) Assay. Cells were seeded into 96-well plates at a density of 4×10^3 cells per well, cultured overnight, and treated with different concentrations of SLT extract solution or taxol solution for 48 h. LDH release was detected by LDH cytotoxicity assay kit (Beyotime, Nantong, Jiangsu, China) based on the manufacturer's instructions. Absorbance levels were measured at 490 nm using a SpectraMax M5 microplate reader.

2.5. Cell Cycle Assay. Cells were collected after 48 h of exposure to SLT, rinsed thrice with PBS, harvested, and fixed in 70% ice-cold ethanol at −4°C overnight. Subsequently, 50 ng/mL propidium iodide (Beyotime) staining solution and 0.1 mg/mL RNase A were added to the cells away from the light for 30 min at room temperature. The cell cycle distribution of cells was analyzed using a flow cytometer (BD Biosciences, Franklin Lakes, NJ, USA).

2.6. Wound Healing Assay. Cells were seeded into 6-well plates and maintained overnight. When cells reached 90% confluence, they were treated with 10 μg/mL mitomycin C for 2 h as described in the literature. The surface layer cells were scratched with a 100 μL sterilized pipette tip on the bottom of each plate after cells reaching 100% confluence. Then, the cell debris was washed, and1 mL fresh serum-free medium was added with SLT at the indicated concentration for 24 h. 0 hours and 24 hours after scratching, use a microscope (Olympus, Tokyo, Japan) to photograph the width of the gap area.

2.7. Transwell Assay. Cells (5×10^4 cells/well) pretreated with SLT were seeded in the top chamber (Millipore, Billerica, MA), which was precoated with Matrigel (BD Biosciences, MA). Serum-free culture medium was added to the top chambers, while the bottom chambers were filled with

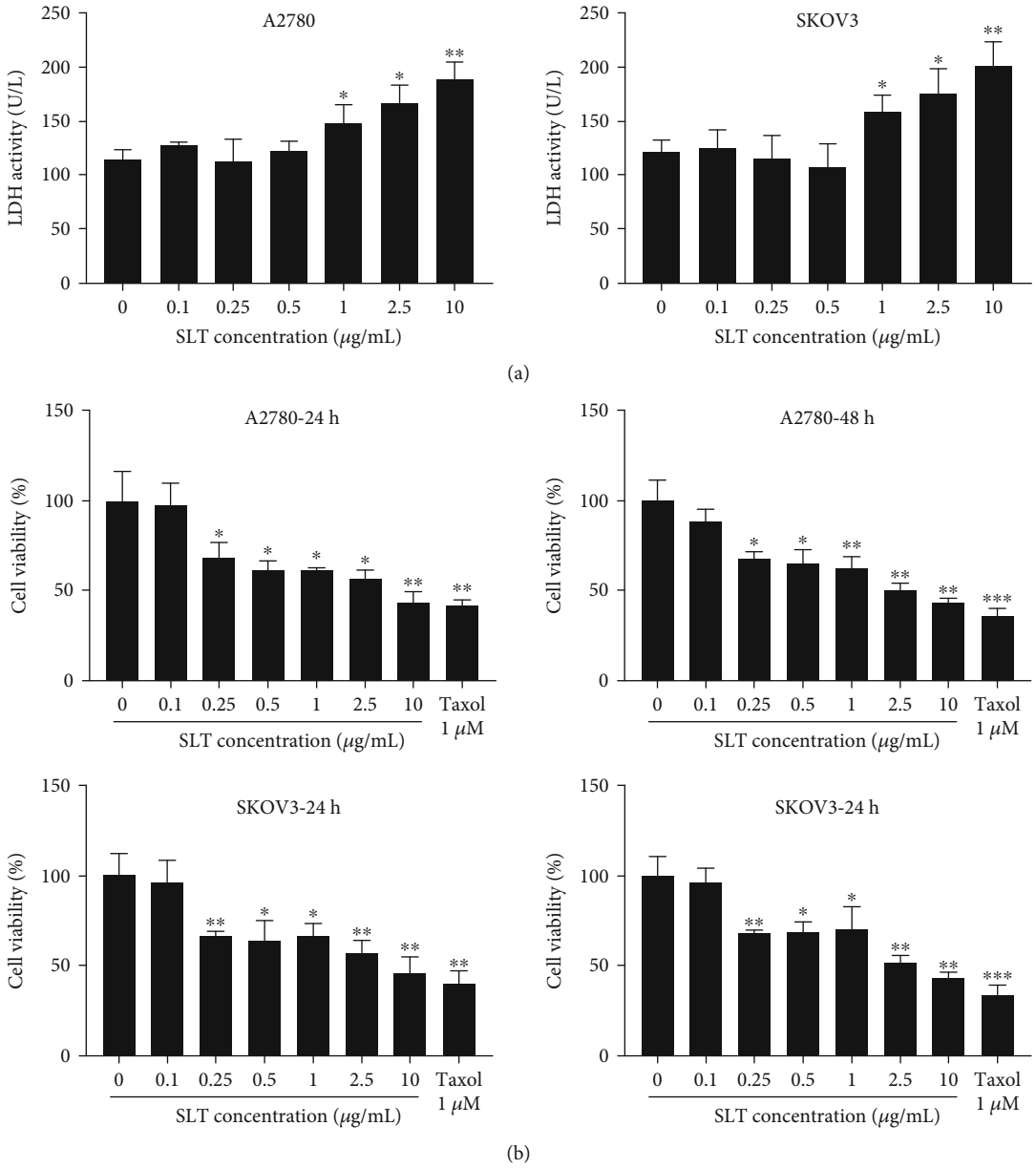

Figure 1: The effects of SLT on ovarian cancer cell viability. (a) The effects of SLT at indicated concentrations on LDH release in A2780 and SKOV3 cells were determined by LDH assay. (b) The effects of SLT at indicated concentrations on the cell viability of A2780 and SKOV3 cells were analyzed by MTT assay. The values were displayed as the mean ± SD. Representative results from three independent experiments were shown ($^{*}P < 0.05$, $^{**}P < 0.01$, and $^{***}P < 0.001$, compared with the control group).

500 μL cultured medium containing 10% FBS. After incubation for 24 h, cells in the bottom chamber were fixed with 4% paraformaldehyde (PFA), stained with 0.1% crystal violet, and counted under a microscope (Olympus, Tokyo, Japan).

2.8. Annexin V-FITC Apoptosis Assay. Cells were harvested and washed thrice with PBS after 48 h of exposure to SLT. Then, cells were incubated with 500 μL of binding buffer containing 5 μL of fluorescein isothiocyanate- (FITC-) labeled Annexin V (Beyotime) and 5 μL of propidium iodide (PI) solution (Beyotime) away from the light for 15 min at room temperature. Then, cell apoptosis rates were analyzed using a flow cytometer (BD Biosciences).

2.9. Measurement of Intracellular Reactive Oxygen Species (ROS). The intracellular levels of ROS were measured using the green fluorescent probe 6-carboxy-2′,7′-dichlorofluorescein diacetates (DCFH-DA, Sigma-Aldrich, MO, USA). 5 $\times 10^3$ cells per well were seeded into a 24-well culture plate and exposed to different concentrations of SLT treatment for 6 h, and then stained with 10 μM DCFH-DA for 30 min under dark at 37°C. After washing with PBS twice and fixing

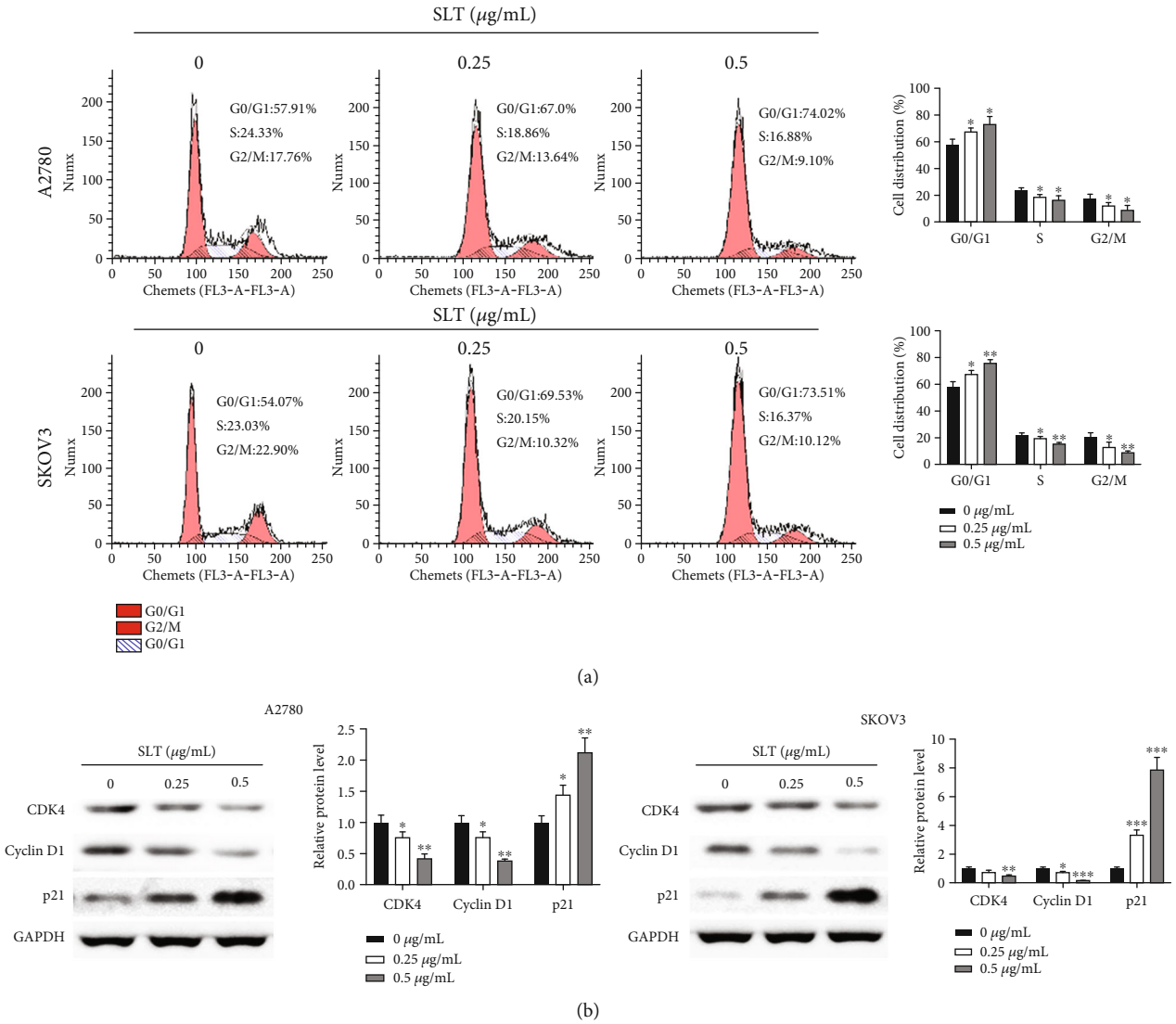

Figure 2: The effects of SLT on cell cycle of ovarian cancer. (a) The effects of SLT on cell cycle distribution of A2780 and SKOV3 cells were analyzed via flow cytometry. (b) The effects of SLT on the expression levels of cell cycle-related proteins in A2780 and SKOV3 cells were evaluated via western blot assay. The values were displayed as the mean ± SD. Representative results from three independent experiments were shown ($^{*}P < 0.05$, $^{**}P < 0.01$, and $^{***}P < 0.001$, compared with the control group).

with 4% paraformaldehyde, the stained cells were observed under a fluorescence microscope. Fluorescence was measured with microplate spectrofluorometer (Synergy 4, Bio-Tek, VT, USA) with 488 nm excitation wavelength and 525 nm emission wavelength. To inhibit ROS, 1 mM N-acetyl-L-cysteine (NAC) was added into the medium for 2 h. The ratio of average fluorescence intensity of each group to that of the control group represents ROS production.

2.10. M0 Macrophage Inducement and Coculture. M0 macrophages were induced from the human monocytes such as THP-1. Briefly, THP-1 cells were seeded in 6-well plates and added with 100 ng/mL phorbol 12-myristate 13-acetate (PMA) in Transwell inserts for 48 h to induce into M0 macrophages. Then, the PMA containing media were removed gently and the activated THP-1 cells were placed into a new 6-well plate adding with 2 mL of fresh RPIM/FCS medium. The differentiated M0-type macrophages were subsequently cocultured with untreated A2780/SKOV-3 cells or A2780/SKOV-3 supplemented with SLT (0.25 and 0.5 μg/mL) to assess the effect of SLT on M1 and M2 polarization of M0 macrophages.

2.11. Flow Cytometry. Flow cytometry assay was performed to detect the expression of CD86 for M1 macrophages and CD206 for M2 macrophages. A2780 or SKOV-3 cells were cocultured with M0-type macrophages, and SLT was coadded at different concentrations (0, 0.25, and 0.5 μg/mL). Then, cell suspension was incubated with FITC, PE-, and allophycocyanin- (APC-) conjugated Abs anti-human CD206 and CD86 (BD Biosciences Pharmingen, USA) for 30 min under the dark; the control isotype corresponding to each primary antibody was also added. Then, cells were washed with PBS and analyzed by flow cytometry (BD, USA).

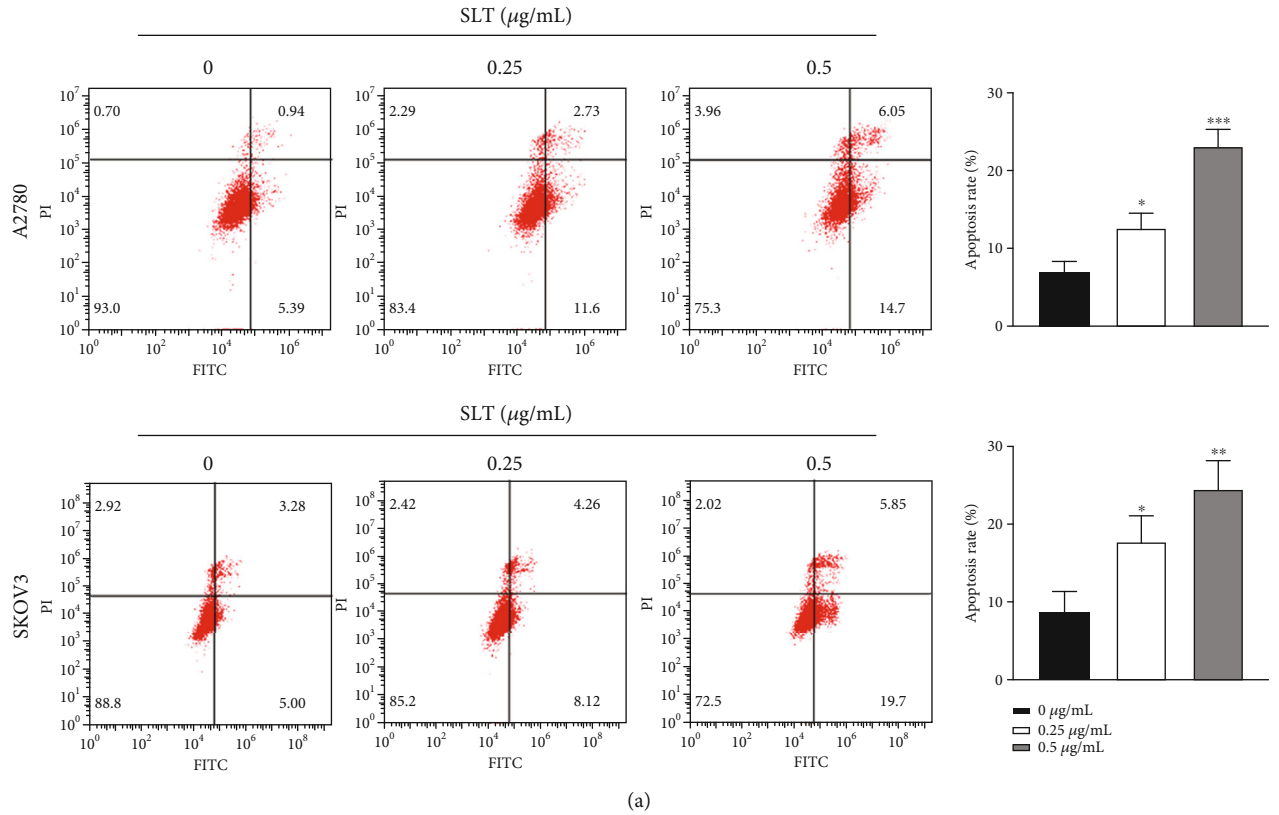

(a)

Figure 3: Continued.

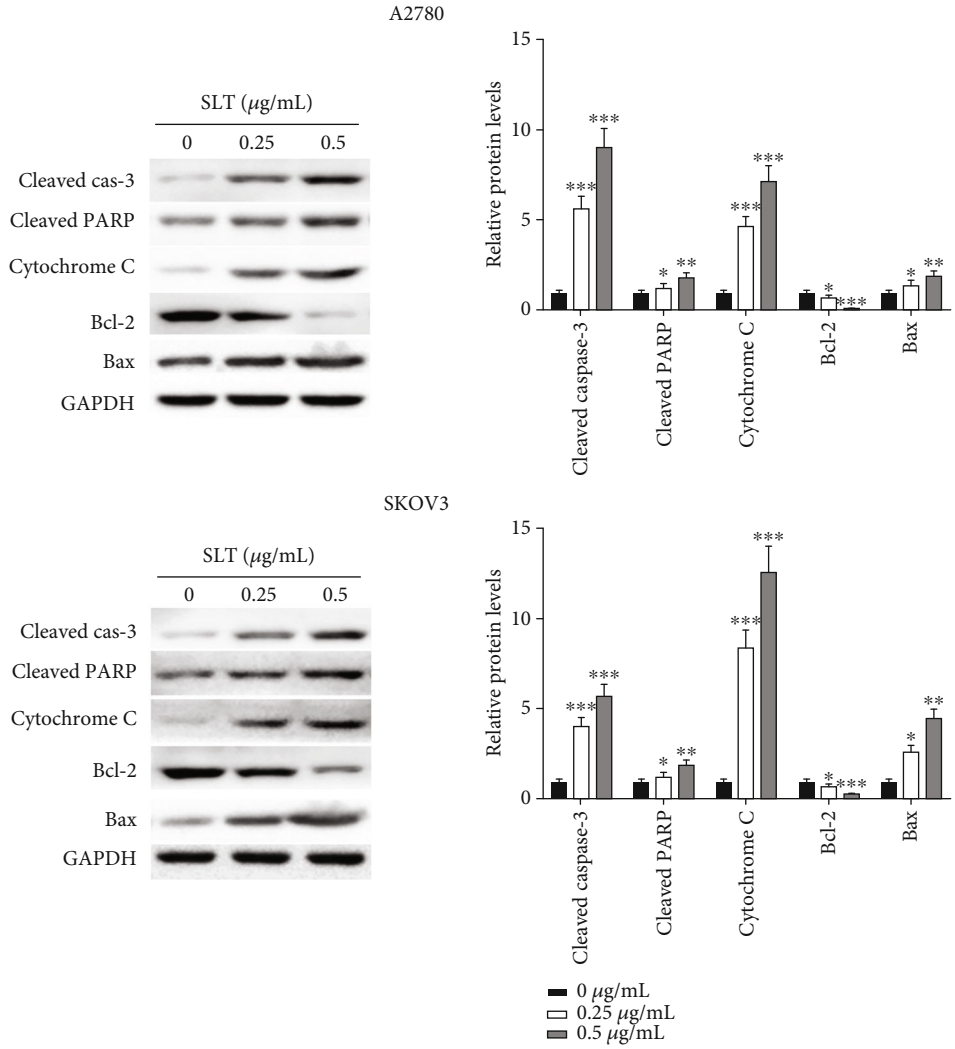

(b)

Figure 3: The effects of SLT on apoptosis of ovarian cancer cells. (a) The effects of SLT on cell apoptosis of A2780 and SKOV3 cells were analyzed via Annexin V-FITC/PI double staining assay. (b) The effects of SLT on the expression levels of apoptosis-related protein in A2780 and SKOV3 cells were evaluated via western blot assay. The values were displayed as the mean ± SD. Representative results from three independent experiments were shown ($^{*}P < 0.05$, $^{**}P < 0.01$, and $^{***}P < 0.001$, compared with the control group).

2.12. Western Blotting. Proteins were extracted using RIPA lysis (Beyotime, Jiangsu, China) buffer and were collected. Then, protein concentration was determined using a BCA assay kit (Thermo Scientific, Waltham, MA, USA). The protein samples were separated by using sodium dodecyl sulfate-polyacrylamide gel electrophoresis (SDS-PAGE) and electrophoretically transferred onto polyvinylidene fluoride (PVDF, EMD Millipore, Billerica, MA, USA) membranes. Membranes were blocked with 5% skim milk for 1 hour and then incubated with primary antibodies against CDK4 (ab199728, 1 : 2000, Abcam), Cyclin D1 (ab226977, 1 : 500, Abcam), p53 (ab131442, 1 : 1000, Abcam), p21 (ab7960, 1 : 2000, Abcam), MMP2 (ab2462, 1 : 5000, Abcam), MMP9 (ab76003, 1 : 2000, Abcam), E-cadherin (ab18203, 1 : 1000, Abcam), N-cadherin (ab18203, 1 : 1000, Abcam), cleaved caspase-3 (ab2302,1 : 1000, Abcam), cleaved PARP (ab32064, 1 : 1000, Abcam), Bcl-2 (ab32124, 1 : 1000, Abcam), Bax (ab7977, 1 : 1000, Abcam), CD86 (ab7977, 1 : 1000, Abcam), CD206 (ab7977, 1 : 1000, Abcam), iNOS (ab7977, 1 : 1000, Abcam), Arg-1 (ab7977, 1 : 1000, Abcam), and GAPDH (ab8245, 1 : 1000, Abcam) at 4°C for overnight. Subsequently, the membranes were probed with horseradish peroxidase-(HRP-) conjugated secondary antibodies (Abcam) at room temperature for 1 hour. The band was visualized using an enhanced chemiluminescence technique (Thermo Fisher Scientific).

2.13. Statistical Analysis. Numerical data are expressed as the mean ± standard deviation (SD) and were analyzed using SPSS 21.0 (Chicago, IL, USA). Statistical analysis between two and multiple groups was performed using Student's *t* -test and one-way analysis of variance(ANOVA) followed by the least significant difference post hoc test. Each experiment was performed independently at least for three times. Differences with values of $P < 0.05$ were considered as statistically significant.

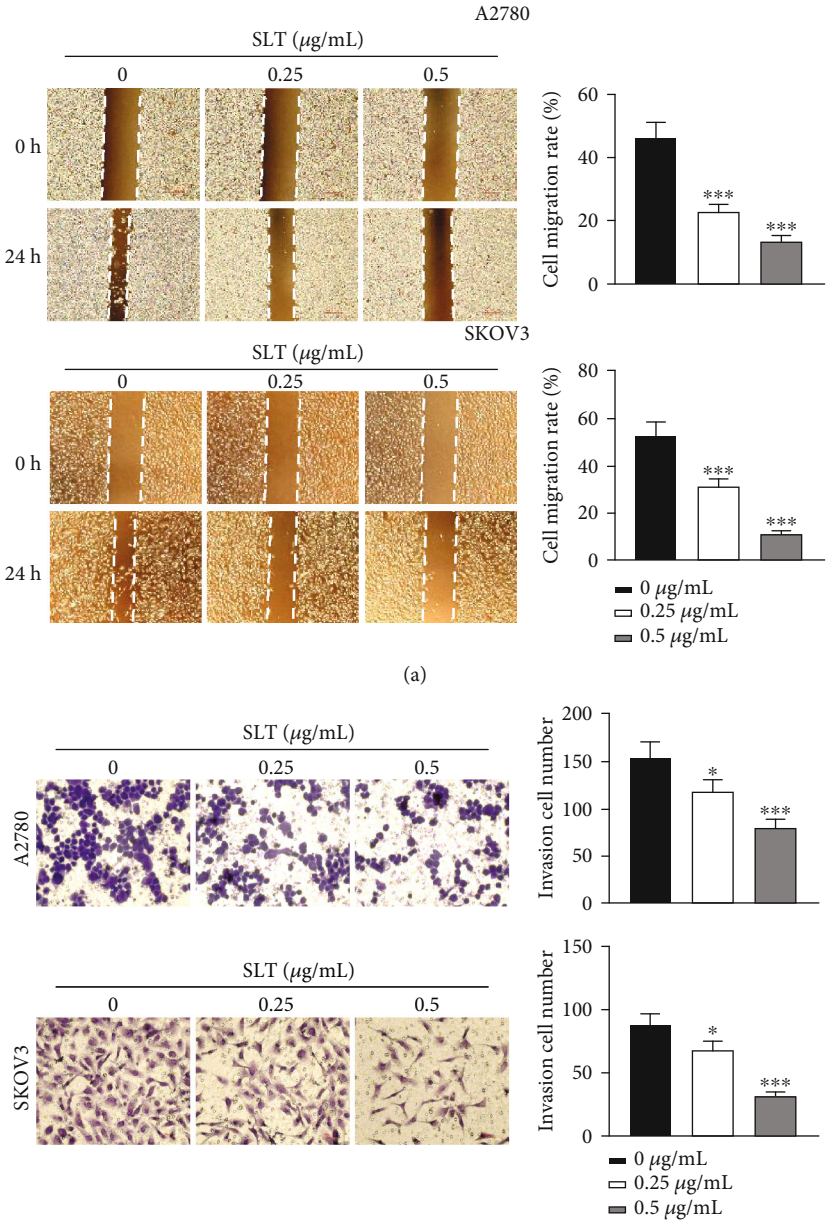

Figure 4: Continued.

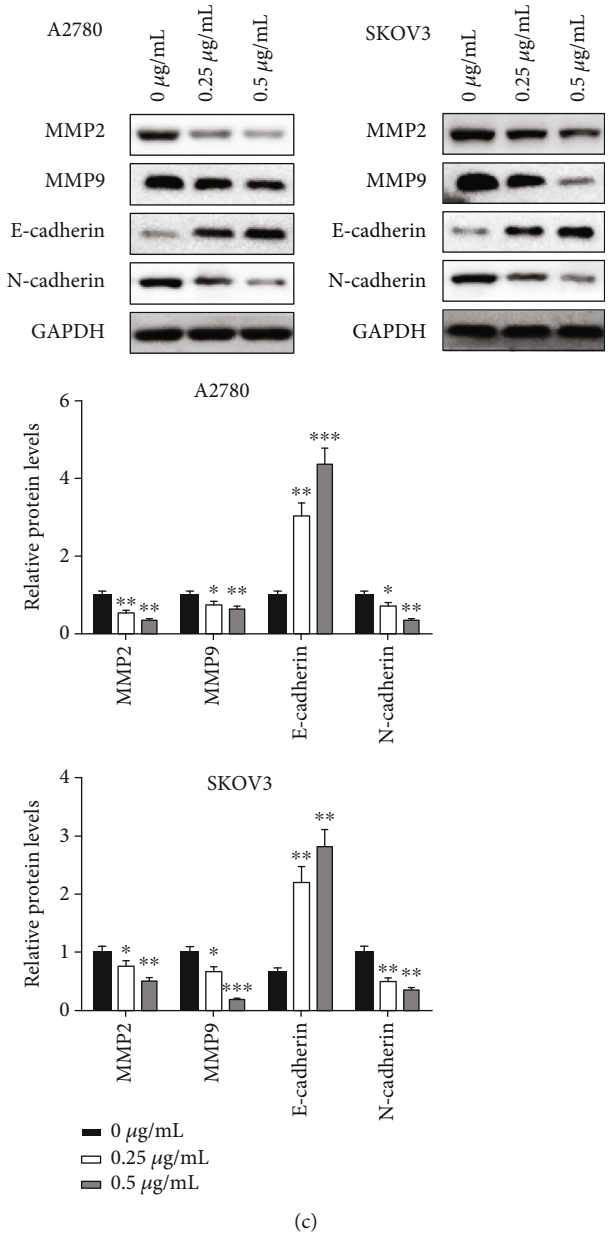

Figure 4: The effects of SLT on migration, invasion, and EMT of ovarian cancer cells. (a) The effects of SLT on cell migration were detected by wound healing assay in A2780 and SKOV3 cells (magnification ×20; scale bar = 1000 μm). (b) The effects of SLT on cell invasion were evaluated by Transwell assay (magnification ×100; scale bar = 200 μm). (c) The effects of SLT on the expression levels of EMT-related protein in A2780 and SKOV3 cells were evaluated via western blot assay. The values were displayed as the mean ± SD. Representative results from three independent experiments were shown ($^{*}P < 0.05$, $^{**}P < 0.01$, and $^{***}P < 0.001$, compared with the control group).

3. Results

3.1. Effects of SLT on Ovarian Cancer Cell Viability. Since the concentration of LDH released into the extracellular environment corresponds to the degree of cell membrane damage, we used the LDH release assay to determine the cytotoxicity of SLT (Figure 1(a)). The results demonstrated that over 1.0 μg/mL of SLT remarkably increased LDH leakage of A2780 and SKOV3 cells, which suggested that high concentration of SLT might be cytotoxic. In addition, MTT assay was used to detect the effect of SLT on cell viabilities (Figure 1(b)). The data indicated that the cell viabilities of A2780 and SKOV3 were significantly inhibited by SLT (0.25, 0.5, 1.0, 2.5, and 10 μg/mL). Therefore, SLT concentrations of 0.25 and 0.5 μg/mL were selected in the following experiments.

3.2. Effects of SLT on Cell Cycle of Ovarian Cancer. Flow cytometry was used to detect the influence of SLT treatment on cell cycle distribution of A2780 and SKOV3 cells. As represented in Figure 2(a), the proportions of G1 phase A2780 and SKOV3 cells in the SLT treatment (0.25 and 0.5 μg/mL) groups were increased compared with the control group. In addition, SLT treatment (0.25 and 0.5 mg/mL) resulted in a

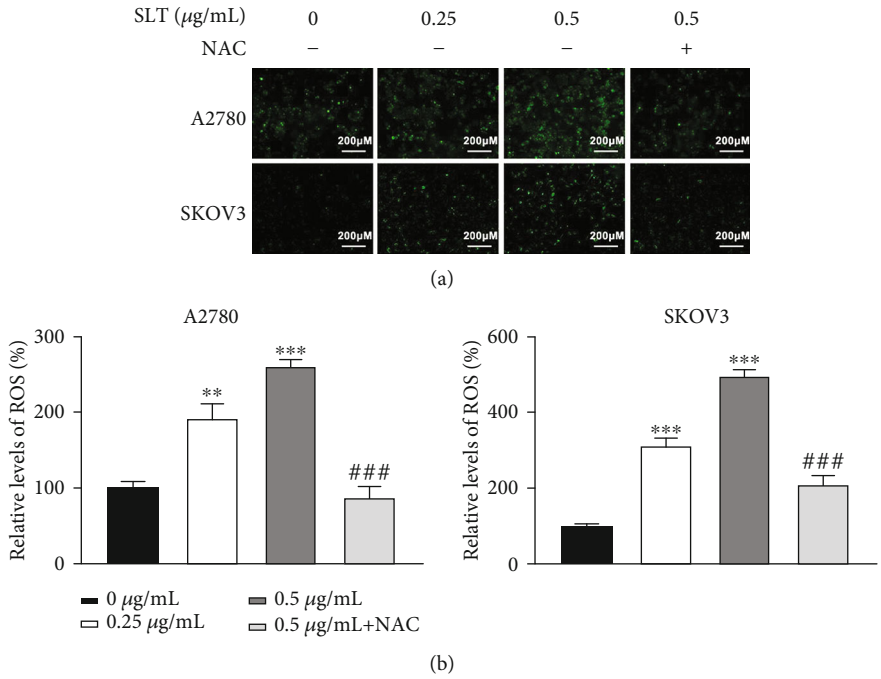

Figure 5: The effects of SLT on ROS production in ovarian cancer cells. (a) The effects of SLT on ROS levels of A2780 and SKOV3 cells were determined using DCF fluorescence by a fluorescence microscope (magnification ×100; scale bar = 40 μm). (b) The DCF fluorescence intensity in A2780 and SKOV3 cells affected by SLT was measured by a fluorescence spectrophotometer. The values were displayed as the mean ± SD. Representative results from three independent experiments were shown ($^{**}P < 0.01$ and $^{***}P < 0.001$, compared with the control group; $^{###}P < 0.001$, compared with the 0.5 μg/mL SLT group).

decrease in the percentage of G2/M cells compared with the untreated cells (the control group). SLT significantly increased G1 phase cells accompanied by a decrease in G2/M phase cells, in a concentration-dependent manner, suggesting that SLT blocks cell cycle in G1 phase. Further western blot assay was used to evaluate the effects of SLT on cell cycle regulation-associated proteins. Consistently, SLT treatment significantly reduced the protein levels of CDK4 and Cyclin D1, but increased the protein level of P21 in both A2780 and SKOV3 cells compared to the control group (Figure 2(b)). These data indicated that the inhibitory activity of SLT on A2780 and SKOV3 cell proliferation may be associated with cell cycle arrest at the G1 phase.

3.3. Effects of SLT on Apoptosis of Ovarian Cancer Cells. Annexin V-FITC/PI double staining assay was used to evaluate the ratio of cell apoptosis after SLT treatment. Results indicated that A2780 and SKOV3 cells after treatment with SLT resulted in a dose-dependent increase of apoptotic cells compared with the control group (Figure 3(a)). The mitochondrial apoptosis pathway plays a key role in the apoptosis signal transduction pathway; hence, we detected changes in apoptosis-related protein levels after SLT treatment. As revealed in Figure 3(b), the protein levels of cleaved caspase-3, cleaved PARP, Bax, and cytochrome C (in the cytoplasm) were significantly increased, and the Bcl-2 level was decreased in the A2780 and SKOV3 cells with SLT treatment compared to the control group (Figure 3(b)). These data suggested that SLT could induce the apoptosis of A2780 and SKOV3 cells which may be partly mediated via a mitochondria-dependent mechanism.

3.4. Effects of SLT on Migration, Invasion, and EMT of Ovarian Cancer Cells. The abilities of migration and invasion of A2780 and SKOV3 cells after treatment with SLT were further determined using wound healing and Transwell assays, respectively. As illustrated in Figure 4(a), A2780 and SKOV3 cells in the SLT treatment group had larger wound areas after 24 hours, indicating that cell migration was significantly decreased compared to the control group. With increasing concentration of the SLT (0.25 and 0.5 μg/mL), the number of invaded cells was significantly reduced as compared to the control group, as shown in Figure 4(b). Further western blot assay results (Figure 4(c)) showed that SLT significantly inhibited the protein levels of MMP2, MMP9, and N-cadherin, and increased the protein level of E-cadherin in A2780 and SKOV3 cells. These results demonstrated that SLT reduces the migration, invasion, and EMT of ovarian cancer cells.

3.5. Effects of SLT on ROS Production in Ovarian Cancer Cells. As ROS can induce caspase-independent cell death, we detected the SLT-induced ROS production in A2780 and SKOV3 cells. As illustrated in Figures 5(a) and 5(b), significant increases in intracellular ROS levels in A2780 and SKOV3 cells exposed to SLT (0.25 and 0.5 μg/mL) were observed by a fluorescence microscope compared to the control cells. Moreover, in this experiment, A2780 and SKOV3 cells were pretreated with N-acetyl-L-cysteine (NAC), an

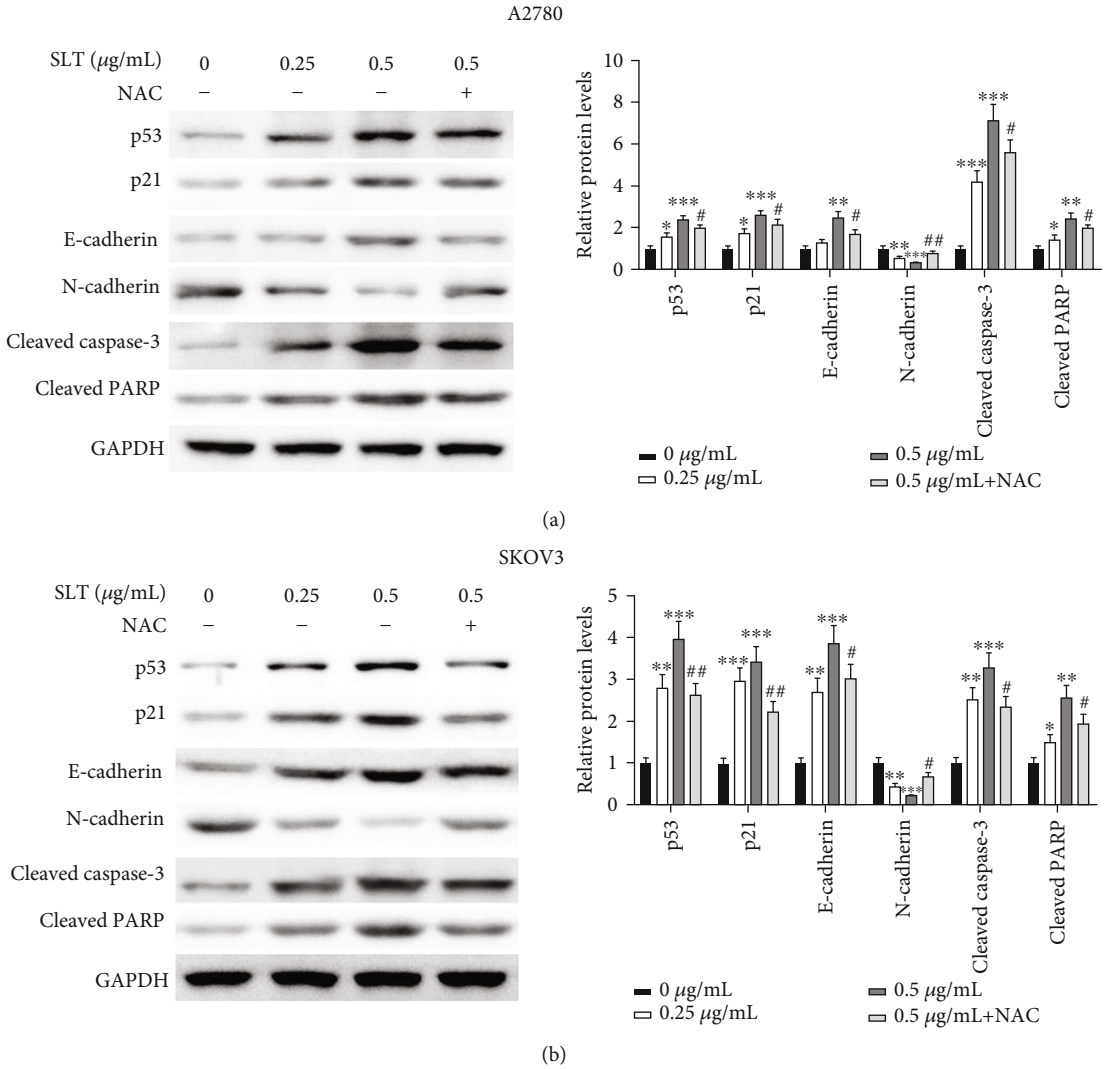

Figure 6: SLT induces the ROS/p53 pathway to regulate ovarian cancer cell proliferation, EMT, and apoptosis. (a) The effects of SLT on the expression levels of p53, p21, E-cadherin, N-cadherin, cleaved caspase-3, and cleaved PARP in A2780 cells were evaluated via western blot assay. (b) The effects of SLT on the expression levels of p53, p21, E-cadherin, N-cadherin, cleaved caspase-3, and cleaved PARP in SKOV3 cells were evaluated via western blot assay. The values were displayed as the mean ± SD. Representative results from three independent experiments were shown ($^{*}P < 0.05$, $^{**}P < 0.01$, and $^{***}P < 0.01$, compared with the control group; $^{\#}P < 0.05$ and $^{\#\#}P < 0.01$, compared with the 0.5 μg/mL SLT group).

inhibitor of ROS generation, and then exposed to SLT. And the results indicated that NAC could partially prevent SLT from inducing the production of ROS. All these data suggested that SLT could promote ROS production in ovarian cancer cells.

3.6. SLT Induces the ROS/p53 Pathway to Regulate Ovarian Cancer Cell Proliferation, EMT, and Apoptosis. p53 is a tumor suppressor protein which can be activated by a variety of cellular stresses, such as cell death, DNA damage, oxidative stress, and hypoxia [20, 21]. It is reported to be a critical molecule that regulates proliferation, EMT, and apoptosis of cancer cells [22–24]. Hence, we used western blot assay to investigate whether p53 plays important role in SLT-induced ROS-mediated ovarian cancer cell proliferation, EMT, and apoptosis in A2780 and SKOV3 cells. The results indicated that SLT inhibited cell proliferation and EMT and induced cell apoptosis, manifested as increased expression of p21, E-cadherin, cleaved caspase-3, and cleaved PARP, and decreased expression of N-cadherin (Figures 6(a) and 6(b)). Moreover, the expression of p53 was significantly upregulated by SLT (Figures 6(a) and 6(b)), indicating that SLT may affect p53-mediated cell proliferation, EMT, and apoptosis. However, the above effects of SLT partially reversed by pretreatment with NAC (Figures 6(a) and 6(b)). Combined with SLT can promote the production of ROS, p53 can be activated by ROS, so SLT can activate ROS/p53 to regulate ovarian cancer progression, which can be reversed by the effect of inhibiting ROS by NAC treatment. Taken together, these results indicated that the increased generation

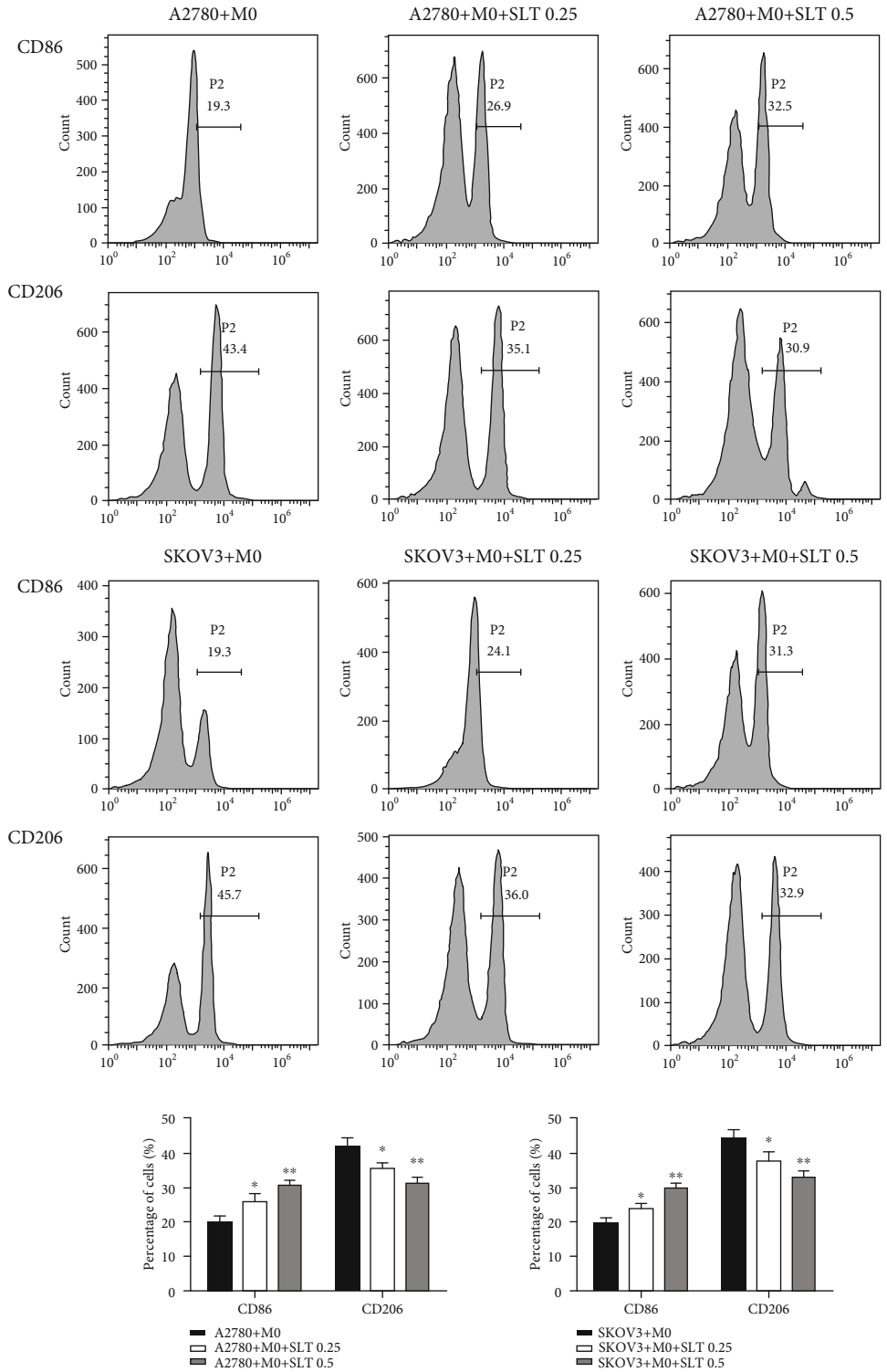

(a)

Figure 7: Continued.

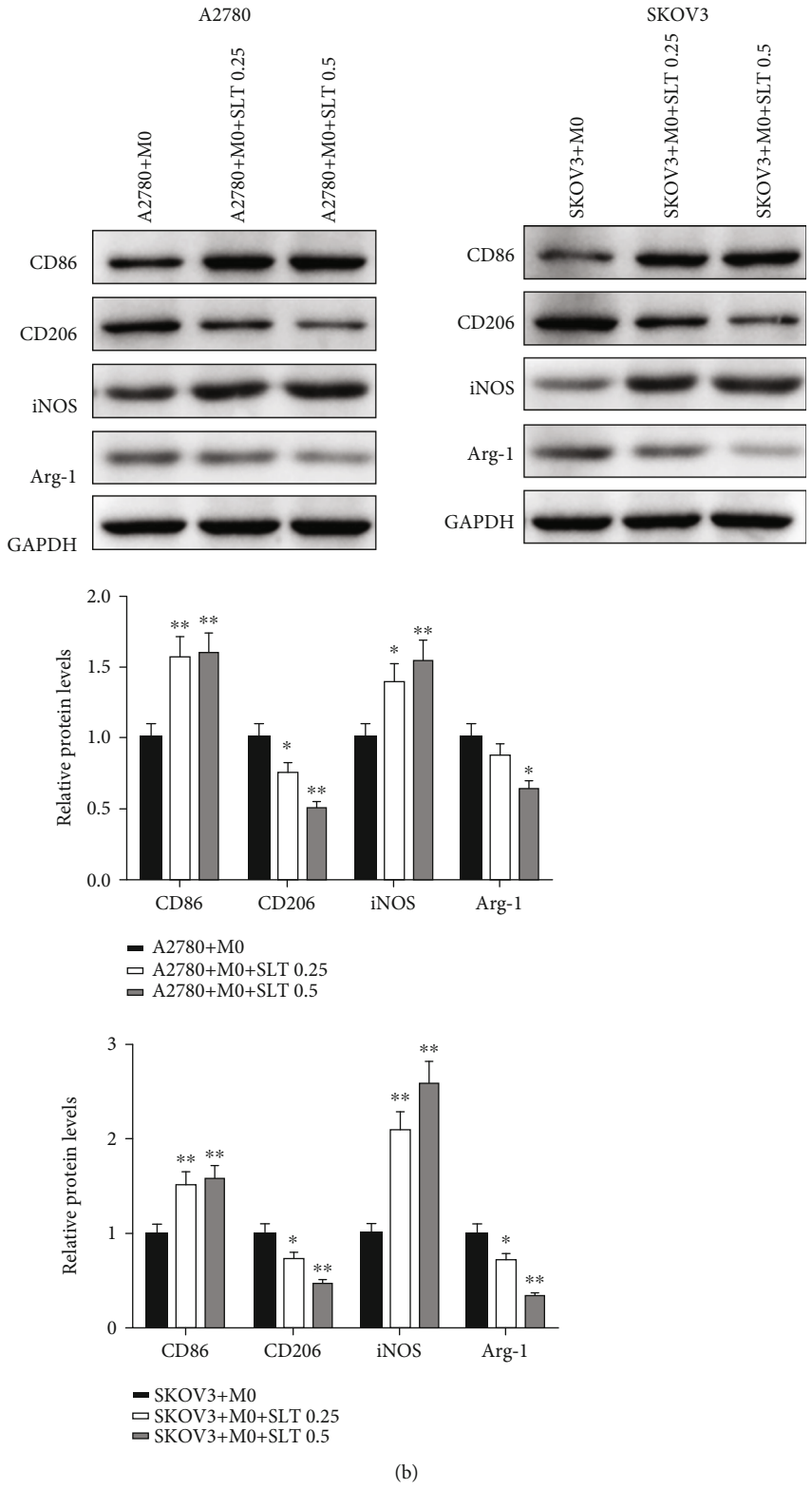

Figure 7: SLT regulates the polarization of M0 macrophages in coculture with ovarian cancer cells. (a) Flow cytometry assay was performed to analyze the M1 and M2 polarization in M0 macrophages, and the percentages of CD86+ and CD206+ cells were detected. (b) The protein expressions of CD86, CD206, iNOS, and Arg-1 were detected using western blotting. The values were displayed as the mean ± SD. Representative results from three independent experiments were shown ($^{*}P < 0.05$, $^{**}P < 0.01$, and $^{***}P < 0.001$ compared with the A2780/SKOV3+M0 group).

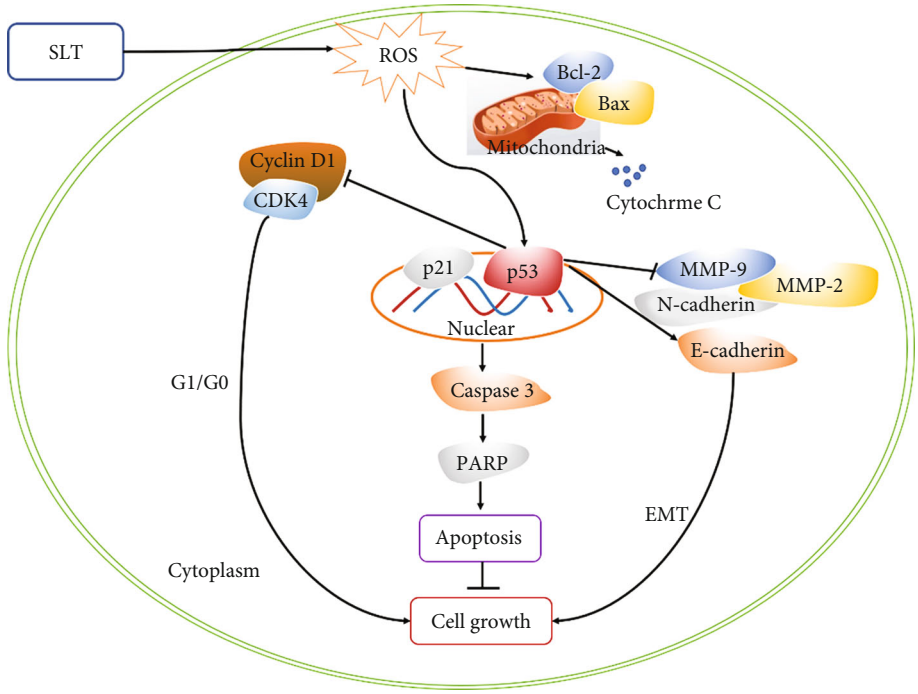

Figure 8: Schematic diagram of the potential molecular mechanism of anticancer effects of SLT on ovarian cancer. →: activation; ⊥: inhibition.

of ROS induced by SLT intensified p53-mediated signaling cascade to regulate cell proliferation, EMT, and apoptosis.

3.7. SLT Regulates the Polarization of M0 Macrophages to Inhibit Ovarian Cancer Progression. As the macrophage polarizations are critically involved in the tumor immune microenvironment and thus affect the biological function of tumor cells, we also detect the effect of SLT on the polarization of M0 macrophages cocultured with A2780 and SKOV3 cells, to investigate the regulation potential of SLT on tumor immune microenvironment. Flow cytometry assay was performed to detect the expression of CD86 of M1 macrophages and CD206 of M2 macrophages. As the results indicated in Figure 7(a), compared to the M0 macrophages cocultured with A2780 or SKOV3 cells, the percentage of CD86+ cells was significantly increased in the A2780/SKOV3+M0 macrophages groups treated with SLT (0.25 and 0.5 μg/mL), but the percentage of CD206+ cells was significantly decreased in the A2780/SKOV3+M0 macrophages groups treated with SLT (0.25 and 0.5 μg/mL). In Figure 7(b), the western blot results showed that compared to those in the A2780/SKOV3+M0 macrophages group, the protein expression of CD86 and iNOS was significantly increased in the A2780/SKOV3+M0 macrophages+SLT groups (0.25 and 0.5 μg/mL), and the protein expression of CD206 and Arg-1 was significantly decreased in the A2780/SKOV3+M0 macrophages+SLT groups (0.25 and 0.5 μg/mL). Taken together, these results indicated that in M0 macrophages cocultured with A2780 or SKOV3, SLT could activate the polarization of M0 macrophages to M1 macrophages, but inhibit the polarization of M0 macrophages to M2 macrophages, thus regulate the tumor immune microenvironment and inhibit the ovarian cancer progression.

4. Discussion

Ovarian cancer is the most common cancer in women and the second cause of gynecologic cancer death among female worldwide [4]. SLT has been proven to have effective anticancer activity against a variety of cancers, but the antitumor activity against ovarian cancer and its underlying mechanism is rare. This study represented the effect of SLT on ovarian cancer and the potential mechanisms. In the present study, we found that SLT could regulate ovarian cancer cell proliferation, migration, invasion, EMT, and apoptosis through activating the ROS-mediated p53 pathway. The effect on macrophage polarization also showed that SLT activated the M0 macrophages polarized to M1 macrophages, and inhibited to M2 macrophages, to regulate the tumor immune microenvironment of ovarian cancer and thus inhibiting tumor progression.

Our results suggested that SLT plays an important role in inhibiting ovarian tumor progression. Previous study reported that the extract of SLT can inhibit the growth of SMMC-7721 cells and induce apoptosis through the mitochondrial pathway in hepatocellular carcinoma [25]. In human colon adenocarcinoma cells, SLT induced cell cytotoxicity and apoptosis, and regulated the expression of CDK1, p27, p53, cyclin B1, cyclin E, caspase-3, caspase-8, caspase-9, Bcl-2, Bax, and cytochrome C activity [18]. Moreover, sesquiterpenoids extracted from SLT can inhibit the proliferation of breast cancer, colon cancer, gastric cancer cells, etc., by inducing mitochondrial-mediated apoptosis [26]. Considering the role of SLT in other cancers, we found that SLT can inhibit the proliferation and induce the G1 phase arrest in ovarian cancer cells. Consistent with the previous study, we found that SLT significantly reduced the

protein levels of CDK4 and Cyclin D1, but increased the protein level of P21. Apoptosis is the process of programmed cell death, which plays a major role in the maintenance of tissue homeostasis and the elimination of tumor cells [27]. Once apoptosis occurs, caspases are activated by proteolytic cleavage and then affect downstream signals, such as PARP [28]. And in this study, SLT was proved to increase the apoptosis rate of ovarian cancer cells through mitochondrial apoptosis pathway with the increased protein levels of cleaved caspase-3, cleaved PARP, Bax, and cytochrome C (in the cytoplasm), while the Bcl-2 level was decreased.

Since most ovarian cancers can only be detected after the cancer has spread to other organs, a promising strategy to fight against this disease is to control the metastasis. EMT is one of the key initiating events of the metastatic cascade, giving tumor cells the ability to invade [29]. EMT and its reverse process mesenchymal transformation to the epithelium (MET) are essential for the metastasis of ovarian cancer; thereby, effective antiovarian cancer treatments can be developed by preventing EMT [30, 31]. MMPs are a family of proteolytic enzymes that include extracellular cell matrix (ECM) modification to accelerate cell migration and cleave cytokines [32]. Increased levels of MMP-2/9 are related to the invasion, metastasis, and poor prognosis of various cancers [33, 34]. A recent study showed that the alkaloid compound solasodine extracted from SLT can induce apoptosis, affect autophagy, and reduce the metastasis of ovarian cancer cells [19]. Therefore, we speculate that SLT can regulate the migration and invasion of ovarian cancer cells. Consistent with our conjecture, SLT was found in this study to inhibit cell migration, invasion, and EMT. Moreover, SLT significantly inhibited the protein levels of MMP2, MMP9, and N-cadherin, and increased the protein level of E-cadherin, indicating that SLT can inhibit EMT in ovarian cancer cells.

ROS are elevated in response to a variety of stimuli and participate in the regulation of the modulation of cancer cell proliferation, invasion, metastasis, and apoptosis [35, 36]. Many studies have shown that ROS activates the expression of p53 in tumor cells, thereby inhibiting tumor growth [37, 38]. p53 is a well-known tumor suppressor that regulates cell cycle progression, which regulates G0/G1 and G2/M cell cycle checkpoints, as well as downstream p21, and also affects apoptosis and EMT processes [39–41]. Yang et al. found that SLT induced G0/G1 phase arrest and triggered apoptosis via p53 activation in the WEHI-3 murine leukemia cells [42]. Therefore, we speculated that the p53 signaling pathway may be a key mechanism regulating the anticancer effects of SLT in ovarian cancer cells. Consistently, SLT was proved to promote ROS accumulation, inhibit cell proliferation, EMT, and induce apoptosis, and the mechanism might be associated with the p53 pathway, whereas the effects can be reversed by inhibiting ROS by NAC treatment. A schematic diagram depicting the hypothetical mechanism required for SLT treatment is illustrated in Figure 8. Taken together, the results suggested that the ROS/p53 pathway might be related to SLT-regulated proliferation, invasion, and apoptosis in ovarian cancer cells.

Tumor-associated macrophages are one of the most abundant and significant innate immune cells in tumor microenvironment; M1 macrophages suppress cancer progression, while M2 macrophages promote it [43]. In *in vitro* simulated tumor microenvironment, study shows that cocultured ovarian cancer cells polarized macrophages to the M2 phenotype, and M2 macrophages enhanced the proliferation, invasion, and migration, and inhibited the apoptosis of ovarian cancer cells, thus playing a stimulation role in ovarian cancer cells [44]. And in ovarian cancer patients, increased overall or intraislet M1/M2 TAM ratios were positively correlated with an improved 5-year prognosis [45]. In this study, we also found that in ovarian cancer cells cocultured with M0 macrophages, that SLT activated the polarization of M0 macrophages to M1 macrophages and inhibited the polarization to M2 macrophages, with the increased percentage of CD86 + cells and decreased percentage of CD206+ cells were detected. It indicated the important role of macrophage polarization as well as the immunoregulation potential of SLT in tumor microenvironment of ovarian cancer cells. Previous study also reported the immunomodulatory activity of SLT extract in tumor, by remarkably promoting splenocyte proliferation, NK cell, and CTL activity in S180 sarcoma tumor-bearing mice, indicated SLT could act as antitumor agent with immunomodulatory activity [46].

In conclusion, our data showed that SLT can inhibit the proliferation, induce apoptosis, inhibit migration, invasion, and EMT, and also regulate macrophage polarization to regulate tumor immune microenvironment in ovarian cancer cells. The results also demonstrate that the mechanism might be achieved by regulating the ROS-mediated p53 signaling pathway. Taken together, these findings may provide insights to better understand the potential mechanisms of the anticancer effects of SLT and help to discover alternative treatment strategies for ovarian cancer.

5. Conclusion

In summary, this study illustrated the anticancer effects of SLT on ovarian cancer cells, suggesting that SLT may have the potential to provide basic evidence for the discovery of antiovarian cancer agents.

Data Availability

All data generated or analyzed during this study are included in this article.

Conflicts of Interest

The authors state that there are no conflicts of interest to disclose.

Authors' Contributions

Chen Zhang and Zheming Li contributed to this work equally.

Acknowledgments

The work was supported by the Zhejiang Traditional Chinese Medicine Science and Technology Plan Project (No. 2019ZA046).

References

[1] C. L. P. Slatnik and E. Duff, "Ovarian cancer," *The Nurse Practitioner*, vol. 40, no. 9, pp. 47–54, 2015.

[2] L. A. Torre, B. Trabert, C. E. DeSantis et al., "Ovarian cancer statistics, 2018," *CA: a Cancer Journal for Clinicians*, vol. 68, no. 4, pp. 284–296, 2018.

[3] C. Stewart, C. Ralyea, and S. Lockwood, "Ovarian cancer: an integrated review," *Seminars in Oncology Nursing*, vol. 35, no. 2, pp. 151–156, 2019.

[4] S. Lheureux, M. Braunstein, and A. M. Oza, "Epithelial ovarian cancer: evolution of management in the era of precision medicine," *CA: a Cancer Journal for Clinicians*, vol. 69, no. 4, pp. 280–304, 2019.

[5] R. Agarwal and S. B. Kaye, "Ovarian cancer: strategies for overcoming resistance to chemotherapy," *Nature Reviews Cancer*, vol. 3, no. 7, pp. 502–516, 2003.

[6] M. Matz, M. P. Coleman, H. Carreira et al., "Worldwide comparison of ovarian cancer survival: histological group and stage at diagnosis (CONCORD-2)," *Gynecologic Oncology*, vol. 144, no. 2, pp. 396–404, 2017.

[7] J. Y. Lee, S. Kim, Y. T. Kim et al., "Changes in ovarian cancer survival during the 20 years before the era of targeted therapy," *BMC Cancer*, vol. 18, no. 1, p. 601, 2018.

[8] G. D. Aletti, M. M. Gallenberg, W. A. Cliby, A. Jatoi, and L. C. Hartmann, "Current management strategies for ovarian cancer," *Mayo Clinic Proceedings*, vol. 82, no. 6, pp. 751–770, 2007.

[9] S. Wang, S. Long, and W. Wu, "Application of traditional Chinese medicines as personalized therapy in human cancers," *The American Journal of Chinese Medicine*, vol. 46, no. 5, pp. 953–970, 2018.

[10] W. W. Hsiao and L. Liu, "The role of traditional Chinese herbal medicines in cancer therapy–from TCM theory to mechanistic insights," *Planta Medica*, vol. 76, no. 11, pp. 1118–1131, 2010.

[11] Q. Ji, Y.-q. Luo, W.-h. Wang, X. Liu, Q. Li, and S.-b. Su, "Research advances in traditional Chinese medicine syndromes in cancer patients," *Journal of Integrative Medicine*, vol. 14, no. 1, pp. 12–21, 2016.

[12] H. Lin, J. Liu, and Y. Zhang, "Developments in cancer prevention and treatment using traditional Chinese medicine," *Frontiers of Medicine*, vol. 5, no. 2, pp. 127–133, 2011.

[13] Y. Hai-long, L. Jian, L. Qing-sheng, and D. Jun-xing, "Chemical constituents from *Solanum lyratum Thunb*," *Bulletin of the Academy of Military Medical Sciences*, vol. 34, no. 1, pp. 65–67, 2010.

[14] L. Yang, F. Feng, and Y. Gao, "Chemical constituents from herb of *Solanum lyratum*," *China Journal of Chinese Materia Medica*, vol. 34, no. 14, pp. 1805–1808, 2009.

[15] S. S. Li, Z. L. Hou, G. D. Yao et al., "Lignans and neolignans with isovaleroyloxy moiety from *Solanum lyratum* Thunb.: chiral resolution, configurational assignment and neuroprotective effects," *Phytochemistry*, vol. 178, p. 112461, 2020.

[16] Z. M. Xiao, A. M. Wang, X. Y. Wang, and S. R. Shen, "A study on the inhibitory effect of *Solanum lyratum Thunb* extract on Lewis lung carcinoma lines," *African Journal of Traditional, Complementary, and Alternative Medicines*, vol. 10, no. 6, pp. 444–448, 2014.

[17] Y. T. Lin, A. C. Huang, C. L. Kuo et al., "Induction of cell cycle arrest and apoptosis in human osteosarcoma U-2 OS cells by Solanum lyratum extracts," *Nutrition and Cancer*, vol. 65, no. 3, pp. 469–479, 2013.

[18] S.-C. Hsu, J.-H. Lu, C.-L. Kuo et al., "Crude extracts of Solanum lyratum induced cytotoxicity and apoptosis in a human colon adenocarcinoma cell line (Colo 205)," *Anticancer Research*, vol. 28, no. 2A, pp. 1045–1054, 2008.

[19] X.-H. Xu, L.-L. Zhang, G.-S. Wu et al., "Solasodine induces apoptosis, affects autophagy, and attenuates metastasis in ovarian cancer cells," *Planta Medica*, vol. 83, pp. 254–260, 2017.

[20] A. Hafner, M. L. Bulyk, A. Jambhekar, and G. Lahav, "The multiple mechanisms that regulate p53 activity and cell fate," *Nature Reviews. Molecular Cell Biology*, vol. 20, no. 4, pp. 199–210, 2019.

[21] J. H. Carter, J. A. Deddens, G. Mueller et al., "Transcription factors WT1 and p53 combined: a prognostic biomarker in ovarian cancer," *British Journal of Cancer*, vol. 119, no. 4, pp. 462–470, 2018.

[22] Y. Kong, L. Zhang, Y. Huang et al., "Pseudogene PDIA3P1 promotes cell proliferation, migration and invasion, and suppresses apoptosis in hepatocellular carcinoma by regulating the p53 pathway," *Cancer Letters*, vol. 407, pp. 76–83, 2017.

[23] W. Tang, K. Dong, K. Li, R. Dong, and S. Zheng, "MEG3, HCN3 and linc01105 influence the proliferation and apoptosis of neuroblastoma cells via the HIF-1α and p53 pathways," *Scientific Reports*, vol. 6, no. 1, 2016.

[24] S. S. Mello and L. D. Attardi, "Deciphering p53 signaling in tumor suppression," *Current Opinion in Cell Biology*, vol. 51, pp. 65–72, 2018.

[25] X.-Q. Mo, H.-Y. Wei, G.-R. Huang et al., "Molecular mechanisms of apoptosis in hepatocellular carcinoma cells induced by ethanol extracts of Solanum *lyratum Thunb* through the mitochondrial pathway," *World Journal of Gastroenterology*, vol. 23, no. 6, pp. 1010–1017, 2017.

[26] M. Chen, J. Wu, X. X. Zhang et al., "Anticancer activity of sesquiterpenoids extracted from *Solanum lyratum* via the induction of mitochondria-mediated apoptosis," *Oncology Letters*, vol. 13, no. 1, pp. 370–376, 2017.

[27] J. S. Long and K. M. Ryan, "New frontiers in promoting tumour cell death: targeting apoptosis, necroptosis and autophagy," *Oncogene*, vol. 31, no. 49, pp. 5045–5060, 2012.

[28] R. Yao, H. Z. Zheng, L. Q. Wu, and P. S. Cai, "Study on effect of glycyrrhizin on apoptosis of HPV18+ human cervical carcinoma HeLa cells induced by mitochondrial membrane depolarization," *Chinese Journal of Modern Applied Pharmacy*, vol. 37, no. 22, pp. 2727–2733, 2020.

[29] T. Brabletz, R. Kalluri, M. A. Nieto, and R. A. Weinberg, "EMT in cancer," *Nature Reviews. Cancer*, vol. 18, no. 2, pp. 128–134, 2018.

[30] M. Takai, Y. Terai, H. Kawaguchi et al., "The EMT (epithelial-mesenchymal-transition)-related protein expression indicates the metastatic status and prognosis in patients with ovarian cancer," *Journal of Ovarian Research*, vol. 7, no. 1, p. 76, 2014.

[31] D. Vergara, B. Merlot, J.-P. Lucot et al., "Epithelial-mesenchymal transition in ovarian cancer," *Cancer Letters*, vol. 291, no. 1, pp. 59–66, 2010.

[32] J. Gaffney, I. Solomonov, E. Zehorai, and I. Sagi, "Multilevel regulation of matrix metalloproteinases in tissue homeostasis indicates their molecular specificity *in vivo*," *Matrix Biology*, vol. 44-46, pp. 191–199, 2015.

[33] D. Karmakar, J. Maity, P. Mondal et al., "E2F5 promotes prostate cancer cell migration and invasion through regulation of TFPI2, MMP-2 and MMP-9," *Carcinogenesis*, vol. 41, no. 12, pp. 1767–1780, 2020.

[34] F. Xu, X. Si, J. Wang, A. Yang, T. Qin, and Y. Yang, "Nectin-3 is a new biomarker that mediates the upregulation of MMP2 and MMP9 in ovarian cancer cells," *Biomedicine & Pharmacotherapy*, vol. 110, pp. 139–144, 2019.

[35] S. Prasad, S. C. Gupta, and A. K. Tyagi, "Reactive oxygen species (ROS) and cancer: role of antioxidative nutraceuticals," *Cancer Letters*, vol. 387, pp. 95–105, 2017.

[36] W.-H. Chiu, S.-J. Luo, C.-L. Chen et al., "Vinca alkaloids cause aberrant ROS-mediated JNK activation, Mcl-1 downregulation, DNA damage, mitochondrial dysfunction, and apoptosis in lung adenocarcinoma cells," *Biochemical Pharmacology*, vol. 83, no. 9, pp. 1159–1171, 2012.

[37] Y.-d. Geng, C. Zhang, J.-l. Lei et al., "Walsuronoid B induces mitochondrial and lysosomal dysfunction leading to apoptotic rather than autophagic cell death via ROS/p53 signaling pathways in liver cancer," *Biochemical Pharmacology*, vol. 142, pp. 71–86, 2017.

[38] H. Zhang, R. Chen, X. Wang, H. Zhang, X. Zhu, and J. Chen, "Lobaplatin-induced apoptosis requires p53-mediated p38MAPK activation through ROS generation in non-small-cell lung cancer," *Frontiers in Oncology*, vol. 9, no. 538, 2019.

[39] C. Li and D. E. Johnson, "Liberation of functional p53 by proteasome inhibition in human papilloma virus-positive head and neck squamous cell carcinoma cells promotes apoptosis and cell cycle arrest," *Cell Cycle*, vol. 12, no. 6, pp. 923–934, 2013.

[40] S. Tudzarova, P. Mulholland, A. Dey, K. Stoeber, A. L. Okorokov, and G. H. Williams, "p53 controls CDC7 levels to reinforce G1 cell cycle arrest upon genotoxic stress," *Cell Cycle*, vol. 15, no. 21, pp. 2958–2972, 2016.

[41] S.-O. Lim, H. Kim, and G. Jung, "p53 inhibits tumor cell invasion via the degradation of snail protein in hepatocellular carcinoma.," *FEBS Letters*, vol. 584, no. 11, pp. 2231–2236, 2010.

[42] J.-S. Yang, C.-C. Wu, C.-L. Kuo et al., "*Solanum lyratum* extracts induce extrinsic and intrinsic pathways of apoptosis in WEHI-3 murine leukemia cells and inhibit allograft tumor," *Evidence-Based Complementary and Alternative Medicine*, vol. 2012, Article ID 254960, 13 pages, 2012.

[43] Y. Yousefzadeh, S. Hallaj, M. Baghi Moornani et al., "Tumor associated macrophages in the molecular pathogenesis of ovarian cancer," *International Immunopharmacology*, vol. 84, p. 106471, 2020.

[44] J. Yi, Y. Lin, W. Yicong, L. Chengyan, Z. Shulin, and C. Wenjun, "Effect of macrophages on biological function of ovarian cancer cells in tumor microenvironment in vitro," *Archives of Gynecology and Obstetrics*, vol. 302, no. 4, pp. 1009–1017, 2020.

[45] M. Zhang, Y. He, X. Sun et al., "A high M1/M2 ratio of tumor-associated macrophages is associated with extended survival in ovarian cancer patients," *Journal of Ovarian Research*, vol. 7, no. 1, p. 19, 2014.

[46] S. H. Liu, X. H. Shen, X. F. Wei, X. H. Mao, and T. Huang, "Immunomodulatory activity of butanol extract from Solanum lyratum in tumor-bearing mice," *Immunopharmacology and Immunotoxicology*, vol. 33, no. 1, pp. 100–106, 2010.

Hindawi
Journal of Immunology Research
Volume 2021, Article ID 6696606, 14 pages
https://doi.org/10.1155/2021/6696606

Research Article

Ganoderma lucidum Spore Polysaccharide Inhibits the Growth of Hepatocellular Carcinoma Cells by Altering Macrophage Polarity and Induction of Apoptosis

Ming Song,[1] **Zhen-hao Li**,[2] **Hong-shun Gu**,[3] **Ru-ying Tang**,[4] **Rui Zhang**,[1] **Ying-li Zhu**,[4] **Jin-lian Liu**,[1] **Jian-jun Zhang**,[1] **and Lin-yuan Wang**[4]

[1]*School of Traditional Chinese Medicine, Beijing University of Chinese Medicine, Beijing 100029, China*
[2]*Zhejiang Shouxiangu Institute of Rare Medicine Plant, Wuyi, 321200, China*
[3]*Beijing Cairui Medicine Technology Institute, Beijing 100094, China*
[4]*School of Chinese Materia Medica, Beijing University of Chinese Medicine, Beijing 100029, China*

Correspondence should be addressed to Jian-jun Zhang; zhangjianjun@bucm.edu.cn and Lin-yuan Wang; wangly@bucm.edu.cn

Received 4 January 2021; Revised 2 February 2021; Accepted 10 February 2021; Published 5 March 2021

Academic Editor: Kai Wang

Background. *Ganoderma lucidum* has certain components with known pharmacological effects, including strengthening immunity and anti-inflammatory activity. *G. lucidum* seeds inherit all its biological characteristics. *G. lucidum* spore polysaccharide (GLSP) is the main active ingredient to enhance these effects. However, its specific biological mechanisms are not exact. Our research is aimed at revealing the specific biological mechanism of GLSP to enhance immunity and inhibit the growth of H22 hepatocellular carcinoma cells. *Methods*. We extracted primary macrophages (Mø) from BALB/c mice and treated them with GLSP (800 μg/mL, 400 μg/mL, and 200 μg/mL) to observe its effects on macrophage polarization and cytokine secretion. We used GLSP and GLSP-intervened macrophage supernatant to treat H22 tumor cells and observed their effects using MTT and flow cytometry. Moreover, real-time fluorescent quantitative PCR and western blotting were used to observe the effect of GLSP-intervened macrophage supernatant on the PI3K/AKT and mitochondrial apoptosis pathways. *Results*. In this study, GLSP promoted the polarization of primary macrophages to M1 type and the upregulation of some cytokines such as TNF-α, IL-1β, IL-6, and TGF-β1. The MTT assay revealed that GLSP+Mø at 400 μg/mL and 800 μg/mL significantly inhibited H22 cell proliferation in a dose-dependent manner. Flow cytometry analysis revealed that GLSP+Mø induced apoptosis and cell cycle arrest at the G2/M phase, associated with the expression of critical genes and proteins (PI3K, p-AKT, BCL-2, BAX, and caspase-9) that regulate the PI3K/AKT pathway and apoptosis. GLSP reshapes the tumor microenvironment by activating macrophages, promotes the polarization of primary macrophages to M1 type, and promotes the secretion of various inflammatory factors and cytokines. *Conclusion*. Therefore, as a natural nutrient, GLSP is a potential agent in hepatocellular carcinoma cell treatment and induction of apoptosis.

1. Introduction

Hepatocellular carcinoma (HCC) is the most life-threatening disease worldwide, having high mortality and poor prognosis and an incidence of more than one million cases per year [1]. At present, the treatments for liver cancer are surgery, radiotherapy, and chemotherapy [2]. Its occurrence and development are closely related to various molecular mechanisms in the cell. Recently, an increasing number of chemical drugs and new targeted drugs have been developed. However, some patients are still resistant to drugs. Therefore, the development of new natural medicines is expected to become another strategy for treating liver cancer. Active extracts of various natural medicinal plants have been tested for cancer treatment and have shown good antitumor efficacy [3].

Nowadays, researches have focused on the immunomodulation and antitumor activity of natural products, and this has become the focus of emerging research [4].

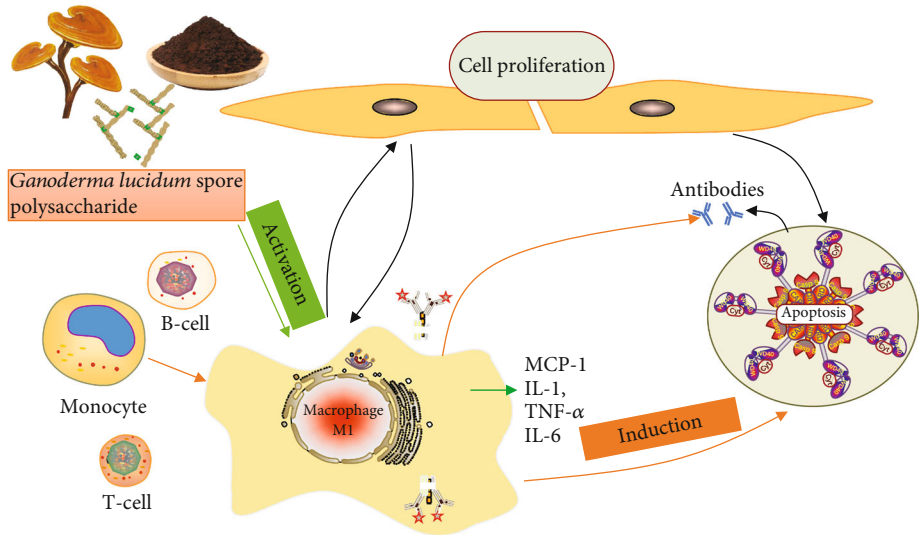

Figure 1: GLSP enhances immunity and induces tumor cell apoptosis by activating macrophages. GLSP: *Ganoderma lucidum* spore polysaccharide.

Naturally sourced antitumor drugs have been shown to exhibit therapeutic effects and few adverse reactions in tumor therapy. They can repair the body's immune system and even cure tumors [5]. *Ganoderma lucidum*, which is also called "Lingzhi" has been used medicinally for more than 2000 years [6] and has been regarded as an effective medicinal compound, reinforcing healthy qi to restore normal function and prolong life and has almost no toxic side effects [7]. *G. lucidum* spores are microscopic and are ejected from the cap during growth and maturation. These germ cells have all of *G. lucidum* genetically active substances [8]. Modern pharmacological studies have shown that *G. lucidum* spores have antitumor effects, increase immune regulation, lower blood sugar and lipid, increase anti-inflammatory and antihypoxia ability, and scavenge free radicals [9].

Macrophages (Mø) play an essential role in humoral and cellular immunity and in maintaining tissue homeostasis [10]. Related studies have found that macrophages are incredibly plastic and can be activated into a series of continuously adjustable functional states under the stimulation of different environments or drugs [11]. Classically activated (M1 type) macrophages and alternatively activated (M2 type) macrophages are the two extremes of this state. The process by which naive (Mφ type) macrophages are stimulated by exogenous factors in specific tissues to differentiate into M1 or M2 macrophages is called macrophage polarization [12]. The dynamic balance between M1 and M2 is vital for maintaining homeostasis. Once the balance is broken, the human body faces a variety of diseases that can sometimes be treated with drugs to regulate these macrophages. The transformation of M1 and M2 macrophages is a dynamic and reversible process. Directional polarization may provide new methods for cancer treatment [13, 14].

Tumor-associated macrophages (TAMs) are similar to the function of immune cells in the tumor microenvironment and mainly infiltrate the tumor matrix to mediate inflammation [15]. The secretion of cytokines, chemokines, growth factors, and proteases and the regulation of intracellular signaling pathways play a vital role in modulating the function of TAMs and tumor cells. The tumor microenvironment combines chronic inflammation, low oxygen levels, nutritional deficiencies, and acidosis, creating extremely complex dynamic systems [16] that regulate tumor growth, proliferation, metastasis, and immune escape. Therefore, we think that the treatment of tumors by reducing the stress state of the tumor's internal environment and then feeding it back to the tumor cells may promote tumor cell apoptosis or autophagy [17, 18]. Supernatant transfer of various cell cocultures in vitro has been used to mimic the tumor microenvironment [19].

By comparing the content and composition of GLSP and *G. lucidum* polysaccharides (GLP), we found that the overall structure is similar, but there are still many differences. At present, more than 200 kinds of substances have been separated, of which the largest is β-glucan and a few are α-glucan [20]. Although there have been many studies on GLP, because the shell of *G. lucidum* spores is hard and difficult to remove completely, we apply a brand-new removal wall technology that makes it possible to extract GLSP with higher purity. GLSP has better physical and chemical properties than GLP, and its application prospects are broader [21, 22]. Besides, GLSP plays a vital role in nourishing and protecting the liver, resisting radiation, resisting gene mutations, and resisting inflammation. Such effects have not been confirmed in GLP-related studies.

In our previous experiments, we found that the *G. lucidum* spore water extract had no inhibitory effect on H22 liver cancer cells and no cytotoxicity. However, when added to macrophages, it had a significant inhibitory effect on H22 liver tumor cells. To clarify the antitumor mechanism of *G. lucidum* spores, we studied the antitumor activity of *G. lucidum* spore polysaccharides (GLSP). We speculate that it is one of the targets of liver cancer, as shown in Figure 1.

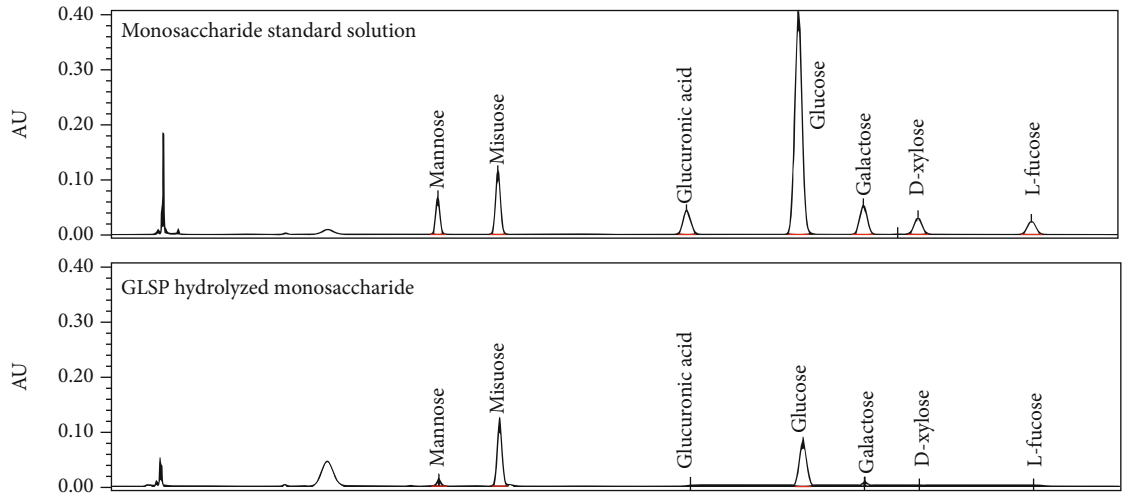

Figure 2: HPLC chromatograms of standard monosaccharide solution and GLSP hydrolysate.

2. Materials and Methods

2.1. Cells and Animals. Mouse H22 cells were obtained from Jiangsu KeyGEN BioTECH Co., Ltd. The culture conditions were 90% RMPI1640 medium + 10% FBS, cultured in an incubator at 37°C, 5% CO_2, and saturated humidity. Sixteen BALB/c mice (male; age range, 4-6 weeks), weighing 20.0 ± 2.0 g, were obtained from the Vital River Laboratory Animal Technology Limited Company (Beijing, China). The laboratory condition is at room temperature (25 ± 2°C) and humidity (65 ± 5%). The ethics committee of Beijing University of Chinese Medicine and the China Academy of Chinese Medicine Sciences approved all the experiments (No. 2016-0012).

2.2. Primary Macrophage Extraction. Mice about six weeks old were shaved on a clean bench for disinfection. The animals were euthanized by cervical dislocation, and they were then immersed in 75% alcohol for 3-5 s by the tail. The mice were then fixed on the dissection table. After scrubbing the peritoneal wall with 75% alcohol, 1 mL precooled PBS was injected into the abdominal cavity with a 5 mL syringe, and the abdomen was gently massaged for 2-3 min. Under aseptic conditions, the abdominal wall was opened, the peritoneum was exposed, and the abdominal wall was scrubbed with 75% alcohol. The peritoneal fluid was aspirated with a syringe and centrifuged at 4°C at 1000 rpm/min for 10 min. Finally, 10% calf serum RPMI-1640 solution was used to suspended cells. Peritoneal macrophages were collected, viable cells > 95% with trypan blue staining were collected, the cell concentration was adjusted to 5.0×10^5 cells/mL with RPMI-1640 medium, and they were inoculated into culture flasks and placed in a 5% CO_2, 37°C incubator. After 4 hours of culture, the nonadherent cells were washed with PBS to obtain purified peritoneal macrophages.

2.3. Preparation of Ganoderma lucidum Spore Powder. A total of 80 g of the wall-removed G. lucidum spore powder was extracted with 95% ethanol in a 5000 mL round flask. After removing ethanol, the residue was added 2400 mL of water (30 times the amount of water) and refluxed for 3 h. The solution was then filtered and concentrated to 80 mL. Then, 425 mL of 95% ethanol diluted to 80% ethanol was added while stirring, let stand for 12 h at 0-4°C, and filtered. The precipitate was taken and dissolved in water and chloroform with n-butanol (5 : 1) mixed solution for extraction according to the Sevag method. Then, the solution was shaken for 15 min, the organic layer was removed, and the extraction was repeated four times, concentrated, and dried to obtain GLSP. The GLSP content was 92.7% according to the test method of the 2015 edition of the "Pharmaceuticals of the People's Republic of China." HPLC chromatograms of standard monosaccharide solution and GLSP hydrolysate are shown in Figure 2.

2.4. Modeling and Drug Delivery. H22 cells were treated for 24 h under different conditions: only DMEM (control), GLSP (800 μg/mL, 400 μg/mL, and 200 μg/mL), macrophage supernatant, and GLSP (800 μg/mL, 400 μg/mL, and 200 μg/mL) +macrophage supernatant combination. The concentrations of GLSP (800 μg/mL, 400 μg/mL, and 200 μg/mL) used in this study resulted in no inhibitory activity on macrophage growth. Culture supernatants were collected to measure levels of TNF-α, TGF-β1, IL-6, and IL-1β. Each group of cells was subsequently harvested to determine intracellular reactive oxygen species (ROS) production for western blot (WB) analyses and other experiments.

2.5. MTT Assay. H22 cells were digested, counted, and prepared into a cell suspension at a concentration of 5×10^4 cells/mL. The plate was placed at 37°C, 5% CO_2 for 24 h in a box. The drug was diluted with complete medium to the required concentration (200 μg/mL, 400 μg/mL, and 800 μg/mL). Then, 100 μL of the corresponding drug-containing medium and 100 μL of macrophage supernatant were added to each well. After 24 h of incubation in the box, 20 μL MTT (5 mg/mL) (Amresco, Solon, Ohio, USA) was added and continued to incubate for 4 h in the incubator. 150 μL DMSO was added to dissolve the MTT and shaken

gently for 10 mins. Absorbance was then measured at $\lambda = 490$ nm; the optical density (O.D.) was determined to calculate the inhibition rate. Inhibitory rate $(\%) = [(C - T)/C] \times 100$, where C is the control group and T is that of the treatment group.

2.6. Cell Cycle Analysis. H22 cells were treated with macrophages and different concentrations of GLSP (200 μg/mL, 400 μg/mL, and 800 μg/mL) for 24 h, collected by digestion, and made into cell suspensions. The cells were washed twice with PBS (centrifuged at 1000 rpm, 5 min). The prepared single-cell suspension was stored at 4°C and washed with PBS before staining the fixing solution. Next, 100 μL RNaseA was added to a 37°C water bath for 30 min and added 400 μL propidium iodide (PI) staining and mixed well. Then, it was incubated at 4°C for 30 min. Flow cytometry analysis (Becton-Dickinson FACSCalibur; Becton-Dickinson, USA) detected the fluorescence of the PI-DNA complex and at 488 nm red fluorescence.

2.7. Annexin V-FITC/PI Double Staining Assay. H22 cells were treated with macrophages and GLSP for 24 h, and the cells were collected. Cells were washed twice with PBS. Then, 500 μL of Binding Buffer was added to suspend the cells, 5 μL of Annexin V-FITC was added and mixed well, and 5 μL of PI was added and mixed with 5 μL propidium iodide (PI) using an Annexin V-FITC/PI staining kit (KeyGEN BioTECH), Cat number: KGA105-KGA108. This was incubated for 15 min in the dark. Flow cytometry analysis was used to detect cell apoptosis.

2.8. Intracellular Reactive Oxygen Species (ROS) Analysis. Cellular ROS were detected using a ROS Assay Kit (KeyGEN BioTECH Co., Ltd., Nanjing, China), Cat number: KGT010-1. DCFH-DA was diluted with serum-free culture medium at 1 : 1000 to a final concentration of 10 μM. After the cells were collected, they were suspended in the diluted DCFH-DA and incubated at 37°C for 20 min. The cells were mixed by inversion every 3-5 min. Cells were washed with serum-free cell culture medium three times to remove the DCFH-DA that had not entered the cells. ROS were analyzed using flow cytometry. Data processing was performed using Cell Quest.

2.9. Mitochondrial Membrane Potential (MMP) Analysis. Mitochondrial membrane potential (MMP) was detected using a JC-1 Apoptosis Detection Kit (KeyGEN BioTECH Co., Ltd., Nanjing, China), Cat number: KGA601-KGA604. H22 cells were treated with macrophages and GLSP for 24 h, before cell collection. 100 μL 10x incubation buffer was diluted with 900 μL sterile deionized water to make 1x incubation buffer. The incubation buffer was mixed and preheated to 37°C. 1 μL JC-1 was added to 500 μL 1x incubation buffer, vortexed, and mixed to prepare JC-1 working solution. A total of 500 μL JC-1 working solution was used to suspend the cells uniformly and incubated for 15-20 min in an incubator at 37°C and 5% CO_2. Washing was made twice with 1x incubation buffer, and 500 μL of 1x incubation buffer was used to resuspend the cells.

Table 1: Primer sequences used in the RT-qPCR analysis.

Gene		Sequences (5′-3′)
PI3K	Forward	AGGGAAGCGAGACGGCACTTT
	Reverse	CCACTACGGAGCAGGCATAGCA
AKT	Forward	CCAAGCACCGTGTGACCATGAA
	Reverse	TGGCGACGATGACCTCCTTCTT
BAX	Forward	CCAGGATGCGTCCACCAAGAAG
	Reverse	CCGTGTCCACGTCAGCAATCAT
BCL-2	Forward	TGCCACCTGTGGTCCATCTGA
	Reverse	CTCTGCGAAGTCACGACGGTAG
Caspase-9	Forward	GCCACTGCCTCATCATCAACAA
	Reverse	AGCGGAATCGGTGCTCAAGTT

2.10. Macrophage Cell Phenotype Detection. Macrophages were inoculated during the logarithmic growth phase into a six-well plate. After the drug was incubated for 24 h, the cells were collected and washed twice with PBS to collect 5×10^5 cells. Then, the supernatant was removed by centrifugation, and 90 μL PBS was added to resuspend the cells. The appropriate amounts of antibodies CD86 (BioLegend 105007) and CD206 (BioLegend 141703) were added. The cells were then incubated for 30 min at 37°C, 400 μL PBS was added, and the cell phenotype was detected by flow cytometry.

2.11. Enzyme-Linked Immunosorbent Assay (ELISA) Analysis. Cytokine levels were determined using a commercial ELISA kit (Proteintech, Rosemont, IL, USA). First, all samples, reagents, and working standards were prepared as instructed by the manufacturer. The required number of microplate strips was removed, and the microwells were placed in the strip holder. Then, 100 μL of each standard and sample was added to the appropriate wells. A cover seal was pressed firmly onto the top of the microwells. The plate was incubated for 90 min at 37°C in a humid environment. Then, the sealing mold was removed, 100 μL was added to each well, and antibody diluent was used to dilute at 1 : 30, except for blanks. And the plates were incubated at 37°C for 1 h. 100 μL of TMB was added to each well, shaken gently, and color developed at 37°C for 15 minutes. 50 μL stop solution was added to each hole. Sample absorbance was read at 450 nm using a Multiskan™ GO (Thermo Fisher Scientific, Waltham, MA, USA) detector system.

2.12. Quantitative Real-Time PCR (RT-qPCR). We continued to explore changes in PI3K, AKT, BAX, BCL-2, and caspase-9 mRNAs. Total RNA from each sample was extracted using a TRIzol reagent (Thermo Fisher Scientific, Waltham, MA, USA). Then, the determination of RNA concentration and purity and synthesis of cDNA first strand was carried out with 20 μL system, using a RevertAid First Strand cDNA Synthesis Kit (Thermo Fisher Scientific). The sequences for primers listed in Table 1 were designed by Primer6 and then synthesized by a biotechnology company (Sangon Biotech Co., Ltd., Shanghai, China). The SYBR® Green PCR Master Mix (Thermo Fisher Scientific) was used to amplify cDNA in the Multicolor Real-time PCR Detection System (Bio-

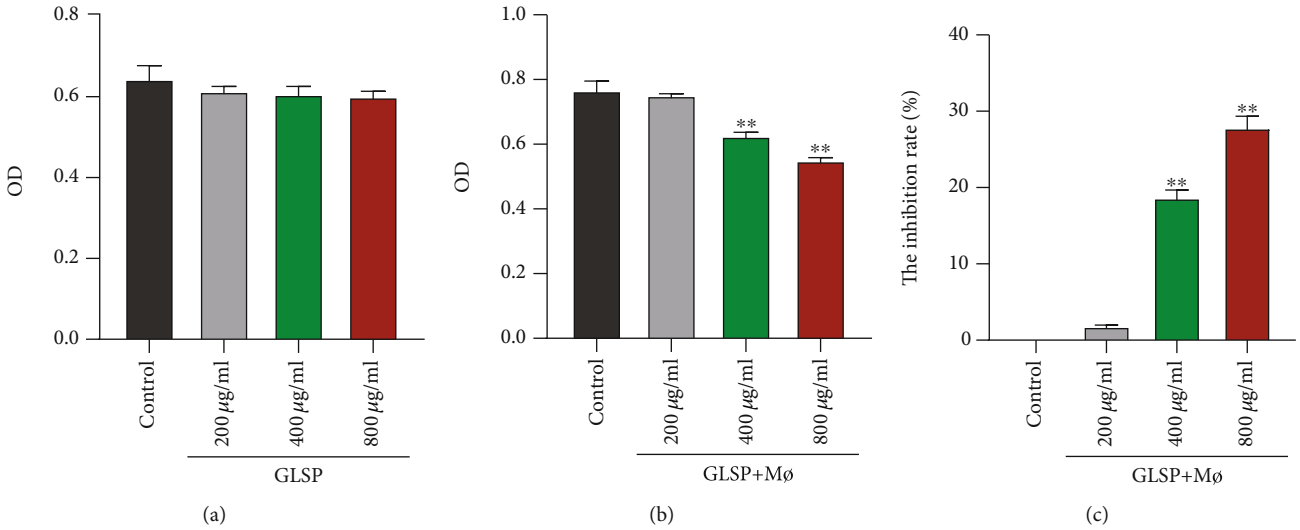

Figure 3: Inhibitory effects of GLSP and GLSP+Mø on the proliferation of H22 cells. (a) MTT assay reveals no effect on the viability of H22 cells treated with GLSP for 24 h; (b) MTT assay reveals a decrease in the viability of H22 cells treated with different concentrations of GLSP +Mø for 24 h, $^{**}P < 0.01$ vs. control group (24 h); (c) the inhibition rate increases in H22 cells treated with different concentrations of GLSP +Mø. $^{**}P < 0.01$ vs. H22 cell control group. GLSP: *Ganoderma lucidum* spore polysaccharide; OD: optical density.

Rad Laboratories Inc.). The PCR parameters were as follows: 95°C for 5 min, followed by 40 cycles of 95°C for 15 s and 72°C for 40 s, followed by 60°C for 1 min and 95°C for 15 s. The $2^{-\Delta\Delta Ct}$ method was used to calculate the results.

2.13. Western Blot Analysis. H22 cells treated with different intervention reagents, including 800 μg/mL GLSP, macrophage culture supernatant, and macrophage culture supernatant containing 800 μg/mL GLSP, were added to the plates and cultured continuously for 24 h. Then, trypsin without EDTA was used for digestion, followed by centrifugation and RIPA lysis solution (Biomiga, Santiago, CA, USA) addition. In line with the molecular weight of the target protein BAX (21 kDa), BCL-2 (26 kDa), CASP-9 (46 kDa), p-AKT (60 kDa), PI3K (85 kDa), and AKT (56 kDa), proteins were transferred onto polypropylene fluoride (PVDF) membranes. Nonfat milk (5%) was used to dilute the antibody. The antibodies used were anti-BAX (50599-2-Ig, mouse polyclonal, diluted 1 : 4,000), anti-CASP-9 (10380-1-AP, rabbit polyclonal, diluted 1 : 1000), anti-PI3K (60225-1-Ig, mouse polyclonal, diluted 1 : 5000), anti-AKT (60203-2-Ig, mouse polyclonal, diluted 1 : 2000), and anti-GAPDH (60004-1-lg, mouse monoclonal, diluted 1 : 5,000). All of the above antibodies were from the Proteintech Group: anti-BCL-2 (ab182858, diluted 1 : 2,000; Abcam Group, Cambridge, MA, USA) and anti-*p*-AKT (CST 4060s, diluted 1 : 2,000; CST, MA, USA). The Tanon-5200 system (Tanon, Shanghai, China) was used for exposure. The intensity of the target protein band was read using Tanon Gis software (Tanon).

2.14. Statistical Analysis. Dates are presented as the mean ± standard deviation (SD). The data were analyzed using SPSS 22.0 and one-way analysis of variance (ANOVA), or a nonparametric test was used for data processing based on the normality test. And a least significant difference (LSD) method was adopted for comparisons between groups. P value < 0.05 was considered a statistically significant difference.

3. Results

3.1. Cytotoxic Effect of GLSP and Macrophage Supernatant on H22 Cells. The activity of GLSP-treated H22 cells was detected using an MTT assay. Results showed that the proliferation of H22 cells was not affected by treatment with GLSP (Figure 3(a)). However, H22 cell proliferation was notably inhibited by macrophage supernatant + 400 μg/mL GLSP or +800 μg/mL GLSP ($P < 0.01$) (Figure 3(b)). The results also showed a dose-dependent increase in the inhibition rate of GLSP (400 μg/mL and 800 μg/mL) + Mø versus the control group ($P < 0.01$) (Figure 3(c)).

3.2. GLSP-Activated Macrophages Induce Cell Cycle Arrest at the G2/M Phase in H22 Cells. We examined the cell cycle distribution after treatment with GLSP and macrophage+GLSP. The percentage of H22 cells treated with macrophages+GLSP (800 μg/mL) in the G2/M phase was significantly higher than that in the control group (Figures 4(a) and 4(b)) ($P < 0.01$), whereas treatment with GLSP alone did not induce the same effect.

3.3. GLSP-Activated Macrophages Promote the Apoptosis of H22 Cells. Results showed that the percentage of apoptotic H22 cells was significantly increased upon macrophage +GLSP treatment (Figures 5(a) and 5(b)) ($P < 0.01$). These results indicated that GLSP-activated macrophages effectively induced H22 cell apoptosis.

We also examined GLSP-induced changes in MMP. GLSP-activated macrophage treatment induced the conversion of red fluorescence to green fluorescence, indicating a decrease in MMP (Figure 5(c)) ($P < 0.01$). As ROS generation

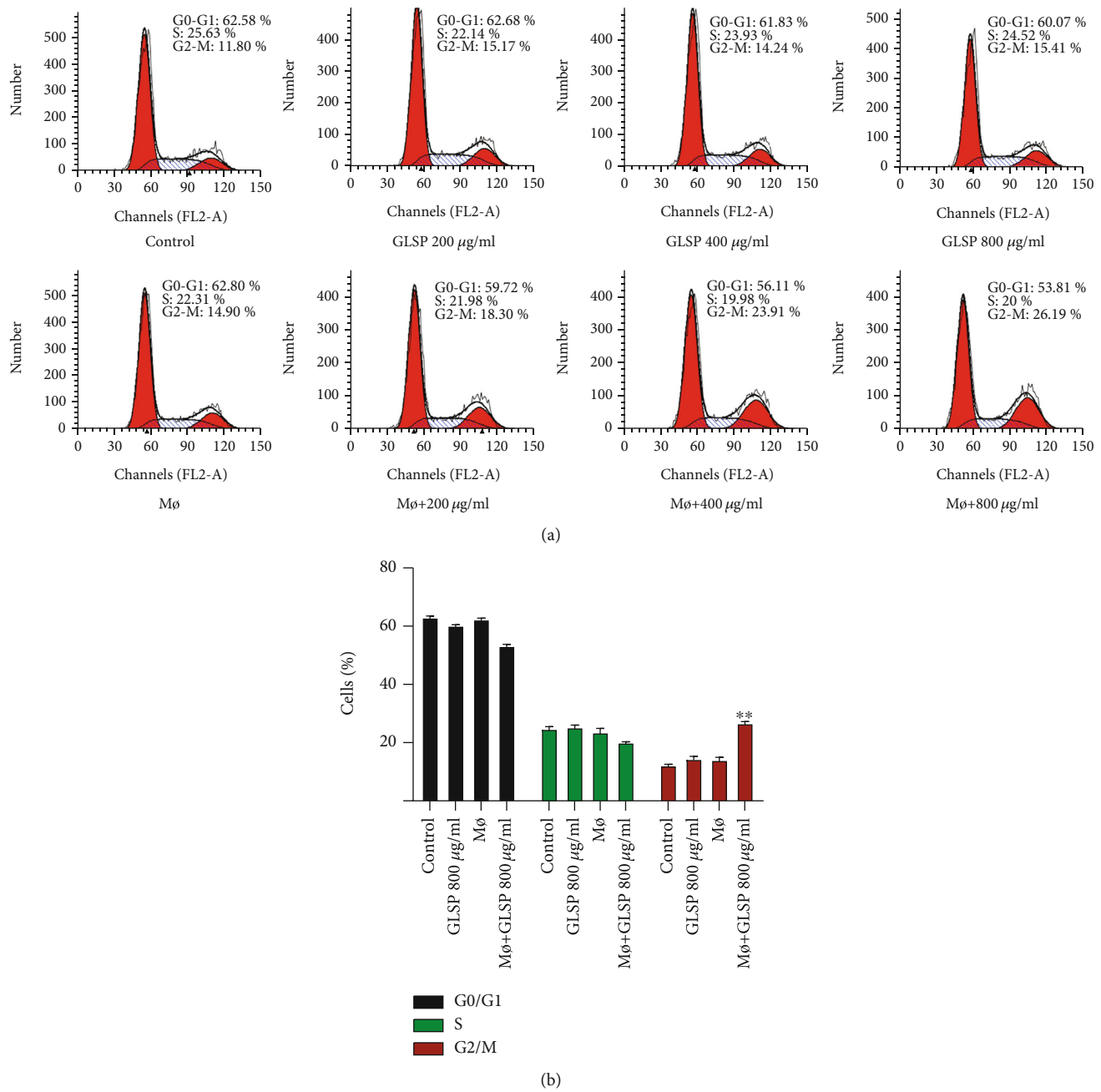

Figure 4: GLSP induces H22 cell arrest at the G2/M phase. (a) Cell cycle distribution of H22 cells treated with GLSP and macrophage supernatant. (b) Percentage in different periods of the cell cycle after GLSP treatment. $^{**}P < 0.01$ vs. H22 cell control group. GLSP: *Ganoderma lucidum* spore polysaccharide.

is closely related to mitochondrial apoptosis, ROS was detected to test whether oxidative stress had an effect on GLSP-activated macrophage-induced apoptosis in H22 cells. As shown in Figures 5(d) and 5(e), GLSP-activated macrophages led to a significant increase in intracellular ROS levels compared to that of the control group ($P < 0.01$). Therefore, the elevation of ROS production may be a relevant cause of GLSP-activated macrophage-induced apoptosis.

3.4. GLSP Activate Macrophage Polarization. Macrophages are dynamic cells that react to different stimuli by adjusting their functional state. Classically activated macrophages, M1 type, and alternatively activated M2 type are the two extremes of this state. We investigated the polarizing effect of GLSP treatment on macrophages. CD86 analysis revealed that H22 tumor cells had no effect on macrophage polarization, but GLSP treatment could activate macrophages, which polarized towards M1 type ($P < 0.01$) (Figures 6(a) and 6(b)). CD206 analysis revealed that H22 tumor cells and GLSP independently could increase M2 type macrophages ($P < 0.01$), but H22 GLSP+macrophages reduced the amount of M2 type (Figures 6(a) and 6(c)). As shown in Figure 5(d),

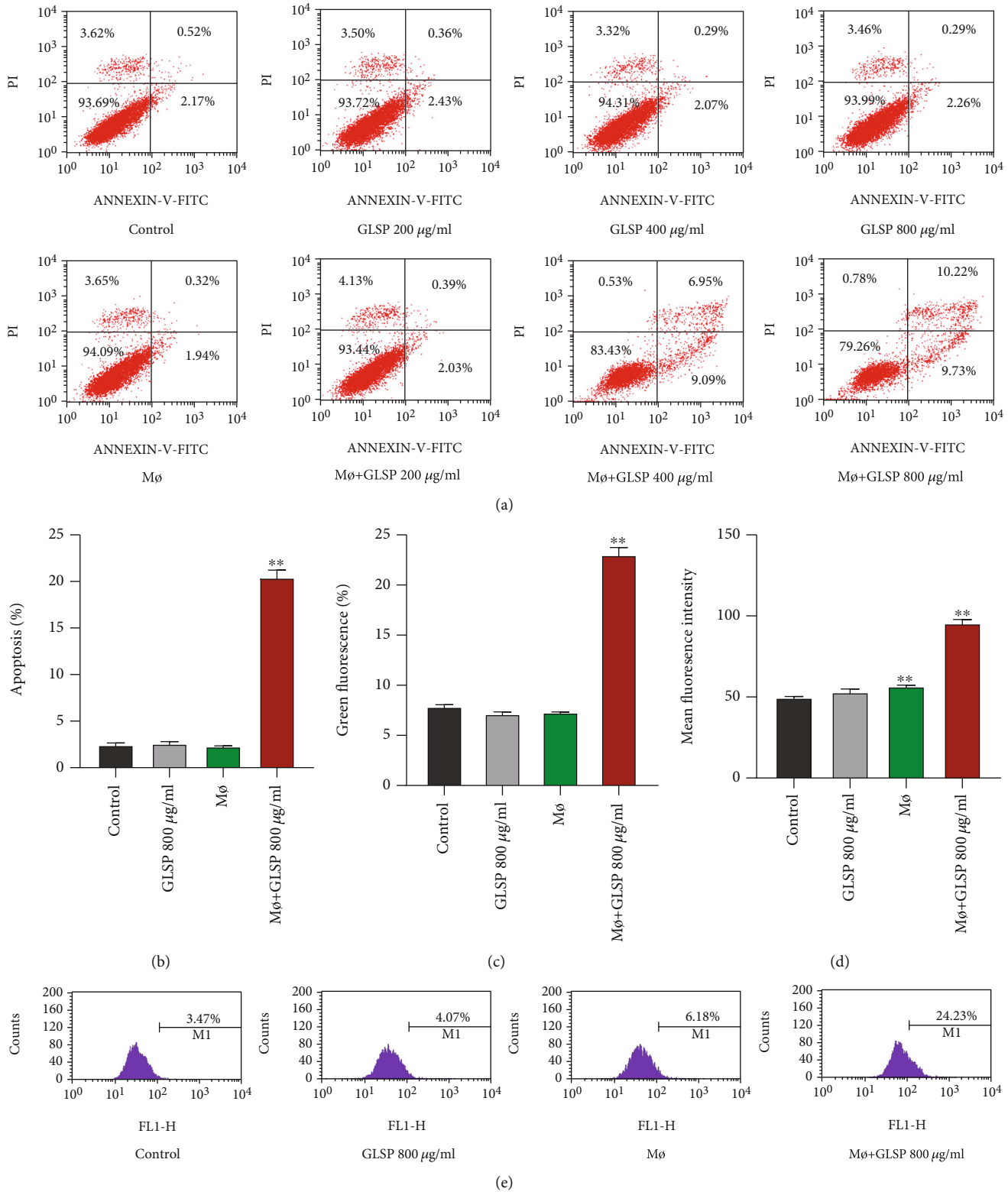

Figure 5: GLSP-activated macrophages induce H22 cell apoptosis. (a) Flow cytometric apoptosis in each group. (b) Percentages of apoptotic cells in each group. (c) FACS assessed MMP based on fluorescent mitochondria. (d) Analyses of ROS levels in H22 cells upon different concentrations of GLSP treatment. (e) Production of intracellular ROS in H22 detected by flow cytometry. Mean Cell Quest Pro analyzed fluorescence intensity. $^{**}P < 0.01$ vs. the control group. GLSP: *Ganoderma lucidum* spore polysaccharide; ROS: reactive oxygen species.

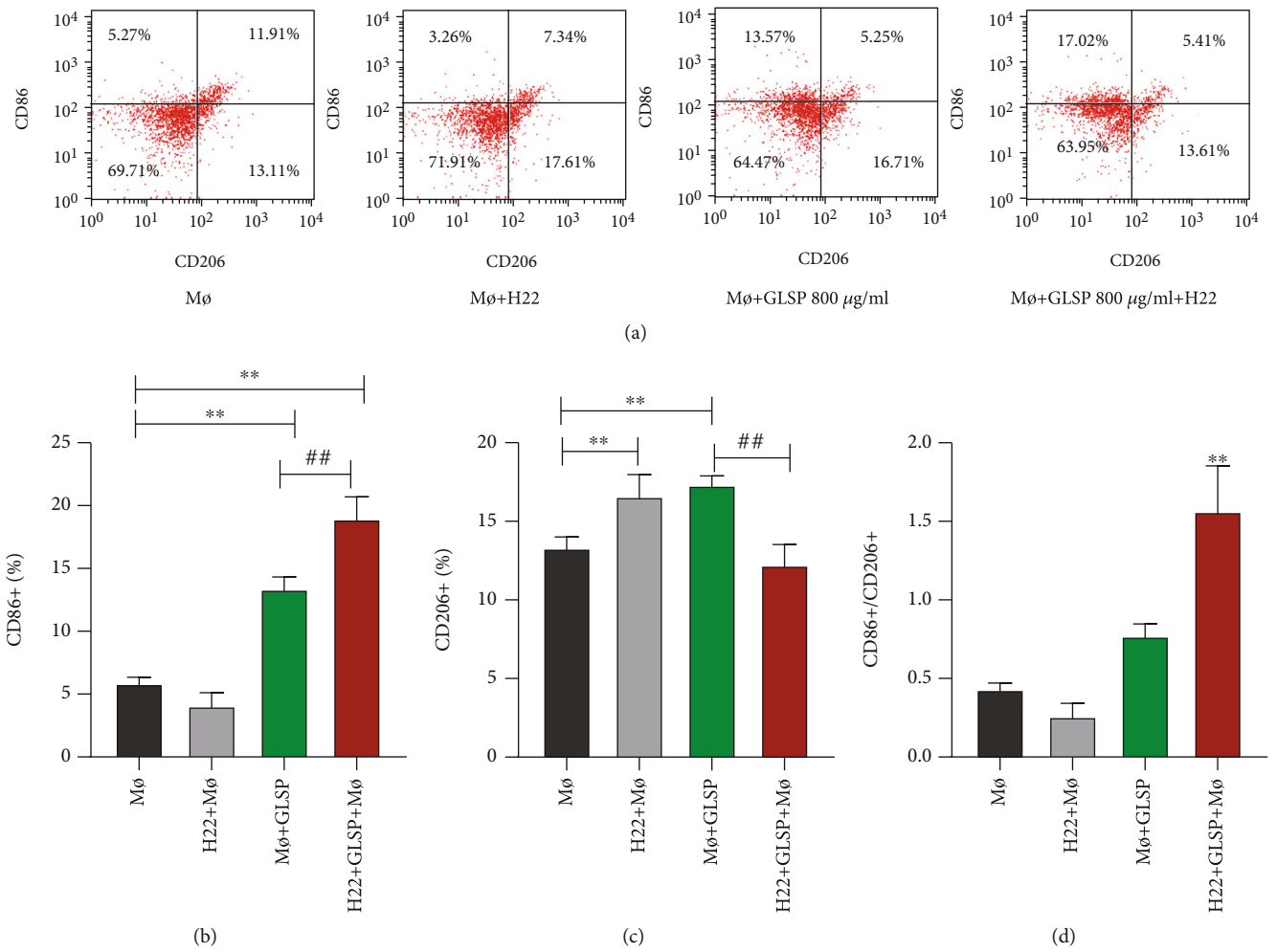

Figure 6: Effect of GLSP on the expression of M1 and M2 macrophage markers: (a) triple staining of flow cytometry analysis of macrophage cells; (b) CD86+ macrophage cells; (c) CD206+ macrophage cells; (d) CD86+/CD206+ macrophage cells. $^{**}P < 0.01$ vs. the control group, $^{\#\#}P < 0.01$ vs. the Mø+GLSP group. GLSP: *Ganoderma lucidum* spore polysaccharide.

H22+macrophages+GLSP improved the ratio of M1/M2. Therefore, GLSP increases the expression of M1 type macrophages and decreases the expression of M2 type macrophages. The cocultivation group improved the ratio of M1/M2, which affects the polarization of macrophages.

3.5. Effect of GLSP on Cytokine Production. As shown in Figure 7, the TNF-α (Figure 7(a)), IL-1β (Figure 7(b)), IL-6 (Figure 7(c)), and TGF-β1 (Figure 7(d)) levels were significantly higher in the macrophage+GLSP group than in the control group ($P < 0.01$) and in the H22+macrophage+GLSP group than in the H22+macrophage group ($P < 0.01$).

3.6. GLSP Activate Macrophages Affecting the PI3K/AKT and Mitochondria-Mediated Apoptotic Signaling Pathways. In the above experiments, GLSP activate macrophages effectively, thereby inducing apoptosis and other changes in H22 cells. Thus, we used RT-qPCR and western blot to explore the differences in apoptotic cell molecules and the PI3K/AKT signaling pathway. At the genetic level, the levels of PI3K were significantly decreased in GLSP+macrophage-treated H22 cells compared with the control group ($P < 0.01$) (Figure 8(a)). In Figure 8(b), the levels of AKT were not affected in GLSP+macrophage-treated H22 cells versus the control group. We measured the levels of BAX, BCL-2, and CASP-9. The levels of proapoptotic BAX were markedly increased, and antiapoptotic BCL-2 was significantly decreased in GLSP+macrophage-treated H22 cells versus the control group ($P < 0.01$) (Figures 8(c) and 8(d)). Levels of CASP-9 were increased in GLSP+macrophage-treated H22 cells versus control cells ($P < 0.01$) (Figure 8(e)).

We continued to explore changes at the protein level. In Figures 8(a) and 8(c), the levels of PI3K were significantly decreased in GLSP+macrophage-treated H22 cells versus the control group ($P < 0.01$). Similarly, the levels of p-AKT were significantly decreased in GLSP+macrophage-treated H22 cells ($P < 0.01$) (Figures 9(a) and 9(d)). In Figure 8(e), the levels of AKT were not affected in GLSP+macrophage-treated H22 cells. We also measured the protein levels of BAX, BCL-2, and CASP-9 and found that the levels of proapoptotic BAX were markedly increased ($P < 0.01$) (Figures 9(b) and 9(f)), and the level of antiapoptotic BCL-2 was significantly decreased in GLSP+macrophage-treated H22 cells versus control groups ($P < 0.01$)

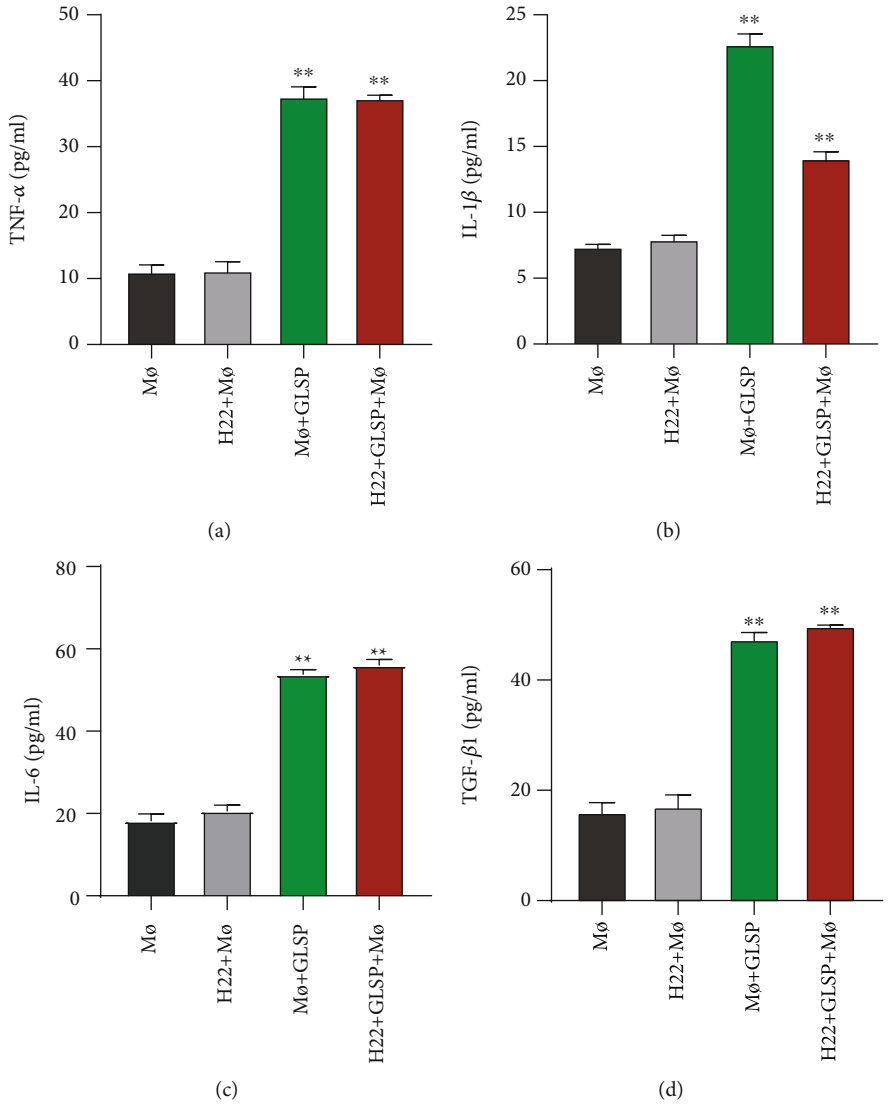

Figure 7: Increasing of proinflammatory cytokine expression by GLSP in macrophages. (a) TNF-α levels; (b) IL-1β levels; (c) IL-6 levels; (d) TGF-β1 levels. Data is expressed as the mean ± SD ($n = 5$), $^{**}P < 0.01$ vs. the control group; $^{\#\#}P < 0.01$ vs. the H22+macrophage group. GLSP: *Ganoderma lucidum* spore polysaccharide.

(Figures 9(b) and 9(g)). Levels of CASP-9 were increased in GLSP+macrophage-treated H22 cells versus control cells ($P < 0.01$) (Figure 9(h)). These results indicated that GLSP +macrophages could simultaneously activate genes and proteins in the mitochondria-mediated apoptotic signaling pathway.

4. Discussion

The primary characteristics of tumors are malignant proliferation and imbalance between cell proliferation and apoptosis [23]. Inhibiting proliferation and inducing apoptosis are excellent strategies for tumor treatment [24]. Previous research has shown that GLSP and *G. lucidum* triterpenes in *G. lucidum* spore powder can effectively inhibit tumors [25, 26]. The antitumor mechanism of *G. lucidum* spore powder includes inhibition of tumor cell proliferation, induction of tumor cell apoptosis, and termination of the tumor cell cycle. Early experiments in our group had found that the water extract of *G. lucidum* spores showed no apparent inhibitory effect on tumor cells and no cytotoxicity change. However, after coculture with immune cells such as macrophages, it showed inhibition of tumor cell characteristics. In order to determine the mechanism of action of the antitumor effect of *G. lucidum* spores, we separately studied GLSP, *G. lucidum* spore triterpene, and *G. lucidum* spore oil. Finally, it was discovered that GLSP is the material basis for activating macrophages to enhance immunity and antitumor activity.

GLSP can activate the immune response. It improved the immune state to achieve the balance of the body's immune state and inhibit the development of tumors [27]. MTT results showed that GLSP alone did not affect the proliferation of H22 tumor cells, showing no cytotoxicity. Nevertheless, it inhibited H22 tumor cells by activating macrophages. In our cell cycle experiments, we found that the

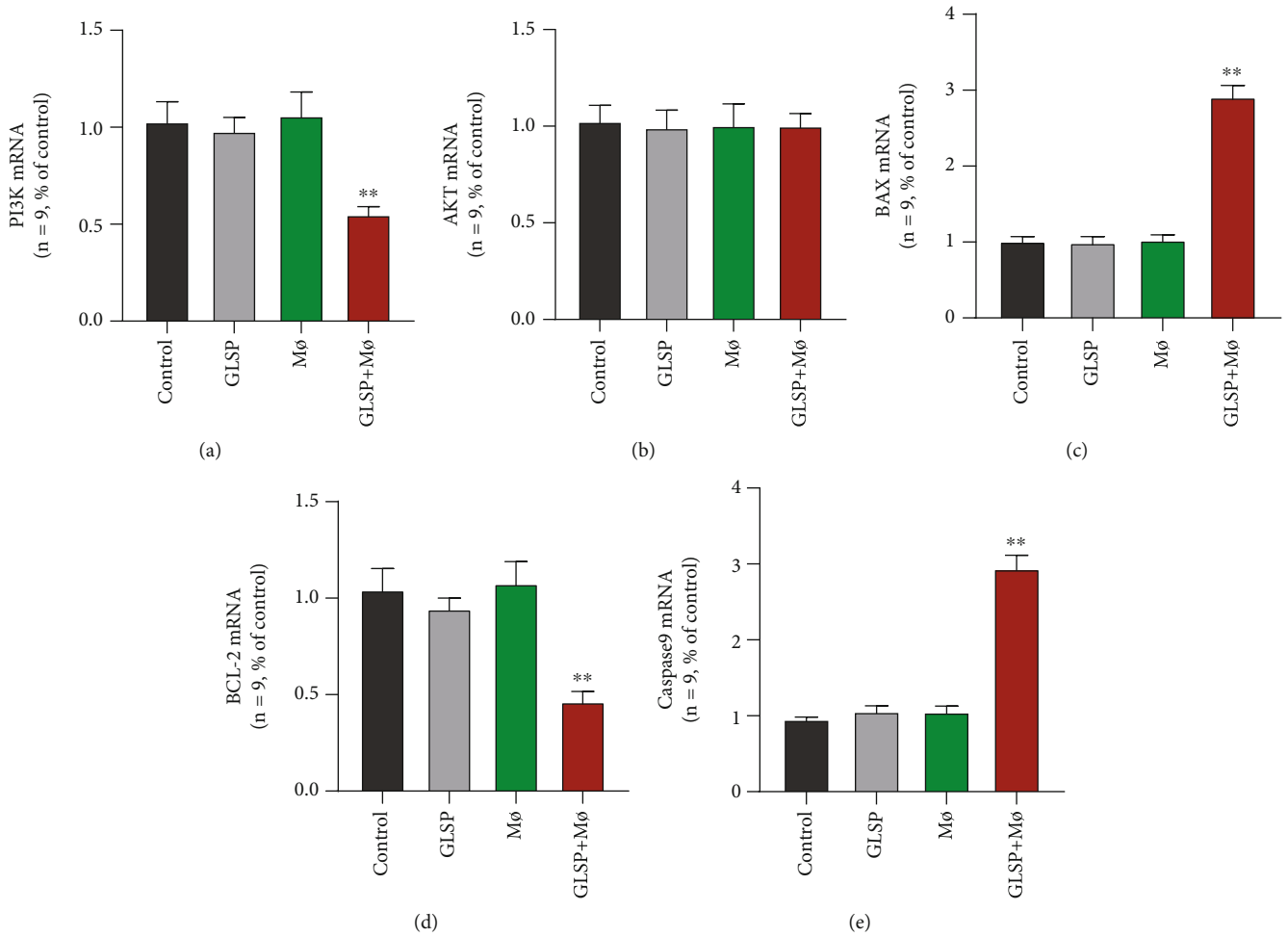

Figure 8: Effect of GLSP and Mø on the mRNA levels of PI3K/AKT and mitochondria-mediated apoptotic signaling pathway genes. H22 was treated with GLSP or Mø for 24 h, and then, the (a) mRNA levels of PI3K, (b) AKT, (c) BAX, (d) BCL-2, and (e) CASP-9 were detected by qPCR. The histogram bars represent three independent experiments, and the values are the mean ± SD. $^{**}P$ value < 0.01 versus the control group. GLSP: *Ganoderma lucidum* spore polysaccharide.

macrophage supernatant containing GLSP can block tumor cells in the G2/M stage, whereas the macrophage supernatant alone had no blocking effect on H22 tumor cells. Cell cycle arrest at the G2/M phase shows that there is damage in the intracellular DNA, which is challenging to repair.

The mitochondrial apoptosis pathway is an integral part of the endogenous cell apoptosis regulation [28]. The endogenous pathway is activated by cellular stress, DNA damage, developmental signals, and loss of survival factors [29]. BCL-2 family proteins are composed of proapoptotic factors (BAX, Bad, Bak, and Noxa) and antiapoptotic factors (BCL-2, BCL-xL, BCL-w, and Mel-1) [30]. The BCL-2 family members are located on the mitochondria and can control its permeability, the release of cytochrome C, the activation of "priming" CASP-9, and the subsequent activation of "executive" CASP-3. Endogenous apoptosis can be inhibited through prosurvival signaling pathways such as PI3K/AKT and MAPK [31, 32]. The PI3K/AKT pathway is an intracellular signaling pathway with phosphatidylinositol kinase and serine/threonine kinase activity. It is involved in regulating cell proliferation, apoptosis, survival, growth, and other cellular physiological functions, and these processes are known to be affected in tumors [33]. The regulation of PI3K/AKT activation is one of the hot topics in tumor pharmacology. As downstream molecules of PI3K/AKT, BCL-2 family proteins play a vital role in regulating apoptosis, mainly through endogenous pathways. Many survival factors can activate the PI3K pathway, leading to the activation of AKT, and AKT plays an essential role in cell survival signal transduction. PTEN has a negative regulatory effect on the PI3K/AKT pathway [34]. Activated AKT can phosphorylate and inhibit Bad, BAX, CASP-9, GSK-3, and FOXO1 [32]. Western blot and RT-qPCR results showed that GLSP downregulated the expression of PI3K and p-AKT genes and proteins in H22 cells. Our results showed a reduced phosphorylation level of AKT by inhibition of the PI3K/AKT signaling pathway, which simultaneously downregulates the expression of BCL-2 in H22 cells at mRNA and posttranslational levels and upregulates the expression of BAX, indicating that GLSP can inhibit the PI3K/AKT signaling pathway and induce apoptosis in liver cancer H22 cells (Figure 10).

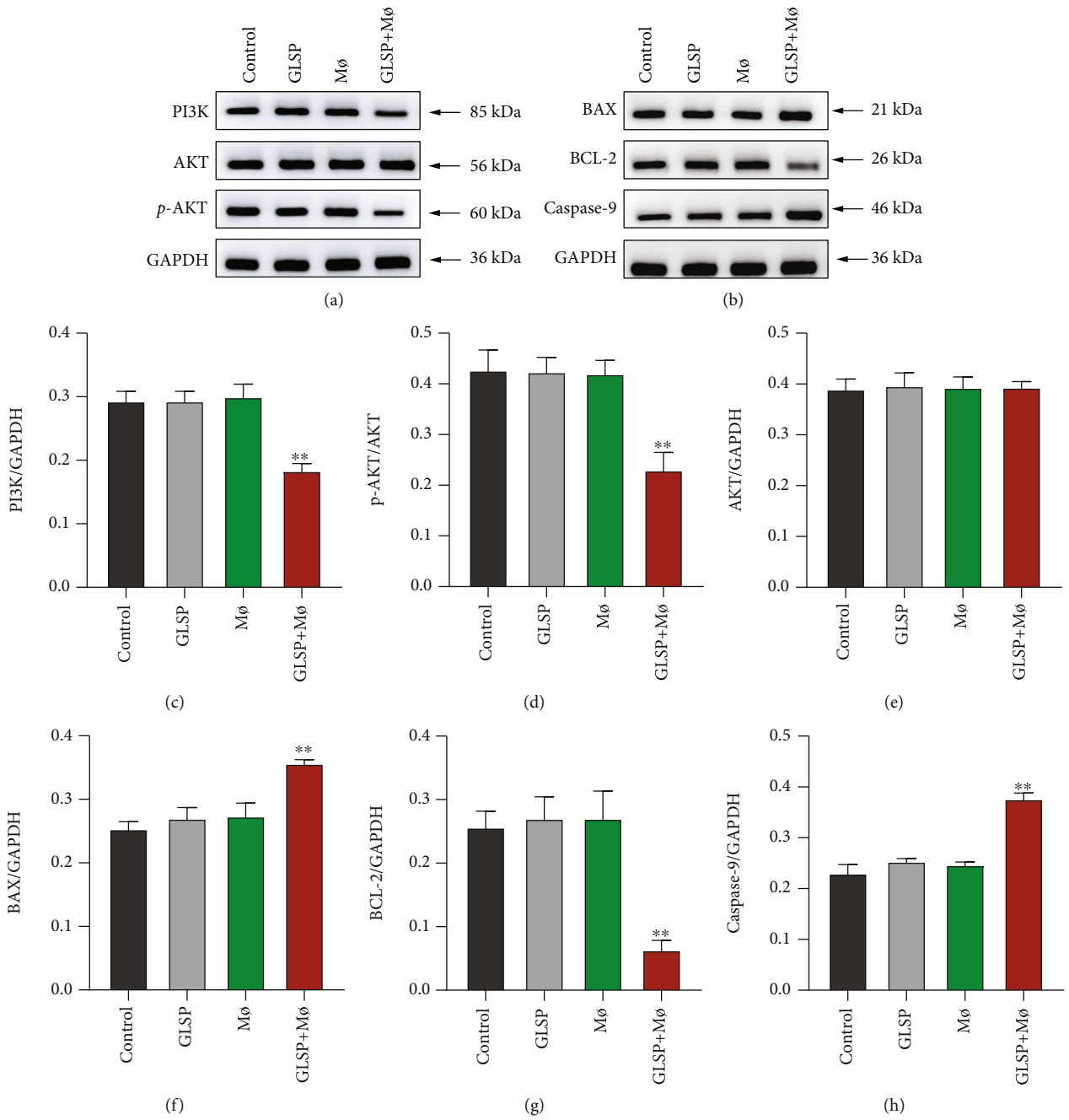

Figure 9: Effect of GLSP and Mø on the expression of PI3K/AKT and mitochondria-mediated apoptotic signaling pathway proteins. H22 cells were treated with GLSP or Mø for 24 h, and then, the protein levels of PI3K, AKT, p-AKT, BAX, BCL-2, and CASP-9 were detected by WB. (a) Protein expression of PI3K/AKT signal pathway; (b) protein expression of BAX, BCL-2, and CASP-9; (c) relative PI3K/GAPDH protein; (d) relative p-AKT/AKT protein; (e) relative AKT/GAPDH protein; (f) relative BAX/GAPDH protein; (g) relative BCL-2/GAPDH protein; (h) relative caspase-9/GAPDH protein, and values are the mean ± SD. $^{**}P$ value < 0.01 vs. control group. GLSP: *Ganoderma lucidum* spore polysaccharide.

The monocyte-macrophage system is an essential part of innate immunity [35, 36]. During inflammation or infection, monocytes in the blood are recruited into the tissue and differentiate into mature macrophages, a group of highly heterogeneous cells. Depending on the microenvironment, macrophages can polarize into different functional phenotypes [37]. According to their different activation states, they are mainly divided into classically activated macrophages (M1 type) and alternatively activated macrophages (M2 type) [38]. The polarization of phagocytic cells is affected by various cytokines in the microenvironment [39]. When the epithelial barrier is destroyed and pathogenic microorganisms invade, a large number of circulating monocytes are recruited under the action of chemokines and differentiate into

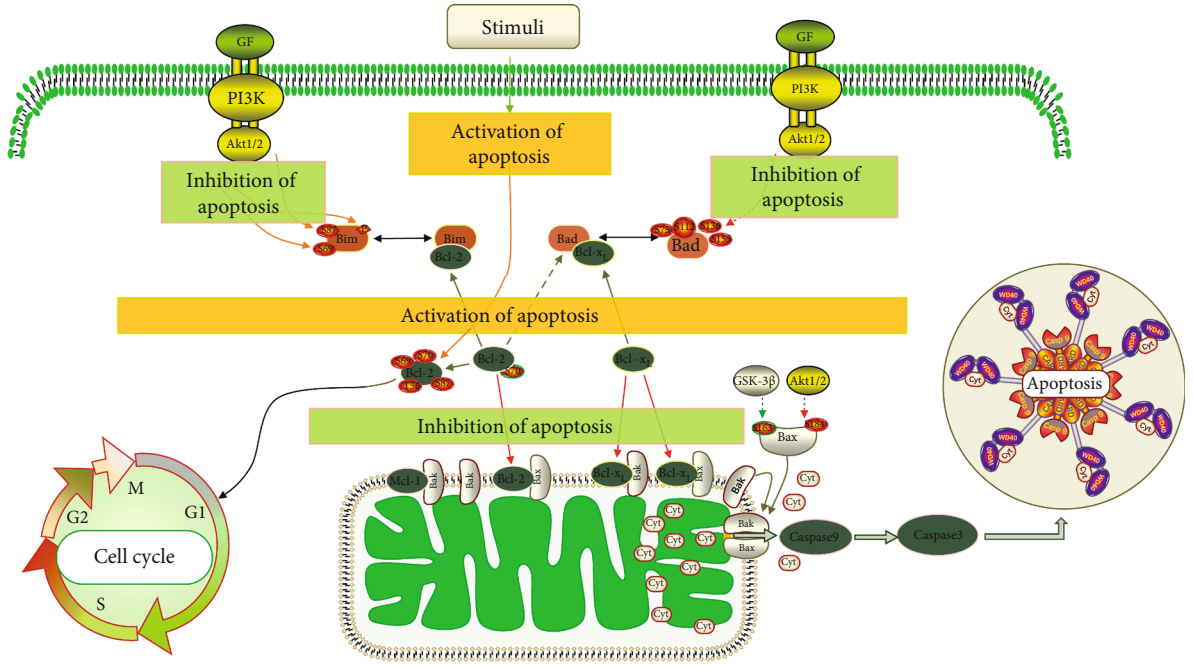

Figure 10: Schematic representation of the endogenous mitochondrial apoptosis pathway.

proinflammatory cells, namely, M1 macrophages, induced by local cytokines [40]. M1 macrophages have potent cytotoxicity; are highly sensitive to LPS; secrete many inflammatory factors and reactive oxygen products, such as IL-6, IL23, and TNF-α; promote inflammation cascades and tissue damage; activate Th1/Th17 adaptive immunity; and promote the elimination of pathogenic microorganisms. M2 type macrophages also increase during the disease, inhibit the inflammatory response, avoid excessive damage to the tissue, and, at the same time, remove pathogenic bacteria and cell debris in the process of inflammation subsiding. They also promote tissue repair and immune balance. The immune balance of the intestine depends on the two types of macrophages working together and coordinating with each other. Therefore, regulating the balance between M1 and M2 macrophages is essential for the occurrence and development of cancer [41].

TAMs are derived from monocytes in the blood system and enter tumor tissues under the action of chemokines [42]. The colony-stimulating factor secreted by tumor cells can prolong the survival time of TAMs. When TAMs are moderately activated in the tumor environment (M1 type), they exert antitumor immune function, which can kill tumor cells and destroy vascular endothelium, thereby inhibiting tumor development. However, if this stimulus is not suppressed in a short time, TAMs will be polarized into M2 type under the action of various cytokines secreted by tumor cells, which is why most TAMs in tumor tissues are M2 type [38]. In contrast to the M1 type, M2 TAMs can secrete growth factors, angiogenesis factors, and proteases, thereby stimulating tumor cell proliferation, promoting angiogenesis and tumor cell invasion and migration, and escaping the surveillance of antitumor immunity [43]. Therefore, the induction of secondary polarization of TAMs in tumor tissues and the transformation of M2 TAMs to M1 have become an essential target for tumor therapy in recent years [44]. Previous research has found that glycopeptide derived from G. lucidum (Gl-PS) could promote polarization of M1 macrophage vs. M2 macrophages [45]. In our macrophage typing experiments, GLSP can increase the number of CD86+ cells, which is an M1 macrophage marker. When H22 tumor cells were cocultured with macrophages, we found that GLSP decreased the number of CD206+ macrophages, an M2 type marker. Overall, when H22 tumor cells are cocultured with macrophages in the TME, GLSP increases the ratio of M1/M2 macrophages. Therefore, we can speculate that GLSP has a regulatory effect on M1 and M2 macrophages in the tumor microenvironment.

Currently, chemotherapy is one of the most common cancer treatments, but it has noticeable side effects [46]. In contrast, "nutritional drugs" are known for their low toxicity. "Nutrition" is a concept that has attracted much attention to prevent and treat diseases [47]. Traditional Chinese medicine (TCM) is a rich source of nutritional medicine that has been used for thousands of years [48]. It has an excellent effect on treating many chronic diseases. Additionally, TCM can also be used as part of a daily diet. TCM is a safe and effective way to prevent and treat diseases. GLSP is one of the foremost effective ingredients in TCM as it has a wide range of therapeutic effects and relatively low toxicity. It is a promising nutritional drug and has attracted wide attention in biomedicine in recent years [49, 50]. The above studies revealed that GLSP activates macrophages to induce apoptosis of H22 hepatocellular carcinoma cell in vitro and the biological mechanism. Next, we will continue to verify the biological activity of GLSP to enhance immunity and antitumor in vivo.

5. Conclusions

In summary, GLSP reshapes the tumor microenvironment by activating macrophages, regulating the polarization of macrophages, and promoting the secretion of various inflammatory factors and cytokines. Moreover, we found that GLSP can block H22 tumor cells in the G2/M phase by activating macrophages and can activate PI3K/AKT signaling pathways to affect the mitochondrial apoptotic pathway and promote tumor cell apoptosis. Therefore, as a natural nutrient, GLSP can alter macrophage polarity and has potential to reshape the tumor microenvironment activity.

Data Availability

The data (original) used to support the findings of this study are available from the authors upon request.

Conflicts of Interest

The authors declare that they have no conflict of interests.

Acknowledgments

This work was supported by the National Key R&D Program of China (2018YFC1706800).

References

[1] H. Jin, S. Wang, E. A. Zaal et al., "A powerful drug combination strategy targeting glutamine addiction for the treatment of human liver cancer," *eLife*, vol. 9, article e56749, 2020.

[2] H. Degroote, A. Van Dierendonck, A. Geerts, H. Van Vlierberghe, and L. Devisscher, "Preclinical and clinical therapeutic strategies affecting tumor-associated macrophages in hepatocellular carcinoma," *Journal of Immunology Research*, vol. 2018, Article ID 7819520, 9 pages, 2018.

[3] H. S. Lee and D. S. Oh, "Assessing the anti-cancer therapeutic mechanism of a herbal combination for breast cancer on system-level by a network pharmacological approach," *Anticancer Research*, vol. 40, no. 9, pp. 5097–5106, 2020.

[4] L. Han, X. Cao, Z. Chen et al., "Overcoming cisplatin resistance by targeting the MTDH-PTEN interaction in ovarian cancer with sera derived from rats exposed to Guizhi Fuling wan extract," *BMC complementary medicine and therapies*, vol. 20, no. 1, article 2825, 2020.

[5] B. B. Zhao, Z. H. Ye, X. Gao, and H. M. Li, "Diwu Yanggan modulates the Wnt/β-catenin pathway and inhibits liver carcinogenesis signaling in 2-AAF/PH model rats," *Current medical science*, vol. 39, no. 6, pp. 913–919, 2019.

[6] M. F. Lau, K. H. Chua, V. Sabaratnam, and U. R. Kuppusamy, "In vitroandin silicoanticancer evaluation of a medicinal mushroom,Ganoderma neo-japonicumImazeki, against human colonic carcinoma cells," *Biotechnology and Applied Biochemistry*, pp. 1–16, 2020.

[7] G. Wang, J. Zhang, T. Mizuno et al., "Antitumor active polysaccharides from the Chinese MushroomSongshan lingzhi, the fruiting body ofGanoderma tsugae," *Bioscience, Biotechnology, and Biochemistry*, vol. 57, no. 6, pp. 894–900, 1993.

[8] D. Li, Q. Zhong, T. Liu, and J. Wang, "Cell growth stimulating effect of Ganoderma lucidum spores and their potential application for Chinese hamster ovary K1 cell cultivation," *Bioprocess and Biosystems Engineering*, vol. 39, no. 6, pp. 925–935, 2016.

[9] Z. Li, Y. Shi, X. Zhang et al., "Screening immunoactive compounds of *Ganoderma lucidum* spores by mass spectrometry molecular networking combined with *in vivo* zebrafish assays," *Frontiers in Pharmacology*, vol. 11, 2020.

[10] S. Tsutsumi, Y. Tokunaga, S. Shimizu et al., "Effects of indole and indoxyl on the intracellular oxidation level and phagocytic activity of differentiated HL-60 human macrophage cells," *The Journal of Toxicological Sciences*, vol. 45, no. 9, pp. 569–579, 2020.

[11] F. Graziano, E. Vicenzi, and G. Poli, "Plastic restriction of HIV-1 replication in human macrophages derived from M1/M2 polarized monocytes," *Journal of Leukocyte Biology*, vol. 100, no. 5, pp. 1147–1153, 2016.

[12] J. Zhou, A. Zhang, and L. Fan, "HSPA12B secreted by tumor-associated endothelial cells might induce M2 polarization of macrophages via activating PI3K/Akt/mTOR signaling," *Oncotargets and Therapy*, vol. 13, pp. 9103–9111, 2020.

[13] Y. le, W. Cao, L. Zhou et al., "Infection of *Mycobacterium tuberculosis* promotes both M1/M2 polarization and MMP production in cigarette smoke-exposed macrophages," *Frontiers in Immunology*, vol. 11, 2020.

[14] F. Zhang, Y. Xuan, J. Cui, X. Liu, Z. Shao, and B. Yu, "Nicorandil modulated macrophages activation and polarization via NF-κb signaling pathway," *Molecular Immunology*, vol. 88, pp. 69–78, 2017.

[15] D. Ma, Y. Zhang, G. Chen, and J. Yan, "miR-148a affects polarization of THP-1-derived macrophages and reduces recruitment of tumor-associated macrophages via targeting SIRPα," *Cancer Management and Research*, vol. 12, pp. 8067–8077, 2020.

[16] J. Kozak, A. Forma, M. Czeczelewski et al., "Inhibition or reversal of the epithelial-mesenchymal transition in gastric cancer: pharmacological approaches," *International journal of molecular sciences*, vol. 22, no. 1, 2020.

[17] H. Lan, W. Zhang, K. Jin, Y. Liu, and Z. Wang, "Modulating barriers of tumor microenvironment through nanocarrier systems for improved cancer immunotherapy: a review of current status and future perspective," *Drug Delivery*, vol. 27, no. 1, pp. 1248–1262, 2020.

[18] Q. Meng, X. Luo, J. Chen et al., "Unmasking carcinoma-associated fibroblasts: key transformation player within the tumor microenvironment," *Biochimica Et Biophysica Acta. Reviews on Cancer*, vol. 1874, no. 2, article 188443, 2020.

[19] J. J. Eyre, R. L. Williams, and H. J. Levis, "A human retinal microvascular endothelial-pericyte co-culture model to study diabetic retinopathy in vitro," *Experimental Eye Research*, vol. 201, article 108293, 2020.

[20] C. H. Yeh, H. C. Chen, J. J. Yang, W. I. Chuang, and F. Sheu, "Polysaccharides PS-G and protein LZ-8 from Reishi (Ganoderma lucidum) exhibit diverse functions in regulating murine macrophages and T lymphocytes," *Journal of Agricultural and Food Chemistry*, vol. 58, no. 15, pp. 8535–8544, 2010.

[21] Y. Wang, Y. Liu, H. Yu et al., "Structural characterization and immuno-enhancing activity of a highly branched water-soluble β-glucan from the spores of _Ganoderma lucidum_," *Carbohydrate Polymers*, vol. 167, pp. 337–344, 2017.

[22] Y. Chen, J. Lv, K. Li et al., "Sporoderm-broken spores of Ganoderma lucidum inhibit the growth of lung cancer: involvement of the Akt/mTOR signaling pathway," *Nutrition and Cancer*, vol. 68, no. 7, pp. 1151–1160, 2016.

[23] L. Gao, H. J. Jin, D. Zhang, and Q. Lin, "Silencing circRNA_001937 may inhibit cutaneous squamous cell carcinoma proliferation and induce apoptosis by preventing the sponging of the miRNA-597-3p/FOSL2 pathway," *International Journal of Molecular Medicine*, vol. 46, no. 5, pp. 1653–1660, 2020.

[24] Y. Sun, Y. Liu, Y. Cai et al., "Downregulation of LINC00958 inhibits proliferation, invasion and migration, and promotes apoptosis of colorectal cancer cells by targeting miR-3619-5p," *Oncology Reports*, vol. 44, no. 4, pp. 1574–1582, 2020.

[25] S. Zhang, S. Nie, D. Huang, J. Huang, Y. Feng, and M. Xie, "*Ganoderma atrum* polysaccharide evokes antitumor activity *via* cAMP-PKA mediated apoptotic pathway and down-regulation of Ca^{2+}/PKC signal pathway," *Food and Chemical Toxicology*, vol. 68, pp. 239–246, 2014.

[26] S. Zhang, S. Nie, D. Huang, J. Huang, Y. Wang, and M. Xie, "Polysaccharide from Ganoderma atrum evokes antitumor activity via toll-like receptor 4-mediated NF-κB and mitogen-activated protein kinase signaling pathways," *Journal of Agricultural and Food Chemistry*, vol. 61, no. 15, pp. 3676–3682, 2013.

[27] K. I. Lin, Y. Y. Kao, H. K. Kuo et al., "Reishi polysaccharides induce immunoglobulin production through the TLR4/TLR2-mediated induction of transcription factor Blimp-1," *The Journal of Biological Chemistry*, vol. 281, no. 34, pp. 24111–24123, 2006.

[28] Y. Xu, J. Zheng, P. Sun et al., "Cepharanthine and curcumin inhibited mitochondrial apoptosis induced by PCV2," *BMC Veterinary Research*, vol. 16, no. 1, 2020.

[29] X. Wang, Q. Liu, D. Kong et al., "Down-regulation of SETD6 protects podocyte against high glucose and palmitic acid-induced apoptosis, and mitochondrial dysfunction via activating Nrf2-Keap1 signaling pathway in diabetic nephropathy," *Journal of Molecular Histology*, vol. 51, no. 5, pp. 549–558, 2020.

[30] C. D. Godwin, O. M. Bates, S. R. Jean et al., "Anti-apoptotic BCL-2 family proteins confer resistance to calicheamicin-based antibody-drug conjugate therapy of acute leukemia," *Leukemia & Lymphoma*, vol. 61, no. 12, pp. 2990–2994, 2020.

[31] B. Dong, Z. Yang, Q. Ju et al., "Anticancer effects of Fufang Yiliu Yin formula on colorectal cancer through modulation of the PI3K/Akt pathway and BCL-2 family proteins," *Frontiers in Cell and Development Biology*, vol. 8, 2020.

[32] A. Robert, A. Pujals, L. Favre, J. Debernardi, and J. Wiels, "The BCL-2 family protein inhibitor ABT-737 as an additional tool for the treatment of EBV-associated post-transplant lymphoproliferative disorders," *Molecular Oncology*, vol. 14, no. 10, pp. 2520–2532, 2020.

[33] K. Ma, C. Zhang, and W. Li, "Gamabufotalin suppressed osteosarcoma stem cells through the TGF-β/periostin/PI3K/AKT pathway," *Chemico-Biological Interactions*, vol. 331, article 109275, 2020.

[34] S. Zhang and R. Cui, "The targeted regulation of miR-26a on PTEN-PI3K/AKT signaling pathway in myocardial fibrosis after myocardial infarction," *European Review for Medical and Pharmacological Sciences*, vol. 24, no. 18, 2020.

[35] B. Al-Sarireh and O. Eremin, "Tumour-associated macrophages (TAMS): disordered function, immune suppression and progressive tumour growth," *Journal of the Royal College of Surgeons of Edinburgh*, vol. 45, no. 1, pp. 1–16, 2000.

[36] W. Yang, Y. Lu, Y. Xu et al., "Estrogen represses hepatocellular carcinoma (HCC) growth via inhibiting alternative activation of tumor-associated macrophages (TAMs)," *The Journal of Biological Chemistry*, vol. 287, no. 48, pp. 40140–40149, 2012.

[37] Z. Shen, H. Seppänen, S. Vainionpää et al., "IL10, IL11, IL18 are differently expressed in $CD14^+$ TAMs and play different role in regulating the invasion of gastric cancer cells under hypoxia," *Cytokine*, vol. 59, no. 2, pp. 352–357, 2012.

[38] S. A. Almatroodi, C. F. McDonald, I. A. Darby, and D. S. Pouniotis, "Characterization of M1/M2 tumour-associated macrophages (TAMs) and Th1/Th2 cytokine profiles in patients with NSCLC," *Cancer Microenvironment*, vol. 9, no. 1, pp. 1–11, 2016.

[39] Y. Komohara and M. Takeya, "CAFs and TAMs: maestros of the tumour microenvironment," *The Journal of Pathology*, vol. 241, no. 3, pp. 313–315, 2017.

[40] S. Bi, W. Huang, S. Chen et al., "*Cordyceps militaris* polysaccharide converts immunosuppressive macrophages into M1-like phenotype and activates T lymphocytes by inhibiting the PD-L1/PD-1 axis between TAMs and T lymphocytes," *International Journal of Biological Macromolecules*, vol. 150, pp. 261–280, 2020.

[41] M. Yin, J. Shen, S. Yu et al., "Tumor-associated macrophages (TAMs): a critical activator in ovarian cancer metastasis," *Oncotargets and Therapy*, vol. 12, pp. 8687–8699, 2019.

[42] Y. Li, F. Cao, M. Li et al., "Hydroxychloroquine induced lung cancer suppression by enhancing chemo-sensitization and promoting the transition of M2-TAMs to M1-like macrophages," *Journal of Experimental & Clinical Cancer Research*, vol. 37, no. 1, 2018.

[43] D. F. Soave, M. P. Miguel, F. D. Tomé, L. B. de Menezes, P. R. Nagib, and M. R. Celes, "The fate of the tumor in the hands of microenvironment: role of TAMs and mTOR pathway," *Mediators of Inflammation*, vol. 2016, Article ID 8910520, 7 pages, 2016.

[44] X. Wang, X. Jiao, Y. Meng et al., "Methionine enkephalin (MENK) inhibits human gastric cancer through regulating tumor associated macrophages (TAMs) and PI3K/AKT/m-TOR signaling pathway inside cancer cells," *International Immunopharmacology*, vol. 65, pp. 312–322, 2018.

[45] L. X. Sun, Z. B. Lin, J. Lu et al., "The improvement of M1 polarization in macrophages by glycopeptide derived from Ganoderma lucidum," *Immunologic Research*, vol. 65, no. 3, pp. 658–665, 2017.

[46] Q. Xu, Y. Yan, S. Gu et al., "A novel inflammation-based prognostic score: the fibrinogen/albumin ratio predicts prognoses of patients after curative resection for hepatocellular carcinoma," *Journal of Immunology Research*, vol. 2018, Article ID 4925498, 11 pages, 2018.

[47] D. J. Richards, "Nutritional products as drugs or food implications for development," *Aging (Milano)*, vol. 5, 2 Supplement 1, pp. 59–64, 1993.

[48] S. Hua, Y. Zhang, J. Liu et al., "Ethnomedicine, phytochemistry and pharmacology ofSmilaxglabra: an important traditional Chinese medicine," *The American Journal of Chinese Medicine*, vol. 46, no. 2, pp. 261–297, 2018.

[49] S. D. Chen, M. C. Hsieh, M. T. Chiou, Y. S. Lai, and Y. H. Cheng, "Effects of fermentation products ofGanoderma lucidumon growth performance and immunocompetence in weanling pigs," *Archives of Animal Nutrition*, vol. 62, no. 1, pp. 22–32, 2008.

[50] S. W. Chiu, Z. M. Wang, T. M. Leung, and D. Moore, "Nutritional value of _Ganoderma_ extract and assessment of its genotoxicity and anti-genotoxicity using comet assays of mouse lymphocytes," *Food and chemical toxicology*, vol. 38, no. 2-3, pp. 173–178, 2000.

Hindawi
Journal of Immunology Research
Volume 2021, Article ID 6641341, 14 pages
https://doi.org/10.1155/2021/6641341

Research Article

Chinese Poplar Propolis Inhibits MDA-MB-231 Cell Proliferation in an Inflammatory Microenvironment by Targeting Enzymes of the Glycolytic Pathway

Junya Li,[1] Hui Liu,[1] Xinying Liu,[2] Shengyu Hao,[3] Zihan Zhang,[1] and Hongzhuan Xuan[1]

[1]*School of Life Science, Liaocheng University, Liaocheng 252059, China*
[2]*Center of Bee Industry on Seed-Breeding and Popularization in Shandong Province, Jinan 250010, China*
[3]*School of Physical Science and Information Technology, Liaocheng University, Liaocheng 252059, China*

Correspondence should be addressed to Hongzhuan Xuan; hongzhuanxuan@163.com

Received 16 December 2020; Revised 24 January 2021; Accepted 2 February 2021; Published 15 February 2021

Academic Editor: Kai Wang

Propolis is rich in flavonoids and has excellent antitumor activity. However, little is known about the potential effects of propolis on glycolysis in tumor cells. Here, the antitumor effects of propolis against human breast cancer MDA-MB-231 cells in an inflammatory microenvironment stimulated with lipopolysaccharide (LPS) were investigated by assessing the key enzymes of glycolysis. Propolis treatment obviously inhibited MDA-MB-231 cell proliferation, migration and invasion, clone forming, and angiogenesis. Proinflammatory mediators, including tumor necrosis factor-alpha (TNF-α), interleukin (IL)-1β, and IL-6, as well as NLRP3 inflammasomes, were decreased following propolis treatment when compared with the LPS group. Moreover, propolis treatment significantly downregulated the levels of key enzymes of glycolysis–hexokinase 2 (HK2), phosphofructokinase (PFK), pyruvate kinase muscle isozyme M2 (PKM2), and lactate dehydrogenase A (LDHA) in MDA-MB-231 cells stimulated with LPS. After treatment with 2-deoxy-D-glucose (2-DG), an inhibitor of glycolysis, the inhibitory effect of propolis on migration was not significant when compared with the LPS group. In addition, propolis increased reactive oxygen species (ROS) levels and decreased mitochondrial membrane potential. Taken together, these results indicated that propolis targeted key enzymes of glycolysis to suppress the proliferation of MDA-MB-231 cells in an inflammatory microenvironment. These studies provide a molecular basis for propolis as a natural anticancer agent against breast cancer.

1. Introduction

Breast cancer (BC) is one of the most common malignant tumors and a major cause of cancer death among women worldwide, and the triple-negative breast cancer (TNBC) subtype is the most aggressive one [1]. Worldwide statistics showed that in 2018, approximately two million new cases were detected, with the total BC cases accounting for 11.6% of all cancers. Therefore, the search for effective anticancer agents is urgent for BC therapy and to improve the quality of life of patients.

In recent years, the antitumor activities of flavonoids have attracted increasing interest among researchers. Propolis, rich in flavonoids, is a resinous substance collected by honeybees (*Apis mellifera*) from various plant sources. It has been used as a folk medicine since ancient times [2].

According to its different plant sources, propolis can be divided into five categories: *Populus* propolis, *Baccharis* propolis, *Clusia* propolis, *Macaranga* propolis, and Mediterranean propolis [3]. More than 200 flavonoids have been identified from various kinds of propolis around the world [4]. Chinese propolis (CP), one of the *Populus* type of propolis, mainly contains flavonoids and phenolic compounds and has exhibited extensive pharmacological activities including antibacterial [5], anti-inflammatory [6], antivirus [7], antitumor [8], antioxidant [9], and immunoregulation activities [10].

We and other researchers demonstrated that propolis has an excellent antitumor activity against various tumor cell lines in vivo and in vitro [8, 11]. Furthermore, we reported that Chinese propolis and its major constituent—caffeic acid phenethyl ester (CAPE)—inhibit breast cancer cell proliferation in an inflammatory microenvironment by inhibiting the Toll-like receptor 4 (TLR4) signal pathway and inducing apoptosis and autophagy [12]. However, these antitumor mechanisms have still not been fully elucidated.

The mitochondria are the center of energy and metabolism in eukaryons. Warburg revealed the unique energy metabolism in cancer cells, suggesting a shift in energy production from mitochondrial oxidative phosphorylation (OXPHOS) to aerobic glycolysis [13]. Alterations in the glucose metabolism are characterized by increased uptake of glucose, hyperactivated glycolysis, decreased OXPHOS component, and the accumulation of lactate. Cancer cells rely on higher rates of aerobic glycolysis as their primary source of energy; thus, aerobic glycolysis becomes a hallmark of cancer cells. Key enzymes of glycolysis, namely, hexokinase 2 (HK2), phosphofructokinase (PFK), pyruvate kinase muscle isozyme M2 (PKM2), and lactate dehydrogenase A (LDHA), are critical glycolysis regulators [14]. Enhanced glycolysis correlates with the upregulation and activation of critical glycolytic enzymes, which, in turn, promotes proliferation, metastasis, and tumorigenesis [15]. Inhibition of glycolysis has been identified as a novel therapeutic focus in cancer therapies.

The levels of HK2, PFK, PKM2, and LDHA have been individually reported to be correlated with cancer cell growth [16–19]. Propolis has excellent antitumor activities, and whether propolis could target crucial glycolytic enzymes to inhibit tumor cell proliferation is still unclear. In the present study, the roles of Chinese propolis on key glycolytic enzymes—HK2, PFK, PKM2, and LDHA—were assessed in MDA-MB-231 cells stimulated with lipopolysaccharide (LPS).

2. Materials and Methods

2.1. Chemicals and Reagents. Leibovitz's L15 medium and fetal bovine serum (FBS) were purchased from Gibco-BRL (USA). LPS from *Escherichia coli* 055 : B5,2′,7′-dichlorodihydrofluorescein diacetate (DCFH-DA) and JC-1 was obtained from Sigma-Aldrich (St. Louis, USA). Matrigel basement membrane matrix was obtained from BD Biocoat (USA). The Enhanced Cell Counting Kit-8 was obtained from Beyotime (China). Primary antibodies against β-actin, GAPDH, HK2, PFK, PKM2, LDHA, NLRP3, and secondary antibody were obtained from ABclonal Biotech (USA). Enzyme-linked immunosorbent assay (ELISA) kits for HK2, PFK, PKM2, and LDHA were obtained Shanghai Enzyme-linked Biotechnology Co., Ltd. (China). A secondary antibody for immunofluorescence and donkey anti-rabbit IgG Alexa Fluor-488 was purchased from Life Technologies (USA).

2.2. Preparation of Chinese Propolis Extract. Chinese propolis was collected from Nanyang in Henan province, located in North China in 2017 (voucher specimen no. CP17110702), and the main plant origin of the propolis sample collected was poplar (*Populus* sp.). The propolis was firstly frozen and then extracted with 95% (v/v) ethanol. The extracted propolis was then ultrasonicated at 40°C for 3 h. The supernatant of the extracted propolis was filtered with filter papers to remove the residues, and then the propolis was extracted again three times. Thereafter, all of the supernatants were combined and evaporated with a rotary evaporator under reduced pressure at 50°C. Then, the concentrate was further evaporated in an oven at 50°C until reaching a constant weight and was stored at -20°C. The ethanol extracted Chinese propolis (EECP) was redissolved in ethanol before use. The major chemical constituents of the EECP were analyzed via HPLC-DAD/Q-TOF-MS as previously described [20].

2.3. Cell Culture. The human breast cancer cell line MDA-MB-231 was purchased from Cell Bank of Typical Culture Preservation Committee, Chinese Academy of Sciences, Shanghai (Shanghai, China). Cells were cultured in Leibovitz's L15 medium supplemented with 10% (v/v) FBS, 100 U/mL of penicillin, and 100 μg/mL streptomycin at 37°C.

2.4. Exposure of MDA-MB-231 to EECP. When the MDA-MB-231 cells reached 80%—90% confluence, they were divided into 3 groups for treatment: (a) culture in L15 medium (control group), (b) culture in L15 medium with 1 μg/mL LPS (LPS group), and (c) culture in L15 medium with 1 μg/mL LPS and EECP (25, 50, and 100 μg/mL) (test group). EECP was dissolved in ethanol and applied to the cells, with a final ethanol concentration in the culture medium of <0.1% (v/v). Ethanol at a concentration of 0.1% (v/v) did not affect the cell viability.

2.5. Cell Viability Assay. Cell viability was measured using the CCK-8 kit. Cells (1×10^5 cells/well) were seeded in 96-well plates. When cells reached 60-70% confluence, they were treated with or without EECP (25, 50, and 100 μg/mL) and LPS (1 μg/mL). At 12, 24, and 48 h, cell viabilities were measured following the manufacturer's instructions. The optical density was determined at 450 nm.

2.6. Transwell Analysis. MDA-MB-231 cells were seeded into 6-wells plates. The medium was replaced with fresh complete medium or medium containing 1 μg/mL LPS alone or LPS with EECP (25, 50, and 100 μg/mL) when cells reached 70% confluence. The cells were further incubated for 24 h. Thereafter, the cells were treated with trypsin, resuspended in serum-free medium, and seeded into the upper chamber of the Transwell. Serum-free medium containing 5×10^4 cells was added to the upper chamber for migration assays, whereas 1×10^5 cells were used for Matrigel invasion assays. L15 medium with 20% FBS was added to the lower chamber. After incubation for 24 h, the cells were fixed with 95% (v/v) ethanol for 10 min, then stained with 0.1% crystal violet solution for 30 min and pictured under a microscope. The migration and invasion rates of cells were counted using Image J software.

2.7. Endothelial Cell Tube Formation Assay. Matrigel was diluted with serum-free medium, and 200 μL of diluent was added into a 24-well plate and maintained at 37°C for 1 hour.

Then, 1×10^5 human umbilical vein endothelial cells (HUVECs) were treated with trypsin, resuspended in serum-free medium, and gently seeded on Matrigel-coated wells. Two hours later, cells were treated with EECP (25, 50, or 100 μg/mL) and LPS (1 μg/mL). Endothelial cell tube formation was photographed through an inverted microscope at 6 h. The total tube numbers and branches were calculated using ImageJ software.

2.8. Colony Formation Assay. MDA-MB-231 cells were seeded into a 6-well plate at 1×10^3 cells/well and cultured for 24 h. Then, cells were treated with EECP (25, 50, and 100 μg/mL) and LPS (1 μg/mL) for 24 h. After that, the medium was replaced with fresh complete medium. The medium was changed every three days. Ten days later, cell colonies were washed with phosphate-buffered saline and fixed with 95% (v/v) ethanol. Then, cells were stained with 0.1% crystal violet and captured under an inverted optical microscope. ImageJ software was used to count the numbers of cells.

2.9. Western Blot Assay. After treatment with EECP (25, 50, and 100 μg/mL) for 24 h, the total protein was extracted using a commercial protein extraction kit. The protein concentration was measured using a BCA protein assay kit. Subsequently, equal amounts of protein (30 μg) were separated via 12% SDS-PAGE. The gels were then transferred to polyvinylidene fluoride (PVDF) membranes. Skim milk (5%) was used to block the nonspecific binding sites for 1 h at room temperature. Primary antibodies (HK2, PFK, PKM2, LDHA, and NLRP3) were incubated with the membranes at 4°C overnight, and horseradish peroxidase- (HRP-) conjugated secondary antibodies were then applied for another 1 h of incubation at room temperature. The immunoreactive signals were detected under an Amersham Image 600 (USA), and the relative quantity of protein was analyzed using ImageJ software.

2.10. Reverse Transcription-Quantitative Polymerase Chain Reaction (RT-PCR) Assay. After treatment with EECP (25, 50, and 100 μg/mL) for 24 h, the total RNA of cells was extracted using an RNA extraction kit (Carry Helix, China) according to the manufacturer's protocol. Then, the cDNA was reversed from RNA using a PrimeScript RT Kit (Thermo #K1622). The primers used in the present study are listed in Table 1. Quantitative real-time PCR was performed using the SYBR Green PCR reagent Kit (Thermo F-415XL). The expression of the housekeeping gene GAPDH was used to normalize the expression levels, and the results were expressed as $2^{-\Delta\Delta Ct}$.

2.11. ELISA Assay. The levels of glycolytic key enzymes-HK2, PFK, PKM2, and LDHA and proinflammatory cytokines-TNF-α, IL-1β, and IL-6 in cell supernatant after EECP (25, 50, and 100 μg/mL) treatment were measured using commercial ELISA kits following standard protocols.

2.12. Immunofluorescence Assay. After treatment with EECP (25, 50, and 100 μg/mL) for 24 h, cells were fixed with 4% paraformaldehyde (w/v) at room temperature for 15 min, then blocked with 5% donkey serum (v/v) for 20 min. After adding the primary antibodies for PKM2 and LDHA (1 : 100) and secondary antibody (1 : 200) (FITC-IgG), a laser scanning confocal microscope (Olympus FV1200, Japan) was used for fluorescence detection. For analysis, ImageJ was used as software. Images are representative of three independent experiments.

Table 1: Primer sequences for genes.

Gene (R)	Sequence
LDHA	F: 5′-TTCAGCCCGATTCCGTTAC-3′
	R: 5′-AGACACCAGCAACATTCATTCC-3′
HK2	F: 5′-GCTTGCCTACTTCTTCACG-3′
	R:5′-TTTCTCCATCTCCTTGCG-3′
PFK	F:5′-ACAGAAGCCTTGGTCTAACAC-3′
	R:5′-GGAGAGTTGGAGGAATCAGTAG-3′
PKM2	F:5′-CCAGGTGAAGCAGAAAGGT-3′
	R:5′-CGGATGAATGACGCAAACA-3′
GAPDH	F:5′-AGAAGGCTGGGGCTCATTTG-3′
	R:5′-AGGGGCCATCCACAGTCTTC-3′
IL-1β	F: 5′-GCTCGCCAGTGAAATGATG-3′
	R: 5′-TGGTGGTCGGAGATTCGTAG-3′

2.13. Reactive Oxygen Species (ROS) and Mitochondrial Membrane Potential Assay. The fluorescent probes, DCFH-DA and JC-1, were used to test ROS production and mitochondrial membrane potential, respectively, according to the manufacturer's protocol. The levels of ROS and mitochondrial membrane potential were quantified using the software accompanying laser scanning confocal microscope (Olympus FV1200, Japan). ROS results were shown as the relative fluorescence intensity ratio compared with the LPS group, and mitochondrial membrane potential results were shown as the ratio of red to green fluorescence as compared with the LPS group.

2.14. Statistical Analysis. All experiments were repeated at least three times independently. Data were expressed as the mean ± SEM. Statistical analysis involved paired Student's t -test and ANOVA via SPSS version 18.0 and Graphpad Prism 5. A P value of <0.05 was considered to indicate a statistically significant difference.

3. Results

3.1. The Major Chemical Components of EECP. The chemical constituents of EECP were measured by HPLC-DAD/Q-TOF-MS analysis, and a total of 16 constituents were identified and quantified (Table 2). Flavonoids such as chrysin, pinocembrin, pinobanksin, apigenin, galangin, and quercin

Table 2: The chemical constituents of EECP identified by HPLC-DAD/Q-TOF-MS analysis.

Compounds	M + H	RT	Content (mg/g)
Chrysin	255.0652	31.264	16.887
Pinocembrin	257.0808	30.431	15.243
Pinobanksin	273.0757	27.11	6.879
Apigenin	271.0601	28.781	4.552
Galangin	271.0601	31.521	23.538
Kaempferol	287.0550	28.418	3.321
Quercin	303.0499	26.811	1.229
Caffeic acid	181.0495	17.172	10.857
Gallic acid	171.0288	26.392	0.470
p-Coumaric acid	165.0546	20.232	4.369
3-O-Acetyl pinobanksin	315.0863	30.708	15.570
Naringin	273.0612	27.11	6.876
Ferulic acid	195.0652	21.391	1.567
3,4-Dimethoxycinnamic acid	209.0808	24.676	9.945
Trans-cinnamic acid	195.0652	21.391	6.222
Caffeic acid phenethyl ester	285.1121	31.273	2.851

were rich in EECP, and previous studies also showed that these compounds have excellent antitumor activities [21–25].

3.2. EECP Decreased Cell Viability in MDA-MB-231 Cells Stimulated with LPS. To investigate the antiproliferation activity of EECP (25, 50, and 100 μg/mL) in MDA-MB-231 cells stimulated with LPS, the cell viabilities at 12, 24, and 48 h were firstly tested using a CCK-8 kit. As shown in Figure 1, there was dramatic decrease in cell viabilities after treatment with different concentrations of EECP, and EECP was found to inhibit MDA-MB-231 cell proliferation in a time- and dose-dependent manner when compared with the LPS group. There was no significant different in cell viabilities between the control and LPS groups ($^{*}P < 0.05$, $^{**}P < 0.01$; Figures 1(a)–1(c)).

3.3. EECP Suppressed Migration, Invasion, and Colony Formation in MDA-MB-231 Cells Stimulated with LPS. To further confirm the effect of EECP on the migration, invasion, and clone formation of MDA-MB-231 cells stimulated with LPS, a transwell experiment and angiogenesis assay were performed. In comparison with the control and LPS groups, treatment with different concentrations of EECP obviously suppressed the cell migration and invasiveness of MDA-MB-231 cells stimulated with LPS. Pretreatment with different concentrations of EECP also dramatically decreased the numbers of colonies formed compared with the LPS group ($^{*}P < 0.05$, $^{**}P < 0.01$; Figures 2(a)–(d)).

3.4. EECP Inhibited Endothelial Cell Tube Formation. Tumor associated angiogenesis plays a crucial role in the growth and metastasis of tumor [26]. To determine the effect of EECP on angiogenesis in vitro, HUVECs were treated with different concentrations of EECP (25, 50, and 100 μg/mL) for 6 h. Compared with the LPS group, endothelial cell tube formation abilities were significantly decreased after treatment with EECP. Correspondingly, the numbers of tubes and tube branches were significantly decreased in a dose-dependent manner after EECP treatment, suggesting that EECP probably inhibits tumor angiogenesis ($^{*}P < 0.05$, $^{**}P < 0.01$; Figures 2(e)–(g)).

3.5. EECP Suppressed the Levels of Inflammatory Mediators in MDA-MB-231 Cells Stimulated with LPS. The levels of IL-6, IL-1β, and TNF-α in the LPS groups were evidently increased. Treatment with EECP resulted in a decrease in these proinflammatory cytokines when compared with the LPS group (Figures 3(a)–3(c)). Furthermore, a decrease in the production of IL-1β was also demonstrated by RT-PCR (Figure 3(d)). More importantly, treatment with a higher concentration of EECP significantly reversed the increase of NLRP3, as shown by Western blotting analysis (Figures 3(e) and 3(f)).

3.6. EECP Decreased the Levels of HK2, PFK, PKM2, and LDHA in MDA-MB-231 Cells Stimulated with LPS. The levels of the key enzymes of glycolysis—HK2, PFK, PKM2, and LDHA—in MDA-MB-231 cells stimulated with LPS were firstly measured using ELISA kits. The levels of HK2, PFK, PKM2, and LDHA after EECP treatment were obviously decreased compared with the LPS group, especially after treatment with a higher concentration of EECP (Figures 4(a)–4(d)).

The decrease in the levels of HK2, PFK, PKM2, and LDHA in MDA-MB-231 cells stimulated with LPS was further confirmed by RT-PCR (Figures 4(e)–4(h)). As expected, EECP treatment dramatically decreased the mRNA levels of HK2, PFK, PKM2, and LDHA in a dose-dependent manner compared with the LPS group.

The protein expression levels of HK2, PFK, PKM2, and LDHA in MDA-MB-231 cells stimulated with LPS were also assessed. As shown in Figures 5(a)–5(e), it was observed that expression levels of the key enzymes of glycolysis were downregulated in the EECP treatment groups compared with the LPS group. The EECP administration alleviated glycolysis by suppressing the levels of HK2, PFK, PKM2, and LDHA.

The immunofluorescence assay of PKM2 and LDHA further confirmed that the EECP administration suppressed the protein expression of PKM2 and LDHA in MDA-MB-231 cells stimulated with LPS. The fluorescence intensities of PKM2 and LDHA evidently decreased in EECP treatment groups compared with the LPS group ($^{*}P < 0.05$, $^{**}P < 0.01$; Figures 5(f)–5(h)).

3.7. EECP Increased ROS Production and Decreased Mitochondrial Membrane Potential in MDA-MB-231 Cells Stimulated with LPS. Mitochondria are the center of energy and metabolism in eukaryons. They are also cellular organs with a critical adjusting function in apoptosis signaling processes. To determine the effect of EECP on mitochondria, the mitochondrial membrane potential and ROS production were analyzed. The functions of mitochondria were damaged, and ROS production was obviously increased after

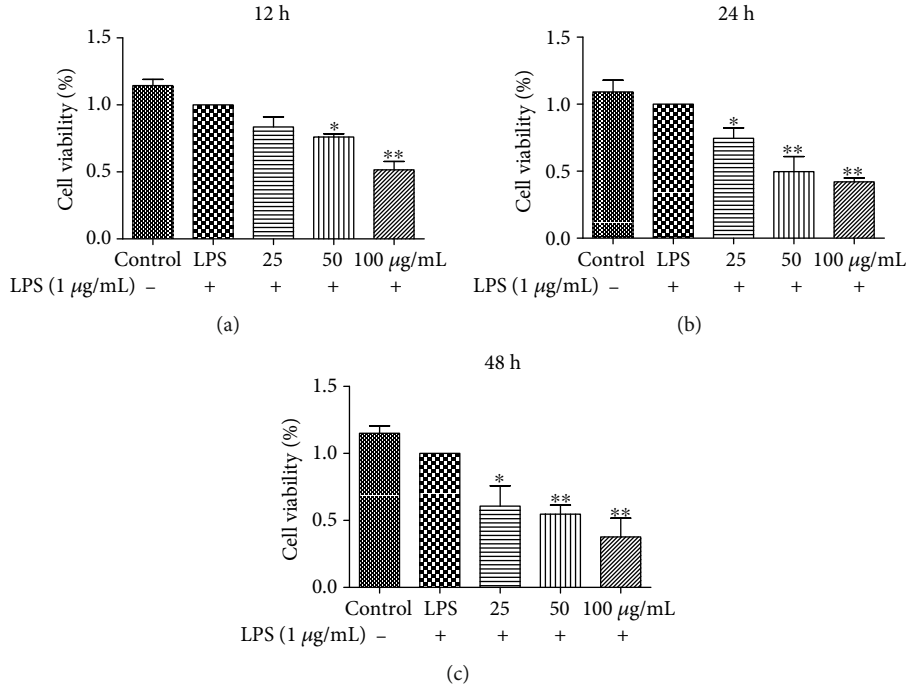

Figure 1: EECP decreased cell viability in MDA-MB-231 cells stimulated with lipopolysaccharide (LPS). (a)–(c) Effect of EECP on the cell viability of MDA-MB-231 cells stimulated with LPS at 12, 24, and 48 h, respectively. 25, 50, and 100 μg/mL: cells treated with EECP at 25, 50, and 100 μg/mL, respectively. Values represent the mean ± SEM from three independent experiments ($^{*}P < 0.05$, $^{**}P < 0.01$ vs. control, $n = 3$).

EECP treatment with the LPS group in MDA-MB-231 cells stimulated with LPS ($^{*}P < 0.05$, $^{**}P < 0.01$; Figures 6(a)–6(c)).

3.8. EECP Inhibited MDA-MB-231 Cell Migration in a Glycolysis—Dependent Manner. To confirm whether EECP inhibited MDA-MB-231 cell migration through inhibiting glycolysis, the scratching assay was performed by adding 2-deoxy-D-glucose (2-DG) into cells. EECP significantly suppressed MDA-MB-231 cell migration without 2-DG in the medium. However, the inhibitory effects in EECP groups were not significant compared with the LPS group after adding 2-DG into the medium, suggesting that EECP's exhibitory effects on MDA-MB-231 cells were probably via the glycolysis pathway ($^{*}P < 0.05$, $^{**}P < 0.01$; Figures 7(a) and 7(b)).

4. Discussion

Although propolis has been shown to have excellent antitumor activities, previous studies assessing antitumor mechanisms by targeting key enzymes of glycolysis were limited. In the present study, we evaluated the antitumor mechanisms of Chinese *populus* propolis in MDA-MB-231 cells stimulated with LPS by studying key glycolysis-related enzymes: HK2, PFK, PKM2, and LDHA. Propolis treatment was able to inhibit MDA-MB-231 cells proliferation, migration, invasion, and angiogenesis, as well as suppress the production of proinflammatory cytokines. More importantly, propolis treatment obviously inhibited the levels of HK2, PFK, PKM2, and LDHA.

The incidence of BC has grown rapidly in recent years. BC can severely decrease a patient's quality of life and has high lethality in women. Tumor glycolysis is crucial for the efficient management of cellular bioenergetics and uninterrupted cancer growth [27]. Although glycolysis is less efficient than oxidative phosphorylation in terms of the net yield of ATP, cancer cells adapt to this mathematical disadvantage by increased glucose uptake, which in turn facilitates a higher rate of glycolysis. Glycolysis in tumor cells produces pyruvate, which is converted to lactic acid in the cytoplasm. These acidic products alter the microenvironment to accelerate tumor proliferation, migration, invasion, and angiogenesis and instigate immunosuppressive networks that are pivotal for cancer cells to escapes immune surveillance [28]. Multiple lines of evidence have established that higher expression levels of key enzymes such as HK2, PFK, PKM2, and LDHA are linked to malignant growth [29, 30]. Thus, targeting glycolysis remains an attractive strategy for therapeutic intervention.

HK catalyzes the first step in glucose metabolism converting glucose to glucose-6-phosphate [29]. HK2 status is clinically linked to recurrence and poor prognosis in BC [31]. This enzyme plays a pivotal role in tumor glycolysis. Inhibition of HK2 has been shown to inhibit the proliferation of cancer cells by shifting the glycolytic pathway with reduced lactate formation [32]. Here, the levels of HK2 were significantly decreased in MDA-MB-231 cells after propolis treatment, as determined by multiple measurement methods.

PFK is crucial in BC cancer progression and is also upregulated in cancer cells; it catalyzes another rate-limiting step of glycolysis, from fructose-6-phosphate to fructose-1,6-bisphosphate [33]. Consistent with the results for HK2,

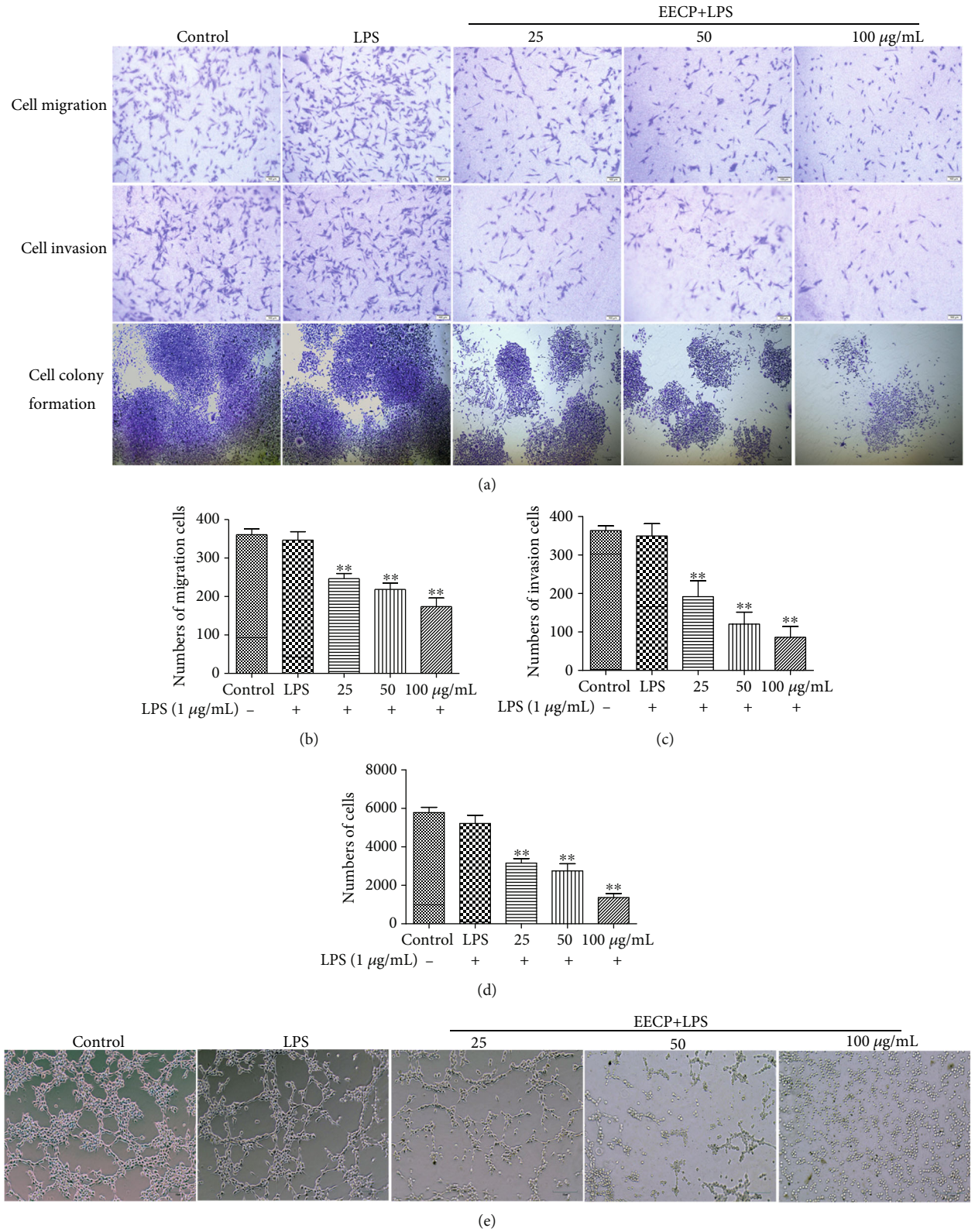

Figure 2: Continued.

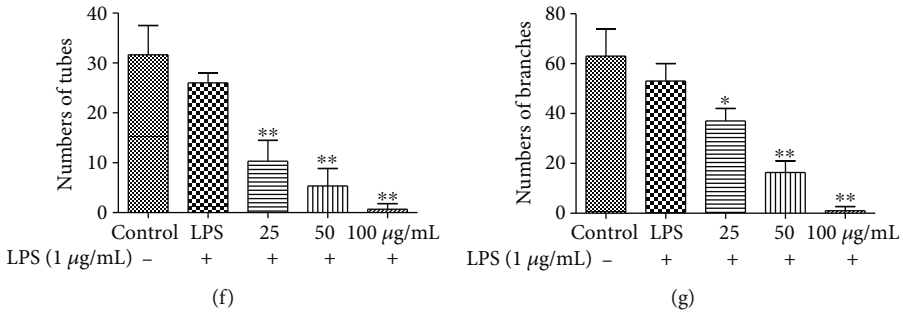

Figure 2: EECP suppressed migration, invasion, and colony formation in MDA-MB-231 cells stimulated with LPS. (a) EECP suppressed migration, invasion, and colony formation in MDA-MB-231 cells. (b)–(d) Quantification of cell migration, invasion, and colony formation in MDA-MB-231 cells after EECP treatment. (e) EECP inhibited angiogenesis in human umbilical vein endothelial cells (HUVECs) at 6 h. (f, g) Quantification of tubes and branches of angiogenesis. Values represent the mean ± SEM from three independent experiments ($^{*}P < 0.05$, $^{**}P < 0.01$ vs. control, $n = 3$).

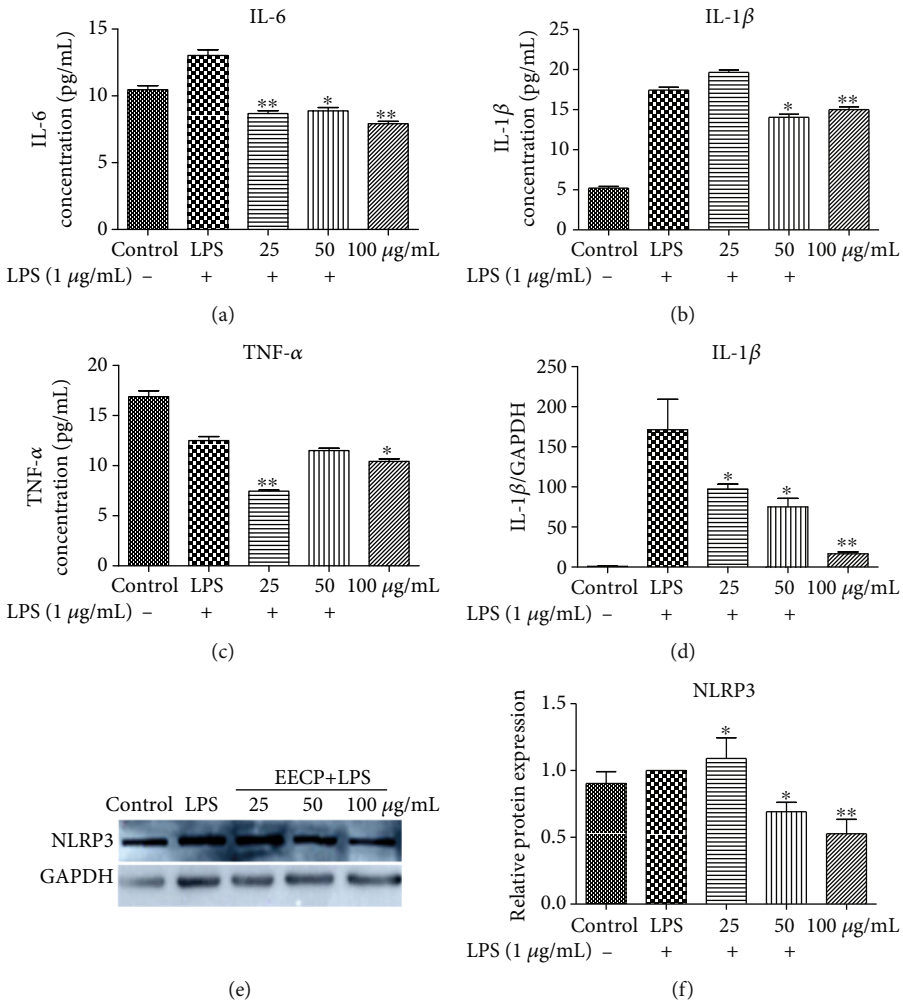

Figure 3: EECP suppressed the levels of inflammatory mediators in MDA-MB-231 cells stimulated with LPS. (a)–(c) EECP inhibited the levels of IL-6, IL-1β, and TNF-α in MDA-MB-231 cells stimulated with LPS, as detected by ELISA kits. (d) EECP inhibited the levels of IL-1β compared with the LPS group, as detected by RT-PCR. (e) EECP inhibited the levels of NLRP3 compared with the LPS group, as detected by Western blotting. (f) Quantification of the relative expression level of NLRP3 in MDA-MB-231 cells. Values represent the mean ± SEM from three independent experiments ($^{*}P < 0.05$, $^{**}P < 0.01$ vs. control, $n = 3$).

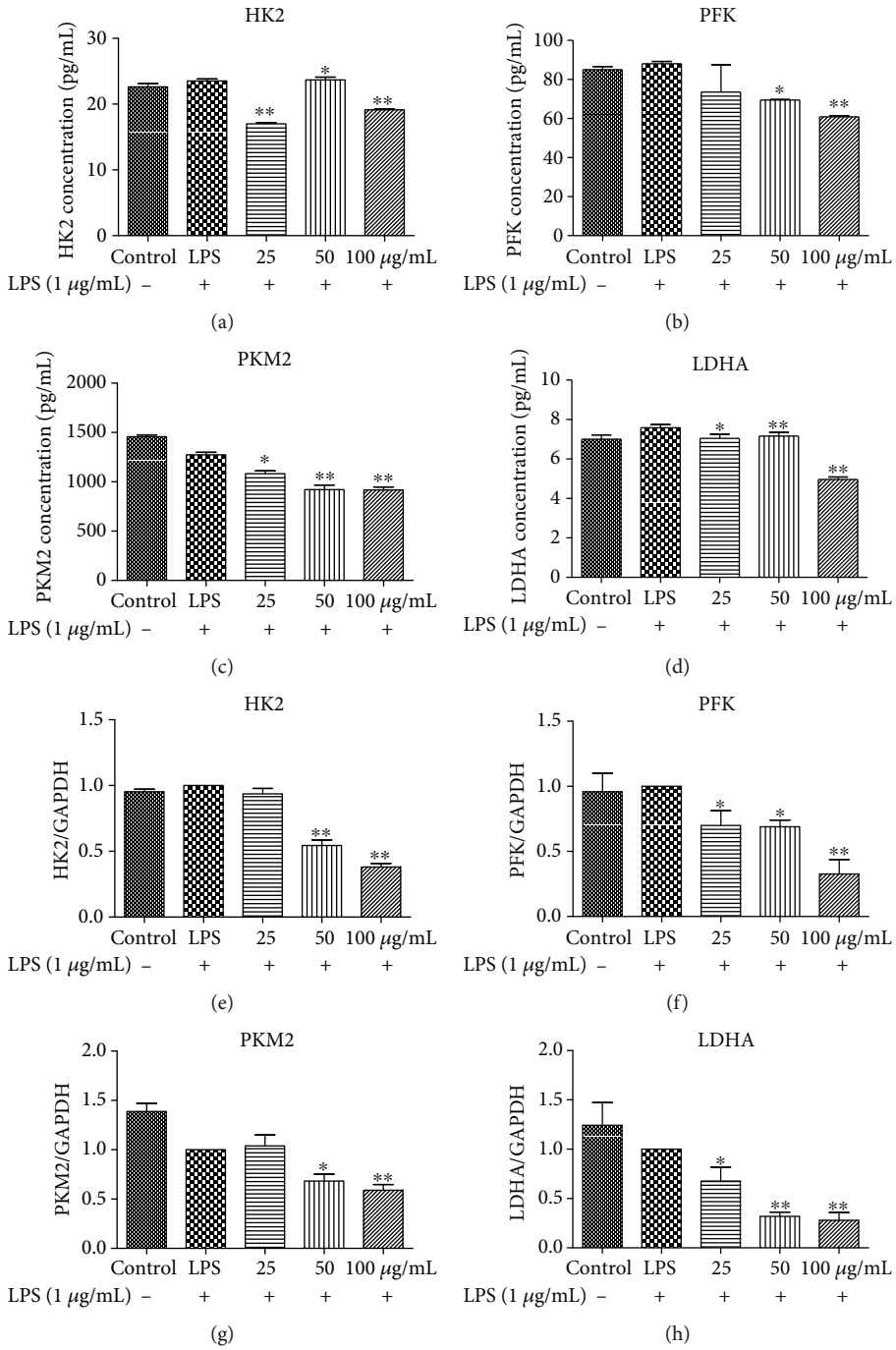

Figure 4: EECP decreased the levels of HK2, PFK, PKM2, and LDHA in MDA-MB-231 cells stimulated with LPS. (a)–(d) EECP decreased the levels of HK2, PFK, PKM2, and LDHA in MDA-MB-231 cells, as detected by ELISA kits. (e)–(h) EECP decreased the levels of HK2, PFK, PKM2, and LDHA in MDA-MB-231 cells, as detected by RT-PCR. Values represent the mean ± SEM from three independent experiments ($^{*}P < 0.05$, $^{**}P < 0.01$ vs. control, $n = 3$).

propolis treatment obviously suppressed the levels of PFK, suggesting that propolis could target key glycolytic enzymes.

PK catalyzes the conversion of phosphoenolpyruvate (PEP) to pyruvate. Among its various isoforms, the M2 isoform has gained much attention due to its higher expression in tumor cells [34]. PKM2 is crucial for aerobic glycolysis and tumor energy metabolism [35]. Emerging preclinical studies have indicated that PKM2 could represent a potential therapeutic target [36]. Here, we also demonstrated that propolis treatment alleviated the levels of PKM2.

LDH catalyzes the final step in the glycolytic pathway that converts pyruvate into lactate, and a higher lactate level significantly correlates with tumor recurrence and the metastatic potential of tumors resulting in poor patient outcomes [37]. Besides this, several studies have identified a prominent role of LDHA in TNBCs [38]. Propolis significantly inhibited

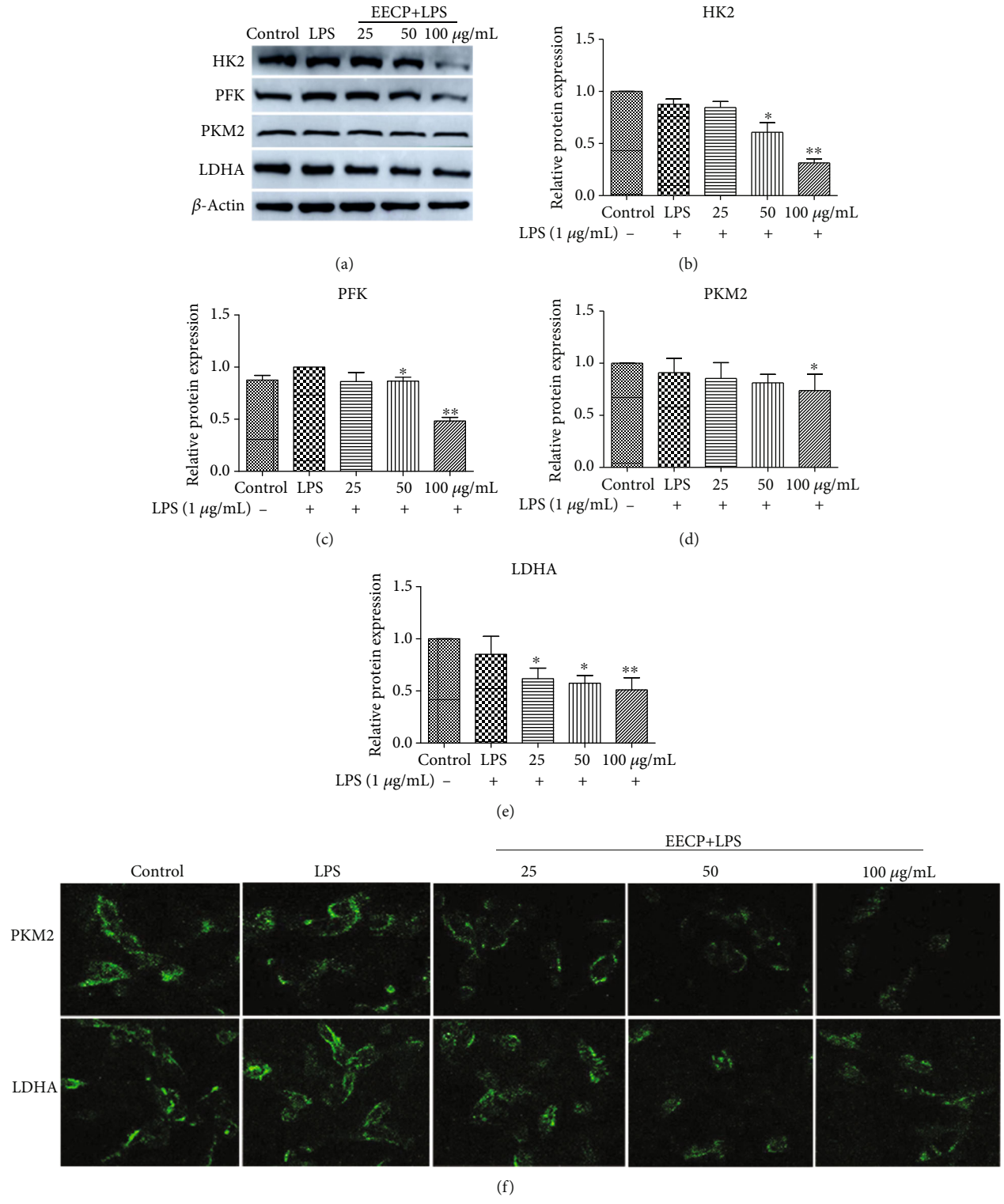

Figure 5: Continued.

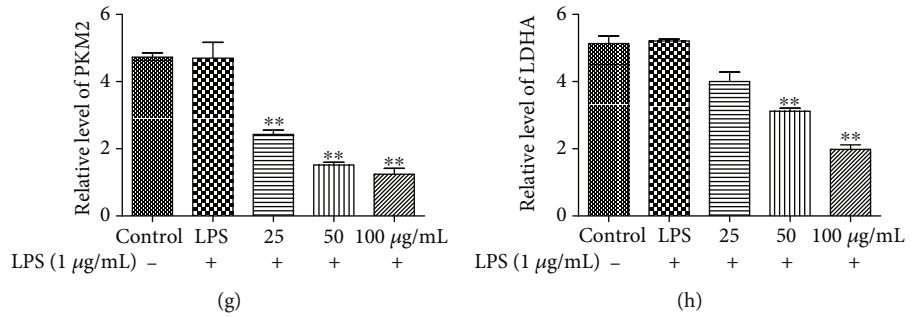

Figure 5: EECP decreased the levels of HK2, PFK, PKM2, and LDHA in MDA-MB-231 cells stimulated with LPS, as detected by Western blotting and immunofluorescence assay. (a) The protein expression levels of HK2, PFK, PKM2, and LDHA in MDA-MB-231 cells. (b)–(e) Quantification of the relative expression levels of HK2, PFK, PKM2, and LDHA in MDA-MB-231 cells. (f) Expression levels of PKM2 and LDHA, as detected by the immunofluorescence assay. (g, h) Quantification of the relative expression levels of PKM2 and LDHA in MDA-MB-231 cells. Values represent the mean ± SEM from three independent experiments ($^{*}P < 0.05$, $^{**}P < 0.01$ vs. control, $n = 3$).

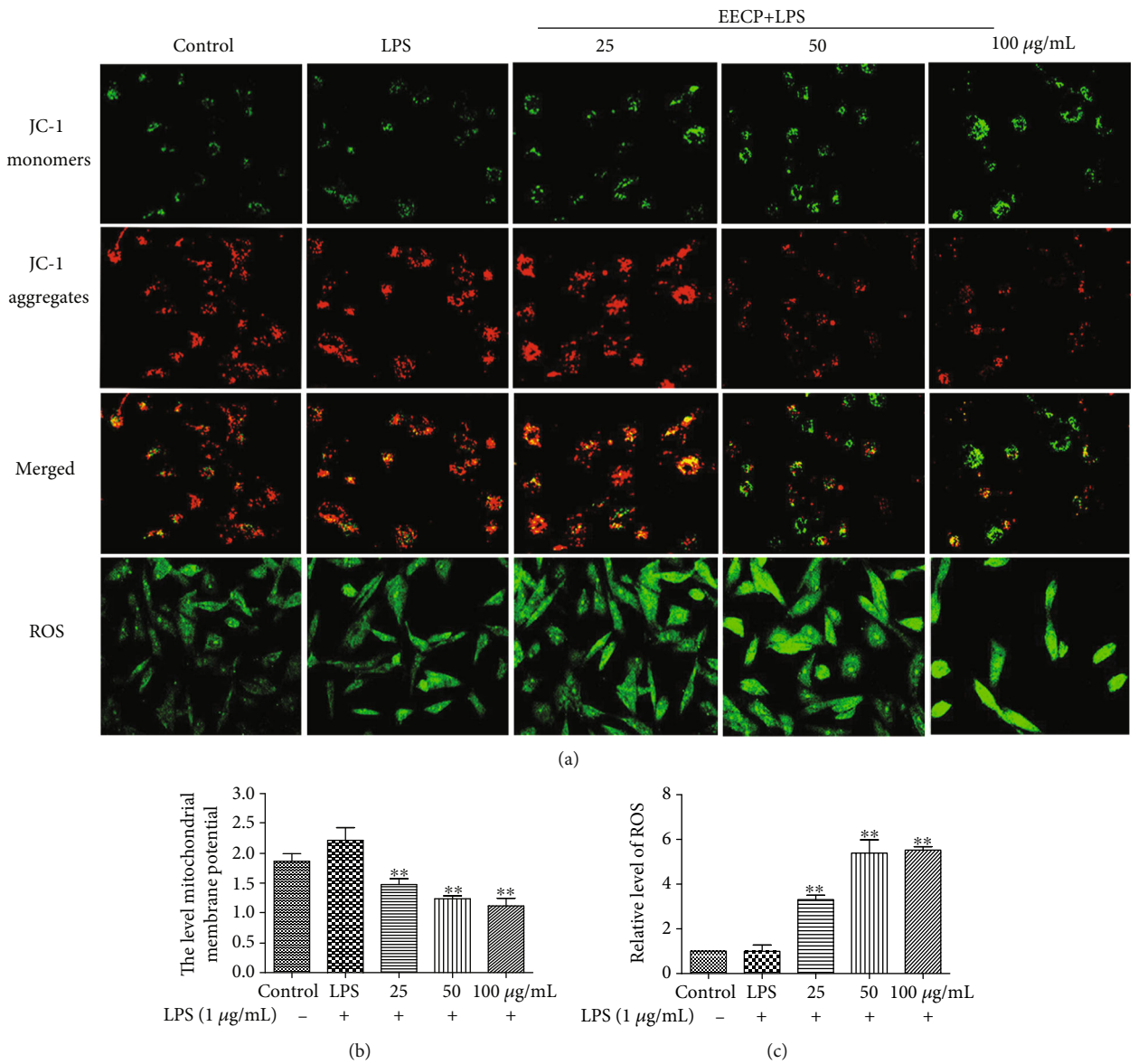

Figure 6: EECP increased reactive oxygen species (ROS) levels and decreased mitochondrial membrane potential in MDA-MB-231 cells stimulated with LPS. (A) Fluorescence micrographs obtained at 24 h. (b, c) Values represent the relative fluorescence intensity per cell determined by laser scanning confocal microscopy. Values represent the mean ± SEM from three independent experiments ($^{*}P < 0.05^{**}P < 0.01$, vs. control, $n = 3$).

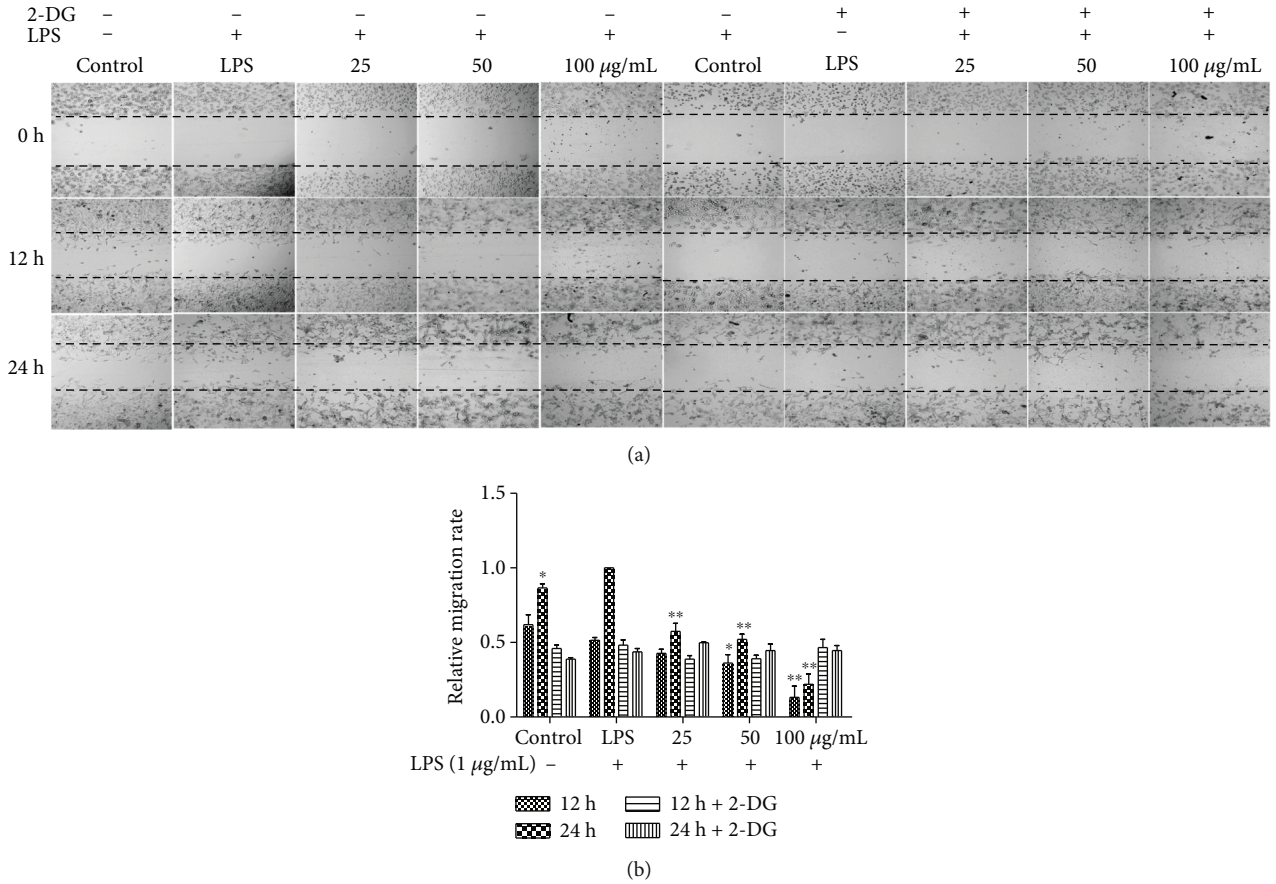

Figure 7: EECP inhibited MDA-MB-231 cell migration in a glycolysis-dependent manner. (a) Effect of EECP on the migration of MDA-MB-231 cells stimulated with LPS with or without 2-deoxy-D-glucose (2-DG). (b) Quantification of the relative migration rate of MDA-MB-231 cells. Values represent the mean ± SEM from three independent experiments ($^{*}P < 0.05$, $^{**}P < 0.01$ vs. control, $n = 3$).

the levels of LDHA, demonstrating promising effects in the prevention of TNBCs.

2-DG, a glucose analog, inhibits glycolysis via its actions on hexokinase [39]. We used 2-DG to inhibit glycolysis in MDA-MB-231 cells to assess the effects of propolis. The results showed that propolis treatment no longer inhibited MDA-MB-231 cell migration compared with the LPS group after inhibition of glycolysis, indicating that propolis exerts the antitumor activity by targeting glycolysis.

ROS are a key determinant of cancer's metabolic phenotype [40]. Maintaining ROS within a narrow range allows malignant cancer cells to enhance their growth and invasion while limiting their apoptotic susceptibility [41]. Cancer cells actively modify their metabolism to optimize intracellular ROS levels and thereby improve survival [42]. Propolis treatment evidently increased the ROS level and decreased the mitochondrial membrane potential in MDA-MB-231 cells stimulated with LPS. The present results are consistent with our original findings, indicating that propolis increases the ROS level to promote cancer cells apoptosis.

The inhibition of glycolysis can also transform tumor cells into forms that are sensitive to immunotherapy and can alter the tumor microenvironment [43]. The NLRP3 inflammasome can be activated by various danger-associated molecular patterns, and the activation of NLPR3 induces caspase-1 activation, IL-1β or IL-18 secretion, and pyroptosis [44]. It has been shown that NLRP3 inflammasome activation in the tumor microenvironment has a critical role in the response to some chemotherapeutic agents [45]. Propolis has excellent anti-inflammatory and immune regulation activities [10]. Here, we also demonstrated that propolis decreased the levels of proinflammatory mediators, including TNF-α, IL-1β, and IL-6, as well as NLRP3 inflammasome to improve the tumor inflammatory microenvironment.

Propolis is rich in flavonoids such as chrysin, pinocembrin, pinobanksin, apigenin, galangin, and quercin, and previous studies also showed that these compounds have excellent antitumor activities. Besides these, CAPE, one of the most important constituent of propolis, also has a strong antitumor activity. In all, these antitumor constituents in propolis account for the strong antitumor activities of propolis.

There are still some limitations in our study. First, although propolis has significant inhibitory effects on glycolytic key enzymes in MDA-MB-231 cells, the effects of propolis on these key enzymes in other tumor cell lines should be

further demonstrated. Second, whether propolis attenuating glycolytic key enzymes suppresses the tumor growth signaling pathway such as PI3K-Akt or propolis inhibiting the PI3K-Akt signaling pathway attenuates glycolytic key enzymes should be further studied.

5. Conclusions

Taken together, the results of this study show that propolis treatment of MDA-MB-231 cells in an inflammatory microenvironment was able to inhibit tumor cell proliferation by targeting key enzymes of glycolysis. As a natural product rich in flavonoids, propolis demonstrated good anti-inflammatory activity in the tumor microenvironment by inhibiting inflammatory cytokines. It was also noted that propolis could target key enzymes of glycolysis to suppress proliferation, migration, invasion, and angiogenesis. Moreover, it was demonstrated that propolis could damage the mitochondrial function by decreasing the mitochondrial membrane potential and increasing ROS production. As a result, Chinese *populus* propolis has excellent potential for use in the prevention and treatment of BC.

Abbreviations

BC: Breast cancer
EECP: Ethanol extract of Chinese propolis
FBS: Fetal bovine serum
HK2: Hexokinase 2
HUVECs: Human umbilical vein endothelial cells
IL-1β: Interleukin-1β
LDHA: Lactate dehydrogenase A
LPS: Lipopolysaccharide
PFK: Phosphate fructose kinase
PKM2: Pyruvate kinase muscle isozyme M2
PVDF: Polyvinylidene difluoride
ROS: Reactive oxygen species
SDS-PAGE: Sodium dodecyl sulfate polyacrylamide gel electrophoresis
TNBC: Triple-negative breast cancer
TNF-α: Tumor necrosis factor-alpha.

Data Availability

The data used to support the findings of this study are included within the article.

Conflicts of Interest

The authors declare no competing conflicts of interest.

Authors' Contributions

H.Z. Xuan and S.Y. Hao designed the study and wrote the manuscript. Y. Jun, H. Liu, and Z.H. Zhang conducted the experiments and analyzed the data. X.Y. Liu and S.Y. Hao revised the manuscript. Y. Jun and H. Liu contributed equally to this work.

Acknowledgments

This work was supported by the grant from the National Natural Science Foundation of China (No. 31672499) and Shandong Province Modern Agricultural Technology System (SDAIT-24-05).

References

[1] O. Golubnitschaja, M. Debald, K. Yeghiazaryan et al., "Breast cancer epidemic in the early twenty-first century: evaluation of risk factors, cumulative questionnaires and recommendations for preventive measures," *Tumour Biology*, vol. 37, no. 10, pp. 12941–12957, 2016.

[2] G. A. Burdock, "Review of the biological properties and toxicity of bee propolis (propolis)," *Food and Chemical Toxicology*, vol. 36, no. 4, pp. 347–363, 1998.

[3] V. Bankova, "Chemical diversity of propolis and the problem of standardization," *Journal of Ethnopharmacology*, vol. 100, no. 1-2, pp. 114–117, 2005.

[4] S. Huang, C. P. Zhang, K. Wang, G. Q. Li, and F. L. Hu, "Recent advances in the chemical composition of propolis," *Molecules*, vol. 19, no. 12, pp. 19610–19632, 2014.

[5] M. C. Fernandez-Calderon, M. L. Navarro-Perez, M. T. Blanco-Roca, C. Gomez-Navia, C. Perez-Giraldo, and V. Vadillo-Rodriguez, "Chemical profile and antibacterial activity of a novel Spanish propolis with new polyphenols also found in olive oil and high amounts of flavonoids," *Molecules*, vol. 25, no. 15, article 3318, 2020.

[6] H. Xuan, Y. Wang, A. Li, C. Fu, and W. Peng, "Bioactive components of Chinese propolis water extract on antitumor activity and quality control," *Evidence-Based Complementary and Alternative Medicine*, vol. 2016, Article ID 9641965, 9 pages, 2016.

[7] V. Bankova, A. S. Galabov, D. Antonova, N. Vilhelmova, and B. Di Perri, "Chemical composition of propolis extract ACF® and activity against herpes simplex virus," *Phytomedicine*, vol. 21, no. 11, pp. 1432–1438, 2014.

[8] Y. Zheng, Y. Wu, X. Chen, X. Jiang, K. Wang, and F. Hu, "Chinese propolis exerts anti-proliferation effects in human melanoma cells by targeting NLRP1 inflammatory pathway, inducing apoptosis, cell cycle arrest, and autophagy," *Nutrients*, vol. 10, no. 9, article 1170, 2018.

[9] Y. Z. Zheng, G. Deng, Q. Liang, D. F. Chen, R. Guo, and R. C. Lai, "Antioxidant activity of quercetin and its glucosides from propolis: a theoretical study," *Scientific Reports*, vol. 7, no. 1, article 7543, 2017.

[10] J. M. Sforcin, "Propolis and the immune system: a review," *Journal of Ethnopharmacology*, vol. 113, no. 1, pp. 1–14, 2007.

[11] K. Wang, J. Zhang, S. Ping et al., "Anti-inflammatory effects of ethanol extracts of Chinese propolis and buds from poplar (Populus×canadensis)," *Journal of Ethnopharmacology*, vol. 155, no. 1, pp. 300–311, 2014.

[12] H. Chang, Y. Wang, X. Yin, X. Liu, and H. Xuan, "Ethanol extract of propolis and its constituent caffeic acid phenethyl ester inhibit breast cancer cells proliferation in inflammatory microenvironment by inhibiting TLR4 signal pathway and inducing apoptosis and autophagy," *BMC Complementary and Alternative Medicine*, vol. 17, no. 1, article 471, 2017.

[13] R. Li, P. Li, J. Wang, and J. Liu, "STIP1 down-regulation inhibits glycolysis by suppressing PKM2 and LDHA and

inactivating the Wnt/beta-catenin pathway in cervical carcinoma cells," *Life Sciences*, vol. 258, article 118190, 2020.

[14] X. Li, J. Sun, Q. Xu et al., "Oxymatrine inhibits colorectal cancer metastasis via attenuating PKM2-mediated aerobic glycolysis," *Cancer Management and Research*, vol. Volume 12, pp. 9503–9513, 2020.

[15] N. Lang, C. Wang, J. Zhao, F. Shi, T. Wu, and H. Cao, "Long non-coding RNA BCYRN1 promotes glycolysis and tumor progression by regulating the miR-149/PKM2 axis in non-small-cell lung cancer," *Molecular Medicine Reports*, vol. 21, no. 3, pp. 1509–1516, 2020.

[16] M. Katagiri, H. Karasawa, K. Takagi et al., "Hexokinase 2 in colorectal cancer: a potent prognostic factor associated with glycolysis, proliferation and migration," *Histology and Histopathology*, vol. 32, no. 4, pp. 351–360, 2017.

[17] E. E. Hackett, H. Charles-Messance, S. M. O'Leary et al., "Mycobacterium tuberculosis limits host glycolysis and IL-1β by restriction of PFK-M via MicroRNA-21," *Cell Reports*, vol. 30, no. 1, pp. 124–136.e4, 2020.

[18] R. Ren, J. Guo, J. Shi, Y. Tian, M. Li, and H. Kang, "PKM2 regulates angiogenesis of VR-EPCs through modulating glycolysis, mitochondrial fission, and fusion," *Journal of Cellular Physiology*, vol. 235, no. 9, pp. 6204–6217, 2020.

[19] H. Wu, X. Wang, T. Wu, and S. Yang, "miR-489 suppresses multiple myeloma cells growth through inhibition of LDHA-mediated aerobic glycolysis," *Genes Genomics*, vol. 42, no. 3, pp. 291–297, 2020.

[20] K. Wang, X. Jin, Y. Chen et al., "Polyphenol-rich propolis extracts strengthen intestinal barrier function by activating AMPK and ERK signaling," *Nutrients*, vol. 8, no. 5, article 272, 2016.

[21] M. F. Tolba, S. S. Azab, A. E. Khalifa, S. Z. Abdel-Rahman, and A. B. Abdel-Naim, "Caffeic acid phenethyl ester, a promising component of propolis with a plethora of biological activities: a review on its anti-inflammatory, neuroprotective, hepatoprotective, and cardioprotective effects," *IUBMB Life*, vol. 65, no. 8, pp. 699–709, 2013.

[22] Y. Zhu, Q. Rao, X. Zhang, and X. Zhou, "Galangin induced antitumor effects in human kidney tumor cells mediated via mitochondrial mediated apoptosis, inhibition of cell migration and invasion and targeting PI3K/AKT/mTOR signalling pathway," *Journal of BUON*, vol. 23, no. 3, pp. 795–799, 2018.

[23] J. Gao, S. Lin, Y. Gao et al., "Pinocembrin inhibits the proliferation and migration and promotes the apoptosis of ovarian cancer cells through down-regulating the mRNA levels of N-cadherin and GABAB receptor," *Biomedicine & Pharmacotherapy*, vol. 120, article 109505, 2019.

[24] H. H. Lee, J. Jung, A. Moon, H. Kang, and H. Cho, "Antitumor and anti-invasive effect of apigenin on human breast carcinoma through suppression of IL-6 expression," *International journal of molecular sciences*, vol. 20, no. 13, article 3143, 2019.

[25] E. R. Moghadam, H. L. Ang, S. E. Asnaf et al., "Broad-spectrum preclinical antitumor activity of chrysin: current trends and future perspectives," *Biomolecules*, vol. 10, no. 10, article 1374, 2020.

[26] P. Gao, L. L. Wang, J. Liu et al., "Dihydroartemisinin inhibits endothelial cell tube formation by suppression of the STAT3 signaling pathway," *Life sciences*, vol. 242, article 117221, 2020.

[27] S. Ganapathy-Kanniappan and J. F. H. Geschwind, "Tumor glycolysis as a target for cancer therapy: progress and prospects," *Molecular Cancer*, vol. 12, article 152, 2013.

[28] S. Cassim, M. Vucetic, M. Zdralevic, and J. Pouyssegur, "Warburg and beyond: the power of mitochondrial metabolism to collaborate or replace fermentative glycolysis in cancer," *Cancers*, vol. 12, no. 5, article 1119, 2020.

[29] M. Haidar, A. Lombes, F. Bouillaud, E. J. Kennedy, and G. Langsley, "HK2 recruitment to Phospho-BAD prevents its degradation, promoting Warburg glycolysis by theileria-transformed leukocytes," *ACS infectious diseases*, vol. 3, no. 3, pp. 216–224, 2017.

[30] M. Hong, X. B. Zhang, F. Xiang, X. Fei, X. L. Ouyang, and X. C. Peng, "MiR-34a suppresses osteoblast differentiation through glycolysis inhibition by targeting lactate dehydrogenase-A (LDHA)," *In Vitro Cellular & Developmental Biology Animal*, vol. 56, no. 6, pp. 480–487, 2020.

[31] E. A. Pudova, A. V. Snezhkina, M. V. Ermoschenkova et al., "HK1 and HK2 gene expression in triple negative and luminal a breast cancer," *Biologicheskie Membrany*, vol. 35, no. 5, pp. 403–406, 2018.

[32] T. Zhang, X. Zhu, H. Wu et al., "Targeting the ROS/PI3-K/AKT/HIF-1α/HK2 axis of breast cancer cells: combined administration of polydatin and 2-deoxy-d-glucose," *Journal of Cellular and Molecular Medicine*, vol. 23, no. 5, pp. 3711–3723, 2019.

[33] X. Shi, L. You, and R. Y. Luo, "Glycolytic reprogramming in cancer cells: PKM2 dimer predominance induced by pulsatile PFK-1 activity," *Physical biology*, vol. 16, no. 6, article 066007, 2019.

[34] R. Tahtouh, L. Wardi, R. Sarkis et al., "Glucose restriction reverses the Warburg effect and modulates PKM2 and mTOR expression in breast cancer cell lines," *Cellular and Molecular Biology (Noisy-le-Grand, France)*, vol. 65, no. 7, pp. 26–33, 2019.

[35] B. Shashni, K. R. Sakharkar, Y. Nagasaki, and M. K. Sakharkar, "Glycolytic enzymes PGK1 and PKM2 as novel transcriptional targets of PPARgamma in breast cancer pathophysiology," *Journal of Drug Targeting*, vol. 21, no. 2, pp. 161–174, 2012.

[36] K. Zhu, Y. Li, C. Deng et al., "Significant association of PKM2 and NQO1 proteins with poor prognosis in breast cancer," *Pathology-Research and Practice*, vol. 216, no. 11, article 153173, 2020.

[37] W. Niu, Y. Luo, X. Wang et al., "BRD7 inhibits the Warburg effect and tumor progression through inactivation of HIF1alpha/LDHA axis in breast cancer," *Cell Death & Disease*, vol. 9, no. 5, article 519, 2018.

[38] X. Huang, X. Li, X. Xie et al., "High expressions of LDHA and AMPK as prognostic biomarkers for breast cancer," *Breast*, vol. 30, pp. 39–46, 2016.

[39] M. Fujita, K. Imadome, V. Somasundaram, M. Kawanishi, K. Karasawa, and D. A. Wink, "Metabolic characterization of aggressive breast cancer cells exhibiting invasive phenotype: impact of non-cytotoxic doses of 2-DG on diminishing invasiveness," *BMC Cancer*, vol. 20, no. 1, article 929, 2020.

[40] S. Rodic and M. D. Vincent, "Reactive oxygen species (ROS) are a key determinant of cancer's metabolic phenotype," *International Journal of Cancer*, vol. 142, no. 3, pp. 440–448, 2018.

[41] J. Cao, X. Liu, Y. Yang et al., "Decylubiquinone suppresses breast cancer growth and metastasis by inhibiting angiogenesis via the ROS/p53/BAI1 signaling pathway," *Angiogenesis*, vol. 23, no. 3, pp. 325–338, 2020.

[42] M. Z. Saleem, M. Alshwmi, H. Zhang et al., "Inhibition of JNK-mediated autophagy promotes proscillaridin A-induced

apoptosis via ROS generation, intracellular Ca(+2) oscillation and inhibiting STAT3 signaling in breast cancer cells," *Frontiers in Pharmacology*, vol. 11, article 01055, 2020.

[43] S. Ganapathy-Kanniappan, "Taming tumor glycolysis and potential implications for immunotherapy," *Frontiers in oncology*, vol. 7, article 36, 2017.

[44] M. S. J. Mangan, E. J. Olhava, W. R. Roush, H. M. Seidel, G. D. Glick, and E. Latz, "Targeting the NLRP3 inflammasome in inflammatory diseases," *Nature Reviews Drug Discovery*, vol. 17, no. 8, pp. 588–606, 2018.

[45] F. Ghiringhelli, L. Apetoh, A. Tesniere et al., "Activation of the NLRP3 inflammasome in dendritic cells induces IL-1β–dependent adaptive immunity against tumors," *Nature Medicine*, vol. 15, no. 10, pp. 1170–1178, 2009.